GREENHOUSE GASES – CAPTURING, UTILIZATION AND REDUCTION

Edited by **Guoxiang Liu**

INTECHWEB.ORG

Greenhouse Gases – Capturing, Utilization and Reduction
Edited by Guoxiang Liu

Published by InTech
Janeza Trdine 9, 51000 Rijeka, Croatia

Publishing Process Manager Maja Bozicevic
Technical Editor Teodora Smiljanic
Cover Designer InTech Design Team

First published March, 2012
Printed in Croatia

A free online edition of this book is available at www.intechopen.com
Additional hard copies can be obtained from orders@intechweb.org

Greenhouse Gases – Capturing, Utilization and Reduction, Edited by Guoxiang Liu
p. cm.
ISBN 978-953-51-0192-5

Contents

Preface

Greenhouse gases, such as carbon dioxide, nitrous oxide, methane, and ozone, play an important role in balancing the temperature of the Earth's surface by absorbing and emitting radiation within the thermal infrared range from the source. However, with the enormous burning of fossil fuels from the industrial revolution, the concentration of greenhouse gases in the atmosphere has greatly increased. The increase has most likely caused serious issues such as global warming and climate change. Such issues urgently request strategies to reduce greenhouse gas emissions to the atmosphere. The main strategies include clean and renewable energy development, efficient energy utilization, transforming greenhouse gases to nongreenhouse gases/compounds, and capturing and storing greenhouse gases underground.

The book entitled Greenhouse Gases - Capturing, Utilization and Reduction covers two parts, a total of 13 chapters. Part 1 (Chapters 1–9) focuses on capturing greenhouse gases by difference techniques such as physical adsorption and separation, chemical structural reconstruction, and biological usage. Part 2 (Chapters 10-13) pays attention to the techniques of greenhouse gases in reduction and storage, such as alternative energy research, energy utilization policy, and geological storage monitoring.

I would like to thank all of authors for their significant contributions on each chapter, providing high-quality information to share with worldwide colleagues. I also want to thank the book managers, Maja Bozicevic and Viktorija Zgela, for their help during the entire publication process.

Guoxiang Liu, Ph.D.
Energy & Environmental Research Center,
University of North Dakota,
USA

Part 1

Greenhouse Gases Capturing and Utilization

1

Carbon Dioxide: Capturing and Utilization

Ali Kargari[1] and Maryam Takht Ravanchi[2]
[1]*Amirkabir University of Technology (Tehran Polytechnic)*
[2]*National Petrochemical Company, Petrochemical Research and Technology Co*
Islamic Republic of Iran

1. Introduction

The global warming issue is one of the most important environmental issues that impacts on the very foundations of human survival.

One person emits about 20 tons of CO_2 per year. Combustion of most carbon-containing substances produces CO_2. Energy utilization in modern societies today is based on combustion of carbonaceous fuels, which are dominated by the three fossil fuels: coal, petroleum, and natural gas. Complete oxidation or combustion of any carbon-based organic matter produces CO_2.

Carbon dioxide makes up just 0.035 percent of the atmosphere, but is the most abundant of the greenhouse gases (GHG) which include methane, nitrous oxide, ozone, and CFCs. All of the greenhouse gases play a role in protecting the earth from rapid loss of heat during the nighttime hours, but abnormally high concentrations of these gases are thought to cause overall warming of the global climate. Governments around the world are now pursuing strategies to halt the rise in concentrations of carbon dioxide and other greenhouse gases (Climate Change 2007). Presently it is estimated that more than 30 billion metric tons of CO_2 is generated annually by the human activities in the whole world. It is reported that approximately 80 percent of the total which is about 24 billion tons is unfortunately originated from only 20 countries. Table 1 shows a list of the most contributed countries in CO_2 emissions. In addition to the efforts for reduction of CO_2, a new technology to collect and store CO_2 is being aggressively developed. The technology is so called CCS which means Carbon dioxide Capture & Storage. Many scientists have concluded that the observed global climate change is due to the greenhouse gas effect, in which man-made greenhouse gases alter the amount of thermal energy stored in the Earth's atmosphere, thereby increasing atmospheric temperatures. The greenhouse gas produced in the most significant quantities is carbon dioxide. The primary source of man-made CO_2 is combustion of fossil fuels. Stabilizing the concentration of atmospheric CO_2 will likely require a variety of actions including a reduction in CO_2 emissions. Since the Industrial Age, the concentration of carbon dioxide in the atmosphere has risen from about 280 ppm to 377ppm, a 35 percent increase. The concentration of carbon dioxide in Earth's atmosphere is approximately 391 ppm by volume as of 2011 and rose by 2.0 ppm/yr during 2000-2009. Forty years earlier, the rise was only 0.9 ppm/yr, showing not only increasing concentrations, but also a rapid acceleration of concentrations. The increase of concentration from pre-industrial concentrations has again doubled in just the last 31 years.

Rank	Country	Annual CO_2 emissions (in 1000 Mt)	% of global total
1	China	7,031,916	23.33%
2	United States	5,461,014	18.11%
3	India	1,742,698	5.78%
4	Russia	1,708,653	5.67%
5	Japan	1,208,163	4.01%
6	Germany	786,660	2.61%
7	Canada	544,091	1.80%
8	Iran	538,404	1.79%
9	United Kingdom	522,856	1.73%
10	South Korea	509,170	1.69%
11	Mexico	475,834	1.58%
12	Italy	445,119	1.48%
13	South Africa	435,878	1.45%
14	Saudi Arabia	433,557	1.44%
15	Indonesia	406,029	1.35%
16	Australia	399,219	1.32%
17	Brazil	393,220	1.30%
18	France	376,986	1.25%
19	Spain	329,286	1.09%
20	Ukraine	323,532	1.07%
21	Poland	316,066	1.05%
22	Thailand	285,733	0.95%
23	Turkey	283,980	0.94%
24	Taiwan	258,599	0.86%
25	Kazakhstan	236,954	0.79%
26	Egypt	210,321	0.70%
27	Malaysia	208,267	0.69%
28	Argentina	192,378	0.64%
29	Netherlands	173,750	0.58%
30	Venezuela	169,533	0.56%
31	Pakistan	163,178	0.54%
32	United Arab Emirates	155,066	0.51%
33	Other countries	3,162,011	11.34%
World		**29,888,121**	**100%**

Table 1. List of countries by 2008 emissions (IEAW, 2010)

Carbon dioxide is essential to photosynthesis in plants and other photoautotrophs, and is also a prominent greenhouse gas. Despite its relatively small overall concentration in the atmosphere, CO_2 is an important component of Earth's atmosphere because it absorbs and emits infrared radiation at wavelengths of 4.26 μm (asymmetric stretching vibrational mode) and 14.99 μm (bending vibrational mode), thereby playing a role in the greenhouse effect, although water vapour plays a more important role. The present level is higher than at any time during the last 800 thousand years and likely higher than in the past 20 million years.

To avoid dangerous climate change, the growth of atmospheric concentrations of greenhouse gases must be halted, and the concentration may have to be reduced (Mahmoudkhani & Keith, 2009).

There are three options to reduce total CO_2 emission into the atmosphere:

- Reduce energy intensity
- Reduce carbon intensity, and
- Enhance the sequestration of CO_2.

The first option requires efficient use of energy. The second option requires switching to using non-fossil fuels such as hydrogen and renewable energy. The third option involves the development of technologies to capture, sequester and utilize more CO_2.

2. Sources of CO_2

About 85% of the world's commercial energy needs are currently supplied by fossil fuels. A rapid change to non-fossil energy sources would result in large disruption to the energy supply infrastructure, with substantial consequences for the global economy. The technology of CO_2 capture and storage would enable the world to continue to use fossil fuels but with much reduced emissions of CO_2, while other low- CO_2 energy sources are being developed and introduced on a large scale. In view of the many uncertainties about the course of climate change, further development and demonstration of CO_2 capture and storage technologies is a prudent precautionary action. Global emissions of CO_2 from fossil fuel use were 23684 million tons per year in 2001. These emissions are concentrated in four main sectors: power generation, industrial processes, the transportation sector and residential and commercial buildings, as shown in Figure 1(a) (IEA, 2003) also, Figure 1 (b and c) depicts the distribution of the flue gases produced by these fuels showing that the major part of the effluent gases is N_2, H_2O, CO_2, and O_2, respectively (Moghadassi et al., 2009).

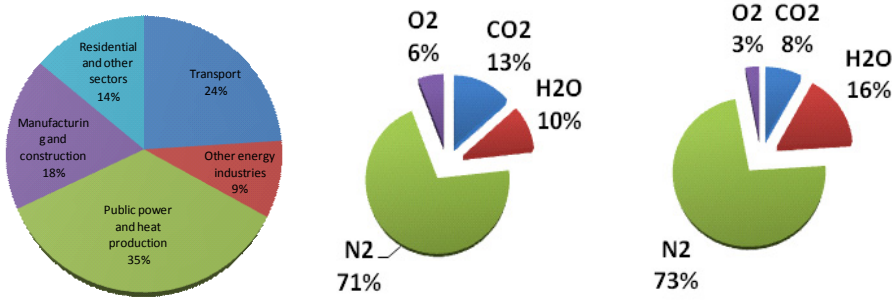

(a) (b) (c)

Fig. 1. (a) The emissions contribution of CO_2 from fossil fuels use in 2001, total emissions 23684 Mt/y and typical power station flue gas compositions, by the use of (a) coal and (b) natural gas as a fuel.

Table 2 shows the worldwide large stationary CO_2 sources emitting more than 0.1 Mt CO_2 per year. Most of the emissions of CO_2 to the atmosphere from the electricity generation and industrial sectors are currently in the form of flue gas from combustion, in which the CO_2 concentration is typically 4-14% by volume, although CO_2 is produced at high concentrations by a few industrial processes. In principle, flue gas could be stored, to avoid

emissions of CO_2 to the atmosphere it would have to be compressed to a pressure of typically more than 10 MPa and this would consume an excessive amount of energy. Also, the high volume of flue gas would mean that storage reservoirs would be filled quickly. For these reasons it is preferable to produce a relatively high purity stream of CO_2 for transport and storage; this process is called CO_2 capture (Lotz & Brent, 2008).

Process	*Number of sources*	*Emissions (Mt CO_2 per year)*
Fossil fuels		
Power	4942	10539
Cement production	1175	932
Refineries	638	798
Iron and steel industry	269	646
Petrochemical industry	470	379
Oil and gas processing	Not available	50
Other sources	90	33
Biomass		
Bioethanol and bioenergy	91	303
Total	***13466***	***7887***

Table 2. Worldwide large stationary CO_2 sources emitting more than 0.1 Mt CO_2 per year (Lotz & Brent, 2008).

2.1 CO_2 large point sources

Power generation is the largest source of CO_2 which could be captured and stored. However, substantial quantities of CO_2 could also be captured in some large energy consuming industries, in particular iron and steel, cement and chemicals production and oil refining.

2.1.1 Cement production

The largest industrial source of CO_2 is cement production, which accounts for about 5% of global CO_2 emissions. The quantity of CO_2 produced by a new large cement kiln can be similar to that produced by a power plant boiler. About half of the CO_2 from cement production is from fuel use and the other half is from calcination of $CaCO_3$ to CaO and CO_2. The concentration of CO_2 in the flue gas from cement kilns is between 14 and 33 vol%, depending on the production process and type of cement. This is higher than in power plant flue gas, so cement kilns could be good candidates for post-combustion CO_2 capture. It may be advantageous to use oxyfuel combustion in cement kilns because only about half as much oxygen would have to be provided per tone of CO_2 captured. However, the effects on the process chemistry of the higher CO_2 concentration in the flue gas would have to be assessed (Henriks et. al., 1999).

2.1.2 Iron and steel production

Large integrated steel mills are some of the world's largest point sources of CO_2. About 70% of the CO_2 from integrated steel mills could be recovered by capture of the CO_2 contained in blast furnace gas. Blast furnace gas typically contains 20% by volume CO_2 and 21% CO, with the rest being mainly N_2. An important and growing trend is the use of new processes for

direct reduction of iron ore. Such processes are well suited to CO_2 capture (Freund & Gale, 2001).

2.1.3 Oil refining

About 65% of the CO_2 emissions from oil refineries are from fired heaters and boilers (Freund & Gale, 2001). The flue gases from these heaters and boilers are similar to those from power plants, so CO_2 could be captured using the same techniques and at broadly similar costs. The same would be true for major fired heaters in the petrochemical industry, such as ethylene cracking furnaces.

2.1.3.1 *Hydrogen and ammonia production*

Large quantities of hydrogen are produced by reforming of natural gas, mainly for production of ammonia-based fertilizers. CO_2 separated in hydrogen plant is normally vented to the atmosphere but it could instead be compressed for storage. This would be a relatively low cost method of avoiding release of CO_2 to the atmosphere. It could also provide useful opportunities for the early demonstration of CO_2 transport and storage techniques.

2.1.3.2 *Natural gas purification*

Some natural gas fields contain substantial amounts of CO_2. The CO_2 concentration has to be reduced to ~2.5% for the market, so any excess CO_2 has to be separated. The captured CO_2 is usually vented to the atmosphere but, instead, it could be stored in underground reservoirs. The first example of this being done on a commercial scale is the Sleipner Vest gas field in the Norwegian sector of the North Sea (Torp & Gale, 2002).

2.1.3.3 *Energy carriers for distributed energy users*

A large amount of fossil fuel is used in transport and small-scale heat and power production. It is not practicable using current technologies to capture, collect, and store CO_2 from such small scale dispersed users. Nevertheless, large reductions could be made in CO_2 emissions through use of a carbon-free energy carrier, such as hydrogen or electricity. Both hydrogen and electricity are often considered as a carrier for energy from renewable sources. However, they can also be produced from fossil fuels in large centralized plants, using capture and storage technology to minimize release of CO_2. Production of hydrogen or electricity from fossil fuels with CO_2 storage could be an attractive transitional strategy to aid the introduction of future carbon free energy carriers (Audus et. al., 1996).

3. Kyoto protocol

The global warming issue forces us to make efforts to use resources and energy efficiently and to reconsider socioeconomic activities and lifestyles that involve large volumes of production, consumption and waste. In June 1992, the Rio de Janeiro United Nations Conference on Environment and Development agreed on the United Nations Framework Convention on Climate Change (UNFCCC), an international treaty aiming at stabilizing greenhouse gas concentrations in the atmosphere. Greenhouse gases such as carbon dioxide (CO_2) or methane are considered responsible for global warming and climate change. Table 3

Gas	*Global warming Potential**	*Contribution to global warming*	*Major sources*
Energy-originated CO_2	1	76%	From fossil fuels both from direct consumption of heating oil, gas, etc. and indirect from fossil fuels for electricity production.
Non-energy-originated CO_2			From use of limestone, incineration of waste, etc. in industrial processes.
CH_4 –(Methane)	21	12%	From anaerobic fermentation, etc. of organic matter in paddy fields and waste disposal sites.
N_2O - (Nitrous oxide)	310	11%	Generated in some manufacturing processes for raw materials for chemical products, the decomposition process of microorganisms in livestock manure, etc.
HFC- (Hydrofluoro-carbons)	140-11700	<1%	Used in the refrigerant in refrigeration and air conditioning appliances, and in foaming agents such as heat insulation materials, etc.
PFC- (Perfluoro Carbons)	7400	<1%	Used in manufacturing processes for semiconductors, etc.
SF_6 – (Sulfur hexafluoride)	25000	<1%	In cover gas when making a magnesium solution, manufacturing of semiconductors and electrical insulation gas, etc.
*Global Warming Potential expresses the extent of the global warming effect caused by each greenhouse gas relative to the global warming effect caused by a similar mass of carbon dioxide.			

Table 3. The global warming potential and major sources subject to the Kyoto protocol.

is a list of most important gases and their global warming potential according to the Kyoto protocol. In 1997, world leaders negotiated the so-called Kyoto protocol as an amendment to the UNFCCC. Under the protocol, industrialized countries committed themselves to a concrete and binding reduction of their collective greenhouse gas emissions (5.2% by 2012 compared to 1990 levels). Currently and within the framework of the UNFCCC, international negotiations try to establish new reduction goals for the post-2012 second commitment period. The December 2009 Copenhagen conference is expected to fix a concrete agreement (UNFCCC, 1992).

The Kyoto Protocol puts a cap on the emissions of these 6 greenhouse gases by industrialized countries (also called Annex I Parties) to reduce their combined emissions by at least 5% of their 1990 levels by the period 2008-2012. In order to minimize the cost of reducing emissions, the Kyoto Protocol has provided for 3 mechanisms that will allow industrialized countries flexibility in meeting their commitments:

- International emissions trading (ET) – trading of emission permits (called Assigned Amount Units or AAUs) among the industrialized countries.
- Joint Implementation (JI) – crediting of emission offsets resulting from projects among industrialized countries (called Emission Reduction Units or ERUs).
- Clean Development Mechanism (CDM) – crediting of emission offsets resulting from projects in developing countries (called Certified Emission Reductions or CERs).

4. Carbon Capture and Storage (CCS)

Carbon capture and storage (CCS) technologies offer great potential for reducing CO_2 emissions and mitigating global climate change, while minimizing the economic impacts of the solution. It seems that along with development of clean technologies, which are a long time program, the need for an emergency solution is vital. Capturing and storage of carbon dioxide is an important way to reduce the negative effects of the emissions. There are several technologies for CCS, some currently are used in large capacities and some are in the research phases. These technologies can be classified, based on their maturity for industrial application, into four classes (IPCC, 2006):

1. "*Mature market*" such as industrial separation, pipeline transport, enhanced oil recovery and industrial utilization.
2. "*Economically feasible*" such as post-combustion capture, pre-combustion capture, tanker transport, gas and oil fields and saline aquifers.
3. "*Demonstration phase*" such as oxy-fuel combustion and enhanced coal bed methane.
4. "*Research phase*" such as ocean storage and mineral carbonation.

Table 4 shows the predicted amounts of CO_2 emission and capture from 2010 to 2050.

Table 5 shows the planned CO_2 capture and storage projects including the location, size, capture process, and start-up date. Figure 2 demonstrates an overview of CO_2 capture processes and systems (IPCC, 2006). There are three known method for capturing of CO_2 in fossil fuels combustion systems. They are applicable in the processes where the main purpose is heat and power generation such as power generation stations. Following is a brief description of there three important capturing processes (WRI, 2008).

Type of data	***Sector***	***2010***	***2020***	***2030***	***2040***	***2050***
CO_2 emission	Power production	12014	13045	10999	7786	4573
	Industry	5399	5715	5277	4385	3493
	Transportation	7080	8211	8237	6733	5228
	Other sources	4589	4894	5072	5072	5072
	Total	***29083***	***31864***	***29586***	***23976***	***18367***
CO_2 capture	Power production	0	340	2750	5963	9176
	Industry	0	66	699	1591	2483
	Transportation	0	148	1046	2550	4055
	Other sources	0	0	0	0	0
	Total	***0***	***554***	***4494***	***10104***	***15713***
Accumulated CO_2 capture (all sectors)		0	1672	28468	104262	236151

Table 4. Predicted CO_2 emission and capture globally in million tones. (Stangeland, 2007).

Project Name	*Location*	*Feedstock*	*Size (MW, except as noted)*	*Capture Process*	*Start-up Date*
Total Lacq	France	Oil	35	Oxf	2008
Vattenfall Oxyfuel	Germany	Coal	30/300/1000*	Oxf	2008–15
AEP Alstom Mountaineer	USA	Coal	30	Poc	2008
Callide-A Oxy Fuel	Australia	Coal	30	Oxf	2009
GreenGen	China	Coal	250/800**	Prc	2009
Williston	USA	Coal	450	Poc	2009–15
Kimberlina	USA	Coal	50	Oxf	2010
NZEC	China	Coal	Undecided	Undecided	2010
AEP Alstom Northeastern	USA	Coal	200	Poc	2011
Sargas Husnes	Norway	Coal	400	Poc	2011
Scottish & Southern Energy Ferrybridge	UK	Coal	500	Poc	2011–12
Naturkraft Kårstø	Norway	Gas	420	Poc	2011–12
Fort Nelson	Canada	Gas	Gas Process	Prc	2011
ZeroGen	Australia	Coal	100	Prc	2012
WA Parish	USA	Coal	125	Poc	2012
UAE Project	UAE	Gas	420	Prc	2012
Appalachian Power	USA	Coal	629	Prc	2012
Wallula Energy Resource Center	USA	Coal	600–700	Prc	2013
RWE power Tilbury	UK	Coal	1600	Poc	2013
Tenaska	USA	Coal	600	Poc	2014
UK CCS Project	UK	Coal	300–400	Poc	2014
Statoil Mongstad	Norway	Gas	630 CHP	Poc	2014
RWE Zero CO2	Germany	Coal	450	Prc	2015
Monash Energy	Australia	Coal	60,000 bpd	Prc	2016
Powerfuel Hatfield	UK	Coal	900	Prc	Undecided
ZENG Worsham-Steed	USA	Gas	70	Oxf	Undecided
Polygen Project	Canada	Coal/ Pcoke	300	Prc	Undecided
ZENG Risavika	Norway	Gas	50–70	Oxf	Undecided
E.ON Karlshamn	Sweden	Oil	5	Poc	Undecided

* 30/300/1000 = Pilot (start time 2008)/Demo/Commercial (anticipated start time 2010–2015)
** 250/800 = Demo/Commercial
bpd = barrels per day; CHP = combined heat and power; Pcoke = petroleum coke; Prc= Pre-combustion; Poc= Post-combustion; Oxf= Oxi-fuel

Table 5. Planned CO_2 capture and storage projects (MIT, 2008).

4.1 Post-combustion capture

In order to separate the CO_2 from the other flue gas components and concentrate the CO_2, it is necessary to add a capture and a compression system (for storage and transport) to the post-combustion system. Advanced post-combustion capture technologies also require significant cleaning of the flue gas before the capture device particularly, sulfur levels have to be low (less than 10 ppm and possibly lower) to reduce corrosion and fouling of the system.

Figure 3 shows a simple block diagram for post-combustion capture from a power plant.

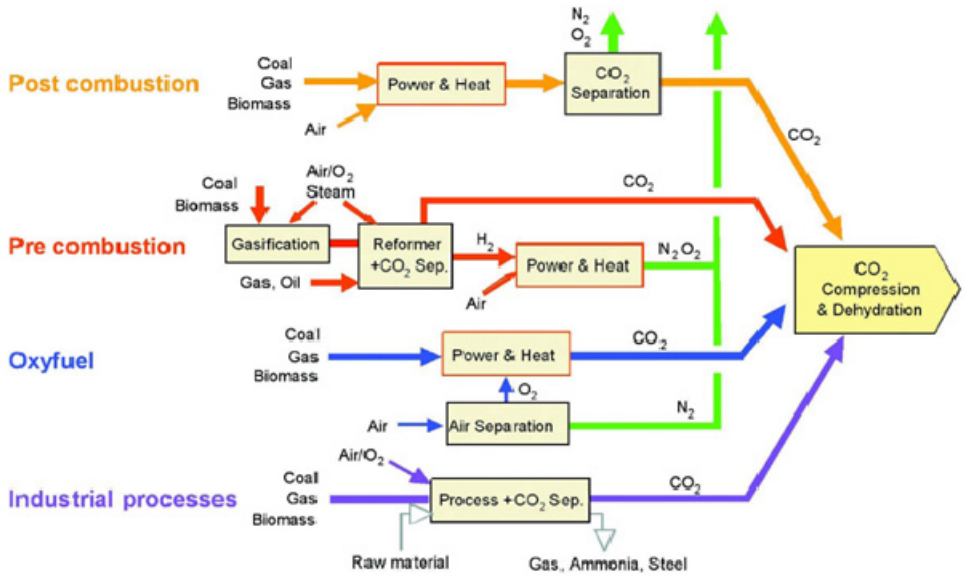

Fig. 2. Overview of CO_2 capture processes and systems.

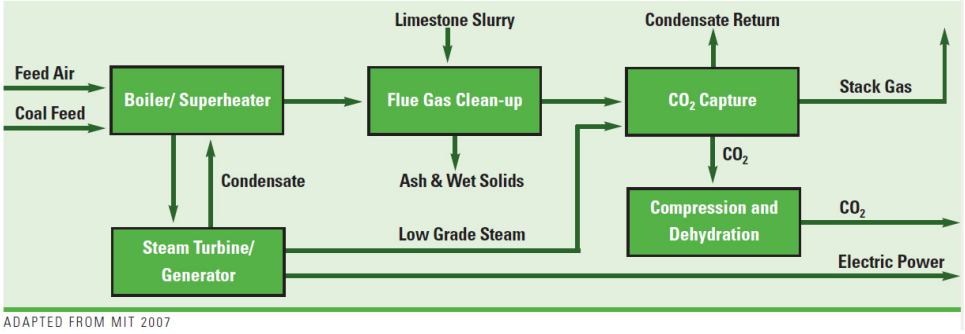

Fig. 3. Post-Combustion Capture from a Pulverized Coal-Fired Power Plant.

4.2 Pre-combustion capture

Pre-combustion capture involves the removal of CO_2 after the coal is gasified into syngas, but before combustion in an Integrated coal Gasification Combined Cycle (IGCC) unit (Figure 4). The first step involves gasifying the coal. Then, a water-gas shift reactor is used to convert carbon monoxide in the syngas and steam to CO_2 and hydrogen. The CO_2 is removed using either a chemical or a physical solvent, such as Selexol™, and is compressed. The hydrogen is combusted in a turbine to generate electricity. Because of technical problems, only 4 GW of IGCC power plants have been built worldwide until the end of 2007.

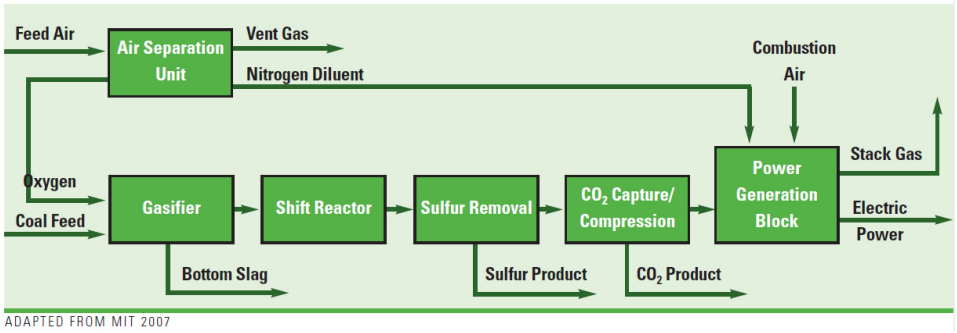

Fig. 4. Pre-Combustion Capture on an IGCC Power Plant.

4.3 Oxy-fuel combustion

Oxy-fuel combustion involves the combustion of fossil fuels in an oxygen-rich environment (nearly pure oxygen mixed with recycled exhaust gas), instead of air. This reduces the formation of nitrogen oxides, so that the exhaust gas is primarily CO_2 and is easier to separate and remove (Figure 5). An air separation unit supplies oxygen to the boiler where it mixes with the recycled exhaust gas. After combustion, the gas stream can be cleaned of PM, nitrogen oxides, and sulfur. After condensing out the water, the flue gas has a CO_2 concentration that is high enough to allow direct compression. As of 2008, oxy-fuel power

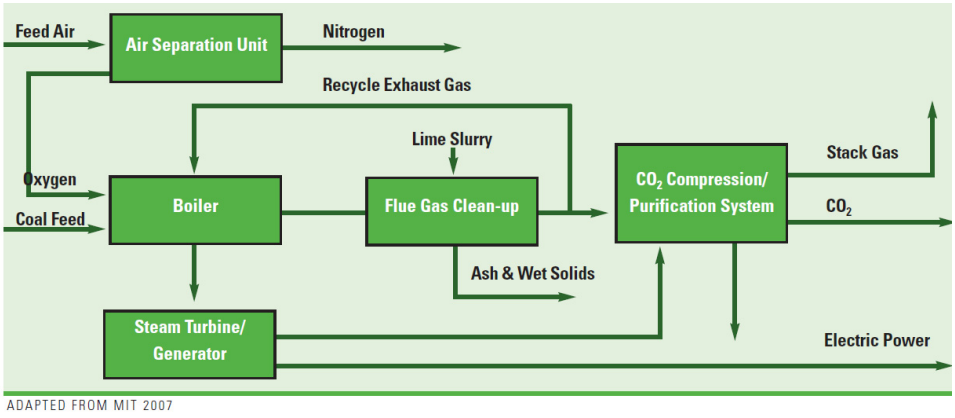

Fig. 5. Oxy-Fuel Combustion with Capture.

plants are in the early stages of development with pilot-scale construction currently underway in Europe and in North America as shown in Table 5 (MIT, 2008).

5. CO_2 removal from gaseous streams

There are three incentives to remove CO_2 from a process stream:

- CO_2 is being removed from a valuable product gas, such as H_2, where it is eventually emitted to the atmosphere as a waste by-product.
- CO_2 is recovered from a process gas, such as in ethanol production, as a saleable product. However, only a modest fraction of the CO_2 produced is marketed as a saleable product, and much of this CO_2 finds its way to the atmosphere because the end use does not consume the CO_2.
- CO_2 is recovered simply to prevent it from being released into the atmosphere, but, this necessarily requires sequestration of the recovered CO_2.

Processes to remove CO_2 from gas streams vary from simple treatment operations to complex multistep recycle systems.

Most of these processes were developed for natural gas sweetening or H_2 recovery from syngas. Recently, interest has built on the capture of CO_2 from flue gas, and even landfill gas and coal bed methane gas. In addition, flue gas, coal bed methane and some landfill gases contain O_2 that can interfere with certain CO_2 separation systems. This complication is generally not present in natural gas, most landfill gas, or H_2 systems. Table 6 lists the licensors of CO_2 separation processes as of 2004 (Ritter & Ebner, 2007; Hydrocarbon Processing, 2004).

For these reasons, commercial CO_2 gas treatment plants are usually integrated gas processing systems; few are designed simply for CO_2 removal. Four different CO_2 removal technologies are widely practiced in industry. These are 1) absorption, both chemical and physical, 2) adsorption, 3) membrane separation, and 4) cryogenic processes (Kohl & Nielsen, 1997). Table 7 shows CO_2 separation techniques including the use of them in CO_2 capture processes.

5.1 Absorption processes

The overwhelming majority of CO_2 removal processes in the chemical and petrochemical industries take place by absorption (see Table 6).

The chemical process industries (CPI) remove CO_2 to meet process or product requirements (e.g., the production of natural gas, ammonia or ethylene oxide manufacturing). A variety of liquid absorbents are being used to remove CO_2 from gas streams.

Absorption processes for CO_2 removal generally can be divided into two categories: (a) *chemical absorption* where the solvent (commonly alkanolamines) chemically reacts with CO_2 and (b) *physical absorption* where the solvent only interacts physically with CO_2 (such as methanol in Rectisol Process and glycol ethers in Selexol Process).

In many industrial applications, combinations of physical solvents and reactive absorbents may be used in tandem. The solvents include monoethanolamine (MEA), diethanolamine (DEA), diisopropanolamine (DIPA), methyldiethanolamine (MDEA), and diglycolamine

Licensor	System	Primary Goal	CO_2 in Tail-gas	Capacity per Unit	Plants world wide
Linde AG	PSA-H_2	H_2-(P)	30-60%	1-100 MMscfd	250
Technip	PSA-H_2	H_2-(P)	30-60%	-	240
Uhde	PSA-H_2	H_2-(P)	30-60%	-110 MMscfd	60
Haldor Topsøe A/S	PSA-H_2	H_2-(P)	30-60%	-20 MMscfd	31
UOP LLC (Polybed)	PSA-H_2	H_2-(P)	30-60%	-200 MMscfd	700
CB&I Howe-Baker	PSA-H_2	H_2-(P)	30-60%	1- 280 MMscfd	170
Foster Wheeler	PSA-H_2	H_2-(P)	30-60%	1- 95 MMscfd	100
Lurgi Oel-Gas-Chemie GmbH	PSA-H_2	H_2-(P)	30-60%	1-200 MMscfd	105
Air Products (PRISM)	PSA-H_2	H_2-(P)	30-60%	15-120 MMscfd	50
Uhde Gmbh	PSA-NH_3	H_2-(P)	30-60%	500-1800 mtpd	14
Haldor Topsøe	PSA-NH_3	H_2-(P)	30-60%	650-2050 mtpd	60
Kellogg Brown & Root, Inc	PSA-NH_3	H_2-(P)	30-60%	-1850 mtpd	200
Axens	Adsorption	GC+CO_2-(R)	1-98%	-	60
Shell Global Solutions International B.V (ADIP)	Scrub (MDEA, DIPA)	AG-(R)	1-98%	-	400
Prosernat-IFP Group Tech. (Advanced Amines)	Scrub (DEA, MDEA)	AG-(R)	1-98%	0.3-25.2 Nm^3/d	120
BASF AG (aMDEA)	Scrub (MDEA)	AG-(R)	1-98%	3.5-700 MMscfd	230
UOP LLC (Amine Guard FS)	Scrub (amine)	AG-(R)	1-98%	-500 MMscfd	500
UOP LLC (Benfield)	Scrub (DEA-K_2CO_3)	AG-(R)	1-98%	-500 MMscfd	700
Exxon Mobil Research & Eng. Co. (FIEXSORB)	Scrub (amine)	AG-(R)	1-98%	-	49
Fluor Enterprises, Inc. (Econamine)	Scrub (DGA) H_2-(P)	CO_2-(R)	+99%	3-400 MMscfd	55
Fluor Enterprises, Inc. (Econamine FG Plus)	Scrub (MEA)	CO_2-(R)	+99%	-300 mtpd	24
Advantica Ltd. (LRS-10)	Scrub (LRS10-K_2CO_3)	CO_2-(R)	+99%	-	30
Lurgi Oel-Gas-Chemie GmbH (Rectisol)	Scrub (Methanol)	AG-(R)	1-98%	-	100
UOP LLC (Selexol)	Scrub (DME, PEG)	AG-(R,P)	1-98%	-	55
Shell Global Solutions International B.V (Sulfinol)	Scrub (sulfolane, amine)	AG-(P)	1-98%	-	200
Air Liquide (Medal)	Membrane	CO_2, H_2O-(R)	2-70%	1-1000 MMscfd	several
NATCO Group Inc. (CYNARA)	Membrane	CO_2-(R)	-95%	5-750 MMscfd	30
UOP LLC (Separex)	Membrane	AG-(R)	-		50
Merichem Chem & Refineries Services (AMINEX)	HFMC	AG-(R)	1-98%	-	10

PSA = Pressure Swing Adsorption; HFMC = hollow fiber membrane contactor; AG = All acid gases (i.e., H_2S, COS and CO_2); P = purification; R = removal; GC= Gas contaminants (Hg, As, H_2O, TBC, NH and Sx)

Table 6. Major Licensors of CO_2 separation processes from gaseous streams (Hydrocarbon Processing, 2004.)

Separation techniques	*Post-combustion*	*Oxy fuel-combustion*	*Pre-combustion*
Chemical & physical absorption	Chemical solvents	-	Physical solvents Chemical solvents
Membrane	Polymer – Ceramic-Hybrid - Carbon	Polymer	Polymer- Ceramic Palladium
Adsorption	Zeolites Active carbons Molecular sieves	Zeolites - Activated carbons - Adsorbents (O_2/N_2)	Zeolites - Activated carbons - Aluminum and silica gel
Cryogenic	-	Distillation	-

Table 7. CO_2 separation techniques (IEAGHG, 2011).

(DGA). Ammonia and alkaline salt solutions are also used as absorbents for CO_2. Water is used as a CO_2 absorbent, but only at high pressures where solubility becomes appreciable. However, in all cases solvent recycling is energy and capital intensive. Among the solvents, MEA has the highest capacity and the lowest molecular weight. It offers the highest removal capacity on either a unit weight or a unit volume basis. When only CO_2 is to be removed in large quantities, or when only partial removal is necessary, a hot carbonate solution or one of the physical solvents is economically preferred. MEA has good thermal stability, but reacts irreversibly with COS and CS_2.

DEA has a lower capacity than MEA and it reacts more slowly. Although its reactions with COS and CS_2 are slower, they lead to different products that cause fewer filtration and plugging problems. TEA has been almost completely replaced in sour gas treating because of its low reactivity toward H_2S. DGA has the same reactivity and capacity as DEA, with a lower vapor pressure and lower evaporation losses. DIPA, which is used in the Sulfinol and Shell Adip processes to treat gas to pipeline specifications, can remove COS and is selective for H_2S removal over CO_2 removal. MDEA selectively removes H_2S in the presence of CO_2, has good capacity, good reactivity, and very low vapor pressure. As a result, MDEA is a preferred solvent for gas treating.

Flue gas from combustion processes associated with burners, flaring, incineration, utility boilers, etc. contain significant amounts of CO_2. However, as discussed above, this CO_2 is generally of low quality because its concentration tends to be low, the flue gas is very hot, and it contains a variety of other gaseous species and particulates that make CO_2 recovery difficult and expensive.

Fluor Enterprises Inc. has 24 Econamine FG plants operating worldwide and producing a saleable CO_2 product for both the chemical and food industries. Randall Gas Technologies, ABB Lummus Global Inc. has four installations of similar technology operating on coal fired boilers. Two of these plants produce chemical grade CO_2 and the other two plants produce food grade CO_2. Mitsubishi Heavy Industries Ltd. also has commercialized a flue gas CO_2 recovery process, based on their newly developed and proprietary hindered amine solvents (KS-1, KS-2 and KS-3).

5.2 Adsorption processes

The adsorption processes include pressure swing adsorption (PSA), temperature swing adsorption (TSA), and hybrid PSA/TSA. Only a few classes of adsorbents and adsorption

processes are being used to remove CO_2 from gas streams. These adsorbents include aluminosilicate zeolite molecular sieves, titanosilicate molecular sieves, and activated carbons. Other classic adsorbents are being used to remove contaminants from CO_2 streams destined for commercial use. In this case, the adsorbents include activated carbons for sulfur compounds and trace contaminant removal, silica gels for light hydrocarbon removal, and activated alumina, bauxite, and silica gels for moisture removal. Of the CO_2 producing processes listed in Table 6, only H_2, syngas, NH_3, fermentation ethanol, natural gas, and combustion are beginning to use adsorption processes for removing or purifying CO_2.

By-product CO_2 from H_2 production via methane steam reforming is recovered using PSA in lieu of absorption. The PSA unit offers advantages of improved H_2 product purity (99-99.99 vol% H_2, 100 ppmv CH_4, 10-50 ppmv carbon oxides, and 0.1-1.0 vol% N_2) with capital and operating costs comparable to those of wet scrubbing.

Modern PSA plants for H_2 purification generally utilize layered beds containing 3 to 4 adsorbents (e.g., silica gel or alumina for water, activated carbon for CO_2, and 5A zeolite for CH_4, CO, and N_2 removal). Depending on the production volume requirements, from four to sixteen columns are used in tandem. The PSA unit is operated at ambient temperature with a feed pressure ranging between 20 and 60 atm. Hydrogen recovery depends on the desired purity, but ranges between 60 and 90%, with the tail gas (i.e., the desorbed gas containing H_2O, N_2, CO_2, CH_4, CO, and H_2) generally being used as fuel for the reformer.

Although PSA systems are increasingly used for H_2 recovery, they yield a by-product CO_2 stream that is only about 50 vol% pure. Low purity makes this tail gas stream less attractive as a commercial CO_2 source.

As the composition of natural gas varies widely depending on the location of the well (the CO_2 concentration in natural gas varies between 3 and 40 vol%; but it could be as high as 80 vol%), and because of the complexity and variability of the composition of natural gas, a train of separation processes, including adsorption, absorption, cryogenic and membrane separation, may be used to process it into pipeline quality methane.

Although the traditional process for removing CO_2 has been the amine process, but PSA technology is beginning to supplant some of the absorption technology in natural gas treatment, especially in the so called shut-in natural gas wells that previously contained too much N_2 to justify processing.

To remove CO_2 from coal bed methane, Engelhard Corporation uses molecular gate adsorption technology with a more traditional PSA mode with compressed feeds ranging in pressure 80-800 psig. Similarly, Axens has commercialized natural gas purification technology, based on alumina and zeolite molecular sieve adsorbents and a TSA regeneration mode. The alumina removes trace and bulk contaminants in the natural gas other than CO_2 through both chemisorption and physisorption mechanisms. The zeolite molecular sieve serves to remove CO_2 and other contaminants via physisorption. Axens has over 60 installations operating worldwide that treat a variety of natural gas and industrial process streams. Table 8 shows the performance characteristics of some common sorbents for CO_2 separation.

Sorbent	Capacity	Feed composition	Ref.
Aqueous ammonia	1.20 g CO_2/g NH_3	15vol% CO_2, 85vol%N_2	Yeh *et al*., 2005
Aminated mesoporous silica	0.45–0.6 molCO_2/mol amine	100% CO_2	Knowles *et al*., 2005
Aminated SBA-15	1528–4188 μmol CO_2/g sorbent	10%CO_2, 90% He, with 2% H_2O	Gray *et al*., 2005
PEI-impregnated MCM-41	45 ml (STP) CO_2/g adsorbent	15% CO_2, 4%O_2, 81% N_2	Xu *et al*., 2005
PEI-impregnated MCM-41	246 mg CO_2/gPEI or 82 mg CO_2/g sorbent	N/A	Xu *et al*., 2002; *Song et al, 2006*
Anthracite activated carbon	65.7 mg CO_2/g adsorbent	N/A	Maroto-Valer *et al*., 2005
Lithium silicate	360 mg CO_2/g sorbent	100% CO_2	Kato *et al*., 2005

Table 8. The CO_2 sorbent performance.

5.3 Membrane processes

Membrane technology for separating gas streams is attractive for many reasons:

1. It neither requires a separating agent nor involves phase changes.
2. No processing costs associated with regeneration and phase change.
3. The systems involve small footprints compared to other processes.
4. They require low maintenance.
5. They are compact and lightweight and can be positioned either horizontally or vertically, which is especially suitable for retrofitting applications.
6. They are modular units and allow for multi-stage operation.
7. They have linear scale up costs (Takht Ravanchi et al., 2009a; Takht Ravanchi & Kargari, 2009).

The major drawbacks associated with this technology are the low capacity and poor thermal properties of the current commercial available membranes. Membranes are an appealing option for CO_2 separation, mainly because of the inherent permeating properties. CO_2 is a fast diffusing gas in many membrane materials, such as glassy and rubbery polymers, molecular sieves, and several other inorganic materials. On the other hand, CO_2 also has a relatively high molecular weight and a large quadruple moment, enabling it naturally to adsorb more strongly to or dissolve at much higher concentrations in these membrane materials compared to many other gas species. These properties give rise to very high CO_2 permeation rates and selectivities over many other gas species, sometimes even higher than H_2 and He. Membrane systems potentially or actually commercialized for gas separations are listed in Table 6. Of the CO_2 producing processes listed, only natural gas production, to a lesser extent landfill gas production, H_2, syngas, and NH_3 production are beginning to use membrane processes for removing or purifying CO_2.

One of the great challenges in membrane-based CO_2 separation technology is the lack of membranes with simultaneous high permeability and selectivity. A wide range of selectivity/permeability combinations are provided by different membrane materials, but for gas separation applications, the most permeable polymers at a particular selectivity are of interest, and the highly permeable polymers exhibit moderate to low selectivity values.

On the other hand, in the application of a membrane with a specific permeability, to meet the desired selectivity using the multi-stage gas separation process is often unavoidable.

Up to now, many studies have been carried out to increase the performance of polymeric membranes. According to these researches, the most important methods for increasing the performance of polymeric membranes are as follows (Sanaeepur et al., 2011a, 2011b; Ebadi et al., 2010, 2011):

1. Incorporation of flexible and polar groups such as amines, carboxyles.
2. Mixing with a carrier (fixed carrier membranes) such as type 1 amino group as a CO_2 carrier.
3. Using a soft segment such as poly (dimethyl siloxane).
4. Addition of a compatibilizer such as polystyrene-block-poly (methylmethacrylate) in polymethylmethacrylate/poly methyl ether blends.
5. Polymer blending and interpenetrating polymer networks.
6. Chemical cross-linking and load-bearing network creation via covalent linkages.
7. Structural modification of block copolymers by block copolymerization with a polymer having specific mechanical properties that form a nanostructure, which has physical cross-linkages with favorite properties.
8. Free volume increasing by adding (nano) particles to polymer matrices.

The first commercial cellulose acetate membrane units for CO_2 removal from natural gas were implemented only few years after the introduction in 1980 of the first commercial PRISM membrane air separation system developed by Monsanto. By the end of the 1980s companies such as Natco (Cynara), UOP (Separex) and Kvaerner (Grace Membrane Systems) were producing membrane plants for this purpose. A few years later, more selective polyimides and only recently polyaramides were slowly introduced to displace the old cellulose acetate systems. Today, commercial membrane technology for CO_2 separation is largely based on glassy polymeric materials (cellulose acetate, polyimides, and polyaramides). Currently, the membrane market devoted to CO_2 separation from natural gas is about 20%, which is only 2% of the total separations market for natural gas. Membranes are used in situations where the produced gas contains high levels of CO_2. However, the membranes are very sensitive to exposure to C5+ hydrocarbons present in wet natural gas streams because these compounds immediately degrades performance and can cause irreversible damage to the membranes. Membranes for large-scale recovery of CO_2 from, for example, natural gas for use as a salable product are a relatively recent development. A variety of membranes, including ones with separating layers made of cellulose acetate, polysulfone, and polyimide, are used for this purpose. Air Products and Chemicals and Ube are marketing membrane systems for EOR and landfill gas upgrading, respectively and they have been commercialized for H_2 purification in reforming processes. For example, membrane processes, such as the POLYSEP membrane systems developed by UOP and the PRISM membrane systems developed by Monsanto and now sold by Air Products and Chemicals recover H_2 from various refinery, petrochemical and chemical process streams. Both are based on polymeric asymmetric membrane materials composed of a single polymer or layers of at least two different polymers, with the active polymer layer being a polyimide. The PRISM system is based on a hollow fiber design and POLYSEP is a spiral-wound, sheet-type contactor. Both are used to recover H_2 from refinery streams at purities ranging from 70 to 99 vol% and with recoveries ranging from 70 to 95%. Relatively

pure H_2 containing a very low concentration of CO_2 leaves these units in the low pressure permeate stream. This stream can be sent to a methanator for CO_2 removal and further purification. The high-pressure retentate stream, consisting of H_2 and CO_2 with low concentrations of CO and CH_4, can be used as fuel.

Figure 6 shows the currently status of the developed membranes for separation of CO_2 from N_2 streams as the selectivity (alpha) versus permeability (P).

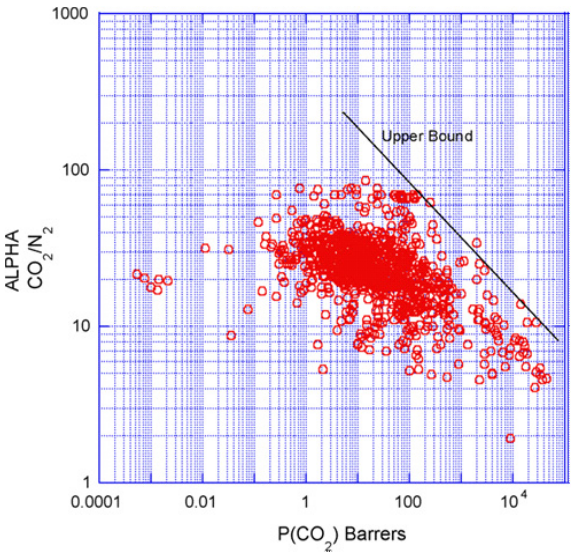

Fig. 6. Upper bound correlation for CO_2/N_2 separation (Robeson, 2008).

Another attractive membrane system is so called "Liquid Membrane" (LM) which have been found many applications in chemical engineering, medicinal and environmental processes (Kaghazchi et al., 2006, 2009; Kargari et al., 2002, 2003a, 2003b, 2003c, 2003d, 2004a, 2004b, 2004c, 2004d, 2004e, 2005a, 2005b, 2006a, 2006b, 2006c ; Mohammadi et al., 2008; Nabieyan et al., 2007; Rezaei et al., 2004).

Separation of gases by LM is a new field in separation science and technology. Separation of olefin/paraffin gases are very attractive and cost effective (Takht Ravanchi, 2008a, 2008b, 2008c, 2008d, 2009a, 2009b, 2009c, 2010a, 2010b, 2010c). CO_2 removal from gas streams especially natural gas is important for increase the heating value of the natural gas and limiting the CO_2 emission in the combustion systems (Heydari Gorji, 2009a, 2009b).

The advantage of the LM over solid (organic or inorganic) membranes are ease of operational conditions and very higher selectivities (in the order of several hundreds), but the instability problems of the LM have limited the industrial applications of this attractive technology.

5.4 Cryogenic liquefaction processes

Recovery of CO_2 by cold liquefaction has the advantage of enabling the direct production of very pure liquid CO_2, which can be readily transported. The disadvantages associated with

the cryogenic separation of CO_2 are the amount of energy required in refrigeration, particularly in dilute gas streams, and the requirement to remove gases, such as water and heavy hydrocarbons, that tend to freeze and block the heat exchangers.

Liquefaction technology for CO_2 recovery is still incipient. Cryogenic CO_2 recovery is typically limited to streams that contain high concentrations of CO_2 (more than 50 vol%), but with a preferred concentration of > 90 vol%. It is not considered to be a viable CO_2 capture technology for streams that contain low concentrations of CO_2, which includes most of the industrial sources of CO_2 emissions. Cryogenic separation of CO_2 is most applicable to high-pressure gas streams, like those available in pre-combustion and oxyfuel combustion processes. Cryogenic CO_2 recovery is increasingly being used commercially for purification of CO_2 from streams that already have high CO_2 concentrations (typically > 90%). Of the CO_2 producing processes listed in Table 6, only ethanol production and H_2, syngas, and NH_3 production utilize cryogenic processes for removing or purifying CO_2.

Currently, Costain Oil, Gas & Process Ltd. has commercialized a CO_2 liquefaction process with around seven units installed worldwide. The process is assisted by membrane technology to treat streams with CO_2 fractions greater than 90 vol.%

Recently, Fluor Enterprises Inc. also developed a CO_2 liquefaction process called CO_2LDSEP. This technology exploits liquefaction to separate CO_2 from H_2 and other gases in the tail gas of a H_2 purification PSA unit. Table 9 demonstrates the CO_2 capture technologies advantages and challenges**.**

6. CO_2 conversion, utilization and fixation

One way to mitigate carbon dioxide emission is its conversion and fixation to value-added products. The main processes for carbon dioxide conversion and fixation in chemical industries are:

a. Hydrogenation
b. Oxidative Dehydrogenation
c. Oxidative Coupling of Methane
d. Dry Reforming of Methane

CO_2 is not just a greenhouse gas, but also an important source of carbon for making organic chemicals, materials and carbohydrates (e.g., foods). As will be discussed below, various chemicals, materials, and fuels can be synthesized using CO_2, which should be a sustainable way in the long term when renewable sources of energy such as solar energy is used as energy input for the chemical processing.

Some general guidelines for developing technologies for CO_2 conversion and utilization can be summarized as below:

- Select concentrated CO_2 sources for CO_2 capture and/or utilization; aim for on-site/nearby uses if possible.
- Use CO_2 to replace a hazardous or less-effective substance in existing chemical processes for making products with significant volumes.
- Use renewable sources of energy or 'waste' energy for CO_2 conversion and utilization whenever possible.

CO_2 Capture Technology	*Capturing method*	*Advantages*	*Challenges*
Pre- Combustion	Physical Solvent	• Recovery process does not require heat. • Common for same solvent to have high H_2S solubility, allowing for combined CO_2/H_2S removal. • System concepts for CO_2 recovery with some steam stripping and delivery at a higher pressure may be optimized for power systems.	• CO_2 pressure is lost during flash recovery. • Must cool down synthesis gas for CO_2 capture, then heat it back up again and re-humidify for firing to turbine. • Low solubilities can require circulating large volumes of solvent, resulting in large pump loads. • Some H_2 may be lost with the CO_2.
	Solid Sorbent	• CO_2 recovery does not require heat. • Common for H_2S to also have high solubility in the same sorbent (combined CO_2/H_2S capture). • System concepts for CO_2 recovery with some steam stripping and delivery at a higher pressure may be optimized for power systems.	• CO_2 pressure is lost during flash recovery. • Must cool synthesis gas for CO_2 capture, then heat it back up again and re-humidify for firing to turbine. • Some H_2 may be lost with the CO_2.
	H_2/CO_2 Membrane	H_2 or CO_2 Permeable Membrane: • No steam load or chemical attrition. H_2 Permeable Membrane Only: • Can deliver CO_2 at high-pressure, greatly reducing compression costs. • H_2 permeation can drive the CO shift reaction toward completion – potentially achieving the shift at lower cost/higher temperatures.	• Membrane separation of H_2 and CO_2 is more challenging than the difference in MW implies. • Due to decreasing partial pressure differentials, some H_2 will be lost with the CO_2. • In H_2 selective membranes, H_2 compression is required and offsets the gains of delivering CO_2 at pressure. In CO_2 selective membranes, CO_2 is generated at low pressure requiring compression.
	Water Gas Shift Membrane	• Promote higher conversion of CO and H_2O to CO_2 and H_2 than in a conventional WGS reactor. • Reduce CO_2 capture and H_2 production costs. • Increase net plant efficiency.	• Single stage WGS with membrane integration • Improved selectivity of H_2 or CO_2 • Optimize membranes for WGS reactor conditions
Post-Combustion	Solvent	• Chemical solvents provide a high chemical potential necessary for selective capture from streams with low CO_2 partial pressure. • Wet-scrubbing allows good heat integration and ease of heat management (useful for exothermic reactions).	• Trade off between heat of reaction and kinetics. • Energy required to heat, cool, and pump nonreactive carrier liquid (usually water) is often significant. • Vacuum stripping can reduce regeneration steam requirements, but is expensive.

CO_2 Capture Technology	Capturing method	Advantages	Challenges
Oxy-fuel Combustion	Solid Sorbent	• Chemical sites provide large capacities/fast kinetics (capture from low CO_2 partial pressure streams). • Higher capacities on a per mass or volume basis than similar wet-scrubbing chemicals. • Lower heating requirements than wet-scrubbing. • Dry process—less sensible heating requirement than wet scrubbing process.	• Heat required to reverse chemical reaction (although generally less than in wet-scrubbing cases). • Heat management in solid systems is difficult, which can limit capacity and/or create operational issues when absorption reaction is exothermic. • Pressure drop can be large in flue gas applications. • Sorbent attrition.
	Membrane	• No steam load. • No chemicals. • Simple and modular designs. • 'Unit operation' versus complex 'process.'	• Tend to be more suitable for processes like IGCC. • Trade off between recovery and product purity. • Requires high selectivity. • Poor economy of scale. • Multiple stages/recycle streams may be required.
	Cryogenic Distillation & Solid Sorbent	• The combustion products are CO_2 and water. The relatively pure CO_2 is easily separated thus making the sequestration process less expensive.	• Current cryogenic air separation plants to produce O_2 are expensive and energy intensive. • High costs of CO_2 recycle. • Converting air-fired systems to oxygen fired. • High temperatures can degrade boiler materials. • Requires high temperature materials. • Excess flue gas constituents contaminating sequestration stream (O_2, SO_2, NOx, Hg).

Table 9. CO_2 capture technologies advantages and challenges (DOE/NETL 2010)

- Convert CO_2 along with other co-reactants into chemical products that are industrially useful at significant scale.
- Fix CO_2 into environmentally benign organic chemicals, polymer materials or inorganic materials.
- Electric power generation with more efficient CO_2 capture and conversion or utilization.
- Take value-added approaches for CO_2 sequestration coupled with utilization.

CO_2 is used as refrigerant for food preservation, beverage carbonation agent, supercritical solvent, inert medium (such as fire extinguisher), pressurizing agent, chemical reactant (urea, etc.), neutralizing agent, and as gas for greenhouses.

Solid CO_2 (dry ice) has a greater refrigeration effect than water ice. Dry ice is also usually much colder than water ice, and the dry ice sublimates to a gas as it absorbs heat. It should be noted that the use of CO_2 for refrigeration does not directly contribute to reduction of CO_2 emissions.

There exist some chemical processes for CO_2 conversion in chemical industry, for which synthesis of urea from ammonia and CO_2 (Eq. (1)) and the production of salicylic acid from phenol and CO_2 (Eq. (2)) are representative examples. Urea is used for making various polymer materials, for producing fertilizers and in organic chemical industry. It is a preferred solid nitrogen fertilizer because of its high nitrogen content (46%). As an example of the usefulness of salicylic acid, acetyl salicylic acid is used for making Aspirin, a widely used common medicine.

$$CO_2 + 2NH_3 \rightarrow H_2N\text{-}CO\text{-}NH_2 \quad (1)$$

$$C_6H_5 - OH + CO_2 \rightarrow C_6H_5(OH)\,COOH \quad (2)$$

Supercritical CO_2 can be used as either a solvent for separation or as a medium for chemical reaction, or as both a solvent and a reactant. The use of supercritical CO_2 ($SC\text{–}CO_2$) allows contaminant free supercritical extraction of various substances ranging from beverage materials (such as caffeine from coffee bean), foods (such as excess oil from fried potato chips), and organic and inorganic functional materials, to herbs and pharmaceuticals. It is also possible to use $SC\text{–}CO_2$ to remove pollutants such as PAHs from waste sludge and contaminated soils and toxics on activated carbon adsorbent (Akgerman et al. 1992).

The dissociation of CO_2 on catalyst surface could produce active oxygen species. Some heterogeneous chemical reactions can benefit from using CO_2 as a mild oxidant, or as a selective source of ''oxygen'' atoms. For example, the use of CO_2 has been found to be beneficial for selective dehydrogenation of ethylbenzene to form styrene, and for dehydrogenation of lower alkanes such as ethane, propane and butane to form ethylene, propylene, and butene, respectively. Some recent studies on heterogeneous catalytic conversion using CO_2 as an oxidant have been discussed in several recent reviews (Song et al, 2002; Park et al, 2001). If renewable sources or waste sources of energy are used, recycling of CO_2 as carbon source for chemicals and fuels should be considered for applications where CO_2 can be used that have desired environmental benefits. CO_2 recycling would also make sense if such an option can indeed lead to less consumption of carbon-based fossil resources without producing more CO_2 from the whole system. Conversion of CO_2 to C1 to C10 hydrocarbon fuels via methanol has also been reported (Nam et al, 1999). There has been

some reported effort on direct synthesis of aromatics from hydrogenation of CO_2 using hybrid catalysts composed of iron catalysts and HZSM-5 zeolite (Kuei and Lee, 1991). Related to the methanol synthesis and Fischer– Tropsch synthesis is the recently proposed tri-reforming process for conversion of CO_2 in flue gas or in CO_2-rich natural gas without CO_2 pre-separation to produce synthesis gas (CO + H_2) with desired H_2/CO ratios of 1.5–2.0 (Song & Pan 2004). For the CO_2 conversion to methanol using H_2, it should be noted that H_2 is currently produced by reforming of hydrocarbons which is an energy-intensive process and accompanied by CO_2 formation both from the conversion process and from the combustion of the fuels which is used to provide the process heat (Armor, 2000). Therefore, methanol synthesis using CO_2 does not contribute to CO_2 reduction unless H_2 is produced by using renewable energy or process waste energy or nuclear energy. BTX hydrocarbons (benzene, toluene, and xylenes) are important sources of petrochemicals for gasoline and other feed-stocks. Aromatization of lower alkanes is an interest in industry, and many efforts have been made in this area. The transformation of CH_4 to aromatics is thermodynamically more favorable than the transformation of CH_4 to C_2H_6, and extensive efforts have also been devoted to the direct conversion along this line in heterogeneous catalysis. To achieve the high activity and stability in methane dehydroaromatization, novel approaches to reduce carbon deposition are being made. The co-feeding of some oxidants (NO, O_2, CO, and CO_2) with CH_4 has been proposed. CO_2 is an acidic oxide, when it is dissolved in water, either as bicarbonate or carbonate (Ayers, 1988), it is slightly acidic. This weak acidity can be used in neutralization processes e.g., in purification of water from swimming pools. Due to its weak acidity, the pH value it can reach is limited (from pH of 12-13 to 6-9). Carbon dioxide can react in different ways with a large variety of compounds. The products that may be obtained are including, e.g., organic carbonates, (amino-) acids, esters, lactones, amino alcohols, carbamates, urea derivatives, and various polymers or copolymers. The limited number of publications in this research area shows that this new territory is still to be exploited. Some of these products are of great technical interest. The major reactions and their products are listed in Table 10. There are both natural and artificial ways to capture or fix the carbon to avoid or delay emission into the atmosphere, such as

reactants	**products with CO_2**	**reactants**	**products with CO_2**
alkane	syngas, acids, esters, lactones	Substituted hydrocarbon[c]	acids, esters, lactones, polycarbonates
cycloalkane	acids, esters, lactones	alkyne	lactones, unsaturated organic carbonates
active-H compound	acids, esters, lactones	epoxide	carbonates, (co)polymers (polycarbonates)
monoalkene	acids, esters, lactones	NH_3 and amine	symmetrical ureas, aminoacids, (co)polymers
diene[a]	acids, esters, lactones[b]	diamine	ureas, carbamates, (co)polymers (polyureas)
cycloalkene	acids, esters, lactones, (co)polymers	imines	carbamates, (co)polymers (urethane)
[a] Allenes and 1,3-dienes; [b] With longer C-C chain than the original monomer; [c] Dihalogen substituted			

Table 10. Reactants and their products in CO_2 reactions

forestation, ocean fertilization, photosynthesis, mineral carbonation, *In-situ* CO_2 capture and hydrate. Interested researcher is referred to (Yamasaki A, 2003; Stewart C, Hessami M, 2005; Maroto-Valer et al., 2005; Druckenmiller and Maroto-Valer, 2005; Liu et al., 2005; Stolaroff et al., 2005) for further details in this subject.

7. Conclusion

CO_2 emission along with its global warming is one of the most important and emergency problem threatens the living on the earth. Although some governmental laws and protocols have limited the emissions, but the emission rates are so high that the accumulation of CO_2 have caused the global climate change. Carbon based fossil fuels have the correct energy concentration and most probably will continue to be the main energy source in the short-medium term but it is necessary to control the CO_2 emission to the atmosphere. The future trends for controlling CO_2 emission and accumulation in the atmosphere should forced on:

1. Reducing fossil fuel use or switching to less CO_2 intense fuels such as biofuls and H_2.
2. Using more efficient energy systems.
3. Increasing the contribution of alternative energies such as solar, wind, etc. in processes.
4. Developing and improving the capture and separation technologies that are economically sound and effective under the operating conditions of CO_2-producing processes.
5. Developing and improving CO_2 storage including terrestrial biomass, deep oceans, saline aquifers, and minerals.
6. Utilizing and sequestering CO_2 by emphasis on fostering and chemical processes.

8. References

Akgerman, C. E.; Ghoreishi, S.M. (1992). Supercritical extraction of hexachlorobenzene from soil, *Ind. Eng. Chem. Res.*, Vol.31, No.1, pp.333–339

Armor, J.N. (2000). Catalytic fixation of CO_2, CO_2 purity, energy, and the environment, *Am. Chem. Soc. Div. Petrol. Chem. Prepr.,* Vol.45, No.1, pp.141–142

Audus, H.; Kaarstad O. & Kowal M. (1996). Decarbonisation of fossil fuels: hydrogen as an energy carrier. *Proc 11th World Hydrogen Energy Conference*, Int. Assoc. of Hydrogen Energy, published by Schon and Wetzel, Frankfurt, Germany

Ayers, W. M. (Ed.) (1988). Catalytic Activation of Carbon Dioxide; ACS Symposium Series 363; American Chemical Society: New York

Climate Change: Forests and Carbon Sequestration (2007). *Temperate Forest Foundation* Vol.16, No.2

DOE/NETL 2010, Carbon Dioxide Capture and Storage RD&D Roadmap, December 2010, http://www.netl.doe.gov/technologies/carbon_seq/refshelf/CCSRoadmap.pdf

Druckenmiller M.L. & Maroto-Valer M.M.; (2005). Carbon sequestration using brine of adjusted pH to form mineral carbonates. *Fuel Processing Technology*, 86: 1599–1614

Ebadi, A.; Sanaeepur, H.; Kargari, A. & Moghadassi, A.R. (2011). Direct determination of concentration-dependent diffusion coefficient in polymeric membranes based on the Frisch method, *Sep. Puri. Technol.*, DOI: 10.1016/j.seppur.2011.08.031.

Ebadi, A.; Sanaeepur, H.; Moghadassi, A.R.; Kargari, A.; Ghanbari, D. & Sheikhi, Z. (2010). Modification of ABS membrane by PEG for capturing carbon dioxide from CO_2/N_2 streams, *Sep. Sci. Technol.*, 45, 1385-1394.

Freund, P. and J. Gale, (2001). Greenhouse gas abatement in energy intensive industries, *Proceedings of the 5th International Conference of Greenhouse Gas Control Technologies, Cairns, Australia, 2001.* CSIRO Publishing

Gray, M.L., et al. (2005). Improved immobilized carbon dioxide capture sorbents. *Fuel Processing Technology*, 86(14-15): 1449–1455

Henriks, C.A., et al., (1999). Emission reduction of greenhouse gases from the cement industry, *Greenhouse Gas Control Technologies, Proceedings of the 4th International Conference of Greenhouse Gas Control Technologies,* Interlaken, Switzerland, Sept. (1998), Elsevier Science Ltd, Oxford, UK

Heydari Gorji, A.; Kaghazchi, T. & Kargari, A. (2009a). Selective Removal of Carbon Dioxide from Wet CO_2/H_2 Mixtures via Facilitated Transport Membranes containing Amine Blends as Carriers, *Chem. Eng. Technol.* Vol. 32, No. 1, pp. 120–128

Heydari Gorji., A.; Kaghazchi, T. & Kargari, A. (2009b) Analytical solution of competitive facilitated transport of acid gases through liquid membranes, *Desalination*, Vol. 235, pp. 245–263

Hydrocarbon Processing (2004). Gas Processes 2004, Gulf Publishing Co.

IEA (2003). *CO_2 emissions from fuel combustion 1997-2001*, IEA/OECD, Paris, France

IEAGHG (2011). Potential for Biomass and Carbon Dioxide Capture and Storage

IEAW (2010), CO_2 Emissions from Fuel Combustion - Highlights ,International Energy Agency website, retrieved 2010-10-06

IPCC (2006). Special Report on Carbon Dioxide Capture and Storage, Edward S. Rubin, Carnegie Mellon University, Pittsburgh, Pennsylvania, USA, Presentation to the RITE International Workshop on CO_2 Geological Storage, Tokyo, Japan February 20

Kaghazchi T.; Kargari, A.; Yegani, R. & Zare, A. (2006). Emulsion liquid membrane pertraction of L-lysine from dilute aqueous solutions by D2EHPA mobile carrier, *Desalination,* Vol. 190, pp. 161-171

Kaghazchi, T.; Takht Ravanchi, M.; Kargari, A. & Heydari Gorji, A. (2009) Application of Liquid Membrane in Separation Processes, *J. Sep. Sci. Eng.*, Vol.1, No. 1, pp. 81-89

Kargari A.; et al., (2003d). Recovery of Phenol from High Concentration Phenolic Wastewater by Emulsion Liquid Membrane Technology, *8th Iranian National Chemical Engineering Conference*, Mashhad, October 2003, Iran

Kargari A.; Kaghazchi, T. & Soleimani, M. (2003a). Application of Emulsion Liquid Membrane in the Extraction of Valuable Metals from Aqueous Solutions, *4th European Congress of Chemical Engineering*, Granada, September 2003, Spain

Kargari A.; Kaghazchi, T. & Soleimani, M. (2003b). Role of Emulsifier in the Extraction of Gold (III) Ions from Aqueous Solutions Using Emulsion Liquid Membrane Technique, *Permea2003 Conference*, Tatranske Matliare, September 2003, Slovakia

Kargari A.; Kaghazchi, T. & Soleimani, M. (2003c). Extraction of gold (III) ions from aqueous solutions using surfactant Liquid Membrane, *8th Iranian National Chemical Engineering Conference*, Mashhad, October 2003, Iran

Kargari A.; Kaghazchi, T. & Soleimani, M. (2004a). Role of Emulsifier in the Extraction of Gold (III) Ions from Aqueous Solutions Using Emulsion Liquid Membrane Technique, *Desalination,* Vol. 162, pp. 237-247

Kargari A.; Kaghazchi, T. & Soleimani, M. (2004b) Mass transfer investigation of liquid membrane transport of gold (III) by methyl iso-butyl ketone mobile carrier, *J. Chem. Eng. & Tech.*, Vol. 27, pp. 1014-1018

Kargari A.; Kaghazchi, T. & Soleimani, M. (2004c). Mass transfer investigation of liquid membrane transport of gold (III) by methyl iso-butyl ketone mobile carrier, *Chisa Conference*, Praha, August 2004, Czech Republic

Kargari A.; Kaghazchi, T. & Soleimani, M. (2005a). Extraction of gold (III) ions from aqueous solutions using emulsion liquid membrane technique, *International Solvent Extraction Conference (ISEC 2005)*, The People's Republic of China, September 2005, China

Kargari A.; Kaghazchi, T. & Soleimani, M. (2006a). Mathematical modeling of emulsion liquid membrane pertraction of gold (III) from aqueous solutions, *J. Memb. Sci.* Vol. 27, pp. 380-388

Kargari A.; Kaghazchi, T.; Kamrani, G. & Forouhar, T. (2005b). Pertraction of phenol from aqueous wastes using emulsion liquid membrane system, *FILTECH Conference*, Wiesbaden, October 2005, Germany

Kargari A.; Kaghazchi, T.; Mardangahi, B. & Soleimani, M. (2006b). Experimental and modeling of selective separation of gold (III) ions from aqueous solutions by emulsion liquid membrane system, *J. Memb. Sci.* Vol. 279, pp. 389-393

Kargari A.; Kaghazchi, T.; Sohrabi, M. & Soleimani, M. (2006c). Application of Experimental Design to Emulsion Liquid Membrane Pertraction of Gold (III) Ions from Aqueous Solutions, *Iranian Journal of Chemical Engineering,* Vol. 3, No. 1, pp. 76-90

Kargari A.; Kaghazchi, T.; Sohrabi, M. & Soleimani, M. (2004d). Batch Extraction of Gold (III) Ions from Aqueous Solutions Using Emulsion Liquid Membrane via Facilitated Carrier Transport, *J. Membr. Sci.,* Vol. 233, pp. 1-10

Kargari A.; Kaghazchi, T.; Sohrabi, M. & Soleimani, M. (2004e). Emulsion liquid membrane pertraction of gold (III) ion from aqueous solutions, *9th Iranian Chemical Engineering Congress*, Iran University of Science and Technology, November 2004

Kargari, A.; Kaghazchi, T.; Mohagheghi, E. & Mirzaei, P. (2002). Application of Emulsion Liquid Membrane for treatment of phenolic wastewaters, *Proceedings of 7th Iranian Congress of Chemical Engineering*, pp. 310-316, Tehran University, October 2002, Iran

Kato M, et al., (2005). Novel CO2 absorbents using lithium containing oxide. *International Journal of Applied Ceramic Technology*, 2(6): 467–475

Knowles G P, et al., (2005). Aminopropyl-functionalized mesoporous silicas as CO2 adsorbents. *Fuel Processing Technology*, 86: 1435–1448

Kohl, A.L. & Nielsen, R.B. (1997). Gas Purification, 4th ed., Gulf Publishing Company, Houston, Texas

Kuei C.K., M.D. Lee, (1991). Hydrogenation of carbon-dioxide by hybrid catalysts, direct synthesis of aromatics from carbon-dioxide and hydrogen, *Can. J. Chem. Eng.* 69 (1), 347–354

Liu N, et al., (2005). Biomimetic sequestration of CO_2 in carbonate form: Role of produced waters and other brines. *Fuel Processing Technology*, 86: 1615–1625

Lotz, M. & Brent, A.C. (2008). A review of carbon dioxide capture and sequestration and the Kyoto Protocol's clean development mechanism and prospects for Southern Africa. *Journal of Energy in Southern Africa*, Vol.19, No.1, pp.13-24

Mahmoudkhani M., D.W. Keith, (2009). Low-energy sodium hydroxide recovery for CO2 capture from atmospheric air—Thermodynamic analysis, *International Journal of Greenhouse Gas Control*, 3, 376–384

Maroto-Valer M.M.; Tang Z.; Zhang Y.; (2005). CO_2 capture by activated and impregnated anthracites. *Fuel Processing Technology*, 86(14-15): 1487–1502

MIT 2008—Massachusetts Institute of Technology (2008). Carbon Capture & Sequestration Technologies Program. Carbon Dioxide Capture and Storage Projects. http://sequestration.mit.edu/tools/projects/index.html

Moghadassi, A.; Ebadi, A. & Kargari, A. (2009). Development of the polymeric blend membrane for CO_2/N_2 separation, *The 6th International Chemical Engineering Congress (IChEC 2009)*, Kish Island, Iran

Mohammadi S.; Kaghazchi, T. & Kargari, A. (2008). A model for metal ion pertraction through supported liquid membrane, *Desalination,* Vol. 219, pp. 324-334

Nabieyan B.; Kaghazchi, T.; Kargari, A.; Mahmoudian, A. & Soleimani, M. (2007). Bench-scale simultaneous extraction and stripping of iodine using bulk liquid membrane system, *Desalination,* Vol. 214, pp. 167-176

Nam S.S., H. Kim, G. Kishan, M.J. Choi, K.W. Lee (2001). Catalytic conversion of carbon dioxide into hydrocarbons over iron supported on alkali ion exchanged Y-zeolite catalysts, *Appl. Catal. A: Gen.* 179 (1–2) (1999) 155–163

Park S.E., J.S. Yoo, J.-S. Chang, K.Y. Lee, M.S. Park, Heterogeneous catalytic activation of carbon dioxide as an oxidant, *Am. Chem. Soc. Div. Fuel Chem. Prepr.* 46 (1), 115–118

Rezaei M.; Mehrabani, A.; Kaghazchi, T. & Kargari, A. (2004). Extraction of chromium ion from industrial wastewaters using bulk liquid membrane, *9th Iranian Chemical Engineering Congress*, Iran University of Science and Technology, November 2004

Ritter J.A.; A.D. Ebner (2007). Carbon Dioxide Separation Technology: R&D Needs For the Chemical and Petrochemical Industries, *Chemical Industries Vision 2020 Technology Partnership*, November 2007

Robeson, L.M. (2008). The upper bound revisited. *J. Membrane Sci.*, vol. 320, pp. 390–400

Sanaeepur, H.; Ebadi, A.; Moghadassi, A. & Kargari, A. (2011a). Preparation and characterization of Acrylonitrile-Butadiene-Styrene/Poly (vinyl acetate) membrane for CO_2 removal, *Sep. and Purif. Technol.*, Vol. 80, pp. 499-508

Sanaeepur, H.; Ebadi, A.; Moghadassi, A.; Kargari, A.; Moradi, S. & Ghanbari, D. (2011b). A novel acrylonitrile-butadiene-styrene/poly (ethylene glycol) membrane: preparation, characterization and gas permeation study, *Polym. Adv. Technol.*, DOI: 10.1002/pat.2031

Song C.S., et al., (Eds.) (2002). CO_2 Conversion and Utilization. American Chemical Society, Washington, DC, *ACS Symposium Series*, vol. 809, pp. 420-427

Song, C. (2006). Global challenges and strategies for control, conversion and utilization of CO_2 for sustainable development involving energy, catalysis, adsorption and chemical processing. *Catal. Today*, Vol.115, pp: 2–32

Song, C.S.; Pan W. (2004). Tri-reforming of methane: a novel concept for catalytic production of industrially useful synthesis gas with desired H_2/CO ratios, *Catal. Today,* 98 (4) 463–484

Stangeland A. (2007). A model for the CO_2 capture potential, *International Journal of greenhouse gas control*, 1,418–429

Stewart C. & Hessami M. (2005). A study of methods of carbon dioxide capture and sequestration–the Sustainability of a photosynthetic bioreactor approach, *Energy Conversion and Management*, 46: 403–420

Stolaroff J K, Lowry G V, Keith D W, (2005). Using CaO- and MgO-rich industrial waste streams for carbon sequestration. *Energy Conversion and Management*, 46: 687–699

Takht Ravanchi, M. & Kargari, A. (2009). New Advances in Membrane Technology, In: *Advanced Technologies*, K. Jayanthakumaran, (Ed.), pp. 369-394, InTech, ISBN 978-953-307-009-4

Takht Ravanchi, M.; Kaghazchi, T. & Kargari, A. (2008a). Separation of a Propylene-Propane Mixture by a Facilitated Transport Membrane, *The 5th International Chemical Engineering Congress (IChEC 2008)*, Jan, 2008, Kish Island, Iran

Takht Ravanchi, M.; Kaghazchi, T. & Kargari, A. (2008b). Immobilized Liquid Membrane for Propylene-Propane Separation, *Proceeding of World Academy of Science, Engineering and Technology*, pp. 696-698, ISSN 1307-6884, Paris, July 2008, France

Takht Ravanchi, M.; Kaghazchi, T. & Kargari, A. (2008c). A new approach in separation of olefin-paraffin gas mixtures by a membrane system, *Amirkabir J. Sci. Res.*, Vol. 19, pp. 47-54

Takht Ravanchi, M.; Kaghazchi, T. & Kargari, A. (2008d). Application of facilitated transport membrane systems for the separation of hydrocarbon mixtures, *18th International Congress of Chemical and Process Engineering*, Praha, August 2008, Czech Republic

Takht Ravanchi, M.; Kaghazchi, T. & Kargari, A. (2009a). Application of Membrane Separation Processes in Petrochemical Industry: A Review, *Desalination*, Vol. 235, pp. 199–244

Takht Ravanchi, M.; Kaghazchi, T. & Kargari, A. (2009b). Separation of Propylene-Propane Mixture Using Immobilized Liquid Membrane via Facilitated Transport Mechanism, *Sep. Sci. Technol.*, Vol. 44, pp. 1198-1217

Takht Ravanchi, M.; Kaghazchi, T. & Kargari, A. (2010a) Facilitated Transport Separation of Propylene-Propane: Experimental and Modeling Study, *J. Chem. Eng. Proc: Process Intensification.,* Vol.49, pp.235-244

Takht Ravanchi, M.; Kaghazchi, T. & Kargari, A. (2010b) Selective Transport of propylene by silver ion complex through an immobilized liquid membrane, *Iranian J. Chem. Eng.*, Vol. 7, No. 1, pp.28-41

Takht Ravanchi, M.; Kaghazchi, T. & Kargari, A. (2010c) Supported Liquid Membrane Separation of Propylene-Propane Mixtures Using a Metal Ion Carrier, *Desalination*, Vol. 250, pp. 130–135

Takht Ravanchi, M.; Kaghazchi, T.; Kargari, A. & Soleimani, M. (2009c). A novel separation process for olefin gas purification, *J. Taiwan. Inst. Chem. Eng.,* Vol. 40, pp. 511-517

Torp, T. & Gale, J. (2002). Demonstrating storage of CO_2 in geological reservoirs: the Sleipner and Sacs projects, *6th International Conference on Greenhouse Gas Control Technologies (GHGT-6), Kyoto, Japan, Oct.2002,* Elsevier Science Ltd, Oxford, UK

UNFCCC, The Kyoto Protocol to the UN Framework Convention on Climate Change (UNFCCC-1992): http://unfccc.int/resource/docs/convkp/kpeng.pdf

WRI, (2008). CCS Guidelines: Guidelines for Carbon Dioxide Capture, Transport, and Storage. Washington, DC: WRI. Published by World Resources Institute

Xu X, Song C S, Andresen J M, Miller B G, Scaroni A W, (2002). Novel polyethyleneimine-modified mesoporous molecular sieve of MCM-41 type as adsorbent for CO_2 capture. *Energy and Fuels*, 16: 1463–1469

Xu X, Song C, Miller B G, Scaroni A W, (2005). Adsorption separation of carbon dioxide from flue gas of natural gas-fired boiler by a novel nanoporous "molecular basket" adsorbent. *Fuel Processing Technology*, 86(14-15); 1457–1472

Yamasaki A., (2003). An overview of CO_2 mitigation options for global warming – Emphasizing CO_2 sequestration options. *J. Chem. Eng. Japan*, 36(4): 361–375

Yeh J T, Resnik K P, Rygle K, Pennline H W, (2005). Semi-batch absorption and regeneration studies for CO_2 capture by aqueous ammonia. *Fuel Processing Technology*, 86(14- 15): 1533–1546

2

Recent Advances in Catalytic/Biocatalytic Conversion of Greenhouse Methane and Carbon Dioxide to Methanol and Other Oxygenates

Moses O. Adebajo and Ray L. Frost
Chemistry Discipline, Faculty of Science & Technology,
Queensland University of Technology, Brisbane
Australia

1. Introduction

Methane gas has been identified as the most destructive greenhouse gas (Liu *et al*., 2004). It was reported that the global warming potential of methane per molecule relative to CO_2 is approximately 23 on a 100-year timescale or 62 over a 20-year period (IPCC, 2001). Methane has high C-H bond energy of about 439 kJ/mol and other higher alkanes (or saturated hydrocarbons) also have a very strong C-C and C-H bonds, thus making their molecules to have no empty orbitals of low energy or filled orbitals of high energy that could readily participate in chemical reactions as is the case with unsaturated hydrocarbons such as olefins and alkynes (Crabtree, 1994; Labinger & Bercaw, 2002). Consequently, only about half of the hydrocarbons containing these ubiquitous C-H bonds are reactive enough to take part in traditional chemical reactions (Bergman, 2007). This is a great challenge that needs to be addressed because several of these un-reactive hydrocarbons are found in petroleum from which several organic products including petrochemicals, fine chemicals, plastics, paints, important intermediates and pharmaceuticals are produced. Methane, besides being a greenhouse gas, is also the major constituent of large, underutilized resources of natural gas (located in remote areas of Asia, Siberia, Western Canada and offshore reservoirs of Australia, and therefore expensive to transport) and coal bed methane (CBM). It is therefore a promising feedstock for producing other value-added products if the problem of C-H activation can be solved. The selective transformation of these ubiquitous but stable C-H bonds to other functional groups could therefore revolutionize the chemicals industry. A clear understanding of the reactions involving C-H activation is therefore an important and interesting challenge.

Generally, there are two routes for converting methane to transportable liquid fuels and chemicals, namely indirect and direct routes. At the moment, commercial catalytic technologies are based on the indirect route that involves a two-step process in which methane is first converted to synthesis gas by steam reforming (Eqn.1), CO_2 reforming (Eqn. 2) or partial oxidation (Eqn. 3) followed by either Fischer-Tropsch synthesis of hydrocarbons (Eqn. 4) or methanol synthesis (Eqns. 5 and 6) and subsequent conversion to hydrocarbons.

$$CH_4 + H_2O \rightarrow CO + 3H_2 \quad (\Delta H^0_{298K} = +206 \text{ kJ mol}^{-1}) \tag{1}$$

$$CH_4 + CO_2 \rightarrow 2CO + 2H_2 \quad (\Delta H^0_{298K} = +247 \text{ kJ mol}^{-1}) \tag{2}$$

$$CH_4 + \tfrac{1}{2}O_2 \rightarrow CO + 2H_2 \quad (\Delta H^0_{298K} = -36 \text{ kJ mol}^{-1}) \tag{3}$$

$$nCO + 2nH_2 \rightarrow (-CH_2)_n + nH_2O \quad (\Delta H^0_{298K} = -165 \text{ kJ mol}^{-1}) \tag{4}$$

$$CO + 2H_2 \rightarrow CH_3OH_{(g)} \quad (\Delta H^0_{298K} = -90.8 \text{ kJ mol}^{-1}) \tag{5}$$

$$CO_2 + 3H_2 \rightarrow CH_3OH_{(g)} + H_2O \quad (\Delta H^0_{298K} = -49.5 \text{ kJ mol}^{-1}) \tag{6}$$

The direct route is a one-step process in which methane or natural gas is reacted with oxygen or another oxidizing species to give the desired product, e.g. methanol or formaldehyde (Eqns. 7 and 8). The direct route is regarded to be more energy efficient than the indirect route since it bypasses the energy intensive endothermic steam reforming step of syngas formation.

$$CH_4 + \tfrac{1}{2}O_2 \rightarrow CH_3OH_{(g)} \quad (\Delta H^0_{298K} = -126.4 \text{ kJ mol}^{-1}) \tag{7}$$

$$CH_4 + O_2 \rightarrow HCHO_{(g)} + H_2O_{(g)} \quad (\Delta H^0_{298K} = -276 \text{ kJ mol}^{-1}) \tag{8}$$

The selective catalytic conversion of methane via partial oxidation into transportable liquids such as methanol, formaldehyde and other oxygenates is one direct route for activating and converting natural gas- or CBM-derived methane to value-added chemicals. This partial oxidation reaction is one of the greatest challenges in heterogeneous catalysis because of the high driving force to full oxidative conversion to CO or CO_2 (Eqns. 9 and 10).

$$CH_4 + {}^3/_2O_2 \rightarrow CO + 2H_2O_{(g)} \quad (\Delta H^0_{298K} = -519.6 \text{ kJ mol}^{-1}) \tag{9}$$

$$CH_4 + 2O_2 \rightarrow CO_2 + 2H_2O_{(g)} \quad (\Delta H^0_{298K} = -802.6 \text{ kJ mol}^{-1}) \tag{10}$$

At the moment, oxygenates such as methanol and formaldehyde are produced via a multi-step process involving first the conversion of methane to syngas followed by the oxygenate formation in a second step. Although this multi-step process is highly efficient, the syngas production is very expensive due to high capital costs and it is therefore only economically viable if it is conducted on a large scale. Thus, a more convenient and economically viable process for small scale methanol production (e.g. at remote locations) would be the direct methane partial oxidation to methanol. Furthermore, it should be noted that methanol, being a precursor to ethylene and propylene, is a primary raw material for the chemical industry (Olah *et al.*, 2009; Beznis *et al.*, 2010a, 2010b). It is produced in large quantities as an intermediate for the production of a wide range of chemicals including formaldehyde, methyl *tert*-butyl ether and acetic acid, most of which are subsequently used to produce many important industrial products such as paints, resins, adhesives, antifreezes and plastics (Olah *et al.*, 2009). Thus, the direct catalytic synthesis of methanol from methane

would open up the possibility of producing a wide range of important chemicals by the chemical industry. Apart from catalytic direct conversion route, an alternative method is the biochemical production of methanol from methane, a process which occurs under mild conditions and atmospheric pressure. This bio-catalytic route is based on the ability of some bacterial species such as methanotrophs and methane monooxygenase (MMO) to oxidize methane to methanol and deeper oxidation products.

Another significant greenhouse gas is carbon dioxide which is considered to be harmful pollutant of our atmosphere and a major source of human-caused global warming (Olah *et al.*, 2009). On the other hand, carbon dioxide is an ubiquitous carbon source from which methanol, dimethyl ether and efficient alternative transportation fuels and their derivatives can be produced (Olah *et al.*, 2009). Thus, it has been suggested that an effective feasible approach for the disposal and recycling of carbon dioxide is its chemical conversion to important chemicals such as methanol, dimethyl ether and liquid fuels (Olah *et al.*, 2009). This approach is considered to have the potential to provide solution to the environmental problem of increasing levels of carbon dioxide in the atmosphere and the accompanying global warming. The chemical transformation of carbon dioxide also makes possible the production of renewable and inexhaustible liquid fuels and other important carbon chemicals, thus allowing an environmentally neutral use of carbon fuels and derived hydrocarbon products (Olah *et al.*, 2009).

The catalytic reductive conversion of carbon dioxide using hydrogen at non-ambient conditions appears to be the most studied direct route to methanol and other oxygenates from carbon dioxide (Eqn. 6). Such catalytic reactions have traditionally been heterogeneous catalytic, photocatalytic and electrocatalytic pathways (Lu *et al.*, 2006). These methods require high temperatures and pressures or additional electric or luminous energy, but both selectivity and yields are usually low. Besides these traditional routes, novel biocatalytic systems have also been shown to be capable of catalysing the reduction of carbon dioxide at ambient conditions (Lu *et al.*, 2006). Such biocatalytic pathways are attractive because they occur with high yields and selectivity at milder reaction conditions without pollution and the processing involves the use of low purity reactants and is very tolerant to many impurities that are toxic to chemical catalysts (Lu *et al.*, 2006; Lu *et al.*, 2010). For example, formate dehydrogenase (FateDH) immobilized in a novel alginate-silica hybrid gel was previously used as the biocatalyst to reductively convert carbon dioxide into formic acid and reduced nicotinamide adenine dinuncleotide (NADH) as the terminal electron donor for the enzymatic reaction (Lu *et al.*, 2006). A combination of biocatalysts has also been used for the reduction of CO_2 to methanol (Lu *et al.*, 2006).

This chapter presents a general overview of recent advances in the development of catalytic and biocatalytic systems for both the direct partial oxidative conversion of methane and the hydrogenation of carbon dioxide to produce methanol and other oxygenates. The review will cover both homogeneous and heterogeneous catalytic systems that have been developed so far. The electrochemical and photocatalytic reductive conversions of carbon dioxide are covered in the review. The chapter also presents a discussion of the progress that has been made on the development of chemical systems like MMO that are capable of oxidizing methane at ambient conditions. One interesting observation in our previous work on catalytic oxidative methylation of aromatics with methane that is directly relevant to the conversion of methane to methanol is that it is possible to inhibit the complete oxidation of

methane to carbon dioxide in the presence of an additive (Adebajo *et al.*, 2000; Adebajo *et al.*, 2004). This chapter also provides a brief summary of such oxidative methylation reaction and its significance to methanol conversion.

2. Conversion of methane to oxygenates

2.1 Recent advances in the catalytic conversion of methane to oxygenates

The direct conversion of methane to oxygenates such as methanol (CH_3OH), formaldehyde (HCHO) and acetic acid (CH_3COOH) has great potential for producing liquid fuels and petrochemicals from natural gas and CBM. This direct conversion route involves partial oxidation at 300-500 °C under fuel-rich mixtures to minimize the extent of the more thermodynamically favourable combustion reaction which produces unwanted CO and CO_2 (Zhang *et al.*, 2003; Navarro *et al.*, 2006; Alvarez-Galvan *et al.*, 2011). Several reviews which provided valuable discussions of various aspects of, and the progress already made in, the direct partial oxidation of methane to methanol and other oxygenates have been published (Foster, 1985; Gesser *et al.*, 1985; Edwards & Foster, 1986; Pitchai & Klier, 1986; Fujimoto, 1994; Yang *et al.*, 1997; Adebajo, 1999; Lunsford, 2000; Tabata *et al.*, 2002; Zhang *et al.*, 2003; Taniewski, 2004; de Vekki & Marakaev, 2009; Holmen, 2009; Alvarez-Galvan *et al.*, 2011). The selective partial oxidation of methane has been carried out in four ways, namely high temperature non-catalytic gas-phase homogeneous oxidation, heterogeneous catalytic oxidation, low temperature homogeneous catalysis in solution and enzymatic or biological catalytic oxidation (Zhang *et al.*, 2003; Holmen, 2009).

The gas-phase non-catalytic reactions usually occur via a free radical mechanism at high temperatures which are unfavourable with respect to the control of selectivity of the desired oxygenates (Navarro *et al.*, 2006; Alvarez-Galvan *et al.*, 2011). Thermodynamic and kinetic analyses have shown that the rate-limiting step of the partial oxidation of methane is the first H-abstraction from the C-H bond to form methyl radicals (Navarro *et al.*, 2006; Alvarez-Galvan *et al.*, 2011). Thus, initiators and sensitizers have been incorporated into the reaction mixture for the purpose of lowering the energy barrier of this H-abstraction (Navarro *et al.*, 2006; Alvarez-Galvan *et al.*, 2011). In particular, nitrogen oxides have been used to promote gas-phase reactions with methane (Otsuka *et al.*, 1999; Tabata *et al.*, 2000; Babero *et al.*, 2002; Tabata *et al.*, 2002). The presence of higher hydrocarbons, especially ethane, in small quantities has also been observed to lower the initiation temperature and increase methanol selectivity and yield (Gesser *et al.*, 1985; Fujimoto, 1994). High selectivities of up to 80% for methanol at up to 10% methane conversion have already been achieved under non-catalytic conditions by Gesser et al. (Yarlagadda *et al.*, 1988; Hunter *et al.*, 1990; Gesser & Hunter, 1998). It is generally accepted that high pressure favours the formation of methanol and high methane/oxygen enhances methanol selectivity but lowers methane conversion in gas phase homogeneous partial oxidation of methane (Zhang *et al.*, 2003, 2008). Most results indicate a selectivity of 30-40% at a conversion of 5-10% under the best conditions which are mainly temperatures of 450-500 °C and pressures of 30-60 bars (Holmen, 2009). The experimental and theoretical evidence obtained so far indicates limited possibilities of producing high yields of methanol in the gas-phase system (Holmen, 2009). The presence of catalysts in such gas-phase reactions carried out at high pressure appears to have no beneficial effect on the reactions. In fact, it has been observed that reactor inertness is critically important for obtaining high selectivity of methanol and that even the feed gas

should be isolated and not be allowed to make contact with the metal wall. Thus, Quartz and Pyrex glass-lined reactors have been shown to yield the best results (Zhang *et al.*, 2008).

Typical experimental results from several studies for the gas-phase partial oxidation of methane are shown in Fig. 1. This figure clearly demonstrates that any improvement in the direct conversion of methane to methanol via the gas phase homogeneous oxidation route must come from the enhancement of selectivity without reducing the conversion per pass which is a great challenge (Holmen, 2009; Alvarez-Galvan *et al.*, 2011). This challenge together with the need to operate the gas-phase reactions at high temperatures which make the control of selectivity to desired products extremely difficult has made it necessary for researchers to make considerable efforts to develop active and selective catalysts for the partial oxidation of methane. This review focuses on providing brief discussions of the progress that has been made in the conversion of methane to methanol and other oxygenates via the heterogeneous catalytic oxidation, homogeneous catalysis in solution and bio-catalytic oxidation routes. Such discussions are presented in the following sections.

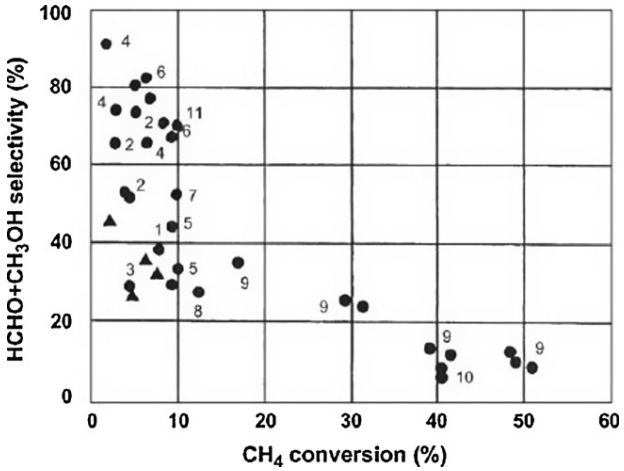

Fig. 1. Gas-phase partial oxidation of methane from several studies. From Tabata et al., 2002.

2.1.1 Heterogeneous catalytic partial oxidation of methane

At much lower pressures (i.e. as low as 1 atm.) than for gas-phase reactions, the catalyst becomes very important for the formation of oxygenates by direct partial oxidation of methane. In spite of the significant efforts that have been devoted to the development of active and selective catalysts, neither the product yield of C_1 oxygenates nor the complete mechanism of the reaction has been clarified (Navarro *et al.*, 2006; Alvarez-Galvan *et al.*, 2011). The selective O-insertion into CH_3 or other species obtained from the first H-abstraction of the CH_4 molecule is normally carried out on redox oxides of molybdenum and vanadium such as MoO_3 and V_2O_3 (Tabata *et al.*, 2002; Navarro *et al.*, 2006; Alvarez-Galvan *et al.*, 2011). In these catalytic systems, the catalytic performances are optimized by keeping isolated metal oxide structures isolated on a silica substrate in a slightly reduced state (Faraldos *et al.*, 1996; Chempath & Bell, 2007; Alvarez-Galvan *et al.*, 2011). The presence of these partially reduced oxides is believed to allow the redox cycles of catalytic surfaces to

proceed more rapidly and smoothly (Alvarez-Galvan *et al.*, 2011). Most results reported to date were obtained at temperatures above 500 °C and formaldehyde has been the main oxidation product. When the reaction was carried out at 600 °C in the presence of excess water vapour on highly dispersed MoO_3/SiO_2, high selectivities (about 90 %) to methanol + formaldehyde oxygenates (or 20% yield) at methane conversions of 20-25% have been reported (Sugino *et al.*, 2000). The improved selectivity which resulted from addition of water vapour was attributed to the formation of silicomolybdic acid (SMA: $H_4SiMo_{12}O_{40}$) over the silica surface.

The performance of V_2O_5/SiO_2 catalyst has been observed to change significantly by adding small amounts of radical initiator in the gas feed (Chempath & Bell, 2007). It was reported that up to 16% yields of oxygenates (methanol + formaldehyde) were obtained by adding about 1 vol.% NO to the feed in the presence of a low specific surface area V_2O_5/SiO_2 catalyst at 650 °C. The strong effect of NO was ascribed to a heterogeneous-homogeneous mechanism involving chain propagation of radical reactions in close vicinity of the catalyst bed (Chempath & Bell, 2007).

It has been reported that isolated molybdate species supported on silica have the highest specific activity and selectivity for the direct oxidation of methane to formaldehyde and a detailed mechanism of methane oxidation to formaldehyde was presented (Ohler & Bell, 2006; Chempath & Bell, 2007).

In addition to MoO_3/SiO_2 and V_2O_5/SiO_2 catalytic systems which have been most widely studied, many other metal oxides have also been investigated. It was observed that when 9.2% of various oxides were deposited onto silica, Ga_2O_3 and Bi_2O_3 which have medium electronegativities exhibited maximum conversion at 650 °C and CH_4:O_2 = 1:1 (Otsuka & Hatano, 1987; Navarro *et al.*, 2006; de Vekki & Marakaev, 2009). The dependence of conversion on electronegativity was found to show extreme behaviour with maximum observed for gallium oxide (Otsuka & Hatano, 1987; de Vekki & Marakaev, 2009). In contrast, the selectivity for formaldehyde exhibited a steady increase with increase in the electronegativity of the additive elements. A possible arrangement of the oxides in decreasing order of selectivity was reported to be P_2O_5, WO_3, B_2O_3 (> 60%) > Sb_2O_3, Nb_2O_3, Al_2O_3, MgO (> 30 %), i.e. the acidic oxides are more selective than the basic oxides (de Vekki & Marakaev, 2009). A binary oxide mixture of Be and B supported on silica (i.e. B_2O_3-BeO/SiO_2) was found to exhibit optimum methane conversion and HCHO yield of 2.8% and 1%, respectively at 600 °C (de Vekki & Marakaev, 2009). The 1% yield corresponds to a selectivity of 35.7%.

Ono and co-workers have previously reported the partial oxidation of methane over various commercial silica catalysts and silica catalysts prepared from Si metal (Ono *et al.*, 1993; Ono & Maruyama, 1996) and over ZSM-5 (MFI) zeolite catalysts (Kudo & Ono, 1997; Ono *et al.*, 2000) at 600-650 °C and low CH_4 pressure of 8-8.5 torr using a closed circulation system and quartz reactor. These workers reported that H-ZSM-5 catalysts with SiO_2/Al_2O_3 ratio of 283 exhibited higher activities than the other commercial silicas. The rate was found to increase with increase in O_2 concentration. The selectivities to CH_3OH were also observed to be higher over NaZSM-5 while selectivities to HCHO were higher over H- and Cs-ZSM-5 catalysts. More recently, these workers investigated the partial oxidation reaction over Al doped silica catalysts and various commercial silica catalysts in a flow reactor system instead of a closed circulation system (Ono *et al.*, 2008). They observed that not only HCHO

and CH_3OH but also other products such as C_2H_6, C_2H_4 and CO were formed over these catalysts and over a quartz reactor without catalysts. The presence of 0.1-0.5 wt% Al in silica enhanced methane conversions even at low O_2 concentrations. However, even over the Al/SiO_2 catalysts, the maximum selectivities to CH_3OH and HCHO obtained were only 3.5% and 7%, respectively. The enhancement of conversion observed over Al/SiO_2 catalysts was attributed to heterogeneous participation of O_2 on sites identified using MAS ^{27}Al NMR as isolated tetrahedrally coordinated Al ions.

Antimony oxides (i.e. Sb_2O_3 or Sb_2O_5) highly dispersed on silica were also reported to be selective for the partial oxidation of methane to HCHO (Zhang *et al.*, 2004). SbO_x/SiO_2 catalysts with SbO_x loadings up to 20 wt% exhibited good HCHO selectivity, even at temperatures as high as 650 °C and the more oxidized Sb_2O_5/SiO_2 catalysts were found to be more selective than the reduced Sb_2O_3 counterpart (Zhang *et al.*, 2004). A HCHO selectivity of up to 41% was obtained for the Sb_2O_5/SiO_2 catalyst at 600 °C but this was reduced to 18% when the reaction temperature was increased to 650 °C

It is unfortunate that experimental studies on the partial oxidation of methane to methanol over a solid catalyst have up till now not been successful. The yield of HCHO on MoO_3/SiO_2 and V_2O_5/SiO_2 which are most widely studied does not exceed 3-4% (de Vekki & Marakaev, 2009). Higher yields have been reported for other catalysts but these could not be confirmed due to poor reproducibility (Zhang *et al.*, 2003; de Vekki & Marakaev, 2009) . Otsuka and Wang (Otsuka & Wang, 2001) have attributed the difficulty in producing methanol at the high temperatures required for activation of methane to immediate decomposition or oxidation of methanol to formaldehyde and carbon oxides. New catalysts that are capable of activating methane at lower temperatures should therefore be developed in future investigations for the direct synthesis of methanol. This is obviously a great challenge in view of the strong C-H bond in methane.

2.1.2 Homogeneous liquid phase catalytic oxidation at low temperatures

The activation of methane at low temperatures has been investigated using homogeneous catalysis. Such low temperature activation of C-H bond does not involve radicals and may lead to more selective reactions than those promoted by heterogeneous catalysts operating at high temperatures. However, the main challenge lies in finding a catalyst system that exhibits suitable reactivity and selectivity while tolerating harsh oxidizing and protic conditions. Shilov and his co-workers pioneered investigations in this area in the 1970s when they showed that methane could be converted to methanol by Pt(II) and Pt(IV) complexes because these complexes do not oxidize methanol to carbon oxides, CO_x (Gol'dshleger *et al.*, 1972; Shilov & Shul'pin, 1997, 2000). Subsequently, organometallic approaches to functionalization of C-H bonds in methane became a subject mainly after the work of Periana et al. (Periana *et al.*, 1993) who proposed a process involving a Hg(II) complex in concentrated H_2SO_4 as the catalyst. Methyl bisulphate is formed as an intermediate and this is then readily hydrolyzed to produce methanol (Eqns. 11 & 12):

$$CH_4 + 2H_2SO_4 \rightarrow CH_3OSO_3H + SO_2 + 2H_2O \quad (11)$$

$$CH_3OSO_3H + H_2O \rightarrow CH_3OH + H_2SO_4 \quad (12)$$

A bipyrimidyl platinum (II) complex and Tl(III), Pd(II) and Au have also been used as oxidation catalysts instead of the mercury complex (Periana *et al.*, 1998). By using the Pt (II) complex, a methane conversion of 90% was obtained with a 72% one-pass yield and 81% selectivity to methylbisulfate at 220 °C and 35 bar. Pd(II) salts are not as effective as Pt(II) complexes because of the reduction of Pd(II) to Pd(0) species and the slow re-oxidation of Pd(0) (Alvarez-Galvan *et al.*, 2011).

The major disadvantages of using H_2SO_4 as a solvent system include the difficulty of separating the methanol product from the sulphuric acid and the need for expensive corrosion-resistant materials and periodic regeneration of spent H_2SO_4 (Alvarez-Galvan *et al.*, 2011). A complete cycle would require the costly regeneration of concentrated H_2SO_4 as indicated in the proposed catalytic cycle shown in Fig. 2 as reported by Periana et al. (Periana *et al.*, 1998). More recent contributions have presented and discussed the key challenges and approaches for the development of the next generation of organometallic, alkane functionalization catalysts based on C-H activation (Periana *et al.*, 2004; Bergman, 2007). One question that remains to be answered is whether a process consisting of several steps such as the ones shown in Fig. 2 can be developed and operated in an economical way. Nevertheless, it illustrates a system where the rate constant for breaking the C-H bond in CH_4 on Pt is much higher than the C-H bond in the methyl bisulfate product (Holmen, 2009).

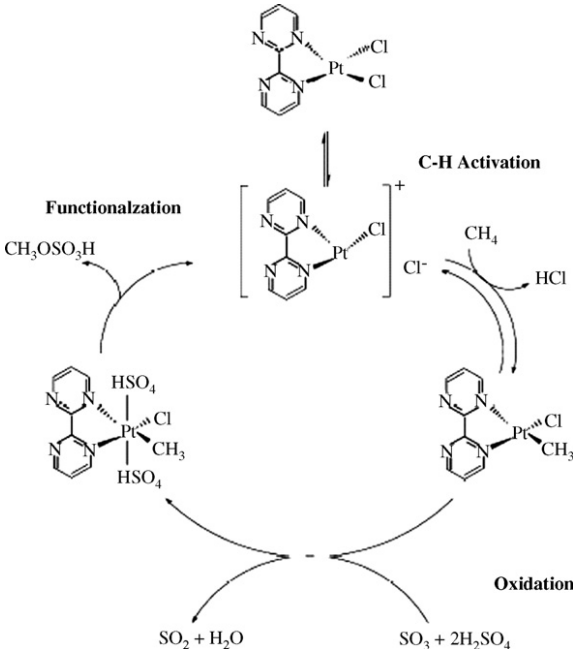

Fig. 2. Reaction mechanism for oxidation of methane to methyl bisulfate using a bipyrimidyl Pt(II) complex in concentrated sulphuric acid (Periana *et al.*, 1998).

Schüth and co-workers (Palkovits *et al.*, 2009) recently reported a new class of solid catalysts for the direct low-temperature oxidation of methane to methanol. The solid catalysts were

synthesized by immobilizing Pt(II) within a covalent triazine-based framework (CTF) containing bipyridyl fragments (Palkovits *et al.*, 2009). Such sold catalysts showed catalytic activity that are comparable to Periana's system at 215 °C in 30% oleum with selectivity to methanol above 75% and were stable over at least five recycling steps.

Most active catalytsts that operate at low temperature normally require the use of strong, environmentally unfriendly oxidizing agents such as SO_3, $K_2S_2O_8$ and $NaIO_4$ (Rahman *et al.*, 2011). Ishihara et al. (Rahman *et al.*, 2011) avoided the use of these oxidants in their very recent study of the synthesis of formic acid by partial oxidation of methane using H-ZSM-5 solid acid catalyst. The reaction was studied at 100 °C and 2.6 MPa pressure using the more benign hydrogen peroxide as the oxidant. They obtained a 13% yield and 66.8% selectivity of formic acid. Triphenylphosphene (Ph_3P) was used as a promoter in the reaction system. However, a fairly large amount of CO_2 was also observed as deep oxidation product. Another green chemical process, which uses gold nanoparticles on silica support as catalyst and ionic liquid (IL) as solvent, has just been reported for direct methane oxidation to methanol (Li *et al.*, 2011). The IL 1-butyl-3-methylimidazolium chloride ([Bmim]Cl) was used as the solvent, trifluoroacetic acid (TFA) and trifluoroacetic anhydride (TFAA) as the acidic reagents and $K_2S_2O_8$ as the oxidant. The reaction was performed at 90 °C and 20 atm methane pressure. In the presence of 0.01g nano-Au/SiO_2 catalyst and 1g IL solvent, optimum methane conversion, selectivity and the yield to methanol obtained were 24.9%, 71.5% and 17.8%, respectively. The selectivity to CO_2 and H_2 obtained were 1.6% and 0.4%, respectively while the yield to these products were 0.6% and 0.1%, respectively. It was reported that 96.9% of the nano-Au/SiO_2 catalyst and the IL system could be recycled and the conversion of methane in the recycled system remained as high as 21.75%.

Metal-containing zeolites (particularly Fe-ZSM-5 and Cu-ZSM-5) have also been observed to show great potential as catalysts for the direct partial oxidation of methane to oxygenates at low or ambient temperatures. Fe-ZSM-5 has been shown to be active for this reaction although the less attractive N_2O was required to be used as the oxidant and this oxidant was observed to lead to the formation of a special type of reactive surface oxygen species known as α-oxygen (Panov *et al.*, 1990; Sobolev *et al.*, 1995; Dubkov *et al.*, 1997). Co-ZSM-5 was also shown recently to be active for the conversion of methane to oxygenates using oxygen (Beznis *et al.*, 2010b). The activity and selectivity were found to be dependent on the nature of cobalt species present in the materials. Cobalt in ion-exchange positions was observed to be selective towards formaldehyde while larger Co-oxide species (CoO and Co_3O_4) prepared by impregnation were selective towards methanol (Beznis *et al.*, 2010b). CuZSM-5 has also been shown to be active for the conversion of methane to methanol at 100 °C using molecular oxygen as oxidant with selectivity >98% (Groothaert *et al.*, 2005; Smeets *et al.*, 2005). Reactivity was found to occur at a small fraction of the total copper sites in the zeolite. The oxygen-activated active site in CuZSM-5 was correlated to a UV-Vis-NIR diffuse reflectance spectroscopy (DRS) absorption band at 22,700 cm^{-1} (Groothaert *et al.*, 2003). Additional information was provided by Woertink et al. (Woertink *et al.*, 2009) on the origin of Cu species using a combination of resonance Raman (rR) spectroscopy and density functional theory (DFT). These workers confirmed that the oxygen activated Cu core is defined as bent mono-(μ-oxo)dicupric cluster (Cu^{II}-O-Cu^{II}) (Woertink *et al.*, 2009). Subsequent investigations by Beznis et al. (Beznis *et al.*, 2010a) have now established a linear relationship between the intensity of the UV-Vis-NIR DRS charge transfer (CT) band at 22,700 cm^{-1} and the amount of methanol produced irrespective of the synthesis route used.

The absolute intensity of the 22,700 cm^{-1} CT band was observed to be always low indicating a low number of active sites in the samples. At least two Cu species were identified to be present in all Cu-ZSM-5 zeolites, namely Cu-O clusters dispersed on the outer surface of ZSM-5 and highly dispersed copper-oxo species inside the channels which are only a minority fraction in the sample (Beznis *et al.*, 2010a). Catalytic experiments and FTIR measurements of adsorbed pivalonitrile revealed that the Cu-O species on the outer surface are inactive for methanol production while the copper species inside the channels are responsible for the selective oxidation of methane to methanol (Beznis *et al.*, 2010a).

2.2 Biological catalytic oxidation at low temperatures

It is well known that methane monooxygenase enzymes (MMO) naturally catalyze the selective oxidation of methane to methanol in water at ambient or physiological conditions. (Labinger, 2004) Two types of this enzyme that provide solution to harnessing methane as an energy source and for synthesis of molecules required for life exists in nature, namely (i) the soluble methane monooxygenase (sMMO) which is a complex of iron found in the cytosol of some methane-metabolizing bacteria and (ii) particulate methane monooxygenase (pMMO) which is a methanotrophic integral protein and a complex of Cu (Kopp & Lippard, 2002; Balasubramanian & Rosenzweig, 2007; Himes & Karlin, 2009). pMMO is a membrane metalloenzyme produced by all methanotrophs and is composed of three protein subunits, pmoA, pmoB and pmoC, arranged in a trimeric $\alpha_3\beta_3\gamma_3$ complex (Balasubramanian *et al.*, 2010; Bollinger Jr., 2010). It is well understood that the soluble enzyme sMMO uses a co-factor containing an active di-iron cluster to bind and activate oxygen in the two-electron oxidation of methane to methanol. In other words, an essential feature of sMMO is an active site containing two iron centres in a non-heme environment (Sorokin *et al.*, 2010; Alvarez-Galvan *et al.*, 2011). This active di-iron centre and the possible mechanistic pathways for sMMO catalysis have been well characterized and studied by Lippard, Lipscomb and their co-workers (Merkx *et al.*, 2001; Kovaleva *et al.*, 2007; Tinberg & Lippard, 2011). The mechanism of sMMO which involves creation of a very strong oxidizing di-iron species that is able to attack a C-H bond in CH_4 is quite different from organometallic CH_4 activation. In contrast to the studies on sMMO, the nature of the pMMO metal active site has been very controversial and was not established until very recently when it was shown that the methane-oxidizing co-factor was a di-copper cluster in the soluble domains of the extramembrane pmoB subunit (Balasubramanian *et al.*, 2010; Bollinger Jr., 2010; Himes *et al.*, 2010). These newly discovered soluble proteins may now be useful tools for investigating the mechanism of oxygen activation and methane hydroxylation at a copper centre (Bollinger Jr., 2010). This new discovery of a di-copper co-factor in pMMO is in agreement with earlier report of direct methane activation by mono-(μ-oxo)dicopper cores in inorganic Cu-ZSM-5 zeolite catalysts (Woertink *et al.*, 2009). Both of these new discoveries appear to have the potential to bring our understanding of copper-mediated methane oxidation to the level achieved for the better studied di-iron sMMO and relevant inorganic models (Bollinger Jr., 2010).

A chemical system that is capable of oxidizing CH_4 at ambient conditions like MMOs would be highly desirable. Complexes mimicking the structural organisation and spectral features of MMO have been reported but di-iron functional synthetic models capable of oxidizing

methane have not yet been created in spite of considerable efforts (Tshuva & Lippard, 2004). However, previous studies have indicated that metallophthalocyanines (MPc), especially iron phthalocyanines (FePc) are good catalysts for clean oxidation processes (Sorokin *et al.*, 2008; Sorokin *et al.*, 2010; Alvarez-Galvan *et al.*, 2011). In particular, it has been shown that μ-nitrido diiron phthalocyanine complexes (Fig. 3) possess remarkable catalytic properties (Sorokin *et al.*, 2008; Sorokin *et al.*, 2010).

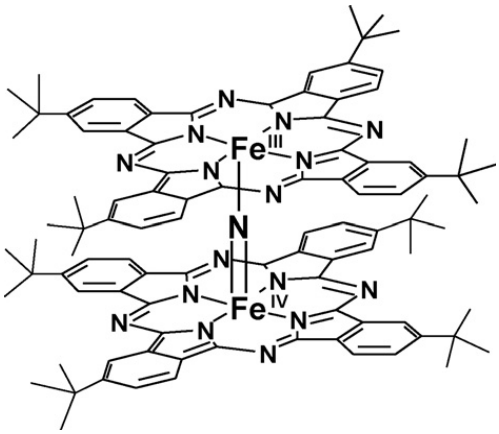

Fig. 3. Structure of μ-nitrido bridged diiron tetra-tert-butylphthalocyanine (Sorokin *et al.*, 2010).

Using ^{13}C and ^{18}O labelling experiments, μ-nitrido diiron tetra-tert-butylphthalocyanine, $(FePc^tBu_4)_2N$ (Fig. 3) supported on silica was shown to activate H_2O_2 to oxidize methane in water at 25-60 °C to methanol, formaldehyde and formic acid under the heterogeneous conditions (Sorokin *et al.*, 2008; Sorokin *et al.*, 2010). The use of H_2O_2 as the clean oxidant, water as the clean reaction medium and easily accessible solid catalyst makes this approach to be green and practical. These features together with the relevance of the binuclear structure of bio-inspired complex to biological oxidation are of great importance from both practical and fundamental points of view. Experimental data indicated that the stable μ-nitrido diiron tetra-tert-butylphthalocyanine complex operates via oxo-transfer mechanism involving a high-valent diiron oxo species which acts as a powerful oxidant in the methane oxidation reaction (Sorokin *et al.*, 2008; Sorokin *et al.*, 2010). The heterolytic cleavage of the O-O bond in $Fe^{IV}NFe^{III}OOH$ complex and the formation of very strong oxidizing $Fe^{IV}NFe^{V}=O$ species are favoured in the presence of acid by the protonation of peroxide oxygen (Sorokin *et al.*, 2008; Alvarez-Galvan *et al.*, 2011). Thus, significant improvement in catalytic activity was observed in the presence of 0.075-0.1 M H_2SO_4 (Sorokin *et al.*, 2008; Sorokin *et al.*, 2010).

Otsuka and Wang (Wang & Otsuka, 1994, 1995; Otsuka & Wang, 2001) have previously shown $FePO_4$ to exhibit a unique catalytic activity when H_2 is added to methane plus oxygen feed at atmospheric pressure. On this catalyst, both methane conversion and selectivity to methanol were enhanced in the presence of H_2 as a reductant. However, only up to 25.7% and 46% selectivities to methanol and formaldehyde, respectively, were obtained at very low conversion of 0.51% even in the presence of hydrogen. Only a trace

amount of methanol was obtained during the oxidation of methane in the absence of hydrogen (Wang & Otsuka, 1994, 1995).

The biochemical formation of methanol by the oxidation of methane was recently investigated using a biocatalyst based on the cells of the bacteria *Methylosinus sporioum B-2121* (Razumovsky *et al.*, 2008). The biocatalyst was suspended in a medium and immobilized in poly(vinyl alcohol) cryogel. It was observed that the use of the immobilized biocatalyst made it possible to enhance the productivity of the process more than 5-fold compared to that of the free cells and to achieve the highest methanol concentration of 62±2 mg L^{-1} in the medium (Razumovsky *et al.*, 2008). A brief review of the classification, characteristics and distribution of methanotrophic bacteria and discussion of the approach of biocatalytic mechanism of the selective oxidation of methane to methanol was presented recently by Liu et al. (Liu *et al.*, 2007).

2.3 Relevance of oxidative aromatics methylation to methane-to-methanol conversion

Recent investigations in our laboratory have demonstrated the formation of methanol intermediate in the oxidative methylation of aromatics in the presence of large excess of methane in a high pressure batch reactor at 400 °C (Adebajo *et al.*, 2000; Adebajo *et al.*, 2004). It appears that the methanol intermediate is formed homogeneously in the gas phase since it was only formed as the major product in the absence of solid catalyst. When zeolite catalysts were introduced into the reactor, the methanol was not detected but was used to methylate the aromatics reactants to produce methylated aromatic products or converted directly to aromatics in the absence of aromatic reactants (Adebajo *et al.*, 2000; Adebajo *et al.*, 2004). Gas phase analysis of reaction products failed to detect any CO_2, CO, H_2, or C_{2+} non-aromatic hydrocarbon products (Adebajo, 1999; Adebajo *et al.*, 2004). Thus, there appears to be no significant complete or incomplete combustion of methane due to failure to detect any CO or CO_2 deep oxidation products in the gas products. This observation implies that it is possible to inhibit the complete oxidation of methane to deep oxidation products in the presence of an additive such as aromatics. This observation is similar to earlier observation that the presence of small amounts of hydrocarbon additives (especially ethane) lowered the initiation temperatures of partial oxidation of methane to methanol and increased the methanol selectivity and yield (Gesser *et al.*, 1985; Fujimoto, 1994). This observation therefore extends the significance of the oxidative methylation reaction and we had earlier suggested that this avenue could be explored further for optimisation of the conversion of methane to methanol (Adebajo *et al.*, 2004).

This work has also demonstrated the possibility of achieving in-situ methylation using methane by combining methanol synthesis by partial oxidation of the methane with methylation of aromatics. This concept is very similar to earlier demonstration by Gesser et al. that methane partial oxidation could be combined with methanol conversion to gasoline in a two-stage continuous flow reactor (Yarlagadda *et al.*, 1987). In the first stage of the reactor, methane and oxygen reacted to produce methanol homogeneously while the methanol was converted by HZSM-5 catalyst in the second stage to produce aromatics (the major components of the liquid products), C_{3+} hydrocarbons, carbon oxides and water (Yarlagadda *et al.*, 1987).

3. Conversion of carbon dioxide to oxygenates

3.1 Recent advances in the catalytic conversion of carbon dioxide to oxygenates

Carbon dioxide is a renewable, non-toxic, abundant (cheap) and inflammable carbonaceous raw material. It is therefore considered attractive as an environmentally friendly chemical reagent or feedstock for the production of a wide range of value-added chemicals and fuels. However, CO_2 is rather inert and its chemical transformations are thermodynamically highly unfavourable. This is illustrated in Figure 4 (Zangeneh *et al.*, 2011). Its inertness is due to its being the most oxidized state of carbon. In other words, it is a raw material in its lowest energy level, thus constituting a major obstacle in establishing industrial processes for its conversion. A large input of energy is therefore required for its transformation into useful chemicals. Nevertheless, several exothermic reactions of CO_2 are known and have been investigated and many reviews of such transformations have been published recently (Jessop *et al.*, 2004; Jessop, 2007; Sakakura *et al.*, 2007; Yu *et al.*, 2008; Olah *et al.*, 2009; Zangeneh *et al.*, 2011). Reduction is the only possible route for the conversion of CO_2 since it is the most oxidized form of carbon. The chemical reduction of CO_2 can be either homogeneous or heterogeneous reduction. According to Sakakura et. al. in their review (Sakakura *et al.*, 2007), four main methodologies for transforming CO_2 into useful chemicals involve:

1. Using high-energy starting materials such as hydrogen, unsaturated compounds, small-membered ring compounds and organometallics.
2. Choosing oxidized low-energy synthetic targets such as organic carbonates.
3. Shifting the equilibrium to the product side by removing a particular compound.
4. Supplying physical energy such as light or electricity.

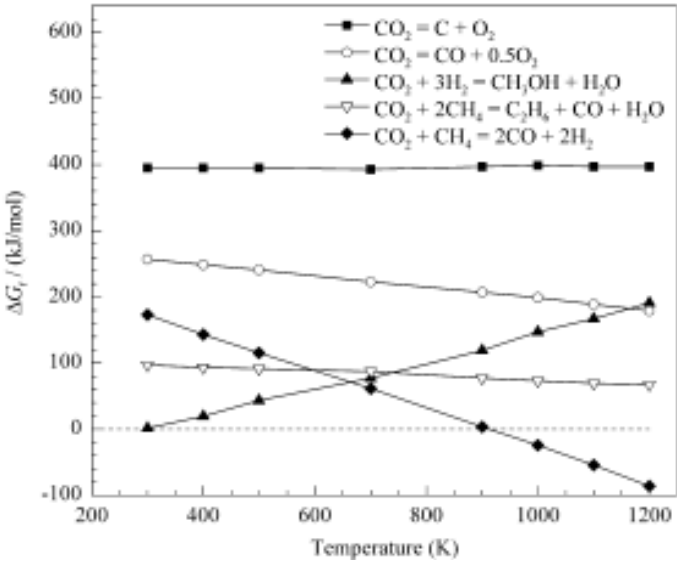

Fig. 4. Thermodynamics of some reactions of carbon dioxide ((Zangeneh *et al.*, 2011).

This review will cover mainly hydrogenation of CO_2 using homogeneous and heterogeneous catalytic and biocatalytic pathways. Photocatalytic and electrochemical reduction of CO_2 will also be discussed.

3.1.1 Homogeneous catalytic hydrogenation of carbon dioxide

Transition metal complexes have been widely used for the homogeneous catalytic hydrogenation of CO_2. The mild conditions used for these reactions make the partial hydrogenation of CO_2 to formic acid and derivatives highly feasible (Eqn. 13) while further reduction of the formic acid is more difficult and only limited examples of formation of other products such as methanol and methane are known (Zangeneh *et al.*, 2011):

$$CO_2 + H_2 \rightarrow HCOOH_{(l)} \; (\Delta H^0_{298K} = -31.8 \text{ kJ mol}^{-1}) \quad (13)$$

Homogeneous hydrogenation of CO_2 has been attracting a lot of interest and the major focus has been to develop active and selective catalysts for the production of valuable organics from this cheap and abundant resource. Two comprehensive reviews of advances in the developments of catalysts for homogeneous hydrogenation of CO_2 to formic acid, formamides, formates, methanol, methane and oxalic acid were published in 2004 and 2007 (Jessop *et al.*, 2004; Jessop, 2007). The earlier review published in 2004 (Jessop *et al.*, 2004) covered the advances in the field since 1995. This earlier review indicated that highly active and efficient catalysts which are mainly transition metal complexes had been developed for the homogeneous hydrogenation of CO_2 to formic acid and its derivatives such as formamides (Jessop *et al.*, 2004). These metal complexes are usually hydrides or halides with phosphines as natural ligands and complexes of Rh and Ru proved to be the most active metals (Jessop *et al.*, 2004; Zangeneh *et al.*, 2011). Such active catalysts were developed for CO_2 hydrogenation in water, organic solvents, supercritical CO_2 and ionic liquids (Jessop *et al.*, 2004). The 2004 review also indicated that the range of formamides that can be produced in high yield had expanded greatly. However, as of the time of this earlier review, very limited work had been done on the development of active and selective homogeneous catalysts for the production of other oxygenates (such as methyl formate, acetic acid, methanol and ethanol) and methane (Jessop *et al.*, 2004). This is so because these other products are more difficult to prepare by the homogeneously hydrogenation reaction. The synthesis of oxalic acid by this homogeneously catalyzed reaction was not yet reported prior to the 2004 review (Jessop *et al.*, 2004).

A novel non-metal-mediated homogeneous hydrogenation of CO_2 to methanol was recently reported by Ashley et al. (Ashley *et al.*, 2009) This was carried out using a Frustrated Lewis pairs (FLP)-based non-metal-mediated process at low pressures (1-2 atm) and a reaction temperature of 160 °C (Ashley *et al.*, 2009). In such FLP systems, the steric environment imposed on the donor and acceptor atoms by the substituents prevents a strong donor-acceptor interaction. The first step in the process involves heterolytic activation of hydrogen and subsequent insertion of CO_2 into a B-H bond of 2,2,6,6-tetramethylpiperidine (TMP) and $B(C_6F_5)_3$ to form $[TMPH][HB(C_6F_5)_3]$ complex (Ashley *et al.*, 2009). Introduction of CO_2 then produced the formatoborate complex $[TMPH]\text{-}[HCO_2B(C_6F_5)_3]$. Subsequent selective

distillation at 100 °C then resulted in the decomposition of the intermediate complex to produce methanol (Ashley *et al.*, 2009).

3.1.2 Heterogeneous catalytic hydrogenation of carbon dioxide

Heterogeneous catalysis is technically more favourable than the homogeneous reaction in terms of the reactor design and the stability, separation, handling and recycling of the catalysts. In spite of these practical benefits, there has only been limited number of compounds that have been synthesized from CO_2 through heterogeneous catalytic pathways and the equilibrium composition is complicated by the simultaneous chemical equilibria (Zangeneh *et al.*, 2011).

Metal-catalyzed heterogeneous hydrogenation of carbon dioxide generally produces methanol or methane directly depending on the reaction conditions. The syntheses of methanol and dimethylether (DME) are generally the most important heterogeneous hydrogenation reactions of CO_2 because of the potential of these oxygenates to become future energy carriers and major feedstock for petrochemical industries through C_1 chemistry (Lunsford, 2000; Olah *et al.*, 2009). Methanol is currently commercially produced on a large scale over heterogeneous catalysts from syngas (Eqns. 5 & 6) obtained from non-renewable natural gas or coal. Syngas contains mainly CO and H_2 along with a small amount of CO_2.

It is well agreed that the $Cu/ZnO/ZrO_2$ catalysts used for syngas production is also active for the direct synthesis of methanol from CO_2 and H_2 and in the steam reforming of methanol (Yu *et al.*, 2008; Olah *et al.*, 2009; Zangeneh *et al.*, 2011). This basic catalyst is often modified by addition of different oxides to improve its activity and stability. Apart from ZrO_2, other irreducible oxides such as Al_2O_3, TiO_2 and Ga_2O_3 have been investigated (Slocynski *et al.*, 2006). The effects of several other metal (e.g. boron, chromium, tungsten and manganese) and metal oxide (e.g. VO_x, MnO_x and MgO) additives have also been reported (Slocynski *et al.*, 2006; Yu *et al.*, 2008). Pd supported on several basic oxides including La_2O_3 and lithium-promoted Pd on SiO_2 have also been found to exhibit considerable activity and selectivity for methanol synthesis (Lunsford, 2000).

DME can be produced by dehydration of methanol (Eqn. 14) or directly from syngas over bifunctional catalysts (Lunsford, 2000; Arena *et al.*, 2004; Sun *et al.*, 2004). The direct synthesis of DME by CO_2 hydrogenation over bifunctional catalysts is a two-step process involving methanol synthesis followed by in situ dehydration of methanol (Eqn. 14) (Arena *et al.*, 2004; Sun *et al.*, 2004). Thus, the bifunctional catalysts contain functionally independent catalysts comprising of the methanol forming component based on CuO-ZnO and a methanol dehydration component based on suitable zeolites e.g. HZSM-5 and HY zeolites (Arena *et al.*, 2004; Sun *et al.*, 2004).

$$2CH_3OH \rightarrow CH_3OCH_3 + H_2O \ (\Delta H^0_{298K} = -23.4 \text{ kJ mol}^{-1}) \quad (14)$$

Very recently, Zhang et al. (Zhang *et al.*, 2009) reported that carbon nanotubes (CNTs) or CNT-based materials doped with some transition metals such as Co, Pd, etc., exhibited good catalytic activity and selectivity for some catalytic processes related to adsorption-activation

and spillover of hydrogen such as CO or CO_2 hydrogenation to alcohols. However, further detailed investigations of the interactions between CNTs and catalytically active host components and between CNTs and reactant molecules are needed in order to gain a better understanding of the nature of the promoter action by CNTs (Zhang *et al.*, 2009).

3.1.3 Photocatalytic reduction of carbon dioxide

Direct photoreduction of CO_2 has recently attracted much attention and many researchers have shown that CO_2 can be reduced in water vapour or solvent by photocatalysts. Photocatalytic systems utilizing semiconductor materials appear to be the most feasible of all the photocatalytic systems and processes that have been investigated. Inoue et al. (Inoue *et al.*, 1979) first reported the possibility of reducing carbon dioxide by photocatalysis in aqueous medium to produce methanol, formic acid, formaldehyde and trace amounts of methane. These workers used photosensitive semiconductors such as TiO_2, WO_3, ZnO, CdS, GaP and SiC. The efficient photoreduction of carbon dioxide in aqueous medium is one of the most challenging tasks due to the rather low solubility of CO_2 at ambient conditions (Sasirekha *et al.*, 2006). TiO_2 has been shown to be the most suitable semiconductor that offers the highest light conversion efficiency due to its excellent physico-chemical properties (Sasirekha *et al.*, 2006). This semiconductor is non-toxic and possesses high stability towards photo-corrosion and relatively favourable band gap energy. Thus, TiO_2 is currently the most widely studied. Two review papers were recently published on the photocatalytic reduction of CO_2 over TiO_2-based photocatalysts (Dey, 2007; Kočí *et al.*, 2008). One problem with TiO_2 is that their photosensitivity is limited to the ultraviolet (UV) region with absorption of only about 4-5% of solar energy due to their relatively large band gap, thus resulting in low quantum efficiencies. A lot of effort has therefore focused on doping TiO_2 with various metals and metal oxides in order to extend their absorption into the visible region (Slamet *et al.*, 2005; Wang *et al.*, 2005; Sasirekha *et al.*, 2006; Wu, 2009; Fan *et al.*, 2011; Wang *et al.*, 2011). In spite of these efforts, both recent reviews (Dey, 2007; Kočí *et al.*, 2008) indicate that the photocatalytic reduction of CO_2 is still in its infancy and that many questions still remain to be answered such as (i) how can the photocatalytic efficiency be improved?, (ii) what is the most suitable form of photocatalysts?, and (ii) how can the utilization of solar energy be greatly increased? Another review suggested that the efficiency of the photocatalytic process for CO_2 reduction can be improved by choosing semiconductors with suitable band-gap energies, developing suitable reductant and optimizing operating conditions such as temperature, pressure, light intensity and operating wavelength (Usubharatana *et al.*, 2006). This other review also suggested that further research should focus on the potential and economics of solar reactor and their design (Usubharatana *et al.*, 2006).

In addition to TiO_2-based photocatalysts, $InTaO_4$ was recently reported to exhibit outstanding photocatalytic reduction of CO_2 into methanol under visible light irradiation (Pan & Chen, 2007; Chen *et al.*, 2008). More recently, the activities of a bifunctional N-doped $InTaO_4$ photocatalyst for the photocatalytic reduction of CO_2 to methanol was demonstrated (Tsai *et al.*, 2011). The photocatalyst was prepared by doping InTaO4 with nitrogen and incorporating a nanostructured Ni@NiO core-shell co-catalyst. Nitrogen doping produced visible-light-responsive photocatalytic activity which further enhanced absorbance. Thus,

methanol yield was enhanced when compared with undoped ones and the rate of the photoreaction was found to increase with visible light irradiation time (Fig. 5). Moreover, the introduction of the co-catalyst enhanced absorbance and methanol yield even further (Fig. 5) and efficiently prevented electron-hole recombination that would otherwise be caused by electrons and holes separated from the crystal (Tsai *et al.*, 2011).

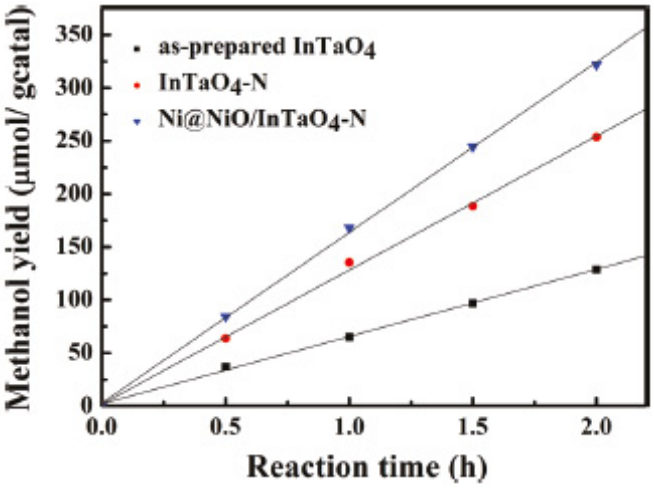

Fig. 5. The variation of methanol yield with reaction time for the as-prepared $InTaO_4$ and the N-doped and co-catalyst treated $InTaO_4$-based samples (Tsai *et al.*, 2011).

3.1.4 Electrochemical reduction of carbon dioxide

Direct electrochemical reduction of CO_2 to produce methanol can be achieved but is rather kinetically complex and needs effective electrocatalysts (Olah *et al.*, 2009). Generally, during the electrochemical reduction of CO_2 to methanol, formaldehyde and formic acid are also produced as shown in Equations 15-17 (Olah *et al.*, 2009). Photoelectrochemical reduction of CO_2 to methanol has also been demonstrated by the use of solar energy at a semiconductor electrode such as p-GaP and such reductive reaction using light energy has been reported to show promise (Barton *et al.*, 2008). Secondary treatment steps for the conversion of formaldehyde and formic acid by-products to methanol over suitable solid catalysts have been developed to overcome the difficulties associated with the formation of product mixtures in the electrochemical reduction of CO_2. Such secondary treatment steps make it possible to significantly increase the overall efficiency of the electrochemical reduction of CO_2 to methanol. However, it is more desirable to develop more effective catalysts that are capable of increasing the selective electrochemical reduction of CO_2 to methanol so as to eliminate or reduce the secondary treatments.

$$CO_2 + 6H^+ + 6\acute{e} \rightarrow CH_3OH + H_2O \quad (15)$$

$$CO_2 + 4H^+ + 4\acute{e} \rightarrow HCHO + H_2O \quad (16)$$

$$CO_2 + 2H^+ + 2\acute{e} \rightarrow HCOOH \quad (17)$$

The electrochemical reduction of carbon dioxide alone has also been found to produce oxalic acid and its derivatives such as glycolic acid, glyoxylic acid, etc., but these reactions have low selectivities (Sakakura *et al.*, 2007).

3.2 Biocatalytic or enzymatic conversion of carbon dioxide

Heterogeneous catalytic, photocatalytic and electrocatalytic routes which are most commonly used for reduction of carbon dioxide with hydrogen to produce methanol and other oxygenates require high temperatures and pressures since the reaction is not thermodynamically favoured at ambient conditions. The selectivity and yields of the desired products are also rather low. Most of the metallic catalysts also require highly pure feedstocks for them to maintain their activities. Thus, the thermochemical reduction of carbon dioxide is not economically viable for industrial use. In contrast to these traditional pathways, novel biocatalytic routes for reduction of CO_2 at ambient conditions have been demonstrated. Such biocatalytic reductions are attractive because they can be very efficient and can make use of low purity reactants and tolerate many impurities that are toxic to chemical catalysts (Lu *et al.*, 2010). For example, a combination of formate dehydrogenase (FateDH), formaldehyde dehydrogenase (FaldDH) and alcohol dehdrogenase (ADH) was used in sequential reduction of CO_2 to methanol (Obert & Dave, 1999; Jiang *et al.*, 2004; Wu *et al.*, 2004). Reduced nicotinamide adenine dinuncleotide (NADH) was used as the terminal electron donor for the enzymatic reaction. This sequential enzymatic conversion pathway is represented by Eqn. 18 below. In a later investigation by Lu et al. (Lu *et al.*, 2006), FateDH immobilized in a novel alginate-silica hybrid gel was used as the biocatalyst to convert CO_2 into formic acid in the presence of reduced NADH as the terminal electron donor (Eqn. 19). The gel was prepared by in-situ hydrolysis and polycondensation of tetramethoxysilane in alginate solution followed by Ca^{2+}-induced gelation (Lu *et al.*, 2006). The reduction of CO_2 by FateDH encapsulated in alginate-silica hybrid gel beads resulted in the high-yield production of formic acid (95.6%) and the relative activity of the immobilized FateDH after 10 cycles was as high as 69% (Lu *et al.*, 2006). Acetogenic bacteria microbes have also been investigated (Song *et al.*, 2011) as biocatalysts for the electrochemical reductive conversion of CO_2 with efficiency of 80-100% in phosphate buffer solution (pH 7) at -0.58 V vs NHE which was near the equilibrium potential of CO_2/formate. Direct bacterial use for electrochemical CO_2 conversion could eliminate expensive enzyme purification steps and widens the choice of catalysts to include the naturally developed and optimized microorganisms (Song *et al.*, 2011).

$$CO_2 \xrightarrow{\text{FateDH, NaDH}} HCOOH \xrightarrow{\text{FaldDH, NaDH}} HCHO \xrightarrow{\text{ADH, NADH}} CH_3OH \quad (18)$$

$$CO_2 + NaDH \xrightarrow{\text{FateDH}} HCOOH + NAD^+ \quad (19)$$

One challenge for the realization of biocatalytic reduction of CO_2 at large scale is the efficiency of the reaction; the reported reaction rates and equilibrium yields are generally low. There is therefore need to develop faster and more efficient biocatalytic systems. Thus, recent research has been focusing on discovery of new enzymes and engineering of the reaction systems for improved catalytic efficiency (Baskaya *et al.*, 2010). Thus, Baskaya et al. (Baskaya *et al.*, 2010) recently investigated the sequential enzymatic conversion of CO_2 to methanol from a thermodynamic point of view with a focus on factors that control the reaction equilibrium. Their results showed that the enzymatic CO_2 conversion is highly sensitive to the pH of the reaction solution and that it is possible to shift the biological

metabolic reactions to favour the synthesis of methanol by conducting the reactions at low pHs (e.g. pH of 5 or 6) and ionic strengths and at elevated temperatures (Baskaya *et al.*, 2010). However, it may be very difficult to reach such favourable conditions with the currently available biocatalysts since native enzymes that catalyze such reactions tend to be denatured and inactivated at acidic and elevated temperatures (Baskaya *et al.*, 2010).

Another major concern for biocatalytic CO_2 conversions is the source of chemical energy used to drive the reactions forward. Lu et al. (Lu *et al.*, 2010) are of the opinion that since the reduced form cofactor NADH carries the energy required for the reactions in the enzymatic reduction of CO_2, a solar power driven regeneration of the co-factor would provide the avenue to use solar energy for production of chemicals and fuels. Thus, these workers believe that the integration of multi-enzyme systems on nanostructured electrodes will provide a unique approach to harvesting solar energy in the forms of renewable chemicals and fuels (Lu *et al.*, 2010).

4. Conclusions

It is evident that the direct conversion of methane to oxygenates such as methanol, formaldehyde and acetic has great potential for producing liquid fuels and petrochemicals while simultaneously reducing the global warming effect of the greenhouse gas. However, the major challenge that needs to be overcome before this can be realised is the difficulty in activating the strong C-H bond in methane at relatively lower temperatures and pressures to make the process economically viable and the problem of achieving high methane conversions without reducing product selectivities at these mild conditions. The homogeneous catalytic conversion of methane at low temperatures is thus highly desirable since the low temperature of activation of C-H bond does not involve radicals and may lead to more selective reactions than those promoted by heterogeneous catalysts operating at high temperatures. However highly active and selective catalysts under the strong oxidizing and protic conditions in which they operate still need to de developed in future investigations. Moreover, these harsh conditions are undesirable because they are environmentally unfriendly. Although, some other catalytic systems that do not operate under such strong oxidizing conditions have been used but their activities and product selectivities still need significant improvement. Among the catalysts that do not require harsh oxidizing conditions, metal-containing zeolites, especially Fe-ZSM-5 and Cu-ZSM-5, have been observed to show great potential for catalytic conversion of methane to oxygenates at low or ambient temperatures. In particular, since the active site in the highly selective CuZSM-5 has recently been identified to be a bent mono-(μ-oxo)dicopper cluster, its catalytic activity and selectivity for the partial methane oxidation should be optimized in future investigations. The biocatalytic oxidation of methane using MMOs or a chemical system that is capable of oxidizing methane at ambient conditions like MMOs is most highly desirable but such biocatalytic systems with desired high activities and selectivities are yet to be created in spite of considerable efforts. Nevertheless, now that the active sites in both pMMO and Cu-ZSM-5 have been identified to be soluble di-copper clusters, efforts should be directed to more detailed investigations of the mechanisms of copper-mediated oxygen activation and methane hydroxylation. A deeper understanding of the mechanism of this important reaction that will be gained from such studies will also underpin the design of novel catalytic systems with high activities and product selectivities, especially now that the active centres are known.

Important observations from studies in our laboratory indicate that it is possible to inhibit the complete oxidation of methane to deep oxidation products in the presence of an additive such as aromatics. It is suggested that this avenue should be explored further for optimizing the conversion of methane to methanol. Our work has also demonstrated the possibility of achieving in-situ methylation or production of aromatics using methane by combining methanol synthesis by partial methane oxidation with methylation of aromatics or methanol-to-aromatics conversion.

Carbon dioxide is a renewable, non-toxic, abundant and inflammable carbonaceous raw material and its reduction therefore also has great potential for both reduction of greenhouse gas emissions to some extent and production of value-added chemicals and fuels. Reduction is the only possible pathway for conversion of CO_2 since it is the most oxidized form of carbon. All types of catalysts (homogeneous, heterogeneous, photocatalysts, electrocatalysts and biocatalysts) are generally observed to play a major or important role in such reduction reactions. However, CO_2 is rather inert and its catalytic reduction and other transformations are highly kinetically and thermodynamically unfavourable. The greatest challenge common to all the different types of catalyst systems therefore lies in developing highly efficient and selective catalysts that do not undergo rapid deactivation and in overcoming the thermodynamic barrier. The thermodynamic limitation could be overcome by adopting either a physical approach (e.g. by using a suitable membrane reactor) or a chemical approach (e.g. by conversion to more stable products). The economic viability of the hydrogenation reactions depends on the sources of energy and hydrogen, thus these should also be taken into consideration in future investigations.

Among the different types of catalytic systems that have been investigated, photocatalytic reduction of CO_2 is highly attractive in view of the utilization of solar energy but the efficiency of the process still needs significant improvement by carefully choosing semiconductors with suitable band gap energy, developing appropriate reductants and optimizing reaction conditions. However, a recently reported bifunctional N-doped $InTaO_2$ photocatalyst containing a nanostructured Ni@NiO core-shell co-catalyst shows some great potential. Thus, other novel photocatalytic systems could be developed using this strategy in future investigations. The biocatalytic pathways for reduction of CO_2 are most attractive because they can operate at ambient temperatures and therefore highly economical. These biocatalytic routes can also be very efficient and can make use of low purity reactants and tolerate many impurities that are toxic to chemical catalysts. However, the reported reaction rates and equilibrium yields are still generally low, thus the efficiency of the reaction still requires significant improvement before it can operate at large scale. Faster and more efficient biocatalytic systems should therefore be developed. Another challenge for biocatalytic conversion is the source of chemical energy for driving the reaction forward. Some workers (Lu *et al.*, 2010) have suggested that the integration of multi-enzyme systems on nanostructured electrodes will provide a unique approach to harvesting solar energy in the forms of renewable chemicals and fuels.

In short, the goal of catalytically and/or biocatalytically converting methane and carbon dioxide to value-added chemicals and fuels while simultaneously reducing greenhouse emissions is far from being realised in terms of efficiency and economic and commercial viability. Nevertheless, the progress that has been made so far cannot be undermined.

5. Acknowledgment

The financial support of this work provided by the Australian Research Council and the Faculty of Science and Technology at QUT is gratefully acknowledged.

6. References

Adebajo, M., Long, M.A. & Howe, R.F. (2000). Methane Activation over Zeolite Catalysts: The Methylation of Benzene. *Res. Chem. Intermed.*, 26, 185-191.

Adebajo, M.O. (1999). *Activation of methane using zeolite catalysts.* PhD Thesis. The University of New South Wales, Sydney, Australia.

Adebajo, M.O., Long, M.A. & Frost, R.L. (2004). Further Evidence for the Oxidative Methylation of Benzene with Methane over Zeolite Catalysts. *Catal. Commun.*, 5, 125-130.

Alvarez-Galvan, M.C., Mota, N., Ojeda, M., Rojas, S., Navarro, R.M. & Fierro, J.L.G. (2011). Direct methane conversion routes to chemicals and fuels. *Catal. Today*, 171, 15-23.

Arena, F., Spadaro, L., di Blasi, O., Bonura, G. & Frusteri, F. (2004). Integrated synthesis of dimethylether via CO_2 hydrogenation. *Stud. Surf. Sci. Catal.*, 147, 385-390.

Ashley, A.E., Thompson, A.L. & O'Hare, D. (2009). Non-metal-mediated homogeneous hydrogenation of CO_2 to CH_3OH. *Angew. Chem. Chem. Int. Ed.*, 48, 9839-9843.

Babero, J.A., Alvarez, M.C., Bañares, M.A., Peña, M.A. & Fierro, J.L.G. (2002). Breakthrough in C_1-oxygenates production via direct methane oxidation. *Chem. Commun.*, 1184-1185.

Balasubramanian, R. & Rosenzweig, A. (2007). Structural and mechanistic insights into methane oxidation by particulate methane monooxygenase. *Acc. Chem. Res.*, 40, 570-580.

Balasubramanian, R., Smith, S.M., Rawat, S., Yatsunyk, L.A., Stemmler, T.L. & Rosenzweig, A.C. (2010). Oxidation of methane by a biological dicopper centre. *Nature*, 465, 115-119.

Barton, E.E., Rampulla, D.M. & Borcarsly, A.B. (2008). Selective solar-driven reduction of CO_2 to methanol using a catalyzed p-GaP based photoelectrochemical cell. *J. Am. Chem. Soc.*, 130, 6342-6342.

Baskaya, F.S., Zhao, X., Flickinger, M.C. & Wang, P. (2010). Thermodynamic feasibility of enzymatic reduction of carbon dioxide to methanol. *Appl. Biochem. Biotechnol.*, 162, 391-398.

Bergman, R.G. (2007). Organometallic chemistry: C-H activation. *Nature*, 446, 391-393.

Beznis, N.V., Weckhuysen, B.M. & Bitter, J.H. (2010a). Cu-ZSM-5 Zeolites for the Formation of Methanol from Methane and Oxygen: Probing the Active Sites and Spectator Species. *Catal. Lett.*, 138, 14-22.

Beznis, N.V., Weckhuysen, B.M. & Bitter, J.H. (2010b). Partial Oxidation of Methane Over Co-ZSM-5: Tuning the Oxygenate Selectivity by Altering the Preparation Route. *Catal. Lett.*, 136, 52-56.

Bollinger Jr., J.M. (2010). Getting the metal right. *Nature*, 465, 40-41.

Chempath, S. & Bell, A.T. (2007). A DFT study of the mechanism and kinetics of methane oxidation to formaldehyde occurring on silica-supported molybdena. *J. Catal.*, 247, 119-126.

Chen, H.-C., Chou, H.-C., Wu, J.C.S. & Lin, H.-Y. (2008). Sol-gel prepared $InTaO_4$ and its photocatalytic characteristics. *J. Mater. Res.*, 23, 1364-1370.

Crabtree, R.H. (1994). Current Ideas and Future Prospects in Metal-Catalyzed Methane Conversion, In: *Studies in Surface Science and Catalysis*, H.E. Curry-Hyde and R.F. Howe, Eds, 81 (Natural Gas Conversion II), pp. 85-92, Elsevier Science B.V., Amsterdam.

de Vekki, A.V. & Marakaev, S.T. (2009). Catalytic partial oxidation of methane to formaldehyde. *Russ. J. Appl. Chem.*, 82, 521-536.

Dey, G.R. (2007). Chemical reduction of CO_2 to different products during photocatalytic reaction on TiO_2 under diverse conditions: an overview. *J. Nat. Gas Chem.*, 16, 217-226.

Dubkov, K.A., Sobolev, V.I., Talsi, E.P., Rodkin, M.A., Watkins, N.H., Shteinman, A.A. & Panov, G.I. (1997). Kinetic isotope effects and mechanism of biomimetic oxidation of methane and benzene on FeZSM-5 zeolite. *J. Mol. Catal. A: Chem.*, 123, 155-161.

Edwards, J.H. & Foster, N.R. (1986). The potential of methanol production from natural gas by direct catalytic partial oxidation. *Fuel Sci. Techol. Intl.*, 4, 365-390.

Fan, J., liu, E.-Z., Tian, L., Hu, X.-Y., He, Q. & Sun, T. (2011). Synergistic effect of N and Ni^{2+} on nanotitania in photocatalytic reduction of CO_2. *J. Environ. Eng.*, 137, 171-176.

Faraldos, M., Bañares, M.A., Anderson, J.A., Hu, H., Wachs, I.E. & Fierro, J.L.G. (1996). Comparison of silica-supported MoO_3 and V_2O_5 catalysts in the selective partial oxidation of methane. *J. Catal.*, 160, 214-221.

Foster, N.R. (1985). Direct catalytic oxidation of methane to methanol - a review. *Appl. Catal.*, 19, 1-11.

Fujimoto, K. (1994). New uses of methane, In: *Studies in Surface Science and Catalysis*, H.E. Curry-Hyde and R.F. Howe, Eds, 81 (Natural Gas Conversion II), pp. 73-84, Elsevier, Amsterdam.

Gesser, H.D. & Hunter, N.R. (1998). A review of C-1 conversion chemistry. *Catal. Today*, 42, 183-189.

Gesser, H.D., Hunter, N.R. & Prakash, C.B. (1985). The direct conversion of methane to methanol by controlled oxidation. *Chem. Rev.*, 85, 235-244.

Gol'dshleger, N.F., Es'kova, V.V., Shilov, A.E. & Shteinman, A.A. (1972). Reactions of alkanes in solutions of platinum chloride complexes. *Zhurnal Fizicheskoi Khimi*, 46, 1353-1354.

Groothaert, M.H., Smeets, P.J., Sels, B.F., Jacobs, P.A. & Schoonheydt, R.A. (2005). Selective oxidation of methane by the bis(mu-oxo)dicopper core stabilized on ZSM-5 and mordenite zeolites. *J. Am. Chem. Soc.*, 127, 1394-1385.

Groothaert, M.H., van Bokhoven, J.A., Battiston, A.A., Weckhuysen, B.M. & Schoonheydt, R.A. (2003). Bis(μ-oxo)dicopper in Cu-ZSM-5 and Its Role in the Decomposition of NO: A Combined in Situ XAFS, UV-Vis-Near-IR, and Kinetic Study. *J. Am. Chem. Soc.*, 125, 7629-7640.

Himes, R.A., Barnese, K. & Karlin, K.D. (2010). One is lonely and three is a crowd: two coppers are for methane oxidation. *Angew. Chem. Chem. Int. Ed.*, 49, 6714-6716.

Himes, R.A. & Karlin, K.D. (2009). A new copper-oxo player in methane oxidation. *Proc. Natl. Acad. Sci. USA*, 106, 18877-18878.

Holmen, A. (2009). Direct conversion of methane to fuels and chemicals. *Catal. Today*, 142, 2-8.

Hunter, N.R., Gesser, H.D., Morton, L.A. & Yarlagadda, P.S. (1990). Methanol formation at high pressure by the catalyzed oxidation of natural gas and by the sensitized oxidation of methane. *Applied Catalysis*, 57, 45-54.

Inoue, T., Fujishima, A., Satoshi, S. & Honda, K. (1979). Photoelectrocatalytic reduction of carbon dioxide in aqueous suspensions of semiconductor powders. *Nature*, 277, 637-638.

IPCC. (2001). In: *Climate Change 2001: The Scientific Basis*, Cambridge University Press, Cambridge.

Jessop, P.G. (2007). Homogeneous hydrogenation of carbon dioxide, In: *Handbook of homogeneous hydrogenation*, J.G. De Vries and C.J. Elsevier, Eds, 1, pp. 489-511, Wiley-VCH Verlag GmbH & Co. KGaA, Weinheim, Germany.

Jessop, P.G., Joó, F. & Tai, C.-C. (2004). Recent advances in the homogeneous hydrogenation of carbon dioxide. *Coord. Chem. Rev.*, 248, 2425-2442.

Jiang, Z., Xu, S. & Wu, H. (2004). Novel conversion of carbon dioxide to methanol catalyzed by sol-gel immobilized dehydrogenases. *Stud. Surf. Sci. Catal.*, 153, 474-480.

Kočí, K., Obalová, L. & Lacný, Z. (2008). Photocatalytic reduction of CO_2 over TiO_2 based catalysts. *Chem. Pap.*, 62, 1-9.

Kopp, D.A. & Lippard, S.J. (2002). Soluble methane monooxygenase: activation of dioxygen and methane. *Curr. Opin. Chem. Biol.*, 6, 568-576.

Kovaleva, E.G., Neibergall, M.B., Chakrabarty, S. & Lipscomb, J.D. (2007). Finding intermediates in the O_2 activation pathways of non-heme iron oxygenases. *Acc. Chem. Res.*, 40, 475-483.

Kudo, H. & Ono, T. (1997). Partial oxidation of CH_4 over ZSM-5 catalysts. *Appl. Surf. Sci.*, 121/122, 413-416.

Labinger, J.A. (2004). Selective alkane oxidation: hot and cold approaches to a hot problem. *J. Mol. Catal. A: Chem.*, 220, 27-35.

Labinger, J.A. & Bercaw, J.E. (2002). Understanding and exploiting C-H bond activation. *Nature*, 417, 507-513.

Li, T., Wang, S.J., Yu, C.S., Ma, Y.C., Li, K.L. & Lin, L.W. (2011). Direct conversion of methane to methanol over nano-[Au/SiO_2] in [Bmin]Cl ionic liquid. *Appl. Catal. A: General*, 398, 150-154.

Liu, C.-J., Hammer, T. & Mallinson, R. (2004). Utilisation of greenhouse gases - Preface. *Catal. Today*, 98, VII-VIII.

Liu, C., Wang, L., Jiang, B., Quan, G., Fan, W. & Wei, D. (2007). Greenhouse gas-methane converts to methanol: advance of bio-catalysis. *Prog. Environ. Sci. Tech.*, 1, 630-636.

Lu, X., Zhao, X. & Wang, P. (2010). High Intensity Enzymatic Biocatalysis for Direct Conversion of Solar Energy into Chemicals and Fuels. *Preprints of Symposia - Am. Chem. Soc., Division of Fuel Chemistry*, 55, 353.

Lu, Y., Jiang, Z.-Y., Xu, S.-W. & Wu, H. (2006). Efficient Conversion of CO_2 to Formic Acid by Formate Dehydrogenase Immobilized in a Novel Alginate-Silica Hybrid Gel. *Catal. Today*, 115, 263-268.

Lunsford, J.H. (2000). Catalytic conversion of methane to more useful chemicals and fuels: a challenge for the 21st century. *Catal. Today*, 63, 165-174.

Merkx, M., Daniel, D.A., Sazinsky, M.H., Blazyk, J.L., Müller, J. & Lippard, S.J. (2001). Dioxygen activation and methane hydroxylation by soluble methane monooxygenase: a tale of two irons and three proteins. *Angew. Chem. Chem. Int. Ed.*, 40, 2782-2807.

Navarro, R.M., Peña, M.A. & Fierro, J.L.G. (2006). Methane oxidation on metal oxides, In: *Metal oxides: Chemistry and applications*, J.L.G. Fierro, Ed, pp. 463-490, CRC Press, LLC Taylor & Francis Group, Boca Raton, FL.

Obert, R. & Dave, B.C. (1999). Enzymatic conversion of carbon dioxide to methanol: enhanced methanol production in silica sol-gel matrices. *J. Am. Chem. Soc.*, 121, 12192-12193.

Ohler, N. & Bell, A.T. (2006). Study of the elementary processes involved in the selective oxidation of methane over MoO_x/SiO_2. *J. Phys. Chem. B*, 110, 2700-2709.

Olah, G.O., Goeppert, A. & Prakash, G.K.S. (2009). Chemical Recycling of carbon dioxide to Methanol and Dimethyl Ether: From Greenhouse gas to Renewable, Environmentally Carbon Neutral Fuels and Synthetic Hydrocarbons. *J. Org. Chem.*, 74, 487-498.

Ono, T., Ikuta, K. & Shigemura, Y. (1993). Partial oxidation of methane at low pressure over silica and silica-supported tin, zirconium and germanium oxides, In: *Studies in Surface Science and Catalysis*, L. Guczi, F. Solymosi and P. Tétényi, Eds, 75 (New Frontiers in Catalysis, Parts A-C), pp. 1967-1970, Elsevier, Amsterdam.

Ono, T., Kudo, H. & Anpo, M. (2000). Partial oxidation of CH_4 and C_2H_6 at low pressure over H- and Na-ZSM-5 catalysts. *Appl. Catal. A: General*, 194-195, 71-78.

Ono, T. & Maruyama, J. (1996). Partial oxidation of CH_4 at low pressure over SiO_2 prepared from Si. *Catal. Lett.*, 39, 73-77.

Ono, T., Nakamura, M., Unno, K., Oyun, A., Ohnishi, J., Kataoka, M. & Masakazu, F. (2008). Partial oxidation of methane over Al/Silica catalysts using molecular oxygen. *J. Mol. Catal. A: Chem.*, 285, 169-175.

Otsuka, K. & Hatano, M. (1987). The catalysts for the synthesis of formaldehyde by partial oxidation of methane. *J. Catal.*, 108, 252-255.

Otsuka, K., Takahashi, R. & Tamanaka, I. (1999). Oxygenates from light alkanes catalyzed by NO_x in the gas phase. *J. Catal.*, 185, 182-191.

Otsuka, K. & Wang, Y. (2001). Direct conversion of methane to oxygenates. *Appl. Catal., A*, 222, 145-161.

Palkovits, R., Antonietti, M., Kuhn, P., Thomas, A. & Schüth, F. (2009). Solid catalysts for the selective low-temperature oxidation of methane to methanol. *Angew. Chem. Chem. Int. Ed.*, 48, 6909-6912.

Pan, P.-W. & Chen, Y.-W. (2007). Photocatlytic reduction of carbon dioxide on $NiO/InTaO_4$ under visible light irradiation. *Catal. Commun.*, 8, 1546-1549.

Panov, G.I., Sobolev, V.I. & Kharitonov, A.S. (1990). The role of iron in nitrous oxide decomposition on ZSM-5 zeolite and reactivity of the surface oxygen formed. *J. Mol. Catal.*, 61, 85-97.

Periana, R.A., Bhalla, B., Tenn, W.J., Young, K.J.H., Liu, X.Y., Mironov, O., Jones, C.J. & Ziatdinov, V.R. (2004). Perspectives on some challenges and approaches for developing the next generation of selective, low temperature, oxidation catalysts for alkane hydroxylation based on the CH activation reaction. *J. Mol. Catal. A: Chem.*, 220, 7-25.

Periana, R.A., Taube, D.J., Evitt, E.R., Loffler, D.G., Wentreck, P.R., Voss, G. & Masuda, T. (1993). A mercury-catalyzed high yield system for the oxidation of methane to methanol. *Science*, 259.

Periana, R.A., Taube, D.J., Gamble, S., Taube, H., Satoh, T. & Fujii, H. (1998). Platinum catalysts for the high-yield oxidation of methane to a methanol derivative. *Science*, 280, 560-564.

Pitchai, R. & Klier, K. (1986). Partial oxidation of methane. *Catal. Rev. - Sci. Eng.*, 28, 13-88.

Rahman, A.K.M.L., Kumashiro, M. & Ishihara, T. (2011). Direct synthesis of formic acid by partal oxidation of methane on H-ZSM-5. *Catal. Commun.*, 12, 1198-1200.

Razumovsky, S.D., Efremenko, E.N., Makhlis, T.A., Senko, O.V., Bikhovsky, M.Y., Podmaster, V.V. & Varfolomeev, S.D. (2008). Effect of immobilization on the the main dynamic characteristics of the enzymatic oxidation of methane to methanol by bacteria *Methylosinus sporium* B-2121. *Russ. Chem. Bull., Intl. Ed.*, 57, 1633-1636.

Sakakura, T., Choi, J.-C. & Yasuda, H. (2007). Transformation of carbon dioxide. *Chem. Rev.*, 107, 2365-2387.

Sasirekha, N., Basha, S.J.S. & Shanthi, K. (2006). Photocatalytic performance of Ru doped anatase mounted on silica for reduction of carbon dioxide. *Appl. Catal. B: Environ.*, 62, 169-180.

Shilov, A.E. & Shul'pin, G.B. (1997). Activation of C-H bonds by metal complexes. *Chem. Rev.*, 97, 2879-2932.

Shilov, A.E. & Shul'pin, G.B. (2000). *Activation and catalytic reactions of saturated hydrocarbons in the presence of metal complexes*. Kluwer Academic, Dordrecht.

Slamet, Nasution, H.W., Purnama, E., Kosela, S. & Gunlazuardi, J. (2005). Photocatalytic reduction of CO_2 on copper-doped titania catalysts prepared by improved impregnation method. *Catal. Commun.*, 6, 313-319.

Slocynski, J., Grabowski, R., Olszewski, P., Kozlowska, A., Stoch, J., Lachowska, M. & Skrzypek, J. (2006). Effect of metal oxide additives on the activity andstability of $Cu/ZnO/ZrO_2$ catalysts in the synthesis of methanol from CO_2 and H_2. *Appl. Catal. A: General* 310, 127-137.

Smeets, P.J., Groothaert, M.H. & Schoonheydt, R.A. (2005). Cu based zeolites: A UV-vis study of the active site in the selective methane oxidation at low temperatures. *Catal. Today*, 110, 303-309.

Sobolev, V.I., Dubkov, K.A., Panna, O.V. & Panov, G.I. (1995). Selective oxidation of methane to methanol on FeZSM-5 surface. *Catal. Today*, 24, 251-252.

Song, J., Kim, Y., Lim, M., Lee, H., Lee, J.I. & Shin, W. (2011). Microbes as electrochemical CO_2 conversionn catalysts. *ChemSusChem*, 4, 587-590.

Sorokin, A.B., Kudrik, E.V., Alvarez, L.X., Afanasiev, A., Millet, J.M.M. & Bouchu, D. (2010). Oxidation of methane and ethylene in water at ambient conditions. *Catal. Today*, 157, 149-154.

Sorokin, A.B., Kudrik, E.V. & Bouchu, D. (2008). Bio-inspired oxidation of methane in water catalyzed by N-bridged diiron phthalocyanine complex. *Chem. Commun.*, 2562-2564.

Sugino, T., Kido, A., Azuma, N., Ueno, A. & Udagawa, Y. (2000). Partial oxidation of methane on silica-supported silicomolybdic acid catalysts in an excess amount of water vapour. *J. Catal.*, 190, 118-127.

Sun, K., Lu, W., Wang, M. & Xu, X. (2004). Low-temperature synthesis of DME from CO_2/H_2 over Pd-modified from $CuO-ZnO-Al_2O_3-ZrO_2$/HZSM-5 catalysts. *Catal. Commun.*, 5, 367-370.

Tabata, K., Teng, Y., Takemoto, T., Suzuki, E., Bañares, M.A., Peña, M.A. & Fierro, J.L.G. (2002). Activation of methane by oxygen and nitrogen oxides. *Catal. Rev. - Sci. Eng.*, 44, 1-58.

Tabata, K., Teng, Y., Yamagushi, Y., Sakurai, H. & Suzuki, E. (2000). Experimental verification of theoretically calculated transition barriers of the reactions in a gaseous selective oxidation of $CH_4-O_2-NO_2$. *J. Phys. Chem. A*, 104, 2648-2654.

Taniewski, M. (2004). The challenges and recent advances in C_1 chemistry and technology. *Polish J. Appl. Chem.*, 48, 1-21.

Tinberg, C.E. & Lippard, S.J. (2011). Dioxygen activation in soluble methane monooxygenase. *Acc. Chem. Res.*, 44, 280-288.

Tsai, C.-W., Chen, H.M., Liu, R.-S., Asakura, K. & Chan, T.-S. (2011). Ni@NiO core-shell structure-modified nitrogen-doped $InTaO_4$ for solar-driven highly efficient CO_2 reduction to methanol. *J. Phys. Chem. C*, 115, 10180-10186.

Tshuva, E.Y. & Lippard, S.J. (2004). Synthetic models for non-heme carboxylate-bridged diiron metalloproteins: strategies and tactics. *Chem. rev.*, 104, 987-1012.

Usubharatana, P., McMartin, D., Veawab, A. & Tontiwachwuthikul, P. (2006). Photocatalytic process for CO_2 emission reduction from industrial flue gas. *Ind. Eng. Chem. Res.*, 45, 2558-2568.

Wang, X.-T., Zhong, S.-H. & Xiao, X.-F. (2005). Photo-catalysis of ethane and carbon dioxide to produce hydrocarbon oxygenates over ZnO-TiO_2/SiO_2 catalyst. *J. Mol. Catal. A: Chem.*, 229, 87-93.

Wang, Y. & Otsuka, K. (1994). Catalytic oxidation of methane to methanol in gas mixture of hydrogen and oxygen. *J. Chem. Soc., Chem. Commun.*, 2209-2210.

Wang, Y. & Otsuka, K. (1995). Catalytic oxidation of methane to methanol with H_2-O_2 gas mixture at atmospheric pressure. *J. Catal.*, 155, 256-267.

Wang, Z., Li, F., Yang, C., Zhang, W. & Wu, J. (2011). Photocatalytic reduction of CO_2 using Cu/S-TiO_2 prepared by eletroless plating method. *Adv. Mater. Res.*, 233-235, 589-595.

Woertink, J.S., Smeets, P.J., Groothaert, M.H., Vance, M.A. & Sels, B.F. (2009). A $[Cu_2O]^{2+}$ core in Cu-ZSM-5, the active site in the oxidation of methane to methanol. *Proc. Natl. Acad. Sci. USA*, 106, 18908-18913.

Wu, H., Huang, S. & Jiang, Z. (2004). Effects of modification of silica gel and ADH on enzyme activity for enzymatic conversion of CO_2 to methanol. *Catal. Today*, 98, 545-552.

Wu, J.C.S. (2009). Photocatalytic reduction of greenhouse gas CO_2 to fuel. *Catal. Surv. Asia*, 13, 30-40.

Yang, K., Batts, B.D., Wilson, M.A., Gorbaty, M.L., Maa, P.S., Long, M.A., He, S.X.J. & Attala, M.I. (1997). Reaction of Methane with Coal. *Fuel*, 76, 1105-1115.

Yarlagadda, P.S., Morton, L.A., Hunter, N.R. & Gesser, H.D. (1987). Direct catalytic conversion of methane to higher hydrocarbons. *Fuel Sci. Techol. Intl.*, 5, 169-183.

Yarlagadda, P.S., Morton, L.A., Hunter, N.R. & Gesser, H.D. (1988). Direct conversion of methane to methol in a flow reactor. *Ind. Eng. Chem. Res.*, 27, 252-256.

Yu, K.M.K., Curcic, I., Gabriel, J. & Tsang, S.C.E. (2008). Recent advances in CO_2 capture and utilization. *ChemSusChem*, 1, 893-899.

Zangeneh, F.T., Sahebdelfar, S. & Ravanchi, M.T. (2011). Conversion of carbon dioxide to valuable petrochemicals: an approach to clean development mechanism. *J. Nat. Gas Chem.*, 20, 219-231.

Zhang, H.-B., Liang, X.-L., Dong, X., Li, H.-Y. & Lin, G.-D. (2009). Multi-walled carbon nanotubes as a novel promoter of catalysts for CO/CO_2 hydrogenation to alcohols. *Catal. Surv. Asia*, 13, 41-58.

Zhang, H., Ying, P., Zhang, J., Liang, C., Feng, Z. & Li, C. (2004). SbO_x/SiO_2 catalysts for the selective oxidation of methane to formaldehyde using molecular oxygen as oxidant, In: *Studies in Surface Science and Catalysis*, X. Bao and Y. Xu, Eds, 147 (Natural Gas Conversion VII), pp. 547-552, Elsevier, Amsterdam.

Zhang, Q., He, D. & Zhu, Q. (2003). Recent progress in direct partial oxidation of methane to methanol. *J. Nat. Gas Chem.*, 12, 81-89.

Zhang, Q., He, D. & Zhu, Q. (2008). Direct partial oxidation of methane to methanol: Reaction zones and role of catalyst location *J. Nat. Gas Chem.*, 17, 24-28.

3

Separation of Carbon Dioxide from Flue Gas Using Adsorption on Porous Solids

Tirzhá L. P. Dantas[1], Alírio E. Rodrigues[2]
and Regina F. P. M. Moreira[3]
[1]*Federal University of Paraná, Department of Chemical Engineering*
[2]*University of Porto, Faculty of Engineering*
[3]*Federal University of de Santa Catarina, Department of Chemical and Food Engineering*
[1,3]*Brazil*
[2]*Portugal*

1. Introduction

The generation of CO_2 is inherent in the combustion of fossil fuels, and the efficient capture of CO_2 from industrial operations is regarded as an important strategy through which to achieve a significant reduction in atmospheric CO_2 levels. There are three basic CO_2 capture routes: (1) pre-combustion capture (via oxygen-blown gasification); (2) oxy-fuel combustion, i.e. removing nitrogen before combustion; and (3) post-combustion capture.

Adopting the post-combustion capture route avoids the potentially long time periods required to develop cost-effective coal-derived syngas separation technologies, hydrogen turbine technology, and fuel-cell technology, etc. It can also provide a means of CO_2 capture in the near-term for new and existing stationary fossil fuel-fired power plants.

Concentrations of CO_2 in power station flue gases range from around 4% by volume for natural gas combined cycle (NGCC) plants to 14% for pulverized fuel-fired plants. In the carbon capture and storage chain (capture, transport and storage) different requirements have been set for the composition of the gas stream mainly containing CO_2, which can vary within the range of 95-97% CO_2 with less than 4% N_2.

There are several post-combustion gas separation and capture technologies currently being investigated, namely: (a) absorption, (b) cryogenic separation, (c) membrane separation, (d) micro-algal bio-fixation, and (e) adsorption.

Current absorption technologies which propose the capture of CO_2 from flue gas are costly and energy intensive. Membrane technology is an attractive CO_2 capture option because of advantages such as energy-efficient passive operation, no use of hazardous chemicals, and tolerance to acid gases and oxygen. However, an important challenge associated with membrane technology is how to create the driving force efficiently, because the feed flue gas is at ambient pressure and contains a relatively low CO_2 content.

Solid sorbents are another promising capture technology. These sorbents can either react with the CO_2 or it can be adsorbed onto the surface. Chemical sorbents that react with the

CO_2 in the flue gas can be comprised of a support, usually of high surface area, with an immobilized amine or other reactant on the surface. Physical adsorbents can separate the CO_2 from the other flue gas constituents, but do not react with it. Instead, they use their cage-like structure to act as molecular sieves. These sorbents can be regenerated using a pressure swing or a temperature swing, although the costs associated with a pressure swing may be prohibitively high. Physisorbents such as activated carbon and zeolites will be safe for the local environment, and are generally relatively inexpensive to manufacture. Conventionally, activated carbon materials have been widely applied in industry for gas separation, and also have been investigated for CO_2 capture. Carbon dioxide emissions are frequently associated with large amounts of nitrogen gas, and thus an adsorbent selective to one of these compounds is required. These adsorbents should also be selective even at high temperatures, i.e., temperatures typical of carbon dioxide emission sources. Activated carbon is a suitable adsorbent and its CO_2 adsorption characteristics are dependent on its surface area and chemical surface characteristics. The surface chemistry of activated carbon is determined by the amount and type of heteroatom, for example oxygen, nitrogen, etc. Therefore, the adsorption capacity of activated carbon for carbon dioxide is a function of its pore structure and the properties of the surface chemistry.

Strategies like PSA (pressure swing adsorption), TSA (temperature swing adsorption) and ESA (electric swing adsorption) processes have been proposed and investigated for adsorption in a cyclic process (Cavenati *et al*., 2006; Grande & Rodrigues, 2008; Zhang et al., 2008). PSA is a cyclical process of adsorption/desorption that occurs through pressure changes and can be very suitable for carbon dioxide separation from exhaust gases due to its easy application in a large temperature range. The most studies presents the CO_2/N_2 separation using PSA process at room temperature, but it has been reported that is possible to obtain high purity CO_2 (~90%) at high temperature (Ko *et al*., 2005). Recently, Grande and Rodrigues (2008) reported that it is possible to recover around 89% of the CO_2 from a CO_2/N_2 mixture using honeycomb monoliths of activated carbon through ESA. However, the temperature of the CO_2/N_2 mixture in a typical exhaust gas can exceed 100°C and at such temperatures the recovery and purity of CO_2 can be significantly modified.

2. Experimental section

2.1 Selection and preparation of adsorbents

The commercial activated carbon used was Norit R2030 (Norit, Netherlands) which was selected due to its high adsorption capacity for CO_2. The nitrogen-enriched activated carbon, denoted as CPHCL, was prepared in a way similar way to that as previously reported (Gray et al., 2004), mixing 10 g of activated carbon with 500mL of 10^{-1}M 3-chloropropylamine hydrochloride solution. The mixture was kept under constant stirring, at ambient temperature for 5 hours. The CPHCL adsorbent was then left to dry for 12 hours in an oven at 105°C.

2.2 Characterization of the adsorbents

The content of carbon, hydrogen and nitrogen was determined by elemental analysis using CHNS EA1100 equipment (CE Instruments, Italy).

Thermogravimetric experiments were carried out with a TGA-50 thermogravimetric analyzer (Shimadzu, Japan) in the temperature range of 30°C – 900°C, at a heating rate of 10°C /min under nitrogen flow.

Fourier transform infrared (FTIR) spectroscopy was used to qualitatively identify the chemical functionality of activated carbon. To obtain the observable adsorption spectra, the solids were grounded to an average diameter of ca. 0.5 mm. The transmission spectra of the samples were recorded using KBr pellets containing 0.1% of carbon. The pellets were 12.7mm in diameter and ca. 1mm thick and were prepared in a manual hydraulic press set at 10 ton. The spectra were measured from 4000 to 400 cm^{-1} and recorded on a 16PC FTIR spectrometer (Perkin Elmer, USA).

X-ray photoelectron spectroscopy (XPS) measurements were carried out with a VG Microtech ESCA3000 MULTILAB spectrometer using monochromatic Al Ka X-rays. The pass energy of the analyzer was 58.7 eV for high-resolution scans. Relative elemental concentrations on the surface of the sorbents were calculated by measuring peak areas in the

high-resolution spectra and then converting to atomic concentrations using sensitivity factors provided by the instrument manufacturer.

2.3 Adsorption equilibrium isotherms

The equilibrium of CO_2 and N_2 adsorption on activated carbon was measured at different temperatures of 30°C, 50°C, 100°C, and 150°C using the static method in a Rubotherm magnetic suspension microbalance (Bochum, Germany) up to approximately 5 bar.

The equilibrium of CO_2 adsorption on CPHCL was measured at different temperatures of 30°C, 50°C, 100°C, and 150°C by the volumetric method, in an automatic sorptometer, Autosorb 1C (Quantachome, USA), up to approximately 1 bar.

Before the adsorption measurements, the solid samples were pre-treated for 12 hours at 150°C under vacuum. This temperature ensures that the amine is homogeneously tethered to the solid surface without devolatilize or decompose it.

2.4 Breakthrough curves: Fixed-bed CO_2 adsorption and CO_2/N_2 mixture adsorption

All the experimental breakthrough curves were obtained by passing the appropriate gas mixture through the packed column with the adsorbent: activated carbon or CPHCL. The solid adsorbent was pre-treated by passing helium at a flow rate of 30 $mL.min^{-1}$ n and at 150°C for 2 hours. These breakthrough curves were obtained 30°C, 50°C, 100°C, and 150°C.

The dynamic of adsorption of CO_2 in a fixed bed was studied using CO_2 diluted in helium (CO_2/He = 20%/80% v/v) in order to obtain the breakthrough curves. For the fixed-bed CO_2/N_2 separation dynamics, the breakthrough curves were obtained by passing the standard gas mixture – 20% CO_2/ 80%N_2 v/v.

The total gas flow rate was maintained at 30 $mL.min^{-1}$ which was controlled by a mass flow unit (Matheson, USA). The column was located inside a furnace with controlled temperature. A gas chromatographic model CG35 (CG Instrumentos Científicos, Brazil) equipped with a Porapak-N packed column (Cromacon, Brazil) and with a thermal

conductivity detector (TCD) was used to monitor the carbon dioxide or nitrogen concentration at the bed exit, using helium as the reference gas. The experimental system – column and furnace – was considered adiabatic because it was isolated with a layer of 0.10m of fiber glass and with a refractory material. The characteristics of the fixed bed and the column are presented in Table 1

	CO_2 and CO_2/N_2 adsorption in a fixed bed [a]	PSA experiments [b]
Bed length, L	0.171 m	0.83 m
Bed diameter, d_{int}	0.022 m	0.021 m
Bed weight, W	0.0352 kg	0.158 kg
Bed voidage fraction, ε	0.52	0.52
Column wall thickness, l	0.0015m	0.0041m
Column wall specific heat, $C_{p,w}$	440 J $kg^{-1}K^{-1}$	500 J $kg^{-1}K^{-1}$
Column wall conductivity, k_w		1.4 W $m^{-1}K^{-1}$
Wall density, ρ_w	7280 kg m^{-3}	8238 kg m^{-3}

Table 1. Characteristics of the fixed bed and the column used in the experiments [[a] Dantas *et al.*, 2010; [b] Dantas *et al.*, 2011].

2.5 Pressure swing adsorption

The PSA experimental setup consisted of one fixed-bed adsorption that simulated the operation of a unit with several fixed-beds, for which more details are given elsewhere (Da Silva & Rodrigues, 2001). The solid adsorbent used was the commercial activated carbon which was pre-treated by passing helium at a flow rate of 1.0 L.min^{-1} and at 150°**C** for 12 hours. The PSA experiments were performed premixed CO_2 to N_2 forming a mixture - 0.15 v/v. The flow rate of each gas was controlled by mass controllers (Teledyne Brown Engineering, USA).

A gas chromatographic model CP9001 (Chrompack 9001, Netherlands) equipped with a Poraplot Q capillary column (Varian, Netherlands), with a thermal conductivity detector (TCD), and with a flame ionization detector (FID) was used to monitor the carbon dioxide or nitrogen concentration at the bed exit, using helium as the reference gas. The experimental system – column and furnace – was considered adiabatic because it was isolated with a layer of 0.10m of fiber glass and with a refractory material. The temperature inside the column was continuously monitored using a K-thermocouple placed at 0.17 m and 0.43 m from the bottom of the column. The column was located inside a convective furnace and thus the system was considered to be non-adiabatic. The characteristics of the fixed bed and the column are presented in Table 1.

The cycles were of the Sharstrom-cycle type and divided by pressurization with pure nitrogen at a flow rate of 3.0 L.min^{-1}, feeding at constant pressure of 1.3 bar and total flow rate of 3.0 L.min^{-1}, countercurrent blowdown decreasing the pressure to 0.1bar and

countercurrent purge with pure nitrogen at constant pressure and a flow rate of 0.5 L.min^{-1}. All experiments were performed with 20 seconds of pressurization and 70 seconds of depressurization. However, different feed and purge times were used. Table 2 summarizes the PSA experimental conditions used in this study.

Run	T, °C	Feed Time, s	Purge time, s
1	50	100	70
2	50	120	50
3	100	120	50
4	100	200	50

Table 2. PSA experimental conditions.

2.5.1 Performance criteria of the PSA process

The definition of the performance criteria provides a common basis for comparing the different experiments. These are; Eq (1) to (3):

$$\text{Purity of } CO_2 = \frac{\int_{t_{blowdown}}^{t_{purge}} F_{CO_2}\,dt}{\sum_{i=1}^{n_{comp}} \int_{t_{blowdown}}^{t_{purge}} F_i\,dt} \tag{1}$$

$$\text{Purity of } N_2 = \frac{\int_{t_{blowdown}}^{t_{purge}} F_{N_2}\,dt}{\sum_{i=1}^{n_{comp}} \int_{t_{blowdown}}^{t_{purge}} F_i\,dt} \tag{2}$$

$$\text{Recovery of } CO_2 = \frac{\int_{t_{blowdown}}^{t_{purge}} F_{CO_2}\,dt}{\int_{0}^{t_{purge}} F_{CO_2}\,dt} \tag{3}$$

where F_i is the molar flow rate of component i – carbon dioxide or nitrogen.

3. Mathematical modelling

3.1 Model description

The model used to describe the fixed-bed experiments is derived from the mass, energy and momentum balances. The flow pattern is described with the axially dispersed plug flow model and the mass transfer rate is represented by a Linear Driving Force model – LDF. It was assumed that the gas phase behaves as an ideal gas and the radial concentration and

temperature gradients are negligible. The fixed-bed model is described by the equations given below.

The mass balance for each component is given by Eq. (4); (Ruthven, 1984):

$$\varepsilon \frac{\partial C_i}{\partial t} + \frac{\partial (uC_i)}{\partial z} = \varepsilon D_L \frac{\partial^2 C_i}{\partial z^2} - (1-\varepsilon)\rho_p \frac{\partial \overline{q}_i}{\partial t} \tag{4}$$

where ε is the bed void fraction, C_i is the gas phase concentration of component *i*, $\overline{q}_i$ is the average amount of component i adsorbed, D_L is the axial mass dispersion coefficient, u is the superficial velocity, and ρ_p is the particle density.

The rate of mass transfer to the particle for each component is given by Eq. (5):

$$\frac{\partial \overline{q_i}}{\partial t} = K_{L,i}(q_i^* - \overline{q}_i) \tag{5}$$

where K_L is the overall mass transfer coefficient of component i and q_i^* is the amount adsorbed at equilibrium, i.e., $q_i^* = f(C_i, T_g)$ given by the adsorption isotherm, and $\overline{q}_i$ is the average amount adsorbed.

The concentration C_i is given by Eq (6):

$$C_i = \frac{y_i P}{R T_g} \tag{6}$$

where y_i is the molar fraction of each gas in the gas phase, P is the total pressure, T_g is the gas temperature and R is the universal gas constant.

The Ergun equation considers the terms for the pressure drop and velocity changes; Eq. (7):

$$-\frac{\partial P}{\partial z} = 150 \frac{\mu_g (1-\varepsilon)^2}{\varepsilon^3 {d_p}^2} u + \ 1.75 \frac{(1-\varepsilon)}{\varepsilon^3 d_p} \rho_g u^2 \tag{7}$$

where μ_g is the gas viscosity, ρ_g is the gas density, and d_p is the particle diameter.

The energy balance is; Eq. (8):

$$\begin{aligned} &\varepsilon C C_{v,g} \frac{\partial T_g}{\partial t} + C C_{p,g} \frac{\partial (uT_g)}{\partial z} = \varepsilon \lambda_L \frac{\partial^2 T_g}{\partial z^2} - \\ &-(1-\varepsilon)\rho_p C_s \frac{\partial T_s}{\partial t} + \ (1-\varepsilon)\rho_p \sum_i \left(-\Delta H_i\right) \frac{\partial \overline{q_i}}{\partial t} - \frac{4 h_w}{d_{\text{int}}} (T_g - T_w) \end{aligned} \tag{8}$$

where $C_{v,g}$ is the molar specific heat at constant volume for the gas phase, $C_{p,g}$ is the molar specific heat at constant pressure for the gas phase, λ_L is the axial heat dispersion coefficient, C_s is the solid specific heat, $\left(-\Delta H_i\right)$ is the heat of adsorption for component i at zero coverage, h_w is coefficient for the internal convective heat transfer between the gas and the column wall, d_{int} is the bed diameter, and T_w is the wall temperature.

The solid phase energy balance is expressed by Eq. (9):

$$\rho_p C_s \frac{\partial T_s}{\partial t} = \frac{6h_f}{d_p}(T_g - T_s) + \rho_p \sum_i (-\Delta H_i) \frac{\partial \overline{q_i}}{\partial t} \tag{9}$$

where h_f is the coefficient for film heat transfer between the gas and the adsorbent.

For the column wall, the energy balance can be expressed by Eq. (10) to (12):

$$\rho_w C_{p,w} \frac{\partial T_w}{\partial t} = \alpha_w h_w (T_g - T_w) - \alpha_{wl} U (T_w - T_\infty) \tag{10}$$

with

$$\alpha_w = \frac{d_{\text{int}}}{l\left(d_{\text{int}} + l\right)} \tag{11}$$

and

$$\alpha_{wl} = \frac{d_{\text{int}}}{\left(d_{\text{int}} + l\right)\ln\left(\frac{d_{\text{int}} + l}{d_{\text{int}}}\right)} \tag{12}$$

where ρ_w is the column wall density, $C_{p,w}$ is the column wall specific heat, α_w is the ratio of the internal surface area to the volume of the column wall, α_{wl} is the ratio of the logarithmic mean surface area of the column shell to the volume of the column (Cavenati *et al.*, 2006), U is the external overall heat transfer coefficient, and T_∞ is the furnace external air temperature. For an adiabatic system, the last term of this equation must not been considered.

3.2 Boundary and initial conditions

The mathematical model was solved using the commercial software gPROMS (Process System Enterprise Limited, UK) which uses the method of orthogonal collocation on finite elements for resolution. The boundary and initial conditions were the show bellow.

3.2.1 For the breakthrough curves

The initial conditions for the adiabatic system are:

$$T_w = T_g = T_s = T_i \,;\; P = P_0 \;\text{ and }\; C_i(z,0) = \overline{q}_i(z,0) = 0 \tag{13}$$

The boundary conditions are described by the equations given below (Eq.14-18).

1. Bed inlet: (z=0)

$$\varepsilon D_L . \left.\frac{\partial C_i}{\partial z}\right|_{z^+} = -u\left(C_i\big|_{z^-} - C_i\big|_{z^+}\right) \tag{14}$$

$$\varepsilon\lambda_L.\left.\frac{\partial T_g}{\partial z}\right|_{z^+} = -uCC_{p,g}(T_g|_{z^-} - T_g|_{z^+}) \tag{15}$$

$$uC|_{z^-} = uC|_{z^+} \tag{16}$$

2. Bed outlet: (z=L)

$$\left.\frac{\partial C_i}{\partial z}\right|_{z^-} = 0 \tag{17}$$

$$\left.\frac{\partial T_g}{\partial z}\right|_{z^-} = 0 \tag{18}$$

3.2.2 For PSA experiments

The initial conditions, only considered for the unused bed, are:

$$T_w = T_g = T_s = T_0 \; ; P = P_0 \;\text{ and }\; C_i(z,0) = \overline{q}_i(z,0) = 0 \tag{19}$$

The initial condition of each new cycle corresponds to the final condition of the previous cycle. The boundary conditions for the mass and energy balances are described by the equations given below (Eq.20-27).

1. Bed inlet: pressurization step (z=0), feed step (z=0) and countercurrent purge step (z=L).

$$\varepsilon D_L \left.\frac{\partial C_i}{\partial z}\right|_{z^+} = -u(C_i|_{z^-} - C_i|_{z^+}) \tag{20}$$

$$\varepsilon\lambda_L.\left.\frac{\partial T_g}{\partial z}\right|_{z^+} = -uC_{p,g}(T_g|_{z^-} - T_g|_{z^+}) \tag{21}$$

2. Bed outlet: pressurization step (z=L), feed step (z=L), countercurrent purge step (z=0), and bed inlet and outlet for countercurrent blowdown step (z=L and z=0, respectively).

$$\left.\frac{\partial C_i}{\partial z}\right|_{z^-} = 0 \tag{22}$$

$$\left.\frac{\partial T_g}{\partial z}\right|_{z^-} = 0 \tag{23}$$

The boundary conditions for the momentum balance are the following:

1. Bed inlet: pressurization step (z=0).

$$P_{z^+} = P_{feed} \tag{24}$$

2. Bed outlet for pressurization step (z=L), and bed inlet for countercurrent blowdown step (z=L).

$$u\big|_{z^-} = 0 \tag{25}$$

3. Bed inlet: feed step (z=0), and countercurrent purge step (z=L).

$$u\big|_{z^-} = u\big|_{z^+} \tag{26}$$

4. Bed outlet: countercurrent blowdown step (z=0), and countercurrent purge step (z=0).

$$P\big|_{z^-} = P_{purge} \tag{27}$$

3.3 LDF global mass transfer coefficient and correlations used to estimation of model parameters

Table 3 summarizes the experimental conditions of temperatures and Reynolds numbers in Runs 1 - 4.

Table 4 shows the LDF global mass transfer coefficient, the axial dispersion coefficient, and the film mass transfer coefficient, should be evaluated using different correlations due different Reynolds numbers in Runs 1 -4 under adiabatic or non-adiabatic systems.

For the all experiments performed at adiabatic system – low Reynols number, the value of the LDF global mass transfer coefficient was estimated using the expression proposed by Farooq and Ruthven (1990) which considers all of the resistances to the mass transfer, i.e., intra- and extraparticle resistances; Eq. (28):

$$\frac{1}{K_L} = \frac{r_p q_o}{3k_f C_o} + \frac{r_p^2 q_o}{15\varepsilon_p D_e C_o} + \frac{r_c^2}{15D_c} \tag{28}$$

where r_p is the particle radius, k_f the external mass transfer coefficient, q_o the value of q at equilibrium with C_o (adsorbate concentration in the feed at feed temperature T_o and expressed in suitable units), ε_P the particle porosity, r_c the radius of activated carbon crystal and D_C is the micropore diffusivity. The micropore diffusivity values were those reported by Cavenati and coworkers (2006) since the micropore distribution of the adsorbents are similar to those of carbon molecular sieves (Cavenati *et al.*, 2006; Vinu & Hartmann, 2005).

For the all experiments performed at non-adiabatic system – high Reynols number, the value of the LDF global mass transfer coefficient was estimated that intraparticke resistance is only controlled by molecular diffusion.

All others correlations used to evaluate the mass and heat transport parameters are summarized in Table 4. The gas phase viscosity was estimated using Wilkes's equation (Bird *et al*., 2007). The axial mass dispersion coefficient (D_L), for the adiabatic system, was evaluated by Leitão & Rodrigues (1995); for the non-adiabatic system, according to Wakao and coworkers (1978). The film mass transfer coefficient (k_f), for the adiabatic system, was evaluated by Seguin et al. (1995); for the non-adiabatic system, according to Wakao and Funazkri (1978). The axial heat dispersion coefficient (λ_L) and the film heat transfer coefficient (h_f) were evaluated by

Wakao and coworkers (1978); the convective heat transfer coefficient between the gas phase and the column wall (h_w) was evaluated according to De Wash & Froment (1972).

		Run	T, °C	Re
Adiabatic System	CO_2 /He	1	28	0.12
		2	50	0.10
		3	100	0.08
		4	150	0.06
Adiabatic System	CO_2 /N_2	1	28	0.36
		2	50	0.32
		3	100	0.25
		4	150	0.20
Non-adiabatic System	PSA	1	50	41.64
		2	50	41.64
		3	100	32.31
		4	100	32.31

Table 3. Experimental conditions of temperature and Reynolds number.

Coefficient	Adiabatic system	Non-adiabatic system
Axial Mass Dispersion	$Pe = 0.508\,\mathrm{Re}^{0.020}\,\frac{L}{d_p}$	$\varepsilon\frac{D_L}{D_m} = 20 + 0.5Sc\,\mathrm{Re}$
Film mass transfer	$Sh = 1.09\,\mathrm{Re}^{0.27}\,Sc^{1/3}$	$Sh = 2 + 1.1\,\mathrm{Re}^{0.27}\,Sc^{1/3}$
Axial Heat Dispersion	$\frac{\lambda_L}{k_g} = 10 + 0.5\,\mathrm{Pr}\,\mathrm{Re}$	
Film heat transfer	$Nu = 2.0 + 1.1\,\mathrm{Re}^{0.6}\,\mathrm{Pr}^{1/3}$	
Internal convective heat transfer	$\frac{h_w d_{\mathrm{int}}}{k_g} = 12.5 + 0.048\,\mathrm{Re}$	
Global heat transfer	$U = \frac{1}{\frac{1}{h_w} + \frac{d_{\mathrm{int}}}{k_w}\ln\left(\frac{d_{ext}}{d_{\mathrm{int}}}\right) + \frac{d_{\mathrm{int}}}{d_{ext}}\frac{1}{h_{ext}}}$	
External convective heat transfer	$\frac{h_{ext}L}{k_{ext}} = 0.68 + \frac{0.67\,Ra^{1/4}}{\left[1 + \left(\frac{0.492}{\mathrm{Pr}}\right)^{9/12}\right]^{4/9}}$	
$Pe = \frac{uL}{D_L}$; $\mathrm{Re} = \frac{\rho_g u d_p}{\mu_g}$; $Sc = \frac{\mu_g}{\rho_g D_m}$; $Sh = \frac{k_f d_p}{D_m}$; $\mathrm{Pr} = \frac{C_{p,g}\mu_g}{k_g}$; $Nu = \frac{h_f d_p}{k_g}$; $Ra = g\beta\frac{(T_w - T_\infty)}{\nu\alpha}L^3$		

Table 4. Correlations used for estimation of mass and heat parameters [Dantas *et al.*, 2011].

The effective diffusivities were calculated by Bosanquet equation and the molecular diffusivities were calculated with the Chapman-Enskong equation (Bird *et al*., 2007). A tortuosity of 2.2 and 1.8 was admitted to the activated carbon particle and CPHCL, respectively.

4. Results and discussion

4.1 Characterization of adsorbents

Textural properties of activated carbon and CPHCL were previously described (Dantas *et al*., 2010). The adsorbents are microporous and the BET surface areas are shown in Table 5.

Modifications with nitrogen-containing species may also result in changes in the porous structure (Arenilas *et al*., 2005). The CPHCL had a lower BET area when compared to the commercial activated carbon. The micropores volume of the CPHCL decreases considerably compared with the commercial activated carbon, suggesting that the nitrogen incorporation partially blocks the access of N_2 to the small pores.

The chemical characteristics of the adsorbents are given in Table 6. As expected, the adsorbent CPHCL has the greater nitrogen content and an N/C atomic ratio which is twice that of the commercial activated carbon.

The FTIR spectra of commercial activated carbon and CPHCL are shown in Figure 1. All spectra show the contribution from ambient water (at about 3600 cm^{-1}) and carbon dioxide (doublet at 2360 cm^{-1} and sharp spike at 667 cm^{-1}) present in the optical bench. The band of O-H stretching vibrations (3600 - 3100 cm^{-1}) was due to surface hydroxyl groups and chemisorbed water. The band at 2844 and 2925 cm^{-1} is frequently ascribed to the C–H stretching. The asymmetry of the band at 3600 – 3100 cm^{-1} indicates the presence of strong hydrogen bonds.

	Commercial activated carbon	**CPHCL**
S_{BET}, m^2/g	1053.0	664.6
S_{micro}, m^2/g	1343.0	753.0
V_{micro}, cm^3/g	0.0972	0.0388
Mean pore radius r_o , nm	1.23	1.54
Particle porosity ε_P	0.47	0.37
N_2 Micropore Capacity, kg/kg	300	155
N_2 Total Capacity, kg/kg	370	260
Particle density $\rho_p .10^3$, kg/m^3	1.14	
Particle diameter $d_p 10^3$, m	3.8	

Table 5. Textural properties of the adsorbents studied [Dantas *et al*., 2010].

	Activated carbon	CPHCL
C	86.2	70.2
H	1.3	2.0
N	0.9	1.4
N/C. 10^2	1	2

Table 6. Chemical characterization of the adsorbents studied. [Dantas *et al*., 2010].

It has been suggested that primary amine can react with the activated carbon surface, forming surface complexes with the presence of NH_2 surface groups (Gray *et al*., 2004). Bands were presence at 3365 and 1607 cm^{-1}, ascribed to asymmetric stretching (νNH_2) and NH_2 deformation, respectively, and at 3303 cm^{-1}. However, the CPHCL spectrum shows that these bands may be overlapped by the OH stretching band (3600-3100 cm^{-1}) and by the aromatic ring bands and double bond (C=C) vibrations (1650-1500 cm^{-1}) (Fanning & Vannice, 1993). The same pattern is observed for CPHCL after CO_2 adsorption at 28°**C** and 150°**C**, indicating that there is no difference in the adsorption behavior.

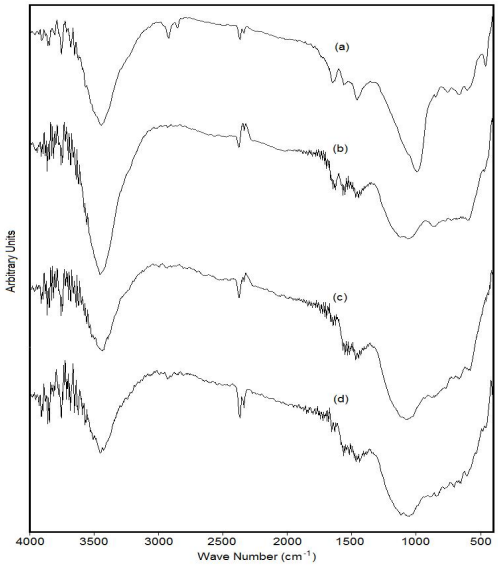

Fig. 1. FTIR spectra of (a) commercial activated carbon; (b) CPHCL; (c) CPHCL after pre-treatment and CO_2 adsorption at 28°**C** and (d) CPHCL after pre-treatment and CO_2 adsorption at 150°**C** [Dantas *et al*., 2010].

4.2 Adsorption equilibrium isotherms

The adsorption equilibrium of CO_2 and N_2 adsorption on activated carbon was previously (Dantas *et al*., 2010) described using the Toth model (Toth, 1971); Eq. (29):

$$q = \frac{q_m K_{eq} P}{\left[1 + (KP)^n\right]^{1/n}} \tag{29}$$

where q_m is the maximum adsorbed concentration, i.e., the monolayer capacity; K_{eq} is the equilibrium adsorption constant and n is the heterogeneity parameter.

The temperature dependence of the equilibrium was described according to the Van't Hoff equation; Eq. (30):

$$K_{eq} = K_o . e^{\left(\frac{-\Delta H_i}{R.T}\right)} \tag{30}$$

where K_o is the adsorption constant at infinite dilution.

Table 7 gives the parameters used for Toth model isotherms of each gas. It should be noted that activated carbon has a high CO_2 adsorption capacity in comparison with the N_2 adsorption capacity. It is worth mentioning that the commercial activated carbon used in this studied has a high CO_2 adsorption capacity in comparison with other adsorbents reported in literature (Grande & Rodrigues, 2008; Glover *et al*., 2008).

The CO_2 adsorption equilibrium isotherms for CPHCL, at low partial pressure, were described according a linear isotherm (Dantas *et al*., 2010); (Eq.31):

$$q = K_p P \tag{31}$$

where K_p is the Henry's Law constant for the adsorption equilibrium which the temperature dependence was also described according to the Van't Hoff equation.

Gas	q_m, 10^{-3}mol/g	*n*	K_o,bar^{-1}	$-\Delta H_i$, kJ/mol
CO_2	*10.05*	*0.68*	*7.62 × 10^{-5}*	*21.84*
N_2	*9.74*	*0.52*	*6.91 × 10^{-5}*	*16.31*

Table 7. Parameters used for fitting of the Toth model for carbon dioxide and nitrogen adsorption o activated carbon.

Table 8 gives the Henry's Law constants for the adsorption equilibrium on CPHCL, at the different temperatures studied, the pre-exponencial factor and heat of adsorption. Table 8 also shows the Henry's constants for the adsorption equilibrium on commercial activated carbon that was fitted at low pressure.

It should be noted, however, that the commercial activated carbon has higher Henry's Law constant indicating that this solid has a greater carbon dioxide adsorption capacity.

The nature of the N functionality is very important because it can affect the basicity of the solid surface (Vlasov & Os'kina, 2002); comparing a primary amine with a secondary amine of the same carbon number, the basic character increases due to the increase in the inductive effect caused by the alkyl groups.

Some authors have reported that although there is a reduction in the BET superficial area which is caused for the partial blockage of the lesser pores, as also observed in this paper, the enrichment of the carbonaceous materials with nitrogen tends to increase the adsorption capacity for CO_2 (Arenillas *et al*., 2005). However, there is no consensus about this issue because sorbents with the high amounts of nitrogen do not have the high CO_2 adsorption capacity reported in recent publications by Arenillas and coworkers (2005) and Pevida *et al*. (2008). In the present study, we show a decrease in the CO_2 adsorption capacity of CPHCL in comparison with non-functionalized activated carbon. The decrease in the CO_2 adsorption capacity is not related to the destruction of basic sites in the CPHCL, as shown in the FTIR studies (Figure 2). In fact, Drage *et al*. (2007) have reported that only an activation temperature higher than 600**°C** can destroy basic sites in the adsorbents.

	Activated carbon	**CPHCL**	
T, °C	**K_p, moles/kg. bar^{-1}**	**K_p, moles/kg. bar^{-1}**	**$-\Delta H_i$, kJ/mol**
28-25	2.89	2.16	20.25
50	1.86	1.55	
100	0.62	0.32	
150	0.29	0.11	

Table 8. Henry's Law constants for the adsorption equilibrium on commercial activated carbon and CPHCL at different temperatures (Dantas *et al*., 2010).

4.3 Fixed-Bed CO_2 adsorption: experimental data and modeling

As previously mentioned, a set of experiments was performed changing the temperature of the carbon dioxide to determine the breakthrough curves of carbon dioxide adsorption on activated carbon and CPHCL.

The Peclet number and the LDF global mass transfer coefficient for the adsorption of carbon dioxide on activated carbon and CPHCL are shown in Table 9.

Run	**T, °C**	*Pe*	**Activated Carbon** K_L **, s^{-1}**	**CPHCL** K_L **, s^{-1}**
1	*28*	21.91	0.0027	0.0041
2	*50*	21.85	0.0043	0.0063
3	*100*	21.75	0.0125	0.0259
4	*150*	21.65	0.0259	0.0719

Table 9. Experimental Conditions and LDF global mass transfer coefficient for CO_2 adsorption on the commercial activated carbon and CPHCL (Adapted from Dantas *et al*., 2010).

Figures 2(a) e 2(b) shows a comparison between the experimental and theoretical curves obtained for the CO_2 adsorption on commercial activated carbon and CPHCL, respectively.

It is observed that, in the case of the mass balance, the model reproduces the experimental data for the different feed concentration and temperatures reasonably well.

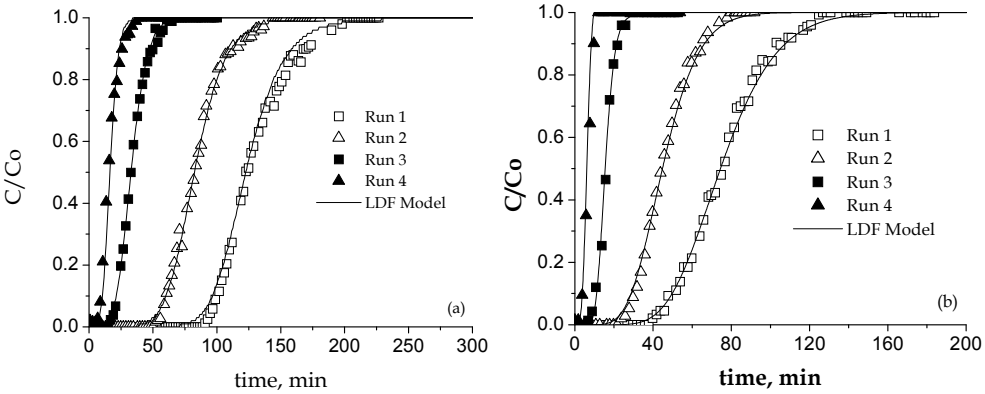

Fig. 2. Breakthrough curves for the CO_2 adsorption (a) on activated carbon and (b) on CPHCL. Symbols: experimental data; Lines: LDF model (Dantas *et al.*, 2010).

The global mass transfer coefficient for CO_2 adsorption on CPHCL in the fixed bed is higher than that for the adsorption on activated carbon (Table 9) which was to be expected because the CPHCL is an adsorbent with less micropores and smaller CO_2 adsorption capacity than the commercial activated carbon. This makes the importance of the external to the internal mass transfer resistance (Eq. (28)) greater in the case of CPHCL than commercial activated carbon.

Figures 3(a) e 3(b) shows the gas simulated temperature profile, at the end of the bed, for the carbon dioxide adsorption at 28°**C** on activated carbon and CPHCL, respectively**.**

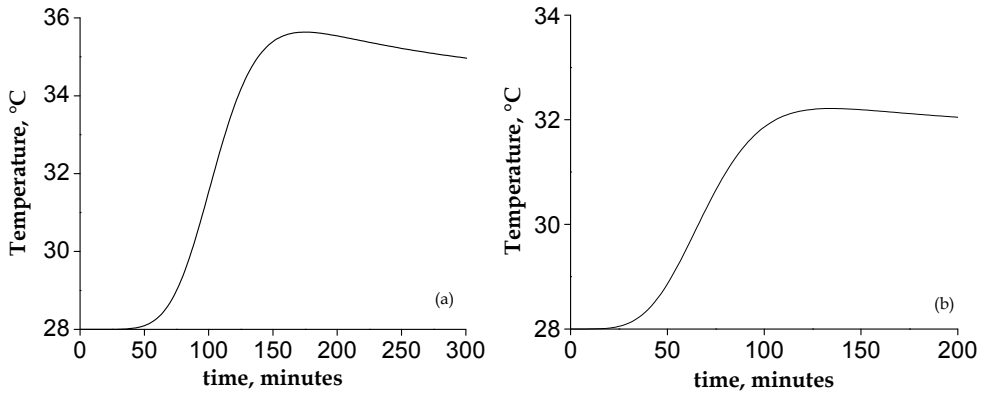

Fig. 3. Gas simulated temperature profile, at the end of the bed, for the carbon dioxide adsorption at 28°C (a) on activated carbon and (b) on CPHCL.

The temperature peaks is about 8°C and 4°C, for activated carbon and CPHCL, respectively. Although as the commercial activated carbon and the CPHCL have about the same heat of

adsorption, but distinct adsorptive capacities, it is also possible to conclude that a higher adsorption capacity leads to a higher temperature peak, since the adsorption is an exothermic phenomenon.

4.4 Fixed-Bed CO_2/N_2 mixture adsorption: Experimental data and modeling

The basic information required to describe the fixed-bed dynamics of the adsorption of carbon dioxide-nitrogen mixtures on activated carbon is the adsorption equilibrium behavior of the single components. The adsorbed equilibrium concentration of carbon dioxide and nitrogen on activated carbon was estimated as a function of the feed concentration from a mass balance in the fixed bed. For each experimental breakthrough curve, the adsorbed concentration is given by:

$$q_i = \frac{1}{\rho_p}\left[\frac{C_{Fi}Q_F t_{st}}{(V-\varepsilon V)} - \frac{C_{Fi}\varepsilon}{(1-\varepsilon)}\right] \tag{32}$$

where *CFi* is the feed concentration of component i, *V* is the bed volume, *QF* is the feed volumetric flow rate and *tst* is the stoichiometric time (Ruthven, 1984).

The resulting adsorbed concentrations are given in Table 10. It can be observed that the activated carbon adsorption capacity for CO_2 and N_2 in the CO_2/N_2 mixtures is the same as that predicted by the single component Toth isotherm using the previously reported adjusted. This is to be expected if the active sites for N_2 and CO_2 are independent, since the amount of CO_2 and/or N_2 adsorbed on the solid at each partial pressure from a CO_2/N_2 mixture is the same as that measured for the pure gases at the same partial pressure, as shown in Table 10. This assumption is in agreement with Siriwardane and coworkers (2001) who observed the same behavior for the adsorption of CO_2/N_2 mixtures on 13X zeolite, although Delgado and coworkers (2006) observed that the nitrogen adsorption can be neglected when it is mixed with carbon dioxide. As the presence of nitrogen in the mixture does not interfere at the CO_2 adsorption on activated carbon, thus the pure component equilibrium isotherms predict very well the equilibrium of each component in the CO_2/N_2 mixture.

Run	T, °C	Adsorbate	q, mol kg$^{-1(a)}$	q, mol kg$^{-1(b)}$
1	***28***	N_2	0.272	0.294
		CO_2	0.734	0.743
2	***50***	N_2	0.178	0.173
		CO_2	0.450	0.466
3	***100***	N_2	0.097	0.096
		CO_2	0.163	0.170
4	***150***	N_2	0.054	0.059
		CO_2	0.072	0.071

Table 10. Experimental conditions and adsorbed concentrations predicted by the Toth model for pure components and from the mass balance of breakthrough experiments on activated carbon. (a) Values calculated from the experimental data; (b) Values calculated using Toth model for single component adsorption.

As previously mentioned, a set of experiments was performed changing the temperature of the carbon dioxide/nitrogen mixture to determine the breakthrough curves of carbon dioxide adsorption and nitrogen adsorption on activated carbon.The axial mass dispersion coefficient and the LDF global mass transfer coefficient for CO_2 and N_2 adsorption on activated carbon are shown in Table 11.

Run	T, °C	D_L , cm² s⁻¹	CO_2	N_2
			K_L , s⁻¹	
1	*28*	0.10	0.0025	0.004
2	*50*	0.10	0.0042	0.011
3	*100*	0.10	0.0138	0.042
4	*150*	0.10	0.0323	0.128

Table 11. Axial mass dispersion coefficient and the LDF global mass transfer coefficient for CO_2 and N_2 adsorption on activated carbon (Adapted from Dantas *et al*., 2011).

Figure 4 shows a comparison between the experimental and theoretical curves obtained for the N_2 and CO_2 adsorption on activated carbon. The model describes quite well the roll-up effect that is caused by the displacement of N_2 by CO_2 (Dabrowski, 1999). The roll-up is a common phenomenon happening in multicomponent adsorption processes when the concentration of one component at outlet of the adsorber exceed it inlet level (Li et al., 2011). It can be observed that, when the temperature is increased, the carbon dioxide and nitrogen breakthrough times are shorter due the exothermic character of adsorption.

The nitrogen breakthrough times are very similar at 28°**C** and 150°**C**. This finding can be explained by the decrease in the amount of nitrogen adsorbed on activated carbon which can be compensated by its faster diffusion at high temperature as observed by Cavenati and coworkers (2006) for nitrogen adsorption on CMS 3K (as mentioned above, this molecular sieve has a similar pore size distribution to that used for the activated carbon in this study). The model reproduces very well the breakthrough curves for the different feed concentrations, including the experimental breakthrough curves obtained for nitrogen. Also, from the breakthrough curves we can note that the adsorbent is very selective towards carbon dioxide.

4.5 PSA: Experimental data and modeling

Figure 5 shows the pressure change as a function of the process time for the experimental conditions of Run 1 (see Table 2). A function was not found to describe with more accuracy the pressure drop during the blowdown step and therefore the model cannot predict very well this process variable.

Figure 6 shows the experimental and simulated changes for CO_2 molar flow rate during the PSA separation. The solid line represents the first cycle and the dashed line the steady-state cycle (CCS).

Figure 7 shows the experimental and simulated N_2 molar flow rate as a function of process time, under the experimental conditions of run 2. The assumption that nitrogen adsorption does not affect the CO_2 adsorption is well represented by the simulation, since the flow rate of nitrogen is not modified during each step.

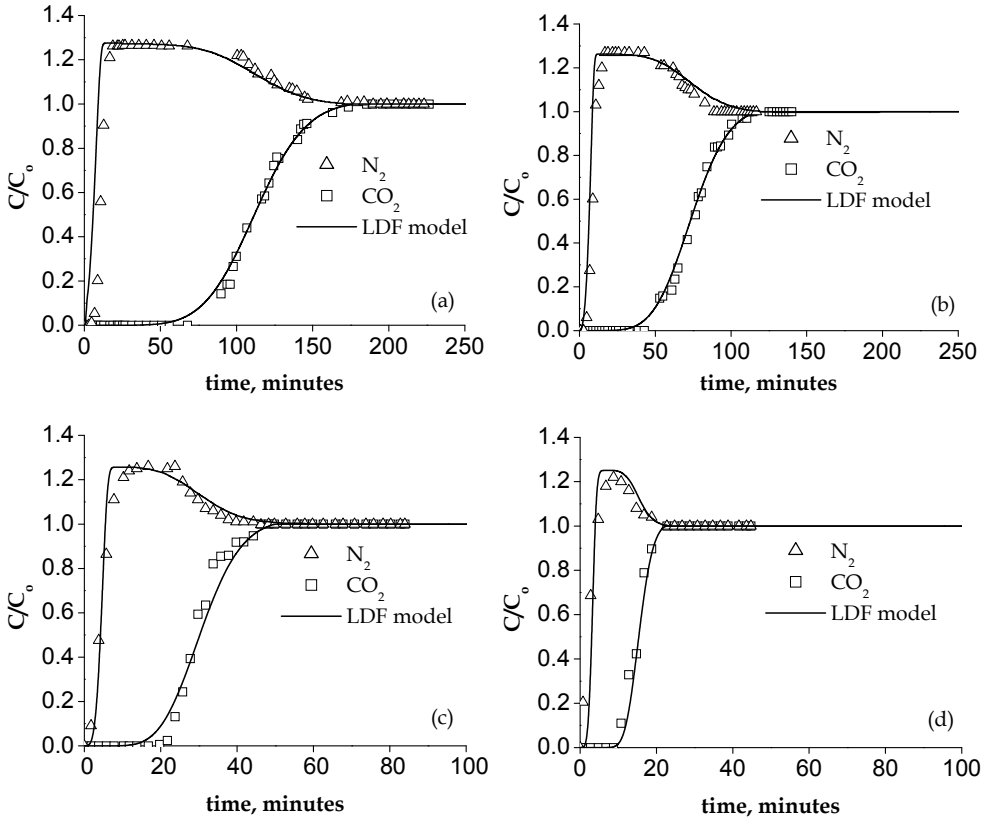

Fig. 4. Breakthrough curves for the N_2 and CO_2 adsorption on commercial activated carbon. Symbols: experimental data; Δ N_2 and □ CO_2. Lines: LDF model. Conditions: (a) run 1; (b) run 2; (c) run 3; and (d) run 4.

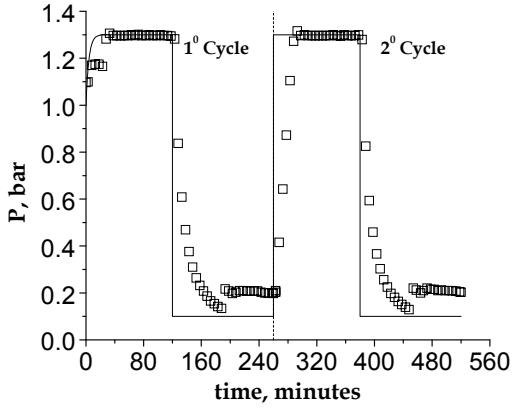

Fig. 5. Pressure change as a function of process time. Experimental conditions: run 1.

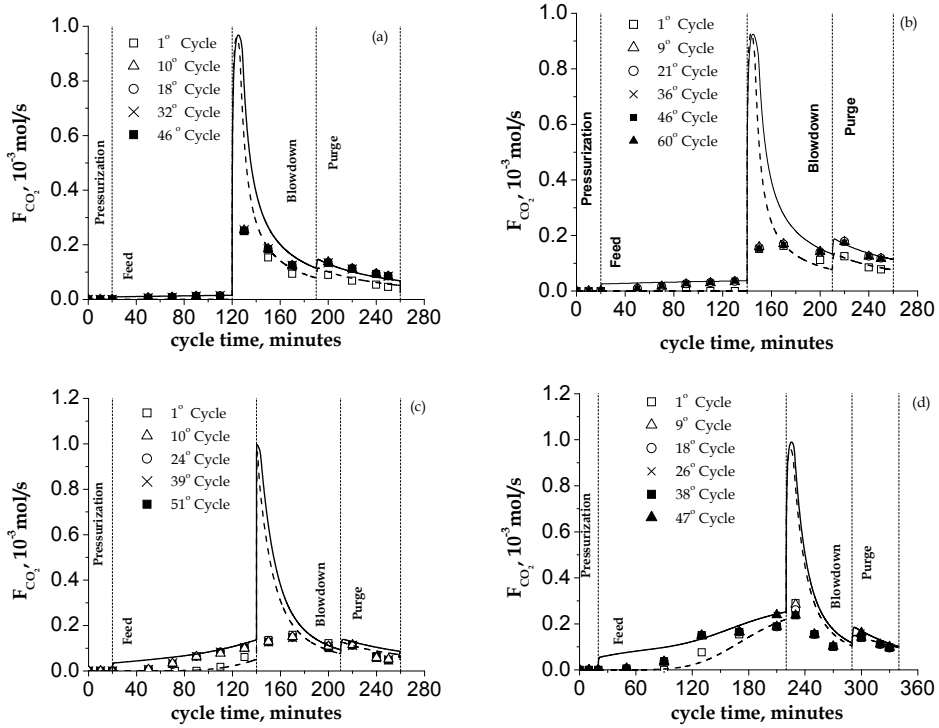

Fig. 6. Carbon dioxide molar flow rate as a function of cycle time. Experimental conditions: (a) run 1; (b) run 2; (c) run 3; and (d) run 4. Solid line: first cycle simulation. Dashed line: CCS simulation.

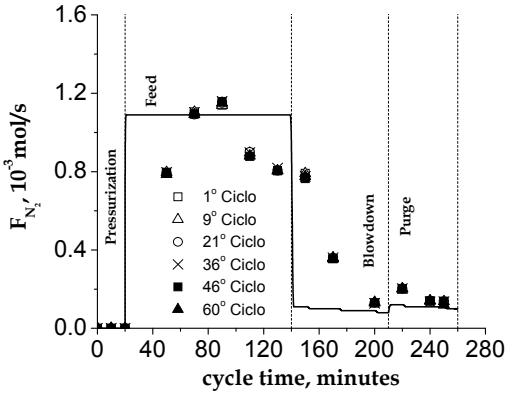

Fig. 7. Nitrogen molar flow rate as a function of cycle time. Experimental conditions: run 2. Solid line: first cycle simulation. Dashed line: CCS simulation.

Figures 8(a) and 8(b) shows the experimental and simulated temperature profile inside the column, at 0.17 m and 0.43 m from the bottom of the column, under the experimental

conditions of run 3. The temperature peak is high due to the exothermic adsorption of CO_2 on activated carbon in a high amount. Therefore heat effects cannot be neglected during adsorption, especially when there is a strong adsorbent-adsorbate interaction.

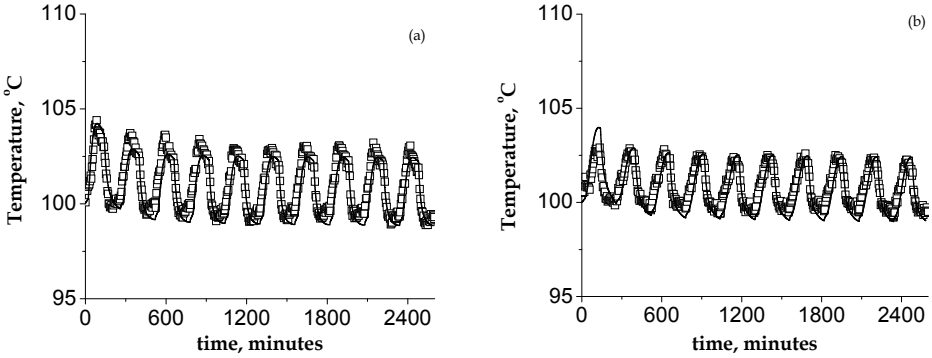

Fig. 8. Temperature profile of the gas phase: (a) at 0.17 m and (b) at 0.43 m from the bottom of the column. Experimental conditions: run 3.

Table 12 shows the performance of the PSA process: carbon dioxide recovery, nitrogen recovery, and carbon dioxide purity obtained for all experimental conditions studied. It is possible note that there is an increase in the carbon dioxide purity with increasing feed time (runs 1 and 2). This indicates that the separation is strongly controlled by the equilibrium. It can be also noted that there is an increase in the carbon dioxide purity with increasing temperature and this is due to the high selectivity of activated carbon. We observed that when the temperature of the CO_2/N_2 mixture was 100°C, a superior CO_2 purity is obtained due to the high selective toward CO_2. This is a good result since it indicates that the cooling of the exhaustion gas before CO_2 separation is not necessary.

Run	Feed time, s	CO_2 purity, %	N_2 purity, %	CO_2 recovery, %
1	100	25.7	87.1	93.1
2	120	31.3	87.5	85.4
3	120	32.3	87.1	73.7
4	200	49.7	78.9	66.8

Table 12. PSA Performance.

As proposed by Grande and Rodrigues (2008) for CO_2 adsorption, adsorbents with a greater adsorption capacity and higher heat of adsorption than the activated carbon honeycomb monolith should be used to achieve a product purity of greater than 16%. Although the CO_2 purity is lower than that is required to transport, the PSA cycle could be optimized in order to increase the CO_2 purity and recovery (Ko *et al.*, 2005). Transport considerations limit the CO_2 purity > 95.5% to ensure a reasonable input of CO_2 compression power (Vinay & Handal, 2010).

5. Conclusion

There are many factors that influence CO_2 capture, some of them are physical and some chemical. Textural properties are important for any adsorption processes but, in the case of CO_2 capture, the surface chemistry is a particularly important factor. The enrichment of activated carbon with nitrogen using amine 3-chloropropylamine hydrochloride blocked some pores of the activated carbon. The increase in the surface basicity was not sufficient to counteract the decrease in the BET superficial area since a reduction in the CO_2 adsorption was observed.

Carbon dioxide adsorption on commercial activated carbon and on a nitrogen-enriched activated carbon, named CPHCL, packed in a fixed bed was studied. The adsorption equilibrium data for carbon dioxide on the commercial activated carbon were fitted well using the Toth model equation, whereas for carbon dioxide adsorption on the CPHCL a linear isotherm was considered. A model using the LDF approximation for the mass transfer, taking into account the energy balance, described the breakthrough curves of carbon dioxide adequately. The LDF global mass transfer coefficient for the adsorption of CO_2 on activated carbon is smaller than that for the CPHCL. Since part of the micropores of the activated carbon are blocked by the incorporation of the amine, probably only the largest pores would be filled by the CO_2, causing a decrease on the capacity of the adsorption and an increase on the adsorption rate.

The fixed-bed adsorption of CO_2/N_2 mixtures on activated carbon was also studied. The adsorption dynamics was investigated at several temperatures and considering the effects caused by N_2 adsorption. It was demonstrated that the solid sorbent adsorbed carbon dioxide and nitrogen to its total capacity, leading to the conclusion that the equilibrium of CO_2 and N_2 adsorption from CO_2/N_2 mixtures could be very well described through the adsorption equilibrium behavior of the single components. The activated carbon used in this study has high selectivity for CO_2 and is suitable for CO_2/N_2 separation processes. The model proposed herein can be used to design a PSA cycle to separate the components of CO_2/N_2 mixtures, where the pressure drop and thermal effects are very important.

The carbon dioxide–nitrogen separation applying PSA process showed that the increase in the inlet temperature of the mixture CO_2/N_2 increases the CO_2 purity due to the great difference between the adsorption capacities of N_2 and CO_2.

6. Acknowledgments

The authors are grateful to CAPES – Comissão de Aperfeiçoamento de Pessoal de Nível Superior (Brazil) – and to CAPES/GRICES for the International Cooperation Project (Brazil/Portugal)

7. References

Arenillas, A.; Rubiera, F; Parra, J.B.; Ania, C.O. & Pis, J.J. (2005). Surface modification of low costs carbons for their application in the environmental protection. *Applied Surface Science*, 252, Vol.252, No.3, pp. 619-624, ISSN 0169-4332.

Bird, R.B.; Stewart, W.E. & Lightfoot, E.H. (2007). Transport Phenomena. Wiley, New York, 2nd Edition, ISBN 0471410772.

Brunauer, S.; Emmett, P.H. & Teller, E. (1938). Adsorption of Gases in Multimolecular Layers. *Journal of American Chemical Society*, Vol. 60, No.2, pp. 309-319, ISSN 00027863.

Cavenati, S.; Grande, C.A. & Rodrigues, A.E. (2006). Separation of $CH_4/CO_2/N_2$ mixtures by layered pressure swing adsorption for upgrade of natural gas. *Chemical Engineering Science,* Vol.61, No.12, pp. 3893-3906, ISSN 0009-2509.

Dabrowski, A. Adsorption and its applications in industry and environmental protection, Vol I. Applications in industry (1999). Elsevier Science, ISBN 044450165-7, Netherlands.

Dantas, T.L.P.; Amorim, S.M.; Luna, F.M.T.; Silva Junior, I. J.; Azevedo, D.; Rodrigues, A. E.; Moreira, R.F.P.M. (2010). Adsorption of carbon dioxide onto activated carbon and nitrogen-enriched activated carbon: Surface Changes, Equilibrium, and Modeling of Fixed-Bed Adsorption. *Separation Science and Technology*, Vol.45, No.1, pp.73 - 84, ISSN 1383-5866.

Dantas, T.L.P.; Amorim, S.M.; Luna, F.M.T.; Silva Junior, I. J.; Azevedo, D.; Rodrigues, A. E.; Moreira, R.F.P.M. (2011). Carbon dioxide-nitrogen separation through adsorption on activated carbon in a fixed bed. *Chemical Engineering Journal*, Vol. 172, No.2-3, pp.698 - 704, 2010, ISSN 1385-8947.

Da Silva, F. A. & Rodrigues, A.E. (2001). Propylene/Propane separation by vacuum swing adsorption using 13X zeolite. *AIChE Journal*,Vol.47, No.2, pp. 341-357, ISSN 1547-5905.

De Boer, J. H.; Lippens, B. C.; Lippens, B.G.; Broekhoff, J.C.P.; Van den Heuvel, A. & Osinga, Th. J. (1966). The T-Curve of Multimolecular N_2-adsorption. *Journal of Colloid and Interface Science*, Vol.21, No.4, pp. 405-414, ISSN 0021-9797.

Delgado, J.A.; Uguina, M.A.; Gómez, J.M; Sotelo, J.L. & Ruíz, B. (2006). Fixed-bed adsorption of carbon dioxide-helium, nitrogen-helium and carbon dioxide-nitrogen mixtures onto silicalite pellets. *Separation and Purification Technology*, Vol.49,No.1, pp. 91-100, ISSN 1383-5866.

De Wash, A.P. & Froment, G. (1972). Heat transfer in packed beds. *Chemical Engineering Science*, Vol.27, No.3, pp. 567-576, ISSN 0009-2509.

Drage, T.C.; Arenillas, A.; Smith, K.M.; Pevida, C.; Piipo, S. & Snape, C.E. Preparation of carbon dioxide adsorbents from the chemical activation of urea-formaldehyde and melamine-formaldehyde resins. *Fuel*, Vol.86, No.1-2, pp.22-31, ISSN 0016-2361.

Dubinin, M.M. & Radushkevich. L.V. (1947). *Proc. Acad. Sci. Phys. Chem. Sec. USSR*, Vol.55, pp. 331.

Fanning, P.E. & Vannice, M.A. (1993). A drift study of the formation of surface groups on carbon by oxidation. *Carbon*, Vol.31, No.5, pp. 721-730, ISSN 0008-6223.

Farooq, S. & Ruthven, D.M. (1990). Heat Effects in Adsorption Column Dynamics. 2. Experimental Validation of the One-dimensional Model. *Industrial & Engineering Chemical Research*, Vol. 29,No.6, pp. 1084-1090, ISSN 0888-5885.

Grande, C.A. & Rodrigues, A. E.(2008). Electric Swing Adsorption for CO_2 removal from flue gases. *International Journal of Greenhouse Gas Control*, Vol.2, No.2, pp. 194-202, ISSN 17505836.

Grant Glover, T.; Dunne, K I.; Davis, R.J. & LeVan, M.D. (2008). Carbon-silica composite adsorbent: Characterization and adsorption of light gases. *Microporous Mesoporous Materials*, Vol.11, No.1-3, pp. 1-11, ISSN 1387-1811.

Gray, M.L.; Soong, Y.; Champagne, K.J.; Baltrus, J.; Stevens Jr, R.W.; Toochinda, P. & Chuang, S.S.C. (2004). CO_2 capture by amine-enriched fly ash carbon sorbents. *Separation and Purification Technology*, Vol. 35, No.1, pp. 31-36, ISSN 13835866.

Ko, D.; Siriwardane, R. & Biegler, L.T. (2005). Optimization of pressure swing adsorption and fractionated vaccum swing adsorption pressure for CO_2 capture. *Industrial & Engineering Chemistry Research*, Vol.44, No. 21, pp. 8084-8094, ISSN 0888-5885.

Leitão, A. & Rodrigues, A.E. (1995). The simulation of solid-liquid adsorption in activated carbon columns using estimates of intraparticle kinetic parameters obtained from continuous stirred tank reactor experiments. *The Chemical Engineering Journal*, Vol.58, No.3, pp. 239-244, ISSN 1385-8947.

Li, G.; Xiao, P.; Xu, D.; Webley, P. A. (2011). Dual mode roll-up effect in multicomponent non-isothermal adsorption processes with multilayered bed packing. *Chemical Engineering Science*, Vol.66, No. 6, pp- 1825-1834, ISSN: 0009-2509.

Mulgundmath ,V. & Tezel ,F.H. (2010). Optimisation of carbon dioxide recovery from flue gas in a TPSA system. *Adsorption*, Vol.16, No.6, pp. 587-598, ISSN 1572-8757.

Pevida, C.; Plaza, M.G.; Arias, B.; Fermoso, J.; Rubiera, F. & PIS, J.J. (2008). Surface modification of activated carbons for CO_2 capture. *Applied Surface Science*, Vol.254, No.2, pp. 7165-7172, 2008, ISSN 0169-4332.

Ruthven, D. M. (1984). Principles of Adsorption and Adsorption Processes. John Wiley & Sons, ISBN 0-471-86606-7.

Siriwardane, R.V.; Shen, M-S. & Fisher, E.P. (2001). Adsorption of CO_2 on Molecular Sieves and Activated Carbon. *Energy Fuels*, Vol.15, No.2, pp. 279-284, ISSN 0887-0624.

Sivakumar, S.V. & Rao, D.P. (2011). Modified duplex PSA. 1. Sharp separation and process intensification for CO_2-N_2-13 X zeolite system. *Industrial & Engineering Chemistry Research*, Vol.50, No.6, pp. 3426-3436, ISSN 0888-5885.

Vinay, M. & Handal, T. (2010). Optimisation of carbon dioxide recovery from flue gas in TPSA system. *Adsorption*, Vol.16, No.6, pp. 587-598, ISSN 1572-8757.

Vinu, A. & Hartmann, M. (2005). Characterization and microporosity analysis of mesoporous carbon molecular sieves by nitrogen and organics adsorption. *Catalysis Today*, Vol.102-103, (May 2005), pp. 189-196, ISSN 0920-5861.

Wakao, N. & Funazkri.T. (1978). Effect of fluid dispersion coefficients on particle-to-fluid mass transfer coefficients in packed beds: Correlation of Sherwood numbers. *Chemical Engineering Science*, Vol. 33,No.10, pp. 1375-1384, ISSN 0009-2509.

Wakao, N.; Kaguei, S. & Nagai, H. (1978). Effective diffusion coefficients for fluid species reacting with first order kinetics in packed bed reactors and discussion on evaluation of catalyst effectiveness factors. *Chemical Engineering Science*, Vol. 33, No.2, p. 183-187, ISSN 0009-2509.

Zhang, J.; Webley, P.A. & Xiao, P. (2008). Effect of process parameters on power requirements of vacuum swing adsorption technology for CO_2 capture from flue gas. *Energy Conversion and Management*, Vol.49, No.2, pp. 346-356, ISSN 0196-8904.

4

The Needs for Carbon Dioxide Capture from Petroleum Industry: A Comparative Study in an Iranian Petrochemical Plant by Using Simulated Process Data

Mansoor Zoveidavianpoor[1], Ariffin Samsuri[1],
Seyed Reza Shadizadeh[2] and Samir Purtjazyeri[2]
[1]*University Teknologi Malaysia, Faculty of Petroleum & Renewable Energy Engineering*
[2]*Petroleum University of Technology, Abadan Faculty of Petroleum Engineering*
[1]*Malaysia*
[2]*Iran*

1. Introduction

The greenhouse effect is the heating of the earth due to the presence of greenhouse gases. According to the Intergovernmental Panel on Climate Change (IPCC), the ongoing emissions of greenhouse gases from human activities are leading to an enhanced greenhouse effect. This may result, on average, in additional warming of the earth's surface (Houghton and Jenkins, 1990). During 2007, global emission of carbon was 7 billion metric tons (Bt), which are expected to increase to 14 Bt per annum by the year 2050 assuming the demand for fossil fuel keeps increasing because of the growing economies around the world (Bryant, 2007). Carbon dioxide (CO_2), is considered as a raw material in chemical industry. So, its recovery from flue gas meets a great prosperity not only for economic point of view but also for its negative effects to the environment. CO_2 emission control by its capturing from fossil-fuel combustion sources is applied widespread in power plants and industrial sectors. By utilization of this approach, fossil fuel could be continually allowed to be used with a lesser degree and/or without contributing significantly to greenhouse-gas warming.

This chapter clearly shows the need for CO_2 capture in downstream petroleum industry by demonstrating its health and environmental effects. These effects are briefly discussed the negative impacts of the increasing trend of CO_2 emission in Iran. Afterward, a comparative study for capturing carbon dioxide in a petrochemical plant in Iran will be presented.

1.1 CO_2 health effects

At 5% concentration in air (500,000 parts per million (ppm)), CO_2 can produce shortness of breath, dizziness, mental confusion, headache and possible loss of consciousness. At 10 % concentrations, the patient normally loses consciousness and will die unless it is removed. With little or no warning from taste or odour, it is possible to enter a tank or a pit full of CO_2 and be asphyxiated in a very short time. Long-term exposure at concentrations of 1-2 % can cause increased calcium deposition in body tissue, and may cause mild stress and

behavioural changes. The National Institute for Occupational Safety and Health (NIOSH) air quality standard for the protection of occupational health sets the limit for CO_2 at 10,000 ppm for 10 hours. The Occupational Safety and Health Administration (OSHA) air quality standards for the protection of occupational health set the limit for CO_2 at 5,000 ppm (Webster, 1995).

Human and environmental impacts of solvent-related emissions at a capture and storage of CO_2 facility were estimated by Veltman et al. (2010). They stated that, although carbon dioxide capture is relatively well-studied in terms of power generation efficiency, CO_2 emission reduction, and cost of implementation, but little is known about the potential impacts on human health and the environment. The U.S. Environmental Protection Agency (EPA) has officially declared that CO_2 and other so-called greenhouse gases are dangerous to public health and welfare, paving the way for much stricter emissions standards (EPA, 2009). The 2009 CO_2 emission shows that the Middle East accounted for 3.3% of the total world CO_2, of which 31% is the share of Iran. Consequently, as shown in Figure 1, the trend of CO_2 emission is progressively increased from 1998 to 2009, which certainly endanger all aspects of life in Iran. The urban environment of Iran is becoming increasingly polluted, with adverse impacts on the health, welfare and productivity of the population. Results indicate that pollution in Tehran, where 20% of Iran's population lives, has well exceeded safe levels (EIA, 2000; Asgari et al., 1998; Masjedi et al., 1998).

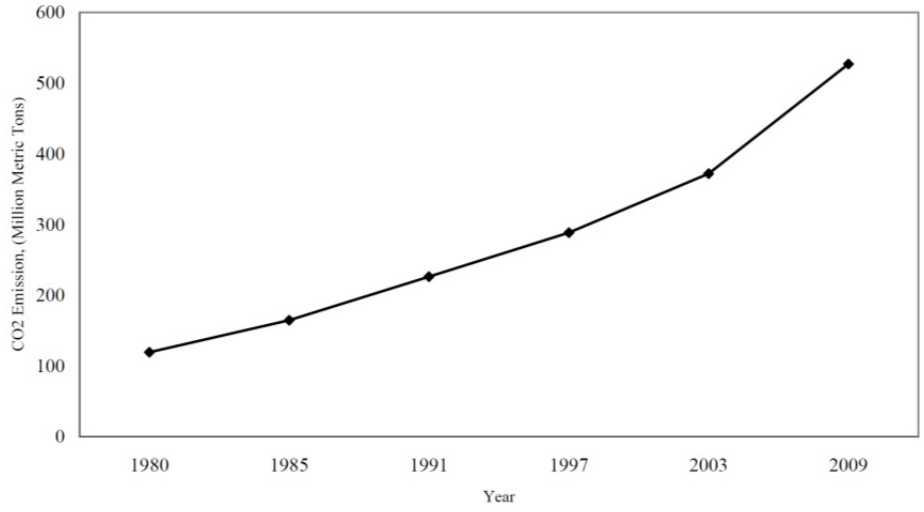

Fig. 1. Increasing trend of total CO_2 emission per Mt from 1980 to 2009 in Iran

1.2 CO_2 emission in Iran

Iran is the second-largest producer and exporter in The Organization of the Petroleum Exporting Countries (OPEC), and in 2008 was the fourth-largest exporter of crude oil globally. Iran holds the world's third-largest proven oil reserves and the world's second-largest natural gas reserves. Figure 2 shows the total fuel consumption in Iran. As it is clear in Figure 3, the combustion of fossil energy contributes with about 84 % to the CO_2 emission in Iran.

The main resource of CO_2 emission is fossil fuels that unfortunately now a day are the basic sources to generate energy in industrial-economic systems. On the other hand, energy is a main factor to achieve economic development, which is highly needed for developing countries. In 2009, Iran consists of 527 million metric tones (Mt) of CO_2 emission and is known to be the 9th worst polluter increasing the emissions by 3.2 per cent to 2009, compared with 2008 levels.

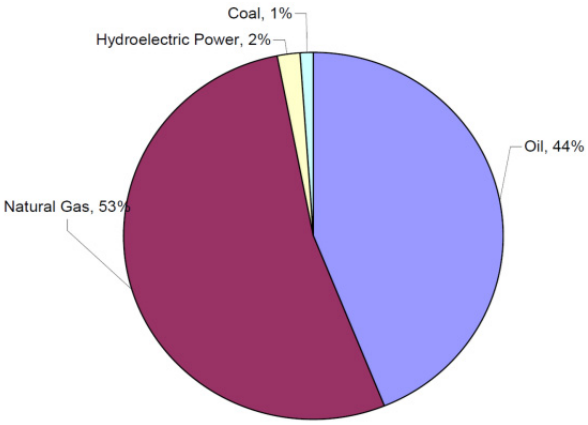

Fig. 2. Total energy consumption in Iran

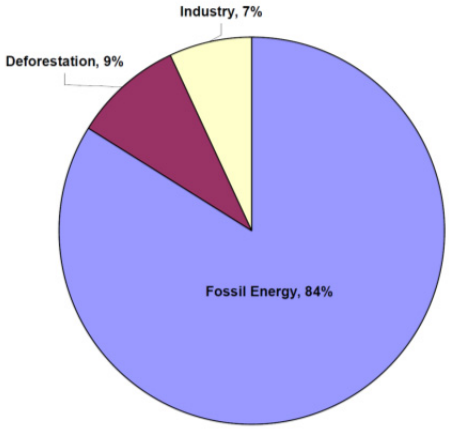

Fig. 3. Overall CO_2 emission in Iran

As shown in Figure 4, the power plant sector with an emission of 28% CO_2 is the largest carbon dioxide emissions source in Iran. Although the consumption of gas has increased in this sector during recent years, still more than 50% of the energy consumption comes from the combustion of heavy fuel oil. The industry sector is the second largest contributor to CO_2 emissions, with about 133 Mt in 2008. The transport sector accounted for 23% of total CO_2 emitted. As Figure 4 shows, the industry sector with about 26% of the total CO_2 emissions was the second major contributor in 2008. The breakdown of the industrial CO_2 emission in

Iran (Figure 5) shows that the petrochemical industry in Iran has more emission contribution in contrast with the other industries such as cement, steel, and gas processing plants. Boilers, process heaters, and other process equipment are the major CO_2 emissions producers in a petrochemical plant. The data presented in Figure 2 through Figure 5 were extracted from different literature; Moradi et al. (2008), Avami and Farahmandpour, (2008), and NIOC (2011).

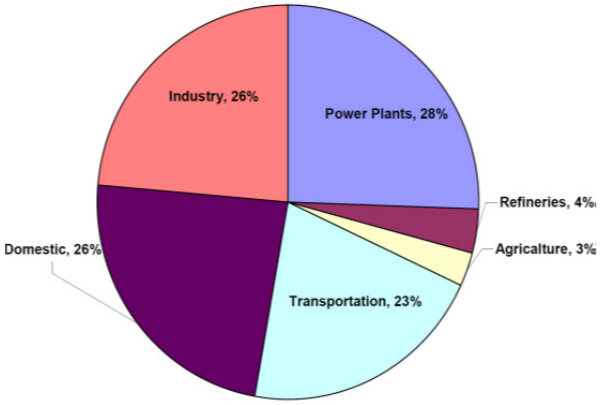

Fig. 4. Iran's Energy Sectors contributed to CO_2 emission in 2008

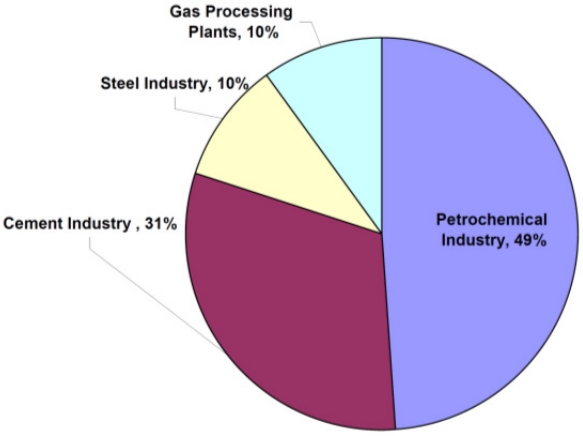

Fig. 5. The breakdown of industrial CO_2 emission in 2008

According to the recent study performed by Roshan et al. (2011), the country's temperature annual trend increment would have an increase of maximum 5.72°C to minimum 3.23°C, while considering the most optimistic case, the country's annual temperature would increased by 4.41 °C till 2100. Figure 6 shows the prediction of the total average of temperature annual and seasonal changes from 2025 to 2100 based on the results of an applied scenario for different regions of Iran. According to Figure 7, the highest amount of CO_2 density, which has been forecasted for the year 2100 is 570 ppm.

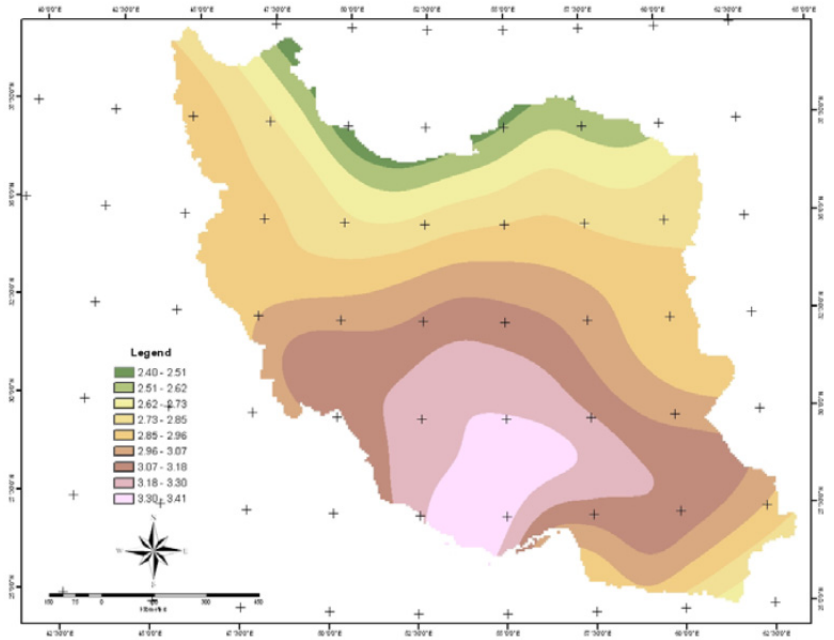

Fig. 6. Prediction of the total average of temperature annual and seasonal changes from 2025 to 2100 based on the results of an applied scenario for different regions of Iran (Roshan et al. 2011)

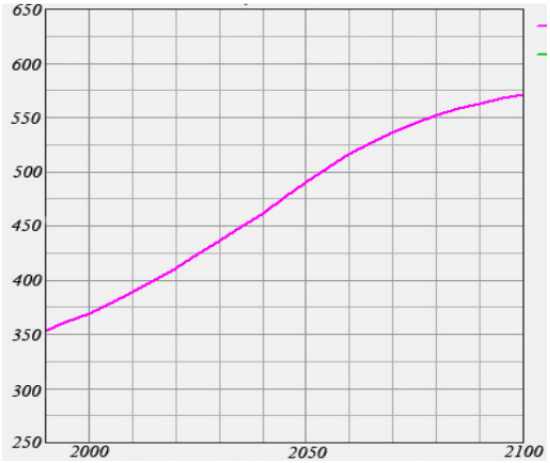

Fig. 7. Prediction of the CO_2 concentration per Mt till 2100 in Iran (Roshan et al. 2011)

2. CO_2 capture technologies

As reported by the United Nations Intergovernmental Panel on Climate Changes (UNIPCH) (1995), CO_2 level has risen 30% to nearly 360 ppm from a pre-industrial era level of 280 ppm.

Judkins et al. (1993) believed that in order to avoid major climate changes, human-generated emissions of CO_2 will have to be reduced by as much as 50-80%. As a result, three strategies had proposed for CO_2 emission control: (1) Exploiting the fuels more efficiently. (2) Replacing coal by natural gas. (3) Recovering and sequestering of CO_2 emissions.

By considering the greenhouse gas effects, it is accepted that natural gas is preferable to other fossil fuels such as coal, and oil. Indeed, removal of CO_2 from natural gas is considered as a practical and more convenience step toward reduction of CO_2 emissions. Removals of CO_2 from gaseous streams have been a current procedure in the chemical industry. Because of the increasing trend of energy consumption globally, removal of CO_2 from natural gas is not easy to be achieved; this task, obviously, required an integrated approach based on modern capturing technologies. The choice of a suitable technology (Figure 8) depends on the characteristics of the flue gas stream, which depend mainly on the chemical or power plant technology. Figure 8 shows the technologies which are currently used for CO_2 capturing.

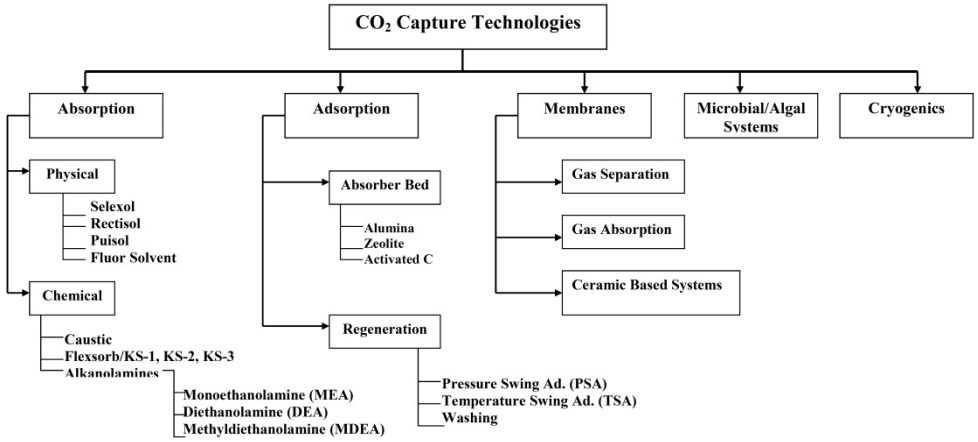

Fig. 8. CO_2 capture technologies

Chemical solvent absorption is based on reactions between CO_2 and one or more basic absorbents such as aqueous solutions of Monoethanolamine (MEA), Diethanolamine (DEA) and Methyldiethanolamine (MDEA). An advantageous characteristic of absorption is that it can be reversed by sending the CO_2-rich absorbent to a stripper where the temperature is raised.

In the present study, simulation of a CO_2 capture from fuel gases of one of the petrochemical plants in Iran was performed by using MEA, DEA and MDEA. In this work, a process by using alkanolamines including CO_2 capture from flue gases was simulated and optimized in a petrochemical plant in Iran. The simulation has been conducted using a commercial software. The required data such as the composition of three type of alcanolamines, were derived in the laboratory. This work consists of six important variables as the output of the simulation process; (1) the amount of CO_2 recovery, (2) amine consumption, (3) mechanical and operational characteristics of the absorption column, (4) CO_2 purity in the stripper column effluent, (5) required energy of the stripper, and (6) mechanical and operational features of the stripper.

In section 3, the applied process in this study for Amine-based CO_2 capture will be described. The results of this work will be presented in Section 4 and discussed in Section 5. Finally, based on different criteria, the selected alkanolamine will be demonstrated.

3. Amine-based CO_2 capture plant: Process description

Amine process is the best and commonest choice for separation of CO_2 from flue gases. Driving force of this process is the reaction between CO_2 and amine in which CO_2 with high purity is acquired by one stage process. This process starts with cooling flue gases applying a water cooler to lessen some of their impurities such as NO_x and SO_x to an acceptable value. Then the chilled gas is pressurized with a blower to the absorption column. Temperature ranges at the top and bottom of the column are about 40-45 and 50-60 °C, respectively. Flue gases and the lean amine are contacted, and CO_2 is absorbed in the amine solution through the absorber. Rich amine at the bottom of the column is pumped into a cross heat exchanger, where its temperature reaches to about 100 °C exchanging heat with the effluent fresh amine of stripping column. Then this solution introduced to the top section of the stripping column. Operating temperature at the top and bottom of the column, operating pressure and column pressure gradient are 110 °C, 120 °C, 1.3 bar and 0.17 bar, respectively.

Required energy for stripping column is supplied from saturated steam at 45 psia. The rich solution of amine and steam are contacted in stripper, and CO_2 is separated from amine. The gas stream containing CO_2 and water steam is exhausted from the top of the column to a condenser where its temperature is lowered to 45 °C. Almost the whole steam is condensed in the condenser and recycled to the top of the column. CO_2 is recovered in a flash drum, then dried and finally compressed to an acceptable pressure. The CO_2-lean solution leaves the reboiler and enters the cross heat exchanger where it is cooled. The solution is then cooled further before it re-enters the absorber.

Packed columns are often employed in the removal of impurities from gas streams and also the removal of volatile components from liquid streams. The dimensionless Robbins correlation factor is actually the Dry Bed Packing Factor issued to calculate the gas and liquid loading factors, which are in turn used to calculate the pressure drop, particularly with newer packing materials. As shown in Table 3 and Table 5, Robbins packing correlation was used as a default correlation. The Height Equivalent to a Theoretical Plate (HETP) relates to packed towers. The value refers to the height of packing that is equivalent to a theoretical plate. As shown in Table 3 and Table 5, Frank correlation was used to determine the equivalent height to theoretical plate.

The entire schematic diagram of the CO_2 absorption process is illustrated in Figure 9. The flow sheet represents a continuous absorption/regeneration cycling process. Note that the reactions of these alkanolamines and CO_2 are mainly occurred by electrochemical reaction in the aqueous solution. Typical reaction mechanism of MEA and CO_2 are as in the following equations.

$$2RNH_2 + CO_2 + H_2O \leftrightarrow (RNH_3)2CO_3 \quad (1)$$

$$(RNH_3)2CO_3 + CO_2 + H_2O \leftrightarrow 2RNH_3HCO_3 \quad (2)$$

$$2RNH_2 + CO_2 \leftrightarrow RNHCOONH_3R \quad (3)$$

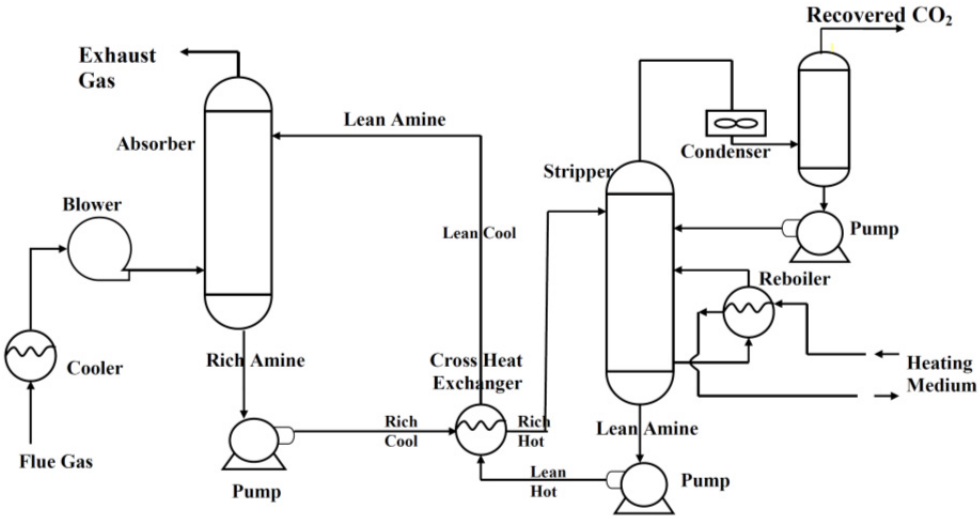

Fig. 9. Flowchart for CO_2 capture from flue gases using MEA, DEA and MDEA.

4. Results

Three different alkanolamines (MEA, DEA, and MDEA) were used in the simulation investigation of CO_2 capture in this work. Composition and thermal specifications of feed (flue gas and amine), entering the first tray at the bottom of the absorber are presented in Tables 1 and 2 respectively.

Component	Molar flow rate (kgmol/h)	Mol .fraction
N_2	7691.244	0.782
CO_2	1208.637	0.123
O_2	205.463	0.021
H_2O	728.561	0,074
Sum	**9833.906**	**1.000**

Table 1. Flue gas composition

Property	Flue gas	MEA	DEA	MDEA
Vapor fraction	1	00	00	00
Temperature (°C)	45.0	35.0	35.0	*35.0*
Pressure (kPa)	130.0	105.5	105.5	105.5
Mass flow (kg/h)	288351.8	596633.4	2010937.5	1990020.5

Table 2. Thermal specification of feed

Many other technologies used for CO_2 capture are based on the MEA process, with changes made in either solvent choice or absorption/stripping methodology. Specifications of the absorber for three types of amines are listed in Table 3. Type and amount of packing are selected so that the maximum recovery is obtained using the minimum consumption of amine. Composition of exit gas and rich amine leaving absorption column is presented in Table 4.

Parameter	MEA	DEA	MDEA
Section diameter (m)	5.944	6.096	6.401
Max flooding (%)	67.4 13	68.985	68.147
X-sectional area	27.745	29.186	32.178
Section height	29.871	42.999	61.086
Section ΔP(kPa)	2.727	10.114	12.072
ΔP per length (kPa)	0.112	0.288	0.242
Flood gas velocity (m^3/m^2h)	14798.038	9479.649	9141.451
Flood gas velocity (m/s)	4.111	2.633	2.539
HETP(m)	0.853	0.860	0.873
HETP correlation	Frank	Frank	Frank
Packing correlation	Robbins	Robbins	Robbins
Packing type	Gempak (metal structured) 0.75 A	Gcmpak (metal random) No._2	Gempak (metal structured) 2 A

Table 3. Specification of absorption column

Component	MEA		DEA		MDEA	
	Exit gas	Rich amine	Exit gas	Rich amine	Exit gas	Rich amine
N_2	99.995	0.005	99.982	0.018	99.98	0.02
CO_2	3.351	96.649	2.062	97.938	30.394	69.606
O_2	99.991	0.009	99.966	0.034	99.961	0.039
H_2O	6.62	93.38	0.459	99.541	0.434	99.566
MEA	0.226	99.774	Nil	Nil	Nil	Nil
DEA	Nil	Nil	Nil	100.00	Nil	Nil
MDEA	Nil	Nil	Nil	Nil	Nil	100.00

Table 4. Upstream and downstream composition of absorption column

As it can be seen almost all the CO_2 in flue gas is recovered by MEA and DEA (above 96 and 97% for MEA and DEA, respectively) through one stage, whereas MDEA amine is observed to be unsuitable for one stage CO_2 recovery (about 30% recovery). Rich amine at the bottom of the column is pumped to a heat exchanger then, achieving appropriate thermal specifications, it is introduced into the stripping column. Specifications of stripper for three types of amines are listed in Table 5.

Parameter	MEA	DEA	MDEA
Section diameter (m)	9.296	5.486	9.906
Max flooding (%)	69.887	50.882	69.777
X-sectional area	67.877	23 .641	77.070
Section height	20.497	18.288	14.922
Section ΔP (kPa)	4.865	16.835	3.242
ΔP per length (kPa)	0.290	----	0.266
Flood gas velocity (m^3/m^2h)	14736.444	----	12316.179
Flood gas velocity (m/s)	4.093	----	3.421
Estimation of pieces of packing	146080059.333	----	1345560.256
Estimation of mass of packing (kg)	292161.187	----	310513.905
HETP (m)	0.976	----	0.995
HETP correlation	Frank	Frank	Frank
Packing correlation	Robbins	Robbins	Robbins
Packing type	Levapacking (plastic) No._2	-------	Ballast Rings (metal). 3&1_2_inch

Table 5. Specification of stripping column

5. Discussion

A brief review on the associated problems of CO_2 emission, such as health and environment effects and the increasing trend of its emission, indicate the seriousness of the CO_2 capture in Iran's energy sector. The Iranian industry sector with about 26% of the total CO_2 emissions was the second major contributor in 2008, and the largest source was the petrochemical industry. The progressively increases of the emission along with its negative effects on the environmental impact, makes the capture of this greenhouse gas a very important issue. The observation of the fact that the combustion of fossil energy contributes with about 84 % to the CO_2 emission in Iran, the general acceptance of gas in contrast with coal or oil, and the advantages of developed technologies applied in the Iranian petrochemical industry, make it possible to take advantages of the Amine-based CO_2 capture in Iran. In order to capture CO_2 from flue gas in one of the petrochemical plants in Iran, three different alkanolamines were utilized in this work.

Today, most of the CO_2 used by the chemical industry is extracted from natural wells. As the extraction price is close to that for recovery from fermentation and other industrial processes, it may be that soon CO_2 recovered from electric energy generation could find a large application in the chemical industry.

To be able to compare the amine processes, the same general configuration of the process, feed composition and flow rate was applied for alkanolamine plant. The amount of CO_2 recovery, amine consumption, mechanical and operational characteristics of absorption column, CO_2 purity in stripper column effluent, required energy of stripper and mechanical and operational features of stripper were compared for three types of amines.

The amount of CO_2 recovery for three types of amines is represented in Figure 10. According to this Figure, CO_2 recovery for MEA and DEA are above 96 % while this value

for MDEA is less than 70%. It means that MDEA is weaker than two other amines and cannot be used for one stage processes.

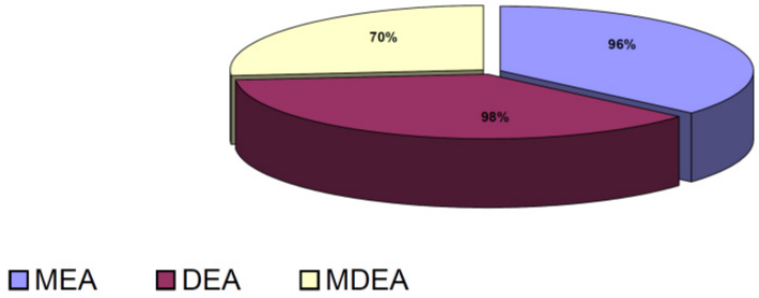

Fig. 10. CO_2 recovery (%) for three types of amine s process.

The amount of amine consumption for three types of amines is represented in Figure 11. As can be seen MEA process uses much fewer amines than other processes (about one fourth), i.e. this process is superior to other processes considering economic aspects. The low MEA consumption raises the reboiler duty substantially. The required pump power increases even more. Since the reboiler heat duty is the most important key to operating costs, this is a significant handicap (Chapel and Mariz, 1999).

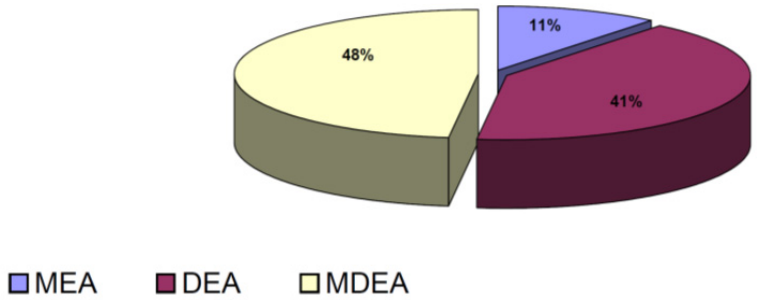

Fig. 11. The percentage of alkanolamine consumption (Kg/h) for three types of amines process.

Mechanical and operational characteristics of absorption column for three types of amines are almost the same, except to column height. Height of absorption column for MEA plant (30 m) is considerably lower than DEA (43 m) and MDEA (61 m) plants. Since, column diameter for all plants are the same, it can be concluded that MEA plant is better than others considering mechanical aspects.

Figure 12 indicates that, CO_2 purity in stripper column effluent is similar to all types of amines (above 97 %). Hence, this parameter could not be used as a criterion for selection of the optimum process.

As it is shown in the Figure 13, required energy of stripper for DEA plant is significantly smaller than other amine plants (about one tenth).

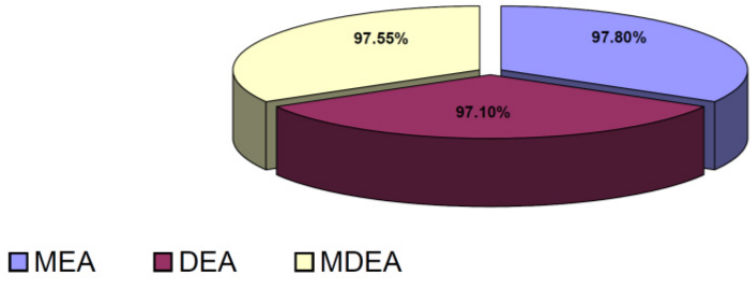

Fig. 12. CO_2 purity (%) for three types of amines process.

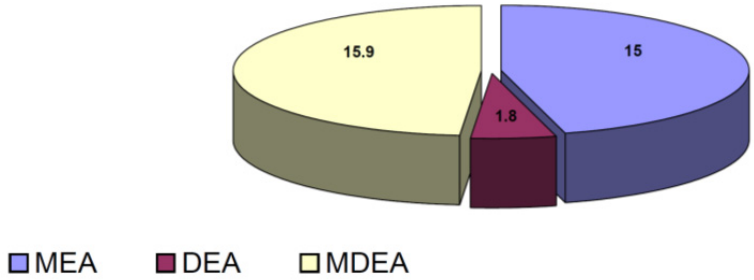

Fig. 13. Energy consumption (Kj/h) for three types of amines process.

Operational features of stripper are alike for all amine plants whereas mechanical characteristics are different to a certain extent. Diameter of MEA, DEA and MDEA stripper columns are 9.3, 5.5 and 10 m and heights of them are 20.5, 18.3 and 15 m, respectively. Taking all parameters into account, it can be concluded that the MEA plant is the best choice for separation of CO_2 from fuel gases.

The removal of CO_2 from flue gases using an amine depends on the gas-liquid mass transfer process. The chemical reactions that permit diffusion of CO_2 in the liquid film at the gas-liquid interface enhance the overall rate of mass transfer. Thus, the CO_2 removal efficiency in the absorber is a function of various parameters that affect the gas-liquid equilibrium (e.g., flow rates, temperature, pressure, flue gas composition, CO_2 concentration, alkanolamine concentration and absorber design). Similarly, the conditions and detailed design of the stripping column affect the energy requirements and overall performance of the system.

MEA is the most frequently used solvent for CO_2 absorption, and the greatest advantage of MEA is its relatively high loading. Two moles of MEA are needed for each mole of CO_2 absorbed, which represents the maximum equilibrium pickup and fixes the minimum circulation rate of MEA for completely treating a given quantity of acid gas.

6. Conclusions

In this chapter, the needs for CO_2 capturing were raised by presenting the negative health and environmental impacts of CO_2 emission in Iran. Direct relationship between fossil-fuel consumption and CO_2 emission was demonstrated in this study. Results show that CO_2 emission, especially from petrochemical plant, will have to be efficiently reduced. So,

chemical absorption technology for CO_2 capture in a petrochemical plant has been selected in this study.

In the present work, CO_2 capture from fuel gases of one of the petrochemical companies in Iran using three alkanolamines (MEA, DEA and MDEA) was simulated and optimized. Specifications of absorber and stripper and composition of exit gas and rich amine leaving absorber were initially reported as simulation results. Then, these alkanolamines were compared considering some parameters such as CO_2 capture amine consumption, mechanical and operational characteristics of absorber and stripper, and CO_2 purity and energy consumption. It was found that, MEA and DEA are capable to recover almost all of CO_2 from flue gases. Amine consumption in an MEA plant is one-fourth of another amine plant where its energy consumption is the same as MDEA plant and ten times larger than DEA plant. Considering mechanical and operational characteristics, it was realized that MEA plant meets economic and aspects better than other amine plants. Finally, taking all parameters into consideration it was deduced that MEA is the best alkanolamine for separation of CO_2 from flue gases in this issue.

7. Acknowledgment

The authors of this chapter would like to express their gratitude to Universiti Teknologi Malaysia due to their supports during this study.

8. References

Al-Baghli, N.A.; Pruess, S.A.; Yesavage, V.F. & Selim, M.S. (2001). A Rate-based Model for the Design of Gas Absorbers for the Removal of CO_2 and H_2S Using Aqueous Solution of MEA and DEA, *Fluid phase equilibria*, Vol. 185, No. 1-2, pp. (31-43), ISSN 0378-3812

Asgari M., DuBois A., et al. (1998). Association of Ambient Air Quality with Children's Lung Function in Urban and Rural Iran, *Archives of Environmental Health*. No. 53.

Avami A. & Farahmandpour B. (2008). Analysis of Environmental Emissions and Greenhouse Gases in Islamic Republic of Iran, *WSEAS TRANSACTIONS on ENVIRONMENT and DEVELOPMENT*, Vol. 4, No.4, pp. (303-312), ISSN: 1790-5079

Blauwhoff, P. M. M.; Versteeg, G. F. & Van Swaaij, W. P. M. (1984). A Study on the Reaction between CO2 and Alkanolamines in Aqueous Solutions. *Chemical Engineering Science*, Vol. 39, No. 2, pp. (207-25), ISSN 0009-2509

Bredesena, R.; Jordal, K. & Bolland, A. (2004). High-Temperature Membranes in Power Generation with CO2 Capture. Chemical Engineering and Processing, Vol. 43, No. 9, pp. (1129–1158), ISSN 0255-2701

Bryant S. (2007). Geologic Storage – Can the Oil and Gas Industry Help Save the Planet, *Journal of Petroleum Technology*. September, pp. (98-105), ISSN: 0149-2136

Chapel, D.G. & Mariz, C.L. (1999). Recovery of CO_2 from Flue Gases: Commercial Trends, presented at the Canadian Society of Chemical Engineers annual meeting October 4-6, Saskatoon, Saskatchewan, Canada.

Energy Information Administration (2000). United States: Iran; Environmental Issues, Apr. 2000, http://www.eia.doe.gov/.

EPA (2009). Endangerment and Cause or Contribute Findings for Greenhouse Gases under Section 202(a) of the Clean Air Act, 210pp

Hart, A. & Gnanendran, N. (2009). Cryogenic CO_2 Capture in Natural Gas. *Greenhouse Gas Control Technol*., Vol. 9, No. 1, pp. (697–706), ISSN 1750-5836

Houghton, J. T.; Jenkins, G. J. & Ephraums, J. J. (1990). *Climate Change*: (ed) The IPCC Scientific Assessment, Cambridge University Press, Cambridge, U.K.

Hu, W. & Chakma, A. (1990). Modeling of Equilibrium Solubility of CO2 and H2S in Aqueous Diglycolamine (DGA) Solutions, *The Canadian journal of chemical engineering*, Vol. 68, No.3, pp.(523-525), ISSN 0008-4034

Judkins, R.; Fulkerson, W. & Sanghvi M.K. (1993). The Dilemma of Fossil Fuel Use and Global Climate Change. Energy and Fuels Vol.7, No.1, pp. (14 – 22), ISSN 0887-0624

Kohl, A. L. & Nielsen, R.B. (1997). *Gas Purification*. (5th edition). Gulf Professional Publishing, ISBN 0884152200, Houston, Texas.

Masjedi, M.; Malek Afzali, H.; Saman Manesh, H.; Ahmadzadeh, Z. & Abdi A. (1998). Survey of Air Pollutants in Tehran, *Journal of Medical Council of Islamic Republic of Iran*, Vol. 15, No. 4, pp. (155-62), ISSN 0254-4571

Merel, J.; Clausse, M. & Meunier, F. (2008). Experimental Investigation on CO_2 Post-combustion Capture by Indirect Thermal Swing Adsorption Using 13x and 5a Zeolites. *Industrial & Engineering Chemistry Research,* Vol. 47, No. 1, pp. (209–215), ISSN 0888-5885

Moradi, A. M.; Akhtarkavan, M.; Ghiasvand, J. & Akhtarkavan, H. (2008). Assessment of Direct Adverse Impacts of Climate Change on Iran. *WSEAS International Conference on CULTURAL HERITAGE AND TOURISM (CUHT'08)*, Heraklion, Crete Island, Greece, July 22-24, pp. (89-94) ISSN 1790-2769

NIOC (National Iranian Oil Company). (2011). CCS Technology, A Report from IOR Research Institute.

Pourjazaieri, S.; Zoveidavianpoor, M. & Shadizadeh, S. R. (2010). Simulation of an Amine-based CO2 Recovery Plant, Petroleum Science and Technology, Vol. 29, No. 1, pp. (39-47), ISSN 1091-6466

Rinker, E.B.; Ashour, S. S. & Sandall, O.C. (2000). Absorption of Carbon Dioxide into Aqueous Blends of Diethanolamine and Methyldiethanolamine. *Industrial & Engineering Chemistry Research*, Vol. 39, No. 11, pp. (4346-4356), ISSN 0888-5885

Roshan, Gh. R.; Khoshakh lagh, F.; Azizi, Gh. & Mohammadi H. (2011). Simulation of Temperature Changes in Iran under the Atmosphere Carbon Dioxide Duplication Condition. *Iranian Journal of Environmental Health Science & Engineering* Vol. 8, No. 2, pp. (139-152), ISSN 1735-1979

Veltman, K.; Singh, B. & Hertwich, E.G. (2010). Human and Environmental Impact Assessment of Postcombustion CO_2 Capture Focusing on Emissions from Amine-Based Scrubbing Solvents to Air, *Environmental Science & Technology,* Vol. 44, No. 4, pp. (1496–1502), ISSN 0013-936X

Webster, J.G. (1995). Chemical Impacts of Geothermal Development. In: Brown, K.L. (convenor), Environmental aspects of geothermal development. World Geothermal Congress, IGA pre-congress course, Pisa, Italy; pp. (79-95)

Zhang, P.; Shi, Y.; Wei, J. W.; Zhao, W. & Ye, Q. (2008). Regeneration of 2-Amino-2-Methyl-1-Propanol used for carbon dioxide absorption. *Journal of Environmental Sciences.* Vol. 20, No. 1, pp. (39–44), ISSN 1001-0742

5

Absorption of Carbon Dioxide in a Bubble-Column Scrubber

Pao-Chi Chen
Graduate School of Engineering Technology
Department of Chemical and Materials Engineering
Lunghwa University of Science and Technology
Taiwan

1. Introduction

In the current stage over 85% of world energy demand is supplied by fossil fuels. Coal-fired plants discharged roughly 40% of the total CO_2 are the main contributors in CO_2 emissions (Kim & Kim, 2004; Yang et al., 2008). Environmental issues caused by exhaust green house gases (GHG) and toxics have become global problems. Through the past studies of five decades, increased GHG levels in atmosphere is believed to cause global warming, in which CO_2 is the largest contributors. International Panel on Climate Change (IPCC) predicts that the CO_2 content in atmosphere may contain up to 570 ppmv CO_2, causing an increase in mean global temperature around 1.9℃ and an increase mean sea level of 38m (Stewart & Hessami, 2005). Also accompanied is species extinction. Therefore, the importance of removing carbon dioxide from exhaust emissions has been recognized around the world. There are three options to reduce total emission into the atmosphere, i. e., to increase energy efficiency, to use renewable energy, and enhance the sequestration or removal of CO_2. However, from the viewpoints of coal-fired plants discharged a lot amount of CO_2-gas, CO_2 gas needs to be removed from the flue gases of such point sources before direct sequestration. There are several processes for CO_2 separation and capture processes, including post-combustion, pre-combustion, oxy-fuel processes, and chemical-looping combustion (Yang et al., 2008). In here, we focus on the treatment of post-combustion processes since they are typical coal-fired plants.

For the removal of exhaust CO_2-gas, several methods have been proposed, such as chemical absorption, physical absorption, membrane separation, biochemical methods, and the catalytic conversion method. In addition to these methods, the absorption of carbon dioxide in an alkaline solution with crystallization has also been adopted to explore the removal of carbon dioxide from waste gas (Chen et al., 2008). This approach, with the production of carbonate by means of reactive crystallization, has been found to be effective. In order to remove of CO_2 gas, several scrubbers were utilized, such as sieve tray column, packed bed column, rotating packed bed and bubble column. Therefore, how to choose an excellent scrubber becomes significant in the removal of CO_2 gas from flue gas. The performances of the scrubbers were always estimated by using overall mass-transfer coefficient. Due to this, they found packed bed with structured packing (Aroonwilas & Tontiwachwuthiku, 1997)

gives a higher overall mass-transfer coefficient as compared with other scrubbers. On the other hand, Chen et al. (2008) found that the performance of scrubber could be estimated by using scrubbing factor, a definition of removal of 1 mole CO_2 gas per mole of absorbent and per liter of scrubber. In this manner, a bubble-column scrubber is the first choice.

In a bubble column, gas is often introduced near the bottom of the column. The liquid may flow through the column either with or against the gas flow. Investigations of bubble-columns from the viewpoints of both environmental problems and industrial use can be found in the literature (Juvekar & Sharma, 1973; Sada et al., 1985; Sauer & Hempel, 1987; Okawa et al., 1999; Chen et al., 2002; Hamid & Jones, 2002; Lapin et al., 2002). Bubble column reactors are widely used in the chemical, petrochemical, biochemical, and metallurgical industries (Degaleesan & Dudukovic, 1998). They were favored because of their simple construction, higher heat and mass transfer coefficients, higher removal efficiency, and effective control of the liquid residence time. In addition, bubble columns may be operated in either batch mode or continuous mode, depending on the requirements, as in processes such as liquid-phase methanol synthesis or continuous-mode Fisher-Tropsch synthesis with a liquid superficial velocity that is lower than the gas superficial velocity by at least an order of magnitude or more. In this manner, the gas flow controls the fluid dynamics of the individual phases of these systems. This in turn controls liquid mixing and inter-phase mass transfer, which subsequently influence conversion and selectivity.

In addition, some investigators (Sauer & Hempel, 1987; Hamid & Jones, 2002) have studied the dynamics, mass transfer, and control of the crystal size and shape of products for industrial purposes. However, these data cannot be utilized effectively. In gas-liquid reaction, the absorption mechanism is controlled by both the mass-transfer and chemical reaction steps, depending on the operating conditions. In order to describe the concentration distributions, several diffusion-with-chemical-reaction models have been proposed in the literature (Sherwood et al., 1975; Shah, 1979; Fan, 1989; Cournil & Herri, 2003). In these reports, the chemical reaction kinetics in gas-liquid reactions was first order or second order, depending on the pH of the solution. However, in some systems the mass action equations were found to be very complicated, and in others, it was found that the pH had an effect on the species (Morel, 1983). Therefore, the absorption of gases was strongly affected by the pH of the solution. Thus, it is clear that controlling the pH of the solution is important for controlling the absorption rates of gases, since the ionic strength and, hence, Henry's constant are affected by the pH of the solution. Additionally, several gas-liquid absorption applications, such as desulfurization processes and the removal of carbon dioxide, involve small particles (Hudson and Rochelle, 1982; Saha and Bandyopadhyay, 1992; Chen et al., 2002; Okawa et al., 1999). However, some of the above papers reported that the size and concentration of solids affected the mass-transfer coefficient, while most studies found larger sizes at higher solid concentrations (Shah, 1979; Cournil & Herri, 2003). These mass-transfer coefficient data cannot be used in absorption with reactive crystallization systems, such as gypsum and carbonates. Therefore, research on the effect of particles on the absorption processes is required. For design purposes, data for the hydrodynamics and mass-transfer coefficients in bubble columns is required (Bukur & Daly, 1987). In order to obtain the mass transfer coefficients in an alkaline solution with and without solids, a two-film model was utilized to describe the absorption of carbon dioxide. The results are also compared here with those reported in the literature.

In this chapter, the materials include absorption models, determination of absorption rate, solution chemistry, determination of mass-transfer coefficients, and scrubbing factors of various scrubbers. Finally, how to estimate the size of bubble-column scrubber is also discussed in this chapter.

2. Absorption models

When gas is blown through the liquid as a stream of bubbles, e. g., in a sparged vessel or on a bubble-plate; diffusion, convection, and reaction proceed simultaneously. A complicated system is formed during gas-liquid contact. Absorption accompanied with chemical reaction not only can enhance the absorption rate but also can reduce the height of scrubber (Levenspiel, 1998). Therefore, in absorption accompanied with chemical reaction system, chemical reaction kinetics play an important role on the overall rate of absorption process. There are eight special cases for the absorption with reaction processes; the absorption efficiency is dependent on fast reaction or slow reaction kinetics. In order to quantitatively evaluate the absorption rate, absorption model proposed is required. Four models are observed in the literature (Danckwerts, 1970; Sherwood et al., 1975); there are the film model, still surface model, surface-renewal model, and the penetration model. In here, a two-film model is introduced, since it is a more practical model for applications, as shown in Figure 1. The gas solute in bulk phase overcomes the resistance of gas film and moves to the gas-liquid interface; later, solute moves across the interface and overcomes the liquid film resistance and goes through the bulk liquid. At the interface the Henry's law is applied:

$$C_i = K_H P_i \tag{1}$$

where C_i is the concentration of solute at liquid side interface, P_i the partial pressure of solute at gas side interface, and K_H the Henry's law constant. The two-film model is widely used in the literature. In here, the Henry's law constant is dependent on the ionic strength and temperature.

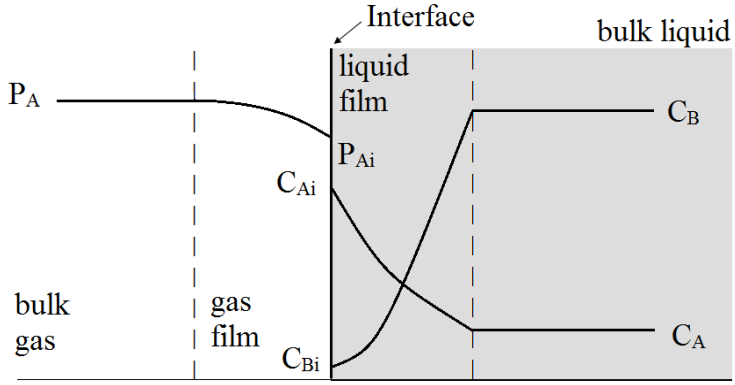

Fig. 1. A schematic diagram for the two-film model.(Levenspiel, 1998)

3. Solution chemistry in carbonate system

When CO_2 dissolves in water, it hydrates to form H_2CO_3. In basic solution, hydrated carbon dioxide ionizes to give hydrated protons [H^+], bicarbonate ion [HCO_3^-], and carbonate ion [CO_2^{2-}]. The solution chemistry for CO_2-H_2O system is expressed in terms of Equations (2)-(4). In here, we will abbreviate [H_2CO_3]+[CO_2] simply as [$H_2CO_3^*$]. The total amount of dissolved carbonate increases with increasing pH because of the ionization equilibrium. In dilute solutions at 25℃, the ionization constants for K_{a1} and K_{a2} are approximately $10^{-6.3}$ and $10^{-16.3}$(Butler, 1982), respectively. The ionization constants depend on temperature and on the presence of other salts.

$$CO_2(g) + H_2O = H_2CO_3^* \tag{2}$$

$$H_2CO_3^* = H^+ + HCO_3^- \tag{3}$$

$$HCO_3^- = H^+ + CO_3^{2-} \tag{4}$$

Figure 2 is a plot of degree of ionization (α)versus pH at 25℃. In here, the total amount of carbonate is the summation of all carbons including $H_2CO_3^*$, HCO_3^- and CO_3^{2-}.We express as C_T. In addition, α_0,α_1, andα_2 are the degree of ionization for species $H_2CO_3^*$, HCO_3^- and

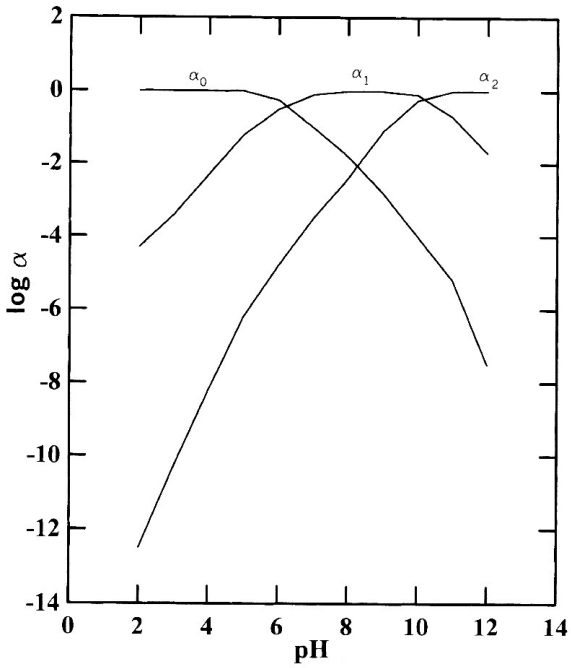

Fig. 2. Ionization of carbon dioxide as a function of pH value $[H_2CO_3^*] = [H_2CO_3] +$ $+[CO_2(aq)]$; $\alpha_0 + \alpha_1 + \alpha_2 = 1$ $\alpha_0 = [H_2CO_3^*]/ C_T$; $\alpha_1 = [HCO_3^-]/ C_T$; $\alpha_2 = [CO_3^{2-}]/ C_T$

CO_3^{2-}, respectively. It is found that α_0 decreases with an increasing in pH on one hand and α_2 increases with pH on the other hand, while α_1 increases with an increasing in pH when the pH is less than 6 on one hand and it decreases with an increasing with pH when the pH is higher than 10 on the other hand. This indicates that the pH value could be adjusted to desired value to control the chemical species, such as $H_2CO_3^*$, HCO_3^- and CO_3^{2-}, presented in the solution. This could be done with an addition of alkaline solution, such as NaOH solution, and acidic solution, such as HCl solution. In order to show the effect of alkaline solution and chemical species on the concentrations of $H_2CO_3^*$, HCO_3^- and CO_3^{2-}, an example will be discussed later.

For the CO_2-H_2O-$BaCl_2$ system with an addition of NaOH solution, there are a lot of chemical species presented in the solution, such as $H_2CO_3^*$, HCO_3^-, CO_3^{2-}, H^+, OH^-, Ba^{2+}, Cl^-, Na^+, and ion pair $BaCO_3^0$. Due to this, the mass action equations, total mass balance equations and charge balance equation are shown in Table 1, Eqs. (5)-(15).

Mass action equations: (Morel, 1983)

$$H_2O = OH^- + H^+ \tag{5}$$

$$CO_2(g) + H_2O = H_2CO_3^* \tag{6}$$

$$H_2CO_3^* = HCO_3^- + H^+ \tag{7}$$

$$HCO_3^- = CO_3^{2-} + H^+ \tag{8}$$

$$BaCO_3^o = Ba^{2+} + CO_3^{2-} \tag{9}$$

$$BaCO_3(s) = Ba^{2+} + CO_3^{2-} \tag{10}$$

Total mass balance equations:

$$TCO = [H_2CO_3^*] + [HCO_3^-] + [CO_3^{2-}] + [BaCO_3{}^0] \tag{11}$$

$$TBa = [Ba^{2+}] + [BaCO_3^o] \tag{12}$$

$$TCl = [Cl^-] \tag{13}$$

$$TNa = [Na^+] \tag{14}$$

Charge balance equation

$$[H^+]+4[Ba^{2+}]+[Na^+]=[OH^-]+[Cl^-]+[HCO_3^-]+4[CO_3^{2-}] \tag{15}$$

Table 1. Mass action, total mass balance, and charge balance equations.

From a given pH value and the total mass balance equations, mass action equations, and activity coefficient equations, the concentrations of chemical species can be obtained by using an ionic strength approximation method (Butler, 1964; Nancollas, 1966; Chen et al., 2004). Due to this, the ionic strength can be determined. The activity coefficients of electrolytes can be estimated from the Bromley correlation equation (Sohnel & Garside, 1992):

$$\frac{1}{z_i^2}\log\gamma_i = -0.511\frac{\sqrt{I}}{1+\sqrt{I}} + \frac{(0.06+0.6B_1)I}{(1+1.5I/z_i)^2} + \frac{B_1 I}{z_i^2} \tag{16}$$

where z_i is the charge number, I is the ionic strength and B_1 is composed of ionic contributions. This equation can be used to estimate activity coefficients in solutions of high ionic strength up to about 6 M. The ionic strength of a solution can be calculated with the following equation:

$$\begin{aligned} I &= \frac{1}{2}\sum z_i^2 C_i \\ &= \frac{1}{2}\left([H^+] + 4[Ba^{2+}] + [Na^+] + [OH^-] + [HCO_3^-] + 4[CO_3^{2-}] + [Cl^-]\right) \end{aligned} \tag{17}$$

For a bubble column, total chloride ion concentration (*TCl*) and total sodium ion concentration (*TNa*) can be determined from material balances, since chloride and sodium ions are both non-reacting components. At steady-state condition, the *TCl* and *TNa* can be evaluated as follows:

$$TCl = \frac{2Q_1C_1}{Q_1 + Q_2} \tag{18}$$

and

$$TNa = \frac{Q_2C_2}{Q_1 + Q_2} \tag{19}$$

where Q_1 and Q_2 are volumetric flow rates for barium chloride solution and sodium hydroxide solution, respectively, C_1 the feed concentration of chloride ion, and C_2 the feed concentration of sodium ion.

Once the ionic strength is obtained, the Henry's law constant, defined in Equation (1), can be evaluated (Butler, 1982). For example, at a temperature of 30℃, Henry's law constant can be expressed as:

$$pK_H = 1.53 + 0.1039I - 0.0148I^2 \tag{20}$$

Where pK_H is defined as:

$$pK_H = -\log K_H \tag{21}$$

Sometime, Henry's law constant is defined as:

$$H = \frac{1}{K_H RT} \tag{22}$$

The Henry's law constant, H, will be used in later.

4. Determination of absorption rate at steady-state

In a bubble column, for a simulated flue gas (CO_2(N_2)-H_2O system), as shown in Figure 3, a gas mixture containing A (carbon dioxide) and B (nitrogen) flowing into a bubble column at the bottom comes into continuous contact with an alkaline solution flowing into the column

at the top. Two streams come into contact with in the column adversely. If we assume that nitrogen gas is essentially insoluble in the liquid phase and that liquid does not vaporize to the gas phase, the gas phase is a binary A-B. The absorption rate of carbon dioxide can be determined by using the material balance under steady state operation, as shown in Figure 3 for a multiple-tube plug-flow model. If we assume plug flow for the gas phase through the tube, the material balance for carbon dioxide in the *i*th tube at steady state is

$$(u_i C_{Ai}\big|_z - u_i C_{Ai}\big|_{z+\Delta z}) S_i - r_{Ai}\pi d_i \Delta z = 0 \tag{23}$$

where u_i is the linear velocity, S_i the cross section of *i*th tube, r_{Ai} the absorption rate per unit area of the *i*th tube, and d_i the diameter of *i*th tube. For a total of N tubes the material balance becomes

$$\sum_{i=1}^{N} S_i (u_i C_{Ai}\big|_z - u_i C_{Ai}\big|_{z+\Delta z}) - \sum_{i=1}^{N} r_{Ai}\pi d_i \Delta z = 0 \tag{24}$$

Equation (24) divided by Δz and taken to the limit, *i.e.*, $\Delta z \to 0$, Equation (24) becomes

$$-\frac{d(\sum u_i S_i C_{Ai})}{dz} - \sum_{i=1}^{N} r_{Ai}(\pi d_i) = 0 \tag{25}$$

or

$$-\frac{dF_A}{dz} - \sum_{i=1}^{N} r_{Ai}(\pi d_i) = 0 \tag{26}$$

where F_A is the overall molar flow rate of the gas phase, which is equal to $\sum u_i S_i C_{Ai}$. Integrating Equation (26), we have

$$-\int_1^2 dF_A - \sum_{i=1}^{N} \int_1^2 r_{Ai}(\pi d_i) dz = 0 \tag{27}$$

and

$$(F_{A1} - F_{A2}) - \int_1^2 \sum_{i=1}^{N} r_{Ai} dA_i = 0 \tag{28}$$

where A_i is the lateral surface area of the *i*th tube. These equations can be rewritten as

$$(F_{A1} - F_{A2}) - \bar{r}_A A = 0\,. \tag{29}$$

and

$$\bar{r}_A = \frac{\sum \int_1^2 r_{Ai} dA_i}{\sum \int_1^2 dA_i} = \frac{\sum \int_1^2 r_{Ai} dA_i}{A} \tag{30}$$

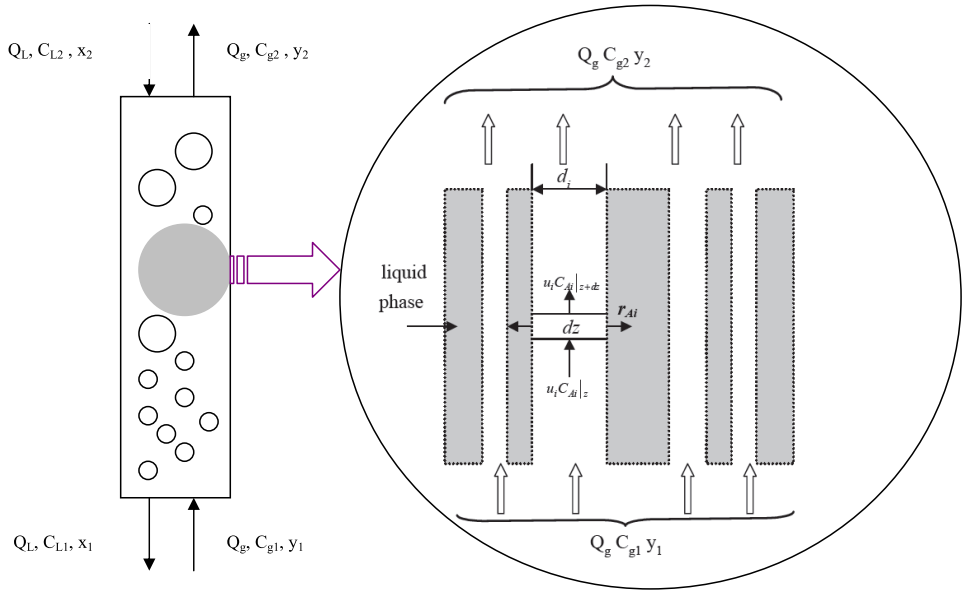

Fig. 3. A multiple-tube plug flow model.

where $\overline{r}_A$ is the mean absorption rate and A is the total surface area of the gas phase in the bubble column, which can not be obtained directly. Equation (29) shows that the absorption rate, $\overline{r}_A A$, is equal to the consumption of carbon dioxide through the bubble column. This value can be determined by measuring the concentration of carbon dioxide and the gas-flow rate:

$$R_A = \frac{F_{A1} - F_{A2}}{V_L} = \frac{F_{A1} - F_{A2}}{\varepsilon_L V_b} \tag{31}$$

and

$$R_A = \frac{\overline{r}_A A}{V_L} \tag{32}$$

where V_L is the volume of the liquid phase, V_b the volume of the bubble column, and ε_L is the hold-up of the liquid phase. Since the molar flow rate of inert gas is equal to $F_{A1}(1-y_1)/y_1$, the molar flow rate of acidic gas at the outlet, F_{A2}, is $F_{A1}[(1-y_1)/y_1][y_2/(1-y_2)]$. Thus, Equation (31) can be rewritten as

$$R_A = \frac{F_{A1}}{V_L}\left[1 - \left(\frac{1-y_1}{y_1}\right)\left(\frac{y_2}{1-y_2}\right)\right] \tag{33}$$

Therefore, the overall absorption rate, R_A, as defined by Cournil & Herri (2003), can be obtained with measurable quantities. Figure 4 exhibits the absorption rate versus gas-flow rate with precipitation at various pH values. The result shows that the absorption rate

increased with an increase in gas-flow rate as well as pH value. In addition, the absorption rate also increased obviously with an increase in gas concentration, y_1, but was only slightly affected by liquid-flow rate.

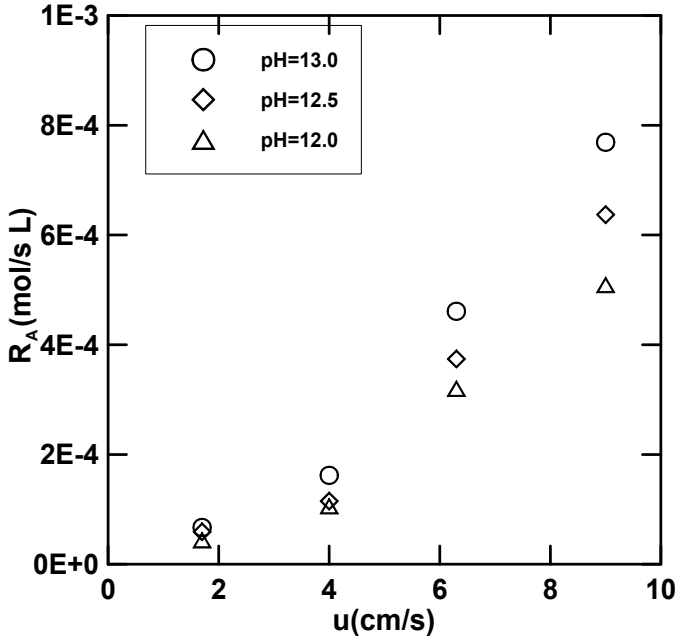

Fig. 4. A plot of R_A versus u at various pH values.

5. Determination of mass-transfer coefficients

According to a two-film model for $CO_2(N_2)$-H_2O system, the relationship between local absorption rate, r_A, and local individual mass-transfer coefficients based on both the gas-side and liquid-side can be written as

$$r_A = k_G a(C_g - C_{gi}) \tag{34}$$

$$= k_L a(C_{Li} - C_L) \tag{35}$$

at the interface $C_{gi} = HC_{Li}$, where H is Henry's law constant defined in Equation (2). Combining Equation (34) and Equation (35) in terms of the overall mass-transfer coefficient, the equation becomes

$$r_A = (K_G a)_{loc}(C_A - HC_{LA}) \tag{36}$$

where, C_A and C_{LA} are concentrations of CO_2-gas in the gas-phase and liquid-phase, respectively. According to Equation (24), we assume plug flow for gas phase and well-mixed flow for liquid phase, the material balance equation between Δz at steady state can be rewritten as:

$$(uC_A\big|_z - uC_A\big|_{z+\Delta z})S - r_A\varepsilon_L S\Delta z = 0 \tag{37}$$

Where, u is the mean gas-superficial velocity based on the column cross-sectional area. Take limit for Equation (37),

$$u\frac{dC_A}{dz} + r_A\varepsilon_L = 0 \tag{38}$$

Substitute Equation (36) into Equation (38),

$$u\frac{dC_A}{dz} + (K_G a)_{loc}(C_A - HC_{AL})\varepsilon_L = 0 \tag{39}$$

In Equation (39), C_{AL} is almost less than 4x10^{-8}M when the pH value is higher than 12. In addition, H value is around 1.5 and C_A is higher than 1mM. Therefore, $C_A >> HC_{LA}$, Equation (39) could be written as

$$u\ \frac{dC_A}{dz} + (K_G a)_{loc} C_A\varepsilon_L = 0 \tag{40}$$

We assume that ε_L is kept constant through the column. Integrating Equation (40), we have

$$u\int_{C_{A1}}^{C_{A2}}\frac{dC_A}{C_A} + \varepsilon_L\int_0^L (K_G a)_{loc}\,dz = 0 \tag{41}$$

and,

$$u\ln\frac{C_{A2}}{C_{A1}} + K_G aL\varepsilon_L = 0 \tag{42}$$

where,

$$K_G a = \frac{1}{L}\int_0^L (K_G a)_{loc}\,dz \tag{43}$$

By multiplying S with Equation (42), the equation becomes

$$K_G a = \frac{Q_g}{V_L}\ln\frac{C_{A1}}{C_{A2}} \tag{44}$$

Using this equation, the average overall mass-transfer coefficient can be evaluated in terms of measurable quantities.

Furthermore, the overall mass-transfer coefficient is correlated with the individual mass-transfer coefficients:

$$\frac{1}{K_G a} = \frac{1}{k_G a} + \frac{H}{k_L a} \tag{45}$$

Here, $1/K_G a$ was overall resistance, $1/k_G a$ the gas-side resistance, and $H/k_L a$ the liquid-side resistance. For a second order reaction, by introducing the enhancement factor into Equation (45), we have

$$\frac{1}{K_G a} = \frac{1}{k_G a} + \frac{1}{((D_A k_2)^{1/2} a)} \frac{H}{C_{B0}^{1/2}}, \tag{46}$$

where k_2 is the second order reaction constant and D_A is the diffusion coefficient for carbon dioxide. Since Henry's constant is a function of the ionic strength and temperature, which can be adjusted with pH values and temperature, a plot of Equation (46) to obtain $k_G a$ and $k_L a$ becomes possible.

5.1 Comparisons of absorption rates overall mass-transfer coefficients

In here, we will compare absorption rate and overall mass transfer coefficient obtained in a bubble-column scrubber for five absorption systems, i.e., $NaOH/BaCl_2/H_2O$, $NaOH/Zn(NO_3)_2/H_2O$, $MEA/CO_2/H_2O$, $MEA/CaCl_2/CO_2$, and $NH_3/CO_2/H_2O$. The process variables are working temperature, gas-flow rate, pH value, and gas concentration. The absorption rates and overall mass transfer coefficients are listed in Table 2. The table shows that the absorption rates obtained for $NaOH/Zn(NO_3)_2/H_2O$ system were in the range of 1.34×10^{-4}-2.88×10^{-3}mol/L.s, which were higher than that the other systems. However, the absorption rates for $NH_3/CO_2/H_2O$ system were in the range of 2.17×10^{-4}-1.09×10^{-3} mol/L.s; the values were comparable with that $NaOH/Zn(NO_3)_2/H_2O$ system. On the other hand, the overall mass-transfer coefficients obtained for $MEA/CO_2/H_2O$ system were higher than the others, while the values for $NH_3/CO_2/H_2O$ and $NaOH/Zn(NO_3)_2/H_2O$ systems were also comparable with the $MEA/CO_2/H_2O$ system. By means of Taguchi's analysis for $MEA/CO_2/H_2O$ system, the significance sequence influencing the absorption rate is $A(CO_2\%) > C(\text{temperature}) > D(\text{gas-flow rate}) > B(\text{pH})$, while the significance sequence for mass-transfer coefficient is $B > A > C > D$.

5.2 Individual mass-transfer coefficients

A plot of $1/K_G a$ vs. $H/(C_{B0})^{1/2}$ at different gas-superficial velocity was shown in Figure 5. A linear plot was obtained in this work. The reciprocal of the intercept at zero $H/(C_{B0})^{1/2}$ was the individual gas-side volumetric mass transfer coefficient. On the other hand, the slope, $1/((D_A k_2)^{1/2} a)$, multiplied by $H/C_{B0}^{1/2}$ was $H/k_L a$, where the liquid-side mass transfer $k_L a$ could be obtained.

Figure 6 is a plot of the liquid-side mass transfer coefficient vs. the gas-superficial velocity at various pH values for both with and without precipitation. The liquid-side mass transfer coefficient increased with an increase in the superficial velocity at various pH values. Both procedures show that the data are close together, larger data points for precipitation and smaller data points for no precipitation. The values obtained in this study were higher than those reported by Fan (1989), as shown in the parallelogram, while the values were close to the values reported by Sada et al. (1985). On the other hand, the trend in our data, extrapolated into smaller gas-superficial velocity, was higher than that reported in Sanchez et al. (2005). A linear regression for $k_L a / [OH^-]^{0.5}$ and u was found to be:

Systems	Operating conditions	R_A (mol/L · s)	K_Ga(1/s)
MEA/CO_2/H_2O	T=25 - 45℃ y_1=15% Q_g=4 - 9.5 L/min C_{MEA}=4 M	1.35×10^{-6}—6.22×10^{-4}	0.027—1.120
MEA/$CaCl_2$/CO_2 (with precipitation)	T=25℃ y_1=10 - 30% pH=9 - 11 C_L=0.2 M C_{MEA}=4 M Q_g =2L/min- 9.5L/min	6.26×10^{-6}—3.69×10^{-4}	0.018-0.249
NH_3/CO_2/H_2O (with precipitation)	T=25 - 60℃ y_1=15 - 60% pH=9.5 - 11.5 C_{NH3}=7.7 M Q_g=2 - 5 L/min	2.17×10^{-4}—1.09×10^{-3}	0.0136—0.567
NaOH/$BaCl_2$/H_2O (with precipitation)	T=25℃ y_1=10 - 30% pH=12 - 13 C_L=0.01-0.2 M C_{NaOH}=1-2 M Q_L=50 - 320 ml/min Q_g=2 – 10.7 L/min	4.4×10^{-5}—7.69×10^{-4}	0.0277—0.196
NaOH/$BaCl_2$/H_2O (without precipitation)	T=25℃ y_1=20% pH=12 - 13 C_{NaOH}=1-2 M Q_L=50 ml/min Q_g=2 – 10.7 L/min	1.03×10^{-4}—1.13×10^{-3}	0.0651—0.339
NaOH/$Zn(NO_3)_2$/H_2O (with precipitation)	T=25 - 45℃ y_1=20% pH=10 -13 C_L=0.2 M C_{NaOH}=2 M Q_L=50 ml/min Q_g=3 - 8 L/min	1.34×10^{-4}—2.88×10^{-3}	0.0145—0.590

Table 2. Absorption rates and overall mass-transfer coefficients in a bubble-column scrubber for different systems.

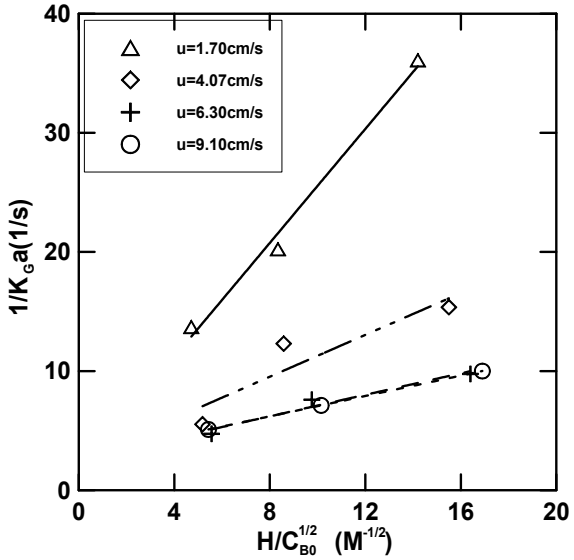

Fig. 5. A plot of $1/K_Ga$ versus $H/C_{B0}^{1/2}$ for obtaining individual mass transfer coefficients (Chen et al., 2008)

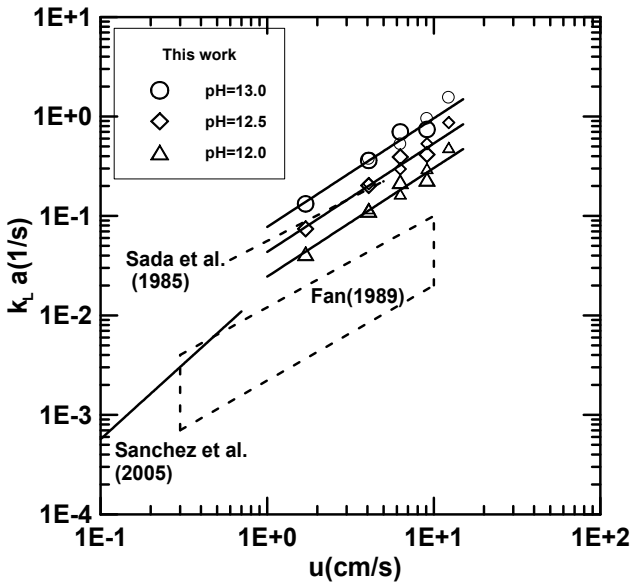

Fig. 6. Effects of process variables on the liquid side mass transfer coefficient.(Chen et al., 2008)

$$k_L a = 0.2449 u^{1.09} [OH^-]^{0.5} \quad (47)$$

The coefficient of determination becomes 0.9670. The exponent of u in here was 1.09, which falls in the exponent range of 0.58 to1.52 reported in the literature. In the same absorption system, a correlation for gas-side mass transfer coefficient obtained by using regression for no precipitation system was shown below:

$$k_G a = 0.29982 u^{0.22} \quad (48)$$

The exponent of u in here was 0.22, which is lower than 0.75 reported in the literature (Sada et al., 1985; Botton et al., 1980). Due to this, the individual mass-transfer coefficients, $k_L a$ and $k_G a$, could be determined when the operating conditions were given; and hence, the overall mass-transfer coefficient was estimated by Equation (45).

6. Scrubbing factor

The scrubbing factor (φ) was defined as $\varphi=(F_g E / F_A V_b)$, which means moles of CO_2-gas to be removed per mole of absorbent and per the volume of the scrubber, estimated values for various scrubbers were also calculated and listed in Table 3. In these systems, F_A is defined as the molar flow rate of absorbent solution. The result showed that φ values in here, both for systems with precipitation and without precipitation, are much higher than those in packed bed systems, indicating that bubble-column scrubbers are indeed more effective than packed bed scrubbers. The scrubbing factors for bubble columns are approximation 5-fold to 20-fold as compared with packed beds. This indicates that the absorption capacity for bubble columns is higher than that for packed beds. Alternatively, comparison for various bubble columns, i.e., NaOH/$BaCl_2$/H_2O system (1), NaOH/$Zn(NO_3)_2$/H_2O system(2), NH_3/CO_2/H_2O system(3), and MEA/CO_2/H_2O system(4), is carried out in here, we find that the magnitude sequence in scrubbing factors are (1) > (3) > (4) > (2). In the current stage system (4) is a more popular system in the removal of carbon dioxide. However, system (3) is a more attractive process since aqueous ammonia absorbent has a lot of advantages, including higher absorption capacity, cheaper, lower energy required from the viewpoint of regeneration, no corrosion problem, and safety, as compared with MEA process (Yeh & Bai, 1999; Yeh et al., 2005). Ammonia scrubbing process is widely applied to produce ammonia bicarbonate (ABC) as a fertilizer in the Chinese chemical industry.

Scrubbers	Operating conditions	$K_G a$(1/s)	$\varphi=(F_g E / F_A V_b)$ (mol/mol-L)
Packed bed (Tontiwachwuthiku et al., 1992)	Q_g=0.87-1.47L/min Q_L=1230-1760ml/min y_1=11.5-19.5% [NaOH]=1.2-2.0M	-	$1.33x10^{-3}$-$6.56x10^{-3}$
Packed bed (Aroonwilas and Tontiwachwuthiku,1997)	-	0.08-0.27*	-
Packed bed with structured packing (Aroonwilas and Tontiwachwuthiku,1997)	Q_g=4.9-10.4L/min Q_L=23-70ml/min y_1=1-15% [NaOH]=1.0-2.0M	0.68-2.74*	0.0176-0.173

	Q_g=4.9-10.4L/min Q_L=46mL/min AMP=1.1M	0.07	-
RPB (Lin et al, 2003)	Q_g=4.4-13.1L/min Q_L=42ml/min y_1=1-10% [NaOH]=2.0M	0.41-0.53**	0.0508-0.151***
	Q_g=4.4-13.1L/min Q_L=42mL/min AMP=1.0M	0.14	-
	Q_g=4.4-13.1L/min Q_L=42mL/min [MEA]=2.0M [MEA+AMP]=2M	0.50-0.75 0.41-0.51	-
Bubble column without precipitation NaOH/$BaCO_3$/H_2O (Chen et al., 2008)	Q_g=4.7-14.5 L/min Q_L=50ml/min y_1=20% [NaOH]= 2.0M T=25℃ pH=9.0-12.0	0.0651- 0.3396	0.178-0.872
Bubble column with precipitation NaOH/$BaCl_2$/H_2O (Chen et al., 2008)	Q_g=2.0-10.27 L/min Q_L=50-320ml/min C_L=0.01-0.2M y_1=10-30% [NaOH]= 2.0M	0.0227- 0.2115	0.0422-0.637
Bubble column without precipitation MEA/H_2O/CO_2 (Chen et al., 2010)	Q_g=4.0-9.5 L/min Q_L=31.35- 215.13ml/min y_1=15-65% [MEA]= 4.0M T=25-45℃ pH=9.0-11.0	0.027-1.1204	0.118-0.494
Bubble column (with precipitation) NH_3/CO_2/H_2O (Chen et al., 2010)	T=25 - 60℃ y_1=15 - 60% pH=9.5 - 11.5 C_{NH3}=7.7 M Q_g=2 - 5 L/min	0.0136－0.56 69	0.0251-0.664
Bubble column (with precipitation) NaOH/$Zn(NO_3)_2$/H_2O (Chen et al., 2010)	T=25 - 45℃ y_1=20% pH=10 -13 C_L=0.2 M C_{NaOH}=2 M Q_L=50 ml/min Q_g=3 - 8 L/min	0.0145－0.59 0	0.0275-0.401

*:'a' is based on volume of packing;**: 'a' is based on dispersion phase; ***: E is assumed to be 0.8.

Table 3. Scrubbing factors for different absorption systems

7. Sizes of bubble-column scrubbers

For a second order instantaneous chemical reaction system, Equation (39) can be applied for gas-side material balance:

$$u\frac{dC_A}{dz}+(K_Ga)_{loc}(C_A-HC_{AL})\varepsilon_L=0 \tag{39}$$

Integrating equation (39) from 0 to Z, we have

$$u\int_{C_{A1}}^{C_{A2}}\frac{dC_A}{C_A-HC_{AL}}+\varepsilon_L K_G a Z=0 \tag{49}$$

where

$$K_Ga=\frac{1}{Z}\int_0^Z(K_Ga)_{loc}dz \tag{50}$$

Combination of overall mass-transfer coefficient, Equation (49) becomes

$$Z=\frac{u}{\varepsilon_L K_G a}\int_{C_{A2}}^{C_{A1}}\frac{dC_A}{C_A-HC_{AL}}=\frac{u}{\frac{\varepsilon_L}{\frac{1}{k_Ga}+\frac{H}{k_La}}}\int_{C_{A2}}^{C_{A1}}\frac{dC_A}{C_A-HC_{AL}} \tag{51}$$

or

$$V_b=\frac{F_{A1}}{C_{A1}\varepsilon_L K_G a}\int_{C_{A2}}^{C_{A1}}\frac{dC_A}{C_A-HC_{AL}}=\frac{F_{A1}}{\frac{C_{A1}\varepsilon_L}{\frac{1}{k_Ga}+\frac{H}{k_La}}}\int_{C_{A2}}^{C_{A1}}\frac{dC_A}{C_A-HC_{AL}} \tag{52}$$

where V_b(=SZ) is the volume of scrubber and F_{A1} is the molar flow rate of input gas. If $C_A>>HC_{LA}$, Equation (52) could be written as:

$$V_b=\frac{F_{A1}}{C_{A1}\varepsilon_L K_G a}\ln\frac{C_{A1}}{C_{A2}}=\frac{F_{A1}}{\frac{C_{A1}\varepsilon_L}{\frac{1}{k_Ga}+\frac{H}{k_La}}}\ln\frac{C_{A1}}{C_{A2}} \tag{53}$$

Equation (53) shows that the size of scrubber is dependent on gas-flow rate, H (ionic strength and temperature), the pH of the solution, liquid hold-up (ε_L), and desired CO_2 output concentration (C_{A2}). In here, k_Ga and k_La can be evaluated by using Equations (47) and (48) if pH and u are given. In addition, liquid hold-up (ε_L) can be estimated according to Figure 7, a plot of 1-ε_L(gas hold-up) versus $u(\frac{1}{\rho}\times\frac{72}{\sigma})^{1/3}$, where ρ and σ are the density and surface tension of the liquid in cgs unit. The final correlation has been given as a curve on

log-log coordinates, which can be represented well by the following Equation (Hikita et al., 1980):

$$1-\varepsilon_L = \frac{1}{2+(0.35/u)[(\rho/1)(\sigma/72)]^{1/3}} \tag{54}$$

Some useful correlations for gas hold-up can be found in the literature (Hikita et al., 1980).

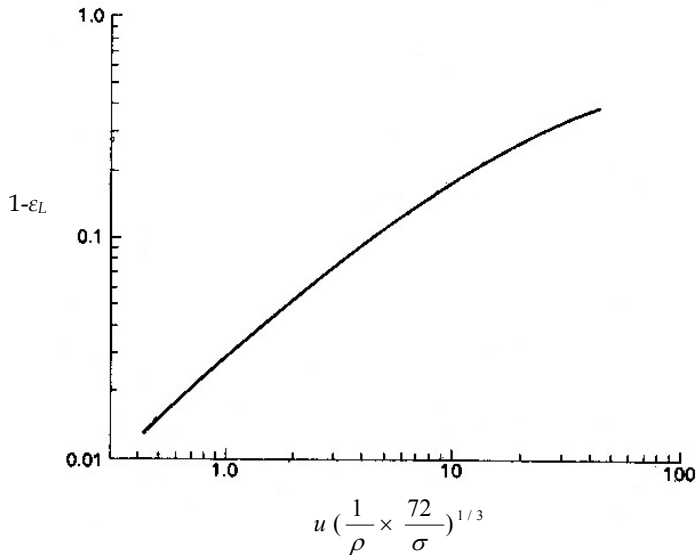

Fig. 7. Gas hold-up in bubble-columns (Danckwerts, 1970)

On the other hand, H can be calculated by using Equations (20) and (22) when the ionic strength and temperature are given. Sometime if overall mass-transfer coefficient correlation is obtained, such as MEA/$CaCl_2$/CO_2 with precipitation system, the overall mass-transfer coefficient can be estimated when u and pH of the solution are available:

$$K_G a = 2.62\times10^{-5}u^{1.76}\exp(0.41pH) \tag{55}$$

8. Conclusion

In this chapter, absorption of CO_2 in a continuous bubble-column scrubber was illustrated for four absorption systems. In order to obtain absorption rate and mass-transfer coefficients in an alkaline solution with and without precipitation, a two-film model with fast reaction case was utilized to study the absorption of carbon dioxide. A multiple-tube plug flow model was developed to determine the absorption rate and overall mass-transfer coefficient. At the gas-liquid interface, the Henry's law is applied to connect between the bulk phases. In order to determine Henry's law constant, the ionic strength can be determined by using an ionic strength approximation method, if the pH of solution, the total mass balance equations, mass action equations, and activity coefficient equations are available.

Combinations of mass-transfer rate, overall mass-transfer coefficient, Henry's law constant and individual mass-transfer coefficients, the overall mass-transfer coefficient can correlate with the individual mass-transfer coefficients. For a second order reaction, by introducing the enhancement factor into correlation equation, we can obtain both gas-side and liquid-side individual mass-transfer coefficients by using measurable data. The effects of process variables on the individual mass-transfer coefficients were discussed and we obtained kinetic expressions for the both. Using Taguchi's analysis for MEA/H_2O/CO_2 system, it was found that the significance sequence influencing the absorption rate is A(CO_2%) > C(temperature) > D(gas-flow rate) > B(pH), while the significance sequence for mass-transfer coefficient is B > A > C > D. According to scrubbing factor defined in here, it was found that the scrubbing factors for bubble columns are always higher than that packed beds. This illustrates a higher scrubbing capacity for bubble columns as compared with packed beds. Finally, according to the material balance model proposed in here, the size of bubble column scrubber could be evaluated when the individual mass-transfer coefficients are available.

9. Acknowledgement

The authors acknowledge the financial support of National Science Council of the Republic of China (NSC-99-2221-E-262-024).

10. Nomenclature

A= total surface area of bubbles in scrubber (cm^2)

a= gas-liquid interfacial area based on the slurry volume (1/cm)

B_1= a constant in Eq.(16)

C_A= concentration of component A (mol/L)

C_B= concentration of component B (mol/L)

C_{A1}= concentration of A in gas phase at inlet (mol/L)

C_{A2}= concentration of A in gas phase at outlet (mol/L)

C_{Ai}= concentration of A at gas side interface (mol/L)

C_{Bi}= concentration of B at liquid side interface (mol/L)

C_1= concentration of chloride ion at the inlet (mol/L)

C_2= concentration of NaOH at the inlet (mol/L)

C_{B0}= concentration of hydroxide ion (mol/L)

C_g=concentration of solute in bulk gas phase (mol/L)

C_{g1}=concentration of CO_2-gas at inlet (mol/L)

C_{g2}=concentration of CO_2-gas at outlet (mol/L)

C_L= concentration of solute in solution (mol/L)

C_{LA}= concentration of component A in liquid phase (mol/L)

C_T=total carbonate concentration (mol/L)

D_A= diffusivity (cm^2/s)

E= removal efficiency

F_{A1}= molar flow rate of the CO_2-gas at the inlet (mol/s)

F_{A2}=molar flow rate of the CO_2-gas at the outlet (mol/s)

F_g= gas-molar-flow rate (mol/s)

F_L= liquid-molar-flow rate (mol/s)

F_A= absorbent A molar-flow rate (mol/s)

H= Henry's law constant

I= ionic strength (mol/L)

k_2= second order reaction constant (L/mol s)

k_La= individual volumetric liquid-side mass-transfer coefficient (s^{-1})

k_Ga= individual volumetric gas-side mass-transfer coefficient (s^{-1})

K_Ga= overall mass-transfer coefficient (s^{-1})

$(K_Ga)_{loc}$= local mass-transfer coefficient (s^{-1})

K_H= Henry's constant defined in Eq.(1)

L=height of the bubble column (cm)

P_i= partial pressure of component i (atm)

P_{Ai}= partial pressure of component A at interface (atm)

Q_1=feed rate of $BaCl_2$ solution (mL/min)

Q_2=feed rate of NaOH solution (mL/min)

Q_g= gas-flow rate (L/min)

Q_L= feed rate of liquid solution (mL/min)

R= universal gas constant (atm-L/K mol)

R_A=absorption rate (mol/s L)

r_A=mass-transfer rate (mol/s cm^2)

$\overline{r}_A$ =average mass-transfer rate defined in Eq.(30)(mol/s cm^2)

S=cross section area (cm^2)

T= absolute temperature (K)

TBa= total barium ion concentration (mol/L)

TCO= total carbonate ion concentration (mol/L)

TCl= total chloride ion concentration (mol/L)

TNa= total sodium ion concentration, mol/L

u= superficial velocity (cm/s)

V_b= volume of the bubble column (L)

V_L= volume of liquid in bubble column (L)

y_1=molar fraction of CO_2-gas at the inlet (%)

y_2=molar fraction of CO_2-gas at the outlet (%)

z= position in the bubble column (cm)

Greek symbols

α_i=degree of ionization, i=0,1,2

γ_i= activity coefficient

ε_L= hold-up of liquid

ρ=density of fluid (g/cm^3)

σ=surface tension (dyn/cm)

φ= scrubbing factor (mol-CO_2/mol·L)

11. References

Aroonwilas, A.; Tontiwachwuthikul, P. (1997). High-efficiency Structured Packing for CO_2 Separation Using 2-amino-2-methyl-1-propanol(AMP). *Separation and Purification Technology*, *12*, pp.67-79.

Botton, R., Cosserrat, D. and Charpentier, J. C. (1980). Mass Transfer in Bubble Columns Operating at High Gas Throughputs, *Chem. Eng. J.*, 20, pp.87-94.

Butler, J. N. (1964). *Ionic Equilibrium*, Addison-Wesley Publishing Company, Inc., USA.

Butler, J. N. (1982). *Carbon Dioxide Equilibriua and Their Applications*, Addison-Wesley Publishing Company, Inc., USA.

Bukur, D. B. and Daly, J. G. (1987). Gas hold-up in bubble columns for Fischer-Tropsch synthesis, *Chem. Eng. Sci.*, 42(12), pp.2967-2969.

Chen, P. C.; Shi, W.; Du, R.; Chen, V. (2008). Scrubbing of CO_2 greenhouse gas accompanying with precipitation in a continuous bubble-column scrubber, *I&EC* , 47, pp.6336-6343.

Chen, P. C.; Chen, C. C.; Fun, M. H.; Liao, O. Y.; Jiang, J. J.; Wang, Y. S.; Chen, C. S. (2004). Mixing and Crystallization Kinetics in Gas-liquid Reactive Crystallization. *Chem. Eng. Tech.*, *27*, pp.519-531.

Chen, P. C.; Kou, K. L. ; Tai, H. K.; Jin, S. L.; Lye, C. L.; Lin, C. Y. (2002). Removal of Carbon Dioxide by Reactive Crystallization in a Scrubber---Kinetics of Barium Carbonate Crystals. *J. Crystal Growth*, *237-239*, pp.2166-2171.

Cournil, M.; Herri, J. M. (2003). Asymptotic Models for Gas-Liquid Crystallization in Two-Film Systems, *AIChE J.*, 49(8), pp.2031-2038.

Danckwerts, P. V. (1970). *Gas-Liquid Reactions*, McGraw-Hill, NewYork, USA.

Degaleesan, S.; Dudukovic, M. P. (1998). Liquid Backing in Bubble Columns and the Axial Dispersion Coefficient, *AIChE J.*, 44(11), pp.2369-2378.

Fan, L. S. (1989). *Gas-Liquid-Solid Fluidization Engineering*; Butterworths: New York, USA.

Hamid, S. N. S.; Jones, A. G. (2002). Scale up of gas-liquid precipitation of calcium carbonate crystals in draft tube bubble columns, *15th Ind. Cry., Serrento, Italy*(2002)(CD-ROM)

Hikita, H.; Asai,S.; Tanigawa, K; Segawa, K; Kitao, M.(1980). Gas hold-up in bubble columns, *The Chemical Engineering Journal*, 20, pp.59-67.

Hudson, J. L.; Rochelle, G. T. (1982). *Flue Gas Desulfurization*, American Chemical Society, ACS Symposium Series 188, Washington, D.C., U.S.A..

Kim, S; Kim, H. T. (2004). Aspen simulation of CO_2 absorption system with various amine solution, *Prepr. Pap.-Am. Chem. Soc., Div. Fuel Chem.*, 49(1), pp.251-252.

Lapin, A.; Paaschen, T.; Junghans, K.; Lubbert, A. (2002). Bubble Column Fluid Dynamics, Flow Structures in Slender Columns with Large-Diameter Ring-Spargers, *Chem. Eng. Sci.*, 57, pp.1419-1424.

Levenspiel, O. (1998). *Chemical Reaction Engineering*, 3rd ed., Chapters 23-24, John Wiley & Sons.

Lin, C. C.; Liu, W. T.; Tan, C. S.(2003). Removal of Carbon Dioxide by Absorption in a Rotating Packed Bed. *Ind. Eng. Chem. Res.*, *42*, pp.2381-2386.

Juvekar, V. A.; Sharma, M.M. Absorption of CO_2 in a suspension of lime, *Chem. Eng. Sci.*, 28, pp.825-837.

Morel, F. M. M. (1983). *Principles of Aquatic Chemistry*; John Wiley & Sons: New York.

Nancollas, G. H.(1966). *Interactions in Electrolyte Solutions*, Elsevier Publishing Company, Amsterdam, Netherlands.

Okawa, T.; Tsuge, H.; Matsue, H. (1999). Reactive crystallization of $CaCO_3$ in a gas-liquid multistage column crystallizer, *14th Ind. Cry.* 1999(CD-ROM)

Sada, E.; Kumazawa, H.; Lee, C.; Fujiwara, N. (1985). Gas-Liquid Mass Transfer Characteristics in a Bubble Column With Suspended Sparingly Soluble Fine Particles, *Ind. Eng. Chem. Process Des. Dev.*, 24, pp.255-261.

Saha, A. K.; Bandyopadhyay, S.S. Absorption of carbon dioxide in alkanolamines in the presence of fine activated carbon particles, *Can. J. Chem. Eng.*, 70, pp.193-196.

Shah, Y. T. (1979). *Gas-Liquid-Solid Reactor Design*; McGraw-Hill; New York.

Sauer, T.; Hempel, D. C. (1987). Fluid dynamics and mass transfer in a bubble column with suspended particles,*Chem. Eng. Technol.* 10, pp.180-189.

Sanchez, O.; Michaud, S.; Escudie, R.; Delgenes, J. P.; Bernet, N.(2005). Liquid Mixing and Gas-liquid Mass Transfer in a Three-phase Inverse Turbulent Bed Reactor. *Chemical Engineering J.*, *114*, pp.114-120.

Shah, Y. T.(1979). *Gas-Liquid-Solid Reactor Design*; McGraw-Hill; New York.

Sherwood, T. K.; Pigford, R. L.; Wilke, C. R. (1975). *Mass Transfer*; McGraw-Hill Inc.; New York.

Sohnel, O.; Garside, J. (1992). *Precipitation*; Butterworth-Heinemann Ltd.: Oxford.

Stewart, C.; Hessami, M. A study of methods of carbon dioxide capture and sequestration---the sustainability of a photosynthetic bioreactor approach, *Energy Conversion and management*, 46, pp.403-420.

Tontiwachwuthikul, P.; Meisen, A.; Lim, J. (1992). CO_2 Absorption by NaOH, Monoethanolamine and 2-amino-2-methyl-1-propanol Solutions in a Packed bed, *Chem. Eng. Sci.*, *47*, pp.381-390.

Yang, H.; Xu, Z.; Fan, M; Cupta, R; Slimane, R. B.; Bland, A. E.; Wright, I. (2008). Process in carbon dioxide sepration and capture: A review, *J. of Environmental Sciences*, 20, pp.14-27.

Yeh, A. C.; Bai, H. (1999). Comparison of ammonia and monoethanolamine solvents to reduce CO_2 greenhouse gas emissions, *The Science of the Total Environment*, *228*, pp.121-133.

Yeh,J. T.; Resnik, K. P.; Rygle, K.; Pennline, H. W. (2005). Semi-batch absorption and regeneration studies for CO_2 capture by aqueous ammonia, *Fuel Processing Technology*, *86*, pp.1533-1546.

6

Ethylbenzene Dehydrogenation in the Presence of Carbon Dioxide over Metal Oxides

Maria do Carmo Rangel[1], Ana Paula de Melo Monteiro[1], Marcelo Oportus[2], Patricio Reyes[2], Márcia de Souza Ramos[1] and Sirlene Barbosa Lima[1]
[1]*GECCAT Grupo de Estudos em Cinética e Catálise, Instituto de Química, Universidade Federal da Bahia*
[2]*Facultad de Ciencias Químicas, Universidad de Concepción, Casilla 3-C, Concepción,*
[1]*Brazil*
[2]*Chile*

1. Introduction

1.1 The use of carbon dioxide for chemicals manufacture

Because of the harmful effects to the environment, there is an increasing concern worldwide for decreasing the amount of atmospheric carbon dioxide. The average temperature of the earth, caused by greenhouse gases, has been increased in such a value that can cause catastrophic events. Several solutions have been proposed to overcome this problem, but they basically involve two approaches: (i) the decrease of carbon monoxide emissions or (ii) the application in innovative technologies to capture and use it. Both alternatives have been studied and discussed and several applications have been proposed (Song, 2006).

The global chemical industry uses about 115 million metric tons of carbon dioxide every year as feedstock in a variety of synthetic processes. This number is insignificant compared to 23.7 billion metric tons estimated annual global emissions of the gas caused by human activities, primarily the burning of fossil fuels. In addition, the total anthropogenic emissions of carbon dioxide, approximately 45%, remain in the atmosphere, as a result of a gradual accumulation of carbon dioxide (Ritter, 2005).

It is believed that the amount of carbon dioxide used by chemical industry could easily be tripled using current technologies, but that still does not solve the problem, since only its use by the chemical industry is not enough to significantly reduce carbon dioxide emissions. Because of the scale of the problem, different strategies need to be used simultaneously, including increasing the efficiency of current processes, as well as the capture and use or storage of carbon dioxide generated by burning fossil fuels and using renewable fuels and energy sources. As a result of the development of the chemistry based on carbon dioxide, a reduction in the use of toxic products in chemical industry is expected with an improvement in health and safety (Ritter, 2005). Therefore, there is a significant effort of scientific and technological community to discuss the use of carbon dioxide in different applications which would provide its elimination from the air and its reuse as raw material for manufacturing other products.

Carbon dioxide can be conveniently used as carbon and/or oxygen sources for the synthesis of chemicals through several processes, both as solvent and/or as reactants. It has potential applications in supercritical conditions, in direct carboxylation reactions, in the conversion of natural gas to liquid (GTL technology) and in methanol synthesis (Aresta and Dibenedetto, 2004). Other studies have shown the use of carbon dioxide as an oxidant in the dehydrogenation of ethane (Murata et al., 2000; Nagakawa et al., 1998), propane (Wang et al., 2000), isobutene (Shimada et al., 1998) and ethylbenzene (Mimura et al., 1998), as well as in methane dry reforming (Wang et al., 2000) and oxidative coupling of methane (Nishiyama and Aika, 1990). Currently, most intermediates in the petrochemical industry are produced from alkenes and aromatics, but their consumption is growing and the existing production capacity is inefficient to provide this market. In addition, alkenes are obtained from cracking processes of natural gas and naphtha which however are very expensive, due to the need of separation and purification of the products (Ogonowski and Skrzynska, 2005).

1.2 The advantages of using carbon dioxide in dehydrogenation reactions

Currently, light alkenes (C2-C4) are obtained by thermal cracking of natural gas and naphtha as well as by catalytic cracking that occurs during oil refining. In addition, they can be produced by catalytic dehydrogenation of hydrocarbons, which has considerable industrial impact, since it provides a route to get the valuable alkenes from low cost feedstock. This process has also the advantage of producing only the desired products, making the plants cheaper to construct and less complicated to operate. Besides alkenes, the dehydrogenation of alkanes can be used to produce hydrogen and oxygenates such as aldehydes and ketones (Nishiyama and Aika, 1990). All these chemicals are important intermediates for the production of polymers, rubbers, detergents and solvents, among other products.

The dehydrogenation of hydrocarbons is reversible and limited by thermodynamic equilibrium and thus the reaction is often performed at high temperatures to increase the conversion. However, this condition leads to hydrocarbons cracking, decreasing the selectivity of the process. These difficulties can be overcome by supplying heat to the reaction by the oxidation of the produced hydrogen or by using an oxidant in the presence of a catalyst, able to perform an oxidation reaction. The reaction thus becomes exothermic and can be carried out at low temperatures, making negligible the formation of cracking products. Another advantage is that the conversion is not strongly limited by thermodynamic factors and then oxidizing agents, such as molecular oxygen, nitrous oxide, halogens, elemental sulfur and carbon dioxide can be used. The use of molecular oxygen or nitrous oxide as oxidants effectively reduces the reaction temperature under atmospheric pressure. Nevertheless, the reaction presents several problems, such as the need of removing the heat of reaction and of controlling the selectivity due to the production of carbon oxides, besides the undesirable flammability of reaction mixtures. Among the oxidizing agents, carbon dioxide has been shown to be the most promising one to be used in dehydrogenation reactions (Bhasin et al., 2001; Krylov et al., 1995; Corberán, 2005).

Chromium oxide (Cr_2O_3) has been used as a commercial catalyst for decades, in the dehydrogenation of light alkanes while chromium-doped hematite is the classical catalyst for ethylbenzene dehydrogenation (Nishiyama and Aika, 1990; Santos et al., 2006; Rangel et al., 2003; Ramos et al., 2008). However, the toxicity of Cr^{+6} ion requires a special care in the

preparation, use and disposal of these catalysts and then there is an interest for developing new green technologies for replacement of these solids. Therefore, several other systems were studied such as cerium oxide (Ikenaga et. al, 2000), manganese oxide (Burri et al., 2006), titanium oxide, vanadium oxide (Burri et al., 2007; Chen et al., 2006) and zirconium oxide among others (Park et al., 2000).

The mechanism of the dehydrogenation reactions of alkanes C_2-C_7 with carbon dioxide over oxide catalysts proved to be different for light and heavy alkanes. The reaction occurs via a redox mechanism but the activation of carbon dioxide can occur by its direct interaction with the reduced catalysts or through the formation of a complex intermediate or by its interaction with the coke produced on the catalyst surface. In the dehydrogenation of ethane and propane, for instance, the removal of oxygen from the oxide-based catalyst occurs as a result of the interaction of the catalyst with the reagent and with the hydrogen which was removed from the alkane molecule. In the case of dehydrogenation of butanes and isobutanes, the reaction occurs through the direct dehydrogenation of alkane followed by the oxidation of hydrogen while for n-heptane both the oxidative function of the catalyst and carbon dioxide lead to coke oxidation. Therefore, it is essential to select catalysts able to adsorb and activate carbon dioxide. The properties of acidic carbon dioxide favor the choice of catalysts with basic properties. However, the alkali and alkaline earth oxides are inefficient because they form carbonate species. Metal oxides of moderate basicity are required and must participate in the redox process with the reduction of carbon dioxide (Krylov at. al, 1995).

The effect of carbon dioxide on the propane and isobutane dehydrogenation is small as compared to ethane dehydrogenation, this can be related to the lower reaction temperatures (600 °C) required to obtain significant conversions, since the dissociation energies for CH_2 or CH groups in propane and isobutane are lower than for CH_3 group in ethane. On the other hand, for ethylbenzene dehydrogenation the produced alkenes contain allylic hydrogen, which has a dissociation energy lower than the starting alkanes. Therefore, the abstraction of hydrogen from the allylic position may favor the formation of coke precursors and the catalyst deactivation cannot be avoided, thereby decreasing the alkenes yield (Wang and Zhu, 2004).

1.3 Ethylbenzene dehydrogenation in the presence of carbon dioxide

Styrene is one of the most used intermediate for organic synthesis, being used as feedstock in the production of synthetic rubbers, plastics and resins copolymers, among other products of high commercial value (Sakurai et al., 2002). This monomer can be obtained by several routes, but the ethylbenzene dehydrogenation in the presence of steam is the main commercial route to produce this monomer. This process allows to supply 90% of the global production of styrene, which is approximately 13 x 10^6 t/year (Sakurai et al., 2002; Cavani and Trifiró, 1995).

Despite being widely used around the world for several years, the ethylbenzene dehydrogenation in the presence of steam (Equation 1) still has some drawbacks, the main one related to the endothermicity and the equilibrium limitation of reaction. As a result, the typical conversion is low, rarely exceeding 50%, even in processes performed at high temperatures (Cavani and Trifiró, 1995). Side reactions also occur, leading to the production of toluene, benzene and coke, which affect the yield of the process and may lead to the

catalyst deactivation (Styles, 1987; Shreve and Brink, 1997). Other problems include the need for recycling of reagents and the use of low ratios steam/ethylbenzene (Cavani and Trifiró, 1995; Styles, 1987; SShreve and Brink, 1997).

$$C_6H_5CH_2CH_{3(g)} + H_2O_{(g)} \rightleftharpoons C_6H_5CH{=}CH_{2(g)} + H_{2(g)} \quad (1)$$

In industrial processes, the catalyst deactivation is minimized by the addition of large amounts of steam, which also shifts the equilibrium increasing the styrene production and eliminates or prevents the formation of coke. In addition, steam oxidizes the catalyst keeping it in a state of highly selective oxidation to styrene (Shreve and Brink, 1997; Herzog et al., 1984).

The most widely used catalysts in ethylbenzene dehydrogenation in the presence of steam are inorganic oxides with promoters (Cavani and Trifiró, 1995; Shreve and Brink, 1997). However, iron oxides containing potassium and chromium oxide are superior to any other known system and have been used in commercial plants, since the first process, for nearly 70 years. Since that time, both the catalyst and the process have undergone several improvements, such as the introduction of beds with radial flow and the use of poison inhibitors (Shreve and Brink, 1997). Several works have been carried out (Santos et al., 2006; Rangel et al., 2003; Ramos et al., 2008; Miyakoshi et al., 2001; Liao et al., 2008) aiming to improve the iron-based catalysts or to find new alternatives systems and process conditions (Holtz et al., 2008; Oliveira et al., 2008; Morán et al., 2007; Ohishi et al., 2005).

A promising alternative to overcome these problems is to perform the process in the presence of carbon dioxide instead of steam. In this case, there is a consumption of 1.5-1.9 x 10^8 cal instead of 1.5 x 10^9 cal per mol of styrene produced, among other advantages of the new process (Mamedov, 1994). In this case, the produced hydrogen is removed as steam by the reverse water gas shift reaction shifting the equilibrium to the formation of dehydrogenation products, as shown in Equation 2. In addition, carbon dioxide removes the coke deposits formed during reaction (Mamedov, 1995).

$$C_6H_5CH_2CH_{3(g)} + CO_{2(g)} \rightleftharpoons C_6H_5CH{=}CH_{2(g)} + CO_{(g)} + H_2O_{(g)} \quad (2)$$

Several authors (Cavani and Trifiró, 1995; Shreve and Brink, 1997; Herzog et al., 1984) have shown that the commercial catalysts based on iron oxide are not satisfactory for ethylbenzene dehydrogenation in the presence of carbon dioxide. Thus, extensive studies have been carried out in order to develop catalytic systems that can operate effectively in the presence of carbon dioxide. Mimura and Saito (Mimura and Saito, 1999; Mimura and Saito, 2000; Saito et. al., 2003) and others (Badstube et al., 1998; Dziembaj et al., 2000), for instance, have investigated iron oxide catalysts promoted with alkali metals supported on alumina and charcoal, respectively, for ethylbenzene dehydrogenation, noting the increased selectivity to the products in the presence of carbon dioxide. Also, the use of carbon dioxide have been studied on iron oxide supported on zirconium oxide and zeolites (Park et al., 2002; Chang et al., 2004), vanadium oxide catalysts and vanadium-antimony supported on alumina (Vislovskiy et al., 2002; Park et al., 2003), in which there was the increased catalytic activity, according to the catalyst. From these studies, they have observed that the effect of carbon dioxide on the activity, selectivity and stability for ethylbenzene dehydrogenation depends on the kind of the catalyst. In the case of zirconia, the positive effect of carbon dioxide was found to be highly dependent on the crystalline phase at 550 °C, the tetragonal one has presented high activity and selectivity to styrene (Vislovsskiy et al., 2002). This

finding was related to differences in specific surface area of the solids and its affinity with carbon dioxide associated with the surface basic sites (Pereira et al., 2004; Sun et al., 2002). In other works, zirconium oxide (Vislovsskiy et al., 2002), mixed oxides of zirconium with titanium or manganese (Park et al., 2000) and mixed oxide of zirconium and cerium supported on SBA-15 (Burri et al., 2006) have led to around 65% of conversion and 95% of selectivity to styrene. On the other hand, Jurczyk and Kania (1989) have found a relationship between the acidic or basic properties and the selectivity of the catalysts by studying binary oxides supported on alumina.

Activated carbons-based catalysts have also proved to be active in ethylbenzne dehydrogenation in the presence of carbon dioxide. Badstube et al. (2000), for instance, have investigated catalysts based on iron supported on activated carbon in ethylbenzene dehydrogenation coupled with the reverse of water gas shift reaction and have found high activity and selectivity to styrene at 550 °C. In addition, Sakurai et al. (2000) have studied active-carbon supported vanadium catalysts at 450-650 °C and also have noted high conversion (67.1%) and selectivity to styrene (80%) at 550 °C. They also found that ethylbenzene conversion in the presence of carbon dioxide was 14% higher than in the presence of argon. Moreover, we have found (Oliveira et al., 2008) that spherical activated carbon-supported copper are promising catalysts for ethylbenzene dehydrogenation in the presence of carbon dioxide. The catalyst with the lowest amount of copper was the most promising one, showing high activity and resistance against deactivation, being able to work up to 600 °C.

In spite of the several studies addressed to metal oxides-based catalysts for ethylbenzene dehydrogenation in the presence of carbon dioxide, there is not a systematic comparison of their behavior in ethybenzene dehydrogenation. In the present work, we compare the activity and selectivity of lanthana, magnesia, niobia, titania and zirconia aiming to state the individual contribution of these pure oxides to the performance of the catalysts for ethylbenzene dehydrogenation in the presence of carbon dioxide.

2. Experimental

2.1 Catalysts preparation

Commercial niobium oxide (Nb_2O_5) and titanium oxide (TiO_2) in rutile phase were kindly supplied by CBMM (HY 340) and Milleniun (T-568), respectively. Lanthanum oxide (La_2O_3), magnesia (MgO) and zirconia (ZrO_2) were prepared in the laboratory.

Zirconium oxide was obtained by the hydrolysis of zirconium oxychloride (250 mL, 1 $mol.L^{-1}$) with ammonium hydroxide (8 % w/w). These solutions were added simultaneously (10 $mL.min^{-1}$) to a beaker containing 50 mL of distilled water, keeping the system under stirring at room temperature. After addition of the reactants, the pH was adjusted to 10 by adding a concentrated ammonium hydroxide solution (30% w/w). The sol was aged for 24 h under stirring and centrifuged at 2500 rpm, for 4 min. The gel obtained was then washed with distilled water. The steps of washing and centrifugation were repeated until no chloride ions detected in the supernatant anymore. The gel was dried at 120 °C, for 12 h, ground and sieved in 100 mesh. In the case of lanthanum oxide and magnesium oxide, lanthanum nitrate and magnesium nitrate solutions (250 mL, 1 $mol.L^{-1}$) were used, respectively, following the method described.

All solids were heated (10 °C.min^{-1}) under air flow (50 mL.min^{-1}) up to 750 °C and kept at this temperature for 5 h to get the L (lanthana), M (magnesia), N (niobia), Z (zirconia) and T (titania) samples.

2.2 Catalysts characterization

Samples were characterized by X-ray diffraction (XRD), specific surface area (Sg) and porosity measurements, thermoprogrammed reduction (TPR) and thermoprogrammed ammonia desorption (NH_3-TPD).

The XRD powder patterns of the solids were obtained in a Shimadzu model XD3A equipment, using CuKα (λ=1.5420 nm) radiation and nickel filter, in a 2θ range between 10-80°, with a scanning speed of 2 °/min.

The specific surface area and porosity measurements were carried out by the BET method in a Micromeritics model TPD/TPR 2900 equipment, using a 30% N_2/He mixture. The sample was previously heated at a rate of 10 °.min^{-1} up to 170 °C, under nitrogen flow (60 mL.min^{-1}), remaining 30 min at this temperature. The TPR profiles were obtained in the same equipment. The samples (0.25-0.3 g) were heated from 27 and 1000 °C, at a rate of 10 °. min^{-1}, under flow of a 5% H_2/N_2 mixture.

The Micromeritics model TPD/TPR 2900 equipment was also used for the acidity measurements by desorption of ammonia (NH_3-TPD). The sample was heated at 110 °C, under nitrogen flow, during 30 min and then saturated with ammonia, injecting this gas through a calibrated loop. After cooling at room temperature, the temperature programmed desorption began, heating the solid from 30 up to 770 °C, under a heating rate of 10°. min^{-1}, using argon as gas carrier (45 mL. min^{-1}).

2.3 Catalysts evaluation

In the catalysts evaluation, the sample (0.3 g) was placed in a fixed bed microreactor and the system was heated under nitrogen flow (20 mL.min^{-1}) up to the reaction temperature (600 °C). The nitrogen flow was then interrupted and a gaseous mixture containing ethylbenzene and nitrogen (coming from a saturator with ethylbenzene at 77 °C) was mixed with a carbon dioxide stream in a chamber and then fed to the reactor. The experiments were performed at atmospheric pressure, using a carbon dioxide to ethylbenzene molar ratio of 10. The gaseous effluent was monitored continuously by a Varian model 3600-X chromatograph with ionization flame detection system, in injection intervals of 30 min. The reaction conditions was adjusted to eliminate the diffusion limitations and to get stable values of 10% of conversion with a commercial catalyst at 600 °C.

3. Results and discussion

3.1 X-ray diffraction

The X-ray diffractograms of the catalysts before (fresh) and after (spent) ethylbenzene dehydrogenation in the presence of carbon dioxide are displayed in Figure 1. It can be seen that fresh lanthana is made of a mixture of hexagonal lanthanum oxide, La_2O_3 (JCPDS 83-1354) and lanthanum hydroxide, $La(OH)_3$ (JCPDS 83-2034) while the spent catalyst has only lanthanum oxide.

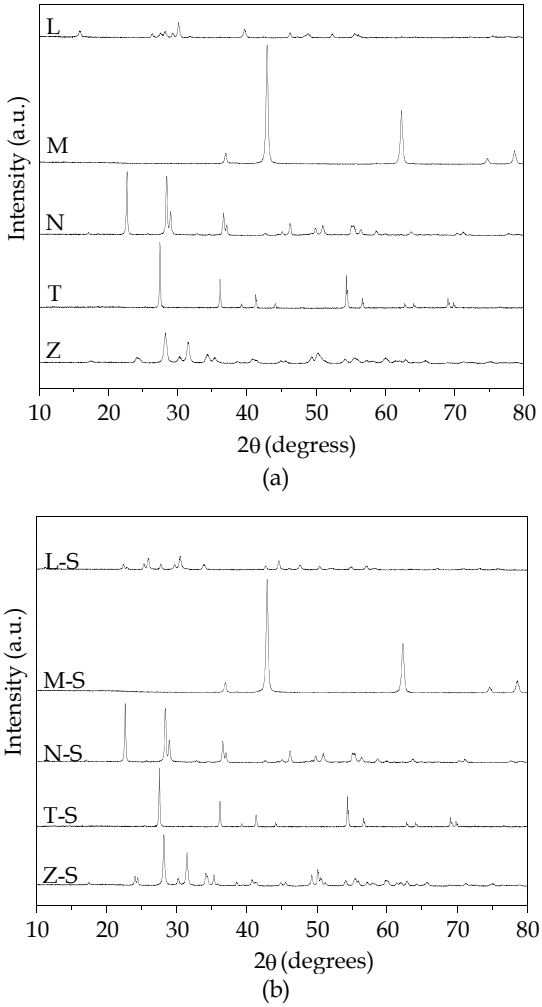

Fig. 1. X-ray diffractograms of the catalysts (a) before and (b) after ethylbenzene dehydrogenation in the presence of carbon dioxide. L= lanthana; M= magnesia; N= niobia; T= titania; Z= zirconia.

On the other hand, the other samples did not go on phase transition during reaction, indicating that they are stable under ethylbenzene dehydrogenation in the presence of carbon dioxide. Moreover, no significant widening or narrowing of the peaks for the fresh and spent catalysts was noted, indicating no change in crystallinity and/or particles size.

For the magnesium-containing solid, cubic magnesium oxide, MgO (JCPDS 87-0652) was found in the catalysts while the monoclinic phase of niobium oxide, Nb_2O_5 (JCPDS 74-0298) was detected for N sample. The tetragonal phase of titanium oxide (rutile), TiO_2 (JCPDS 88-1172) was found for T sample. Zirconium oxide (ZrO_2) showed a typical profile of the monoclinic phase (JCPDS 86-1450) but with several peaks coincident with those of the

tetragonal (JCPDS 88-1007) or cubic (JCPDS 81-550) phases and then the presence of these phases cannot be discarded.

3.2 Thermoprogrammed reduction

Figure 2 shows the reduction profiles of the catalysts. As we can see, the L sample shows a curve with only one reduction peak around 636 °C, which can be related to the reduction of nitrate species and/or the reduction of lanthanum oxide (Santos et al. 2005; Hoang et al., 2003).

On the other hand, the solid based on niobium (N sample) displays a curve with two reduction peaks, the first one at 645 °C can be attributed to the formation of carbon monoxide and dioxide produced from the carbon residue of the precursor, used in the commercial preparation. The second peak, at 894 °C, is related to the reduction of Nb^{+5} to Nb^{+4} species (Pereira et al., 2000).

The sample containing titanium (T sample) displays a curve with a small and broad reduction peak at 487 °C, assigned to a small reduction of titania (Lenzi et al., 2011). The solid based on magnesium oxide (M sample) presents a curve with a reduction peak centered at 318 °C, related to the reduction of nitrate species and another in the range of 400-850 °C. The curve of zirconium oxide (Z sample) presents two reduction peaks, the first centered at 665 °C and the second one centered at 786 °C (Maity et al., 2000). These results are in agreement with previous works (Santos et al. 2005; Hoang et al., 2003; Pereira et al., 2000; Lenzi et al., 2011; Maity et al., 2000) and indicate that the reducibility increases in the sequence T <N <Z <L <M.

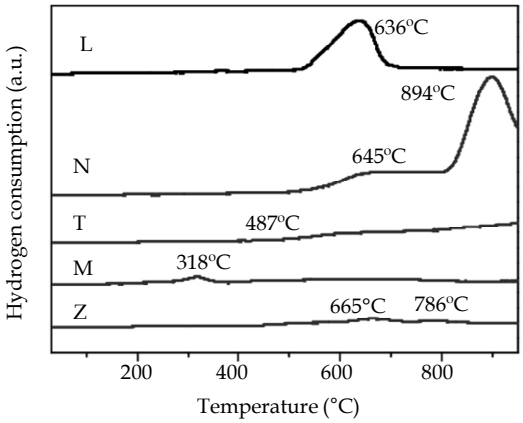

Fig. 2. Curves of thermoprogrammed reduction of the catalysts. L= lanthana; M= magnesia; N= niobia; T= titania; Z= zirconia.

3.3 Specific surface areas and porosity

All samples showed type III isotherms, as shown in Figure 3, which are typical of macroporous solids. Magnesia and zirconia showed curves with a small hysteresis loop (type H3), indicating the presence of some mesopores.

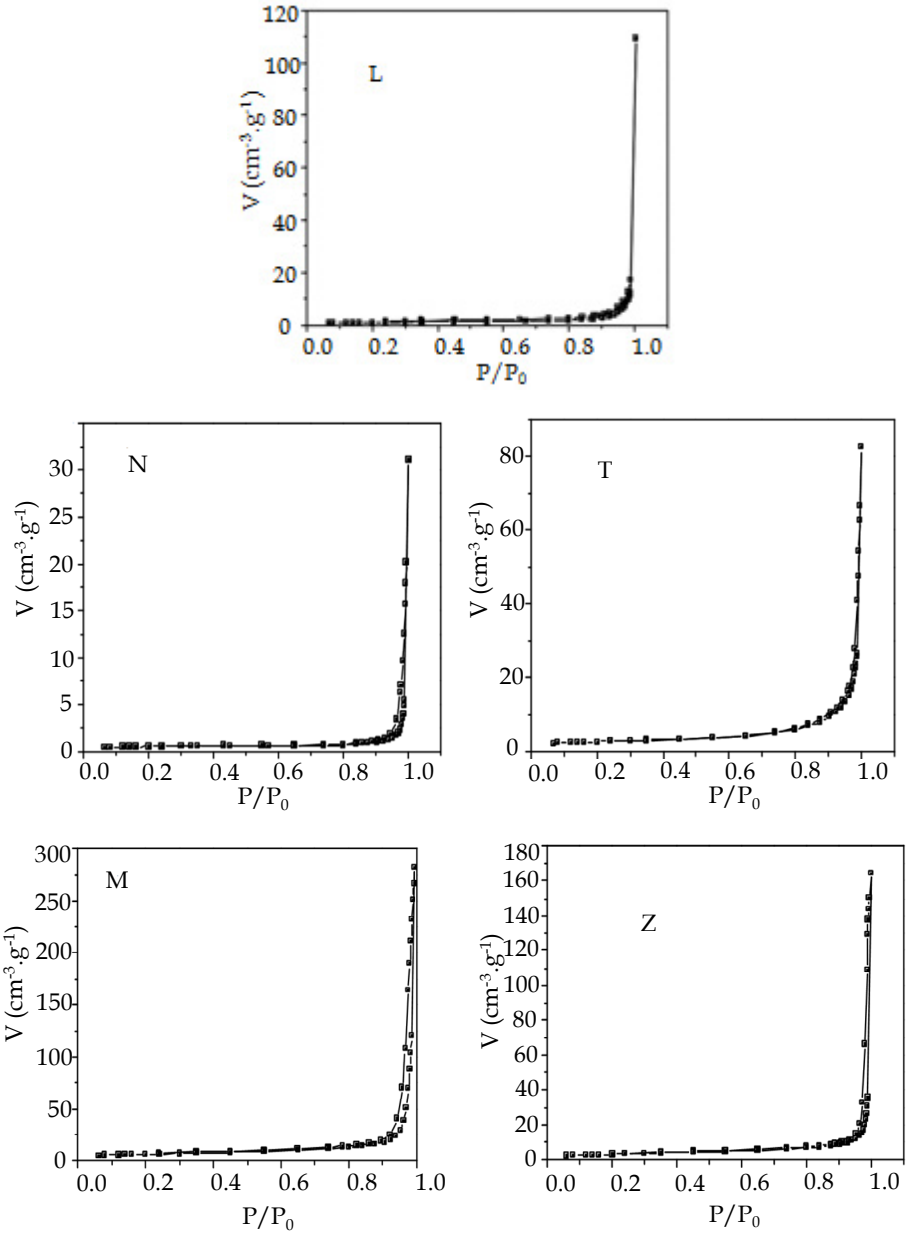

Fig. 3. Adsorption/desorption nitrogen isotherms of the samples. L= lanthana; M= magnesia; N= niobia; T= titania; Z= zirconia.

The specific surface areas of fresh and spent catalysts are shown in Table 1. All fresh catalysts showed low values, this can be assigned to the high calcination temperature of the

solids. During reaction, the specific surface area of titania, magnesia and zirconia showed no significant change, indicating that they were stable under the reaction conditions.

On the other hand, lanthana and niobia showed an increase of this parameter after ethylbenzene dehydrogenation, a fact that can be related to the reduction of the solids during reaction, by carbon monoxide (Equation 2) producing smaller and/or more porous particles. The easiness of these samples for going on reduction is confirmed by the reduction termoprogrammed profiles, which showed that lanthanum oxide and niobium oxide have consumed the highest amount of hydrogen.

3.4 Thermoprogrammed ammonia desorption

The profiles of temperature programmed desorption of ammonia (NH_3-TPD) for the catalysts are shown in Figure 4 and the total number of moles of ammonia desorbed by the samples is shown in Table 2. As previously stated (Ohishi et al., 2005), the amount of ammonia desorbed below 200 °C is related to weak acidic sites; in the range of 200-350 °C it corresponds to moderate acidic sites, while in temperatures higher than 350 °C it can be associated to strong acidic sites.

Samples	Sg ($m^2.g^{-1}$)	Sg* ($m^2.g^{-1}$)
L	3.0	15
N	1.6	3.4
T	10	9.2
M	21	18
Z	11	12

Table 1. Specific surface areas of the catalysts before (Sg) and after (Sg*) ethylbenzene dehydrogenation. L= lanthana; M= magnesia; N= niobia; T= titania; Z= zirconia.

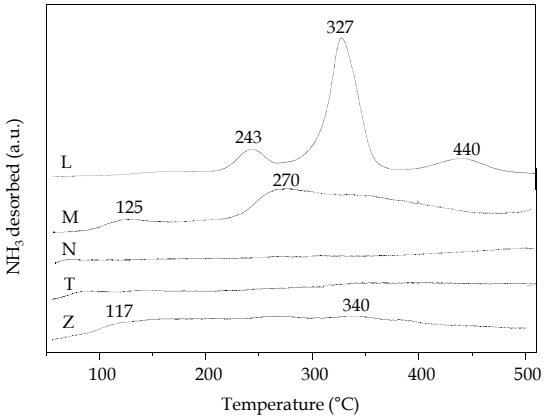

Fig. 4. Curves of thermoprogrammed ammonia desorption for the catalysts. L= lanthana; M= magnesia; N= niobia; T= titania; Z= zirconia.

Samples	$n(NH_3)x10^5$ (g^{-1})
L	20.89
M	3.10
N	0.73
T	0.72
Z	2.79

Table 2. Total acidity of the catalysts, expressed as number of moles of ammonia, n (NH_3) desorbed per gram of catalyst. L= lanthana; M= magnesia; N= niobia; T= titania; Z= zirconia.

Niobia and titania showed a very low hydrogen consumption (Table 1), indicating almost the absence of acidic sites. For zirconia and magnesia weak and moderate sites were detected, which correspond to a low ammonia consumption. For lanthana, the amount of ammonia desorbed is much greater than for other oxides, showing that it is the most acidic solid. The desorption peaks are centered at 243, 327 and 440 °C and the most sites are those of moderate strength.

3.5 Activity and selectivity of the catalysts

All catalysts were active in ethylbenzene dehydrogenation, in the presence of carbon dioxide, as shown in Figure 5. In the beginning of reaction, lanthana was the most active one followed by the others in the order: L>Z>M≅N>T. This behavior can be related to both the intrinsic activity of these solids and their specific surface areas. As these catalysts are mass,

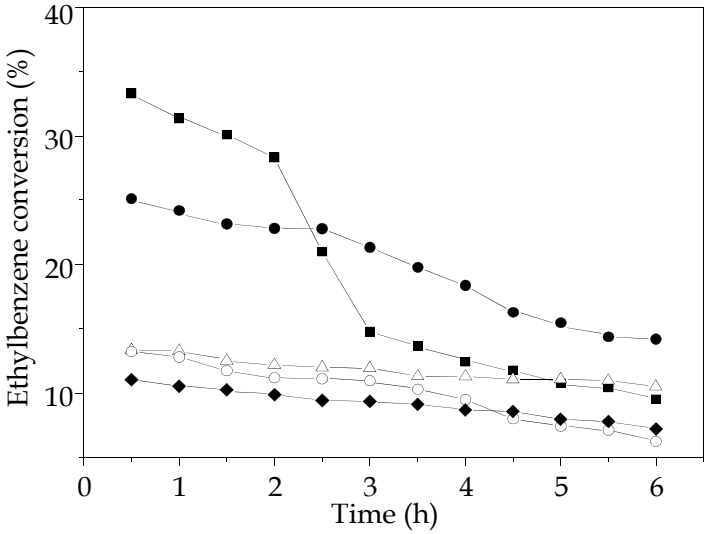

Fig. 5. Ethylbenzene conversion as a function of time over the catalysts during dehydrogenation reaction in the presence of carbon dioxide. (■) L= lanthana; (Δ) M= magnesia; (o) N= niobia; (♦) T= titania; (●) Z= zirconia.

Sample	$a_i \times 10^3$ (mol.g^{-1}.h^{-1})	$a_i/S_g \times 10^4$ (mol.m^{-2}.h^{-1})	$a_f \times 10^3$ (mol.g^{-1}.h^{-1})	$a_f/S_g \times 10^4$ (mol.m^{-2}.h^{-1})	ΔX (%)
L	3.8	12.7	1.1	0.7	23.5
N	1.5	9.2	10.7	2.3	4.8
T	1.3	1.3	1.1	1.2	1.6
M	2.9	1.4	2.5	1.4	1.9
Z	2.7	2.5	1.6	1.3	10.6

Table 3. Initial (a_i) and final (a_f) activity, initial (a/Sg) and final (a*/Sg) specific surface area of the catalysts and the drop in conversion (ΔX) during ethylbenzene dehydrogenation in the presence of carbon dioxide. ΔX= X(initial) – X (final). L= lanthana; M= magnesia; N= niobia; T= titania; Z= zirconia.

their intrinsic activity can be conveniently expressed as the activity per specific surface area. As shown in Table 3, the intrinsic activity decreases in the order: L>N>T≅M≅Z, indicating that titania, magnesia and zirconia have the same activity in ethylbenzene dehydrogenation while lanthana and niobia showed the highest values, a fact that is closely related to the kind of metallic oxide. In addition, it is well known the ability of lanthana for adsorbing carbon dioxide (Yue et al., 2007) favouring the activity in the reaction. Niobia showed the lowest activity due to its low specific surface area, since it has intrinsic activity close to zirconia.

During ethylbenzene dehydrogenation, all catalysts go on deactivation but in different ways, according to their kind (Figure 5 and Table 3). The lanthanum-based sample showed the highest deactivation, the conversion decreases sharply after 2 h of reaction achieving values close to magnesia, at the end of reaction. On the other hand, zirconia deactivates slowly during reaction while the other samples deactivates even more slowly.

Zirconia was the most selective catalysts towards styrene production, as shown in Figure 6, while titania was the least selective one; the other samples showed similar intermediate values of selectivity. During reaction, the selectivities change according to the kind of the catalysts, in such way that at the end of reaction the selectivity decreases in the order: Z>M≅L>T>N. This finding suggests that the active sites go on transformations during reaction probably related to changes in acidity. As found previously (Qiao et al., 2009), the selectivity of the catalysts in ethylbenzene dehydrogenation is closely related to the acidity/basicity of the sites.

The selectivities of the catalysts to benzene and toluene are shown in Figures 7 and 8, respectively. As we can see, titania and niobia were the most selective catalysts to toluene, in agreement with the results of ammonia desorption. According to previous authors (Qiao et al., 2009), if the basic sites are strong enough to remove the β-hydrogen, the rupture of the lateral bond C-C will be favored and then the toluene selectivity will increase. On the other hand, if the acidity is high, the α-hydrogen will be preferentially removed, the phenil-C bond will be favored and benzene selectivity will increased. Therefore, benzene and toluene are formed on different kinds of sites.

The selectivities to benzene and toluene change during ethylbenzene dehydrogenation, as noted in Figures 7 and 8. It is interesting to note that after 5 h of reaction, the selectivity of niobia to toluene increased sharply as the expenses of a decrease in ethylbenzene selectivity. It suggests that the basicity of niobia increases even more during reaction.

The values of styrene yield as a function of reaction time in ethylbenzene dehydrogenation are shown in Figure 9. One can note that the values follow the same tendency as the conversion both in the beginning and in the end of reaction. Zirconia led to the highest yield, followed by lanthana, which leads to yield similar to magnesia and lightly higher than titania and niobia.

These results show that zirconia is the most promising catalyst for ethylbenzene dehydrogenation in the presence of carbon dioxide, as compared to lanthana, niobia, titania and magnesia. These findings are mostly related to the kind of oxide as well as to the acidic/basic properties of the catalysts.

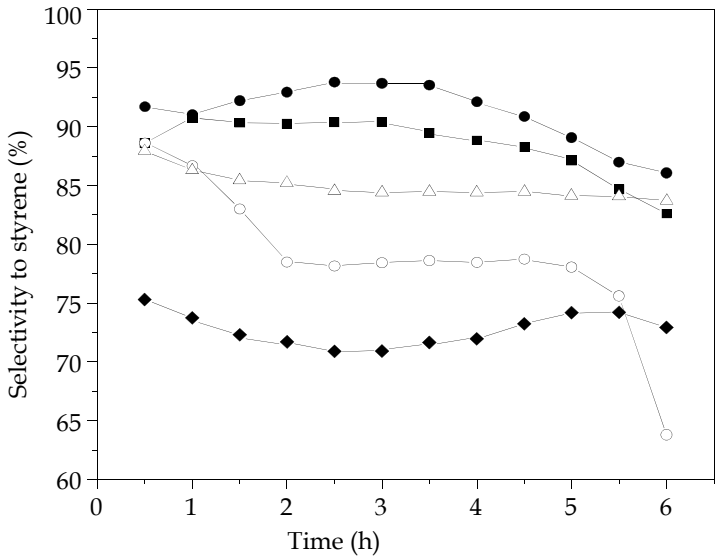

Fig. 6. Selectivity of the catalysts to styrene as a function of time during dehydrogenation reaction in the presence of carbon dioxide. (■) L= lanthana; (Δ) M= magnesia; (o) N= niobia; (♦) T= titania; (●) Z= zirconia.

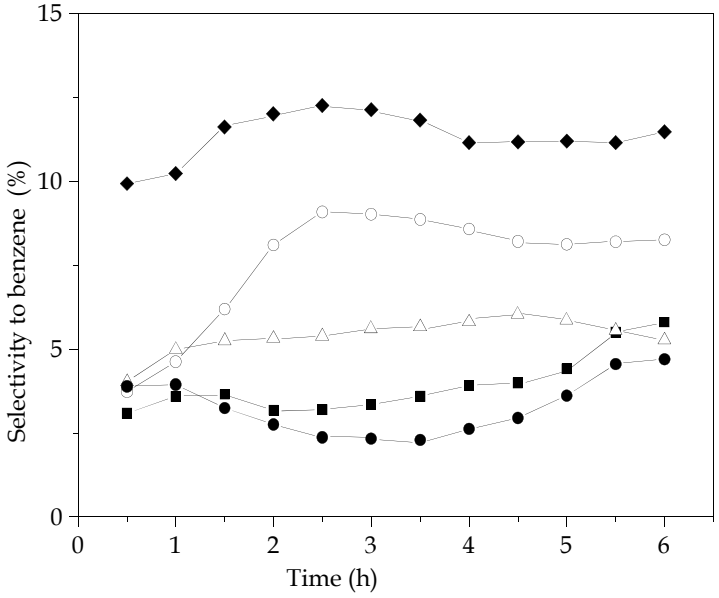

Fig. 7. Selectivity of the catalysts to benzene as a function of time during dehydrogenation reaction in the presence of carbon dioxide. (■) L= lanthana; (Δ) M= magnesia; (o) N= niobia; (♦) T= titania; (•) Z= zirconia.

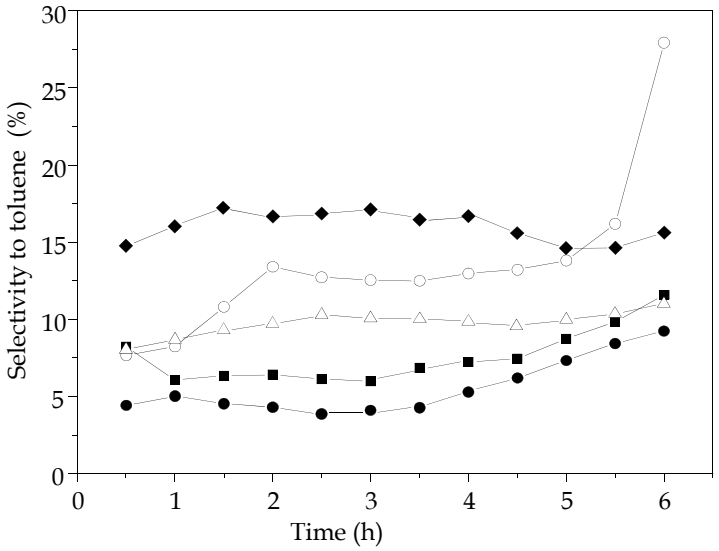

Fig. 8. Selectivity of the catalysts to toluene as a function of time during dehydrogenation reaction in the presence of carbon dioxide. (■) L= lanthana; (Δ) M= magnesia; (o) N= niobia; (♦) T= titania; (•) Z= zirconia.

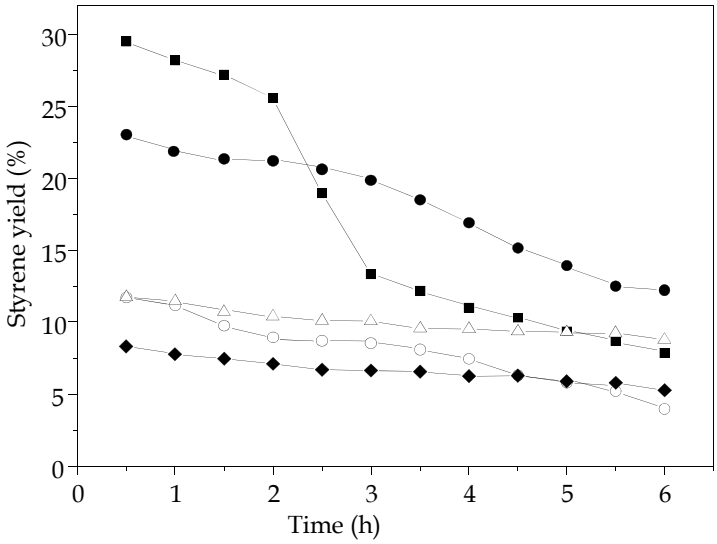

Fig. 9. Styrene yield as a function of time over the catalysts during ethylbenzene dehydrogenation in the presence of carbon dioxide. (■) L= lanthana; (Δ) M= magnesia; (o) N= niobia; (♦) T= titania; (•) Z= zirconia.

4. Conclusion

Metal oxides such as lanthana (La_2O_3), magnesia (MgO), niobia (Nb_2O_5), titania (TiO_2) and zirconia (ZrO_2) are catalytically active in ethylbenzene dehydrogenation in the presence of carbon dioxide to produce styrene. These solids are stable during reaction, showing the same phases before and after reaction, except for the lanthanum-based solid, which went on phase transition during reaction. Except for zirconia and titania, all specific surface areas changed during reaction. All catalysts have shown styrene selectivities higher than 60 % and were typically basic, producing more toluene than benzene. Zirconia was the most active and selective catalyst and this was related to its highest intrinsic activity. It was also the most selective to styrene, leading to the highest styrene yield. Therefore, it is the most promising catalyst to produce styrene by ethylbenzene dehydrogenation in the presence of carbon monoxide, among the samples studied.

5. Acknowledgment

APMM, MSR and SBL acknowledge CAPES, FAPESB and CNPq for their graduate fellowships. The authors thank CNPq and FINEP for the financial support and CBMM and Millenium for supplying niobia and titania, respectively.

6. References

Aresta, M. & Dibenedetto, A. (2004). Product review. The Contribution of the Utilization Option to Reducing the CO_2 Atmospheric Loading: Research Needed to Overcome

Existing Barriers for a Full Exploitation of the Potential of the CO_2 Use. *Catalysis Today*, Vol.98, issue 4, (December 2004), pp. 455-462, ISSN: 09205861.

Badstube, T., Papp, H., Dziembaj, R. & Kustrowski, P. (2000). Screening of Catalysts in the Oxidative Dehydrogenation of Ethylbenzene with Carbon Dioxide. *Applied Catalysis A*, Vol.204, issue 1, (November 2000), pp. 153-165, ISSN: 09205861.

Badstube, T., Papp, H., Kustrowski, P. & Dziembaj, R. (1998). Oxidative Dehydrogenation of Ethylbenzene with Carbon Dioxide on Alkali-Promoted Fe/Active Carbon Catalysts. *Catalysis Letters*, Vol.55, issues 3-4, (September 1998), pp. 169-172, ISSN: 1011-372X.

Bhasin, M. M., McCain, J. H., Vora, B. V., Imai, T. & Pujadó, P. R. (2001). Dehydrogenation and Oxydehydrogenation of Paraffins to Olefins. *Applied Catalysis A*, Vol.221, issues 1-2, (November 2001), pp. 397-419, ISSN: 09205861.

Burri, D. R., Choi, K-M., Han, S-C., Burri, A., Park, S-E. Selective Conversion of Ethylbenzene into Styrene Over K_2O/TiO_2-ZrO_2 Catalysts: Unified Effects of K_2O and CO_2. *Journal of Molecular Catalysis A*, Vol.269, issues 1-2, (May 2007), pp. 58-63, ISSN: 1381-1169.

Burri, D. R., Choi, K.M., Han, D.-S., Koo, J.-B. & Park, S.-E (2006). CO_2 Utilization as an Oxidant in the Dehydrogenation of Ethylbenzene to Styrene over MnO_2-ZrO_2 Catalysts. *Catalysis Today*, Vol.115, issue 1-4, (June 2006), pp. 242-247, ISSN: 0920-5861.

Cavani, F. & Trifiro, F. (1995). Review Alternative Processes for the Production of Styrene. *Applied Catalysis A*, Vol. 133, issue 2, (December 1995), pp. 219-239, ISSN: 0926-860X.

Chang, J.-S., Hong, D.-Y., Park, Y.-K. & Park, S.-E. (2004). Selective Formation of Styrene via Oxidative Dehydrogenation of 4-Vinylcyclohexene over ZrO_2-Supported Iron Oxide Catalysts. *Studies in Surface Science and Catalysis*, Vol.153, (2004), pp. 347-350, ISBN13: 978-0-444-53601-3.

Chen, S., Qin, Z. Sun, A., Wang, J. Theoretical and Experimental Study on Reaction Coupling: Dehydrogenation of Ethylbenzene in the Presence of Carbon Dioxide. *Journal of Natural Gas Chemistry*, Vol.15, issue 1, (March 2006), pp. 11-20, ISSN: 1003-9953.

Corberán, V. C. (2005). Novel Approaches for the Improvement of Selectivity in the Oxidative Activation of Light Alkanes. *Catalysis Today*, Vol.99, issues 1-2, (January 2005), pp. 33-41, ISSN: 09205861.

Dziembaj, R., Kustrowski, P., Badstube, T. & Papp, H. (2000). On the Deactivation of Fe, K/Active Carbon Catalysts in the Course of Oxidative Dehydrogenation of Ethylbenzene with Carbon Dioxide. *Topics in Catalysis*, Vol. 11-12, issues 1-4, pp. 317-326. ISSN: 1572-9028.

Farrauto, R. J. &Bartholomew, C.H. (1997). *Fundamentals of Industrial Catalytic processes*, Blackie Academic & Professional: Hydrogenation and Dehydrogenation of Organic Compound, New York.

Herzog, B. D., Raso, H. F. Industrial and Engineering Chemistry Process Design and Development, Vol.23 (April 1984), pp. 187-196, ISSN: 0196-4305.

Hoang, D.L., Dittmar, A. J., Radnik, K.-W., Brzezinka & Witke, K. (2003). Redox Behaviour of La-Cr Compounds Formed in $CrOx/La_2O_3$ Mixed Oxides and

$CrOx/La_2O_3/ZrO_2$ Catalysts. *Applied Catalysis A*, Vol.239, issues 1-2, (January, 2003), pp. 95-110, ISSN: 0926-860X.

Holtz, R. D., Oliveira, S. B., Fraga, M. A. & Rangel, M. C. (2008). Synthesis and Characterization of Polymeric Activated Carbon-Supported Vanadium and Magnesium Catalysts for Ethylbenzene Dehydrogenation. *Applied Catalysis A*, Vol. 350, issue 1, (November 2008), pp. 79-85, ISSN: 0926-860X.

Ikenaga, N., Tsuruda, T., Senma, K., Yamaguchi, T., Sakurai, Y. & Suzuki, T. (2000). Dehydrogenation of Ethylbenzene with Carbon Dioxide Using Activated Carbon-Supported Catalysts. *Industrial & Enginnering Chemistry Research*, Vol. 39, nº5, (March 2000), pp. 1228–1234. ISSN 0888-5885.

Jurczyk, K. & Kania, W. (1989). Base Properties of Modified y-Alumina. *Applied Catalysis*, Vol.56, issue 1, (August 1989), pp. 253-261, ISSN: 0926-860X.

Krylov, O.V., Mamedov, A.Kh. & Mirzabekova, S.R. (1995). The Regularities in the Interaction of Alkanes with CO2 on Oxide Catalysts. *Catalysis Today*, Vol.24, issues 3, (June, 1995), pp. 371-375, ISSN: 0920-5861.

Lenzi, G.G., Fávero, C.V.B., Colpini, L.M.S., Bernabe, H., Baesso, M.L., Specchia, S. & Santos, O.A.A. (2011). Photocatalytic Reduction of Hg(II) on TiO_2 and Ag/TiO_2 Prepared by the Sol–Gel and Impregnation Methods. *Desalination*, Vol.270, issues 1-3, (April 2011), pp. 241-247, ISSN: 0011-9164.

Liao, S.-J., Chen, T., Miao, C.-X., Yang, W.-M., Xie, Z.-K., Chen & Q.-L. (2008). Effect of TiO_2 on the Structure and Catalytic Behavior of Iron–Potassium Oxide Catalyst for Dehydrogenation of Ethylbenzene to Styrene. *Catalysis Communications*, Vol.9, issue 9, (May, 2008), pp. 1817-1821, ISSN: 1566-7367.

Maity, S.K., Rana, M.S., Srinivas, B.N., Bej, S.K., Dhar, G. Murali, Rao & Prasada, T.S.R. (2000). Characterization and Evaluation of ZrO_2 Supported Hydrotreating Catalysts. *Journal of Molecular Catalysis A*, Vol.153, issues 1-2, (March 2000), pp. 121–127, ISSN: 1381-1169.

Mamedov, .E. A. (1994). Beneficial Influences of the Reactive Atmosphere on Selective Oxidation Catalysts. *Applied catalysis A*, Vol.116, issues 1-2, (September 1994), pp. 49-70, ISSN: 0926-860X.

Mamedov, E.A. & Corberan, V.C. (1995). Oxidative Dehydrogenation of Lower Alkanes on Vanadium Oxide-Based Catalysts. *Applied Catalysis A*, Vol.127, issues 1-2, (June 1995), pp. 1-40, ISSN: 0926-860X.

Mimura, N. & Saito, M. (1999). Dehydrogenation of Ethylbenzene to Styrene over Fe_2O_3/Al_2O_3 Catalysts in the Presence of Carbon Dioxide. *Catalysis Letters*, Vol.58, issues 1, pp. 59-62, ISSN: 1011-372X.

Mimura, N. & Saito, M. (2000). Dehydrogenation of Ethylbenzene to Styrene Over Fe_2O_3/Al_2O_3 Catalysts in the Presence of Carbon Dioxide. *Catalysis Today*, Vol.55, issues 1-2, (January 2000), pp. 173-178, ISSN: 0920-5861.

Mimura, N., Takahara, I., Saito, M., Hattori, T., Ohkuma, K., & Ando, M. (1998). Dehydrogenation of Ethylbenzene Over Iron Oxide-based Catalyst in the Presence of Carbon Dioxide. *Catalysis Today*, Vol.45, issues 1-4, (October 1998), pp. 61-64, ISSN: 09205861.

Miyakoshi, A., Ueno, A. & Ichikawa, M. (2001). XPS and TPD Characterization of Manganese-Substituted Iron–Potassium Oxide Catalysts Which are Selective for

Dehydrogenation of Ethylbenzene Into Styrene. *Applied Catalysis A*, Vol.219, issues 1-2, (October 2001) pp. 249-258, ISSN: 0926-860X.

Morán, C., González, E., Sánchez, J., Solano, R., Carruyo, G. & Moronta, A. (2007). Dehydrogenation of Ethylbenzene to Styrene Using Pt, Mo and Pt-Mo Catalysts Supported on Clay Nanocomposites. *Journal of Colloid and Interface Science*, Vol.315, issue 1, (November 2007), pp. 164-169, ISSN: 0021-9797

Murata, W. K., Hayakawa, T., Hamakawa, S. & Suzuki, K. (2000). Dehydrogenation of Ethane with Carbon Dioxide Over Supported Chromium Oxide Catalysts. *Applied Catalysis A*, Vol.196, issue 1, (March 2000), pp. 1-8, ISSN: 09205861.

Nakagawa, K., Okamura, M., Ikenaga, N., Suzuki, T. & Kobayashi, T. (1998). Dehydrogenation of Ethane Over Gallium Oxide in the Presence of Carbon Dioxide. *Chemical Communications*, issue 9, (January 1998) pp. 1025-1026. ISSN: 1364-548X

Nishiyama, T. & Aika, K. (1990). Mechanism of the Oxidative Coupling of Methane Using CO_2 as an Oxidant Over PbO-MgO. *Journal of Catalysis*, Vol.122, issue 2, (April 1990), pp. 346-351, ISSN 0021-9517.

Ogonowski, J. & Skrzyńska, E., (2005). Catalytic Dehydrogenation of Isobutene in the Presence of Carbon Dioxide. *Reaction Kinetics and catalysis Letters*, Vol.86, nº 1, (June 2005), pp. 195-201, ISSN: 0133-1736.

Ohishi, Y., Kawabata, T., Shishido, T., Takaki, K., Zhang, Q., Wang, Ye & Takehira, K. (2005). Dehydrogenation of Ethylbenzene With CO_2 Over Cr-MCM-41 Catalyst. *Journal of Molecular Catalysis A*, Vol.230, issues 1-2, (April 2005), pp. 49-58, ISSN: 0021-9797.

Oliveira, S. B., Barbosa, D. P., Monteiro, A. P. M., Rabelo, D. & Rangel, M. C. (2008). Evaluation of Copper Supported on Polymeric Spherical Activated Carbon in the Ethylbenzene Dehydrogenation. *Catalysis Today*, Vol.133-135, (Abril 2008), pp. 92-98, ISSN: 09205861.

Park, J-N., Noh, J., Chang, J-S., Park, S-E. Ethylbenzene to Styrene in the Presence of Carbon Dioxide Over Zirconia. *Catalysis Letters*, Vol.65, nº 1-3, (January 2000), pp. 75-78, ISSN: 1011-372X.

Park, M. S., Chang, J.-S., Kim, D. S. & Park, S.-E. (2002). Oxidative Dehydrogenation of Ethylbenzene with Carbon Dioxide over Zeolite-Supported Iron Oxide Catalysts. *Research on Chemical Intermediates*, Vol.28, nº 5, (November 2001), pp. 461-469.

Park, M.-S., Vislovskiy, Vladislav P., Chang, J.-S., Shul, Y.-G., Yoo, Jin S. & Park S.-E. (2003). Catalytic Dehydrogenation of Ethylbenzene with Carbon Dioxide: Promotional Effect of Antimony in Supported Vanadium–Antimony Oxide Catalyst. *Catalysis Today*, Vol.87, issues 1-4, (November 2003), pp. 205-212, ISSN: 0920-5861.

Pereira, E. B., Pereira, M. M., Lam, Y.L., Perez, C. A.C. & Schmal, M. (2000). Synthesis and Characterization of Niobium Oxide Layers on Silica and the Interaction with Nickel. *Applied Catalysis A*, Vol.197, issue 1, (April 2000), pp. 99-106, ISSN: 0926-860X.

Pereira, M. F. R., Órfão, J. J. M. & Figueiredo J. L. (2004). Influence of the Textural Properties of an Activated Carbon Catalyst on the Oxidative Dehydrogenation of Ethylbenzene. *Colloids and Surfaces A: Physicochemical and Engineering Aspects*, Vol.241, issues 1-3, (July 2004), pp. 165-171, ISSN: 0927-7757.

Qiao, Y., Miao, C., Yue, Y., Xie Z., Yang, W. & Gao, Z. (2009). Vanadium Oxide Supported Mesoporous MCM-41 as New Catalysts for Dehydrogenation of Ethylbenzene with CO_2. *Microporous and Mesoporous Materials*, Vol.119, issues 1-3, (March 2009), pp. 150-157, ISSN: 1387-1811.

Ramos, M. S., Santos, M. S., Gomes, L. P., Albornoz, A. & Rangel, M. C. (2008). The influence of Dopants on the Catalytic Activity of Hematite in the Ethylbenzene Dehydrogenation. *Applied Catalysis A:General*, Vol.341, issue 1-2, (June 2008), pp. 12-17, ISSN: 0926-860X.

Rangel, M. C., Oliveira, A. C.; Fierro, J. L. G.; Valentini, A. & Nobre, P. S. S. (2003). Non Toxic Fe-Based Catalysts for Styrene Synthesis. The Effect of Salt Precursor and Aluminum Promoter on the Catalytic Properties. *Catalysis Today*, Vol.85, issue 1, (September 2003), pp. 49-57, ISSN: 09205861.

Ritter, S. K. (2005). What Can We Do With Carbon Dioxide? *Chemical and Engineering News*, Vol.85, (April, 2007), pp. 11-17, ISSN 0009-2347.

Saito, M., Kimura, H., Mimura, N., Wu, J. & Murata, K. (2003). Dehydrogenation of Ethylbenzene in the Presence of CO_2 Over an Alumina-Supported Iron Oxide Catalyst. *Applied Catalysis A*, Vol.239, issues 1-2, (January 2003), pp. 71-77, ISSN: 0926-860X.

Sakurai, Y., Suzaki, T., Ikenaga, N. & Suzuki, T. (2000). Dehydrogenation of Ethylbenzene with an Activated Carbon-Supported Vanadium Catalyst. *Applied Catalysis A*, Vol.192, issue 2, (February 2000), pp. 281-288, ISSN: 09205861.

Sakurai, Y., Suzaki, T., Nakagawa, K., Ikenaga, N.-O., Aota, H., Suzuki, T. (2002). Dehydrogenation of Ethylbenzene over Vanadium Oxide-Loaded MgO Catalyst: Promoting Effect of Carbon Dioxide. *Journal of Catalysis*, Vol.209, issue 1, (July 2002), pp. 16-24, ISSN: 0021-9517.

Santos, M. S., Albornoz, A. & Rangel, M. C. (2006). The Influence of the Preparation Method on the Catalytic Properties of Lanthanum-Doped Hematite in the Ethylbenzene Dehydrogenation. *Studies and Surface Science and Catalysis*, Vol.162, pp. 753-760, ISBN13:978-0-444-53601-3.

Santos, M. S., Berrocal, G. P., Fierro, J. L. G. & Rangel, M. C. (2005). Effect of Aluminum Content on the Properties of Lanthana-Supported Nickel Catalysts to WGSR. *Studies in Surface Science and Catalysis*, Vol.167, pp. 493-498, ISBN 13: 978-0-444-53601-3.

Shimada, H., Akazawa, T., Ikenaga, N. & Suzuki, T. (1998). Dehydrogenation of Isobutane to Isobutene with Iron-Loaded Activated Carbon Catalyst. *Applied Catalysis A*, Vol.168, issue 2, (March 1998), pp. 243-250, ISSN: 0926-860X.

Shreve, R. N. & Brink, J. A. (1997). *Indústrias de Processos Químicos*, (4ª Edição), Guanabara 34 Koogan, ISBN: 8527714191, Rio de Janeiro.

Song, C. (2006). Global Challenges and Strategies for Control, Conversion and Utilization of CO_2 for Sustainable Development Involving Energy, Catalysis, Adsorption and Chemical Processing. *Catalysis Today*, Vol.115, issues 1-4, (June 2006), pp. 2-32, ISSN: 0920-5861.

Styles, A. B. In *Applied Industrial Catalysis*; Leach, B.E. Academic Press, (1987), pp. 137-153, New York.

Sun, A., Qin, Z. & Wang, J. (2002). Reaction Coupling of Ethylbenzene Dehydrogenation with Water-Gas Shift. *Applied Catalysis A*, Vol.234, issues 1-2, (August 2002), pp. 179-189, ISSN: 0926-860X.

Vislovskiy, V. P., Chang, J.-S., Park, M.-S. & Park, S.-E. (2002) Ethylbenzene into Styrene with Carbon Dioxide over Modified Vanadia–Alumina Catalysts. *Catalysis Communications*, Vol.3, issue 6, (June 2002), pp. 227-231, ISSN: 1566-7367.

Wang, S., Murata, K., Hayakawa, T., Hamakawa, S. & Suzuki, K. (2000). Dehydrogenation of Ethane with Carbon Dioxide over Supported Chromium Oxide Catalysts. *Applied Catalysis A*, Vol.196, issue 1, (March 2000), pp. 1-8, ISSN: 0926-860X.

Wang, S. & Zhu, Z. H. (2004). Catalytic Conversion of Alkanes to Olefins by Carbon Dioxide Oxidative Dehydrogenation – A Review. *Energy & Fuels*, Vol.18, nº4, (April 2004), pp. 1126-1139. ISSN: 1520-5029

Yue, Y., Li, H., Miao, C., Xie, Z., Hua, W., Gao, Z. Dehydrogenation of Ethylbenzene and Propane over Ga_2O_3-ZrO_2 Catalysts in the Presence of CO_2. *Catalysis Communications*, Vol.8, issues 9, (September 2007), pp. 1317-1322, ISSN: 1566-7367.

7

Sustainable Hydrogen Production by Catalytic Bio-Ethanol Steam Reforming

Vincenzo Palma[1], Filomena Castaldo[1],
Paolo Ciambelli[1] and Gaetano Iaquaniello[2]
[1]*Dipartimento di Ingegneria Industriale, Università di Salerno*
[2]*Tecnimont KT S.p.A. Italy, Roma*
Italy

1. Introduction

Energy is an essential input for social development and economic growth. At present, globally the demand for energy is increasing in consonance with socio-economic development, though in developing countries it increases a little bit more quickly than developed countries. Energy consumption in developed countries grows at a rate of approximately 1% per year, and that of developing countries, 5% per year.

The International Energy Agency estimates that world energy demand will increase by half again between now and 2030, with more than two-thirds of this increase coming from developing and emerging countries. Moreover, global population is predicted to further increase by 2050, and global primary energy consumption is projected to considerably increase during the same time period.

Nowadays, our energy requirements are almost fully provided for carbon containing-fossil sources such as oil, coal and natural gas, which have been formed during many millions of years from plant biomass. According to the recently released 1008 BP Statistical Review of World Energy, the world's total proven oil, natural gas and coal reserves are respectively 169 billion tons, 177 trillion cubic meters and 847 billion tons by the end of 2007. With current consumption trends, the reserves to oil lower than of the world proven reserves of natural gas and coal- 42 years versus 60 and 133 years, respectively.

Known petroleum reserves are limited resources and are estimated to be depleted in less than 50 years at the present rate of consumption. The dramatic increase in the price of petroleum, the finite nature of fossil fuels, increasing concerns regarding environmental impact, especially related to climate change from greenhouse gas emissions, and health and safety considerations are forcing the search for renewable energy sources. (Mustafa Balat & Mehmet Balat, 2009).

Hydrogen has many social, economic and environmental benefits to its credit. It has the long-term potential to reduce the dependence on foreign oil and lower the carbon and criteria emissions from the transportation sector. Only in the last decade the idea of a post-fossil fuel hydrogen-based economy started to gain mainstream interest (Ni et al., 2007).

Hydrogen can be used either as a fuel for direct combustion in an internal combustion engine or as the fuel for a polymer electrolyte membrane (PEM) fuel cell (Kotay & Das, 2008). It can be produced through different methods but the steam reforming of hydrocarbons (mainly natural gas) is the most commonly used.

From an environmental point of view, steam reforming is not a sustainable method for hydrogen production due to the use of fossil fuel-based feedstock and the transformation of almost all the carbon of the hydrocarbons into carbon dioxide. Taking these aspects into considerations, bio-mass derived ethanol is suited to substitute the conventional fossil fuels based on petroleum or natural gas and to perform the ethanol steam reforming (ESR) reaction, that is a fuel well-adapted to the production of hydrogen.

Since the 1970s, Brazil has led the way in developing ethanol as a major fuel source. More recently, the USA has become a major producer of ethanol, with production doubling from 8 billion L yr^{-1} (B L yr^{-1}) in 2002 to 15 B L yr^{-1} in 2005 and increasing further by 25% to 20 B L yr^{-1} in 2006 (Institute for Agriculture and Trade Policy, 2006).

The EU has a similarly ambitious plan. Nowadays, the Italian ethanol production has a lower area of application respect to the European context, in particular in comparison with Spain, Germany, France and Poland. However, the communitarian potentialities of bioethanol are higher than the biodiesel ones (Figure 1) and the predicted trend in the ethanol production will probably lead to a considerably reduction in the production costs.

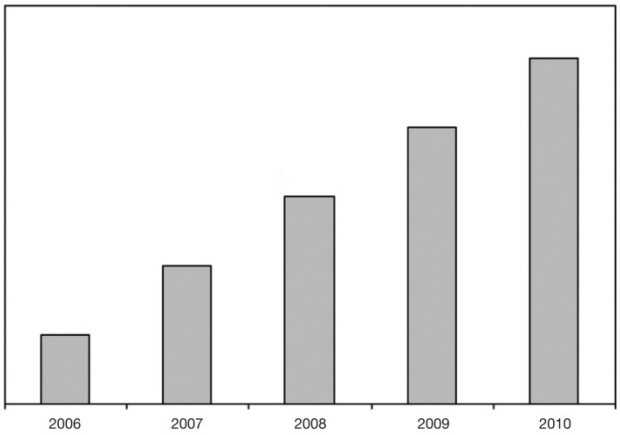

Fig. 1. Trend of ethanol production in application of the 81/06 Law (AssoDistil, Bioetanolo in Italia, BIOFUEL EXPO 2006)

Recently, intensive researches have been devoted to the ESR reaction performed at high temperature. In a catalytic steam reforming process the ethanol is converted in combination with water into a hydrogen rich gas which consist of H_2, CO, CO_2, CH_4 and H_2O. The CO in the reforming product gas will deactivate the anode catalyst of the PEM fuel cell. Therefore a gas cleaning process is necessary: a catalytic high and low temperature water shift reaction (WGS) reduces the CO content of the reforming product gas to about 0.2 vol%. Since this reaction is exothermic, it is favoured at low temperature, then the high temperature-ESR

reaction coupled with the low temperature-WGS reaction whole process could suffer from thermal inefficiencies. When using a low temperature operating range, in order to minimize the CO amount in the outlet gas stream and to reduce the thermal duty, a decrease of the H_2 selectivity and the catalyst deactivation, due to coke formation, are quite unavoidable.

This chapter deals for a great part with the ESR process. For the reformer process, a catalyst screening is carried out. The influence of different parameters on the reforming reaction and catalyst performance is evaluated.

2. Hydrogen production

Hydrogen is the simplest, lightest, most plentiful and most abundant element in the universe. It is colourless, odourless, tasteless and nontoxic gas found in air at concentrations of about 100 ppm (0.01%). It is made up of one proton and one electron revolving around the proton. It has the highest specific energy content per unit weight among the known gaseous conventional fuels (143 GJ ton^{-1}) and is the only carbon-free fuel which ultimately oxidizes to water as a combustion product (some nitrogen oxized are formed at very high combustion temperatures). Therefore burning hydrogen not only has the potential to meet a wide variety of end use applications but also does not contribute to greenhouse emissions, acid rain or ozone depletion. The use of hydrogen will contribute to significant reduction of these energy-linked environmental impacts.

The properties that contribute to hydrogen use as a combustible fuel are reported in Table 1 (Mustafa Balat, 2008).

Characteristic	**Details**
Limits of flammability	Wide range
Ignition energy	Very low (0.02 M)
Detonation limits	Detonable over a wide range of concentrations when confined. Difficult to detonate when unconfined
Ignition temperature	Higher than other fuels
Flame speed	An order of magnitude higher (faster) than that of gasoline
Diffusivity	Very high
Density	Very low

Table 1. Hydrogen properties (Mustafa Balat, 2008)

There are different production technologies, schematically reported in Figure 2.

All methods can, generally, fall into four broad categories (Haryanto et al., 2005):

i. Thermochemical technologies:

they involve thermally assisted chemical reactions that release the hydrogen from hydrocarbons or water. The advantage of the

thermochemical process is that its overall efficiency (thermal to hydrogen) is higher (about 52%) and production cost is lower.

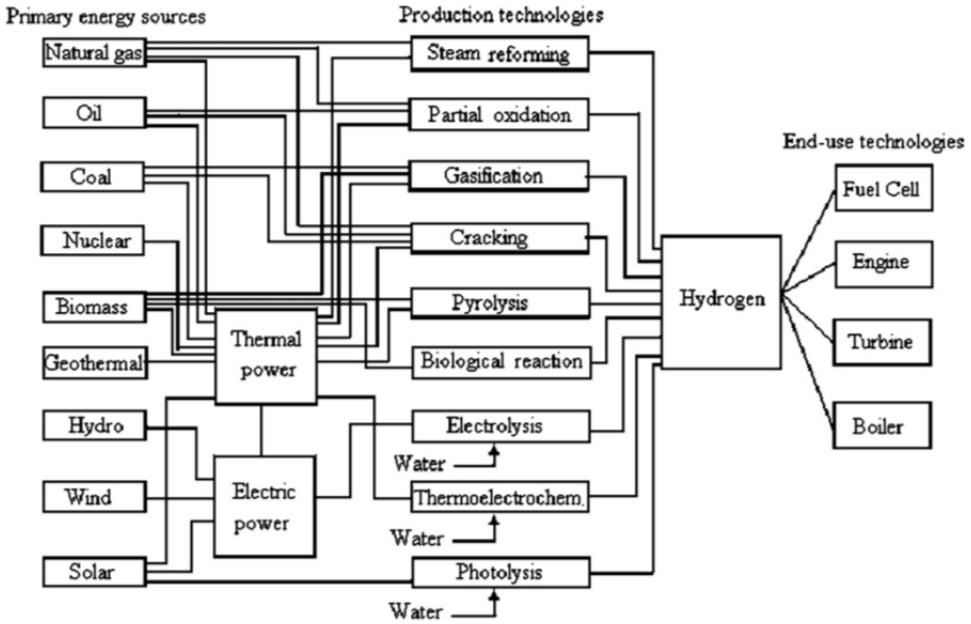

Fig. 2. The main alternative methods of hydrogen production from energy sources (Mustafa Balat et al., 2008)

Thermochemical technologies can be divided into two categories:

a. steam reforming from raw materials such as natural gas (Eq. 1), coal, methanol, ethanol, or even gasoline.

$$CH_4 + 2H_2O = 0.5O_2 \rightarrow CO_2 + 4H_2 \tag{1}$$

b. gasification (Eq 2, carbon gasification), partial oxidation (Eq 3) and pyrolysis from solid or semisolid feedstocks.

$$CH_{1.8} + H_2O = 0.5O_2 \rightarrow CO_2 + 1.9H_2 \tag{2}$$

$$CH_{0.8} + 0.6H_2 + 0.7O_2 \rightarrow CO_2 + H_2 \tag{3}$$

ii. Electrochemical technologies:

by these processes, the hydrogen is produced by electrochemically splitting water molecules into their constituent hydrogen and oxygen through the electrolysis of water (reported in Eq. 4)

$$2H_2O_2 \rightarrow H_2 + O_2 \tag{4}$$

The decomposition of water takes places in a so-called electrolysis cell and consists of two partial reactions that take place at two electrodes. To achieve the desired production capacity, numerous cells are connected in series forming a module: larger systems can be assembled by adding up several modules. It depends on cheap power, which is regionally

dependent on the presence of limited and inexpensive hydroelectric sources of power. This technology would be competitive only if low-cost electricity is available.

iii. Photobiological technologies:

These techniques use natural photosynthetic activity of bacteria and green algae. These processes are still immature and in the experimental stage. There are several types of photobiological processes, mainly:

a. biophotolysis;
b. photofermentation;
c. dark-fermentation.

iv. Photoelectrochemical technologies:

They consist in the production of H_2 in one step, splitting water by illuminating a water-immersed semiconductor with sunlight. They are in the early stage of development; so the pratical applicabilities are unclear. Interest in the production of hydrogen continues unabated because of the additional reason that hydrogen is perceived as the energy of the future. Extensive research is being carried out in many other processes for hydrogen production such as high temperature electrolysis of steam, solar photovoltaic water electrolysis and plasma decomposition of water. At present, approximately 96% of the hydrogen produced coming from fossil fuel-based processes, in particular steam reforming.

3. The steam reforming of hydrocarbons

Reforming separates hydrogen from hydrocarbons by adding heat; the reforming efficiency is obtained through studying of physical-chemical properties of feedstock, thermodynamic conditions (temperature and pressure of reaction, technical configurations of reformer such as dimensions and catalysts), and feedstock and water flows (Mustafa Balat & Mehmet Balat, 2009).

Heavy hydrocarbons are very active and water activation may be the rate determining step in the steam reforming, specially at lower temperatures (400-600°C).

The steam reforming reaction for a generic hydrocarbon is:

$$C_nH_{2n+2} + nH_2O \Leftrightarrow nCO + (2n+1)H_2 \tag{5}$$

For methane, n=1, the above equation becomes:

$$\begin{aligned} &CH_4 + H_2O \Leftrightarrow CO + 3H_2 \\ &\Delta H^0_{298} = +206 KJmol^{-1} \end{aligned} \tag{6}$$

It is typically followed by the water gas shift (WGS) reaction

$$\begin{aligned} &CO + H_2O \Leftrightarrow CO_2 + H_2 \\ &\Delta H^0_{298} = -41 KJmol^{-1} \end{aligned} \tag{7}$$

The methane steam reforming (MSR) reaction is strongly endothermic with an increase of the number of molecules, thus it is favoured at high temperatures and low pressures.

Since methane is a very stable molecule, the steam reforming of natural gas should be carried out at high temperatures (around 800-850°C) and it can be expected that methane activation is a critical step of the reaction. In fact, the critical steps having the highest energy barriers on most metals are CH_4 dissociation and CO formation, but the first effect is predominant, specially at high temperature (Wei & Iglesia, 2004). For all metals used as active species of the catalyst, the reaction is of first-order in CH_4 and virtually of zero order in H_2O and CO_2. Moreover, since the turnover frequency of the steam reforming is very close to that of dry reforming, probably neither H_2O activation nor CO_2 activation intervenes in the rate determining steps of methane conversion (Tavazzi et al., 2006, Donazzi et al., 2008 , Maestri et al., 2008).

However, some undesired C-containing intermediates cannot be excluded even though the formation of these compounds would be strongly dependent on the reaction conditions.

Currently, the steam reforming of natural gas comprises almost 60% of the world feedstock for H_2 production; in the United States, about 96% of H_2 is currently produced through steam reforming. It is clear that natural gas is the most commonly used and generally the most economically competitive method for hydrogen production. Natural gas is a kind of fossil fuel, and its usage fails to provide a solution to deal with the huge amount of carbon dioxide emissions during the reforming processes. In addition the use of fossil fuels for secondary energy production is non-sustainable.

As a result, there is a growing interest in the search for effective alternatives to produce renewable hydrogen cleanly and safety.

Hydrogen can be produced from biorenewable feedstocks via thermo-chemical conversion processes such as pyrolysis, gasification, steam gasification, supercritical water gasification of biomass and steam reforming of bio-fuels. The term biofuel is referred to liquid, gas and solid fuels predominantly produced from biomass. Biofuels include energy security reasons, environmental concerns, foreign exchange savings, and socioeconomic issues related to the rural sector. Biofuels include bioethanol, biomethanol, vegetable oils, biodiesel, biogas, bio-synthetic gas (bio-syngas), bio-oil, bio-char, Fischer-Tropsch liquids, and biohydrogen.

Most traditional biofuels, such as ethanol from corn, wheat, or sugar beets, and biodiesel from oil seeds, are produced from classic agricultural food crops that require high-quality agricultural land for growth.

The biofuel economy will grow rapidly during the 21st century; in the most biomass-intensive scenario, modernized biomass energy contributes by 2050 about one half of total energy demand in developing countries.

Among the various feedstocks, ethanol is a very attractive for hydrogen production from a renewable source thanks to its following features:

- it has a relatively high hydrogen content;
- it is available,
- it is non-toxic;
- it is easy to carry, storage and handle;
- it can be produced renewably by fermentation of biomass;

- it is a clean fuel;
- it doesn't contain sulphur compounds and heavy metals (Demirbas et al. 2008).

Moreover, in the ESR process, ethanol can be used without necessity of water separation, called in this case bio-ethanol.

4. Ethanol steam reforming

The reaction stoichiometry of the steam reforming of a generic alcohol:

$$C_nH_{2n+1}OH + (n-1)H_2O \rightarrow nCO + 2nH_2 \tag{8}$$

Coupled with the WGS reaction, the reaction leads to carbon dioxide and hydrogen:

$$C_nH_{2n+1}OH + (2n-1)H_2O \rightarrow nCO_2 + 3nH_2 \tag{9}$$

The C_1 compound, that in the hydrocarbons steam reforming is methane, is methanol in this case. It is the most reactive alcohol. It decomposes spontaneously at relatively low temperatures with-out water in the reacting gases (n=1). For this reason, methanol is considered as a "liquid" syngas, much easier to transport than the syngas itself.

Comparing the Gibbs free energy of the steam reforming reaction for n=1 and n=4, it is evident that the steam reforming reaction is more facile on alcohols than on corresponding alkanes.

4.1 Thermodynamic analysis

The thermodynamic aspects of the ethanol steam reforming system have received great attention (Freni et al., 1996; Ioannides, 2001; Benito et al., 2005; Vaidya & Rodriguez, 2006; Fatsikostas & Verykios, 2004; Aupretre et al., 2005, 2004; Garcia & Laborde, 1991; Vasudeva et al., 1996; Fishtik et al., 2000; Mas et al., 2006; Rossi et al., 2009; Rabenstein & Hacker, 2008; Alberton et al., 2007; Ni et al., 2007).

The ethanol-steam mixtures can give rise to numerous reactions, even if the desired one is the Eq. 10 with n=1:

$$\begin{aligned} &C_2H_5OH + 3H_2O \rightarrow 2CO_2 + 6H_2 \\ &\Delta H^0_{298} = +173 kJmol^{-1} \end{aligned} \tag{10}$$

However, the reaction pathway is complex: several secondary reactions could occur, among which the ethanol dehydrogenation to acetaldehyde, the ethanol dehydration to ethylene, the ethanol decomposition to acetone, that are by-products, possible precursors of coke formation.

The main reactions are reported as follows:

1. The steam reforming leading to CO and H_2:

$$\begin{aligned} &C_2H_5OH + H_2O \Leftrightarrow 2CO + 4H_2 \\ &\Delta H^0_{298} = +255 kJmol^{-1} \end{aligned} \tag{11}$$

2. The hydrogenolysis to methane

$$C_2H_5OH + 2H_2 \Leftrightarrow 2CH_4 + H_2O$$
$$\Delta H_{298}^0 = -157 kJmol^{-1} \quad (12)$$

3. The ethanol dehydration to ethylene

$$C_2H_5OH \Leftrightarrow C_2H_4 + H_2O$$
$$\Delta H_{298}^0 = +45 kJmol^{-1} \quad (13)$$

4. The dehydrogenation to acetaldehyde

$$C_2H_5OH \Leftrightarrow C_2H_4O + H_2$$
$$\Delta H_{298}^0 = +68 kJmol^{-1} \quad (14)$$

5. The cracking to methane, CO and H_2

$$C_2H_5OH \Leftrightarrow CO + CH_4 + H_2$$
$$\Delta H_{298}^0 = +49 kJmol^{-1} \quad (15)$$

6. The cracking to methane and CO_2

$$C_2H_5OH \Leftrightarrow \frac{1}{2}CO + \frac{3}{2}CH_4$$
$$\Delta H_{298}^0 = -74 kJmol^{-1} \quad (16)$$

7. The cracking to carbon, CO and H_2

$$C_2H_5OH \Leftrightarrow C + CO + 3H_2$$
$$\Delta H_{298}^0 = +124 kJmol^{-1} \quad (17)$$

8. The cracking to carbon, water and H_2

$$C_2H_5OH \Leftrightarrow 2C + H_2O + 2H_2$$
$$\Delta H_{298}^0 = -7 kJmol^{-1} \quad (18)$$

9. The cracking to carbon, methane and water

$$C_2H_5OH \Leftrightarrow 2C + H_2O + 2H_2$$
$$\Delta H_{298}^0 = -7 kJmol^{-1} \quad (19)$$

10. The cracking to carbon, methane and water

$$C_2H_5OH \rightarrow CH_4 + C + H_2O$$
$$\Delta H_{298}^0 = -82 kJmol^{-1} \quad (20)$$

It was found that high temperature (>600°C), high water to ethanol-molar-ratio (in the range 4-10) and low pressure (atmospheric) led to an increase in hydrogen yield and reduced the concentration of by-products (Erdohely et al., 2006; Hernandez & Kafarov et al., 2009; Silveira et al., 2009).

The equilibrium composition of the gases corresponding to the stoichiometric feed ratio, in a low temperature operating range (T=100-600°C), has been calculated.

Eight gaseous species, C_2H_5OH, H_2O, O_2, H_2, CO, CO_2, CH_4, C_2H_4O, C_3H_6O, C_2H_4 and one in solid phase, carbon, have been considered as product. In order to analyze coke formation for a thermodynamic point of view it is assumed that carbon formed is elemental, in the graphitic form, hence, free energy of carbon formation (ΔG_f) is zero and vapour pressure is zero in the range of temperature analyzed, thus the total Gibbs free energy can be considered to be independent of carbon. However the amount of carbon can be included in the elemental mass balance.

The results are reported in terms of ethanol conversion, selectivity to products and hydrogen yield, defined as follows (Eqs. 21 – 30):

$$X_{C_2H_5OH}[\%] = \frac{n_{in\,C_2H_5OH} - n_{out\,C_2H_5OH}}{n_{in\,C_2H_5OH}} \cdot 100 \tag{21}$$

$$S_{H_2}[\%] = \frac{n_{H_2} / 6}{n_{in\,C_2H_5OH} - n_{out\,C_2H_5OH}} \cdot 100 \tag{22}$$

$$S_{CO}[\%] = \frac{n_{CO} / 2}{n_{in\,C_2H_5OH} - n_{out\,C_2H_5OH}} \cdot 100 \tag{23}$$

$$S_{CO_2}[\%] = \frac{n_{CO_2} / 2}{n_{in\,C_2H_5OH} - n_{out\,C_2H_5OH}} \cdot 100 \tag{24}$$

$$S_{CH_4}[\%] = \frac{n_{CH_4} / 2}{n_{in\,C_2H_5OH} - n_{out\,C_2H_5OH}} \cdot 100 \tag{25}$$

$$S_{C_3H_6O}[\%] = \frac{n_{C_3H_6O} / (2/3)}{n_{in\,C_2H_5OH} - n_{out\,C_2H_5OH}} \cdot 100 \tag{26}$$

$$S_{C_2H_4O}[\%] = \frac{n_{C_2H_4O}}{n_{in\,C_2H_5OH} - n_{out\,C_2H_5OH}} \cdot 100 \tag{27}$$

$$S_{C_2H_4}[\%] = \frac{n_{C_2H_4}}{n_{in\,C_2H_5OH} - n_{out\,C_2H_5OH}} \cdot 100 \tag{28}$$

$$S_C[\%] = \frac{n_C / 2}{n_{in\,C_2H_5OH} - n_{out\,C_2H_5OH}} \cdot 100 \tag{29}$$

$$Y_{H_2}[\%] = \frac{n_{H_2} / 6}{n_{in\,C_2H_5OH}} \cdot 100 \tag{30}$$

In all cases examined ethanol conversion was total in the whole range of temperature, thus hydrogen selectivity and hydrogen yield coincide. At low temperatures, the cracking into methane and carbon dioxide is thermodynamically favoured. Hydrogen and CO contents progressively increase with temperature. Moreover, even if all compounds present in equations are included in the thermodynamic calculations, acetaldehyde and ethylene are never favoured, thus in the following section it has been reported the results as selectivity to major products formed.

The effect of two important parameters, defined as follows, have been calculated:

- Water-to-ethanol molar Feed ratio:

$$r.a. = \frac{molesH_2O}{molesEtOH} \tag{31}$$

- Feed dilution ratio:

$$r.d. = \frac{molesN_2}{molesEtOH + molesH_2O} \tag{32}$$

4.1.1 Effect of water to ethanol molar ratio

Equilibrium selectivity to H_2, CH_4, CO, CO_2, C_2H_4O, C_2H_4, C_3H_6O as a function of temperatures has been investigated. The range of operating conditions used is reported in Table 2.

• Temperature [°C]	• 100 ÷ 1000
• Water to ethanol molar ratio • r.a. H_2O:C_2H_5OH [mol:mol]	• 1:1 ÷ 10:1
• Dilution ratio • r.d. N_2:(H_2O+C_2H_5OH) [mol:mol]	• 4

Table 2. Operating condition for thermodynamic analysis: effect of water-to-ethanol molar ratio

Figure 3 shows the H_2 selectivity as a function of temperature for different values of the S/C (steam-to-carbon) ratio. The results of thermodynamic evaluations indicate that, in the overall temperature range, by increasing the feed ratio, the H_2 selectivity increases. By considering the temperature effect, the behaviour is quite different and in particular it is interesting to note that there is a maximum in the H_2 selectivity in the range 550-700°C, excepted for the S/C ratio lower than 3.

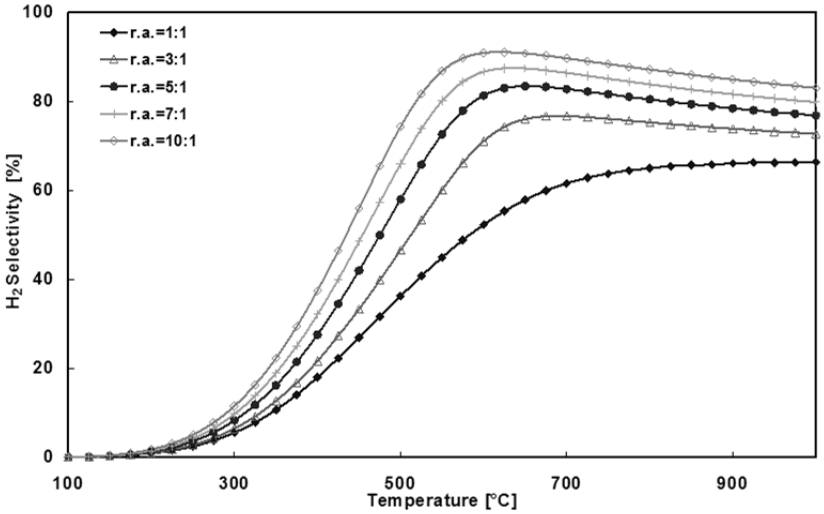

Fig. 3. H_2 selectivity as a function of temperature at different water-to-ethanol molar ratios

CH_4 selectivity has the opposite tendency. It is possible to observe in Figure 4 that the tendency to produce methane decreases by increasing the water content in the feed stream. In particular, at temperatures higher than 750°C, CH_4 selectivity is zero.

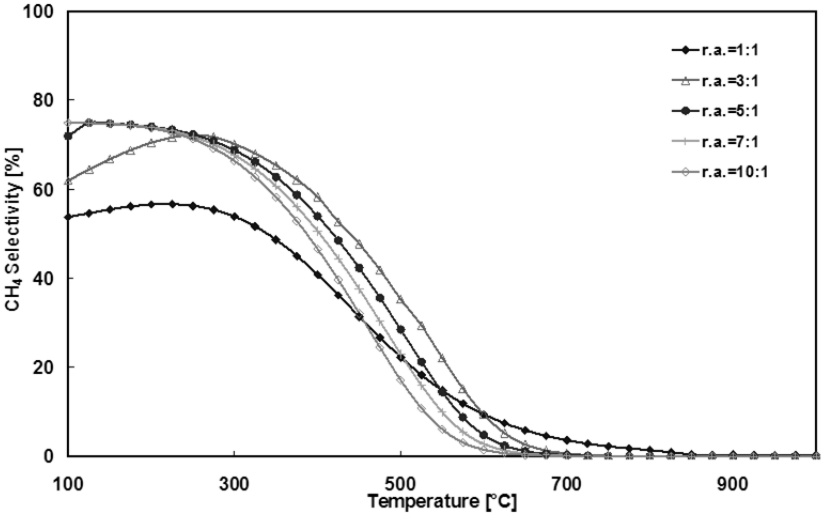

Fig. 4. CH_4 selectivity as a function of temperature at different water to ethanol molar ratios

CO selectivity (Figure 5), at T< 400°C, is not influenced by the presence of water because the CO-WGS reaction is favoured at lower temperatures. With temperature increasing, CO selectivity increase with a more evident tendency for lower water to ethanol molar ratios: at 1000°C, with r.a.= 1, CO selectivity is total, while with r.a.= 10, it results 50%.

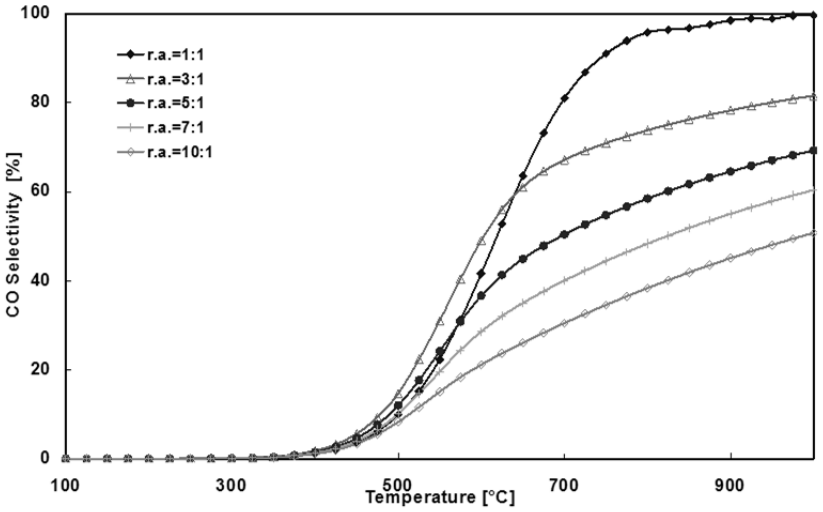

Fig. 5. CO selectivity as a function of temperature at different water to ethanol molar ratios

The data concerning the CO_2 selectivity are reported in Figure 6 as a function of temperature for different r.a. values, showing that S_{CO2} has a maximum in the range 500-700°C and that, by increasing the r.a. value, the CO_2 selectivity increase in the overall temperature range.

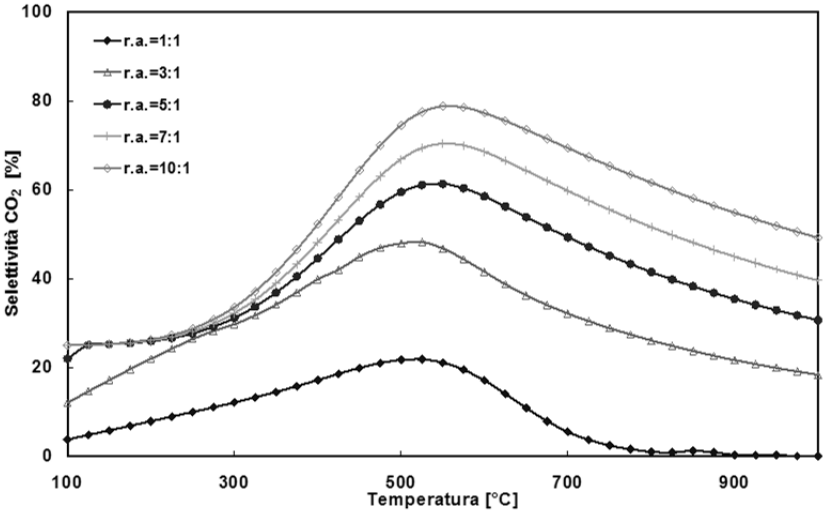

Fig. 6. CO_2 selectivity as a function of temperature at different water to ethanol molar ratios

Coke formation has also been studied at various T and r.a. values (Figure 7). At atmospheric pressure for a fixed temperature, r.a< 4:1 favour coke formation until 900°C. This effect is more obvious lowering temperature below 500 °C, in fact for r.a.= 3, coke formation may

occur only if T< 200 °C. It is worth to note that in the literature is also reported that by increasing the pressure, the S_C is lower, in particular at higher temperature (Hernandez et al. 2009).

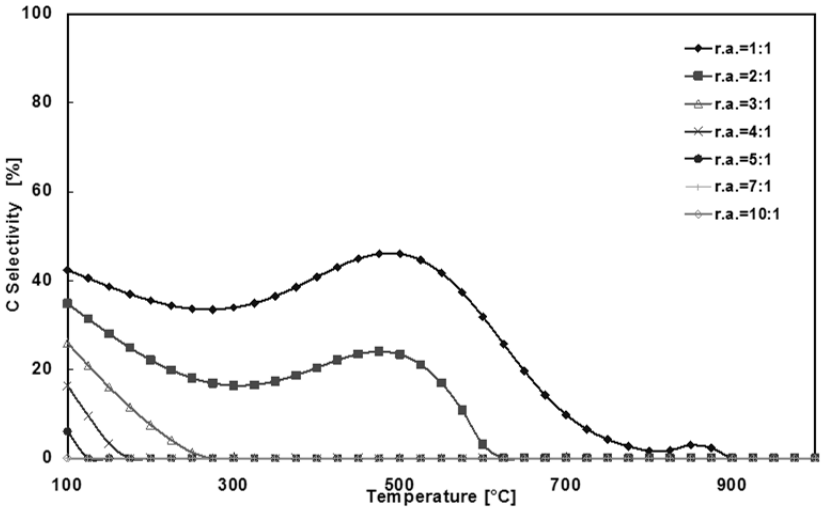

Fig. 7. C selectivity as a function of temperature at different water to ethanol molar ratios.

Since ethanol conversion is complete, H_2 yield and selectivity coincide (Figure 8) and, consequently, the comments are the same of Figure 3.

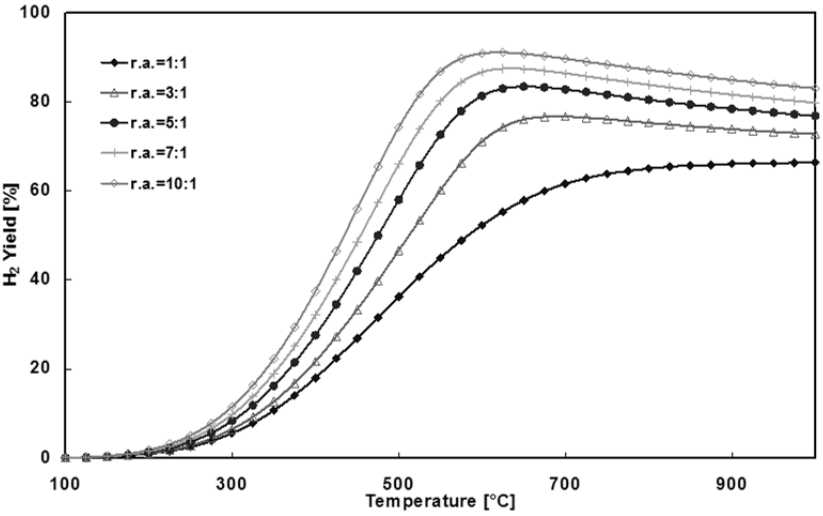

Fig. 8. H_2 yield as a function of temperature at different water to ethanol molar ratios

4.1.2 Effect of dilution ratio

Equilibrium selectivity to H_2, CH_4, CO, CO_2, C_2H_4O, C_2H_4, C_3H_6O as a function of temperature was studied. The range of operating conditions covered for the thermodynamic analysis is reported in Table 3.

Temperature [°C]	100 ÷ 1000
Water to ethanol molar ratio r.a. = H_2O:C_2H_5OH [mol:mol]	3
Dilution ratio r.d. = N_2:(H_2O+C_2H_5OH) [mol:mol]	0 ÷ 49

Table 3. Operating conditions for thermodynamic analysis-effect of dilution ratio

In Figure 9, 10 and 11 are reported results concerning the H2, CH4 and CO selectivity, respectively. Figure 9 shows that , in the range 100-600°C, hydrogen selectivity is favoured when temperature increases, the yield shows a slightly negative trend. Moreover, by increasing the r.d., the selectivity also increases because the reaction takings place with an increase in moles number. The presence of gaseous nitrogen has the same effect of the pressure decreasing (Khedr et al., 2006). Moreover, it is clear that methane selectivity has a complementary behaviour (Figure 9) with respect to CO and H_2, and it decreases when temperature and dilution increase. This result can be explained considering that, by increasing the temperature and the dilution ratio, the methane steam reforming reaction is progressively more favoured and CO and H_2 are produced.

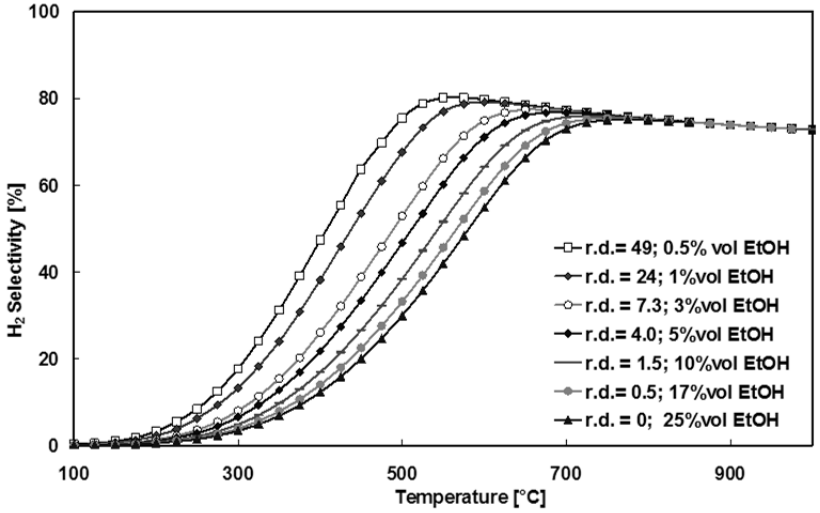

Fig. 9. H_2 selectivity as a function of temperature at different dilution ratios

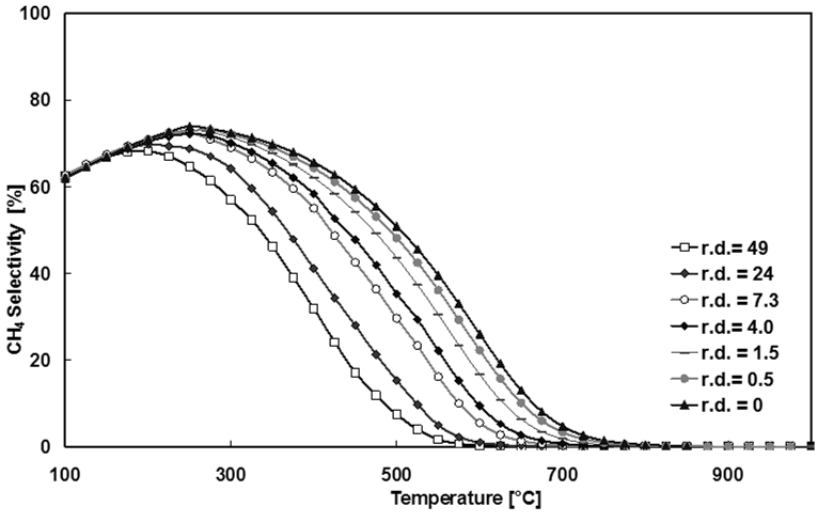

Fig. 10. CH_4 selectivity as a function of temperature at different dilution ratios

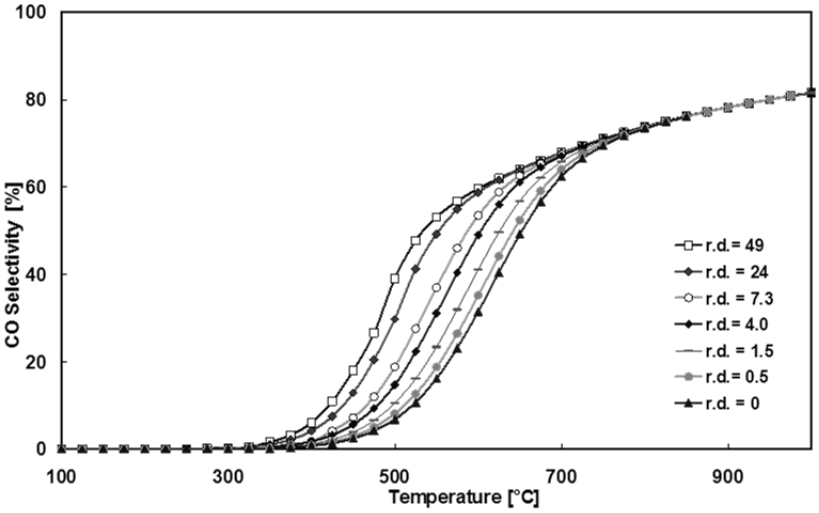

Fig. 11. CO selectivity as a function of temperature at different dilution ratios

The CO_2 selectivity is reported in Figure 12 as a function of temperature at different r.d. values. It is interesting to note that S_{CO2} has a maximum in the range 400-600°C, in agreement with the shoulder observed in the SH_2 profile.

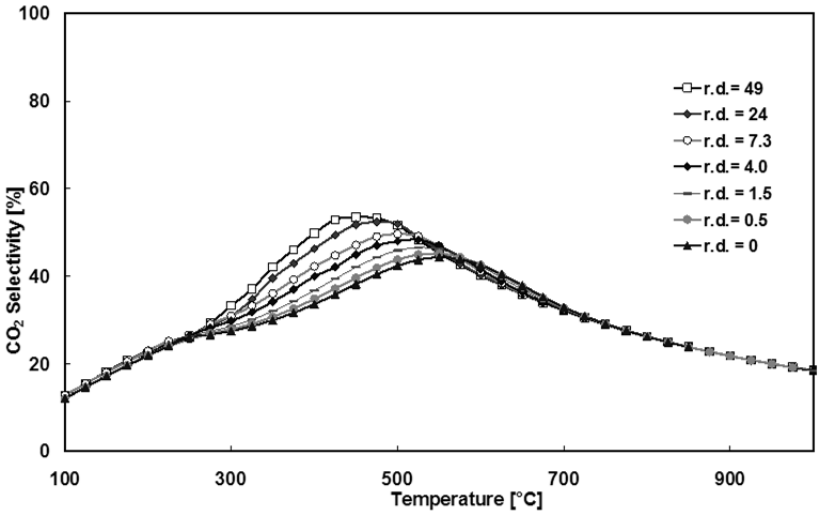

Fig. 12. CO_2 selectivity as a function of temperature at different dilution ratios

About the formation of different HC product, the results showed that, in the operating range considered, there isn't C_3H_6O, C_2H_4O, C_2H_4 formation, at any dilution ratio.

There is, instead, coke formation for temperature lower than 250°C, with a selectivity that decreases from 26% at 100°C, with temperature increasing (Figure 13).

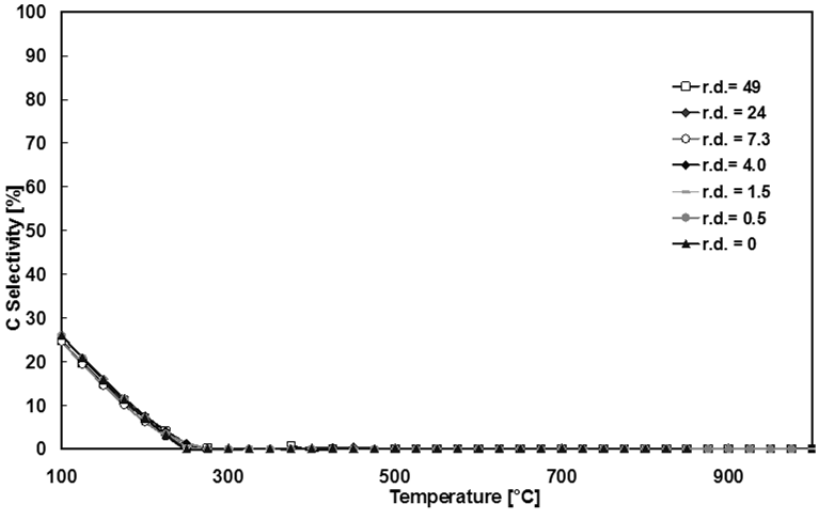

Fig. 13. C selectivity as a function of temperature at different dilution ratios

Since ethanol conversion is complete, hydrogen yield has the same tendency and values of the hydrogen selectivity (Figure 14).

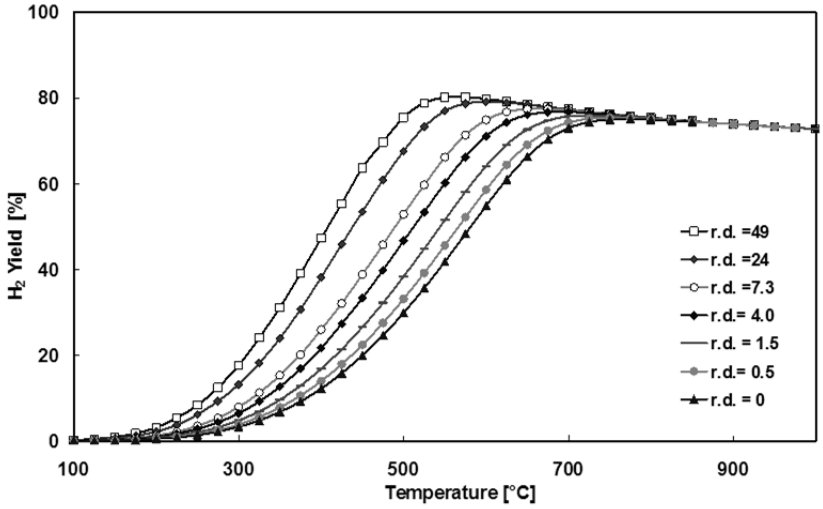

Fig. 14. H_2 yield as a function of temperature at different dilution ratios

4.1.3 ΔH of reaction

Considering the same system, composed of nine species, it has been estimated ΔH of reaction. The effect of temperature and water-to-ethanol molar ratio is shown in Figure 15.

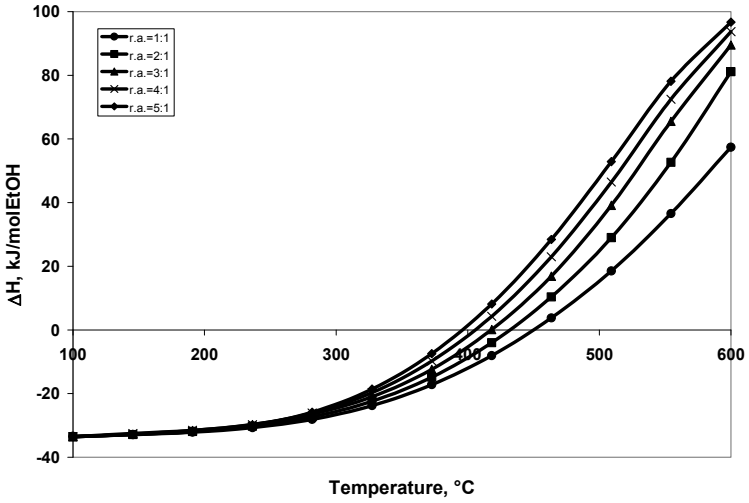

Fig. 15. Effect of temperature and water to ethanol and oxygen to ethanol molar ration on ΔH of reaction

At atmospheric pressure and for a fixed temperature, ΔH increases with water to ethanol molar ratio but it is very interesting to note the effect of temperature: ΔH increases with

temperature for all operating conditions examined but, in the temperature range 400-450°C, the reaction is almost athermic, then in this range the reaction needs a very low thermal duty. This behaviour could better explain the choice of the low temperature operating range.

4.1.4 Selected thermodynamic conditions

From the thermodynamic analysis reported, it may be concluded that hydrogen production through bioethanol steam reforming is favoured at temperatures higher than 600°C, because high H_2 and CO selectivity can be thermodynamically achieved at these high temperatures.

The results obtained are in agreement with other previous studies (Garcia & Laborde, 1991, Vasudeva et al., 1996). High temperatures and water to ethanol molar ratio favour hydrogen production; the tendency of methane is exactly the opposite of that of hydrogen.

There isn't a remarkable effect of the dilution ratio on products selectivities. Instead, the presence of water in the feed system is in favour of hydrogen yield. A stoichiometric water to ethanol molar ratio (3:1) is the minimum value enough to avoid coke formation in a wide range of temperature, so it has been selected in order to consider the most severe case.

Based on these considerations, ethanol steam reforming has been more widely studied over the high temperature range. Since CO is a poison for the anode of the fuel cells, it is necessary to remove it through the exothermic WGS reaction. For this purpose, it would be necessary to pass the reformate through a bed of low-temperature water-gas shift catalyst in order to generate further hydrogen and eliminate CO. This adversely affects overall system efficiency due to heat losses and increases the capital cost for necessary hardware. As a result, low temperature ethanol steam reforming is an attractive alternative (Roh et al., 2006a; Roh et al., 2006b; Ciambelli et al., 2009; Ciambelli et al., 2010a; Ciambelli et al., 2010b; Palma et al., 2011). This operating range could be useful to obtain a H_2 rich gas stream, also reducing the overall thermal duty. However, at low temperature hydrogen yield is lower and the reaction produces a wide range of undesirable secondary products but the main detrimental effect is related to the catalyst deactivation during ethanol steam reforming at low temperature has been reported to be severe.

Then a proper selection of a suitable catalyst is very important for the low temperature bio-ethanol steam reforming. Catalysts play an important role in the reactivity toward complete conversion of ethanol. However, each catalyst induces different pathways and, therefore, the selection of a suitable catalyst plays a vital role in ethanol steam reforming for hydrogen production. Active catalysts should maximize hydrogen selectivity and inhibit coke formation as well as CO production (Armor, 1999).

The literature surveys presented above reveal that the ethanol conversion and selectivity to hydrogen highly depend on the type of metal catalyst used, type of precursors, preparation methods, type of catalyst support, presence of additives, and operating conditions, i.e. water/ethanol molar ratio and temperature (Ni et al., 2007).

The steam reforming of ethanol over Ni, Co, Cu and noble metal (Au, Pd, Pt, Rh, Ru, Ir), supported on ionic oxides (CeO_2, Al_2O_3, MgO, TiO_2 but also Fe-Cr and Fe-Cu mixed oxides) has been extensively studied. The greatest concern lies in developing an active catalyst that inhibits coke formation and CO production, while there are few studies about low temperature ethanol steam reforming catalysts. In the follow sections it has been taken an overview of the published literature.

4.2 Noble metals-based catalysts

Noble metals on various supports are well-known for their high catalytic activity and have been studied extensively.

The catalytic performance of supported noble metal (Ru, Rh, Pd, Pt, Ir, Au) catalysts for the steam reforming of ethanol has been investigated in the temperature range of 600–850°C with respect to the nature of the active metallic phase, the nature of the support (Al_2O_3, MgO, TiO_2) and the metal loading. Different authors (Breen et al., 2002; Aupretre et al., 2005; Erdohelyi et al., 2006; Frusteri et al., 2004; Men et al., 2007; Diagne et al., 2002; Romero-Sarria et al., 2008; Domok et al., 2010; Basagiannis et al., 2008; Yamazaki et al., 2010) used Rh, Pd, and Pt on different supports such as alumina and ceria/zirconia: the noble metals activity decreased in the order of Pt-loaded catalyst, Rh-loaded catalyst, Pd-loaded catalyst. Dehydration of ethanol to ethylene was noted on alumina-supported noble metal catalysts. The catalyst stability was also monitored with and without the presence of oxygen. It was found that water enhanced the stability of ethoxide surface species formed by the dissociation of ethanol.

4.2.1 Rhodium catalysts

The ethanol steam reforming over Rh/Al_2O_3 catalysts have been investigated. The reaction was carried out at temperatures between 50 and 650°C with a water-to-ethanol molar ratio of 4.2-8.4 with or without O_2 addition for autothermal process, concluding that methane is a primary product whose selectivity decreases with contact time. The mechanism is composed by the following steps:

- ethanol dehydrogenation and/or dehydration
- gasification of acetaldehyde or ethylene formation.

The performance of Rh-based catalysts supported on alumina was compared with other metals: Rh appears as the most active one, but a further performance is obtained when it is doped with Ni or Ru (Breen et al., 2002; Liguras et al., 2003)

Aupetre et al. classified the metal activity in the order:

$$Ni> Rh>> Pd>Pt>Cu>Ru$$

A lot of studies suggest that Rh-based catalysts are promising (Freni et al., 2000, Wanat et al., 2004, Diagne et al., 2004).

$Rh/\gamma\text{-}Al_2O_3$ with 5 wt% loading was found to degrade considerably after operation for 100 h. Moreover, it was found that coke formation could be prevented at high temperatures by sufficiently large amounts of Rh and strong excess of water; in particular, at 650°C, only C_1 products were present at the exit of the stream, less coke was formed and the catalyst was more stable in presence of O_2. It is possible to suggest the occurrence of several reactions: acethaldehyde formed by dehydrogenation of ethanol is decomposed to CH_4 and CO (Eq. 33) or undergoes steam reforming (Eq. 34). Then water reforms the C_1 products to hydrogen (Eq. 35, 36). In addition, when O_2 is present, the reactions in Eqs 37-40 occur (Cavallaro et al., 2003).

$$CH_3CHO \Leftrightarrow CH_4 + CO \tag{33}$$

$$CH_3CHO + H_2O \Leftrightarrow 2CO + 3H_2 \quad (34)$$

$$CH_4 + H_2O \Leftrightarrow CO + 3H_2 \quad (35)$$

$$CO + H_2O \Leftrightarrow CO_2 + H_2 \quad (36)$$

$$CO + 0.5O_2 \Leftrightarrow CO_2 \quad (37)$$

$$C_2H_5OH + 0.5O_2 \Leftrightarrow CH_3CHO + H_2O \quad (38)$$

$$CH_4 + 2O_2 \Leftrightarrow CO_2 + 2H_2O \quad (39)$$

$$C + O_2 \Leftrightarrow CO_2 \quad (40)$$

$Rh/\gamma\text{-}Al_2O_3$ catalyst was studied to evaluate the complex reaction mechanism, at least at the preliminary stage. When a mixture of ethanol and water is used to supply a heated coil reactor, the reagents are transformed according to the reaction behavior pattern provided by the chemical nature of the catalyst. In the case where a dual function acid-dehydrogenant catalyst is used, it is reasonable to think that the main reactions will be those described in the scheme shown in Figure 16 (Cavallaro, 2000).

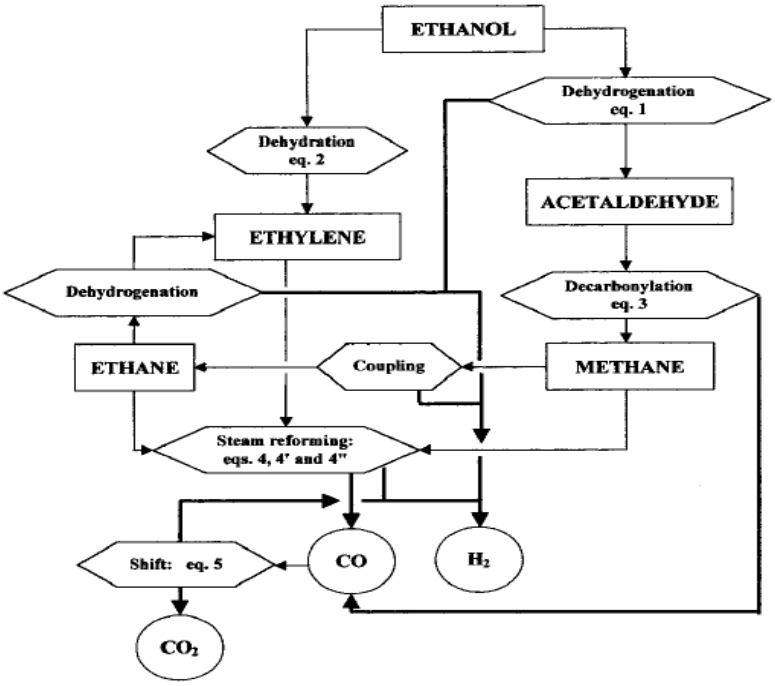

Fig. 16. Pathways for the steam reforming of ethanol over Rh/Al_2O_3 catalysts (Cavallaro, 2000)

In the case of ethanol steam reforming over Rh/Al_2O_3 under pressure (1.1 MPa), the catalysts is highly active, selective and stable in the ethanol at 700°C. Up to 4 g of hydrogen per hour and per gram of catalyst could be produced with a high selectivity towards CO_2 formation. The nature of the metal precursor salt (in terms of metal phase dispersion), metal loading and the reaction conditions influenced the performance of the catalyst (Aupretre et al., 2004).

Depositing Rh on MgAl-based spinel oxide supports (Figure 17) exhibited higher basicity, compared with alumina-supported Rh, whereas the surface acidity was strongly reduced, resulting in improved stability.

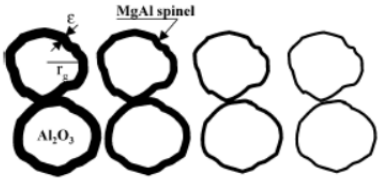

Fig. 17. Schematic picture of the morphology of the $MgAl_2O_4/Al_2O_3$ support (Aupretre et al., 2005)

Rh/ZrO_2 catalysts, in which the catalyst support is decorated with CeO_2, Al_2O_3, La_2O_3 and Li_2O, respectively, were studied for ethanol steam reforming reactiom. The catalyst using ZrO_2 without any decoration as the support exhibits the highest catalytic activity for H_2 production. Moreover it was found that Rh particle size and distribution as well as the surface area of the catalyst are not important factors in determining the catalytic performance.

It was evaluated the catalytic performance of MgO-supported Pd, Rh, Ni, and Co for hydrogen production by ethanol steam reforming. Rh/MgO showed the best ethanol conversion and stability at 650°C, while Ni/MgO exhibited the highest hydrogen selectivity (>95%). The activity of the catalysts reduced in the order Rh> Co> Ni> Pd. Coke formation rate on Rh/MgO was very low as MgO was basic. It was also found that the deactivation was mainly due to metal sintering. It was proposed a reaction mechanism for ethanol steam reforming: ethanol is first dehydrogenated to acetaldehyde which subsequently decomposes to CH_4 and CO. These lead to the formation of H_2 and CO_2 by steam reforming and water gas shift (WGS) reactions. Thus, the exit stream composition is governed by CH_4 steam reforming and WGS reactions (Frusteri et al. 2004).

Some studies (Diagne et al., 2002; Rogatis et al., 2008) deal with the hydrogen production by ethanol steam reforming over Rh catalysts supported on CeO_2, ZrO_2 and various $CeZrO_x$ oxides (Xe/Zr= 4,2, or 1). In the range 300-500°C, with a very Ar-diluted feed stream, with a high water-to-ethanol molar ratio, the H_2 yield resulted not favoured by a high basicity of support. Another paper (Idriss, 2004) outlined the complexity of the ethanol reactions on the surfaces of noble metals/cerium oxide catalysts, suggesting that hydrogen production is directly related to two main steps: the first involves breaking the carbon-carbon bond, and Rh appears the most suitable compound for this reaction at reasonable operating temperatures; the second involves CO oxidation to CO_2. Ethanol reforming on Rh/CeO_2–ZrO_2 does not appear to be sensitive to Rh dispersion. Up to 5.7 mol H_2 can be produced per

mol ethanol at 350-450°C on Rh/CeO_2-ZrO_2 in presence of excess of water (Diagne et al., 2002).

Rh/ZrO_2-CeO_2 catalysts appears to favour ethanol dehydrogenation rather than dehydration during the ethanol steam reforming reaction. They exhibit higher H_2 yield at low temperatures, possibly due to the efficient oxygen transfer from ZrO_2-CeO_2 to Rh. Higher Rh loadings enhance not only the WGS reaction but also CH_4 formation (Roh et al. 2008). Rh/ZrO_2 catalysts, in which the catalyst support is decorated with CeO_2, Al_2O_3, La_2O_3 and Li_2O, respectively, were studied for ethanol steam reforming reaction. The catalyst using ZrO_2 without any decoration as the support exhibits the highest catalytic activity for H_2 production. Moreover it was found that Rh particle size and distribution as well as the surface area of the catalyst are not important factors in determining the catalytic performance.

$CeZrO_x$ is an interesting support for Rh and Ni (Aupretre et al., 2005) since it

- significantly increased the H_2 yield;
- strongly favours the acetaldehyde route to CO_x and H_2 instead of its decomposition into CO and methane, due to the fast oxidation of the CH_3 groups of acetaldehyde, related to the well know oxygen storage capability and mobility of the support;
- favours the direct composition of water into hydrogen and not only into OH groups;
- inhibits the dehydration route to ethylene, that is a coke precursor, and promotes CH_x oxidation and surface cleaning along the steam reforming process. For this reasons, the catalysts stability is improved.

Rh/TiO_2 catalysts were also studied (Rasko at al., 2004): it was found that ethanol dissociation forms ethoxides at ambient temperature. Dehydrogenation leads to acetaldehyde.

4.2.2 Platinum

There is a scarse information in literature on Pt-based catalysts for low temperature ethanol steam reforming. It was studied oxidative steam reforming of ethanol over a Pt/Al_2O_3 catalyst modified by Ce and La. The presence of Ce as an additive was found to be beneficial for hydrogen production. The presence of La however did not promote ethanol conversion. When both Ce and La were present on the support, poorer catalyst behaviour was observed due to lower Pt-Ce interaction with respect to La-free ceria-alumina support (Navarro et al., 2005).

The reaction of ethanol and water has been investigated over K doped 1% Pt/Al_2O_3 catalysts. The presence of K resulted at room temperature in upward shift of the IR band of CO formed in the ethanol adsorption. At higher temperature the presence of surface acetate species was also detected which, according to the TPD results decomposed above 300°C to form CH_4 and CO_2. The K destabilized these forms. In the catalytic reaction the H_2 selectivities were similar and much higher over all promoted Pt/Al_2O_3 than on the pure catalyst. It was proved that the K had a destabilizing effect onto the surface acetate groups and thus improved the steam reforming activity of 1% Pt/Al_2O_3. The potassium caused significant changes in the product distribution of the steam reforming reactions (Figure 18): over K containing catalysts, higher selectivity of H_2, CO_2, and CH_4 was obtained in the steady state than over pure 1% Pt/Al_2O_3, and the potassium also suppressed the formation of ethylene.

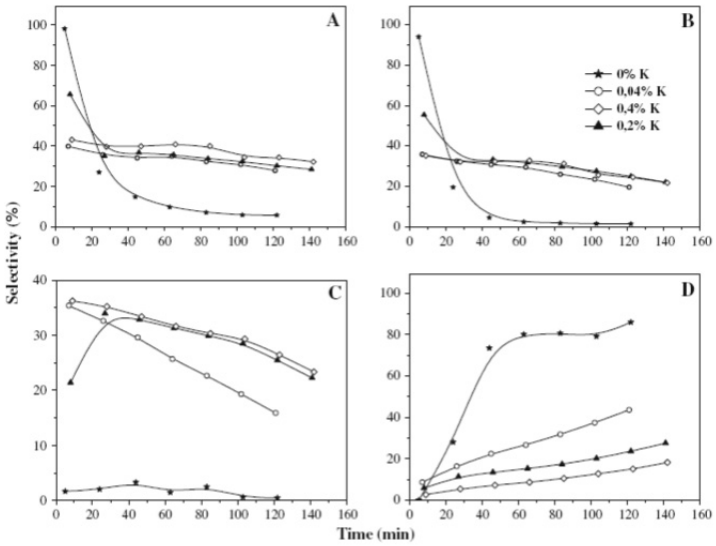

Fig. 18. The selectivity of H_2 (A), CO_2 (B), CH_4 (C), and C_2H_4 (D) formation in the ethanol steam reforming reaction at 450°C on Pt/Al_2O_3 catalysts with different K loading (Domok et al., 2008)

The effect of the support nature and metal dispersion on the performance of Pt catalysts during steam reforming of ethanol was studied (de Lima et al., 2008). H_2 and CO production was facilitated over Pt/CeO_2 and $Pt/CeZrO_2$, whereas the acetaldehyde and ethane formation was favoured on Pt/ZrO_2. According to the reaction mechanism, some reaction pathways are favoured depending on the support nature, which can explain the differences observed on the resulting product distribution. At high temperature, the forward acetate decomposition is promoted by both steam and Pt and is favoured over the CeO_2-based catalyst. These results are likely due to the higher Pt dispersion on Pt/CeO_2 catalyst.

The steam reforming reactions for bio-ethanol and reagent ethanol over several Pt/ZrO_2 catalysts with 1–5 wt% Pt loadings were examined. For the reaction with reagent ethanol, the main products were H_2, CO_2, CO, and CH_4; production of acetone, acetaldehyde, and ethylene at 400°C was very low. The partial ethanol steam reforming reaction and the ethanol decomposition reaction occur competitively in the catalytic system. The activities of the catalysts with larger Pt loadings were higher and more stable. The H_2 yield on the Pt/ZrO_2 catalyst reached 29% at 400°C, but at 500°C the activity of H_2 formation rapidly decreased with time-on-stream. The activity for the ethanol steam reforming reaction decreased more rapidly than that for the ethanol decomposition reaction (Yamazaki et al., 2010).

The effects of the support (alumina or ceria) on the activity, selectivity and stability of 1 wt% Pt catalyst for low temperature ethanol steam reforming have been investigated. Experimental results in the range 300-450°C showed a better performance of ceria supported catalyst, especially with reference to deactivation rate. Moreover, Pt/CeO_2 catalyst performance increase by increasing the Pt load in the range 1-5 wt% (Figure 19). The best catalytic formulation (5 wt% Pt on CeO_2) was selected for further studies. It is worthwhile

that this catalyst is also active for the water gas shift conversion of CO to CO_2, resulting in the absence of CO in the reformate product. (Ciambelli et al., 2010a).

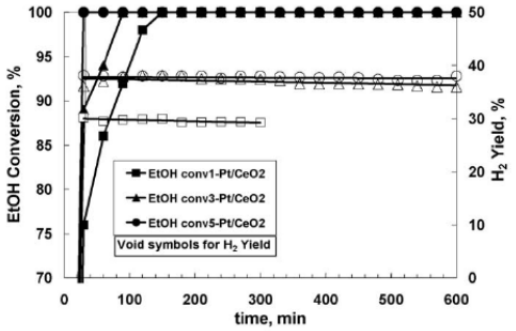

Fig. 19. Effect of Pt load on ethanol conversion and H_2 yield versus time on stream for Pt/CeO_2 catalysts. Experimental conditions: T = 300°C; C_2H_5OH = 0.5 vol%; $C_2H_5OH:H_2O:N_2$ = 0.5:1.5:98; Q_{Tot} = 1000 (stp)cm^3/min; GHSV: 15,000 h^{-1} (Ciambelli et al., 2010a)

Some preliminary results of a kinetic investigation of SR of ethanol on the selected Pt/CeO_2 catalyst and a proposed reaction mechanism are also reported (Ciambelli et al., 2010b). The main promoted reactions are ethanol decomposition, ethanol steam reforming and CO water gas shift, and the apparent reaction orders are 0.5 and 0 for ethanol and steam respectively, with an apparent activation energy of 18 kJ mol^{-1} evaluated in the range 300–450°C. Kinetic evaluations and temperature programmed desorption experiments suggest a surface reaction mechanism reported in Figure 20 and involving the following steps:

i. ethanol dissociative adsorption on catalyst surface to form acetaldehyde intermediate;
ii. decarbonylation to produce mainly H_2, CH_4 and CO;
iii. WGS reaction of CO adsorbed on Pt sites to produce H_2 and CO_2.

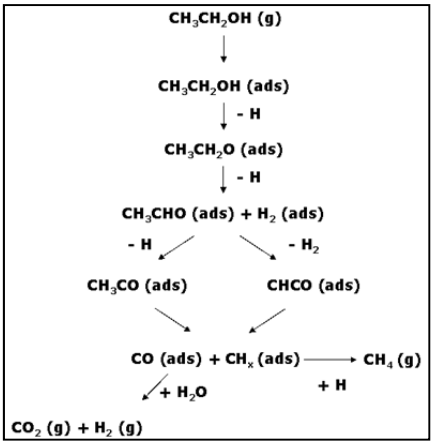

Fig. 20. Scheme of the surface reaction mechanism proposed (Ciambelli et al., 2010b)

4.2.3 Palladium

Few studies on Pd catalyzed steam reforming of ethanol have also been reported earlier. In another such study on Pd/Al_2O_3, these researchers reported that CO concentration was minimum at 450°C and the amount of coke formed was negligible even at stoichiometric water-to-ethanol ratios (Goula et al., 2004).

Pd catalysts supported on a porous carbonaceous material in presence of steam in the range of temperatures 330-360°C was found to have high activity and stability (Galvita et al., 2002). However, it was observed that a Pd/MgO catalyst drastically deactivated during reaction due to metal sintering at 650°C. Coke formation on Pd/MgO occurred at higher rate than on MgO-supported Rh, Ni and Co catalysts (Frusteri et al., 2004).

Unlike Rh, co-deposition of Pd and Zn on ZnO support led to formation of PdZn alloy, which favored dehydrogenation and hydrogen production (Casanovas et al., 2006).

4.2.4 Ruthenium

The catalytic performance of supported Ru-based catalysts for the steam reforming (SR) of ethanol has been studied. The catalytic performance is significantly improved with increasing metal loading; in particular, although inactive at low loading, Ru showed comparable catalytic activity with Rh at high loading. There was a marked increase in conversion of ethanol and selectivity to H_2 over Ru/Al_2O_3 with an increase in the Ru content (Figure 21). The Ru/Al_2O_3 with 5 wt% loading could completely convert ethanol into syngas with hydrogen selectivity above 95%, the only byproduct being methane (Figure22).

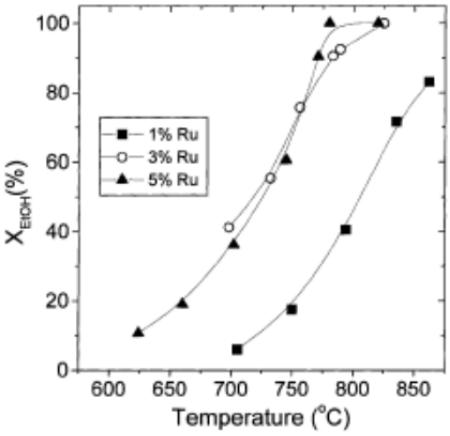

Fig. 21. Effect of reaction temperature on the conversion obtained over Ru/Al_2O_3 catalysts of variable metal content (1-5%) (Liguras et al., 2003)

High dispersion of catalyst atom at the support surface was found to enhance the activity of catalysts. The catalyst was stable and had activity and selectivity higher than Ru/MgO and Ru/TiO_2. The selection of support played an important role in long-term catalytic operation. Acidic supports, such as γ-Al_2O_3, induced ethanol dehydration to produce ethylene, which

was a source of coke formation. Dehydration can be depressed by adding K to neutralize the acidic support or by using basic supports, i.e. La_2O_3 and MgO. About 15% degradation in ethanol conversion was detected for Ru/Al_2O_3 with 5 wt% after operation for 100 h (Liguras et al., 2003).

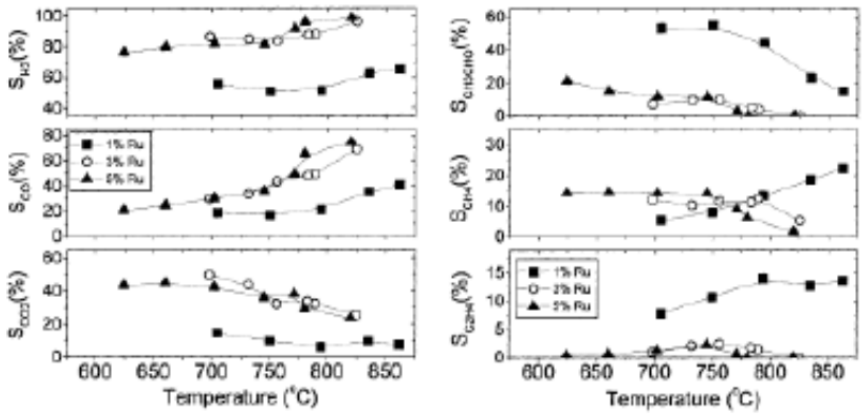

Fig. 22. Effect of reaction temperature on the selectivity toward reaction products over Ru/Al_2O_3 catalysts of variable metal content (1-5%) (Liguras et al., 2003)

4.2.5 Iridium

Steam reforming of ethanol over an Ir/CeO_2 catalyst has been studied with regard to the reaction mechanism and the stability of the catalyst. It was found that ethanol dehydrogenation to acetaldehyde was the primary reaction, and acetaldehyde was then decomposed to methane and CO and/or converted to acetone at low temperatures. Methane was further reformed to H_2 and CO, and acetone was directly converted into H_2 and CO. Addition of CO, CO_2, and CH_4 to the water/ethanol mixture proved that steam reforming of methane and the water gas shift were the major reactions at high temperatures (Figure 23). The Ir/CeO_2 catalyst displayed rather stable performance in the steam reforming of ethanol at 650°C even with a stoichiometric feed composition of water/ethanol, and the effluent gas composition remained constant for 300 h on-stream. Significant deactivation was detected at 450°C. The CeO_2 in the catalyst prevented the highly dispersed Ir particles from sintering and facilitated coke gasification through strong Ir–CeO_2 interaction (Zhang et al., 2008).

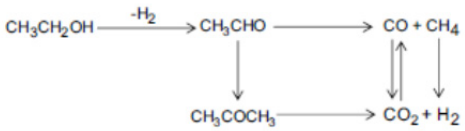

Fig. 23. Proposed reaction scheme of ethanol steam reforming on the Ir/CeO_2 catalyst (Zhang et al., 2008)

Figure 24 shows the concentrations of H_2, CO_2, CH_4, and CO in the outlet gas as a function of time-on-stream (TOS) (Zhang et al., 2008).

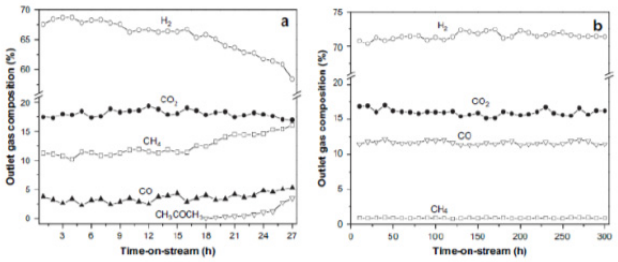

Fig. 24. Long-term stability test of the Ir/CeO_2 catalyst (Zhang et al., 2008)

La_2O_3-supported Ir catalyst was tested for the oxidative steam reforming of ethanol (OSRE). La_2O_3 would transform into hexagonal $La_2O_2CO_3$ during OSRE, which suppress coking. Reduced Ir metal can interplay with $La_2O_2CO_3$ to form Ir-doped $La_2O_2CO_3$. It dynamically forms and decomposes to release active Ir nanoparticles, thereby preventing the catalyst from sintering and affording high dispersion of Ir/La_2O_3 catalysts at elevated temperatures. By introducing ultrasonic-assisted impregnation method during the preparation of a catalyst, the surface Ir concentration was significantly improved, while the in situ dispersion effect inhibited Ir from sintering. The Ir/La_2O_3 catalyst prepared by the ultrasonic-assisted impregnation method is highly active and stable for the OSRE reaction, in which the Ir crystallite size was maintained at 3.2 nm after 100 h on stream at 650°C and metal loading was high up to 9 wt%.

Catalytic activity of a ceria-supported Iridium catalyst was investigated for steam reforming of ethanol within a temperature range of 300–500°C. The results indicated that only less sintering influences the catalytic activities for high temperature reduction. The ethanol conversion approached completion around 450°C via reduction pretreatment for Ir/CeO_2 samples under H_2O/EtOH molar ratio of 13 and 22,000 h^{-1} GHSV. Not only was a high dispersion of both catalysts present but also no impurities (e.g., boron) interfered with the catalytic activities. The hydrogen yield (H_2 mole/EtOH mole) exceeds 5.0 with less content of CO and CH_4 (<2%) (Siang et al., 2010).

4.3 Non noble metals

However, the high cost of noble metals is a major limiting factor in their use for hydrogen production via steam reforming. Some selected studies on ethanol steam reforming over non-noble metal catalysts are reported.

4.3.1 Nickel catalysts

Because of its high performances, its low cost and its high activity, nickel is one of the most studied metals for ethanol steam reforming for catalysts on different supports (Table 4).

The reforming reaction was carried out using various catalysts with Ni on La_2O_3, Al_2O_3, yttria-stabilised zirconia (YSZ), and MgO (Fatsikostas et al., 2002). According to their observations, from among the different catalytic systems selected, Ni/La_2O_3 catalyst exhibited the highest activity in hydrogen production. The ESR activities of three nano-size nickel catalysts, Ni/Y_2O_3, Ni/La_2O_3, and Ni/Al_2O_3, using nickel oxalate as precursor in the

impregnation-decomposition – reduction method, were investigated (Sun et al., 2005). It was found that the Ni/Y_2O_3 and Ni/La_2O_3 catalysts exhibited relatively high activity in ethanol steam-reforming at 250°C. An increase in the reaction temperature to 320 °C resulted in increased conversion as well as selectivity. In their study, Ni/Al_2O_3 exhibited comparatively lower activity in ethanol steam-reforming and hydrogen selectivity.

However, all three catalysts exhibited long-term stability in the ethanol steam-reforming reaction.

Studies on the steam-reforming of ethanol on Ni/B_2O_4 (B = Al, Fe, Mn) focusing on the influence of the B site metal and crystallinity on the catalytic performance of spinel-type oxide catalysts were carried out (Muroyama et al., 2010). All the spinel-type oxides promoted ethanol steam-reforming regardless of the reduction treatment, indicating that the nickel species were gradually reduced during the reaction.

The Ni/Al_2O_4 catalyst exhibited stable ethanol conversion, H_2 yield, and C_1 selectivity. The decrease in the activity of Ni/Fe_2O_4 and Ni/Mn_2O_4 catalysts was found to be due to carbon deposition.

Ni/MgO catalyst has been studied in steam reforming of ethanol (Freni et al., 2002), showing high activity and selectivity to H_2. Frusteri et al. (2004) reported high H_2 selectivity (> 95 %) at a space velocity 40000 h^{-1} over Ni/MgO at MCFC operating conditions (650°C). The performance of alkali-doped Ni/MgO catalysts on bio-ethanol steam reforming was also studied. The addition of Li and K enhanced the catalyst stability mainly by depressing Ni sintering. It was found that, because of the presence of the MgO support, there was a reduction in the amount of carbon decomposition on the catalyst. At higher temperatures (above 600°C), nickel-based catalysts became more effective in ethanol steam-reforming giving H_2, CO, CO_2, and CH_4 as the main reaction products (Fatsikostas & Verykios, 2004; Fatsikostas et al., 2002; Benito et al., 2007).

The steam-reforming of ethanol was investigated on alumina supported nickel catalysts modified with Ce, Mg, Zr, and La (Sanchez-Sanchez et al., 2009). They found that the addition of these promoters directly affected the acidity, structure, and morphology of Ni particles. The presence of Mg decreased the surface acidity of Al_2O_3 and modified the degree of interaction between Ni and Al_2O_3. The addition of Zr to the Al_2O_3 support resulted in a decrease in surface acidity as well as a decrease in the dispersion of Ni phases in the catalyst as compared with that achieved on Al_2O_3 alone; in addition, strong Ni – ZrO_2 interactions were observed in these systems. The addition of Ce to the Al_2O_3 support led to a moderate decrease in the surface acidity of Al_2O_3 and resulted in nickel phases with a better dispersion.

The ethanol steam reforming was also studied over Ni/Al_2O_3 in the range of temperatures 300-500 °C (Comas et al., 2004): it was not find any evidence of the water gas shift reaction occurring over Ni. They proposed a reaction scheme for ethanol reforming on Ni-based catalyst at 500°C. In this scheme acetaldehyde and ethylene formed as intermediates during reaction produces CO, CO_2, CH_4 and H_2 as the final products by steam reforming while the effluent composition is determined by methane steam reforming.

Ni/La_2O_3 exhibited high activity and stability in steam reforming of ethanol to hydrogen. This was attributed to the formation of lanthanum oxycarbonate species ($La_2O_2CO_3$), which

reacts with the surface carbon deposited during reaction and prevents deactivation (Fatsikostas et al., 2001; Fatsikostas et al., 2002).

Ethanol reforming was studied over Ni catalysts supported on γ -Al_2O_3, La_2O_3 and La_2O_3/γ-Al_2O_3 (Fatsikostas and Verykios, 2004). The impregnation of Al_2O_3 with La_2O_3 reduced carbon deposition. The presence of La_2O_3 on the catalyst, high water to ethanol ratios and high temperatures offered high resistance to carbon deposition.

The influence of the support nature (TiO_2, ZnO, Al_2O_3 and Al_2O_3–Fe_2O_3) of nickel catalysts on their activity, selectivity and coking phenomenon in the steam reforming of ethanol in the range of 300–600°C was investigated (Denis et al., 2008). An improvement of the selectivity of the process to hydrogen generation and diminishing of the formation of undesirable products (especially of hydrocarbons, including ethylene, and carbonaceous deposit) may be obtained by promoting nickel catalysts with sodium. On the basis of both ethanol conversions and hydrogen selectivities one may get the following order of hydrogen productivity in the steam reforming of ethanol: Ni/Zn > Ni/ Ti > Ni/Al–Fe > Ni/Al (Figure 25).

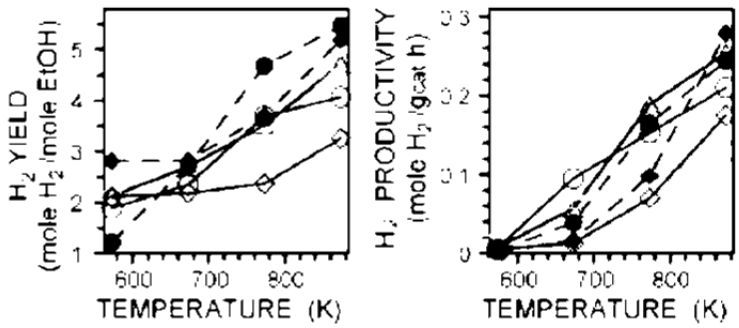

Fig. 25. Effect of nickel catalyst support and sodium promoter on the yield and productivity of hydrogen formation in the steam reforming of ethanol: (◊) Ni/Al; (Δ) Ni/Ti; (○) Ni/Zn; (□) Ni/Al–Fe; (♦) Ni/Al + Na; (● Ni/Zn + Na (Denis et al., 2008)

Perovskite-type oxide supported nickel catalysts, namely NiO/$LaFe_yNi_{1-y}O_3$ are promising candidate for the steam reforming of ethanol. The NiO/$LaFe_yNi_{1-y}O_3$ catalysts show high activity, selectivity as well as very good stability both in terms of anti-sintering of active species of nickel and anti-carbon deposition (Chen et al., 2009; Zhang et al., 2009; de Lima et al., 2010). Ni/ITQ-2 delaminated zeolite was found to be active in the ethanol steam reforming reaction. Deposition of coke occurs; however deactivation was not detected during the experimental time (72 h) (Chica & Sayas, 2009).

The Ni-based spinel-type oxides, NiB_2O_4 (B=Al, Fe, Mn), were investigated for their catalysis of the ethanol steam reforming reaction. Ethanol conversion over spinel-type oxides without reduction treatment was comparable to that over γ-alumina supported Ni catalyst reduction. The spinel oxide of $NiAl_2O_4$ showed extremely stable performance for 48 h, while the activity of $NiFe_2O_4$ and $NiMn_2O4$ catalysts was reduced by carbon deposition. Catalyst stability for reforming reaction was closely related to the stability of the nickel metal dispersed on the catalyst surface and the spinel structure. Differences in crystallinity and

surface area among the catalysts were not crucial factors for determining ethanol conversion for $NiAl_2O_4$ calcined between 800°C and 1100°C. the catalyst calcined at 900°C exhibited the highest activity for the reforming reaction (Muroyama et al., 2010).

Al_2O_3, MgO, SiO_2 and ZnO supported nickel catalysts were prepared and evaluated in the steam reforming for hydrogen production. Comparing the conversion of ethanol and selectivity to hydrogen over nickel-based catalysts, at a reaction temperature of 400°C, the result was: Ni/SiO_2>>Ni/Al_2O_3>Ni/ZnO>Ni/MgO. The highest conversion over Ni/SiO_2, could indicate that there is a greater amount of active sites available for this catalyst. However, selectivity to hydrogen was affected by the support used and occurred in the following order: Ni/SiO_2 ~ Ni/MgO>Ni/ZnO>>Ni/Al_2O_3. The low H_2 selectivity presented by Ni/Al_2O_3 could be due to the great C_2H_4 formation promoted by this catalyst. In addition, according to the results, it is possible to conclude that at 400°C only Ni/SiO_2 was active for ethanol steam reforming and at 500°C of reaction temperature, Ni/SiO_2 and Ni/MgO showed activity for ethanol steam reforming (Fajardo et al., 2010).

The reforming of crude ethanol was studied over Ni/Al_2O_3 catalysts (Akande et al. 2005a; Akande, 2005b) suggesting a power law model in the range of temperatures 320 ÷ 520°C. Thus the rate could be expressed as in Eq. 41:

$$-r_A = k_0 e^{-\frac{E}{RT}} C_A^n \tag{41}$$

where "$-r_A$" is in kmol $kgcat^{-1}s^{-1}$, "k_0" is in $kmol^{0.57}(m^3)^{0.43}kg_{cat}^{-1}s^{-1}$, "$C_A$" is crude ethanol concentration in kmol m^{-3}, "n" denotes order with respect to ethanol. The order with respect to ethanol was found to be 0.43 while the energy of activation "E" was found to be 4.41 kJ mol^{-1}. The Eley Rideal type kinetic model was also reported for catalytic reforming of crude ethanol over Ni/Al_2O_3 for temperatures in the range 320 - 520°C (Aboudheir et al., 2006), assuming dissociation of adsorbed crude ethanol as the rate-determining step (Eq. 42):

$$-r_A = \frac{k_0 e^{-\frac{E}{RT}} (C_A - C_C^2 C_D^6 / K_P C_B^3)}{(1 + K_A C_A)^2} \tag{42}$$

where "$-r_A$" is the rate of disappearance of crude ethanol in kmol $kgcat^{-1}s^{-1}$, "k_0" is in m^3 $kgcat^{-1}s^{-1}$, "A" = ethanol, "B" = water, "C" = CO_2, "D" = H_2, "C_i" denotes concentration of species "i" in kmol m_{-3}, "K_P" denotes the overall equilibrium constant in $(kmol\ m^{-3})^4$, "K_A" denotes the absorption constant of A in m^3 $kmol^{-1}$. A kinetic study of ethanol steam reforming to produce hydrogen within the region of kinetic rate control was carried out. A Ni(II)–Al(III) lamellar double hydroxide as catalyst precursor was used. The catalyst, working in steady state, does not produce acetaldehyde or ethylene; H_2, CO, CO_2 and CH_4 were obtained as products. Using the Langmuir–Hinshelwood (L–H) approach, two kinetic models were proposed. The first was a general model including four reactions, two of them corresponding to ethanol steam reforming and the other two to methane steam reforming. When high temperatures and/or high water/ethanol feed ratios were used, the system could be reduced to two irreversible ethanol steam reforming reactions (Mas et al., 2008).

Ni content (wt.%)	Support	r.a.	T (°C)	X_{EtOH} (%)	S_{H2} (%)
10	γ-Al_2O_3	4	600	100	75
10		8	650	100	78.2
15		6	750	100	87
17		3	750	100	93
16.1		3	250	76	44
20		3	700	77	87
20		3	800	100	96
35		6	500	100	91
10	La_2O_3	8	650	100	89.3
15.3		3	250	80.7	49.5
17		3	600	93	87
17		3	700	100	95
17		3	750	100	90
20		3	800	35	70
20		3	500	100	95
15	La_2O_3-Al_2O_3	6	600	100	87
10	TiO_2	4	600	100	86
10	$Ce_{0.5}Ti_{0.5}O_2$	3	600	100	58
30	$Ce_{0.74}Ti_{0.26}O_2$	8	600	98	88
30	$Ce_{0.74}Ti_{0.26}O_2$	8	650	100	93
10	ZnO	4	600	95	80
10		8	650	100	89.1
10	MgO	8	650	100	82.2
17		3	750	100	79
17	YSZ	3	750	100	92
20.6	Y_2O_3	3	250	81.9	43.1

Table 4. Ethanol conversion and initial selectivity to hydrogen obtained on various nickel supported catalysts and different reaction conditions (temperature, water-to-ethanol molar ratio r.a.), at atmospheric pressure

4.3.2 Cobalt

Cobalt (Co) is another non-noble metal catalyst under extensive investigation (Table 5) as supported Co could break C–C bond. Earlier, Co-based catalysts were deemed as appropriate system for steam reforming of ethanol. The use of ZnO-supported cobalt-based catalysts has been proposed for the steam reforming of ethanol (Llorca et al., 2002, 2003, 2004). The use of $Co(CO)_8$ as precursor produced a highly stable catalyst that enabled of the production of CO-free H_2 at low temperatures (350°C). They concluded that the method of catalyst preparation affected its performance and structural characteristics.

The catalytic properties of Co among other metals was also studied (Haga et al., 1998): it was found that selectivity to H_2 was in the order Co>Ni>Rh>Pt, Ru, Cu. In another study found that the supports vastly influenced the properties of Co catalysts (Haga et al., 1997). The formation of H_2 decreased in the order: Co/Al_2O_3>Co/ZrO_2>Co/MgO>Co/SiO_2>Co/C. The Co/Al_2O_3 catalyst exhibited the highest selectivity to H_2 (67% at 400°C) by suppressing

methanation of CO and decomposition of ethanol. Similarly, it was found that Co/MgO is more resistant to coke formation than Co/Al_2O_3 at 650°C (Cavallaro et al., 2001).

It was reported high catalytic activity of Co/SiO_2 and Co/Al_2O_3 for steam reforming of ethanol (Kaddouri & Mazzocchia, 2004), concluding that the product distribution was dependent on both the nature of the support and the method of catalyst preparation, thereby suggesting metal-support interaction. The ethanol steam reforming over Co/Al_2O_3 and Co/SiO_2 was studied (Batista et al., 2004), the catalysts showed average conversion higher than 70 % at 400°C. The metal loading influenced ethanol conversion and product distribution.

The catalytic activity for the ethanol steam reforming of Co_3O_4 oxidized, reduced and supported on MgO, and of CoO in MgO solid solution was investigated. Only samples containing metallic cobalt are found to be active for reforming reaction. It appears that samples containing metallic cobalt are active for the steam reforming of ethanol, whereas Co^{+2} stabilized in MgO solid solution, is able for ethanol dehydrogenation. It has been evidenced that coke deposition is always present in spite of different kinetic conditions and of low ethanol concentration (Tuti & Pepe, 2008).

An excellent ethanol reforming catalysts was performed with cobalt oxides at atmospheric pressure. Apparently, the dehydrogenation of ethanol to acetaldehyde is the first step with cobalt oxides.

$$2C_2H_5OH \rightarrow CH_3CHO_{(ads)} + H_2 \tag{43}$$

The acetaldehyde can be transformed in different pathways: decomposes to methane and carbon monoxide or on the surface of cobalt oxide it can be oxidized to acetate and follow decomposes into methyl group and CO_2.

$$CH_3CHO_{(a)} \rightarrow CH_4 + CO \tag{44}$$

$$CH_3CHO_{(a)} \rightarrow CH_3COO_{(asd)} \tag{45}$$

$$CH_3CHO_{(a)} \rightarrow CH_{3(asd)} + CO_2 \tag{46}$$

In addition, the methyl group can further react with surface OH species or water to form carbon monoxide and hydrogen

$$CH_{3(asd)} + OH_{(asd)} \rightarrow 2H_2 + CO \tag{47}$$

$$2CH_{3(asd)} + 2H_2O \rightarrow 5H_2 + 2CO \tag{48}$$

In the presence of water, the side-reactions of water gas shift (WGS) and methane steam reforming may also occur

$$CO + H_2O \rightarrow H_2 + CO_2 \tag{49}$$

$$CH_4 + H_2O \rightarrow 3H_2 + CO \tag{50}$$

CoO_x catalysts at low temperature possessed high activity. The best sample approached the H_2 yield theoretical value around 375°C. At a molar feed ratio $EtOH/H_2O$ of 1/13 and 22,000 h^{-1}GHSV, the H_2 yield reached 5.72 and only low CO (<2%) and CH_4 (<0.8%) concentrations were detected (Wang et al., 2009).

Also Co/CeO_2-ZrO_2 catalysts were characterized and tested for ESR reaction. It was found that the catalyst reducibility was influenced by the preparation methods; at 450°C, the impregnated catalyst gives a hydrogen production rate of 147.3 mmol/g-s at a WHSV of 6.3 h^{-1} (ethanol) and a steam-to-carbon ratio of 6.5 (Lin et al., 2009).

The ethanol steam reforming was studied at 500 and 600°C on CoZnAl catalysts with different Co loading (9 and 25 wt%) and a Zn:Al atomic ratio nearly constant (about 0.6). the catalysts were active in the ethanol steam reforming at atmospheric pressure in the temperature range studied, but with significant differences in their performance. High hydrogen selectivities, better than 80%, were obtained on catalyst with high Co loading (25 wt%). CO, CO_2 and minor amount of CH_4 were the only carbon produced at 600°C. The catalysts without a previous reduction were very active in the steam reforming of ethanol, with 100% of ethanol conversion at 500 and 600°C. the increase in Co loading decreased the formation of intermediates compounds and improved the H_2 selectivity. At 600°C, the hydrogen selectivity increases from 31 to 86% when Co loading increases from 9 to 25%. This improved behavior was related to the presence of Co_3O_4 on CoZA25 which was mostly reduced to Co^0 and CoO under reforming conditions (Barroso et al., 2009).

Co/ZnO catalyst was applied for ethanol steam reforming, showing high activity with an ethanol conversion of 97% and a H_2 concentration of 73% at a gas hourly space velocity of 40,000 h^{-1} and a moderately low temperature of 450°C. Results on product concentrations at low temperature of 450°C confirm a good and stable performance of Co/ZnO catalyst with H_2, CO_2, CO and CH_4 of 72, 22-25, 2-3, and 1%, respectively (Lee et al., 2010).

Studies using temperature-programmed reaction and isotopic labeling techniques have shown that the reaction network involved in ethanol steam reforming is complex (Song et al., 2010), with many competing reactions taking place depending on the temperature range used, probably in the order reported in Figure 26.

The effect of oxygen mobility on the bio-ethanol steam reforming of ZrO_2- and CeO_2-supported cobalt catalysts was investigated. The catalyst undergoes deactivation; this was due mostly to deposition of various types of carbon on the surface although cobalt sintering could also be contributing to the deactivation. The addition of ceria was found to improve the catalytic stability as well as activity, primarily due to the higher oxygen mobility of ceria. Its use allows gasification/oxidation of deposited carbon as soon as it forms. Although Co sintering is also observed, especially over the ZrO_2-supported catalysts, it does not appear to be the main mode of deactivation. The high oxygen mobility of the catalyst not only suppresses carbon deposition and helps maintain the active surface area, but it also allows delivery of oxygen to close proximity of ethoxy species, promoting complete oxidation of carbon to CO_2, resulting in higher hydrogen yields (Song et al., 2009).

Catalysts based on Co supported on pure silica ITQ-2 delaminated zeolite have been prepared and tested in the bioethanol steam reforming; it exhibited the highest hydrogen selectivity and the lowest CO selectivity. Deposition of coke occurs; however deactivation was not detected during the experimental time (72 h) (Chica & Sayas, 2009).

$$CH_3CH_2OH \rightarrow CH_3CHO + H_2 \quad (1)$$
$$CH_3CH_2OH \rightarrow CH_4 + CO + H_2 \quad (2)$$
$$CH_3CH_2OH \rightarrow C_2H_4 + H_2O \quad (3)$$
$$CH_3CHO \rightarrow CH_4 + CO \quad (4)$$
$$2CH_3CHO \rightarrow CH_3COCH_3 + CO + H_2 \quad (5)$$
$$CH_3CHO + 3H_2O \rightarrow 2CO_2 + 5H_2 \quad (6)$$
$$CH_3CH_2OH + H_2O \rightarrow 2CO + 4H_2 \quad (7)$$
$$CH_3CH_2OH + 3H_2O \rightarrow 2CO_2 + 6H_2 \quad (8)$$
$$CO + 3H_2 \rightarrow CH_4 + H_2O \quad (9)$$
$$CH_4 + 2H_2O \rightarrow CO_2 + 4H_2 \quad (10)$$
$$CO + H_2O \rightarrow CO_2 + H_2 \quad (11)$$
$$CO_2 + H_2 \rightarrow CO + H_2O \quad (12)$$
$$C_2H_4 \rightarrow \text{coke} \quad (13)$$
$$CH_4 \rightarrow C + 2H_2 \quad (14)$$
$$2CO \rightarrow CO_2 + C \quad (15)$$

Fig. 26. Reactions Involved in Ethanol Steam Reforming over Co-Based Catalysts (Song et al., 2010)

Co content (wt.%)	Support	r.a.	T (°C)	X_{EtOH} (%)	S_{H2} (%)
8	Al_2O_3	13	400	74	60-70
18		13	400	99	63-70
8	SiO_2	3	400	89	62-70
18		3	400	97	69-72
10	ZnO	4	350	100	73.4
10 (with Na 0.06 wt% addition)		13	400	100	72.1
10 (with Na 0.23 wt% addition)		13	400	100	73.4
10 (with Na 0.78 wt% addition)	YSZ	13	400	100	74.2

Table 5. Ethanol conversion and hydrogen selectivity obtained on various cobalt supported catalysts and different reaction conditions (temperature, water-to-ethanol molar ratio r.a., in the presence or not of inert gas), at atmospheric pressure

4.3.3 Copper

Cu-based catalyst have received particular attention. The methanol reforming system for industrial H_2 production uses $Cu/ZnO/Al_2O_3$ catalyst (Cavallaro & Freni, 1996): the catalyst exhibited good activity with CO, CO_2 and H_2 as the main product above 357°C.

The steam reforming of ethanol over CuO/CeO_2 to produce acetone and hydrogen has also been studied (Oguchi et al., 2005). The amount of hydrogen produced was not large over CuO, CuO/SiO_2 and CuO/Al_2O_3, indicating that water is not effectively utilized in the reaction. Figure 27 shows that 2 mol of hydrogen was formed from 1 mol of ethanol over CuO/CeO_2 above 380°C; the amount of hydrogen was found to be twice that over CuO/SiO_2 and CuO/Al_2O_3 without KOH treatment. Acetone and CO_2 were also produced. By-products were ethylene, butanal, ethyl acetate, acetal (1,1-diethoxyethane), and a minute amount of unknown compounds. Molar ratios of acetone, CO_2, and H_2 produced per reacted ethanol were 1/2, 1/2, and 2, respectively (Nishiguchi et al., 2005). The formation of acetone could be described by following reaction (Eq. 51):

$$2C_2H_5OH + H_2O \rightarrow CH_3COCH_3 + CO_2 + 4H_2 \tag{51}$$

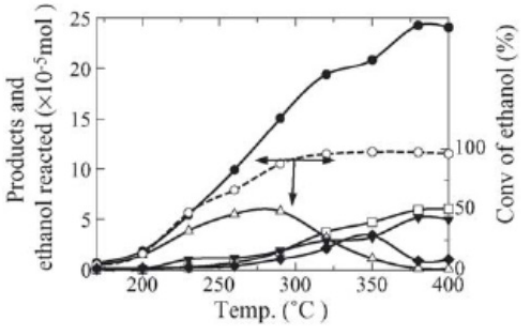

Fig. 27. Steam reforming of ethanol over 20 mol% CuO/CeO_2 (0.5 g): (O) ethanol, (●) hydrogen, (Δ) acetaldehyde, (▼) acetone, (□) CO_2 and (♦) others (Nishiguchi et al., 2005)

4.4 Bimetallic

There is an increasing interest in bimetallic or alloy metal catalysts for ethanol steam reforming; bimetallic catalysts are often used because they have significantly different catalytic properties than either of the parent metals. For example, PtRu catalysts are used in fuel cell applications because of their tolerance to carbon monoxide poisoning. However, it is not easy to predict what to change in catalytic activity will be for a particular bimetallic catalyst.

Ethanol reforming was studied over $Ni/Cu/Cr/Al_2O_3$ catalyst at 300 ÷ 550°C, suggesting that the catalytic effect was more pronounced at lower temperatures (Luengo et al., 1992).

It was found that $Ni\text{-}Cu/SiO_2$ catalyst is more active and selective toward H_2 production in bio-ethanol oxidative steam reforming than Ni/SiO_2 which rapidly deactivates due to coke formation (Fierro et al., 2003). In previous studies, these researchers presented optimization of oxidative steam reforming of ethanol over $Ni\text{-}Cu/SiO_2$ (Fierro et al., 2002; Klouz et al., 2002).

NiZnAl catalysts was prepared by citrate sol–gel method for ethanol reforming at 500–600°C (Barroso et al., 2009). The product distribution was found very sensitive to the alloy

composition. With a Ni loading of 18–25 wt%, high hydrogen selectivity of around 85% was obtained. Ethanol reforming by CeO_2-supported Ni–Rh bimetallic catalyst was studied (Kugai et al., 2005). However, dispersed Ni–Rh redox couple was found instead of a NiRh alloy. The presence of Ni could improve Rh dispersion. Smaller CeO_2- support-crystallite size also improved Rh dispersion and led to strong Rh-CeO_2 interaction.

Cu/Ni/K/γ-Al_2O_3 catalyst exhibited acceptable activity, stability and selectivity to H_2 at 300°C (Mariño et al., 1998, 2001, 2003, 2004). Ethanol dehydrogenation and C–C bond rupture were favored by Cu and Ni, respectively. In addition, K neutralized acidic sites of γ-Al_2O_3, reducing the possibility of coke formation.

A series of Cu–Ni–Zn–Al mixed oxide catalysts were prepared by the thermal decomposition of $Cu_{1-x}Ni_xZnAl$-hydrotalcite-like precursors for ethanol steam reforming. The CuO and NiO were found to distribute on the support ZnO/Al_2O_3. The addition of Cu species facilitated dehydrogenation of ethanol to acetaldehyde, while the presence of Ni led to C–C bond rupture (Velu et al., 2002).

Cu-plated Raney nickel is an active and stable catalyst for low temperature steam reforming of ethanol (250-450°C) (Morgenstern & Fornango, 2005). Methanation was not observed but WGS activity was very poor. The kinetics were modelled by a sequence of two first order reactions: dehydrogenation of ethanol to acetaldehyde (E = 149 kJ/mol) and decarbonylation of acetaldehyde.

Ni–Cu catalysts supported on different materials were tested in ethanol steam reforming reaction for hydrogen production at reaction temperature of 400°C under atmospheric pressure; they were found to be promising catalysts for ethanol steam reforming. Prevailing products can be related to main reactions over catalysts surface. During 8 h of reaction this catalyst presented an average ethanol conversion of 43%, producing a high amount of H_2 by steam reforming and by ethanol decomposition and dehydrogenation parallel reactions. Steam reforming, among the observed reactions, was quantified by the presence of carbon dioxide. About 60% of the hydrogen was produced from ethanol steam reforming and 40% from parallel reactions.

Analysis of reaction products indicated that strong acid sites are responsible for the ethanol dehydration reaction, forming ethylene and diethyl ether, while metallic Ni is responsible for breaking the carbon–carbon bond, increasing the production of C_1 compounds.

The importance of the support for the performance of the Ni–Cu catalysts was evident and indicated a straight relation between support acidity and catalyst efficiency. It was shown that support acidity promotes metal–support interaction, which is a necessary step for the synthesis of catalysts with good stability, high activity and selectivity to the ethanol reforming reaction. However, the acid sites should not be too strong in order to avoid dehydration products, such as ethylene and ethyl ether, which reduce the selectivity to reforming reaction (Furtado et al., 2009).

A parametric study was conducted over Pt-Ni/δ-Al_2O_3 to explore the effect of Pt and Ni contents on the ethanol steam reforming characteristic of the bimetallic catalyst. The best ethanol steam reforming performance is achieved over 0.3wt%Pt-15wt%Ni/δ-Al_2O_3. Kinetic of ethanol steam reforming was studied over this catalyst in the 400-550°C interval using differential and integral methods of data analysis. A power function rate expression was

obtained with reaction orders of 1.01 and -0.09 in ethanol and steam, respectively, and the apparent activation energy of ethanol steam reforming was calculated as 59.3 ± 2.3 kJ mol^{-1} (Soyal-Baltacioglu et al., 2008).

Monometallic Ru and bimetallic Ru-Pt supported nanoparticles, derived from organometallic cluster precursors, were found to be highly efficient ethanol steam reforming catalysts, outperforming all others that were tested under the identical reaction conditions. The high catalytic efficiencies of cluster-derived catalysts are attributed to the very small sizes of the metallic nanoparticles (Koh et al., 2009).

Steam reforming of ethanol was examined over $Co/SrTiO_3$ addition of another metal -Pt, Pd, Rh, Cr, Cu, or Fe- for promotion of the catalytic activity. Ethanol conversion and H_2 yield were improved greatly by adding Fe or Rh at 550°C. Although Rh addition promoted CH_4 formation, Fe addition enhanced steam reforming of ethanol selectively. A suitable amount of Fe loading was in the window of 0.33-1.3 mol%. A comparative study of the reaction over a catalyst supported on SiO_2 was conducted, but no additional effect of Fe was observed on the Co/SiO_2 catalyst. High activity of $Fe/Co/SrTiO_3$ catalyst came from interaction among Fe, Co, and $SrTiO_3$ (Sekine et al., 2009).

Mechanistic aspects of the ethanol steam reforming on Pt, Ni, and PtNi catalysts supported on γ-Al_2O_3 are investigated. The main reaction pathway for ethanol steam reforming over the three catalysts studied was found to be the ethanol dehydrogenation and subsequent acetaldehyde decomposition. For Ni and PtNi catalysts, a second reaction pathway, consisting in the decomposition of acetate intermediates formed over the surface of alumina support, became the main reaction pathway operating in the steam reforming of ethanol once the acetaldehyde decomposition pathway is deactivated (Sanchez-Sanchez et al., 2009).

The influence of the addition of Ni on the catalytic behaviour of a Rh/Y_2O_3-Al_2O_3 catalyst (Rh/Y-Al) was evaluated in the ethanol steam reforming reaction in the presence of methyl-2-propan-1-ol as impurity. It was established that the catalytic behaviour of the Rh/Y-Al base catalyst is widely improved by the addition of Ni. Nickel incorporation leads to the formation of both dispersed nickel phase and nickel aluminate species. Basic properties of the support were not modified by the addition of Ni but it was concluded to a rearrangement of acid sites. $NiAl_2O_4$ phase leads to an increase of the Lewis acid sites (LAS) of weak strength, generating a decrease of the production of coke and higher catalytic stability. It has been shown that the incorporation of Ni on the Rh/Y-Al catalyst increases the rhodium accessibility and stabilizes the rhodium particles size. The higher performances of RhNi/Y-Al catalyst were correlated to an increase in the methane steam reforming activity (Le Valant et al., 2010).

The effect of Fe, Ni, Cu, Cr, and Na (1%) addition over ZnO-supported Co (10%) honeycomb catalysts in the steam reforming of ethanol (ESR) and water gas shift reaction (WGS) for the production of hydrogen was studied. Catalysts promoted with Fe and Cr performed better in the ESR, and the sample promoted with Fe showed high activity for WGS at low temperature. Alloy particles in catalysts promoted with Fe and Cr exhibited a rapid and higher degree of redox exchange between reduced and oxidized Co, which may explain the better catalytic performance (Casanovas et al., 2010).

The catalytic activity of NiM/La_2O_3-Al_2O_3 (M= Pd, Pt) catalysts with different noble metal contents was investigated in the steam reforming of ethanol. Experimental tests of ethanol

steam reforming showed that the catalysts produced a hydrogen-rich gas mixture It was seen that the addition of noble metal stabilized the Ni sites in the reduced state throughout the reaction, increasing ethanol conversion and decreasing coke formation, irrespective of the nature or loading of the noble metal. In the experiments performed at 450°C, the catalysts showed lower H_2 formation and higher acetaldehyde production than the promoted catalysts. Moreover, the bimetallic catalysts showed a higher ethanol conversion and higher hydrogen yield than he Ni/La_2O_3-Al_2O_3 catalyst, irrespective of the nature or concentration of the noble metal (Profeti et al., 2009).

Steam reforming of ethanol for H_2 production was studied over a catalyst prepared by copper and nickel retention on zirconia microsphere. It was concluded that high temperature (550°C), higher water/ethanol molar ratio (3:1) promote on $Ni/Cu/ZrO_2$ high hydrogen yield (60 %) (Bergamaschi et al., 2005).

A series of Co-Ni catalysts has been studied for the hydrogen production by ethanol steam reforming. The total metal loading was fixed at 40% and the Co-Ni composition was varied (40-0, 30-10, 20-20, 10-30 and 0-40). All the catalysts were active and stable at 575°C during the course of ethanol steam reforming with a molar ratio of H_2O:EtOH=3:1. The 40Ni catalyst displayed the strongest resistance to deactivation, while all the Co-containing catalysts exhibited much higher activity than the 40Ni catalyst. The hydrogen selectivities were high and similar among the catalysts, the highest yield of hydrogen was found over the 30Co-10Ni catalyst (He et al., 2009).

Ni-based catalysts doped with copper additives were studied on their role in ethanol steam reforming. The effects of Cu content, support species involving Al_2O_3-SiO_2, Al_2O_3-MgO, Al_2O_3-ZnO, and Al_2O_3-La_2O_3, on the catalytic performance were studied. Activity tests showed that Ni-Cu-based bimetallic catalyst had the best catalytic performance when Cu content was 5 wt%, with the H_2 selectivity for 61.2% at 400°C and 92.0% at 600°C. TPR showed much higher Cu content made the interaction between the support and NiO weak. On the basis of the optimal Cu content, Ni-Cu-based bimetallic catalysts supported on Al_2O_3-M_yO_z (M=Si, La, Mg, or Zn) were prepared to study the effect of composited support on the catalytic performance in the steam reforming reaction of ethanol. The catalysts supported on Al_2O_3-MgO and Al_2O_3-ZnO have much higher H_2 selectivity than that on Al_2O_3-SiO_2 (Zhang et al., 2009).

Ni/Al-SBA-15 mesoporous catalysts have been synthesized in order to study the influence of Al incorporation on their properties and catalytic performance in ethanol steam reforming. It was found that several properties such as mesostructure ordering, acidity, Ni dispersion and nickel-support interaction of Ni/SBA, depend on the Si/Al ratio of SBA-15 support. Ni/Al- SBA presents larger Ni phase particles size and stronger of the metal-support interaction. All catalyst were active in ethanol steam reforming and were selective to hydrogen, but although Ni/Al-SBA catalysts keep almost complete ethanol conversion for Si/Al ratios lower than 60, they showed lower selectivity towards main products. The incorporation of Al atoms into SBA-15 structure is responsible for the formation of catalyst acid sites; therefore Al has a great influence on the product distribution. Support acidity promotes ethanol dehydration, generating high coke amounts and disminishing hydrogen selectivity. Thus, the best catalytic results, in terms of highest hydrogen selectivity and lower coke deposition, were reached with Ni/SBA-15 catalyst (Lindo et al., 2010).

ZnO-supported Ni and Cu as well as bimetallic Co-Ni and Co-Cu catalysts containing ca. 0.7 wt% sodium promoter and prepared by the coprecipitation method were tested in the ethanol steam-reforming reaction at low temperature (250-450°C), using a bioethanol-like mixture diluted in Ar. Monometallic ZnO-supported Cu or Ni samples do not exhibit good catalytic performance in the steam-reforming of ethanol for hydrogen production. Copper catalyst mainly dehydrogenates ethanol to acetaldehyde, whereas nickel catalyst favours ethanol decomposition. However, the addition of Ni to ZnO-supported cobalt has a positive effect both on the production of hydrogen at low temperature (<300°C), and on catalyst stability (Homs et al., 2006).

Since on Pt/CeO_2 catalysts the maximum amount of hydrogen produced is limited by the inability to activate CH_4 at low temperature, a possibility is adding a secondary metal to catalyst composition: nickel, cobalt and silver were selected as secondary metal. The bimetallic Pt-Ni and Pt-Co catalyst supported on CeO_2 exhibited a synergic effect of the active species, giving a H_2 and CH_4 rich stream without any catalyst deactivation, in very diluted reaction conditions. When platinum is present along with nickel, acetaldehyde is converted into H_2 and carbon oxides. Increasing platinum loading the hydrogenation capability of nickel is enhanced; this is confirmed by an increasing in CH_4 selectivity. Higher temperature is not favorable in order to obtain an H_2 and CH_4 rich stream. Over bimetallic Pt-Ni catalyst the formation of CO is favored increasing temperature to 450°C. Long term stability tests reveals that the catalyst 3 wt.% $Pt/10$ wt.% Ni/CeO_2 is very effective in ethanol steam reforming reaction at 300 °C exhibiting no deactivation in about 13 h of time on stream with no CO formation. No improvement in the performance of Pt-Ni catalysts is observed substituting nickel with cobalt or silver in bimetallic catalysts. The cobalt performance in ethanol steam reforming reaction at 300°C was similar to nickel in bimetallic Pt based catalysts supported on CeO_2. The catalyst 3 wt.% $Pt/10$ wt.% Co/CeO_2 is highly selective to steam reforming products, also CH_4 selectivity is higher with a stability of about 13 h of time on stream without CO production. The best temperature condition in the low and middle temperature range is 300°C (Ruggiero A., PhD Thesis, University of Salerno, 2009).

The performance of bimetallic PtNi and PtCo catalysts supported on CeO_2 has been investigated in low temperature ethanol steam reforming in both diluted and concentrated reaction mixtures. The catalysts were prepared by two different method, wet impregnation and coprecipitation, to monitor the effect of the preparation technique on the catalysts performances: the catalytic activity is deeply affected by the preparation method, leading to prefer the impregnated samples. The influence of reaction temperature (in the range 250-600°C), dilution ratio, water-to-ethanol molar ratio (in the range 3-6), space time (in the range 7500h-15000h^{-1}) was also studied with respect to catalysts activity, selectivity and durability. The results, in very concentrated conditions, close to the raw bio-ethanol stream conditions, showed that the Pt/Ni catalyst seems to be very promising for the low temperature ESR reaction, since it shows the best performance in terms of activity and selectivity among the investigated catalysts, yet at low contact times (Palma et al., 2010).

A comparative study between the different tendency to produce coke of all the catalysts were also performed, showing that coke formation occurs using the Pt/Ni sample, even if the products distribution doesn't change in an appreciable way during the experiment. This effect can be explained considering that the formation of carbonaceous fibers occurs in the catalytic bed, causing the reactor plugging. Since the gas products distribution is not

affected during the experiment, it could be desumed that the plugging effect is not directly linked to the catalytic site. In fact there aren't evidence of any loss of activity by site blockage or support degradation effect.

From some characterization after the stability test, it could be assumed that the reactor plugging (due to the high pressure drop values reached) is related to the coke deposited on the catalyst, since, about 1% of the overall carbon fed during the test has been found as coke in the sample analysed after the stability test.

A higher water to ethanol seems to be helpful to improve the catalyst durability since the pressure drops increasing occur at higher reaction times, probably due to the strong influence of water in the coke gasification reactions.

The cobalt-based catalysts, despite their not perfect agreement with the equilibrium products distribution, seems to be more durable, in the same operating conditions.

A deeper study of the coke formation mechanism together with the evaluation of the kinetic parameters will be necessary to better know the proposed process, that appears economically feasible and industrially attractive.

5. Conclusion

Although catalytic steam reforming is widely used for hydrogen production, it is not a green process since hydrocarbons are not a renewable source and harmful emissions are produced. Bioethanol is an excellent candidate to replace in the perspective of a hydrogen-based economy. Thermodynamically, the ethanol steam reforming requires relatively high temperatures and low pressures. When the reaction is carried out at moderate temperatures, in order to reduce the thermal duty and the CO amount in the outlet gas stream, the catalyst role is particularly crucial.

Starting from the catalysts proposed in this and other papers, the development of a more advanced catalyst formulation, is necessary and is still a challenge for the scientific research. It is recommended to pay more attention to the reaction mechanism, since there are few studied on this aspect, particularly at low temperatures.

Moreover, the literature mainly deals with the steam reforming of bio-ethanol in which the feed stream is simulated through a mixture of ethanol and water, prepared with the desired water-to-ethanol-molar ratio. Nevertheless, the steam reforming of crude ethanol differs from that of pure ethanol by the fact that the impurities present in the crude ethanol feed may influence the hydrogen yield and the catalyst stability. Very few studies report the use of crude ethanol for hydrogen production by steam reforming but this aspect is very important to consider, since a catalyst more resistant to deactivation could be necessary.

6. Acknowledgment

The authors thank Tecnimont for financial assistance.

7. References

Aboudheir, A.; Akande, A.; Idem, R. & Dalai, A. (2006). Experimental studies and comprehensive reactor modeling of hydrogen production by the catalytic

reforming of crude ethanol in a packed bed tubular reactor over a Ni/Al_2O_3 catalyst. International Journal of Hydrogen Energy, 31, 752 – 761

Akande, A. J.; Idem, R. O. & Dalai, A.K. (2005a) Synthesis, characterization and performance evaluation of Ni/Al2O3 catalysts for reforming of crude ethanol for hydrogen production, Appl. Catal. A: Gen., 287, 159–175

Akande, A.J. (2005b) Production of hydrogen by reforming of crude ethanol, M. Sc. Thesis, University of Saskatchewan

Alberton, A. L., Souza, M. M. V. M. & Schmal M. (2007) Carbon formation and its influence on ethanol steam reforming over Ni/Al_2O_3 catalysts, Catalysis Today 123, 257–264

Amphlett, J. C.; Leclerc, S.; Mann, R. F.; Peppley, B. A. & Roberge, P. R. (1998) Fuel Cell Hydrogen Production by Catalytic Ethanol Steam Reforming, Proceedings of the 33rd Intersociety Energy Conversion Engineering Conference, Colorado Springs, CO, Paper No. 98-269

Armor, J. N. (1999) Review: The Multiple Roles for Catalysis in the Production of Hydrogen, Appl. Catal. A: Gen., 176, 159-176

Aupretre, F.; Descorme, C. & Duprez, D. (2004) Hydrogen production for fuel cells from the catalytic ethanol steam reforming, Topics Catal., 30/31, 487-491

Aupretre, F.; Descorme, C.; Duprez, D.; Casanave, D. & Uzio D. (2005) Ethanol steam reforming over $Mg_xNi_{1-x}Al_2O_3$ spinel oxide-supported h catalysts, Journal of Catalysis 233 , 464–477

Balat, Mustafa & Balat Mehmet (2009) Political, economic and environmental impacts of biomass-based hydrogen, International Journal of Hydrogen Energy, 34, 3589-3603

Balat, Mustafa (2008) Potential importance of hydrogen as a afuture solution to environmental and transportation problems, International Journal of Hydrogen Energy, 33, 4013-4029

Barroso, M. N.; Gomez, M. F.; Arrua, L. A. & Abello, M. C. (2009) Steam reforming of ethanol over a NiZnAl catalyst. Influence of pre-reduction treatment with H_2, Reaction Kinetics and Catalysis Letters 97, 27-33

Basagiannis, A. C.; Panagiotopoulou, P. & Verykios, X. (2008) Low Temperature Steam Reforming of Ethanol Over Supported Noble Metal Catalysts, Top Catal. 51:2–12 DOI 10.1007/s11244-008-9130-z

Batista, M. C.; Santos, R. K. S.; Assaf, E. M.; Assaf, J. M. & Ticianelli, E.A. (2004) High efficiency steam reforming of ethanol by cobalt-based catalysts, J.Power Sources 134, 27-32

Benito, M.; Padilla, R.; Sanz., J. L. & Daza L. (2007) Thermodynamic analysis and performance of a 1kW bioethanol processor for a PEMFC operation, Journal of Power Sources 169, 123–130

Benito, M.;. Sanz, J. L.; Isabel, R.; Padilla, R.; Arjona, R. & Dazaa L. (2005) Bio-ethanol steam reforming: Insights on the mechanism for hydrogen production, Journal of Power Sources 151, 11–17

Bergamaschi, V. S.; Carvalho, F. M. S.; Rodrigues, C. & Fernandes, D.B. (2005) Preparation and evaluation of zirconia microspheres as inorganic exchanger in adsorption of copper and nickel ions and as catalyst in hydrogen production from bioethanol, Chem. Eng. J., 112, 153-158

Breen, J. P.; Burch, R. & Coleman, H. M. (2002) Metal-catalysed steam reforming of ethanol in the production of hydrogen for fuel cell application, Appl. Catal. B: Environ., 39, 65-74

Casanovas, A.; Llorca, J.; Homsa, N.; Fierro, J. L. G. & de la Piscina, P. R. (2006) Ethanol reforming processes over ZnO-supported palladium catalysts: Effect of alloy formation, Journal of Molecular Catalysis A: Chemical 250, 44–49

Casanovas, A.; Roig, M.; de Leitenburg, C.; Trovarelli, A. & Llorca, J. (2010) Ethanol steam reforming and water gas shift over Co/ZnO catalytic honeycombs doped with Fe, Ni, Cu, Cr and Na, International Journal of Hydrogen Energy 35, 7690 – 7698

Cavallaro, S. & Freni, S. (1996) Ethanol steam reforming in a molten carbonate fuel cell. A preliminary kinetic investigation, International Journal of Hydrogen Energy 21, 465-469.

Cavallaro, S. (2000) Ethanol steam reforming on Rh/Al_2O_3 catalysts, Energy & Fuels 14, 1195-1199

Cavallaro, S.; Chiodo, V.; Freni, S.; Mondello, N. & Frusteri, F. (2003) Performance of Rh/Al_2O_3 catalyst in the steam reforming of ethanol: H_2 production for MCFC, Appl. Catal. A: Gen., 249, 119-128

Cavallaro, S.; Mondello, N. & Freni S. (2001) Hydrogen produced from ethanol for internal reforming molten carbonate fuel cell, Journal of Power Sources 102, 198–204

Chen, Y.; Cui, P.; Xiong, G. & Xu, H. (2009) Novel nickel-based catalyst for low temperature hydrogen roduction from methane steam reforming in membrane reformer, Asia-Pac. J. Chem. Eng. 5, 93–100

Chica, A. & Sayas S. (2009) Effective and stable bioethanol steam reforming catalyst based on Ni and Co supported on all-silica delaminated ITQ-2 zeolite, Catalysis Today 146, 37–43

Ciambelli, P.; Palma, V. & Ruggiero A. (2010a) Low temperature catalytic steam reforming of ethanol. 1. The effect of the support on the activity and stability of Pt catalysts, Applied Catalysis B: Environmental 96, 18–27

Ciambelli, P.; Palma, V. & Ruggiero A. (2010b) Low temperature catalytic steam reforming of ethanol. 2. Preliminary kinetic investigation of Pt/CeO_2 catalysts, Applied Catalysis B: Environmental 96, 190–197

Ciambelli, P.; Palma, V.; Ruggiero A. & Iaquaniello G. (2009) Platinum catalysts for the low temperature catalytic steam reforming of ethanol, Chemical Engineering Transactions 17, 19-24 DOI 10.3303/CET 0917004

Comas, J.; Marino, F.; Laborde, M. & Amadeo, N. (2004) Bio-ethanol steam reforming on Ni/Al_2O_3 catalyst. Chem. Eng. J., 98, 61-68

de Lima, S.M.; da Silva, A. M.; Jacobsb, G.; Davisb, B.H.; Mattosa, L.V. & Noronhaa F.B. (2010) New approaches to improving catalyst stability over Pt/ceria during ethanol steam reforming: Sn addition and CO_2 co-feeding, Applied Catalysis B: Environmental 96, 387–398

De Rogatis L.; Montini T.; Casula M. F. & Fornasiero P. (2008) Design of $Rh@Ce_{0.2}Zr_{0.8}O_2 - Al_2O_3$ nanocomposite for ethanol steam reforming, Journal of Alloys and Compounds 451, 516 – 520

Denis, A.; Grzegorczyk, W.; Gac, W. & Machocki, A. (2008) Steam reforming of ethanol over Ni/support catalysts for generation of hydrogen for fuel cell applications, Catalysis Today 137,453–459

Diagne, C.; Idriss, H. & Kiennemann, A. (2002) Hydrogen production by ethanol reforming over $Rh/CeO_2–ZrO_2$ catalysts, Catal. Commun. 3, 565–571.

Diagne, C.; Idriss, H.; Pearson, K.; Gómez-García, M. A. & Kiennemann, A. (2004) Efficient hydrogen production by ethanol reforming over Rh catalysts. Effect of addition of Zr on CeO_2 for the oxidation of CO to CO_2, C. R. Chimie 7, 617–622

Domok, M., Oszko, A., Baan, K., Sarusi, I. & Erdohelyi, A. (2010) Reforming of ethanol on Pt/Al_2O_3-ZrO_2 catalyst, Applied Catalysis A: General 38, 33–42

Domok, M.; Baa´n, K.; Kecske´s T. & Erdohelyi A. (2008) Promoting Mechanism of Potassium in the Reforming of Ethanol on Pt/Al_2O_3 Catalyst, Catal Lett 126:49–57 DOI 10.1007/s10562-008-9616-0

Donazzi A.; Beretta A.; Groppi G. & Forzatti P. (2008) Catalytic partial oxidation of methane over a 4% Rh/α-Al2O3 catalyst Part I: Kinetic study in annular reactor, Journal of Catalysis 255, 241 – 258

Erdohelyi, A;. Raskó, J.; Kecskés, T.; Tóth, M.; Dömök, M. & Baán, K. (2006) Hydrogen formation in ethanol reforming on supported noble metal catalysts. Catalysis Today 116, 367-376

Fajardo, H.V.; Longo, E.; Mezalire, D.Z.; Nuerberg, G.B.; Almerindo, G.I.; Collasiol, A.; Probst L. F. D.; Garcia I. T. S. & Carreno N. L. V. (2010) Influence of support on catalytic behaviour of nickel catalysts in the steam reforming of ethanol for hydrogen production, Environ Chem Lett 8, 79-85

Fatsikostas, A. N. & Verykios, X. E. (2004) Reaction Network of Steam Reforming of Ethanol over Ni-Based Catalysts, J. Catal. 225, 439-452

Fatsikostas, A. N.; Kondarides, D. I. & Verykios, X. E (2001) Steam Reforming of Biomass-Derived Ethanol for the Production of Hydrogen for Fuel Cell Applications, Chem. Commun. 9, 851-852

Fatsikostas, A. N.; Kondarides, D. I. & Verykios, X. E. (2002) Production of hydrogen for fuel cells by reformation of biomass-derived ethanol, Catalysis Today 75, 145-155

Fierro, V.; Akdim, O. & Mirodatos, C. (2003) On-board hydrogen production in a hybrid electric vehicle bybio-ethanol oxidative steam reforming over Ni and noble metal based catalysts, Green Chemestry 5, 20–24

Fierro, V.; Klouz, V.; Akdim, O. & Mirodatos C. (2002) Oxidative reforming of biomass derived ethanol for hydrogen production in fuel cell applications, Catalysis Today 75, 141–144

Fishtik, I.; Alexander, A.; Datta, R. & Geana, D. (2000) A thermodynamic analysis of hydrogen production by steam reforming of ethanol via response reaction. International Journal of Hydrogen Energy, 25, 31-45

Freni, S.; Cavallaro, S.; Mondello, N.; Spadaro, L. & Frusteri F. (2002) Steam reforming of ethanol on Ni/MgO catalysts: H_2 production for MCFC, Journal of Power Sources 108, 53–57

Freni, S.; Maggio, G. & Cavallaro, S. (1996) Ethanol steam reforming in a molten carbonate fuel cell: a thermodynamic approach, Journal of Power Sources 62, 67-73.

Freni, S.; Mondello, N.; Cavallaro, S.; Cacciola, G.; Parmon, V. N. & Sobyanin, V.A. (2000) Hydrogen production by steam reforming of ethanol: a two step process, React. Kinet. Catal. Lett., 71, 143-152.

Frusteri, F.; Freni, S.; Chiodo, V.; Spadaro, L.; Blasi, O.D.; Bonura, G. & Cavallaro, S. (2004) Steam reforming of Bio-ethanol on Alkali- Doped Ni/MgO Catalysts: Hydrogen Production for MC Fuel Cell, Appl. Catal. A: Gen., 270, 1-7

Furtado, A. C.; Gonc, C.; Alonso, C. G., Cantao, M.P. & Fernandes-Machado N. R. C. (2009) Bimetallic catalysts performance during ethanol steam reforming: Influence of support materials, International Journal of Hydrogen Energy 34, 7189 – 7196

Galvita, V. V.; Belyaev V. D.; Semikolenov V. A.; Tsiakaras P., Frumin A. & Sobyanin V.A. (2002)*Ethanol decomposition over Pd-based catalyst in the presence of steam, React.Kinet.Catal.Lett 76, 2, 343-351

Garcia, E.Y. & Laborde, M.A. (1991) Hydrogen production by steam reforming of ethanol: thermodynamic analysis, International Journal of Hydrogen Energy 16, 307-312.

Goula, M. A.; Kontou, S. K. & Tsiakaras, P. E. (2004) Hydrogen Production by Ethanol Steam Reforming over a Commercial Pd/ γ -Al_2O_3 Catalyst, Appl. Catal. B: Environ. 49, 135-144.

Haga, F.; Nakajima, T.; Miya, H. & Mishima, S. (1997) Catalytic properties of supported cobalt catalysts for steam reforming of ethanol, Catal. Lett. 48, 223-227

Haga, F.; Nakajima, T.; Yamashita, K. & Mishima, S. (1998) Effect of crystallite size on the catalysis of alumina-supported cobalt catalyst for steam reforming of ethanol, React. Kinet. Catal. Lett. 63, 253-259

Haryanto, A.; Fernando, S.; Naveen, M. & Adhikari S. (2005) Current status of hydrogen production techniques by steam reforming of ethanol, Energy & Fuels, 19, 2098-2106

He, L.; Berntsen, H.; Ochoa-Fernandez; Walmsey, J.C.; Blekkan, E.A. & Chen D. (2009) Co-Ni catalysts derived from hydrotalcite-like materials for hydrogen production by ethanol steam reforming, Top Catal. 52, 206-217

Hernàndez, L. & Kafarov, V. (2009) Thermodynamic evaluation of hydrogen production for fuel cells by using bio-ethanol steam reforming: Effect of carrier gas addition, Journal of Power Sources 192, 195–199

Homs, N.; Llorca, J. & de la Piscina, P.R. (2006) Low-temperature steam-reforming of ethanol over ZnO-supported Ni and Cu catalysts. The effect of nickel and copper addition to ZnO-supported cobalt-based catalysts; Catalysis Today 116, 361–366

Idriss, H. (2004) Ethanol Reactions over the Surfaces of Noble Metal/Cerium Oxide Catalysts, Platinum Met. Rev. 48, 105-115

Ioannides, T. (2001) Thermodynamic analysis of ethanol processors for fuel cell applications, Journal of Power Sources 92, 17-25

Kaddouri, A. & Mazzocchia, C. (2004) A study on the influence of the synthesis conditions upon the catalytic properties of Co/SiO_2 or Co/Al_2O_3 catalyst used for ethanol steam reforming, Catal. Commun. 5, 339-345

Khedr, M.H.; Omarb, A. A. & Abdel-Moaty S.A. (2006) Magnetic nanocomposites: Preparation and characterization of Co-ferrite nanoparticles. Colloids and Surfaces A: Physicochem. Eng. Aspects 281, 8–14

Klouz, V.; Fierro, V.; Denton, P.; Hatz, H; Lisse, J. P.; Bouvot-Mauduit, S. & Mirodatos C. (2002) Ethanol reforming for hydrogen production in a hybrid electric vehicle: process optimisation, Journal of Power Sources 105, 26-34

Koh, A. C. W.; Chen, L.; Leong, W. K.; Ang, T. P.; Johnson, B. F. G.; Khimyak, T. & Lin, J. (2009) Ethanol steam reforming over supported ruthenium and ruthenium–

platinum catalysts: Comparison of organometallic clusters and inorganic salts as catalyst precursors, International Journal of Hydrogen Energy 34, 5691 – 5703

Kotay, S. M. & Das, D. (2008) Biohydrogen as a renewable energy resource—Prospects and potentials, International Journal of Hydrogen Energy 33, 258 – 263

Kugai, J.; Velu, S. & Song, C. (2005) Low-temperature reforming of ethanol over CeO2-supported Ni-Rh bimetallic catalysts for hydrogen production, Catal. Lett. 101, 255-264

Le Valant, A.; Bion, N.; Can, F.; Duprez, D. & Epron F. (2010) Preparation and characterization of bimetallic Rh-Ni/Y_2O_3-Al_2O_3 for hydrogen production by raw bioethanol steam reforming: influence of the addition of nickel on the catalyst performances and stability, Applied Catalysis B: Environmental 97, 72–81

Lee, Y.-K.; Kim, K.-S.; Ahn, J.-G.; Son, I.-H. & Shin W.C. (2010) Hydrogen production from ethanol over Co/ZnO catalyst in a multi-layered reformer, International Journal of Hydrogen 35, 1147 – 1151

Liguras, D.K.; Kondarides, D. I. & Verykios, X.E. (2003) Production of hydrogen for fuel cells by steam reforming of ethanol over supported noble metal catalysts, Appl. Catal. B: Environ., 43, 345–354

Lin, S.S.-Y.; Daimon, H. & Ha, S.Y. (2009) Co/CeO_2-ZrO_2 catalysts prepared by impregnation and coprecipitation for ethanol steam reforming, Applied Catalysis A: General 366, 252-261.

Lindo, M.; Vizcaìno, A. J.; Calles, J. A & Carrero, A. (2010) Ethanol steam reforming on Ni/Al-SBA-15 catalysts: Effect of the aluminium content, International Journal of Hydrogen Energy 35, 5895 – 5901

Llorca, J.; Homs, N.; Sales, J. & Ramirez de la Piscina, P. (2002) Efficient production of hydrogen over supported cobalt catalysts from ethanol steam reforming, J. Catal. 209, 306-317

Llorca, J.; Homs, N.; Sales, J.; Fierro, J.-L. G. & de la Piscina, P.R. (2004) Effect of sodium addition on the performance of Co-ZnO-based catalysts for hydrogen production from bioethanol, J. Catal. 222, 470-480.

Llorca, J.; Ramirez de la Piscina, P.; Dalmon, J.; Sales, J. & Homs, N. (2003) CO-free hydrogen from steam reforming of bioethanol over ZnO-supported cobalt catalysts. Effect of the metallic precursor, Appl. Catal. B: Environ., 43, 355-369

Luengo, C. A.; Ciampi, G.; Cencig, M. O.; Steckelberg, C. & Laborde M.A. (1992) A novel catalyst for ethanol gasification, International Journal of Hydrogen Energy 17, 677-681

Maestri M.; Vlachos D. G.; Beretta A.; Groppi G. & Tronconi E. (2008) Steam and dry reforming of methane on Rh: Microkinetic analysis and hierarchy of kinetic models, Journal of Catalysis 259, 211–222

Mariño, F.; Baronetti, G.; Jobbagy, M. & Laborde, M. (2003) Cu-Ni-K/-Al_2O_3 supported catalysts for ethanol steam reforming. Formation of hydrotalcitetype compounds as a result of metal–support interaction, Appl. Catal. A: Gen., 238, 41–54

Mariño, F.; Boveri, M.; Baronetti, G. & Laborde, M. (2001) Hydrogen production from steam reforming of bioethanol using Cu/Ni/K/ γ- Al_2O_3catalysts. Effect of Ni, International Journal of Hydrogen Energy 26, 665-668.

Marinõ, F.; Boveri, M.; Baronetti, G. & Laborde, M. (2004) Hydrogen production via catalytic gasification of ethanol. A mechanism proposal over copper-nickel catalysts. International Journal of Hydrogen Energy 29, 67-71

Mariño, F.; Cerella, E. G.; Duhalde, S.; Jobbagy, M. & Laborde, M. (1998) Hydrogen from steam reforming of ethanol. Characterization and performance of copper-nickel supported catalysts, International Journal of Hydrogen Energy 23, 1095-1101.

Mas, V.; Bergamini, M. L.; Baronetti, G.; Amadeo, N. & Laborde M. (2008) A Kinetic Study of Ethanol Steam Reforming Using a Nickel Based Catalyst, Top Catal Llorca, J. Homs, N. Sales, J. Fierro, J.-L. G. de la Piscina, P.R. (2004) Effect of sodium addition on the performance of Co-ZnO-based catalysts for hydrogen production from bioethanol. J. Catal., 222, 470-480.

Mas, V.; Kipreos, R.; Amadeo, N. & Laborde, M. (2006) Thermodynamic analysis of ethanol/water system with the stoichiometric method, International Journal of Hydrogen Energy, 31, 21-28

Men, Y.; Kolb, G.; Zapf, R.; Hessel, V. & Loewe, H. (2007) Ethanol steam reforming in a microchannel reactor, Process Safety and Environmental Protection 85(B5), 413-418

Morgenstern, D.A. & Fornango, J.P. (2005) Low-temperature reforming of ethanol over copper-plated Raney nickel: a new route to sustainable hydrogen for transportation, Energy & Fuels 19 1708-1716

Muroyama, H.; Nakase, R.; Matsui, T.& Eguchi, K. (2010) Ethanol steam reforming over Ni-based spinel oxide, International Journal of Hydrogen Energy 35, 1575-1581

Navarro, R. M.; Alvarez-Galvan, M. C.; Cruz Sanchez-Sanchez, M., Rosa F. & Fierro J. L. G. (2005) Production of hydrogen by oxidative reforming of ethanol over Pt catalysts supported on Al_2O_3 modified with Ce and La, Appl. Catal. B: Environ. 55, 229-241

Ni, M.; Leung, D. Y. C. & Leung, M. K. H D. (2007) A review on reforming bio-ethanol for hydrogen production, International Journal of Hydrogen Energy, 32, 3238-3247

Nishiguchi, T.; Oka, K.; Matsumoto, T.; Kanai, H., Utani, K. & Imamura, S. (2006) Durability of WO_3/ZrO_2-CuO/CeO_2 catalysts for steam reforming of dimethyl ether, Applied Catalysis, A: General 301(1), 66-74.

Oguchi, H.; Nishiguchia, T.; Matsumoto, T.; Kanaia, H.; Utania, K.; Matsumurab, Y. & Imamura S. (2005) Steam reforming of methanol over $Cu/CeO_2/ZrO_2$ catalysts, Applied Catalysis A: General 281, 69–73

on Pt/Al2O3 Catalyst

Palma, V.; Palo, E.; Castaldo F.; Ciambelli P. & Iaquaniello G. (2011) Catalytic activity of CeO_2 supported Pt-Ni and Pt-Co catalysts in the low temperature bio.ethanol steam reforming, Chemical Engineering Transactions, 17(2011)947-952 DOI 10.3303/ CET1125158

Profeti, L. P. R.; Diasb, J. A. C.; Assafc, J. M. & Assafa, E.M. (2009) Hydrogen production by steam reforming of ethanol over Ni-based catalysts promoted with noble metals, Journal of Power Sources 190, 525–533

Rabenstein, G. & Hacker V. (2008) Hydrogen for fuel cells from ethanol by steam-reforming, partial-oxidation and combined auto-thermal reforming: A thermodynamic analysis, Journal of Power Sources 185, 1293–1304

Raskó, J.; Hancz, A. & Erdohelyi A. (2004) Surface species and gas phase products in steam reforming of ethanol on TiO_2 and Rh/TiO_2, Applied Catalysis A: General 269, 13–25

Roh, H.-S.; Platon, A.; Wang, Y. & King, D. L. (2006a) Catalyst deactivation and regeneration in low temperature ethanol steam reforming with $Rh/CeO_2 – ZrO_2$ catalysts, Catalysis Letters 110, 1–2

Roh, H.-S.; Wang Y.; King D. L., Platon A. & Chin Y.-H. (2006b) Low temperature and H2 selective catalysts for ethanol steam reforming, Catalysis Letters 108, 1–2

Romero-Sarria, F.; Vargas, J. C. ; Roger, A.-C. & Alain, K. (2008) Hydrogen production by steam reforming of ethanol, Catalysis Today 133-135, 149-153

Rossi, C. C. R. S.; Alonso C.G.; Antunes, O. A. C.; Guirardello, R. & Cardozo-Filho L. (2009) Thermodynamic analysis of steam reforming of ethanol and glycerine for hydrogen production, International Journal of Hydrogen Energy 34, 323-332

Ruggiero A., PhD Thesis, University of Salerno (2009)

Sanchez-Sanchez, M. C.; Navarro Yerga, M.; Kondarides, D. I.; Verykios, X. E. & Fierro, J.L.G. (2009) Mechanistic Aspects of the ethanol steam reforming reaction for hydrogen production on Pt, Ni, and PtNi supported on γ-Al_2O_3, J. Phys. Chem. A

Sekine, Y.; Kazama, A.; Izutsu, Y.; Matsukata; M. & Kikuchi E. (2009) Steam reforming of ethanol over cobalt catalyst modified with small amount of iron, Catal. Lett. 132, 329–334

Siang, J.-Y., Lee, C.-C., Wanga, C.-H.; Wanga, W.-T.; Deng, C.-Y.; Yeh, C.-T. & Wanga C-B. (2010) Hydrogen production from steam reforming of ethanol using a ceria-supported iridium catalyst: Effect of different ceria supports, International Journal of Hydrogen and Energy 35, 3456 – 3462

Silveira, J. L.; Braga, L. B.; de Souza, A. C. C. & Antunes J. S. (2009) The benefits of ethanol use for hydrogen production in urban transportation, Renewable and Sustainable Energy Reviews 13, 2525-2534

Song, H. & Ozkan, U. S. (2009) Ethanol steam reforming over Co-based catalysts: Role of oxygen mobility, Journal of Catalysis 261, 66 – 74

Song, H. & Ozkan, U. S. (2010) Economic analysis of hydrogen production through a bio-ethanol steam reforming process: Sensitivity analyses and cost estimations, International Journal of Hydrogen 35, 127 – 134

Soyal-Baltacıoglu,F.; Aksoylu, A. E. & Onsan, Z. I. (2008) Steam reforming of ethanol over Pt–Ni Catalysts, Catalysis Today 138, 183–186

Sun, J.; Qiu, X.; Wu, F. & Zhu, W. (2005) H_2 from steam reforming of ethanol at low temperature over Ni/Y_2O_3, Ni/La_2O_3 and Ni/Al_2O_3 catalysts for fuel cell application, International Journal of Hydrogen Energy 30, 437-445

Tavazzi I.; Beretta A.; Groppi G. & Forzatti, P. (2006) Development of a molecular kinetic scheme for methane partial oxidation over a Rh/α-Al_2O_3 catalyst, Journal of Catalysis 241, 1 – 13

Tuti, S. & Pepe, F. (2008) On the Catalytic Activity of Cobalt Oxide for the Steam Reforming of Ethanol, Catal Lett 122,196-203

Vaidya, P. D. & Rodrigues, A. E. (2006) Insight into steam reforming of ethanol to produce hydrogen for fuel cells, Chemical Engineering Journal 117, 39-49

Vasudeva, K.; Mitra, N.; Umasankar, P. & Dhingra, S.C. (1996) Steam reforming of ethanol for hydrogen production: thermodynamic analysis, International Journal of Hydrogen Energy, 21, 13-18.

Velu, S.; Satoh, N.; Gopinath, C.S. & Suzuki, K. (2002) Oxidative reforming of bio-ethanol over CuNiZnAl mixed oxide catalysts for hydrogen production, Catal. Lett. 82, 145-152

Wanat, E. C.; Venkataraman K. & Schmidt L. D. (2004) Steam reforming and water–gas shift of ethanol on Rh and Rh–Ce catalysts in a catalytic wall reactor, Applied Catalysis A: General 276, 155–162

Wang, C.-B.; Lee, C.-C.; Bi, J.-L.; Siang, J.-Y.; Liu, J.-Y. & Yeh C.-T. (2009) Study on the steam reforming of ethanol over cobalt oxides, Catalysis Today 146, 76–81

Wei, J. & Iglesia E. (2004) Structural and Mechanistic Requirements for Methane Activation and Chemical Conversion on Supported Iridium Clusters, Angew. Chem. Int. Ed. 43, 3685 –3688

Whitaker, F. L. & Lueckel, W. J. (1994) The phosphoric acid PC25 fuel cell power plant - and beyond, Proceedings of the American Power Conference 56(1), 177-8

Yamazaki, T.; Naoko, K.; Katoh, M.; Hirose, T.; Saito, H.; Yoshikawa T. & Mamoru, W. (2010) Behavior of steam reforming reaction for bio-ethanol over Pt/ZrO_2 catalysts, Applied Catalysis B: Environmental 99, 81–88

Yamazaki, T.; Naoko, K.; Katoh, M.; Hirose, T.; Saito, H.; Yoshikawa, T. & Mamoru, W. (2010) Behavior of steam reforming reaction for bio-ethanol over Pt/ZrO_2 catalysts, Applied Catalysis B: Environmental 99, 81–88

Zhang, B.; Cai, W.; Li Y., Xu, Y. & Shen, W. (2008) Hydrogen production by steam reforming of ethanol over an Ir/CeO_2 catalyst: Reaction mechanism and stability of the catalyst, International Journal of Hydrogen and Energy 33, 4377-4386

Zhang, L.; Li, W.; Liu, J.; Guo, C.; Wang, Y. & Zhang J. (2009) Ethanol steam reforming reactions over Al_2O_3/SiO_2-supported Ni–La catalysts, Fuel 88, 511–518

8

Destruction of Medical N_2O in Sweden

Mats Ek and Kåre Tjus
IVL Swedish Environmental Research Institute
Sweden

1. Introduction

The potent greenhouse gas nitrous oxide (N_2O) is widely used in Sweden and many other countries as a mild anaesthetic or pain relief for mothers in labour. The Stockholm County Council (SCC) realized that the nitrous oxide used was responsible for a significant part of the total emission of greenhouse gases from their activities, including public transport. In 2002 SCC started to look for economically and environmentally sound ways to stop or lower the emission. Since nitrous oxide is effective, cheap, easy to use and without risks for mother or baby the maternity wards wanted to continue to use it as one of several methods for pain relief.

Different ways to collect and destroy the used nitrous oxide were therefore investigated in co-operation with IVL Swedish Environmental Research Institute (IVL). Efforts were soon concentrated on an existing Japanese unit treating mixed anaesthetic gases from operation (Kai et al, 2002). This was rebuilt for the new purpose by Showa Denko K.K., and installed in one of Stockholm's main hospitals in 2004. The unit called Anaesclean-SW was effective and reliable from start, and destroyed more than 95 % of the collected gas. Life Cycle Assessment (LCA) and Life Cycle Cost (LCC) showed that the method was both environmentally and economically sound (Ek & Tjus 2008). The results were so good that SCC as one of their environmental goals said that the emission of nitrous oxide from the hospitals in 2011 should have decreased by 75 % as compared to that in 2002.

This chapter will discuss the development in Stockholm and the rest of Sweden up till now. It includes

- Choice of destruction method
- Tests of systems to capture as much of the gas as possible from the delivery rooms
- Different ways to reduce the energy demand
- Competition with more suppliers
- Lower prices and adaptation to smaller hospitals
- Continuous information to other county councils in Sweden

There are now 12 units running in Sweden. LCA and LCC for the latest ones will be given, and the future development discussed.

2. Different ways to decrease the emission of N_2O from hospitals

The use of N_2O in Swedish hospitals has decreased during the last years, but it was still about 155 tons in 2009 (Borgendahl, 2011). Since 1 kg N_2O has the same effect as greenhouse

gas as 298 kg CO_2, this corresponds to about 46 000 tons of CO_2. It is a small part of the total emission of N_2O from Sweden, that was reported to be about 23 000 tons N_2O in 2009 (UNFCCC, 2011) but it is easier to influence than the emissions from agriculture which is the totally dominating source. About 90 % of the total amount of N_2O used in the Swedish hospitals is estimated to be used for pain relief during labour, and the rest mainly for surgical operation and special dental care. N_2O is stable in the patient lung and blood system, and all the used gas is finally emitted from the body.

In 2002 the environmental director of SCC, Åke Wennmalm, pointed out that N_2O used in delivery in Stockholm was responsible for a significant part of the total globing warming potential from the SCC. Electricity was mainly from renewable sources, and the transport sector was rapidly going over to non-fossil fuel. A broad and long-term work was started to decrease the emissions of N_2O. Several steps in the chain of N_2O use were studied.

2.1 Decreased use of N_2O

The most direct way to reduce the emission of N_2O is to reduce the use. In surgical operation N_2O is now used just in small quantities, combined with other anaesthetics. The use is minimized by circulation of the anaesthetics in the breathing air. This is possible since the patient is anaesthetised and the breathing mask is firmly attached to the patient. Recirculation of N_2O is much more difficult in delivery or dental care with more open systems. It is important that the mother in labour pain can dose the pain relieve herself, without the aid of medical professionals. This means that she just uses the mask with gas when she is in pain, most of the time she doesn't use the mask.

If it is difficult to reduce the use of N_2O in delivery, why not use other methods? There are several, like epidural, uterine and pelvic anaesthesia. However, most anaesthetics in Sweden consider N_2O to be the best method in normal birth, since it can be handled by the mother herself, it is cheap and it is without known negative side effects on children and mothers. N_2O is now used in about 70 % of the births in Sweden (Borgendahl, 2011). Other countries with more than 50 % use of N_2O are Finland, Norway, England, Australia and New Zealand. In Canada it is used in 20-30 % of all births, while it is very rare now in USA. There is a debate now in USA to again start to offer N_2O as an alternative method, mainly due to the low cost and easy handling by the mothers themselves. But there are also two negative aspects when using N_2O. Besides the strong effect as a greenhouse gas, it can also affect the health of the delivery ward personnel negatively during long time exposure (Berge, 2001). The occupational health 8 h limit value in Sweden is 100 ppm N_2O.

Of course all N_2O that is purchased should be used by the patients. However, a survey of the often old distribution systems in many hospitals revealed leakage points responsible for up to 20 % of the purchased amount, or even more in some hospitals. Another point of loss of N_2O is the residual in pressurised bottles returned to the supplier. Since gases for medical use have to be filled in clean, empty bottles, the residue has to be let out. This can be 5-10 % of the total amount, depending on the practice of the hospital. There has to be a certain safety margin so that there is always gas available. The residual gas is sometimes used for other purposes by the supplier, but in many cases it is (was) just released to the atmosphere. Many County Councils now demand that their supplier destroy the residual N_2O that is not used for other purposes.

2.2 Collection of used N_2O

Since the negative effect on occupational health has been known for a long time, the delivery wards already have systems to reduce the concentration of N_2O in the delivery rooms. The distributing masks are also collecting most of the gas in the exhalation, and this is ventilated out of the room in different ways.

In Sweden different types of masks and suction systems are used. In the so called single masks there is just one compartment in the mask, and both inlet of N_2O and suction of exhalation gas are connected to this. The suction is normally via an ejector pump in the main ventilation shaft, and the capacity is about 25 L/min. The collected N_2O is considerably diluted in the shaft, to concentrations of about 50-100 ppm. As will be discussed later this is a serious drawback for destruction.

In many hospitals there is a more powerful and separate exhaust system. This uses double masks, with one central compartment where the gas is distributed, and a surrounding compartment where the exhaled air is collected, mixed with some of the surrounding air, and sucked out with a fan. This fan normally has a capacity of about 500 L/min, and it has its own outlet tube to the atmosphere. This system can collect more of the exhaled N_2O, and the concentration is higher in spite of the high air flow.

Fig. 1. A midwife demonstrates the use of a double mask. (Photo Mattias Ahlm)

Studies of systems with double masks have shown that 70-75 % of the used gas is collected by the mask (SLL, 2008). The figure varies a lot between deliveries, dependent on the handling of the mask. As much as 25-30 % of the used N_2O is lost to the room atmosphere

and evacuated by the main ventilation. One reason is imperfect handling of the mask; this is not the main concern of the mother at the time. Some gas leaks out beside the mask.

Another reason is that the gas dissolved in the mothers blood is ventilated out during several exhalations after she has stopped inhaling the gas. This means that the mask should be used for exhalation for half a minute or more, without inhalation through it, after the pain has decreased. With special instruction about this the collection ratio was shown to increase to 80-85 % (SLL, 2010).

A small step in this direction is the new practice with the mask in a string around the mother's neck. In this way the mask continues to suck out some of the exhalation air even if the mother is walking around in the room.

2.3 Ways to destruct N_2O

When most of the used N_2O is collected in a relatively concentrated stream it is possible to destroy it in different ways. It is also possible to separate N_2O from the air stream for purification and reuse. However, the relatively low capacity of e.g. zeolites, cost of purification of a medical gas and the low price of new N_2O make this less interesting.

N_2O is a quite stable gas, but like most chemical compounds, it can be oxidised or reduced, depending on conditions.

2.3.1 Oxidation

Oxidation here means introduction of more oxygen in the molecule, giving compounds like NO_2, or in general NO_X with $X > 0.5$. Just mixing N_2O and oxygen (or air) is not enough, but in conventional combustion the temperature is enough. High concentrations of N_2O can be incinerated without extra fuel, but for the concentrations in the delivery exhaust external fuel has to be added. This fuel and the incinerator are of course extra costs, and can only be justified if the heat energy is needed close to the hospital. Today most of the Swedish hospitals are connected to district heating systems, and don't have furnaces. However, experiments with combustion in a hospital furnace still in use have been performed. It showed that the NO_X production was so high that the experiments were stopped (Engman, 2011).

N_2O can also be oxidised at lower concentrations by using a heated catalyst. No extra fuel is needed, but the catalyst has to be heated in some way all the time, since the reaction is not exothermic enough. Also in this process NO_X is formed, with its negative environmental impact.

2.3.2 Catalytic reduction

Reduction here means removal of oxygen, and the result is N_2, nitrogen gas that constitutes most of our atmosphere. On the catalyst something else has to be oxidised, like any organic gas or hydrogen gas. The temperature of the catalyst doesn't have to be so high, but the problem is the high concentration of oxygen in the collected exhaust gas. This is about 20 %, compared to about 0.2 % of N_2O. This means that a lot of organic material or hydrogen gas has to be added to reduce the oxygen to water before most of the N_2O is reduced. To be of interest the catalyst has to very selective for N_2O.

2.3.3 Catalytic splitting

A third method to break the N_2O molecule is to split it into nitrogen gas, N_2, and oxygen, O_2. This can be done with a catalyst at temperatures about 400-500°C, without any addition. As with the other methods the catalyst has to be heated all the time, so energy recovery from the treated gas is important in order to improve the environmental performance and reduce cost. In 2002, when the method had to be decided, this seemed to be the most promising method. At that time there was a presentation of a Japanese system that treated exhaust gas from surgical operation (Kai et al., 2002). It removed other anaesthetic gases and split N_2O catalytically. After discussions between SCC and Showa Denko K.K. the Japanese company started to investigate the possibilities to treat N_2O in much lower concentration than in Japan, and without other anaesthetic gases. After it was shown that the process created no or very little NO_X the process was a candidate for delivery wards in SCC.

3. Installed destruction units

3.1 Generation 1

Early in 2004 SCC made an international enquiry for tenders. The only final offer was given by Showa Denko. There were obviously no other systems close to commercialisation. The first unit, called Anesclean SW, was installed at Huddinge hospital in southern Stockholm in December 2004.

Anesclean SW consisted of
Inlet N_2O concentration meter (IR based flow through system),
Textile particle filter to minimise clogging of the catalyst bed,
Fan with manual speed control,
Air flow meter,
Heat exchanger between inlet and outlet gas to the catalyst bed,
The catalyst bed with electric heating,
Outlet N_2O concentration meter and
A fan to dilute the treated gas, to cool it further before discharge to atmosphere.

Heat recovery was from start considered to be important, due to the great amount of air that passed the catalyst and cooled it down. The temperature of the treated air stream before mixing with ambient air was about 80°C when the catalyst temperature was 400°C. The catalyst, being the heart of the system, had a secret composition and manufacturing process, but was mainly 5 % rhodium on aluminium oxide.

The 11 delivery rooms at Huddinge hospital already had double masks and efficient exhaust system (Anevac) so Anesclean SW could just be connected to the suction system outlet. The Anevac system is common to all 11 rooms, but the valve to each room is closed as long as no N_2O is used there. When a mother wants pain relief the first time the personnel activates the system, and the mother can breathe in a mixture of oxygen and N_2O whenever she wants. The suction system is automatically activated and about 500 L/min is from now on sucked out through the mask. This continues until the N_2O system is turned off, normally after the birth. This means that the 500 L/min for long periods, between the worst labour pains, is mainly air. When the mother uses N_2O the concentration can be up to 30 000 ppm in peaks.

500 L/min is not an exact figure; it is regulated by certain under pressure in the system. When there is no room activated there is still a base air flow, due to small intentional leaks in the system. This is illustrated in figure 2. There were hours with no N_2O to destroy, but still there was an air flow of 1 m^3/min in this period. For short periods there were up to 5 or 6 rooms connected. This is a problem since the fan in Anesclean had to be changed manually. In practice you had to decide which air flow to set in order to collect most of the exhaust gas most of the time. In this case it was set to 2.3 m^3/min, based upon flow rates and concentrations measured over a long period.

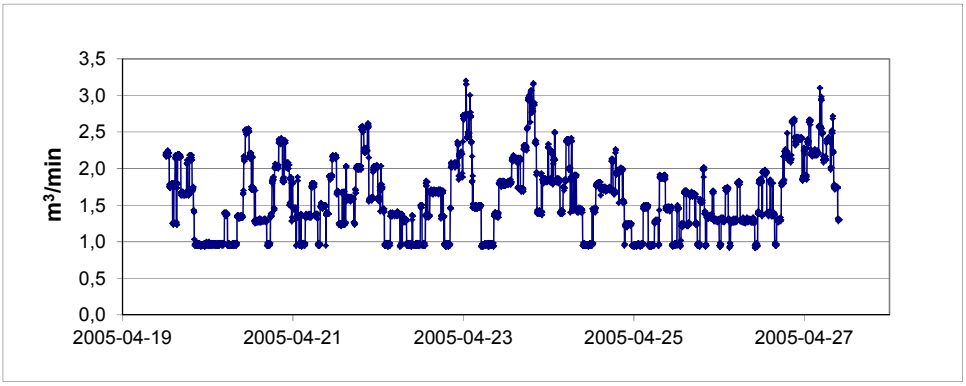

Fig. 2. Variation of gas flow rate in the Anevac system dependent on the number of mothers using N_2O.

Not just the flow rate varies quickly over time. The concentration of N_2O varies even more, for this installation between 0 and about 10 000 ppm. This is illustrated in figure 3. The reason to have constant flow rate in Anesclean SW was fear about the temperature control of the catalyst not being able to follow fast variations in flow rate, and thus cooling. With this fixed air flow rate of 2.3 m^3/min in average about 5 % of the collected N_2O from the Anevac system wasn't taken into the Anesclean SW, it was directly led to the atmosphere.

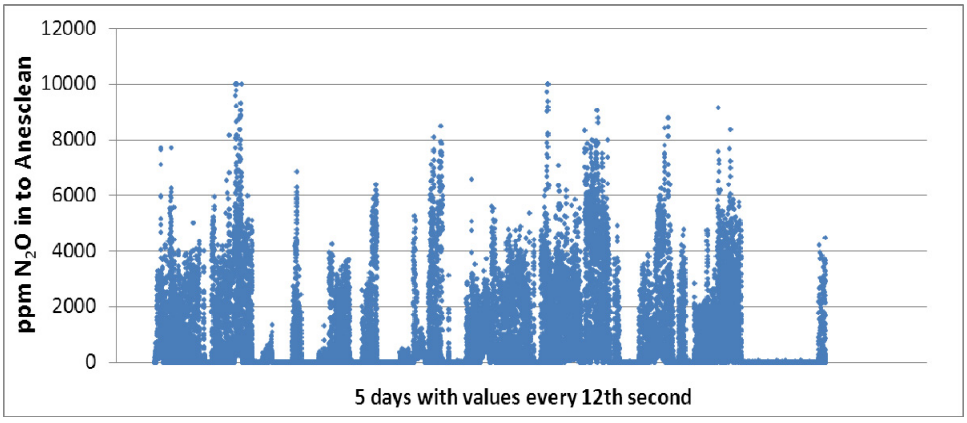

Fig. 3. Variation of concentration of N_2O in the Anevac system, average concentration about 700 ppm.

Of the N_2O entering the Anesclean SW over 97 % was destroyed during the first year of operation. The availability of the system was high, over 99 %, without any maintenance. The short stop periods were due to testing of the back-up energy system at the hospital each month. Then the unit had to be restarted manually.

The only problem with this first generation was the high consumption of energy. Due to the constantly high air flow rate it used about 35 kWh/kg N_2O destroyed. This is coupled to the relatively low average concentration of about 900 ppm N_2O in the treated air.

3.2 Generation 2

After the successful installation of this first unit SCC decided to go on with installations in other hospitals. After some discussion about licence fees the Swedish company QMT in 2008 installed the second unit in Danderyd hospital in the northern part of Stockholm. The design was similar to the original one delivered by Showa Denko at Huddinge hospital, with the same catalyst.

There were some important differences however. The one big unit was divided in two, with a separate part for gas analyses and regulation of the unit. This was mainly to make it easier to install in crowded areas. Extra heat exchangers were added to recover as much as possible of the energy used. But the most important change was on line regulation of the amount of air that was actually treated. This was done by measuring the airflow from the exhaust system Anevac, and setting the fan capacity slightly higher. In this way all the collected air was treated and very little air from outside was added. This resulted in average N_2O concentration about 2 400 ppm, compared to about 900 ppm in the first generation unit with the same number of delivery rooms connected.

Experience showed no problems to keep the temperature in the catalyst bed constant, and the overall destruction of collected N_2O was more than 98 %. Mainly due to the regulation of air flow the specific energy demand was decreased to about 10 kWh/kg N_2O destroyed.

3.3 Generation 3

One remaining drawback with the unit was the big size, which made it difficult to install in some hospitals. The price was also relatively high, especially for smaller hospitals with fewer deliveries. By now a new Swedish company Nordic Gas Cleaning, NGC, had developed their own system, with another catalyst without rhodium or other rare metals, built in modules and with simpler casing. The typical NGC unit is smaller and considerably lighter, about 1.0 x 3.3 m footprint, 2 m high and 1 400 kg (figure 4), compared to the first Anesclean SW with footprint 1.6 x 3.0 m, 2 m high and about 3 500 kg for the same number of delivery rooms.

The later NGC units also have another system for heat recovery. Instead of the conventional gas/gas heat exchangers it uses ceramic heat storage systems, one on each side of the catalyst. Heating is still just in the catalyst itself, to about 500°C in their case. Hot air leaving the catalyst heats up ceramic bed 2. When the temperature in ceramic bed 1 has dropped to about 60°C, the flow direction changes and ceramic bed 1 is heated by the treated air while bed 2 is preheating air going in to the catalyst bed. Flow direction is changed about every 2-3 minutes. When changing flow direction a small amount of air doesn't pass the catalyst, but

this is led through a bed of activated carbon. This N_2O is then immediately desorbed and passed through the catalyst before the next change of direction.

Fig. 4. The unit from NGC installed at Södertälje hospital. (Photo Anette Andersson)

In these units the fan and the air flow is regulated by a certain under pressure at the inlet, this means that just a little more air is treated than the amount given by the collection system from the masks. About 98 % of the collected gas is destroyed.

In spite of the higher temperature in the catalyst the specific energy demand is still lower than in the second generation Anesclean SW. With the same loading (i.e. the same number of delivery rooms connected) it is about 5 kWh/kg N_2O destroyed. The smaller and more flexible units with both lower energy demand and lower price has resulted in just this third generation type being sold the last two years.

4. Energy savings

The most important factor for energy demand is the amount of air treated. However, a very good recovery of heat from the treated air also influences the energy used. The specific energy demand, kWh/kg destroyed N_2O, is highly dependent on the mean concentration of N_2O in the treated air.

The air flow per connected breathing mask is a compromise between working environment and energy saving. Low air flow means less N_2O captured, but less energy needed to

destroy this. High air flow collects more N_2O, gives better working environment, but takes a lot of energy for destruction. In all three systems in table 1 the collection system had the same design with double masks and roughly the same air flow per mask (400-500 m^3/min).

Type of unit	Delivery rooms	Average air flow, m^3/min	Average concentration, ppm N_2O	Specific energy demand, kWh/kg N_2O
Generation 1 (2004)	11	2.3	900	35
Generation 2 (2008)	12	1.9	2 400	10
Generation 3 (2010)	12	1.5	1 500	5

Table 1. Energy demand in N_2O destruction systems at three hospitals of similar size.

The development over time is obvious, and this has also been the main reason for designing new systems. The destruction ratios for N_2O have been 98-99 % in all three systems.

These are relatively big hospitals and delivery wards. With the same system the specific energy demand increases rapidly for smaller units, with longer periods without N_2O used and lower concentrations. To change this a new generation with smart regulation of air flow to the unit has to be developed. Much could be saved by not treating the air completely without N_2O. This is both in periods without any birth with N_2O (the system not activated) and in periods where the exhaust system is activated but no mother at the moment is breathing N_2O. However, as will be seen later, the energy demand in the new units has very little influence on the total cost.

5. LCA

LCA, or Life Cycle Assessment, has been used to evaluate the total environmental impact of the destruction units. Methods and results for the first installation have been reported (SLL, 2005a). All steps are included, from production of equipment material and electricity needed, period of use and finally discharge of the equipment. In all stages use of resources and emissions of different kinds are calculated and sorted into different impact categories. The most important impact categories here are

- Global warming
- Acidification
- Photochemical ozone formation
- Nutrient enrichment/eutrophication and
- Stratospheric ozone depletion

The functional unit in these calculations was 1 kg of N_2O collected by the exhaust gas system. In the case of no destruction the only impact is the potential global warming effect, and this is for 1 kg N_2O 298 kg CO_2-equivalents.

With a destruction unit the direct emission of N_2O is decreased by about 98 %, leaving 0.02 kg N_2O or 5.96 kg CO_2-equiv. But production of material needed, transports and electricity also contributes to global warming. This is added to get the total impact of this kind. The same is done for all relevant impact categories.

This is a hard work, but still quite scientifically based. The problem comes when you want to compare the possible impacts from one process with another, or in this case no

destruction compared to destruction with a well-defined process. The impacts have different units, and some of them are local or regional, while others are global. Which one is most important? Now it is not strictly scientific any more, you can choose different suggested methods to compare the total impact. In this case we show the method with the average annual impact of one person in the world for global impacts and in the EU for regional impacts, table 2. The absolute impacts from the delivery room and the destruction unit are divided by these reference quantities. This is called normalisation. The unit of the normalised values is (European) annual person equivalent. (Hauschild & Wenzel, 2001)

	Global warming (global impact)	Acidification (regional impact)	Photochemical ozone formation (regional impact)	Eutrophication (regional impact)	Stratospheric ozone depletion (global impact)
Unit	kg CO_2 equiv.	kg SO_2 equiv.	kg C_2H_4 equiv.	kg PO_4^{3-} equiv.	kg CFC11 equiv.
No treatment	298	0	0	0.27	0
Destruction	6.45	0.00117	0.000128	0.00581	$2.9 \cdot 10^{-8}$
Normalisation references[1]	6 310	34	5.3	37	0.029
No treatment, annual milliperson equiv.	47	0	0	7.3	0
Destruction, annual milliperson equiv.	1.0	0.034	0.024	0.16	0.001

[1] kg of the respective impact / year/ person (in the world or in the EU). References per year from the Centre of Environmental Science – Leiden University (CML), version CML2001 – Dec. 07, divided by data from population statistics.

Table 2. Summarized LCA for destruction of N_2O in a big hospital with a generation 3 unit, compared to direct emission of 1 kg N_2O.

The different units make it impossible to compare the impact of treatment in a strict scientific way. By transforming all impacts to units of annual person equivalents one can at least see the different impacts compared to the impact of an average person in the world or in the EU, as appropriate. The impacts on global warming and eutrophication have the highest figures. For global warming potential it is obvious that treatment of N_2O is to prefer, while it is slightly negative for acidification, for photochemical ozone formation near the ground and for the stratospheric ozone destruction potential. If the effect of the destruction unit on eutrophication is positive or negative depends on the fate of the nitrogen of the N_2O which is emitted to the environment. If this nitrogen actually contributes to eutrophication, then the destruction unit obviously has a positive impact on eutrophication.

Since the aim of the treatment is to reduce global warming, this category is obviously important, and it is possible to say that this method can decrease the global warming potential from the use of N_2O without any strong negative impacts on some of the other common environmental impacts. The same was shown also for the first generation unit from Showa Denko (SLL, 2005a). A complete assessment should, however, also consider the possible discharge of toxic compounds from the manufacture and use of the destruction equipment, as well as the necessary use of resources.

The figures used in the LCA are as far as possible based upon actual material production and transports in this case. For electricity Nordic average electricity is used, that is mainly hydropower and nuclear power. This specific hospital uses "green electricity", mainly hydropower, with even less environmental impact. If electricity was based more upon coal, the impact would be higher, but destruction of N_2O still appears to perform better than no destruction.

6. LCC

Even if the treatment of N_2O is environmentally sound, it also has to be economically realistic. If it is too expensive per kg avoided CO_2-equivalent, the money should be used for other methods to decrease global warming. To evaluate this LCC, Life Cycle Cost, with the annuity method has been used. This was done for the first Anesclean unit before further investments were decided (SLL, 2005b).

LCC has also been calculated for generation 3 units. Investment cost is here the price of the unit and all costs for installation. Maintenance costs are electricity, service contract and a few hours for local check. The service contract includes changes of catalyst (every 4th year) and fans, and calibration of meters. The residual value is based upon scrap prices and costs for disposal of some components.

Table 3 shows the result for a big hospital (12 delivery rooms) and equipment from NGC, generation 3. The electricity price for SCC is now about 0.115 €/kWh, and also the double price was used in calculations. The technical and economic lifetime was set to 10 or 15 years, and the interest to 4 or 6 %. Electricity costs, service contract and other personnel costs were supposed to increase by 3 % each year.

Life time years	Interest rate	Electricity price €/kWh (2011)	**Specific cost €/kg CO_2-eq.**	Capital cost	Electricity cost
10	4 %	0.115	**0.073**	84 %	2.6 %
10	4 %	0.23	**0.074**	81 %	5.1 %
10	6 %	0.115	**0.079**	85 %	2.4 %
10	6 %	0.23	**0.081**	83 %	4.7 %
15	4 %	0.115	**0.057**	78 %	3.6 %
15	4 %	0.23	**0.059**	75 %	6.9 %
15	6 %	0.115	**0.063**	80 %	3.2 %
15	6 %	0.23	**0.065**	78 %	6.2 %

Table 3. Life Cycle Cost for destruction of N_2O with generation 3 equipment in a big hospital, with different life time, interest rate and electricity cost.

A total cost below 0.1 or even 0.2 €/kg CO_2-equivalent is considered as a good investment in SCC for reduction of climate change potential. It is obvious that the totally dominating cost is the capital cost while other factors have little influence. Personnel costs (mainly service contract) and spare parts are 10-15 % of the total cost. For the first unit from Showa Denko the total cost was about 0.099 €/kg CO_2-equivalent, and higher proportions on capital cost and electricity (SLL, 2005b). Cheaper units and better energy efficiency has paid off.

For smaller hospitals the cost will rise rapidly. So far the smaller units from NGC are almost as expensive as their bigger ones, they have higher specific energy demands, and destroy much less N_2O/year. The unit installed at Södertälje hospital with 6 delivery rooms have a life cycle cost of 0.20 €/kg CO_2-equivalent destroyed (15 years, 4 % interest and the lower electricity price). 72 % of this is capital costs, and the service cost has now reached 24 % of the total cost. With the design and technique used today installation in hospitals with less than 5 delivery rooms will have a high cost for each kg CO_2-equivalent.

7. Overall emission of N_2O in 2010 in SCC

The total emission of N_2O from medical use in SCC has decreased from 33 386 kg in 2002 to 15 959 kg in 2010 (SLL, 2011). This is about 52 % decrease, or about 5 200 tons of CO_2-equivalents less than in 2002. This is still far from the environmental goal 75 % decrease to 2011 in SCC. However, with the three new units installed late in 2010 it is quite possible to reach the goal. With the expected destruction in these the calculated decrease from 2002 will be about 72 %. If the emission is related to the number of births in SCC the decrease will be over 75 % since more children are born 2010 and 2011 than in 2002.

Most of the decrease is due to the 5 installed destruction units, but also better control of usage and leaks have contributed. As long as the collected N_2O is not more than about 75 % of the used amount it is difficult to reach much further. Now just a few small users like special dentist care are without treatment, and for these new techniques are necessary.

8. Spreading of experience

After the successful installation and evaluation of the first unit in Stockholm the SCC decided to spread its knowledge and experience to other County Councils. Now all County Councils in Sweden are represented in a N_2O consortium that meets via electronic conferences 4-6 times every year and physically at least once a year.

Now in 2011 there are 12 units installed, spread over 4 counties. Discussions are held in others, and there is also interest from other countries.

9. Conclusion

The focus upon emitted N_2O as a significant part of the total greenhouse gas emission from SCC has led to development and installation of several units to destroy N_2O used in child delivery. The units have become less expensive, and especially less energy demanding. In big hospitals with many births the installation of destruction units is positive to the

environment and the cost per avoided CO_2-equivalent is competitive with other ways to decrease emission of greenhouse gases.

The results from the latest generation of units from NGC show that for small hospitals, with 4 or less delivery rooms, much cheaper units with even less need of service and maintenance have to be developed to give acceptable costs for N_2O degradation.

The interest in collection of N_2O for destruction has also led to increased efforts to minimize the negative effect on occupational health. The exhaust gas collection has improved, and several measurements of residual concentrations in delivery rooms have been done.

10. References

Berge, T. I. (2001) Nitrous oxide in dental surgery. *Best Practice & Research Clinical Anaesthesiology,* 15 (3), 477 – 489.

Borgendahl J. (2011). www.webbhotell.sll.se/lustgaskonsortiet/ Sammanställning över lustgasförbrukningen inom Sveriges regioner och landsting. (Compilation of laughing gas consumption in Swedish regions and county councils) In Swedish.

Ek, M. &Tjus, K. (2008). Decreased emission of nitrous oxide from delivery wards – case study in Sweden. Mitig Adapt Strateg Glob Change 13:809-818.

Engman J. (2011) ÅF Division Infrastructure, personal communication.

Hauschild, M. Z. & Wenzel, H. (2001). The European Personal Equivalent: Measuring the personal environmental space. Annual report NATO/CCMS Pilot Study, Clean Products and Processes (Phase 1). Report no. 242 US EPA.

Kai, T.; Kanmura Y.; Takahashi S.; Atobe H. &Hotta M. (2002). Development and utilization of a system for treating waste anaesthetic gases, ASA abstract. Anaesthesiology 96:A574.

SLL (2005a)
http://www.webbhotell.sll.se/sv/lustgaskonsortiet/Rapporter-och-artiklar/Rapporter-från-olika-lustgasprojekt , Lustgasdestruktion, SLL – LCA of a method to decompose laughing gas.

SLL (2005b)
http://www.webbhotell.sll.se/sv/lustgaskonsortiet/Rapporter-och-artiklar/Rapporter-från-olika-lustgasprojekt , Lustgasdestruktion, SLL – LCC for laughing gas destruction.

SLL (2008).
http://www.webbhotell.sll.se/sv/lustgaskonsortiet/Rapporter-och-artiklar/Rapporter-från-olika-lustgasprojekt /Förbättrad insamling, SLL – Insamlingsgrad av lustgas vid förlossning 2008.pdf (Degree of collection of N2O from deliveries) In Swedish.

SLL (2010).
http://www.webbhotell.sll.se/sv/lustgaskonsortiet/Rapporter-och-artiklar/Rapporter-från-olika-lustgasprojekt/ Förbättrad insamling, SLL – Insamlingsgrad med och utan Västeråsmetoden 2010 (Degree of collection with and without the Västerås method) In Swedish.

SLL (2011). Miljöredovisning 2010 (Environmental account). In Swedish.
UNFCCC (2011).
http://unfccc.int/national_reports/annex_i_ghg_inventories/national_inventories_submissions/items/5888.php

9

Dietary Possibilities to Mitigate Rumen Methane and Ammonia Production

Małgorzata Szumacher-Strabel and Adam Cieślak
Poznań University of Life Sciences,
Department of Animal Nutrition and Feed Management,
RUMEN PULS
Poznań
Poland

1. Introduction

Efficiency of ruminal metabolism is a significant factor affecting production and release of pollutants, i.e. methane and ammonia. Efficient and balanced ruminal fermentation reduces the emission of gases, particularly methane, to the atmosphere. Losses of energy from the feed ration, connected with the production of methane, are particularly significant in ruminants, since approx. 2/3 production costs are generated by feeds (including forages), fed to animals. Actions aiming at a limitation of methanogenesis in ruminants, at the simultaneous monitoring of quantitative and qualitative changes in methanogens, are justified from the scientific and economic point of view. Proposals of legislative changes include the intention expressed by the European Commission to introduce the so-called *cow tax*, a tax on kept ruminants.

Constant temperature on Earth is maintained thanks to a certain type of the greenhouse effect. Solar radiation with a wavelength of 0.1 - 4 μm, reaching the Earth's surface, results in its natural heating, causing the emission of thermal radiation with a wavelength of 4 to 80 μm. Greenhouse gases (GHG) are found in the atmosphere and absorb radiation with an identical wavelength, at the same time causing an elevation of temperature in the lower layers of the atmosphere (IPCC, 2007). Thanks to the above, the mean temperature of the troposphere is by 33°C higher than in case of the absence of an atmosphere, facilitating the development and preservation of life forms on Earth (IPCC, 2007). However, it is estimated that excessive emission of greenhouse gases, caused by human activity, in the last century resulted in the global temperature increasing by 0.5°C. In view of the above the Intergovernmental Panel on Climate Change (IPCC) forecasts that by the year 2100 the temperature on Earth will increase by 1.8 - 3.9°C. This may lead to the melting of ice caps in the Arctic and Antarctic, elevation of sea and ocean levels, continentality of climates, elongation or shortening of the vegetation seasons depending on the latitude, disturbances in air circulation in the atmosphere. Moreover, the above mentioned changes may contribute e.g. to the intensification of tropical cyclones and such phenomena as El Niño or the Quasi-Biennial Oscillation (QBO; Topping, 2007).

The most important greenhouse gases, affecting the above mentioned climatic changes, include carbon (IV) oxide, methane and nitrogen (I) oxide (Steinfeld et al. 2006). Since other greenhouse gases are converted into carbon dioxide equivalents, public attention is focused on this gas. However, it needs to be stressed that CH_4 and N_2O have much higher global warming potentials (GWP) in comparison to CO_2, i.e. 23 and 296, respectively (Paustian et al., 2006, Steinfeld et al., 2006). GWP is an index presenting quantitatively the effect of individual substances on the greenhouse effect, referred to CO_2 (GWP = 1) in the assumed time horizon, typically 100 years. The concentration of GHG within the last several years has changed drastically. It is estimated that since 1750 the concentration of methane in the atmosphere increased by 1060 ppm, which amounts to 151%. As a result of human activity, which for decades has been aiming at the development of industry and agriculture, the consequences of global warming have been manifested with increasing intensity, caused e.g. by excessive emission of greenhouse gases to the atmosphere. In the opinion of some authors the primary sources of methane emission may be divided into natural (accounting for 29%) and anthropogenic (71%; Wuebbles & Hayboe, 2002). Thus the effect of anthropogenic factors on climate change is much greater than that of natural factors, such as volcanic eruptions or solar bursts.

Among anthropogenic factors agriculture, including animal production, is a major sector with a highly significant contribution to environmental pollution, as it has been increasing with an increase in the human population worldwide.

Agriculture is considered to be responsible for about two-thirds of the anthropogenic sources and among them enteric microbial fermentation in ruminants is the main producer of methane and other greenhouse gasses, as well as ammonia. According to the Report of the Food and Agriculture Organization FAOSTAT (FAO, 2008) approx. 56 billion animals are kept worldwide as slaughter animals, while according to some data a 2-fold increase in the population is forecasted by 2050 (Steinfeld et al., 2006). It was shown that greenhouse emission is connected with the population of farm animals (USDA, 2011). Methane produced by ruminants contributes to 95% of the anthropogenic total methane and 18% of the total greenhouse gasses in the atmosphere. Production and emission of greenhouse gases from ruminants is strongly correlated with rumen energy and protein metabolism, as well as changes occurring in manure. According to Steinfeld et al. (2006) 86 million ton methane are released annually to the atmosphere from animal production. Of that pool as much as 95 to 97% originate from ruminants, including 63 to 64% produced by cattle, 9 to 10% buffaloes, 8% sheep, while 3.8 to 3.9% by goats (Johnson & Ward, 1996). The other 3 to 5% are produced by monogastric animals (Crutzen et al., 1986). Methane in ruminants is formed as a result of ruminal and intestinal fermentation, of which 90% of this amount comes from the rumen (Khalil, 2000).

The energy necessary for the ruminants is derived mostly from plant polysaccharides such as cellulose, whereas nitrogen originates from ruminal ammonia and amino acids. As a result of ineffective carbohydrate and protein digestion in the rumen, methane and ammonia are formed. Production of methane during fermentation of feeds in the rumen is connected with the loss of crude energy from the consumed feed ration. Thus limitation of these losses, resulting from the process of methane formation, is becoming increasingly important both in view of environmental protection and the economic aspect.

The international community, perceiving the need to counteract the negative effects of greenhouse gases, organized in 1992 in Rio de Janeiro the UN Conference on the Environment and Development. During the conference assumptions were developed for international cooperation to reduce greenhouse emissions responsible for the phenomenon of global warming. However, to date the Kyoto protocol of 1997, which entered into force on 16 February 2005 and which has been approved by 174 countries, is the most important document introducing limits to gas emissions. On the power of the resolutions of this Protocol the countries, which decided to ratify it, declared to reduce by the year 2012 their emissions by negotiated amounts listed in the appendix to the protocol (at least 5% of the emission level from 1990 - art. 3 item 1) for carbon dioxide, methane, nitrogen oxide, HFC and PFC, i.e. greenhouse gases. In case of the lower or excessive emissions of these gases, signatories of the agreement declared to engage in the trade exchange consisting in the sale or purchase of quotas from other countries. If the Kyoto protocol is fully implemented, it is forecasted that as a result of its resolutions the mean global temperature is going to be reduced by 0.02°C to 0.28°C by 2050. Moreover, Poland was a participant of the Earth Summit in Rio de Janeiro in 1992 and one of the countries, which approved the Framework UN Convention on Climate Change, thanks to which it could sign the Kyoto Protocol. In comparison to the level from 1988, i.e. the basal year for former COMECON countries, Poland is to reduce its emission by 6%. Out of the total amount of 350 million ton methane emitted annually to the atmosphere, approx. 80 million ton is generated by animal production, which constitutes as much as 23% of the methane pool resulting from human activity (Islam & Begum, 1997).

Actions aiming at a reduction of the amount of methane produced by ruminants are of interests for researchers worldwide. However, methods to limit production and emissions have to be adapted to local conditions, i.e. the feed base in each of the countries, etc. Also the scientific community systematically organizes conferences on methane emission from the agricultural sector. The first such conference was organized in Japan in 2001, with 200 delegates from 20 countries, while as many as 400 delegates from 36 countries participated in the latest one held in 2010 in Canada.

Moreover, the European Union and many other countries see the necessity to introduce common fees for emitted methane, at similar principles as those for the already implemented fees for CO_2 emissions. Low profitability of agricultural production and the relatively low investment potential – as a result of considerable fragmentation – suggests that taxation of CH_4 emission will result in a situation when agriculture, primarily animal breeding, will suffer most from these additionally financial burdens. One of the current proposal assumes fees of €5 for 1 ton of emitted gas, which implies a fee proposals of €13 per dairy cow, €7 per head of non-dairy cattle and €1 per 1 sheep. This constitutes an integral part of the adopted strategy recorded in the so-called Kyoto protocol. These resolutions constitute a supplement to the United Nations Framework Convention on Climate Change, and at the same time they are an international agreement concerning counteractions to global warming.

2. Rumen metabolism – Microorganisms involved in hydrogen and nitrogen metabolism

Microorganisms colonizing the rumen participate in the digestion of basic nutrients. Particularly thanks to the presence of bacteria all changes in the fermentation processes are made possible. Rumen bacteria are capable of producing specific enzymes participating in the digestion process. In case of ruminants bacterial enzymes are very important, since these

animals are not able to synthesize their own digestive enzymes in their forestomachs. Depending on the type of microorganisms, their interrelations and efficiency, they influence metabolic changes in animals.

In ruminants, such as domestic cattle, sheep and goats, the main fermentation processes of nutrients in the consumed feed ration occur in the first forestomach, i.e. the rumen. These processes to a most part are possible thanks to the microorganisms colonizing it. The microbial population in the rumen consists of bacteria at 10^{10} cells/ml, protozoans at 10^{6} cells/ml, fungi at 10^{3}-10^{7} cells/ml and methanogens at 10^{9} cells/ml (Kamra, 2005). However, it needs to be remembered that according to some data so far only approx. 10% microbial population have been identified in the ruminal ecosystem (Pers-Kamczyc et al., 2011). Most microorganisms participating in the production of methane for their adequate growth and development require the following environmental conditions: pH between 6 and 8 (Jones et al., 1987) and redox potential at –300 mV (Stewart & Bryant, 1988).

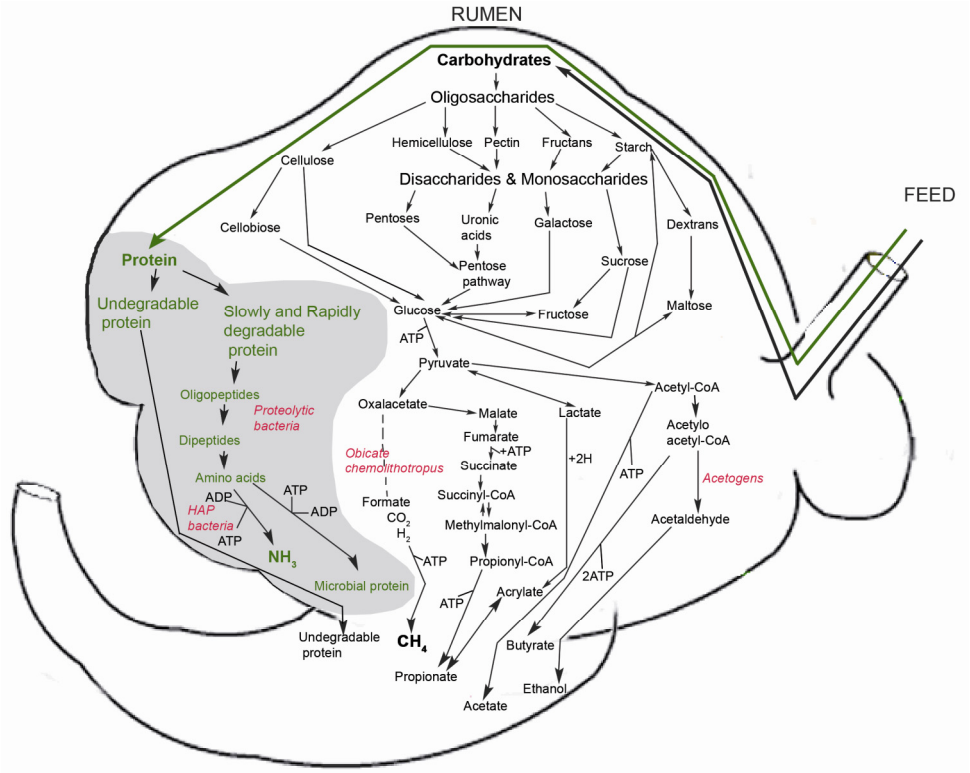

Fig. 1. A schematic pathways of carbohydrates and protein rumen fermentation (Van Soest, 1994 with modifications)

2.1 Rumen methanogens

Methanogens are microorganisms, which are directly responsible for the formation of methane in this ecosystem. They belong to the group of *Archaea* within the kingdom of

Euryarcheota. *Archaea* differ fundamentally from bacteria belonging to the group of eubacteria both in terms of their structural traits and metabolism. Murein, a peptidoglycan characteristic of the cell wall, in case of *Archaea*, is replaced by pseudomurein (Cheong et al., 1991). Due to that fact *Archaea* is not sensitive to antibiotics inhibiting the synthesis of the cell walls, such as valinomycin, penicillin or cycloserine (Hilpert et al., 1981). Moreover, in contrast to the bacterial wall composed of glycerol esters and fatty acids, the bilayer lipid wall of *Archaea* consists of di- or tetra-esters of glycerol and isoprenoid chains (Hafenbrandl et al., 1996). Such a structure of the cell wall, among other things, facilitates the growth and development of these microorganisms under extreme conditions such as e.g. protozoan cells. Another trait differentiating methanogens from eubacteria is related with the base sequence in the ribosomal RNA (Stewart et al., 1997). Only in methanogens the occurrence of the following was detected: deazariboflavin derivative of F_{420}, methanopterin, methanofuran, nickel tetrapyrol factor F_{430} and coenzyme M. These enzymes and their prosthetic groups are required for the transformation of H_2 and CO_2 to methane. Also vitamin B_{12} is necessary for the appropriate course of this process.

McAlister et al. (1996) described 5 species of methanogens living in the rumen from among 66 found in nature. According to Stewart et al. (1997) the most important species include *Methanobacterium formicicum, Methanobrevibacter ruminantium, Methanosaricina barkeri, Methanosaricina mazei* and *Methanomicrobium mobile.* Methanogenesis may occur only under anaerobic conditions at the participation of methanogens using hydrogen, being a by-product of metabolism in the other groups of microorganisms. Methanogens belong to the biggest population of microorganisms using hydrogen formed in metabolic processes in the alimentary tract of ruminants. Concentration of hydrogen ions in the ruminal environment affects the efficiency of methane production due to the loss of H+ binding capacity by *Archaea* at pH 5.5, thus leading to further acidification (Van Kessel & Russel, 1995). As a consequence, the population of methanogens is reduced (Russel et al., 1988). The process of methanogenesis serves essential functions in the appropriate functioning of the ruminal ecosystem, maintaining the concentration of hydrogen ions at 10^{-6} – 10^{-7} mol/dm^3, which has an advantageous effect on carbohydrate metabolism in the rumen (Wolin & Miller, 1988; Ushida & Jouany, 1996). According to Morvan et al. (1996), growth and development in *Achaea* is correlated with the population of microorganisms degrading cellulose, leading to an increase in the concentration of hydrogen ions (the substrate to the process of methanogenesis), being a by-product in the hydrolysis of crude fiber. A synthropy was shown between bacteria and methanogens in the rumen in *in vitro* cultures (Wolin et al., 1997), consisting in the dependence resulting from metabolism of the analyzed group of microorganisms. Bacteria provide the substrate for methanogenesis in the form of hydrogen and formate, while methanogens reduce the concentration of products of bacterial metabolism (e.g. in the process of horizontal hydrogen transfer). These products in high amounts may be harmful for other microorganisms living in the ruminal environment. Methanogens utilize carbon dioxide for hydrogen reduction and the generated energy is used for ATP production. Thus methanogens use methane formation as the sole energy-generating mechanism. Methane formation facilitates the maintenance of a low hydrogen concentration in the rumen and improves carbohydrate metabolism (Wolin & Miller, 1988; Ushida & Jouany, 1996). It has been estimated that the amount of H_2 used daily by a cow in the process of methanogenesis is approximately 800 L. However, none of the carbohydrate-fermenting bacteria and protozoa produce methane, but many of them synthesize substrates to be transformed into methane.

2.2 Rumen protozoa

Protozoans are another group of microorganisms participating in the process of methanogenesis. Similarly, as in the case of bacteria, the degradation of crude fiber being the effect of protozoan activity results in an increased concentration of hydrogen in the ruminal environment, which is used in the so-called horizontal hydrogen transfer by methanogens to the reduction of carbon (IV) oxide. Vogels et al. (1980) and Lloyd et al. (1996) showed that cells of ciliates may be colonized by *Archaea*. This indicates that the population of methanogens is connected with the numbers of protozoans. According to Stewart et al. (1997) the most important species of methanogens living in symbiosis with protozoans include *Methanobacterium formicicum, Methanobrevibacter ruminantium, Methanosaricina barkeri, Methanosaricina mazei* and *Methanomicrobium mobile.* However, it needs to be remembered that due to a different structure of cell surface in protozoan cells species preferences may occur in methanogens (Vogels et al., 1980). This seems to be confirmed by studies conducted by Regensbogenova et al. (2004a), which showed that *Methanomicrobium mobile* is found mainly in single-species cultures of *Metadinium medium*, *Entodinium furca monolobum* and *Diplodinium dentatum*. In turn, Kamra (2005) reported 4 other ruminal ciliate species from the group of *Entodiniomorpha*, which remain in close symbiosis with methanogens, i.e. *Entodinium elonginucleatum*, *Entodinium bursa*, *Eudiplodinium maggii* and *Eremoplastron bovis*. In other studies it was shown that the symbiosis of protozoans and methanogens may be observed in the ruminal ecosystem in case of *Dasytricha ruminantium*, *Entodinium caudatum*, *Entodinium furca monolobum*, *Diplodinium dentatum*, *Eremoplastron dilobum*, *Metadinium medium*, *Epidinium ecaudatum* and *Ophyroscolex caudatus* (Finlay et al., 1994; Kisidayova et al., 2000; Regensbogenova et al., 2004b; Cieślak et al., 2006a). Literature data seem to be ambiguous e.g. due to such factors as latitude, at which a given study was conducted, the applied feed ration or the species of animals. According to some studies (Vogels et al., 1980) methanogens may be both ecto- and endo-symbionts of protozoans. Thus, by reducing the population of protozoans we also reduce the population of *Archaea,* leading to a decreased methane emission (Ushida & Jouany, 1996; Dohme et al., 2001; Machműller et al., 2003; Soliva et al., 2003; Hu et al., 2005; Cieślak et al., 2006b; Goel et al., 2008; Karnati et al., 2009). Cieślak et al. (2009a) found different metabolic responses in case of rumen ciliates *Entodinium caudatum* and *Diploplastron affine* and their associated bacteria. In addition, the same group of authors stated that the rumen protozoa may produce different levels of methane, that is correlated with population size. For example, the *Epidinium ecaudatum* monoculture was characterized by the lowest cell population (386 cells per ml) producing 0.77 mmol methane, whereas *Entodinium caudatum* with the highest cell population (6183 cells per ml) was the lowest methane producer (0.54 mmol; Cieślak et al., unpublished).

2.3 Rumen fungi

Another example of horizontal hydrogen transfer is provided by the symbiosis between fungi and methanogens. According to Joblin et al. (2002), the primary products of metabolism in *Fungi imperfecta*, such as hydrogen, carbon (IV) oxide or formate, similarly as in case of the previously mentioned microorganisms, may be used by methanogens in the process of methanogenesis. It was shown that in fungal monocultures, concentrations of metabolic products, i.e. formate, hydrogen, lactate and methanol, were drastically reduced, while the amount of acetate was increasing (Joblin et al. 2002). Moreover, in other studies, it was shown that in the culture of fungi with methanogens cellulolytic and xylanolytic

activity of eucaryota was much higher than in case of pure cultures (Williams et al., 1995). In turn, according to Nakashimada et al. (2000) incubation of *Neocallimastix frontalis* and methanogens leads directly to the transformation of cellulose into methane.

2.4 Rumen bacteria

When analyzing the process of methanogenesis occurring in the rumen in terms of the participating microorganisms we need to take into consideration the fact that this environment is a highly dynamic ecosystem, still not completely clarified by researchers even when using state-of-the-art techniques of microorganism identification (Pers-Kamczyc et al., 2011). The final composition of the biocenosis in the rumen ecosystem is the effect of various factors, e.g. diet, feed additives, health, species, age and condition of the animal, season, or geographical conditions (Stewart et al., 1997; Graeme et al., 1998; Wright et al., 2007; Cieślak et al., 2009a; Szumacher–Strabel et al., 2009a).

Enteric fermentation of livestock, mainly in ruminants, is responsible also for ammonia emission that represents the loss of dietary nitrogen and is the reason of environmental pollution. In spite of the fact that ruminants can utilize almost all nitrogen sources, the limits of the ability of dairy animals and other high producing animals to recycle N are rarely reached in commercial herds and excess of dietary protein leads to ammonia formation (Place & Mitloehner, 2010). The process of ammonia formation in the rumen involves mostly proteolytic bacteria, including the hyper ammonia producing bacteria. Ineffective retention of nitrogen leads in turn to the excretion of nitrogen-rich wastes. Proteolytic bacteria as well as hyper ammonia producing bacteria (HAP) indicate a potential action in degrading protein and producing ammonia in ruminants. Although HAP are not abundant, they are characterized by high activity. According to literature data they are responsible for the degradation of protein in the rumen and thus for the amount of 50% ammonia production (Hart et al., 2008). A total of 14 morphologically differing species have been identified. The highest activity is attributed to *Clostridium sticklandii, Clostridium aminophilum* and *Bacteroides ruminicola.* They are gram-positive bacteria, sensitive e.g. to ionophore antibiotics. For the first time hyper-ammonia producing bacteria were isolated in New Zealand and Australia in sheep, cows and deer fed green forage (Attwood et al., 1995). The presence of these bacteria in the rumen fluid depends on the type of feed ration, as well as latitude at which animals live. Moreover, the group of bacteria exhibiting under specific conditions, similar properties include universal *Megasphaera elsdenii* and *Butyrivibrio fibrisolvens*, bacteria participating e.g. in the process of biohydrogenation of unsaturated fatty acids. As a result of their action excessive degradation of protein from the feed ration takes place. An addition of investigated additives to the feed ration may inhibit the development of the above mentioned bacterial species. Limitation of protein degradation in the rumen by a reduction of the population and activity of HAP is of paramount practical economic importance, since protein is one of the most expensive nutrients and an appropriate management of nitrogen in the rumen determines the productivity of animals. Limitation of protein losses and ammonia production will also contribute to a reduction of environmental pollution.

Changes in the fermentation profile of nitrogen compounds, i.e. metabolism of crude protein, are to a considerable degree dependent on the requirement of microorganisms colonizing the rumen as well as the ruminant itself. Changes of crude protein in the rumen occur in two directions. On the one hand, they are reactions of synthesis of protein in microorganisms, where non-protein compounds, such as e.g. urea, or feed protein are

substrates for these biochemical changes. On the other hand, a reaction of degradation of feed protein, which is rich in exogenous amino acids, valuable for the intermediary metabolism of the ruminant. Unfortunately, rumen bacteria degrading feed protein reduce the amount of exogenous amino acids available to the host. Thus in order to supply an adequate level of protein and in this way important amino acids in the gastric contents its degradation by microorganisms needs to be partly reduced, thus enhancing its availability in the small intestine. Protein, transferred to the duodenum, is digested by proteolytic enzymes and is utilized by them (Kamra, 2005).

3. Effect of feeding strategies on methane and ammonia production

3.1 Dietary carbohydrates

3.1.1 Type of feed

The most promising approach is connected with the modulation of rumen microbial populations by proper dietary formulation. Feeding of ruminants with feeds of high nutritive value increases nutrient concentration in the feed ration, thus resulting in the increased dry matter digestibility, degradable in the rumen as well as farther sections of the digestive tract. This causes a reduced emission of CH_4 per 1 kg DMD (dry matter digestibility) (Hegarty, 1999a). This effect may be obtained, e.g. using silage from high quality maize, which constitutes the main component of the daily feed ration used in the feeding of ruminants. Appropriate preparation of silages considerably improves nutrient availability, thus limiting the amount of produced methane per 1 kg milk (Moss et al., 2000; Cieślak et al., 2005). Use of higher quality feeds also causes an increase in the ad-lib consumption of dry matter from feed, thus increasing the total nutrient uptake by animals. Among other things it influences an improved milk yield of cows. However, in such a case increased production is not accompanied by a proportional increase in methane emission. This was confirmed by a study of Kirchgessner et al. (1995) indicating that a two-fold increase in milk yield (from 5 000 l to 10 000 l annually) results in an increase in the production of methane by only 5%. Thus the total amount of methane produced by ruminants may be reduced by a decrease in the population size of dairy cattle at an increase in their productivity.

3.1.2 Type of carbohydrates

It was shown that the composition of the feed ration may be a factor strongly limiting the production of methane, which is directly connected with the type of carbohydrates applied in the feed ration (Moss et al. 2000). It is estimated that 1 kg of crude fiber gives 79 g of methane, whereas 1 kg of starch about 10 g CH_4 (Cieślak et al., 2005). In general, soluble carbohydrates reduce methanogenesis when compared to fiber fermentation. On the other hand, the feed ration for cows with the predominant proportion of structural carbohydrates causes an increase in the rate of methanogenesis (Moss et al., 2000). Our research also proved that methane production reached a higher level in the full forage diet, while it was lower in mixed forage-concentrate diets, and the lowest values were recorded in the mixed concentrate-forage diet (Jalč et al., 2006a, b).

3.1.2.1 Structural carbohydrates

For example, the control diet consisting of fresh alfalfa was characterized by the highest methane production (9.77 mMd^{-1}) when compared with the control diets rich in concentrates

(4.75 mMd^{-1}; Jalč et al., 2006c). We also need to mention here another structural carbohydrate, i.e. lignin. Lignin is not readily digestible in the process of ruminal fermentation. Limitation of digestion causes a reduced production of VFA, thus reducing methanogenesis (Van Soest, 1982). Moreover, the type of the used straw as well as refining processes of straw-containing feeds, such as ammonia treatment or leaching, result in a change in the molar proportions of acetic acid to propionic acid in ruminants (Hvelplund et al., 1978). Feeding of sheep using ammonia-treated wheat straw reduces the production of methane in comparison to wheat straw or barley straw, subjected to leaching or ammonia treatment (Moss et al., 1994).

3.1.2.2 Nonstructural carbohydrates

The limitation of the methanogenesis process may be caused by the transformation of readily digestible carbohydrates (starch) first of all to propionic acid, which may disturb horizontal hydrogen transfer and as a consequence limit the rate of the process. Moreover, a higher proportion of concentrate usually means a higher amount of starch in the feed ration, thus affecting a change towards fermentation. By lowering pH of the ruminal contents the capacity of methanogens to form methane is reduced (Lana et al., 1998; Russel, 1998). The level of pH in the rumen may also change depending on the frequency of feeding. If animals are fed the daily feed ration in two separate doses, pH in the rumen changes within the range from 5.85 to 6.65, whereas in case of six doses fluctuations are lower, from 6.15 to 6.40 (Kaufmann et al., 1980). Less stable pH causes a reduction of methane emission by ruminants through an increased production of propionic acid (Jensen & Wolstrup, 1977; Sutton et al., 1986), however, in modern feeding regimes such practices are used less frequently.

3.2 Dietary fat

Another method potentially influencing the process of methanogenesis consists in the addition of fatty acids, both saturated and unsaturated. Fat by affecting many metabolic processes may modify the amount of produced methane, and thus increase the energy value of the feed ration. In many countries nutrition standards for ruminants recommend an addition of fat at 2% to 8% in dry matter of the feed ration. The amount of added fat depends on its form and type (Cieślak et al., 2001; Szumacher-Strabel et al., 2009b; Martin et al., 2010). Palmquist & Jenkins (1980) suggested feeding from 3 to 5% fat in diets for adult ruminants, thus increasing energy uptake at the simultaneous maintenance of the level of consumed fiber, in this way reducing the amount of fed starch. Substitution of starch with fat may result in the stabilization of ruminal processes (Palmquist, 1994; Szumacher-Strabel et al., 2001 a, b). Grant & Weidner (1992) were of an opinion that in the diets of adult cattle the amount of added fat should not exceed 700 - 900 gram per head, which constitutes from 6 to 8% in dry matter of the feed ration. Tackett et al. (1996) defined the maximum addition of rapeseed oil in the feed ration at 10%. Enriching the feed ration with vegetable oils not only increases the amount of available energy, but also the amount of unsaturated fatty acids (UFA) in final products (Szumacher-Strabel et al., 2001c; Potkański et al., 2009; Cieślak et al., 2010). It needs to be stressed that UFA have a toxic effect on microbial cell walls by enhancing their permeability, as well as a gradual degradation, potentially reducing the numbers of microorganisms participating in changes, in which hydrogen is a by-product. For this reason the amount of available hydrogen will have a direct effect on the scale of

methanogenesis. Moreover, methanogenesis may directly compete for hydrogen with the process of biohydrogenation occurring in the ruminal environment and deactivating UFA (unsaturated fatty acids). A common characteristic of both processes may be competition for the atom of hydrogen (Czerkawski et al., 1966). Plascencia et al. (1999) reported that the scale of ruminal biohydrogenation of fatty acids may be directly proportional to the estimated methane production. As a result of biohydrogenation UFA reduce the concentration of hydrogen ions in the environment, thus decreasing methanogenesis (Johnson & Johnson, 1995; Cieślak et al., 2001). However, the total amount of hydrogen used in the saturation of UFA bonds is small (0.01) in comparison to the reduction of CO_2 to methane (0.48), synthesis of volatile fatty acids (0.33) or the utilization of hydrogen by bacterial cells (0.12). For this reason in some studies no dependence was found between the process of biohydrogenation and methanogenesis (Czerkawski et al., 1966; Van Nevel & Demeter, 1996).

On the basis of comparisons prepared to date, concerning the effect of the addition of fat to feed rations for ruminants, it was shown that every 1% added fat reduces methanogenesis by 2.2 to 5.6% (Eugene et al., 2008; Beauchemin et al., 2008; Martin et al., 2010). According to the same data it may be stated that the influence of FA contained in fat depends on their nature. Other literature data point to the fact that the applied addition of fat in the nutrition of ruminants results in a modification of fermentation processes in the rumen; however, the amount of the addition depends on many factors and needs to be optimized continuously (Szumacher-Strabel et al., 2001c; Giger-Reverdin et al., 2003; Cieślak et al., 2004; Eugene et al., 2008). The European Union recommends the use of oils in feeding of ruminants, as a perfect alternative for other feed additives such as antibiotic growth stimulants, influencing microorganisms living in the rumen and participating e.g. in methanogenesis (Boadi et al., 2004; Monteny et al., 2006; Szumacher-Strabel et al., 2011b).

3.2.1 Saturated fatty acids

Studies concerning the effect of saturated fatty acids (SFA) on the process of methanogenesis in ruminants are typically based on oils containing considerable amounts of these acids. On the basis of conducted analyses it needs to be stressed that short chain fatty acids (SCFA) do not exhibit such properties in comparison to medium chain fatty acids (MCFA) C12:0, C14:0, which may significantly reduce methanogenesis (Dohme et al., 2004). Coconut oil is one of such SFA carriers constituting an important source of saturated medium chain fatty acids, i.e. lauric acid C12:0 and myristic acid C14:0 (Laureles et al., 2002). These acids were identified as substances strongly reducing microorganisms participating in methanogenesis (Dohme et al., 1999; Machmüller et al., 2003a). Thus, e.g. in studies conducted using a 7% addition of coconut oil to the sheep feed ration a reduction of the protozoan count amounted to as much as 97% (Machmüller & Kreuzer 1999). Results of previous experiments indicate that not all species of protozoans (e.g. *Epidinium* spp.) are eliminated from the rumen ecosystem after the application of the above mentioned experimental factor (Matsumoto et al., 1991). Moreover, Cieślak et al. (2006b) showed that a 5% addition of coconut oil while reducing the population of protozoans increases the total count of bacteria in the RUSITEC system. In turn, Yabuuchi et al. (2006) recorded a considerable limitation of the ciliate population at the application of 2.0 g coconut oil per 1 l ruminal fluid in comparison to the control as well as the experimental group with an addition of soybean oil. The reduction of the protozoan population in case of the application of coconut oil led to a

reduction of methanogenesis. In studies conducted by Cieślak et al. (2006b) it was found that irrespective of the adopted proportion of concentrates in relation to forages the reduction of the protozoan count after the application of coconut oil at 5% was comparable. In turn, differences were recorded in the amount of formed methane at the application of the experimental factor in the feed rations with different proportions of structural carbohydrates. The authors were of an opinion that it suggests the potential effects of varying action of MCFA contained in coconut oil on the population of other microorganisms than protozoans, and participating in the formation of methane in the ruminal ecosystem. In earlier conducted investigations it was found that MCFA not only have a negative effect on the population of protozoans, but also methanogens. Another example presenting the effect of fat on the population of methanogens is provided by the experiment, in which coconut oil was added to the feed ration (Ipharraguerre & Clark, 2003). Those researchers stated that the reduction of methanogenesis occurred through a direct action of acids contained in coconut oil on the population of methanogens in contrast to ionophore antibiotics, which reduced the production of CH_4 inhibiting the activity of bacteria producing hydrogen (Ipharraguerre & Clark, 2003). As it was shown in the other studies, conducted by Soliva et al. (2003a), lauric acid (C12:0) is more effective in the limitation of methanogenesis in comparison to myristic acid (C14:0). Additionally it was observed that the population of *Archaea* is reduced with the increase of content of lauric acid in the feed ration. For the first time in this study it was documented that the order-specific composition of the methanogenic population will be changed by MCFA, which directly indicated the effect of MCFA not only on the population of microorganisms (e.g. protozoa) producing a substrate for methanogenesis in the form of hydrogen. In other studies conducted by the same research team it was stated that a 24-h incubation of a mixture of C12:0 and C14:0, through a synergistic action, considerably reduces the production of methane in comparison to C12:0 applied individually (Soliva et al., 2003b). A confirmation for this hypothesis is provided by further studies, in which it was shown that myristic acid may increase the negative effect of C12:0 on the emission of methane (Soliva et al., 2004a). In a review paper (Machmüller, 2006) a summary was presented concerning the results obtained to date on the effect of MSFA on methanogenesis occurring in ruminants both *in vitro*, and *in vivo*. It was shown in the analysis of the recorded results that the application of an amount even below 3% MCFA of C12:0 and C14:0 in the feed ration results in the reduction of methanogenesis by 50%. The author stressed that the limitation of methanogenesis in ruminants may be greater if: i) MCFA with higher proportions of C12:0 and C14:0 are applied, ii) animals are fed with feed rations containing higher proportions of concentrates, iii) feed rations are supplemented with soap-forming minerals and if the daily amount of MCFA is divided into smaller portions, thus providing a cyclical supply of MCFA to the rumen environment. It results from the above mentioned information that the application of MCFA is more effective in relation to methanogenesis at intensive feeding than in case of extensive feeding.

3.2.2 Unsaturated fatty acids

Feeds of plant origin contain varied amounts of ether extract, while unsaturated fatty acids (UFA) are the dominant acids in the fatty acid profile. The greatest amounts of ether extract are found in seeds of oil crops (approx. 45%) as well as their oils (even up to 99%). The primary source of oleic acid is e.g. rapeseed oil (approx. 62%), for linoleic acid it is sunflower oil (approx. 64%), while for linolenic acid it is linseed oil (approx. 53%). UFA may

have a multifaceted effect on the production of methane in the ruminal ecosystem through a direct action on the population of bacteria, protozoa or methanogens, as well as - to a limited degree - by a reduction of the amount of available hydrogen (biohydrogenation). Machmüller (2006) stated that the range of action of fatty acids on microorganisms living in the rumen depends on the following factors: the type of used acid source, amount and frequency of its application as well as the share of concentrates in the feed ration. This confirms earlier observations reported by Henderson (1973), who stated that the count of microorganisms in the rumen is influenced not only by the composition, but also by the fatty acid profile of the feed ration as well as the amount of applied fatty acids. According to Dong et al. (1997), it also depends on the type of applied fatty acids. Most frequently FA have a negative effect on the population of cellulolytic bacteria, hindering the access of these microorganisms to feed particles, or directly through their toxic effect on bacterial cells (Dong et al., 1997; Hristov et al., 2004). In other experiments it was shown that the negative effect of the addition of long chain fatty acids (LCFA) is probably caused through an action on the cell membrane, particularly of gram-positive bacteria. It has been shown *in vitro* that linolenic acid is particularly toxic for the 3 cellulolytic bacterial species (*Fibrobacter succinogenes, Ruminococcus albus, and Ruminococcus flavefaciens*), because it disrupts cell integrity (Maia et al., 2007). Here it needs to be stressed that the previously conducted studies showed a dependence between cellulolytic bacteria and methanogens (Morvan et al., 1996). In other studies it was found that the *F. succinogenes* population was reduced markedly by an increasing degree of unsaturation and inclusion level of unsaturated C18-fatty acids, while *R. flavefaciens* was inhibited only by linoleic and linolenic acids at a high level (Zhang et al., 2008). Those authors indicated an ambiguity in the response of microorganisms on the applied acids. The observed reduction of the bacterial population may be explained by chemical properties of fatty acids. Due to the long non-polar carbon chain, as well as the polar hydroxyl group, FA behave similarly to detergents. These substances as a result of interaction with the cell membrane of microorganisms cause a reduced surface tension in the lipid bilayer and the generation of "holes", through which ions escape to the medium, thus leading the cell to destruction. Moreover, in the presence of long chain fatty acids (LCFA) in the medium genes engaged in LCFA transport through the cell membrane. Membrane proteins FadL and FACS are responsible for the transfer of FA through the lipid bilayer (Black & DiRusso, 2003). In certain bacteria, e.g. *Escherichia coli*, excessive accumulation of fatty acids in the cell leads to the activation of genes engaged in β-oxidation, which facilitates FA utilization and their use as a source of energy and carbon (Hearn et al., 2009). At the time when excess LCFA are found in the medium, this mechanism is disturbed, which as a consequence leads to cell death (Black & DiRusso, 2003). The action of long chain fatty acids on selected species of bacteria that take part e.g. in ammonia formation was also confirmed by Maczulak et al. (1981). In studies conducted by those authors it was shown that palmitic as well as stearic acids reduce the growth and development of *Bacteroides ruminicola* and *Butyrivibrio fibrisolvens*, while oleic acid stimulates the development of *Selenomonas ruminantium*, *Bacteroides ruminicola* and *Butyrivibrio fibrisolvens.* Moreover, we may find in literature other examples than only negative for the influence of vegetable oils on the bacterial population. Dohme et al. (2001) observed that an addition of stearic acid as well as linoleic acid at 50g kg^{-1} DM does not have a negative effect on the total count of discussed microorganisms. In turn, other studies showed a positive

effect of oils on the synthesis of microbial proteins reflected in the activity of microorganisms, including bacteria (Broudiscou et al., 1994, Szumacher-Strabel et al., 2001a; Jalč et al., 2006d). A lack of definite results concerning the effect of an addition of vegetable oils on the population of bacteria may be e.g. related with the type of applied carbohydrates in the feed ration. A smaller negative effect of the addition of used oils was observed in feed rations with the predominance of structural carbohydrates in comparison to non-structural carbohydrates (Cieślak et al., 2006 b; Jalč et al., 2006a; Machmüller et al. 2006). It needs to be remembered that it is possible to provide such supplementation with fat that it does not have a negative effect on the processes occurring in the rumen as well as the composition of fat in animal products (Cieślak et al., 2010; Cieślak et al., 2009b; Szumacher-Strabel et al., 2011b). According to other data, only the addition of fat at an amount greater than 5.0% dry matter has a toxic effect on ruminal microorganisms, including bacteria (Woolcock, 1991). In case of the influence of the addition of oil on the population of protozoans the dependence between the population size of these microorganisms and the extent of methanogenesis seems closer due to the fact that protozoans are the greatest producers of hydrogen in the rumen ecosystem. It was found that there is also a physical link between protozoans and methanogenesis, thus protozoans are responsible in 9 to 37% for methanogenesis in the rumen (Finlay et al., 1994; Newbold et al., 1995). For this reason the reduction of the population of protozoans, accounting for up to 35% of the rumen microbial mass (Williams & Coleman, 1992) may cause a direct reduction of the population of methanogens, and in this way also the extent of methanogenesis. Similarly as in case of the unclear effect of fatty acids contained in oils on bacterial counts, and similarly as it is the case with the population of protozoans data are also ambiguous.

Most frequently to date a negative effect of both SFA and UFA has been reported, in the pure form and in mixtures, in the liquid and solid form, *in vitro* and *in vivo* on the total population of protozoans or individual dominant species (Ivan et al., 2001; Hristov et al., 2004; Soliva et al., 2004b, Zhang et al., 2008; Beauchemin et al., 2009). In studies conducted by Szumacher-Strabel et al. (2004) it was shown that a 5% addition of rapeseed oil (a source of C18:1), sunflower oil (source of C18:2) or linseed oil (source of C18:3) caused a limitation of total protozoan counts in the rumen by 19%, 31% and 35%, respectively, which was connected with a reduction of methanogenesis by 27, 35 and 50%, respectively. The authors pointed to the fact that with an increase in the number of unsaturated bonds in analyzed oils, the degree of the effect on the process of methane formation increased in the rumen ecosystem. These results were confirmed by studies conducted by Varadyova et al., (2007). A significant effect was observed of 5% linseed oil added to the diet with a meadow hay:barley grain ratio (80:20%) on the rumen ciliate population; the total protozoan concentration and the number of *Entodinium* spp. were reduced as well as *Dasytricha ruminantium*, *Isotricha* spp., *Polyplastron multivesciculatum*, *Ophryoscolex tricoronatus* and *Eremoplastron dilobum*. Similarly as in case of a study by Ivan et al. (2001), in which it was found that the use of 6% sunflower oil caused a considerable reduction of the population of protozoans *Entodiniomorpha* as well as the total defaunation of ciliates *Holotricha*. In both above mentioned cases, the limitation of the counts of protozoans could have been connected with a reduction of methanogenesis. However, both in studies conducted by a team of Varadyova et al., (2007) and Ivan et al., (2001) unfortunately methane production was not determined. In other studies a 6% addition of soybean lipids caused a 37%

reduction of methane emission (Jordan et al., 2006a), while a 5.8% addition of linseed oil reduced it by as much as 52% (Martin et al., 2008). Due to above, the authors (Martin et al., 2008) stated that the application of linseed oil as an FA carrier seems a highly promising addition to feed rations for ruminants in terms of ruminal methanogenesis. Beauchemin et al. (2009) reported that the emission of methane by dairy cows to a higher degree was limited in case of the application of linseed or rapeseed in comparison to sunflower seeds, by 17 and 10%, respectively. On the basis of studies conducted by other research teams, in which pure linoleic acid was added to the feed ration, only a statistically significant reduction was found of both total protozoan count and the production of methane (Dohme et al., 2001), and such conclusions need to be drawn with caution. According to Cieślak et al. (2011, unpublished data) the effect of FA on protozoan counts depends not only on the type, but also the concentration of the discussed experimental factor, as well as particular species of protozoa. This study showed a varying effect of pure forms of fatty acids applied at different concentrations on populations of *Entodinium caudatum* (EC), *Eudiplodinium maggii* (EM) and *Epidinium ecaudatum* (EE) in long-term (28 days) monocultures. The most toxic effect was exerted by the following FA: stearic acid, linolenic acid, oleic acid and linoleic acid for the EC population, and linolenic, oleic and stearic for EE. The linoleic acid was not toxic to the EE population. The EM population was the most resistant to the investigated FA and only stearic and linolenic fatty acids reduced protozoan numbers. In those investigations it was also stated that individual analyzed monocultures differ in the amounts of produced methane. The EE and EM control monocultures produced on the average higher amounts of methane (0.77 and 0.74 mmol, respectively) when compared to the EC control (0.54 mmol). The above hypotheses may be partly explained by a lack of a negative effect of the addition of oils on the population of the analyzed rumen ciliates in case of some studies (Matsumoto et al., 1991; Cieślak et al., 2006a; Kisidayova et al., 2006; Cieślak et al., 2009a). A 5% addition of evening primrose oil containing considerable amounts of C18:2 and C18:3 caused a reduction of the counts of *Dasytricha ruminantium*, *Isotricha* spp. as well as *Polyplastron multivesciculatum*, while on the other hand increasing the population of *Entodinium* spp. by 32% and *Diploplastron affine* by 21% (Kisidayova et al., 2006). In other studies, in which a carrier of the C18:2 acid was used, it was shown that *Isotricha* spp. and *Dasytricha* spp. as well as cellulolytic protozoans (*Polyplastron* spp., *Diplodinium* spp., *Enoploplastron* spp.) are more sensitive to the action of the discussed acid than protozoans *Entodinium* spp (Ivan et al., 2001). In case of oleic acid a 5% addition of rapeseed oil (the primary carrier of this acid) in dry matter of the substrate to the culture medium of *Eremoplastron dilobum* in short-term (24 h) incubation, limiting the production of methane by 14% did not have a negative effect on the population of analyzed protozoans (Cieślak et al., 2006a). In the opinion of those authors it suggests that other microorganisms participating in methanogenesis or their metabolic activity were in a certain way reduced, thus influencing the reduction of the amount of methane formed in the rumen. Similar results were previously recorded by Wettstein et al. (2000), who as a result of a 7.7% addition of canola seeds and a 3.1% addition of canola oil caused a reduction of methanogenesis by approx. 26% without the reduction of protozoan counts in the rumen. In other studies it was found that rumen ciliates *Entodinium caudatum* and *Diploplastron affine* and their associated bacterial populations exhibited different metabolic responses to the form and concentration of linoleic acid (Cieślak et al., 2009a). Differences in the observations may additionally result e.g. from different rumen fluids used in analyses (species and

individual differences). Moreover, some authors suggest that the discussed microorganisms have a limited ability to assimilate, transform and utilize fat in the feed ration (Ivan et al., 2001). However, to date the level of FA addition has not been determined, which would influence the above mentioned factors. According to Ivan et al. (2001), this level is 10 mg/L in case of linoleic acid, while Kisidayova et al. (2005) suggested that an inhibition of growth and development of *Diplodinium* spp. and *Entodinium* spp. is caused already by 3 μg/L of this acid. Such differences may have been caused by conditions (*in vitro* vs. *in vivo*), under which the experimental factor, i.e. the fat addition, was applied. Martin et al. (2010) reported that in case of experiments conducted *in vitro*, it may be definitely stated that the emission of methane is reduced with an increase in the level of fat addition. Differences in recorded results depending on the experimental conditions were also shown in case of the application of other long chain fatty acids. In *in vivo* experiments, in which an addition of fish oil (a carrier of eicosapentaenoic acid – C20:5; docosahexaenoic acid – C22:6) was used in the mixture with other oils, a slight effect was found on the production of methane (Woodward et al., 2006). In turn, in studies conducted *in vitro* a considerable reduction of CH_4 level was observed under the influence of the applied experimental factor in the form of fish oil (Dong et al., 1997; Fievez et al., 2003). Similar results were shown in investigations conducted by Jalč et al. (2006c), in which the reduction of ruminal methanogenesis through an addition of fish oil was 23%. However, the authors showed that this limitation was comparable in its extent as in case of the application of linseed oil. It is suggested that there are still many ambiguities in the influence of FA on the populations of individual protozoan species and thus the process of methanogenesis.

Development of modern molecular techniques extended the range of identifiable microorganisms in different media, e.g. in the rumen ecosystem. State-of-the-art methods of molecular biology, based on rRNA analysis and independent of *in vitro* cultures, facilitate a better characteristic of the quantitative and qualitative composition of the ruminal methanogen population (Pers-Kamczyc et al., 2011).

Thus, the possibility to determine the effect of LCFA was extended to other microorganisms participating in methanogenesis, such as methanogens. Similarly as bacteria, methanogens are one of the earliest organisms colonizing the rumen. *Archaea* are found in the forestomach of lambs already 30 h after birth (Morvan et al., 1994). The population of these microorganisms in lambs in the first week of life is 10^4 cells/g contents, while in the third week of life it is already 10^8-10^9 cells/g (Skillman et al., 2006). Methanogens appearing the earliest in the rumen belong to the genus *Methanobrevibacter* (Skillman et al., 2006). In case of *Methanobacterium*, representatives of this family rapidly colonize the rumen environment; however, in contrast to *Methanobrevibacter* they rapidly disappear, i.e. at day 12 - 19 after birth (Zhu et al., 2007). Similarly as bacteria, *Archaea* living on solid particles may represent a considerable portion of the total population of methanogens in the rumen (Tajima et al., 2001). Zhu et al. (2007) mentioned *Methanobrevibacter* spp., *Methanosphaera* spp. as well as unidentified methanogens as species characteristic of that fraction. In turn, Shin et al. (2004) indicated that the most numerous group of *Archaea* living on solid particles comprises the families of *Methanomicrobiaceae* and *Methanobacteriaceae*. *Methanomicrobium mobile, Methanobacterium aarhusense* as well as *Methanosphaera stadtmanii* are species found only as forms floating in the rumen fluid, which constitute a slight percent of the total population of *Archaea* (Zhu et al., 2007).

A 10% addition of rapeseed oil as an LCFA carrier in feed rations composed mainly of concentrate under *in vitro* conditions caused a statistically highly significant decrease in the production of methane, amounting to 44% (Dong et al., 1997). The authors in their investigations showed that the main cause of such a high reduction of methanogenesis was connected with the negative influence of fat on the population of methanogens. This is confirmed by the experiences of other researchers, in which using pure forms of fatty acids from the C18 group a reduction in the population of methanogens was recorded (Zhang et al., 2008). However, the authors of those studies stressed that the degree of the effect of applied fatty acids depends on their type as well as concentrations. Among the used acids linolenic acid turned out to be the most toxic acid. In turn, stearic acid irrespective of the applied concentration (35 or 70 g/kg dry matter) caused an increase in the population size of methanogens without a limitation of the amount of produced methane. Moreover, it was found that protozoans in case of the application of C18 fatty acids are more sensitive than methanogens. In other experiments using wild dog rose seed oil an 8% decrease in methane production was recorded after 48 h of fermentation, whereas the methanogen concentration tended to increase by 14.5% (Szumacher-Strabel et al., 2011b). These studies may indicate the fact that other factors, such as the activity of individual species of methanogens should be taken into consideration. It was previously confirmed in studies on the activity of bacteria after the application of feed rations containing both saturated and unsaturated acids (Kowalczyk et al., 1977, Ivan et al., 2001).

3.3 Phytogenic dietary additives as a source of secondary plant metabolites

Since 1 January 2006 legal regulations concerning animal feeds issued by the European Union prohibited the application in animal nutrition of feed additive antibiotics, frequently called antibiotic growth promotors (Directive EU 1831/2003). The main reason for the introduction of this regulation was connected with the increasingly negative attitude of the public to the feed additives used so far. Reports appeared on a dependence between antibiotics used in animal nutrition and growth of antibiotic-resistant bacterial strains, including also those pathogenic to humans (Barton, 2000; Hurd, 2005). Increasing problems resulting from the implementation of the EU directive 1831/2003 forced dairy cattle breeders and producers to search for new alternative solutions, which application would improve production performance, contribute to higher feed conversion ratios, greater body weight gains, appropriate regulation of gastrointestinal microflora, as well as reduce emissions of ammonia and methane.

An alternative which could ensure the development of new, non-antibiotic growth stimulants, mainly of plant origin, comprises e.g. herbs and plant extracts together with the contained bioactive compounds.

The field of science investigating biologically active substances in herbs, that means secondary metabolites of plants is called pharmacognosis. To date we have discovered approx. 35 000 secondary metabolites and 50% production of the pharmaceutical industry is based on the utilization of bioactive substances.

Secondary metabolites serve an important ecological function acting as chemical communicators between plants and the environment (Calsamiglia et al., 2007). Gershenzon & Croteau (1991) discovered and published the antimicrobial and antiseptic effect of biologically active substances.

Secondary metabolites are difficult to classify and it is connected with the problems in the determination of the proper and complete mechanism of their action and pathways of their synthesis. In the recent period 3 groups of compounds were identified, to which on the basis of conducted studies different types of secondary metabolites are classified.

The following groups were identified:

- essential oils
- saponins
- tannins.

All the above classes of defined compounds are characterized by a specific biological activity. In case of these compounds the accumulated knowledge, the effects and manner of action on microbial fermentation in the rumen have become relatively well-known but still series of studies are required together with a confirmation, not only *in vitro,* but first of all *in vivo*.

Effects of phytogenic additives, rich in secondary plant metabolites on methane and ammonia production are not yet clear (Benchaar et al., 2008). Some data proved potentially antimicrobial properties of secondary plant metabolites against a wide range of rumen microorganisms and hence rumen microbial fermentation e.g. decreased ammonia production (Busquet et al., 2006), some indicated no effect on the ammonia concentration (Busquet et al., 2005). Effect of active components depends on their chemical structure, constituents and concentration (Śliwinski et al., 2002, Castillejos et al. (2006). Calsamigila et al., (2007) concluded that essential oils being the source of secondary plant metabolites may inhibit the deamination and methanogenesis that results in lower ammonia and methane concentration.

3.3.1 Essential oils

Essential oils are a mixture of secondary metabolites. They are connected with plants described as 'herbal', 'spice' or 'aroma' (Greathead, 2003). They are responsible for the characteristic aroma (*'quinate essentia'*) of these plants and may be obtained using steam distillation or extraction with the application of solvents. Many of them seem to have bactericidal and bacteriostatic effects. They act against bacteria, as well as fungi, viruses and protozoans (Greathead, 2003). Studies by Covan (1999) indicate that 60% preliminarily tested essential oils indicate an inhibitory action in relation to the development of fungi and 30% in relation to bacteria. Studies on the antibacterial action were also conducted by Chao & Young (2000), Smith-Palmer et al. (1998), Dorman & Deans (2000), Wallace et al. (1994), Wang et al. (2000) and Goel et al. (2008). One of the potential mechanisms of action in these compounds is related with the inactivation of extracellular enzymes (Bruel & Coote, 1999) and damage of cell walls (Greathead, 2003). Essential oils also influence electron transport, ion gradients, protein translocation and other enzyme-dependent reactions (Greathead, 2003).

Studies published in 2006 by Casteillejos et al. and Busquet et al. indicate a highly advantageous effect of biologically active components on ruminal fermentation. However, they also showed the adaptability of certain groups of microorganisms to applied factors in case of their long-term action. The best effects were observed in investigations conducted in

the closed management system, which is characterized by a limited duration of the experiment. Previously conducted studies suggested the influence of essential oils on ruminal fermentation processes maintained to the advantage of propionic fermentation. By influencing the modification of the fermentation process they contribute to changes in the composition of animal origin products, providing them with health-promoting properties.

Results of investigations conducted to date do not yield definite answers taking into consideration the type and concentration of the applied oil, or the secondary metabolite itself, which could effectively replace feed antibiotics. Appearing discrepancies as well as literature data suggest the advisability of further studies in order to gain insight into the problem and broaden our knowledge on the application of additions of appropriate essential oils in feed rations for ruminants.

Essential oils in terms of their chemical structure comprise multi-component mixtures of compounds. All these compounds are hydrocarbons, alcohols, aldehydes, ketones, esters or ethers (Hristov et al., 2007). Essential oils may contain derivatives of acetylene, phenylpropan, as well as sulfur and nitrogen compounds, coumarins and other rarely found compounds with a non-terpene structure. The most active components contained in these mixtures belong to two most important chemical groups (Casteillejos et al., 2007):

- terpenoids (terpenes)
- phenylpropanoids.

Essential oils are a group of compounds among secondary metabolites of plant origin (tannins and saponins), which selected properties are still to be discovered and identified. However, knowledge gained in recent years makes it possible to state that essential oils are a highly varied pool of compounds exhibiting high chemical reactivity and biological activity. We define them as compounds which:

- are soluble in ethanol, fats and solvents of fatty acids
- have a polar structure and are composed of lipophilic and hydrophilic ionic groups
- density is usually lower than that of water
- are practically insoluble in water
- at room temperature are liquids, most frequently oily
- boiling point ranges from 50 to 320˚C
- are optically active substances, which means that they are found in the D and L forms
- most frequently are colorless substances, but they are also brown, bluish and greenish
- in the plant world are used to attract insects, serve a defense function, facilitate wound closure and hinder evaporation from leaf surface
- within the entire family of essential oils there are also oils, which products are used in aromatherapy and pharmacological industry
- constitute substrates for the production of pigments and vitamin A
- exhibit extensive applications in medicine:
  - are used in the control of cardiovascular diseases
  - exhibit carcinogenic action, neutralizing the negative, rapid and uncontrolled increase in the numbers of free radicals
- improve taste, have an advantageous effect on digestion processes and thus contribute to the inhibition of excessive intestinal fermentation in the organisms of ruminants

- essential oils, similarly as the other group of secondary metabolites (saponins, tannins) have been proven to exhibit major antimicrobial and antiseptic properties. These specific properties are directed against a wide range of microorganisms, including bacteria, protozoans and fungi (Benchaar et al., 2007) and hence may have antimethanogenic and antiammonia formation properties.

Certain plant extracts, including essential oils, similarly as most antibiotics exhibit bacteriostatic and bactericidal properties. The broad range of their antibacterial action is connected with their chemical structure. Essential oils are derivatives of phenols (aromatic hydrocarbons), thus to a considerable degree they have comparable chemical and biological properties. Phenols and other surfactants have the ability to inhibit bacterial development and growth and to kill bacterial cells. These compounds, as well as the identified essential oils at an adequate concentration act as bactericidal agents. This antibacterial activity is a consequence of their ability to contact with the membrane of bacterial cells. Essential oils as lipophilic compounds change the structure of the cell membrane, which also has a similar polar structure (membranes are composed mainly of lipids and proteins), disturbing their functions by leading to a drop in ion gradient and loss of its stability (Griffin et al., 1999; Calsamiglia et al., 2007). In most cases bacteria may prevent such a phenomenon by using appropriate ionic pumps, equalizing occurring changes in the gradient of concentrations. Such a response on the part of bacteria would protect cells from death (Griffin et al., 2001; Cox et al., 2001). Unfortunately, such an action in which a cell loses large amounts of energy contributes to a reduction of growth and development, which as a consequence leads to more serious changes in the fermentation profile of the rumen.

When analyzing the mechanism of action of essential oils it may be stated that they should be more effective in their antibacterial action against strains of gram-positive bacteria, which cell membranes interact directly with the hydrophobic compounds of essential oils (Smith-Palmer et al., 1998). Similarly, Burt in 2004 suggested that gram-positive bacteria seem to be more sensitive to the antimicrobial action of essential oils than gram-negative bacteria. Gram-negative bacteria have an additional, bilayer inner membrane, lining the cell wall from the inside. This membrane is characterized by a complex structure (proteins, phospholipids, liposaccharides), and apart from the mechanical function, which it serves in the cell, it also plays the role of a certain permeability barrier limiting access of hydrophobic compounds. However, some biological agents contained in essential oils, such as e.g. thymol and carvacrol, caused growth inhibition also in gram-negative bacteria by disturbing the proper function of the inner membrane. Conclusions stemming from the above observations show that in case of selected essential oils and specific contained biologically active compounds (e.g. thymol and carvacrol) an effective action against both gram-positive and gram-negative bacteria is possible (Calsamiglia et al., 2007). However, effects of secondary plant metabolites on methane and ammonia emission are still unexplored areas. For example our findings on the effect of essential oils and particular secondary plant metabolites did not confirm the direct antimethanogenic effect when eugenol and vanillin were supplemented to dairy cow ratio analyzed in Rusitec system (Szumacher-Strabel et al., 2009), whereas limonene affected rumen methanogenesis inhibiting the methanogens populations (Cieślak et al., 2009c).

3.3.2 Saponins

Saponins comprise a numerous group of glycosides, found in angiospermous plants. The property distinguishing them from the other glycosides is the reduction of surface tension

(Sparg et al., 2004). The name "saponin" originates from the Latin word *sapo* [soap], since saponins are water-soluble substances, capable of forming foam and saponification (Oleszek, 2002; Vincken et al., 2007). These properties result from their structure. Saponins are composed of hydrophobic sapogenin, i.e. aglycone and the hydrophilic part of the saccharide, i.e. glycone, most frequently comprised by glucose, arabinose, xylose and galactose. Ages ago plants containing saponins were considered valuable and used in medicine, herbology, pharmacology as well as cosmetology. They were used e.g. as detergents, for example root of soapwort *Saponaria officinalis* L., and thanks to traditional Chinese medicine worldwide acclaim was given to properties of saponins contained in roots of ginseng *Panax ginseng* C. A. Mey. (Sparg et al., 2004). Saponins are substances which protect plants against bacterial and fungal infections. Saponins by changing the structure of cell membranes (and thus also that of epithelia) make them more readily permeable for organic components. They trigger the secretion of gastric fluid, bile and intestinal fluid. Saponins exhibit antibacterial, antiprotozoal and antiviral properties. Some of them are capable of binding toxins and metabolites. Properties of saponins are to a considerable degree influenced by the volume of the applied feed ration. In case of saponin overdose they exhibit a disadvantageous effect on the organism. This type of action comprises the following effects: hemolytic, nephrotoxic, hepatotoxic, as well as antinutritional, consisting in the inhibition of active nutrient transport.

The potentially advantageous action of saponins in the rumen, including the antibacterial, antiprotozoal, antifungal as well as antimethanogenic effect, is indicated by the results of studies conducted in recent years by many authors (Agarwal et al., 2006; Goel et al., 2008; Patra and Saxena, 2009). However, those researchers pointed to the fact that the effects of saponin administration depend on many factors, including the time of application (Wina et al., 2006).

Many studies conducted to date showed that the addition of saponins to feed rations for ruminants, irrespective of their source (*Yucca schidigera, Sapindus saponaria, Sapindus rarak*) reduces methanogenesis (Śliwiński et al., 2002; Ningrat et al., 2002; Hess et al., 2003a, 2004; Wang et al., 2009). Similarly as in case of fat supplementation, saponins added directly to feed rations may influence microorganisms participating in the process of methane formation in the rumen. This effect is multifaceted, affecting both microorganisms participating in the production of hydrogen, e.g. protozoans, and microorganisms utilizing this hydrogen to produce methane (Szumacher-Strabel & Cieślak, 2010). This hypothesis is confirmed by earlier studies, in which antimicrobial action of saponins was shown in case of organisms colonizing the rumen (Benchaar et al., 2007a). The population of protozoans, ruminal microorganisms indirectly connected with methanogenesis, was completely reduced thanks to the addition of saponins coming from *Yucca schidigera* (Wallace et al., 1994). The probable cause of the destruction of protozoan cells was the chemical structure of saponins. Saponins are composed of hydrophobic sapogenin, i.e. an aglycone, and a hydrophilic saccharide part, i.e. a glycone, which may comprise glucose, arabinose, xylose and galactose. Saponins are classified on the basis of their aglycone structure into two groups: steroid (C27), derivative of spirostane or furostane, and triterpene (C30), having triterpene aglycone (Sparg et al., 2004). These compounds may interact with cholesterol found in membranes of eukaryotic cells, causing cell destruction (Cheeke, 1999; Wina et al., 2005). In studies on the effect of saponins coming from tea on pure cultures of methanogens predominating in the ruminal fluid (*Methanobrevibacter ruminantium*) no negative influence

was observed on the counts of these microorganisms (Guo et al., 2008). Similarly, in a study conducted by a team of Mao et al. (2010) it was shown that the reduction of methane emission from growing lambs was not caused by a direct action of tea saponins on methanogens, but rather on the population of protozoans, in this way limiting the amount of available hydrogen for the process of methanogenesis. The authors indicated that those observations were consistent with the previously reported results of *in vitro* experiments, in which methanogenesis was reduced with no decrease in the population of methanogens under the influence of the same saponin carrier (Hu et al., 2005). The lack of a negative action of saponins on the population of methanogens was also recorded in other studies, where *Sapindus saponaria* was applied at 100 mg/g dry matter (Hessa et al., 2003b). Similarly as in case of the earlier reports a 20% reduction of methanogenesis was directly connected with a 54% reduction of the protozoan population. However, not all literature data confirm a lack of a negative influence of saponins on populations of methanogens. An experiment conducted using saponins from fruits of *Sapindus rarak* showed that a reduction of methanogen RNA concentration was obtained at the application of the highest concentration of the tested experimental factor in the feed ration (4 mg/ml), while lower concentrations did not have an effect on the populations of these microorganisms (Wina et al., 2005). A reduction of protozoan populations, both *in vitro* and *in vivo*, was also recorded after the application of an extract from *Yucca schidigera* (YSE; Hristov et al., 1999; Pen et al., 2006). However, it needs to be remembered that the use of YSE did not always reduce the populations of protozoans. In investigations conducted by Benchaar et al. (2008) no negative effect was found of 60 g YSE (containing 10% saponin) per cow a day on the total numbers and the distribution by genera of ruminal ciliate protozoa. Similarly, other authors did not show any such effect (Hristov et al., 2003; Bahh et al., 2007). The observed differences may have been caused by the amount of applied saponins (Hristov et al., 2004). This hypothesis may be confirmed by the investigations conducted by our research team. The use of an extract from *Knautia arvensis* only at higher doses (50.0 and 100.0 mg/40 mL of culture) caused a reduction of methanogenesis. In contrast, lower concentrations (0.5, 2.5, 5.0, 12.5 and 25.0 mg/40 mL of culture) did not reduce the amount of produced methane (Szumacher-Strabel et al., unpublished data). In other studies conducted by our team using roots of *Saponaria officinalis* as a saponin carrier at 0, 4, 10, 20, 40, 100 and 200 mg per 40 ml of culture the reduction of methanogenesis was as low as 12 to 26% at higher concentrations (from 40 to 200 mg; Zmora et al., unpublished data). Moreover, it was shown that the limitation of methane production was caused by the reduction of the population of protozoans, both *Entodiniomorhpa* and *Holotricha*. These studies also showed that lower concentrations of saponins coming from roots of *Saponaria officinalis* may have a stimulating effect on the population of protozoans, increasing slightly the amount of formed methane. Other causes of a lack of the effect of saponins on processes occurring in the rumen as well as counts of protozoans may be related with the total degradation of saponins (Makkar & Becker 1997), hydrolysis (Miles et al., 1992; Teferedegne et al., 1999) or deglycosylation (deglycosylate) (Wang et al., 1998). Odenyo et al. (1997) stated that the manner of saponin administration influenced the population of microorganisms in the rumen. In the conducted experiment 300 g *Sesbania sesban* introduced directly to the rumen had a toxic action on the population of protozoans, while saponins administered to animals together with feed did not show such properties. According to the researchers, the result may be explained by

rumination of feed by animals, since in this way amylase contained in saliva causes detoxication of saponins.

Goel et al. (2008) additionally pointed to differences in the composition of feed rations as a factor potentially differentiating the effect of saponins on methanogenesis. When feeding a feed ration with a predominance of concentrates rich in starch we may more effectively inhibit methanogenesis in comparison to the effect of a feed ration, in which forages predominated. When using saponins as the agent limiting the production of methane by the reduction of protozoan counts we also need to consider the passing antiprotozoal action, directly dependent on the time of action (Newbold et al., 1997, Teferedegne et al., 1999). As it was already mentioned, protozoans are not resistant to saponins; however, theses substances through the action of bacteria in the rumen environment may be subjected to the process of detoxication, and the time during which it takes place is a significant element of this process (Teferedegne et al., 1999; Teferedegne, 2000).

Many studies also indicated the action of saponin on populations of anaerobic fungi in the rumen ecosystem (Mao et al., 2010; Wang et al., 2011). *In vitro* experiments showed that the counts of fungi were reduced under the influence of saponins coming from *Yucca schidigera* or *Sesbania pachycarpa* (Wang et al., 2000; Muetzel et al., 2003). Saponins from fruits of *Sapindus rarak* completely eliminated fungal RNA already at the lowest concentration (1 mg/ml) of the experimental factor in the feed ration, while the highest concentration (4 mg/ml) caused a reduction of the methanogen RNA concentration (Wina et al., 2005). This suggests, similarly as in case of protozoans, that fungi are more sensitive to the action of saponins than methanogens. Thus saponins reducing the populations of fungi cause a reduction of available hydrogen in the rumen environment. In another experiment, in which gynosaponins extracted from *Gynostemma pentaphyllum* were applied at 50, 100 as well as 200 mg/l in the co-culture of a fungus *Piromyces* sp. F1 and a methanogen *Methanobrevibacter* sp., a reduction was stated both for the counts of methanogens and the production of methane at all the applied doses (Wang et al., 2011). In contrast, lower concentrations (50 mg/l) did not reduce the population of fungi. The increased fungi numbers in case of low doses of gynosaponins are probably due to the sugar moiety of saponin as a nutrient for microorganisms (Wang et al., 2011). This suggests that researchers when interpreting recorded results have to take into consideration the potential occurrence of an interaction between substances or compounds contained in extracts and a biologically active agent. An example of these interactions was presented in a study conducted using garlic (Kamel et al., 2008). An addition of garlic to the rumen fluid caused a reduction of methanogenesis by 19.5%, whereas an addition of allicin, one of the compounds of garlic oil, did not change CH_4 production. On the basis of that experiment it may be concluded that allicin alone does not exert an inhibitory effect; however, its interaction with some unidentified garlic components cannot be ruled out. In turn, in other studies after the application of 0.1, 0.2 or 1.0 mg of xanthohumol (an isolated biologically active agent from hops) it was found that all concentrations of the applied experimental agent caused a reduction of methanogenesis in the rumen environment (Zmora et al., 2012). Presented examples suggest that in the analysis of the effect of individual biologically active substances on processes occurring in the rumen environment, in the pure form or e.g. in extracts, we need to consider the possibility of such interactions as those mentioned above. In view of the above, an interpretation of recorded results is sometimes very difficult.

3.3.3 Tannins

Tannins are polyphenolic compounds, with a high molecular weight and capacity to form complexes with other compounds, especially proteins (Barszcz & Skomiał, 2011). Tannins are formed via shikimic pathway and are divided into hydrolyzable and condensed (non-hydrolysable; proanthocyanidins). The basic unit for hydrolyzable tannins is gallic acid (3, 4, 5-trihydroxyl benzoic acid), and flavone (oligomers or polymers of flavonoid units) for condensed one. Hydrolyzable tannins comprise two classes: gallotannins and ellagitannins (Figure 1). Gallotannins are formed of units of gallic acid surrounding a polyolic core. The most common source of gallotannins is tannic acid, whereas ellagitannins may exist in the form of ellagic acid units surrounding a polyolic core but at least 2 of them are linked through carbon-carbon bonds. Proanthocyanidins are polymers of flavon-3-ol (catechin) units (Figure 2) and exist most often as cyaniding and delphinidin. According to Kowalik et al. (2009) tannins are known for their antimicrobial activity and the growth and enzyme activity of many microorganisms. They may reduce the digestibility of cell walls by binding bacterial enzymes and (or) forming ingestible complexes with cell wall carbohydrates. They also create complex protein. Tannin-protein interactions depend on the structure either of protein or of tannins. Tannins, similarly as essential oils or saponins, exhibit antimicrobial action. However, as with other biologically active compounds, the mechanism of their action depends on the one hand on their chemical structure and on the other hand on the group of microorganisms which it influences.

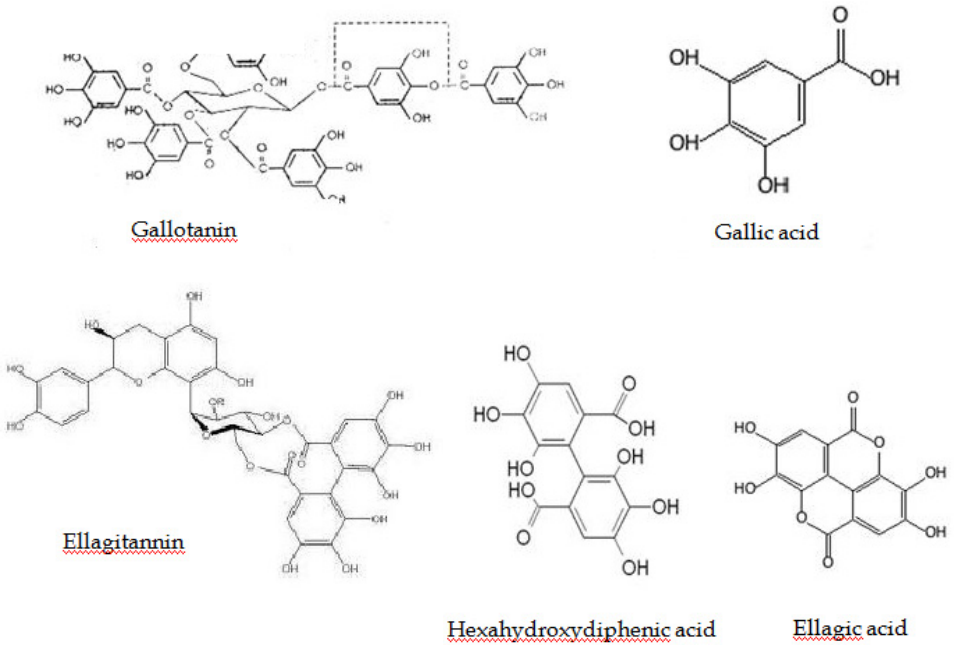

Fig. 2. Structure of hydrolysable tannins (www.ansci.cornell.edu)

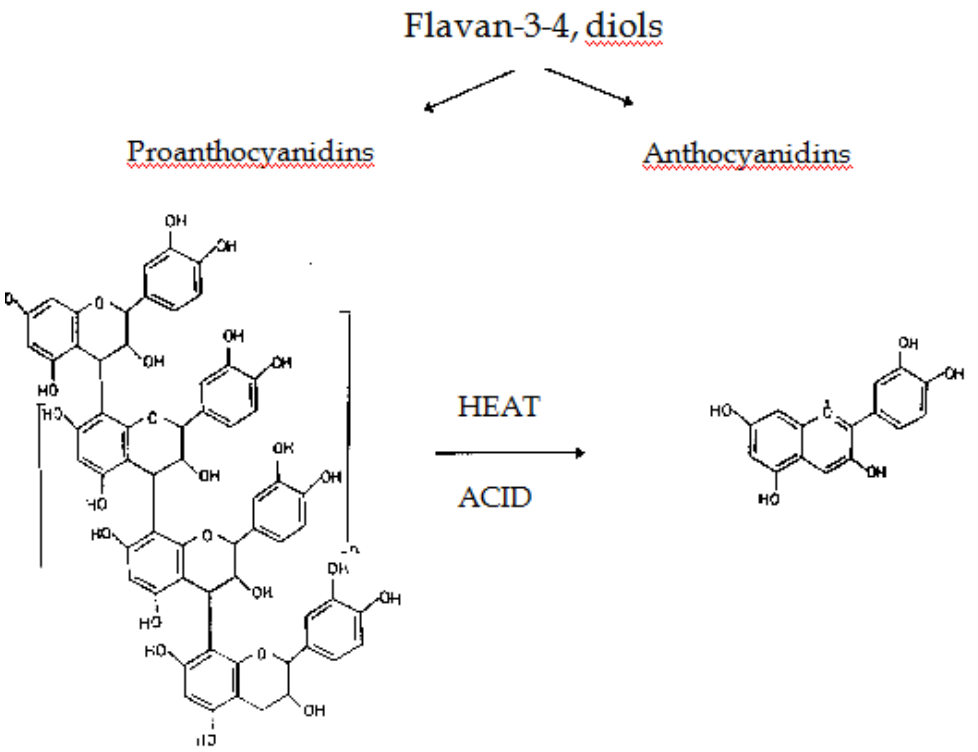

Fig. 3. Structure of condensed tannins (www.ansci.cornell.edu)

Thus the applications of biologically active plant origin substances, including tannins, to mitigate enteric ruminal CH_4 emissions and ammonia production are becoming increasingly extensive (Szumacher-Strabel & Cieślak, 2010). Unfortunately, the reduction of methane production through the application of forages containing condensed tannins (CT), recorded in many studies (Woodward et al., 2001; 2002; Hess et al., 2003a; Animut et al., 2008), may have been caused by the negative effect of tannins on the digestibility of nutrients. This results from the fact that tannins exhibit an antinutritional effect. It consist in their ability to form complexes with proteins and sugars, as a result of which the digestibility of nutrients contained in feed is limited, reducing the utilization of nutrients from the feed ration. Another cause of the reduced digestibility may be connected with the reduction of activity of cellulase and xynalase, i.e. enzymes degrading structural carbohydrates (Salawu et al., 1999). However, it needs to be mentioned here that other studies on the effect of tannins on the rumen environment did not show a limitation of activity of cellulolytic bacteria (Animut et al., 2008). Moreover, the amount of tannins in feed exceeding 60 g/kg^{-1} gives it a bitter taste, deteriorating palatability and thus reducing feed uptake by animals.

An addition of tannins to feed rations used in the nutrition of ruminants may influence the process of methanogenesis, similarly as in case of other biologically active substances, either indirectly or directly (Tavendale et al., 2005; Bhatta et al., 2009). Indirectly tannins may reduce the populations of microorganisms participating in fermentation processes in the

rumen environment, and thus reducing the concentration of H_2, a necessary substrate for the formation of methane. This action may be also direct on the populations of methanogens, thanks to which methane is formed in the rumen ecosystem. In studies conducted using methanogens commonly found in the rumen environment (*Methanobrevibacter ruminantium*), a deactivation of these microorganisms was found, which caused a reduction of methanogenesis in the rumen environment (Tavendale et al., 2005). The authors of those studies suggested that a reduced growth of methanogens could have been caused by the bacteriostatic and bactericidal effects of CT. In other studies it was shown that CT has a greater potential to reduce the process of methanogenesis in comparison to hydrolyzing tannins (HT; Bhatta et al., 2009). A team of Tavendale et al. (2005) showed that the reducing action of tannins on the populations of methanogens may depend on the chemical structure of tannins. In their studies they used CT. In other experiments attention was focused on feeds containing both HT and CT, exhibiting a greater potential to reduce methanogenesis than feeds containing only HT (Bhatta et al., 2009). According to those authors, one of the causes of the differences resulting from the effect of HT and CT is connected with the action on the populations of protozoans. However, Śliwiński et al. (2002) stated that extracts containing HT did not have a negative effect on protozoan populations, whereas Leinműller et al. (1991) showed that HT influences the counts of protozoans, although its action was smaller in comparison to CT, which is consistent with previously cited data (Bhatta et al., 2009). In view of the above, Beauchemin et al. (2007) suggested the use of a CT extract to reduce CH_4 emissions, as an alternative to the use of tannin-rich forages. Literature data concerning the limitation of ciliate populations in the rumen, and thus the amount of formed methane in the rumen after the application of tannins, are ambiguous (Patra & Saxena, 2009; Szumacher-Strabel & Cieslak, 2010). Most studies indicate that tannins reduce populations of protozoans (Salawu et al., 1999; McSweeney et al., 2001; Patra et al., 2006; Animut et al., 2008). Similar dependencies were shown in studies conducted using CT of leucaena, acacia and eucalyptus (Sallam et al., 2010). Moreover, in another experiment it was shown that CT from leucaena not only reduces the counts of protozoans, but also populations of methanogens, thus significantly reducing the amount of formed methane (Tan et al., 2011). According to Makkar et al. (1995), a reduction of the protozoan population as a result of a tannin addition to feed rations not only causes a limitation of the amount of produced methane, but also influences the scale of synthesis of microbial protein in this environment. However, it needs to be remembered that the reduction of the amount of methane formed in the rumen depends on many factors, including e.g. the amount of applied tannins, administration time of tannin carriers, or animal species given the feed with an addition of tannins (Szumacher-Strabel & Cieslak, 2010). However, such sources of tannins are being continuously searched for, which while reducing methane production in the rumen would not have a negative effect on the rumen ecosystem. An example of such analyses may be provided by experiments conducted by Monforte-Briceno et al. (2005). Those researchers analyzed 15 plants, tannin carriers, in terms of their antiprotozoal action. However, only three plants turned out to be effective. Other studies determined e.g. the dependence between the content of biologically active compounds (*i.e.,* total phenols, total tannins, condensed tannins and tannin activity using a tannin bioassay) in 17 plant materials and the production of methane. It was shown that among them only 6 (leaves of *Rheum undulatum*, *Vaccinium vitis-idaea*, *B. crassifolia*, *Rhus typhina* and *P. peltatum*, and roots of *B.*

crassifolia) have considerable potential (*i.e.*, >25%) to decrease enteric methane production from ruminants (Jayanegara et al., 2009). In turn, in another experiment screening unconventional feeds and various supplements for their ruminal methane mitigation potential only a trend towards a reduction of the amount of produced methane (by 15%) was shown in case of the application of a high-tannin extract from *Acacia mearnsii* (50 g/kg diet; Staerfl et al., 2010). This points to the fact that researchers searching for an ideal agent reducing the amount of produced methane still face a long way to go before they obtain satisfactory results not only from the scientific, but also practical point of view.

3.4 Antibiotics growth promoters

Antibiotic growth promoters (AGP) started to be used in mid fifties of XX century. They are actually applied in United States of America, China and Argentina. AGP were utilized in animal nutrition in Europe until 2006 when the ban on their use (Directive 1831/2003/CEE, European Commission 2003), implemented in 2003 and effective since 1st January 2006, has been introduced. The principal reason for this directive was connected with the increasingly negative attitude of the public to feed additives applied so far. Reports appeared on a dependence between antibiotics used in animal nutrition and growth of antibiotic-resistant bacterial strains, including those pathogenic to humans (Barton, 2000; Hurd, 2005), which was confirmed several years later, when evidence was presented on an increased resistance of certain strains, e.g. *Salmonella typihimurium DT104, Campylobacter spp.* and *Escherichia coli.* Until the moment antibiotic growth stimulants were withdrawn, they had been used on a broad scale in order to improve the composition of ruminal microflora, thus eliminating or inhibiting microorganisms and their products (toxins), having a potentially deteriorating effect on digestion processes. The growth stimulating effect, which was caused by subtherapeutic doses of antibiotics in feed rations was discovered in the 1940's, when for the first time a fermentation extract of *Streptomyces aureofaciens* was applied in feeding chickens. Over the last thirty years a positive effect of AGP was found in terms of increased body weight gains, particularly in the period before weaning, as well as more advantageous feed conversion ratios (Gaskin et al., 2002). Thanks to the effective application of antibiotics in feeds for monogastric animals, as well as in feeding of ruminants, the use of AGP led to advances in this technology, production and practical applications.

Monensin, was the first ionophore antibiotic allowed in animal nutrition by Food and Drug Administration in 1971 (McGuffy et al., 2001). AGP have also potential to decrease green house gasses production and emission to the atmosphere, as well as to decrease the digestive tract pathogens activity. They are active against gram-positive bacteria, protozoa and fungi inhabiting the digestive tract. Also some gram-negative bacteria are sensitive to ionophores. Their utilization may have positive effect on rumen nitrogen metabolism, nitrogen retention and as the consequence may decrease protein degradation and ammonia production and emission. Ionophores reduce ruminal degradation of peptides and deamination of amino acids thus decreasing rumen ammonia production (Hobson & Stewart, 1997). This lead to increased protein concentration and absorption in the further part of digestive tract and improved feed utilization (McGuffy et al., 2001). It was noticed in *in vitro* studies that, microbial efficiency expressed per mol ATP (g/mol) was increased by monensin from 7.8 to 12.6. Moreover, protein conversion ratio, degradability of protein and microbial protein synthesis efficiency were increased and non protein utilization ratio

decreased in the presence of monensin (Jalč et al., 1992). However ionophore antibiotics are not harmful to methanogens, it is proved that they reduce methane precursors, hydrogen and formate (Hobson & Stewart, 1997). Ionophores act by interrupting transmembrane movement and intracellular equilibrium of ions in certain classes of bacteria and protozoa (McGuffy et al., 2001; Heydari et al., 2008). Many of them are not selective in acting. The commonly increasing use of antibiotic growth stimulants in the feed rations for animals was caused first of all by an improvement of productivity and a limitation of incidence of certain wide-spread diseases related with the alimentary tract of animals. However, in the early 1990's the first reports appeared on the potential acquisition of cross immunity by humans towards antibiotics used in animal feeding. The probability of such antibiotic resistance in certain bacteria turned to be slight, but fateful, as in case of e.g. vancomycin. Its long-term use in feeding of slaughter animals caused the development of vancomycin-resistant enterococci. This type of bacteria does not cause any disease in animals, whereas in the human organism it contributes to the development of inflammatory conditions in the urinary system and may cause endocarditis. Moreover, an increased resistance to vancomycin was found for certain bacterial strains pathogenic to humans, such as e.g. *Staphylococcus ureus* (Van den Bogaard et al., 2000). In view of the presented examples, with the concern for the quality of life and health safety of the general public, and in connection with the ineffectiveness of antibiotic therapy a complete ban was passed on the use of "unnatural" feed additives to feed rations for farm animals in the European Union. The presently increasing consumer awareness has led to the elimination of all non-plant origin compounds added to animal feeds. Today consumers require food to be not only of high health safety quality, but mainly free from any additives, which may potentially lead in the future to an increase in resistance of animal organisms to certain pathogenic bacterial strains. That situation resulted in an intensive development of research on searching and using effective natural compounds displaying similar properties, that were discussed above.

4. Conclusions

It can be concluded that it is possible to mitigate rumen methane and ammonia production by modulation of dietary nutrients, however, more studies are needed to determine the impact of particular component, the interaction among components (synergistic and antagonistic reactions) as well as interaction among the dietary nutrients and particular microbial population. Of course, each research should be verified in *in vivo* condition with mixed ruminal microflora, taking under consideration environmental factors. What is more, studies on compounds found in plants, potentially influencing ruminal metabolism and as a consequence - also the productivity of animals, should not only be strategic, but rather fundamental objectives, making it possible to broaden our knowledge on the interdependencies between animals and the cocktail of phytochemical compounds they consume with feed every day.

5. References

Agarwal, N.; Shekhar, C.; Kumar, R.; Chaudhary, L.C.; Kamra, D.N. (2009) Effect of peppermint (*Mentha piperita*) oil on in vitro methanogenesis and fermentation of feed with buffalo rumen liquor. *Anim. Feed Sci. Technol.*, 148, 321–327

Animut, G.; Goetsch, A.L.; Puchala, R.; Patra, A.K.; Sahlu, T.; Varel, V.H.; Wells, J. (2008) Methane emission by goats consuming different sources of condensed tannins. *Anim. Feed. Sci. Technol*., 144, 228–241

Attwood, G.T. & Reilly K. (1995) Identification of proteolytic rumen bacteria isolated from New Zealand cattle. *J. Appl. Bacteriol.,* 79, 22-29

Ban Salem, H.; Krzeminski, R.; Ferlay, A.; Doreau, M. (1993) Effect of lipid supply on in vivo digestion in cows: comparison of hay and silage diets. *Can. J. Anim. Sci.,* 73, 547-557

Barszcz, M. & Skomiał, J. (2011) Possibilities of tannins utilization in the protection of animals and human health. *Post. Nauk. Roln*., 2, 95-110, in Polish

Barton, M.D. (2000) Antibiotic use in animal feed and impact on human Health. *Nutr. Res. Rev.,* 13, 279-299

Beauchemin, K.A.; Kreuzer, M.; O'Mara, F. & McAllister T.A. (2008) Nutritional management for enteric methane abatement: a review. *Aust. J. Experim. Agric.,* 48, 21–27

Beauchemin, K.A.; McGinn, S.M.; Benchaar,C.; Holtshausen, L. (2009) Crushed sunflower, flax, or canola seeds in lactating dairy cow diets: Effects on methane production, rumen fermentation, and milk production. *J. Dairy Sci*., 92, 2118-2127

Beauchemin, K.A.; McGinn, S.M.; Martinez, T.F.; McAllister, T.A.; (2007) Use of condensed tannin extract from quebracho trees to reduce methane emissions from cattle. *J. Anim. Sci.,* 85, 1990–1996

Benchaar, C.; Calsamiglia, S.; Chaves, A.V.; Fraser, G.R.; Colombatto, D.; McAllister, T.A.; Beauchemin, K.A.; (2008) A review of plant-derived essential oils in ruminant nutrition and production. *Anim. Feed Sci. Technol.,* 145, 209-228

Benchaar, C. ; Petit, H.V. ; Berthiaume ,R. ; Ouellet, D.R. ; Chiquette, J. ; Chouinard, P.Y. (2007) Effects of essential oils on digestion, ruminal fermentation, rumen microbial populations, milk production, and milk composition in dairy cows fed alfalfa silage or corn silage. *J. Dairy Sci*., 90, 886-897

Benchaar, C.; Petit, H.V.; Berthiaume, R.; Quellet, D.R.; Chiquitte, J.; Chouinardt, P.Y. (2007) Effects of Essential Oils on Digestion, Ruminal Fermentation, Rumen Microbial Populations, Milk, Production, and Milk Composition in Dairy Cows Fed Alfalfa Silage or Corn Silage. *J. Dairy Sci.,* 90, 886-897

Bhatta, R.; Uyeno, Y.; Tajima, K.; Takenaka, A.; Yabumoto, Y.; Nonaka, I.; Enishi, O.; Kurihara, M. (2009) Difference in the nature of tannins on in vitro ruminal methane and volatile fatty acid production and on methanogenic archaea and protozoal populations. *J. Dairy Sci.,* 92, 5512-5522

Black, P.N. & DiRusso, C.C. (2003) Transmembrane Movement of Exogenous Long-Chain Fatty Acids: Proteins, Enzymes, and Vectorial Esterification. *Microbiol. Molecul. Biol. Rev.,* 67, 454-472

Boadi, D.; Benchaar, C.; Chiquette, J. Masse, D. (2004) Mitigation strategies to reduce enteric methane emissions from dairy cows: Update review. *Can. J. Anim. Sci*., 84, 319-335

Broudiscou, L.; Pochet, S.; Poncet, C. (1994) Effect of linseed oil supplementation on feed degradation and microbial synthesis in the rumen of ciliate-free and refaunated sheep. *Anim. Feed Sci. Technol*. 49, 189-202

Bruel, S. & Coote, P. (1999) Preservative agents in foods – Mode of action and microbial resistance mechanisms. *Int. J.Food Microbiol.*, Amsterdam, v. 50, p.1-17

Burt S., (2004) Essentials oils: Their antibacterial properties and potential applications in food-a review. *Int. J. Ford Microbiol.,* 94, 223-253

Busquet, M.; Calsamiglia, S.; Ferret, A.; Kamel, C. (2006) Plant extracts affect *in vitro* rumen microbial fermentation. *J. Dairy Sci*., 89, 761-771

Busquet, M.; Calsamiglia, S.; Ferret, S.; Kamel, C. (2005) Screening for the effects of natural plant extracts and secondary plant metabolites on rumen microbial fermentation in continuous culture. *Anim. Feed Sci. Technol.* 123, 597-613

Calsamigilia, S.; Busquet, M.; Cardozo, P.W.; Castillejos, L.; Ferret, A. (2007) Invited Review: Essential Oils As Modifiers of Rumen Microbal Fermentation *J. Dairy Sci.,* 90, 2580-2595

Castillejos, L.; Calsamiglia, S.; Ferret, A.; Losa R. (2007) Effects of dose and adaptation time of a specific blend of essential oil compounds on rumen fermentation *Anim. Feed Sci. Technol.,* 132, 186-201

Castillejos, L.; Calsamiglia, S.; Ferret, A. (2006) Effect of essential oils active compounds on rumen microbial fermentation and nutrient flow in *in vitro* systems. *J. Dairy Sci.,* 89, 2649-2658

Chao, S.C.; Young, D.G. (2000) Screening for inhibitory activity of essential oils on selected bacteria, fungi and viruses. *J. Essent. Oil Res.,* 12, 639-649

Cheeke, P.R. (1999) Actual and potential application of *Yucca schidigera* and *Quillaja saponaria* saponins in human and animal nutrition. *Proc. Am. Soc. Anim. Sci*., pp. 1-10

Cheong, G.W.; Cejka, Z.; Peters, J.; Stetter, K.O.; Baumeister W. (1991) The surface protein layer of *Methanoplanus limicola*: three-dimensional structure and chemical characterization. *System App. Microbiol*., 14, 209-27

Cieślak, A.; Kowalczyk, J.; Czauderna, M.; Potkański, A.; Szumacher – Strabel, M. (2010) Enhancing unsaturated fatty acids in ewe's milk by feeding rapeseed or linseed oil. *Czech. J. Anim. Sci.,* 55, 496-504

Cieślak, A.; Miltko, R.; Bełżecki, G.; Szumacher-Strabel, M.; Michałowski, T. (2009b) Rumen ciliates *Entodinium caudatum*, *Eudiplodinium maggii* and *Diploplastron affine*: a potential reservoir of unsaturated fatty acids for the host. *Acta Protozool*., 48, 335-340

Cieślak, A.; Miltko, R.; Bełżecki, G.; Szumacher-Strabel, M.; Potkańki, A.; Kwiatkowska, E.; Michałowski, T. (2006a) Effect of vegetable oils on the methane concentration and population density of the rumen ciliate, *Eremoplastron dilobum*, grown *in vitro. J. Anim. Feed Sci*., 15, 15-18

Cieślak, A.; Potkański, A.; Kowalczyk, J.; Szumacher-Strabel, M.; Czaczyk, K.; Gubała, A.; Janicki M. & Szymankiewicz E. (2005) Methane production in *in vitro* studies as an effect of different additives to grass silage. *J. Anim. Feed Sci.,* 14, Suppl. 1, 307-310

Cieślak, A.; Potkanski, A.; Szumacher-Strabel M. & Kowalczyk J. (2004) Blood parameters of lambs fed diets with vegetable oil supplements *J. Anim. Feed Sci*., 13 Suppl. 2, 21-24

Cieślak, A.; Szumacher-Strabel, M.; Potkański, A.; Kowalczyk J.& Czauderna M. (2001) The effects of different amounts and types of fat on the extent of C18 unsaturated fatty acid hydrogenation in the rumen of sheep. *J. Anim. Feed Sci.,* 10, Suppl. 2, 123-128

Cieślak, A.; Szumacher-Strabel, M.; Szymankiewicz, E.; Piękniewski, M,; Oleszak, P.; Siwiński, Ł.; Potkański A. (2006b) Coconout oil reduces protozoa amount and methane release during fermentation in a RUSITEC system. *J. Anim. Feed Sci*., 15, 19-22

Cieślak, A.; Váradyová, Z.; Kišidayová, S.; Szumacher-Strabel M. (2009a) The effects of linoleic acid on the fermentation parameters, population density, and fatty-acid profile of two rumen ciliate cultures, *Entodinium caudatum* and *Diploplastron affine. Acta Protozool.*, 48, (1) 51-61

Cieślak, A.; Zmora, P.; Nowakowska, A.; Szumacher-Strabel, M. (2009c) Limonene affect rumen methanogenesis inhibiting the methanogens populations. *Acta Bioch. Pol.*, 56, Suppl. 2, 59-60

Cowan, M.M. (1999) Plant products as antimicrobial agent. *Clin. Microbiol.* Reviews 12, 564-582

Cox, S.D.; Mann, C.M.; Markam, J.L. (2001) Interaction between components of the essential oil of *Melaleuca alternifolia. J. Appl. Microbiol.*, 91, 492-49

Crutzen, P.J.; Aselmann, I. & Seiler W. (1986) Methane Production by Domestic Animals, Wild Ruminants, other Herbivorous Fauna, and Humans. Tullus 33B, pp.271-284

Czerkawski, J.W.; Blaxter, K.L. & Wainman F.W. (1966) The metabolism of oleic , linoleic, and linolenic acids by sheep with reference to their effects on methane production. *Br. J. Nutr.*, 20, 349 -362

Dohme, F.; Machmüller, A.; Sutter, F.; Kreuzer, M. (2004) Digestive and metabolic utilization of lauric, myristic and stearic acid in cows, and associated effects on milk fat quality. *Arch. Anim. Nutr.*, 58, 99-116

Dohme, F.; Machmüller, A.; Wasserfallen, A.; Kreuzer, M. (2001) Ruminal methanogenesis as influenced by individual fatty acids supplemented to complete ruminant diets. *Lett. Appl. Microbiol.*, 3, 47-51

Dong, Y.; Bea, H.D.; McAllister, T.A.; Mathison, G.W.; Cheng, K.G. (1997) Lipid induced depreession of methane production and digestibility in the artificial rumen system (RUSITEC). *Can. J. Anim. Sci.*, 77, 269-278

Dorman, H.J.D. & Deans S.G. (2000)Antimicrobial agents from plants: Antibacterial activity of plant volatile oils. *J. Appl. Microbiol.*, 88, 308-316

Eugene, M.; Masse, D.; Chiquette, J.; Benchaar, C. (2008) Meta-analysis on the effect of lipid supplementation on methane production in lactating dairy cows. *Can. J. Anim. Sci.*, 88, 331-334

European Commission (2003) Regulation (EC) No. 1831/2003 of the European Parliament and of the Council of 22 September 2003 on Additives for Use in Animal Nutrition. *Off. J. Eur. Union,* L268/29-L268/43

FAO - Food and Agriculture Organization of the United Nations (2008) FAOSTAT, Available from http://faostat.fao.org/

Fievez, V.; Dohme, F.; Danneels, M.; Raes, K.; Demeyer, D. (2003) Fish oils as potent rumen methane inhibitors and associated effects on rumen fermentation *in vitro* and *in vivo. Anim. Feed Sci. Technol.*, 104, 41–58

Finlay, B.J.; Esteban, G.; Clarke, K.J.; Williams, A.G.; Embley, T.M.; Hirt, R.R (1994) Some rumen ciliates have endosymbiotic methanogens. *FEMS Microbiol. Lett.,* 117, 157-162

Finlay, B.J.; Esteban, G.; Clarke, K.J.; Williams, A.G.; Embley, T.M.; Hirt, R.R. (1994) Some rumen ciliates have endosymbiotic methanogens. *FEMS Microbiol. Lett.,* 117, 157-162

Gaskin, H.R.; Collier C.C.; Anderson, D.B. (2002) Antibiotics as growth promoters mode of action. *Anim. Biotechnol.*, 13, 29-42

Gershenzon J. & Croteau R. (1991) Terpenoids. Their Interactions with Secondary Plant Metabolites. Vol. 1. G.A. Rosenthal, M.R. Berenbaum, Academic Press, San Diego, CA. pp. 165-219

Giger-Reverdin, S.; Morand-Fehr, P.; Tran, G. (2003) Literature survey of the influence of dietary fat composition on methane production in dairy cattle. *Livest. Prod. Sci.,* 82, 73-79

Goel, G.; Makkar, H.P.S.; Becker K. (2008) Changes in microbial community structure, methanogenesis and rumen fermentation in response to saponin-rich fractions from different plant materials. *J. Appl. Microbiol.,* 105, 770-777

Graeme, T.; Attwood, G.T.; Klieve, A.V.; Ouwerkerk, D.; Patel, B.K.C. (1998) Ammonia-hyperproducing bacteria from New Zealand ruminants. *Appl. Environ. Microbiol.*, 64, 1796-1804

Grant, R.J. & Weidner, S.J. (1992) Effect of fat from whole soyabeans on performance of dairy cows fed rations differing in fiber level and particle size. *J. Dairy Sci.,* 75, 2742 – 2751

Greathead, H. (2003) Plants and plant extracts for improving animal productivity. *Proc. Nutr. Soc.*, 62, 279-290

Griffin, S.G.; Wyllie, S.G.; Markham, J.L.; Leach D.N. (1999) The role of structure and molecular properties of terpenoids in determining their antimicrobial activity. *Flavour Fragr. J.,* 14, 322-332

Guo, Y.Q.; Liu, J.X.; Lu, Y.; Zhu, W.Y.; Denman, S.E.; McSweeney, C.S. (2008) Effect of tea saponin on methanogenesis, microbial community structure and expression of mcrA gene, in cultures of rumen microorganisms. *Lett. Appl. Microbiol.*, 47, 421-426

Hafenbradl, D.; Keller, M.; Stetter, K.O. (1996) Lipid analysis of *Methanopyrus kandleri*. *FEMS Microbiol. Lett.* 136, 99-202

Hart, K.J.; Yáñez-Ruiz, D.R.; Duval, S.M.; McEwan, N.R.; Newbold, C.J. (2008) Plant extracts to manipulate rumen fermentation. *Anim. Feed Sci. Technol.*, 147 (1-3), 8-35

Hearn, E.M.; Patel, D.R.; Lepore, B.W.; Indic, M.; van Berg, B. (2009) Transmembrane passage of hydrophobic compounds through a protein channel wall. *Nature,* 458, 367-70

Hegarty, R. S. (1999a) Mechanisms for competitively reducing ruminal methanogenesis. *Aust. J. Agric. Res*. 50, 1299-1305

Henderson, C. (1973) The effects of fatty acids on pure cultures of rumen bacteria. J. *Agric. Sci.,* 81, 107-112

Hess, H.D.; Kreuzer, M.; Diaz, T.E.; Lascano, C.E.; Carulla, J.E.; Soliva, C.R.; Machműller, A. (2003a) Saponin rich tropical fruits affect fermentation and methanogenesis in faunated and defaunated rumen fluid. *Anim. Feed Sci. Technol.*, 109, 79-94

Hess, H.D.; Monsalve, L.M.; Lascano, C.E.; Carulla, J.E.; Diaz, T.E.; Kreuzer, M. (2003b) Supplementation of a tropical grass diet with forage legumes and Sapindus saponaria fruits: effects on in vitro ruminal nitrogen turnover and methanogenesis. *Aust. J. Agric. Res*., 54, 703–713

Heydari, K.H.; Dabiri, N.; Fayazi, J.; Roshanfekr, H. (2008) Effect of ionophores monensin and lasalocid on performance and carcass characteristics in fattening Arabi lambs. *Pak. J. Nutr.,* 7, 81-84

Hilpert, R.; Winter, J.; Hammes, W.; Kandler O. (1981) The sensitivity of archaebacteria. *Zentralbl. Bacteriol. Microbiol. Hyg. Abt. 1 Orig Reihe* C3, 228-244

Hristov, A.N.; Ivan, M.; Neill, L.; McAllister, T. A. (2003) A survey of potential bioactive agents for reducing protozoal activity in vitro. *Anim. Feed Sci. Technol.*, 105, 163–184

Hristov, A.M.; Ivan, M.; McAlister, T.A. (2004) *In vitro* effects of individual fatty acids on protozoal numbers and on fermentation products in ruminal fluid from cattle fed a high-concentrate, barley-based diet. *J. Anim. Sci.*, 82, 2693-2704

Hristov, A.N.; Ropp, J.K.; Zaman, S.; Melgar, A. (2008) Effects of essential oils on *in vitro* ruminal fermentation and ammonia release. *Anim. Feed Sci. Tech.*, 144, 55-64

Hristov, N.A.; McAllister, T.A.; Van Herk, F.H.; Cheng, K.J.; Newbold, C.J.; Cheeke, P.R. (1999) Effect of *Yucca schidigera* on ruminal fermentation and nutrient digestion in heifers. *J. Anim. Sci.,* 77, 2554–2563

Hu, W.L.; Guo, Y.Q.; Liu, J.X.; Wu, Y.M.; Ye J.A. (2005) Tea saponins affect methanogenesis and fermentation in faunated and defaunated rumen *in vitro* RPT system. *J. Zhejing Univ. Sci.,* 6B, 787-792

Hurd, H.S. (2005) Can antibiotic use in ford animals actually reduce consumer risk? *Food Safety Asia*, pp. 120-122

Hvelplund, T.; Stigsen, P.; Moller, P. D. & Jensen, K. (1978) Propionic acid production rate in the bovine rumen after feeding untreated and sodium hydroxide-treated straw. *Z. Tierphys. Tierernahr. Fuutermittelkde.* 40, 183 – 190

IPCC (Intergovernmental Panel on Climate change) (2007) The Physical Science Basis, Contribution of Working Group I to the Fourth, Available from http://www.ipcc.ch/publications_and_data/publications_ipcc

Ipharraguerre, I. R. & Clark, J. H. 2003. Usefulness of ionophores for lactating dairy cows: A review. *Anim. Feed Sci. Technol.*, 106, 39-57

Islam, M. R. & Begum J. (1997) Short review of global methane situation and of facilities to reduce in ruminants in third world countries. *AJAS* 10 (No.2), 157-163

Ivan, M.; Mir, P.S.; Koeing, K.M.; Rode, L.M.; Neill, L.; Entz, T.; Mir, Z. (2001) Effects of dietary sunflower seed oil on rumen protozoa population and tissue concentration of conjugated linoleic acid in sheep. *Small Rumin. Res.,* 41, 215-227

Jalč, D.; Baran, M.; Vendrák T. & Siroka P. (1992) Effect of Monensin on Fermentation of Hay and Wheat Bran Investigated by the Rumen Simulation Technique (RUSITEC) *Arch. für Tiererna.* 42, 2, 153-158

Jalč, D.; Cieślak, A.; Potkański, A.; Szumacher-Strabel M. & Kowalczyk J. (2006c) The effect of different oils and diets on methane release in an artificial rumen (Rusitec). *J. Anim. Feed Sci.,* 15, Suppl. 1, 149-152

Jalč, D.; Potkański, A.; Szumacher-Strabel, M.; Kowalczyk J. & Cieślak A. (2006a) The effect of a high concentrate diet and different fat sources on rumen fermentation in vitro. *J. Anim. Feed Sci.,* 15, Suppl. 1, 137-140

Jalč, D.; Potkański, A.; Szumacher-Strabel, M.; Kowalczyk J. & Cieślak A. (2006b) The effect of a high forage diet and different oil blends on rumen fermentation in vitro. *J. Anim. Feed Sci.,* 15, Suppl. 1, 141-144

Jalč, D.; Potkański, A.; Szumacher-Strabel, M.; Kowalczyk J. & Cieślak A. (2006d) The effect of a forage diet and different fat sources on rumen fermentation in vitro. *J. Anim. Feed Sci.,* 15, Suppl. 1, 129-134

Jayanegara, A,; Togtokhbayar, N.; Makkar, H.P.S.; Becker, K. (2009) Tannins determined by various methods as predictors of methane production reduction potential of plants by an *in vitro* rumen fermentation system. *Anim. Feed Sci. Technol.,* 150, 230–237

Jensen, K. & Wolstrup P. (1977) Effect of feeding frequency of fermentation pattern and microbial activity in the bovine rumen. *Act Vet. Scand*., 18, 108-121

Joblin, K.N.; Matsui, H.; Naylor, G.E.; Ushida K. (2002) Degradation of fresh ryegrass by methanogenic co-culture of ruminal fungi grown in the presence or absence of *Fibrobacter succinogenes*. *Curr. Microbiol.,* 45, 46-53

Johnson, K.A. & Johnson, D.E. (1995) Methane emissions from cattle. *J. Anim. Sci*. 73, 2483-2492

Jones, W.J.; Nagle, D.P.Jr. & Whitman W.P. (1987): Methanogens and the diversity of archaebacteria. *Microbiol. Rev.,* 51, 135-177

Jonson, D.E.& Ward G.M. (1996) Estimates of animal methane emissions. Environmental Monitoring and Assessment 42, pp. 133-141. Kluwer Academic Publishers. Printed in the Netherlands

Jordan, E.; Kenny, D.; Hawkins, M.; Malone, R.; Lovett, D.K. & O'Mara F.P. (2006) Effect of refined soy oil or whole soybeans on intake, methane output, and performance of young bulls. *J. Anim. Sci*., 84, 2418–2425

Kamel, C.; Greathead, H.M.R.; Tejido, M.L.; Ranilla, M.J.; Carro, M.D. (2008) Effects of allicin and diallyldisulfideon *in vitro* rumen fermentation of a mixed diet. *Anim. Feed Sci. Technol.,* 145, 351–363

Kamra, D.N. (2005) Rumen microbial system, *Curr. Sci.,* 89 (1), 124-135

Karnati, S.K.R.; Yu, Z.; Firkins, J.L. (2009) Investigating unsaturated fat, monensin, or bromoethanesulfonate in continuous cultures retaining ruminal protozoa. II. Interaction of treatment and presence of protozoa on prokaryotic communities. *J. Dairy Sci*., 92, 3861-3873

Kaufmann, W.; Hagemeister, H. & Dirksen G. (1980) Adaptation to changes in dietary composition, level and frequency of feeding. In: Y. Ruckebusch and P Thivend (Eds.). Digestive Physiology and Metabolism in Ruminants. MTP Press, Lancaster, England. pp. 587-602

Khalil, M. A. K. (2000): Atmospheric methane: an introduction. In Atmospheric Methane: Its Role in the Global Environment, pp.1-8. Springer-Verlag, Berlin, Germany

Kirchgesser, M.; Windisch, W.; Muller, H.L. (1995) Nutrional factors for the quantification of methane production. In: Engelhardt W. V., Leonhard-Marek S., Breves G., Giesecke D. (Eds.) Ruminant physiology: Digestion, metabolism, growth and reproduction, Proceedings of the Eighth International Symposium on Ruminant Physiology, Ferdinad Enke Verlag, Stuttgart, pp. 333-348

Kisidayova, S.; Mihalikova, K.; Varadyova, Z.; Potkański, A.; Szumacher-Strabel, M.; Cieślak, A.; Certik, M.; Jalč, D. (2006) Effect of microbial oil, evening primrose oil and borage oil on rumen ciliate population in artificial rumen (Rusitec) *J. Anim. Feed Sci.*, 15, 153-156

Kisidayova, S.; Varyadova, Z.; Michałowski, T.; Newbold, C.J. (2005) Regeneration of cryoresistance of *in vitro* rumen ciliate cultures. *Cryobiology,* 51, 76-84

Kisidayova, S.; Varyadova, Z.; Zelenak, I.; Siroka P. (2000) Methanogenesis in rumen ciliate cultures of *Entodinium caudatum* and *Epidinium ecaudatum* after long-term cultivation in a chemically defined medium. *Folia Microbiol*., 45, 269-274

Kowalczyk, J.; Orskov, E.R.; Robinson, J.J.; Stewart, C.S. (1977) Effects of fat supplementation on voluntary food intake and rumen metabolism in sheep. *Brit J. Nutr.,* 37, 251

Kowalik, B.; Pająk, J.J.; Skomiał, J. (2009) The effect of tannins on processes in the rumen. *Post. Nauk Roln*., 1, 91-102

Lana, R. P.; Russell, J. B.; Van Amburgh M. E. (1998) The role of pH in regulating ruminal methane and ammonia production. *J. Anim. Sci.*, 76, 2190-2196

Laureles, L.R.; Rodriguez, F.M.; Reano, C.E.; Santos, G.A.; Laurena, A.C.; Mendoza, E.M. (2002) Variability in fatty acid and triacylglycerol composition of the oil of coconut (*Cocos nucifera* L.) hybrids and their parentals. *J. Agric. Food Chem.,* 50, 1581-1586

Lloyd, D.; Williams, A.G.; Amann, R.; Hayes, A.J.; Durrant, L.; Ralphs, J.R. (1996) Intracellular prokaryotes in rumen ciliate protozoa: detection by confocal laser scanning microscopy after *in situ* hybridization with fluorescent 16S rRNA probes. *Europ. J. Protist*., 32, 523–531

Machmuller, A. & Kreuzer M. (1999) Methane suppression by coconut oil and associated effects on nutrient and energy balance in sheep. *Can. J. Anim. Sci*., 79, 65-72

Machmuller, A. (2006) Medium-chain fatty acids and their potential to reduce methanogenesis in domestic ruminants. *Agr. Ecosyst. Environ*., 112,107-114

Machmuller, A.; Solva, C.R.; Kreuzer, M. (2003) Effect of coconut oil and defaunation treatment on methanogenesis in sheep. *Reprod. Nutr. Dev*., 43, 41-55

Maczulak, A.E.; Dehority, B.A.; Palmquist, D.L. (1981) Effects of long-chain fatty acids on growth of rumen bacteria. *Appl. Environ. Microbiol*., 42, 856-862

Maia, M.R.G.; Chaudhary, L.C.; Figueres, L. & Wallace, R.J. (2007) Metabolism of polyunsaturated fatty acids and their toxicity to the microflora of the rumen. *Antonie Van Leeuwenhoek*, 91, 303–314

Makkar, H.P.S. & Becker K. (1997) Degradation of Quillaja saponins by mixed culture of rumen microbes. *Lett. Appl. Microbiol*., 25, 243-245

Mao, H-L.; Wang, J-K.; Zhou, Y-Y.; Liu, J-X. (2010) Effects of addition of tea saponins and soybean oil on methane production, fermentation and microbial population in the rumen of growing lambs. *Livest. Sci.,* 129, 56–62

Martin, C.; Morgavi, D.P.; Doreau, M.; (2010) Methane mitigation in ruminants: from microbe to the farm scale. *Anim*., 4:3, 351-365

Martin, C.; Rouel, J.; Jouany, J.P.; Doreau, M. & Chilliard, Y. (2008) Methane output and diet digestibility in response to feeding dairy cows crude linseed, extruded linseed, or linseed oil. *J. Anim. Sci*., 86, 2642–2650

Martin, S.A. & Jenkins, T.C. (2002) Factors affecting conjugated linoleic acid and trans - C18:1 fatty acid production by mixed ruminal bacteria. *J. Anim. Sci.,* 80, 3347-3352

Matsumoto, M.; Kobayashi, T.; Takenaka, A.; Itabashi, H. (1991) Defaunation effects of medium-chain fatty acids and their derivatives on goat rumen protozoa. *J. Gen. Appl. Microbiol.* 37, 439-445

McAllister, T.A.; Okine, E.K.; Mathison, G.W. & Cheng K. J. (1996) Dietary, environmental and microbiological aspects of methane production in ruminants. *Can. J. Anim. Sci*., 76, 231-243

McGuffy, R.K.; Richardson, L.F.; Wilkinson, J.I.D. (2001) Ionophore for dairy cattle: Current status and future outlook. *J. Dairy Sci.,* 84 (E. Suppl.), E194-E203

Miles, C.O.; Wilkins, A.L.; Munday, S.C.; Holland, P.T.; Smith, B.L.; Lancaster, M.J.; Embling, P.P. (1992) Identification of the calcium salt of epismilagenin beta-D-glucuronide in the bile crystals of sheep affected by *Panicum-dichotomiflorum* and *Panicum-schinzii* toxicoses. *J. Agric. Food Chem*., 40, 1606-1609

Monforte-Briceno, G.E.; Sandoval-Castro, C.A.; Ramirez-Aviles, L.; Capetillo-Leal, C.M. (2005) Defaunating capacity of tropical fodder trees: effects of polyethylene glycol and its relationship to in vitro gas production. *Anim. Feed. Sci. Technol*., 123–124, 313–327

Monteny, G.J.; Bannink, A. Chadwick D. (2006) Greenhouse gas abatement strategies for animal husbandry. *Agric. Ecosyst. Environ*., 112, 163-170

Morvan, B.; Bonnemoy, F.; Fonty, G.; Gouet P. (1996) Quantitative determination of H2-utilizing acetogenic and sulfate-reducing bacteria and methanogenic archaea from digestive track of different mammals. *Curr. Microbiol.,* 32, 129-133

Morvan, B.; Dore, J.; Rieulesme, F.; Foucat, L.; Fonty, G.; Gouet, P. (1994) Establishment of hydrogen-utilizing bacteria in the rumen of the newborn lamb. *FEMS Microbiol. Lett.,* 117, 249-256

Moss, A. R.; Deaville, E. R. & Givens, D. I. (1994) Effect of supplementing grass silage with sugar beet feed on methane production by sheep. *Proc. Brit. Soc. Anim. Prod.,* Paper No. 53

Moss, A.R.; Jouany, J.P.; Newbold, C.J. (2000) Methane productions by ruminants: its contribution to global warming. *Annal Zootech.,* 49, 231-253

Muetzel, S.; Hoffmann, E.M.; Becker, K. (2003) Supplementation of barley straw with Sesbania pachcarpa leaves in vitro: effects on fermentation variables and rumen microbial concentration structure quantified by ribosomal RNA-targeted probes. *Br. J. Nutr.,* 89, 445–453

Nakashimada, Y.; Srinivasan, K.; Murakami, M.; Nishio N. (2000) Direct conversion of cellulose to methane by anaerobic fungus *Neocallimastix frontalis* and defined methanogens. *Biotech. Lett.,* 22, 223-227

Newbold, C.J.; ElHassan, S.M.; Wang, J.; Ortega, M.E.; Wallace, R.J. (1997) Influence of foliage from African multipurpose trees on activity of rumen protozoa and bacteria. *Br. J. Nutr*., 78, 237-249

Newbold, C.J.; Lassalas, B. & Jouany, J.P. (1995) The importance of methanogens associated with ciliate protozoa in ruminal methane production in vitro. *Lett. Appl. Microbiol*., 21, 230–234

Odenyo, A.A.; Osuji, P.O.; Karanfil, O. (1997) Effect of multipurpose tree (MPT) supplements on ruminal ciliate protozoa. *Anim. Feed Sci. Technol*., 67, 169-180

Oleszek, W.A. (2002) Chromatographic determination of plant saponins. J. *Chromatogr., A* 967, 147-162

Palmquist, D. L. & Jenkins T.C. (1980) Fat in lactation rations: review. *J. Dairy Sci.* 63, 1 – 14

Palmquist, D.L. (1994) The role of dietary fats in efficiency of ruminants. American Institute of Nutrition

Patra, A.K.; Kamra, D.N.; Agarwal, N. (2006) Effect of plant extracts on in vitro methanogenesis, enzyme activities and fermentation of feed in rumen liquor of buffalo. *Anim. Feed. Sci. Technol*., 128, 276–291

Patra, A.K.; Saxena, J. (2009) Dietary phytochemicals as rumen modifiers: a review of the effects on microbial populations. *Antonie van Leeuwenhoek*, 96, 369-375

Paustian, K.; Antle, M.; Sheehan, J.; Eldor; P. (2006) Agriculture's Role in Greenhouse Gas Mitigation. Washington, DC: Pew Center on Global Climate Change

Pen, B.; Sar, C.; Mwenya, B.; Kuwaki, K.; Morikawa, R.; Takahashi, J. (2006) Effects of *Yucca schidigera* and *Quillaja saponaria* extracts on in vitro ruminal fermentation and methane emission. *Anim. Feed Sci. Technol*., 129, 175–186

Pers-Kamczyc, E.; Zmora, P.; CieślakA. & Szumacher-Strabel M. (2011) Development of nucleic acid based techniques and possibilities of their application to rumen microbial ecology research *J. Anim. Feed Sci., 20, 315–337*

Place, S.E. & Mitloehner F.M. (2010) Invited review: Contemporary environmental issues: A review of the dairy industry's role in climate change and air quality and the potential of mitigation through improved production efficiency. *J. Dairy Sci.,* 93, 3407-3416

Plascencia, A.; Estrada, M. & Zinn, R.A. (1999) Influence of Free Fatty Acids Content on the Feeding Value of Yellow Grease in Finishing Diets for Feedlot Cattle. *J. Anim. Sci*., 77, 2603 – 2609

Potkański, A.; Szumacher-Strabel, M,; Cieślak A. (2009) Effect of rapeseed and fish oil blend supplementation to dairy cows summer feeding on rumen parameters and milk fatty acid profile. *Anim. Sci. Pap. Rep*., 27, 83-93

Regensbogenova, M.; Kisidayova, S.; Michalowski, T.; Javorsky, P.; Moon-Van Der Staay, G.W.M.; Moon-Van Der Staay, S.Y.; Hackstein, J.H.P.; McEwan, N.R.; Jouany, J.P.; Newbold, J.C.; Pristas P. (2004b) Rapid Identification of Rumen Protozoa by Restriction Analysis of Amplified 18S rRNA Gene. *Acta Protozool.,* 43, 219 – 224

Regensbogenova, M.; McEwan, N.R.; Javorsky, P.; Kisidayova, S.; Michalowski, T.; Newbold, C.J.; Hackstein, J.H.P.; Pristas P. (2004a) A re-appraisal of the diversity of the methanogens associated with the rumen ciliates. *FEMS Microbiol. Lett*., 238, 307-313

Russel J. B. (1998) The importance of pH in the regulation of ruminal acetate to propionate ratio and methane production in vitro. *J. Dairy Sci.,* 81, 3222-3230

Russell, M.J.; Hall, A.J.; Cairns-Smith, A.G. & Braterman P.S. (1988) Submarine hot springs and the origin of life. *Nature,* 336,117

Salawu, M.B.; Acamovic, T.; Stewart ,C.S.; Hovell, F.D.; De, B. (1999) Effects of feeding quebracho tannin diets, with or without a dietary modifier, on rumen function in sheep. *Anim. Sci.,* 69, 265–274

Scott A. M. (2002) Basic of rumen microbiology. Course materials 21-24.10.2002. Poznań, Poland.

Shin, E.C.; Choi, B.R.; Lim, W.J.; Hong, S.Y.; An, C.L.; Cho, K.M.; Kim, Y.K.; An, J.M.; Kang, J.M.; Lee, S.S.; Kim, H.;, Yun, H.D. (2004) Phylogenetic analysis of archaea in three fractions of cow rumen based on the 16S rDNA sequence. *Anaerobe,* 10, 313-319

Skillamn, L.C.; Evans, P.N.; Stromp, C.; Joblin, K.N. (2006) 16S ribosomal DNA-directed PCR primers for ruminal methanogens and identification of methanogens colonizing young lambs. *Anaerobe* 10, 277-285

Śliwiński, B.; Kreuzer, M.; Wettstein, H.R.; Machmüller, A. (2002) Rumen fermentation and nitrogen balance of lambs fed diets containing plant extracts rich in tannins and saponins, and associated emission of nitrogen and methane. *Arch. Anim. Nutr*., 56, 379-392

Smith-Palmer, A.; Stewart, J.; Fyfe, L. (1998) Antimicrobial properties of plant essentials oils and essence against five important food-borne pathogens. *Lett. Appl. Microbial*., 26, 118-122

Soliva, C.R.; Hindrichsen, I.K.; Meile, L.; Kreuzer, M.; Machmüller, A. (2003) Effects of mixtures of lauric and myristic acid on rumen methanogens and methanogenesis *in vitro*. *Lett. App. Microbiol.,* 37, 35-9

Soliva, C.R.; Meile, L,; Cieślak, A.; Kreuzer, M., Machmuller, A. (2004a) Long-term Rusitec study on the interactions of dietary lauric and miristic acid supplementation in suppressing ruminal methanogenesis *Br. J. Nutr.,* 92, 689-700

Soliva, C.R.; Meile, L,; Hindrichsen, I.K,; Kreuzer, M., Machmuller, A. (2004b) Myristic acid supports the immediate inhibitory effect of lauric acid on ruminal methanogens and methane release. *Anaerobe,* 10, 269-276

Sparg, S. G.; Light, M. E.; van Staden, J. (2004) Biological activities and distribution of plant saponins. *J. Ethnoph.,* 94, 219-243

Staerfl, S.M.; Kreuzer M. & Soliva C.R. (2010) In vitro screening of unconventional feeds and various natural supplements for their ruminal methane mitigation potential when included in a maize-silage based diet *J. Anim. Feed Sci*., 19, 651–664

Steinfeld, H.; Gerber, P.; Wassenaar, T.; Castel, V.; Rosales, M.; de Haan, C. (2006) Livestock's Long Shadow: Environmental Issues and Options. Rome: Food and Agriculture Organization of the United Nations.

Stewart, C.S. & Bryant M.P. (1988) The rumen bacteria. W: Barnes E.M., Mead G.C. Anaerobic bacteria in habitats other than man. Palo Alto, CA Blackwell Scientific Publications, pp. 21-75

Stewart, C.S.; Flint, H.J.; Bryant M.P. (1997) The rumen bacteria. W: Hobson P.N., Stewart C.S. The Rumen Microbial Ecosystem. London Blackie Academic & Professional, pp. 10-72

Sutton, J.D.; Hart, I.C.; Broster, W.H.; Elliott R.J. & Schuller E. (1986) Feeding frequency for lactating dairy cows: effects on rumen fermentation and blood metabolites and hormones. *Brit. J. Nutr.*, 56, 181-192

Szumacher – Strabel, M. & Cieślak, A. (2010) Potential of phytofactors to mitigate rumen ammonia and methane production *J. Anim. Feed Sci*., 19, 3, 319-337

Szumacher-Strabel, M.; Cieślak, A.; Potkański, A,; Kowalczyk J. & Czauderna M. (2001a) The effects of different amounts and types of fat on rumen microbial protein synthesis in sheep. *J. Anim. Feed Sci*., 10, Suppl. 2, 97-101

Szumacher-Strabel, M.; Cieślak, A.; Nowakowska A. (2009a) Effect of oils rich in linoleic acid on *in vitro* rumen fermentation parameters of sheep, goats and dairy cows. *J. Anim. Feed Sci.,* 18, 3, 440-452

Szumacher-Strabel, M.; Cieślak, A.; Nowakowska, A.; Potkański, A. (2009b) Feeding plant and fish oils to improve polyunsaturated fat concentrations in intramuscular, perirenal and subcutaneous lambs' fat. *Schriftenreihe der Deutschen Gesellschaft Für Züchtungskunde*, 81, (2), 133-140

Szumacher-Strabel, M.; Cieślak, A.; Zmora, A.; Pers-Kamczyc, E.; Bielińska, S.; Stanisz, M. & Wójtowski, J. (2011b) *Camelina sativa* cake improved unsaturated fatty acids in ewe's milk *J. Sci. Food Agric.,* 91, 2031–2037

Szumacher-Strabel, M.; Martin, S.A.; Potkański, A.; Cieślak, A.; Kowalczyk, J. (2004) Changes in fermentation processes as the effect of vegetable oil supplementation in *in vitro* studies. *J. Anim. Feed Sci*., 13, 215-218

Szumacher-Strabel, M.; Nowakowska, A.; Zmora, P.; Cieślak, A. (2009c) Essentials oils and secondary plant metabolites in dairy cow feeding. *Acta Bioch. Pol*., 56, Suppl. 2, 57-58

Szumacher-Strabel, M.; Potkański, A.; Cieślak, A.; Kowalczyk J. & Czauderna M. (2001c) The effects of different amounts and types of fat on metabolites in the rumen of sheep. *J. Anim. Feed Sci.,* 10, Suppl. 2, 91-96

Szumacher-Strabel, M.; Potkański, A.; Cieślak, A.; Kowalczyk J. & Czauderna M. (2001b) The effects of different amounts and types of fat on the level of conjugated linoleic acid in the meat and milk of sheep. *J. Anim. Feed Sci*., 10, Suppl. 2, 103-108

Szumacher-Strabel, M.; Zmora, P.; Roj, E.; Stochmal, A.; Pers-Kamczyc, E.; Urbańczyk, A.; Oleszek, W.; Lechniak, D. & Cieślak A. (2011a) The potential of the wild dog rose (*Rosa canina*) to mitigate *in vitro* rumen methane production. *J. Anim. Feed Sci. 20, 285–299*

Tackett, V.L.; Bertrand, T.C.; Jenkins, T.C.; Pardue, F.E. & Grimes L.W. (1996) Interaction of dietary fat and acid detergent fiber diets of lactating dairy cows. *J. Dairy Sci.,* 79, 270-275

Tajima, K.; Nagamine, T.; Matsui, H.; Nakamura, M.; Animov, R.I. (2001) Phylogenetic analysis of archaeal 16S rRNA libraries from the rumen suggests the existence of a novel group of archaea not associated with known methanogens. *FEMS Microbiol. Lett*., 200, 67-72

Tavendale, M.H.; Meagher, L.P.; Pacheco ,D.; Walter, N.; Attwood, G.T.; Sivakumaran, S. (2005) Methane production from in vitro rumen incubations with *Lotus pedunculatus* and *Medicago sativa*, and effects of extractable condensed tannin fractions on methanogenesis. *Anim. Feed Sci. Technol*., 123-124, 403-419

Teferedegne, B. (2000) New perspectives on the use of tropical plants to improve ruminant nutrition. *Proc. Nutr. Soc*., 59, 209–214

Teferedegne, B.; McIntosh, F.; Osuji, P.O.; Odenyo, A.; Wallace, R.J.; Newbold, C.J. (1999) Influence of foliage from different accessions of the sub-tropical leguminous tree, *Sesbania sesban*, on ruminal protozoa in Ethiopian and Scottish sheep. *Anim. Feed Sci. Technol*., 78, 11-20

Topping, J.C. (2007) *Study by NASA and University Scientists Shows World Temperature Reaching a Level Not Seen in Thousands of Years and Raises Grave Concern of Irreparable Harm,* Available from http://www.climate.org/2002/programs/washington_summit_temperature_rise.

USDA (2011) U.S. Agriculture and Forestry Greenhouse Gas Inventory: 1990–2008. Washington, DC: U.S. Department of Agriculture. Technical Bulletin No. 1930, pp. 159

Ushida, K. & Jouany, J. P., (1996) Methane production associated with rumen-ciliated protozoa and its effect on protozoan activity. *Lett. Appl. Microbiol*., 23, 129-132

Van den Bogaard, A.E.; Bruinsma, N.; Stalberingh, E.E. (2000) The effect of banning avoporacin on VRE carriage in the Netherlands. *J. Antimicrob. Chemother*., 46, 146-147

Van Kessel, J.S. & Russel J.B. (1995) The effect of pH on in vitro methane production from ruminal bacteria. *Proc. Conf. Rum. Funct*., 23, 7-29

Van Nevel, C.J. & Demeyer D.I. (1996) Control of rumen methanogenesis. *Environm. Monitor. Assessm.,* 42, 73–97

Van Soest, P. J. (1982) Nutritional ecology of the ruminant. Corvallis, Oregon. Books Inc.

Van Soest, P. J. (1994) Nutritional ecology of the ruminant (2nd ed.). Ithaca NY Cornell Univ. Press

Varadyova, Z.; Kišidayova, S.; Siroka, P.; Jalč, D. (2007): Fatty acid profiles of rumen fluid from sheep fed diets supplemented with various oils and effect on the rumen ciliate population. *Czech. J. Anim. Sci.,* 52, 399–406

Vincken, J.P.; Heng, L.; de Groot, A.; Gruppen, H. (2007) Saponins, classification and occurrence in the plant kingdom. *Phytochem.,* 68, 275-297

Vogels, G.D.; Hoppe, W.F.; Stumm C.K. (1980) Association of methanogenic bacteria with rumen ciliates. *Appl. Environ. Microbiol.,* 47, 219-221

Wallace, R.J.; Arthaud, L.; Newbold, C.J. (1994) Influence of *Yucca-schidigera* extract on ruminal ammonia concentrations and ruminal microorganisms. *Appl. Environ. Microbiol*., 60, 1762-1767

Wang, C.J.; Wang, S.P.; Zhou, H. (2009) Influences of flavomycin, ropadiar, and saponin on nutrient digestibility, rumen fermentation, and methane emission from sheep. *Anim. Feed Sci. Technol*., 148, 157–166

Wang, X.F.; Mao, S.Y.; Liu, J.H.; Zhang, L.L.; Cheng, Y.F.; Jin W. & Zhu W.Y. (2011) Effect of *yucca schidigera* extract on ruminal fermentation and mathonogens *in vitro J. Anim. Feed Sci*., 20, 259–271

Wang, Y.X.; McAllister, T.A.; Newbold, C.J.; Rode, L.M.; Cheeke, K.J. (1998) Effects of *Yucca schidigera* extract on fermentation and degradation of steroidal saponins in the rumen simulation technique (RUSITEC). *Anim. Feed Sci. Technol*., 74, 143-153

Wang, Y.X.; McAllister, T.A.; Yanke, L.J.; Xu, Z.J.; Cheeke, P.R.; Cheng, K.J. (2000) In vitro effects of steroidal saponins from *Yucca schidigera* extract on rumen microbial protein synthesis and ruminal fermentation. *J. Sci. Food Agric.,* 80, 2114-2122

Wettstein, H. R.; Machmüller, A;, Kreuzer, M. (2000) Effects of raw and modified canola lecithin compared to canola oil, canola seed and soy lecithin on ruminal fermentation measured with rumen simulation technique. *Anim. Feed Sci. Technol.,* 85, 153-169

Williams, A.G. & Coleman, G.S. (1988) The rumen protozoa. W: Hobson P.N. The Rumen Microbial Ecosystem. London Elsevier Applied Sciences. pp. 77-128

Williams, A.G.; Joblin, K.N.; Fonty, G. (1995) Interactions between the rumen chytrid fungi and other microorganisms. W: Mounffort D.O., Orpin C.G. Anaerobic Fungi: Biology, Ecology and Function. New York Marcel Dekker

Wina, E.; Muetzel, S.; Becker, K. (2006) The dynamics of major fibrolytic microbes and enzyme activity in the rumen in response to short- and ling-term feeding of *Sapindus rarak* saponins. *J. Appl. Microbiol.,* 100, 114-122

Wina, E.; Muetzel, S.; Hoffmann, E.; Makkar, H.P.S.; Becker, K. (2005) Saponins containing methanol extract of Sapindus rarak affect microbial fermentation, microbial activity and microbial community structure in vitro. *Anim. Feed Sci. Technol*., 121, 159–174

Wolin, M.J. & Miller, T.L. (1988) Microbe-microbe interactions. W: Hobson P.N., The rumen microbial ecosystem. New York Elsevier Science Publishers, pp. 343-359

Wolin, M.J.; Miller, C.; Stewart C.J. (1997) Microbe-microbe interactions. W: Hobson P.N., Stewart C.J. The Rumen Microbial Ecosystem. London Blackie Academic & Professional, pp. 467-491

Woodward, S. L.; Waghorn G. C.; Ulyatt M. J.; Lassey K. R. (2001) Early indications that feeding Lotus will reduce methane emission from ruminants. *Proc. N.Z. Anim. Prod*., 61, 23–26

Woodward, S.L.; Waghorn, G.C. & Thomson, N.A. (2006) Supplementing dairy cows with oils to improve performance and reduce methane – does it work? *Proceedings of the New Zealand Society of Animal Production,* 66, 176–181

Woodward, S.L.; Waghorn, G.C.; Lassey, K.R.; Laboyrie, P.G. (2002) Does feeding sulla (*Hedysarum coronarium*) reduce methane emission from dairy cows? *Proc. N. Z. Soc. Anim. Prod*., 62, 227–230

Woolcock, J.P. (1991) Microbiology of animals and animal products. Elsevier Scientific Publishers B.V.

Wright, A.D.; Auckland, C.H.; Lynn, D.H. (2007) Molecular diversity of methanogens in feedlot cattle from Ontario and Prince Edward Island, Canada. *Appl. Environ. Microbiol*., 73, 4206-4210

Wuebbles, D.J.; Hayhoe, K. (2001) Atmospheric methane and global change. *Earth-Sci. Rev.,* 57, 177-210

Yabuuchi, Y.; Matsushita, Y.; Otsuka, H.; Fukamachi, K.; Kobayashi, Y. (2006) Effects of supplemental lauric acid-rich oils in high-grain diet on *in vitro* rumen fermentation. *Anim. Sci. J.,* 77, 300-307

Zhang, C.M.; Guo, Y.Q., Yuan, Z.P.; Wu, Y.M.; Wang, J.K.; Liu, J.X.; Zhu, W.Y. (2008) Effect of octadeca carbon fatty acids on microbial fermentation, methanogenesis and microbial flora *in vitro*. *Anim. Feed Sci. Technol.,* 146, 259-269

Zhu, W.Y.; Mao, S.Y.; Liu, J.X.; Cheng, Y.F.; Iqbal, M.F.; Wang, J.K. (2007) Diversity of methanogens and their interactions with other microorganisms in methanogenesis in the rumen. *The Proceedings of the VII International Symposium on the Nutrition of Herbivores. China Agric. Univ. Press*, 17-22

Zmora, P., Cieślak, A., Jędrejek, D., Stochmal, A., Pers-Kamczyc, E., Oleszek, W., Nowak, A., Szczechowiak, J., Lechniak, D., Szumacher-Strabel, M. (2012) Preliminary in vitro study on the effect of xanthohumol on rumen methanogenesis. *Arch. Anim. Nutr*., 66, 66-71

Part 2

Greenhouse Gases Reduction and Storage

10

Effective Choice of Consumer-Oriented Environmental Policy Tools for Reducing GHG Emissions

Maria Csutora and Ágnes Zsóka
Corvinus University of Budapest
Hungary

1. Introduction

Due to the perceived and expected environmental impacts of climate change there is an urgent need to reduce Greenhouse Gasses (GHG) at each and every point of emission (see World Research Institute, 2010). The ongoing efforts of governments to establish and implement policies include investigating changes in consumer behaviour and attitudes towards sustainability. The often very high costs of measures makes economic analysis necessary in order to find out which technologically feasible abatement options are capable of realizing the largest emission reductions at least social cost (Csutora and Zilahy 1998, Ürge-Vorsatz and Füle 1999, Creyts et al. 2007, Stern 2008). According to recent studies there is even space for "win-win" solutions as a number of options exist which can result in huge GHG reductions at a "negative cost", meaning that those solutions are both beneficial from environmental and economic points of view. However, organisations often ask for external governmental support in order to implement those measures (Zilahy 2004) and individuals also regularly seem slow and inconsistent in transforming their positive environmental attitudes into environmentally aware consumption habits and reducing their levels of consumption (Rubik et al., 2009, Thøgersen and Crompton, 2009, Nemcsicsné Zsóka, 2005).

This chapter puts forward a model which allows a more effective choice of consumer-oriented environmental policy tools for GHG emission reduction and mitigation. As a first step, the marginal social cost curve is constructed for GHG mitigation options. Then, based on the marginal social cost curve and the marginal private cost curve, different – green, yellow, and red – zones of action are identified. GHG mitigation options chosen from those zones are then evaluated with the help of a profiling method which addresses barriers to implementation. Profiling may help in designing an implementation strategy for the selected options in order to overcome those barriers and make consumer policy more effective and acceptable to society. Opportunities for consumer policy are evaluated using several policy tools based on the literature and practical examples.

2. The marginal social cost curve and the three zones of action in GHG mitigation

It is very important — regarding the climate-related environmental impacts of consumer behaviour segments — which have the highest added value, or, differently formulated,

which products can provide the biggest efficiency gains. According to the research of Tukker and Jansen (2006) – who reviewed 11 studies focusing on the life-cycle impacts of total consumption at the level of society – the greatest environmental impacts are caused by a small number of product categories. "Food, housing and related energy use, and transport are in total responsible for some 70% or more of the total lifecycle impacts of all products and services used for final household and government consumption, whereas these categories are responsible for only 55% of the final expenditure" (Tukker and Jansen, 2006, pp. 175). Raaij and Verhallen (1983) also found the residential sector responsible for a considerable quantity – about 30% – of total energy demand in The Netherlands. Obviously, energy saving initiatives can provide considerable benefits for the environment.

The so-called 20-20-20% energy targets of the European Union (including Hungary) to be met by 2020 suggest a reduction in EU greenhouse gas emissions of at least 20% below 1990 levels; 20% of EU energy consumption to come from renewable resources; and a 20% reduction in primary energy use compared with projected levels, to be achieved by improving energy efficiency (http://ec.europa.eu/environment/climat/climate_action.htm). This energy policy is quite ambitious for several countries and makes efficient GHG mitigation measures necessary.

The maximisation of social welfare is the main guiding principle in the allocation of social resources. This means that actions to mitigate climate change can be justified only if they; a) contribute to an increase in social welfare (Stern, 2008); and, b) if resources are used in the most efficient way at the least possible cost.

The model we propose is based on a cost-efficiency approach. This means that we focus on reaching the maximum possible energy savings through using a given set of resources. Hence, the horizontal axis of the curve reflects climate change impacts which are considered proportional to energy saving potential. As further benefits like the external societal benefits of energy savings, inter-sectoral impacts, or benefits for future generations are estimated in controversial ways and result in a very wide range of outcomes, we decided to exclude benefit estimation problems from our analysis.

The Marginal Social Cost Curve for mitigation options presents the costs of mitigation options in an explicit way, covering only financial costs in our model. The reason why we omit indirect costs related to GHG mitigation options (concerning their analysis, see Zilahy et al. 2000) is uncertainty about their magnitude due to estimation techniques. The construction of the marginal social cost curve of mitigation is the following (see Csutora and Zsóka 2011, p. 73-74):

1. Construction of the baseline scenario representing the "without policy" option. If no policy is adopted, the increasing income and energy demand of society will result in an increase in GHG emissions.
2. Identification of mitigation options (e.g., improving insulation, replacing windows, switching to Compact Fluorescent Lamp (CFL) *or* light-emitting diode (LED) bulbs, photovoltaic cells, etc).

3. Evaluation of the mitigation potential for each option as well as the assessment of the marginal social costs of that option. Construction of the marginal social cost curve for selected mitigation options. Construction of mitigation scenarios that integrate multiple mitigation options.

As a first step, abatement potential and costs are calculated for each significant abatement option. Then all the options are arrayed from lowest to highest costs in order to construct the **Marginal Abatement Cost Curve** of GHG reduction options (for an example of this, see Figure 1).

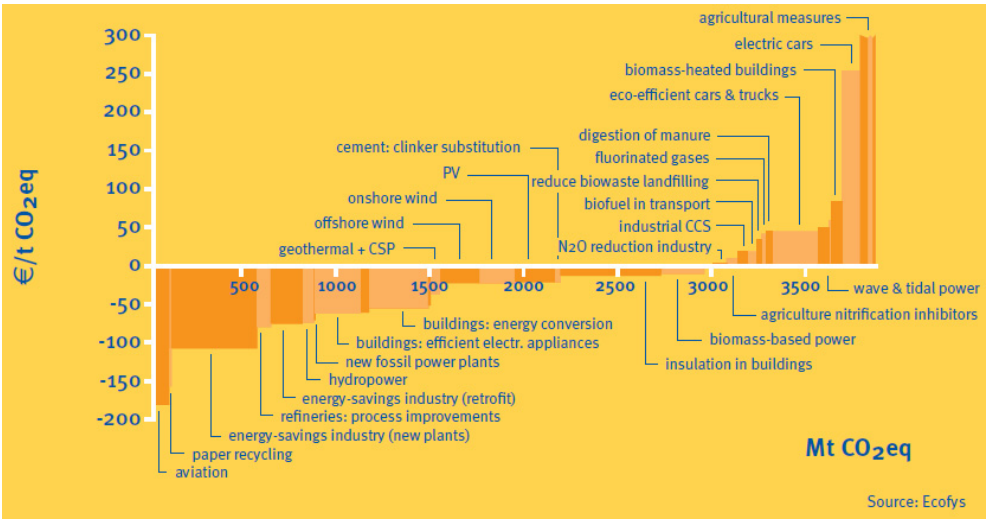

Fig. 1. Cost curve scenario for the EU27 in 2030. Cumulative abatement is relative to the FTRL reference emission in 2030. Technologies are aggregated into clusters for clarity. (Source: Wesselink and Deng, 2009).

Marginal abatement cost curves (MACs) reflect the relationships between the tons of greenhouse gas emissions abated and the unit price of abatement. The *total social cost* of abatement is the area under the positive side of the MAC curve minus the area under the negative side of the curve.

According to the McKinsey report (Creyts et al. 2007), almost 40 percent of abatement could be achieved at *negative social cost* in the United States (ergo, the return on investment is positive over a lifecycle) making these options "no-regret." Similarly, for the EU27, Wesselink and Deng (2009) analysed cost scenarios. As Figure 1 shows, half of the options can be found in the negative social cost zone. Both reports concluded that buildings and appliances are the areas with greatest abatement potential for improving energy efficiency.

A similar calculation has been made for Hungary, the result of which is a marginal social cost curve for mitigation GHG options, illustrated in Figure 2.

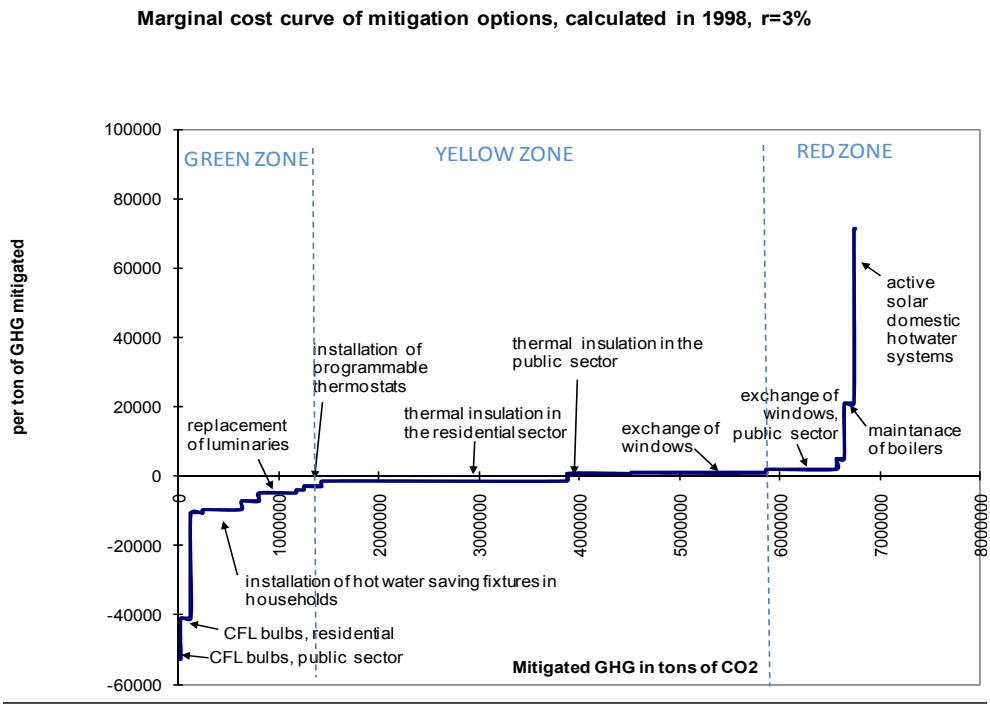

Fig. 2. Marginal social costs of energy-savings options (based on Csutora and Zilahy 1998)

Despite the several "no regret" options, implementation is often restricted by the fact that negative marginal social costs do not necessarily result in negative private costs (see Figure 3).

Implementing these options is desirable for society, but not for individuals. In our model we use a traffic light analogy (see Csutora and Zsóka 2011, p. 75-76):

- "**Green zone options** pay back for both society and for the individual. Such initiatives and activities are likely to penetrate the market without intervention, although this penetration may take time depending on the technology involved.
- **Yellow zone options** pay back for the society, but not the individual. This is the major arena for policy intervention. These options definitely need public policy support and investment but such effort will pay back for the society.
- **Red zone options** neither pay back for the society nor for the individual. They can only be promoted under very special circumstances, (e.g. as spin-off technologies).

The existence of green, yellow and red zones suggests a gap between the energy saving potential and the implementation of options which fall into the different zones. This makes further assessment necessary from the point of view of designing consumer policy. A profiling method is used to identify barriers and opportunities for dealing with these different scenarios, especially for the case of yellow zone options.

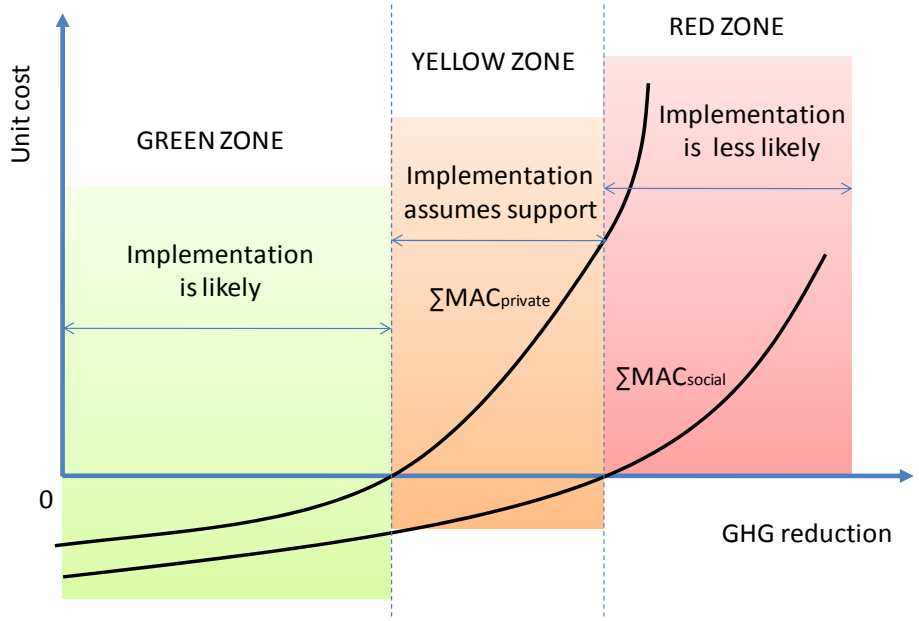

Fig. 3. Implementation likelihood of GHG reduction options based on marginal social and marginal private costs (Csutora and Zsóka, 2011, p. 75).

3. Use of the Profiling Concept for assessing GHG mitigation options

The **Profiling Concept** originates from risk management (see hazard profiles reflecting public perception of new, unknown, or high scale risks in Slovic, 1987 as well as Slovic and Weber, 2002) and will be used in this case for evaluating the public perception of GHG mitigation options. Furthermore, realising the implementation barriers and the beneficial side of the selected options, the public perception of proposed consumer policy actions can also be anticipated and evaluated. Based on the assessment, an implementation strategy can be formulated for new, innovative GHG mitigation options.

Figure 4 and Figure 5 include the most important elements for assessing introduction of CFL bulbs or LED bulbs as a GHG mitigation option. Both types of bulbs are compared to conventional incandescent bulbs. Specific scores are given in each evaluation aspect for each option, the result of which is an assessment profile for each option. It is very important that scores and assessment are policy-specific and country-specific. The same level of cost might be judged acceptable in richer countries yet prohibitive in developing countries. Attitudes and behavioural aspects are also different in different cultures. Thus no single solution or profile exists — even for the same GHG mitigation option.

Implementation barriers can be divided into four categories: cost, benefit, cooperation, and risk factors. The **cost factor** includes up-front investment costs, the net private cost of implementation (or payback) and the net social costs of implementation. According to Baden et al. (2006), *up-front investment costs* are regarded as major barriers for the private sector because families with lower incomes will not dispose of the capital to invest into specific

energy-saving solutions (see Jakob 2007) even if an investment (e.g. additional insulation) would in fact pay back over a reasonable time. CFL bulbs fall into the green zone, but they are still too expensive for some. In Hungary, the widely accepted *payback* period of investments seems to be up to 6 years for the society, even in the case of long-term projects (e.g. retrofit projects such as insulation; see: http://www.napkollektor-info.hu/component/poll/16). Central and local government often drive these investments through providing subsidies – otherwise the market would be too small, even if public awareness of the importance and payback period of those types of investments exists among society.

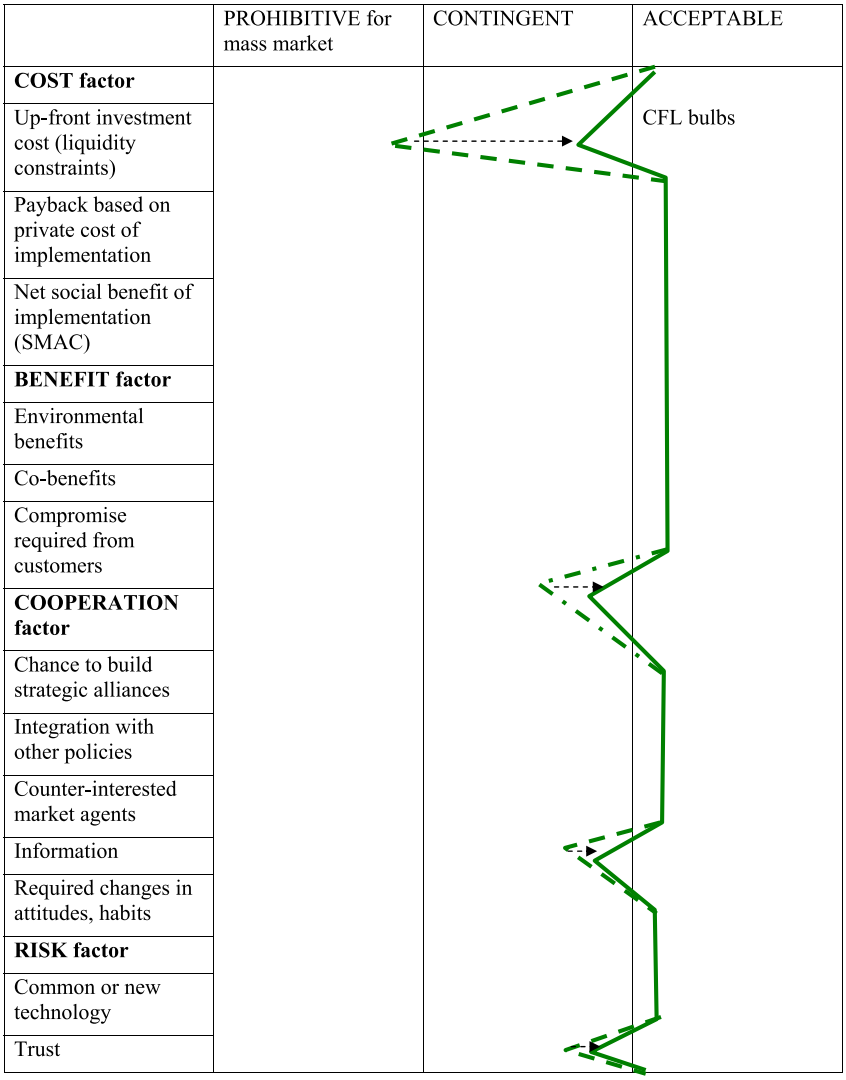

Fig. 4. Changing consumer perception profile of CFL bulbs

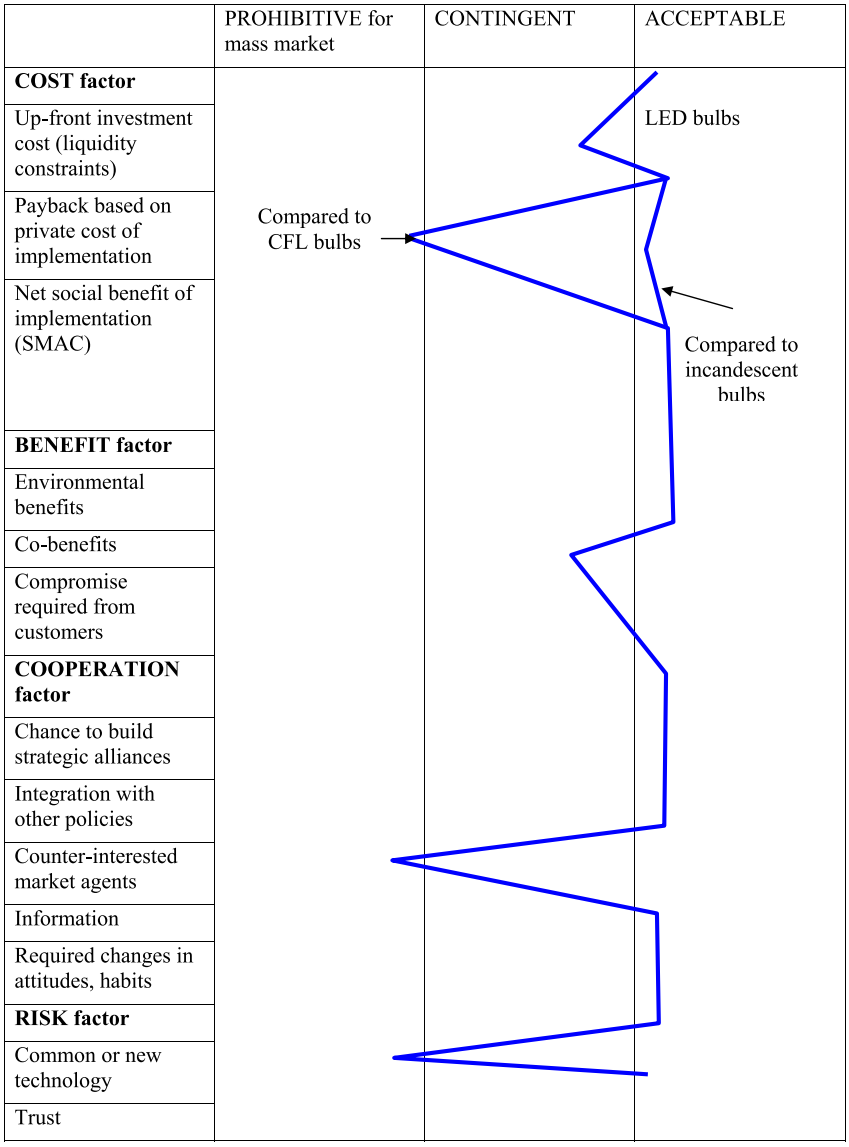

Fig. 5. Consumer perception profile of LED bulbs

Benefits can be *environmental benefits* representing the environmental potential of the solution; *co-benefits* are reflected in the longer lifetime of CFL bulbs, for example, or in the increased value of homes, comfort level, or prestige. *Compromise required from the customers* means the non-monetary sacrifices which derive from a poor institutional system and infrastructure, low availability of the product or solution, compromise in product features compared to substitutes, etc. For acceptance of CFL bulbs shape was a major barrier, just

following cost, hindering penetration on the EU market. (Bertoldi and Bogdan 2006a). Later, CFL bulbs became smaller and less awkwardly-shaped due to technological innovation, resulting in higher acceptability on the consumer side. Thus the consumer perception profile of CFL bulbs changed showing a reduced peak in the contingent zone. (Figure 4.) A compromise element reduces the potential benefits and can be a real barrier, as market penetration is usually slow even in the case of "green zone" options (Bertoldi and Bogdan 2006a, 2006b).

Studying the payback of LED bulbs (Figure 5) leads to interesting conclusions. LED bulbs *do* pay back when they replace incandescent bulbs. Once you have bought and installed CFL bulbs, however, they are not worth replacing with LED bulbs. LED bulbs cannot save enough energy to justify the early jettisoning of CFL bulbs. CFL bulbs are characterised by having a long life, *so high market penetration rate of CFL bulbs may create a market barrier to LED bulbs.* Thus countries with low market share of CFL bulbs may have higher potential for achieving a higher penetration rate of LED bulbs. LED bulbs can be considered a green or yellow label option in areas when they replace conventional bulbs but a 'red' option when they replace CFL bulbs.

The **cooperation factor** includes barriers and opportunities for cooperating in order to penetrate the market with a solution. The *chance to build strategic alliances* is a real potential in the case of LED bulbs as the automotive industry promotes their spread through the building of highly positioned cars with LED lighting systems. Indirectly, this measure makes the technology more widespread and (step-by-step) cheaper. Ürge Vorsatz (2001) found that the high penetration rate of CFL bulbs in Hungary, when compared to other EU countries, is a result of the integrated forceful marketing efforts of competing manufacturers trying to bite out the biggest possible market share in a new market. "To address the market barriers, a residential CFL campaign was launched by ELI-Hungary in co-operation with manufacturers, retailers, wholesalers and NGOs. The campaigns addressed awareness and information barriers to the adoption of CFLs by residential customers. In 2003 the foreseen CFL sales doubled as compared to 1999, of which 60% was produced by the three major lamp manufacturers" (Bertoldi and Bogdan Atanasiu, 2007, p. 10).

Integration with other policies is also very important and may exert positive or negative impact on the spread of new technologies. "Inadequate or inefficient policies often create more barriers rather than ease them" (Hinostroza et al. 2007, pp. 31).

Counter-interested market agents can make it difficult to push through beneficial solutions. In several countries – including Hungary – the workers in plants manufacturing conventional bulbs could temporarily slow down the market penetration process of CFL bulbs through use of lobbying power and protests against them. Of course, the new EU regulation which gradually phases out traditional light bulbs by 2012 (http://ec.europa.eu/news/energy/090901_en.htm) helps accelerate the spread of new technologies and has lead to the liquidation of some producers who stick to manufacturing traditional bulbs.

Lack of information on options, potential and cost effectiveness can also function as barrier to market penetration of new technologies. The same applies to lack of awareness (see Jakob 2007) even when information is available – for example in the case of LED bulbs. Lack of a sufficient marketing budget often makes producers unable to disseminate information about

new solutions. Lack of information was identified by Ürge-Vorsatz (2001) as being the number one hidden barrier behind false perceptions about high costs.

New technologies may *require changes in attitudes and habits* which can also be a considerable barrier when considering, for example, the unusual shape of CFL or LED bulbs and the tendency for humans to insist on the familiar.

The **risk factor** includes *perceived risks involved in new solutions* when compared to common technologies – e.g. financial and technological risks (see Jakob 2007) – as well as the question of *trust*. There is a risk that the bulbs will have a shorter lifetime than promised by the manufacturer. Being a new technology, the actual lifetime of these bulbs has not been tested in real life yet.

Based on the scores for each factor, a consumer policy profile of the selected GHG mitigation options can be drawn. As explained, Figure 4 and 5 show two examples which are significantly different in their profiles. Designing policy implementation involves pushing the curve into the acceptable zone. Pushing the string at a certain point influences other profile factors as well. For example, special purpose CFL bulbs were invented to fight consumer disapproval of odd bulb shapes, thus requiring less of a compromise, although at a cost.

Thus eliminating the factors which keep the regarded solution in the prohibitive zone is not the only approach the policy may take when addressing barriers to implementation. The policy may rely on and take advantage of features where the option was given a high score. The costs of consumer policy can be significantly reduced if there are economic agents who find co-benefits in the proposed solution and are willing to invest in promoting it. Figure 5 suggests that LED bulbs have a consumer perception profile very similar to that which CFL bulbs had in the past. This similarity calls for similar policy actions to be taken for LED bulbs.

4. Application of consumer policy tools

As a next step, consumer-oriented environmental policy tools are analyzed with regard to their effectiveness in evoking GHG reductions. In the authors' opinion, most consumer policy tools work best for mitigation options which fall into the yellow zone. This is especially true for tools that represent major intrusions into existing market structures. For example, **environmental taxation** may correct externalities (e.g. the price of energy which does not include the impact of climate change) in order to close the gap between the marginal social cost curve and the marginal private cost curve. If this option is unacceptable for political reasons, products with less impact on climate can be supported.

Environmental labelling works best in the red or yellow zone as it builds on the added value of environmental quality to the consumer. It is the only tool able to address issues and reach consumers even when the cost of product is high related to substitutes, either in private or in social terms. For example, hybrid cars are expensive compared to the energy saved, and no cost payback can be expected. Still, as they represent environmental or prestige value for a certain segment of environmentally aware consumers, they have achieved a premium price position and a small but significant market share. Active solar systems and photovoltaic cells are other examples of this kind, as mentioned above. The role

of voluntary environmental labelling is important as it can succeed in situations when all other tools fail, but it will not be able to make an impact on a mass market mainly consisting of uninterested consumers. Of course, products positioned in the "green" zone are not always priced higher than other products so labelling may work in the green or yellow zone as well. Of course, compulsory labelling may have a wider scale impact on consumer behaviour. Directive 2010/30/EU sets compulsory minimum efficiency requirements for household appliances to motivate producers to improve product design in order to lower the energy consumption during the use phase (http://ec.europa.eu/energy/efficiency/labelling/labelling_en.htm).

Table 1 summarises the effectiveness of consumer policy tools in different zones of action, illustrating the effectiveness of each consumer policy tool (using zero to three X's for each zone to indicate level of efficiency).

	Green zone	Yellow zone	Red zone
Environmental labelling	X	XXX	XXX
Taxation	X	XXX	XX
State aid policy	X	XXX	X
Substance bans	XXX	X	
Voluntary agreement		XX	
Product design guidelines		XXX	
Information dissemination	XXX	XX	X
Extension of producer responsibility		XXX	
Public procurement	XXX	XXX	
Standardization	XXX	XX	

Table 1. Effectiveness of consumer policy tools in different zones of action

Getting the price right is probably the single most effective measure available to stimulate markets for greener products (see Green Paper on Integrated Product Policy, published by the Commission of the European Communities, 2001). Tools, such as **differentiated taxation** according to the environmental performance of products**, extended producer responsibility** or **green public procurement** work best in the yellow zone where there is a significant discrepancy between marginal social costs and marginal private cost as private costs do not reflect the total price of externalities. Using these tools in the red zone is not justifiable, except for in the rare cases of spin-off technologies which show the potential to reduce both environmental burden and costs in the long run. According to the French Sustainable Development Strategy for 2010-2013 "France sees a strong role for eco-labels in making greener products more credible and attractive to consumers, aiming to double sales of products carrying the French or EU eco-label by 2012. Green products must also be incentivised by EU agreement on reduced VAT rates, extended bonus-malus schemes to reward the best and punish the worst, and green public-procurement requirements". (http://ec.europa.eu/environment/etap/). The same idea has been formulated by the Danish EPA regarding products carrying the Nordic Swan label and the European eco-label

(http://www.mst.dk). These strategies are in the spotlight of policy making, waiting for the decisions to be made for their implementation. In Hungary, the holders of the Hungarian eco-label are given the opportunity to claim back part of the tax (a so-called product fee) imposed on products like packaging, tyres, batteries, refrigerants, etc.

Public procurement accounts for 19% of GDP in the European Union (http://www.epractice.eu/en/library/5280576) suggesting that green public procurement represents a huge market for environmentally friendly products. Since 2008, environmental criteria have been set for at least 18 product groups – including several energy-related ones (http://ec.europa.eu/environment/gpp), – and there are ongoing consultation processes such as the one on the proposed Green Public Procurement (GPP) criteria for indoor lighting and tissue paper which is currently ongoing (http://ec.europa.eu/environment/consultations/gpp_en.htm). Green Public Procurement is a voluntary tool, although there are numerous EU directives supporting it and accelerating the market penetration of more energy efficient products. Directive 2010/31/EU on the energy performance of buildings requires member states to ensure that "after 31 December 2018, new buildings occupied and owned by public authorities are nearly zero-energy buildings" (http://ec.europa.eu/environment/gpp/eu_related_en.htm).

Extension of producer responsibility influences both the design phase of products in a more preventative direction, as well as making the take-back of end-of-life products easier for consumers (see different stages of the 94/62/EC Directive on Packaging and Packaging Waste http://europa.eu/legislation_summaries/environment/waste_management/l21207_en.htm or the 2002/95/EC Directive on Waste Electrical and Electronic Equipment, http://ec.europa.eu/environment/waste/weee/index_en.htm, etc). This tool is very important in the yellow zone.

State aid policy – being part of the price correction mechanism – can be used as a second best solution when taxing polluting products is not acceptable to society or to politicians. Taxing energy, for example, evokes a lot of concern regarding social justice and low income families. Higher market penetration of "green zone" options should not be promoted by subsidies. As these options pay the individual back, other measures would be more effective such as making credit and loan opportunities easier available, providing information, making widespread use of marketing tools, product standards or labelling. However, it should be noted that consumers tend not to replace household items (e.g., light bulbs, washing machines, etc.) until they become unusable, which makes the penetration of even "green zone" options rather slow.

Substance bans may work in the green zone only if a good substitute is available at a reasonable price. The ban on mercury in glass thermometers is a good example. Digital thermometers are available and affordable substitutes. Nonetheless, mercury based thermometers would probably remain on the market without a strict regulation to phase them out. Asbestos insulation or Mercury-Cadmium batteries are other examples of the same kind.

Voluntary agreements as supply-side policy tools also work best in the yellow zone as they embody company measures based on a mutual agreement procedure between them and regulatory authorities for the sake of the environment. For green zone options there seems to be no need of such agreements while at the other end of the spectrum, red zone options can not be managed using voluntary agreements.

Product design guidelines also include climate-related legislative elements, like the Directive 2009/125/EC on ecodesign requirements for energy-related products. The aim of the Ecodesign Directive is „to reduce the environmental impact of products, including life-cycle energy consumption by providing EU-wide rules for the design of energy-related products" (http://ec.europa.eu/environment/gpp/eu_related_en.htm). The Directive inter alia promotes the development and application of technical or performance-based specifications for green public procurement.

Standardization also belongs to the group of supply side measures, making the organisational background and production activities of companies more suitable from a climate-friendly perspective and indirectly creating more sustainable consumption.

This list can be extended and there is a space for analysing the effectiveness of different consumer policy tools more deeply case by case, utilising practical examples.

6. Conclusions

Keeping climate change under control increasingly appears to be one of the most urgent and ambitious challenges for mankind now and in the future, making innovative solutions and sacrifices necessary. Consumer-oriented environmental policy tools are becoming widespread, especially in the more developed countries, in order to tackle the problem through reducing GHG emissions. The above chapter aimed to present a model which is appropriate for evaluating the effectiveness of consumer policy tools which can be implemented to put GHG mitigation solutions into action. Political support is very important, but it can be expected only when the social costs of GHG emission abatement are low and the climate change strategy can be implemented in a cost-efficient way.

As a framework for the analysis we constructed the marginal private and the marginal social cost curves, and identified three zones of action for GHG emission reduction. Then we introduced the profiling technique to identify barriers and opportunities for selected options. In the authors' opinion, special attention should be paid to options with high environmental potential and negative, zero, or slightly positive social costs. These are the typical "yellow" and "green zone" options which are most likely to be implemented although some barriers may hinder and slow down this process. We illustrated the profiling method using the example of different light bulbs.

Our suggestion for consumer policy is to use the profiling method in order to both compare the selected GHG mitigation options based on the identified barriers and to find the most relevant tools to demolish those implementation barriers. Pushing or pulling the profile string can be achieved by using appropriate consumer policy measures which can provide parallel solution for even more than one implementation problem simultaneously, moving the selected option into a more favourable position; a zone where action is easier and the option becomes more acceptable to society. Consumer policy tools can be classified based on their GHG emission abatement applicability and effectiveness for options which fall into different zones.

One future direction for research is a thorough analysis of consumer policy tools for several "green," "yellow" or even "red zone" options in order to find out how exactly the existing barriers to implementation can be dismantled in order to realise more effective climate strategies.

7. Acknowledgements

The research was financially supported by the project called TAMOP-4.2.1/B-09/1/KMR-2010-005.

8. References

Baden, S., Fairey, P., Waide, P., de T'serclaes, P., Lautsen, J. (2006). Hurdling Financial Barriers to Low Energy Buildings: Experiences from the USA and Europe on Financial Incentives and Monetizing Building EnergySavings in Private Investment Decisions, *Proceedings of 2006 ACEEE Summer Study of Energy Efficiency in Buidings*, American Council for an Energy Efficent Economy, Washington

Bertoldi, P. and Bogdan A (2006a). Residential Lighting Consumption and Saving Potential in the Enlarged EU, European Commission – DG Joint Research Centre, Institute for Environment and Sustainability, European Commission Joint Research Centre

Bertoldi, P. and Bogdan A: (2006b). Electricity Consumption and Efficiency Trends in the Enlarged European Union, - *Status report 2006*-, European Commission Directorate-General Joint Research Centre Institute for Environment and Sustainability

Commission of the European Communities (2001). Green Paper on Integrated Product Policy COM 68 final, http://eur-lex.europa.eu/LexUriServ/site/en/com/2001/com2001_0068en01.pdf

Creyts, Y., Derkach, A., Nyquist, S, Ostrowski, K. and Stephenson, J. (2007). U.S. Greenhouse Gas Abatement Mapping Initiative, McKinsey & Company.

Csutora, M. and Zilahy, G. (1998). Economic Analysis of Greenhouse Gas Mitigation Options in Hungary, Budapest University of Economic Sciences, Ph.D. Conference

Csutora, M., Zsóka, Á. (2011). Maximizing the efficiency of greenhouse gas related consumer policy, Journal of Consumer Policy, Volume 34, Issue 1 (2011), Page 67-90, DOI:10.1007/s10603-010-9147-0, www.springerlink.com/content/94j20g7223060p35/

Hinostroza, M.; Cheng, C.; Zhu, X.; Fenhann, J.; Figueres, C.; Avendano, F. (2007).; Potentials and barriers for end-use energy efficiency under programmatic CDM, Working Paper No. 3, CD4CDM Working Paper Series, UNEP Risø Centre on Energy, Climate and Sustainable Development, Roskilde, available at: http://www.cd4cdm.org/Publications/pCDM&EE.pdf

Jakob, M. (2007). The drivers of and barriers to energy efficiency in renovation decisions of single-family home-owners, CEPE Working paper series 07-56, CEPE Center for Energy Policy and Economics, ETH Zürich

Nemcsicsné Zsóka, Á. (2005). Consistency and gaps in pro-environmental organisational behaviour, PhD dissertation, Corvinus University of Budapest

Raaij, W. van, Verhallen, T. (1983). A behavioral model of residential energy use, Journal of Economic Psychology, 3, 1, 39-63.

Rubik, F., Scholl G., Biedenkopf, K., Kalimo, H., Mohaupt, F., Söebech, Ó., Sto, E., Strandbakken, P., Turnheim, B. (2009). Innovative Approaches in European Sustainable Consumption Policies, Schriftenreihe des IÖW 192/09, Berlin

Slovic, P. (1987). Perception of risk, Science, 236, 280-285

Slovic, P. and Weber, E.U. (2002). Perception of Risk Posed by Extreme Events, The Conference on Risk Management Strategies in an Uncertain World, Held In April 12-13, 2002, Palisades, New York, 1-21

Stern, N.: (2008). The Economics of Climate Change, American Economic Review, 98, 1-37

Thøgersen, J. and Crompton, T. (2009). Simple and Painless? The Limitations of Spillover in Environmental Campaigning, *Journal of Consumer Policy*, 32, 141-163

Tukker, A. and Jansen, B. (2006). Environmental Impacts of products, A Detailed Review of Studies, Journal of Industrial Ecology, 10 (3), 159-182

Ürge-Vorsatz, D. – Füle, M (1999). Economics of Greenhouse Gas Limitations, Hungary Country Study, UNEP Collaborating Centre on Energy and Environment and Riso National Laboratory, Denmark

Ürge-Vorsatz, Jochen Hauff, (2001). Drivers of market transformation: analysis of the Hungarian lighting success story, Energy Policy, 29, 10, Pages 801-810, ISSN 0301-4215, DOI: 10.1016/S0301-4215(01)00013-1.,

Wesselink, B. and Deng, I. (2009): Sectoral Emission Reduction Potentials and Economic Costs for Climate Change, ECOFYS.

World Research Institute (2010). Global Climate Trends 2005, http://earthtrends.wri.org/pdf_library/data_tables/cli5_2005.pdf

Zilahy, G. (2004). Organisational Factors Determining the Implementation of Cleaner Production Measures in the Corporate Sector, Journal of Cleaner Production, 12,4, 311-319

Zilahy G., Nemcsicsné Zsóka Á., Szeszler, Á., Ürge-Vorsatz, D., Markandya, A., Hunt, A. (2000). The Indirect Costs and Benefits of Greenhouse Gas Limitation: Hungary Case Study, Handbook Reports, UNEP Collaborating Centre on Energy and Environment and Riso National Laboratory, Denmark

URL-sources:

http://www.napkollektor-info.hu/component/poll/16
http://ec.europa.eu/environment/climat/climate_action.htm
http://ec.europa.eu/news/energy/090901_en.htm
http://ec.europa.eu/energy/efficiency/labelling/labelling_en.htm
http://ec.europa.eu/environment/etap/inaction/policynews/577_en.html
http://www.mst.dk/English/SustainableConsumptionandProductionintheNordicRetailSector/WhatCanPolicymakersDo/SelectedPolicyInstruments/DifferentiatedVAT/
http://ec.europa.eu/environment/gpp/eu_related_en.htm
http://www.epractice.eu/en/library/5280576
http://ec.europa.eu/environment/gpp
http://ec.europa.eu/environment/consultations/gpp_en.htm
http://europa.eu/legislation_summaries/environment/waste_management/l21207_en.htm
http://ec.europa.eu/environment/waste/weee/index_en.htm

11

Livestock and Climate Change: Mitigation Strategies to Reduce Methane Production

Veerasamy Sejian and S. M. K. Naqvi
Division of Physiology and Biochemistry, Central Sheep and Wool Research Institute
Avikanagar
India

1. Introduction

Global warming refers to a significant rise in the planets temperature making it uninhabitable. It happens thus: the earth is warmed by energy from the sun. In order to maintain its temperature, the earth must radiate some of that energy back into the atmosphere. However, certain atmospheric gases form a blanket around the earth, allowing solar radiation to penetrate, but preventing it from escaping. The more these green house gases, the hotter the earth (Sarmah, 2010).

Climate change is seen as a major threat to the survival of many species, ecosystems and the sustainability of livestock production systems in many parts of the world. Green house gases (GHG) are released in the atmosphere both by natural sources and anthropogenic (human related) activities. An attempt has been made in this article to understand the contribution of ruminant livestock to climate change and to identify the mitigation strategies to reduce enteric methane emission in livestock. The GHG emissions from the agriculture sector account for about 25.5% of total global radiative forcing and over 60% of anthropogenic sources. Animal husbandry accounts for 18% of GHG emissions that cause global warming. Reducing the increase of GHG emissions from agriculture, especially livestock production should therefore be a top priority, because it could curb warming fairly rapidly. Methane with the global warming potential of 25 and longer residence time is an important GHG (Wuebbles and Hayhoe 2002; Forster et al. 2007). The rising concentration of CH4 is strongly correlated with increasing populations, and currently about 70% of its production arises from anthropogenic sources (Moss et al. 2000; IPCC 2007). Ruminant livestock such as cattle, buffalo, sheep and goats contributes the major proportion of total agricultural emission of methane. Although the reduction in GHG emissions from livestock industries is on high priorities, strategies for reducing emissions should not reduce the economic viability of enterprises if they are to find industrial acceptability.

Ruminant livestock has been recognized as a major contributor to greenhouse gases (Steinfeld et al., 2006). Livestock account for mainly 80% of all emissions from the agricultural sector. Emissions into the air by any animal production system can be problematic in terms of pollutants and toxicity and in terms of odour and the perception of air quality by human neighbours. The three major greenhouse gases (GHGs) are carbondioxide (CO_2), methane (CH_4) and nitrous oxide (N_2O). CH_4 also has serious impact

on high atmosphere ozone formation. It is important to reduce methane production from the rumen, because methanogenesis corresponds to 2-12% of dietary energy loss as well as contributing to global warming. Enteric CH_4 emissions represent an economic loss to the farmer where feed is converted to CH_4 rather than to product output.

There is a growing interest in decreasing the potential threat of global warming by reducing emissions of GHGs into the atmosphere (Moss et al., 2000). Agricultural activities contribute significantly to global GHG emissions, namely CO_2, CH_4, N_2O and ammonia (NH_3), which are major GHGs contributing to global warming (IPCC, 2001). There is mounting awareness worldwide of the necessity to protect the environment (Meadows et al., 1992), minimize the contamination of air with CO_2, CH_4, NH_3, and N_2O and other GHGs that contribute to the radiative forcing (Tamminga, 1996). The consequences of increasing the atmospheric concentration of GHGs responsible for the radiative forcing are gradual elevation of average global temperatures, altered viability of plants, animals, insects and microbes with numerous adverse consequences to human well being. The degree to which these changes are projected to occur is dependent upon a reliable GHG policy models with a range of scenarios for the levels of GHG emissions (Moss et al., 2000).

Offering relatively fewer cost-effective options than other sectors such as energy, transport and buildings, agriculture has not yet been a major player in the reduction of GHG emissions (UNFCCC, 2008). Agriculture and livestock are nevertheless poised to play a greater role in post-2012 climate agreements (UNFCCC, 2008), and indeed wide-ranging policy action will certainly be needed (McAlpine et al., 2009). Adapting to climate change and reducing GHG emissions may require significant changes in production technology and farming systems that could affect productivity. Many viable opportunities exist for reducing methane emissions from enteric fermentation in ruminant animals and from livestock manure management facilities. To be considered viable, these emissions reduction strategies must be consistent with the continued economic viability of the producer, and must accommodate cultural factors that affect livestock ownership and management.

2. Sources of GHGs from agriculture and livestock

CH_4 is emitted from a variety of anthropogenic and natural sources. More than 70 percent of global CH_4 emissions are related to anthropogenic activities. Anthropogenic sources include fossil fuel production and use, animal husbandry (enteric fermentation in livestock and manure management), paddy rice cultivation, biomass burning, and waste management. Emissions from enteric fermentation of the domestic livestock contribute significantly to GHGs inventories. Emissions from animal facilities primarily consist of animal respiration and enteric fermentation. In addition, emissions from manure storage are also believed to be a potential source of CH_4 (Sejian et al., 2011a).

3. Impact of global warming

Many impacts of global warming are already detectable. As glaciers retreat, the sea Level rises, the tundra thaws, hurricanes and other natural calamities occur more frequently, and penguins, polar bears, and other species struggle to survive (Topping, 2007), experts anticipate even greater increases in the intensity and prevalence of these changes as the 21st century brings rises in GHG emissions (Sarmah, 2010). The five warmest years since the

1890s were 1998, 2002, 2003, 2004, and 2005 (NASA, 2006). Indeed, average global temperature have risen considerably, and the Intergovernmental panel on climate change (IPCC, 2007a) predicts increases of 1.8-3.9ºC (3.2-7.1º F) 2100. These temperature rises are much greater than those seen during the last century, when average temperatures rose only 0.06º C (0.12F) decade (NOAA, 2007). Since the mid -1970s, however, the rate of increase in temperature rise has tripled. The IPCC' s latest report (IPCC, 2007b) warns that climate change ″ could lead to some impacts that are abrupt or irreversible.″ According to FAOSTAT (FAO, 2008) globally approximately, 56 billion land animals are reared and slaughtered for human consumption annually, and livestock inventories are expected to double by 2050, with most increases occurring in the developing world (Steinfeld et al., 2006). As the numbers of farm animal reared for meat, egg and dairy production rise, so do their GHG emissions (Sarmah, 2010).

4. Livestock and climate change

The major global warming potential (GWP) of livestock production worldwide comes from the natural life processes of the animals. Table 1 describes the salient features of the three major GHGs. Methane production appears to be a major issue although it presently contributes only 18 % of the overall warming. It is accumulating at a faster rate, and is apparently responsible for a small proportion of the depletion of the protective ozone layer. Methane arises largely from natural anaerobic ecosystems, rice/paddy field and fermentative digestion in ruminant animal. In fact, CH_4 is considered to be the largest potential contributor to the global warming phenomenon (Johnson et al., 2002; Steinfeld et al., 2006). It is an important component of GHG in the atmosphere, and is associated with animal husbandry (Leng 1993; Moss et al., 2000). Much of the global GHG emissions currently come from enteric fermentation and manure from grazing animals and traditional small-scale mixed farming in developing countries. The development of management strategies to mitigate CH_4 emissions from ruminant livestock is possible and desirable. Not only can the enhanced utilization of dietary 'C', improve energy utilization and feed efficiency hence animal productivity, but a decrease in CH_4 emissions and also reduce the contribution of ruminant livestock to the global CH_4 inventory.

GHG	Chemical Formula	Lifetime (years)	Radiative efficiency (W $m^{-2}ppb^{-1}$)	Global Warming Potential
Carbon dioxide	CO_2	Up to 100 years	1.4×10^{-5}	1
Methane	CH_4	12	3.7×10^{-4}	23
Nitrous Oxide	N_2O	114	3.03×10^{-3}	310

Table 1. Global warming potential (GWP) of the GHGs

5. Enteric methane production

Livestock are reared throughout the world, and are an important agricultural product in virtually every country. CH_4 is emitted as a by-product of the normal livestock digestive process, in which microbes resident in the animal's digestive system ferment the feed consumed by the animal. This fermentation process, also known as enteric fermentation,

produces CH_4 as a by-product. The CH_4 is then eructated or exhaled by the animal. Within livestock, ruminant livestock (cattle, buffalo, sheep, and goats) are the primary source of emissions. Other livestock (swine and horses) are of lesser importance for nearly all countries. The number of animals and the type and amount of feed consumed are the primary drivers affecting emissions. Consequently, improvements in management practices and changes in demand for livestock products (mainly meat and dairy products) will affect future CH_4 emissions.

Among the livestock, cattle population contributes most towards enteric CH_4 production (Johnson & Johnson, 1995). Enteric fermentation emissions for cattle are estimated by multiplying the emission factor for each species by the relevant cattle populations. The emissions factors are an estimate of the amount of CH_4 produced (kg) per animal, and are based on animal and feed characteristics data, average energy requirement of the animal, the average feed intake to satisfy the energy requirements, and the quality of the feed consumed. The district or country level emission from enteric fermentation is computed as a product of the livestock population under each category and its emission coefficient (Chhabra et al. 2009). The emission coefficients for CH_4 emissions from enteric fermentation are country-specific, and these coefficients should conform to IPCC guidelines (IPCC, 2007b).

5.1 Contribution of ruminants to GHGs through enteric methane emission

Ruminant livestock such as cattle, buffalo, sheep and goats contributes the major proportion of total agricultural emission of methane (Leng, 1993; Lassey, 2007; Chhabra et al., 2009). Ruminants are categorized by the presence of rumen, a special digestive organ, in the body. Besides having unique ability to digest fibrous and low grade roughages/plant material, it is also a major producer of methane, a potent green house gas. The enteric fermentation in rumen is highly useful for humankind because it converts coarse and fibrous plants into food and fiber for humankind. However, enteric fermentation in rumen also produces methane through bacterial breakdown of feeds called as methanogenesis. The animals release methane into atmosphere through exhaling or ruminating through mouth or nostrils. Methane production and release accounts for release of digestible energy to atmosphere and therefore inefficient utilization of feed energy. Enteric fermentation also produces volatile fatty acids. Among the volatile fatty acids, acetate and butyrate promote methane production. Global emission of methane from the digestion process of ruminants is about 80 Million tones per year (Gibbs & Johnson, 1994) and considered to be single largest source of anthropogenic methane emission (IPCC, 2001). Methane emission from ruminants provides enough scope of easy and practical management for reduction in methane emission (McMichael et al., 2007).

5.2 Enteric fermentation-process description

Enteric fermentation is the digestive process in herbivores animals by which carbohydrates are broken down by micro-organisms into simple molecules for absorption into the bloodstream. CH_4 is produced as a waste product of this fermentation process. CH_4 production through enteric fermentation is of concern worldwide for its contribution to the accumulation of greenhouse gases in the atmosphere, as well as its waste of fed

energy for the animal. CH_4 is produced in the rumen and hindgut of animals by a group of *Archaea* known collectively as methanogens, which belong to the phylum *Euryarcheota*. Among livestock, CH_4 production is greatest in ruminants, as methanogens are able to produce CH_4 freely through the normal process of feed digestion. Ruminant animals are the principal source of emissions because they produce the most CH_4 per unit of feed consumed. What makes ruminant animals unique is their "fore-stomach" or rumen, a large, muscular organ. The rumen is characterized as a large fermentation vat where approximately 200 species and strains of micro organisms are present. The microbes ferment the plant material consumed by the animal through a process known as enteric fermentation. The products of this fermentation provide the animal with the nutrients it needs to survive, enabling ruminant animals to subsist on coarse plant material. CH_4 is produced as a byproduct of the fermentation and is expelled. "Monogastric" animals produce small amounts of CH_4 as the result of incidental fermentation that takes place during the digestion process. "Non-ruminant herbivores" produce CH_4 at a rate that is between monogastric and ruminant animals. Although these animals do not have a rumen, significant fermentation takes place in the large intestine, allowing significant digestion and use of plant material.

Methane producing bacteria reside in the reticulo-rumen and large intestine of ruminant livestock. These bacteria, commonly referred to as methanogens, use a range of substrates produced during the primary stages of fermentation to produce CH4, thus creating generated energy required for their growth. All methanogen species can utilize hydrogen ions (H2) to reduce CO2 in the production of CH4 as this reaction is thermodynamically favorable to the organisms. Availability of H2 in the rumen is determined by the proportion of end products resulting from fermentation of the ingested feed. Processes that yield propionate and cell dry matter act as net proton-using reactions, whereas a reaction that yields acetate results in a net proton increase. Other substrates available to methanogens include formate, acetate, methanol, methylamines, dimethyl sulfide and some alcohols, however, only formate has been documented as an alternative CH_4 precursor in the rumen. Figure 1 describes the number of factors affecting methane production from rumen.

The principal methanogens in the bovine rumen utilize hydrogen and carbon dioxide, but there is a group of methanogens of the genus *Methanosarcina* that grow slowly on H2 and CO2 and therefore maintain a distinct niche by utilizing methanol and methylamines to produce CH_4. Formate, which is formed in the production of acetate, can also be used as a substrate for methanogenesis, although it is often converted quickly to H2 and CO2 instead. Volatile fatty acids (VFA) are not commonly used as substrates for methanogenesis as their conversion into H2 and CO2 is a lengthy process, which is inhibited by rumen turnover. Therefore, methanogenesis often uses the H2 and CO2 produced by carbohydrate fermentation, as VFAs are formed. By removing H2 from the ruminal environment as a terminal step of carbohydrate fermentation, methanogens allow the microorganisms involved in fermentation to function optimally and support the complete oxidation of substrates. The fermentation of carbohydrates results in the production of H2 and if this end product is not removed, it can inhibit metabolism of rumen microorganisms.

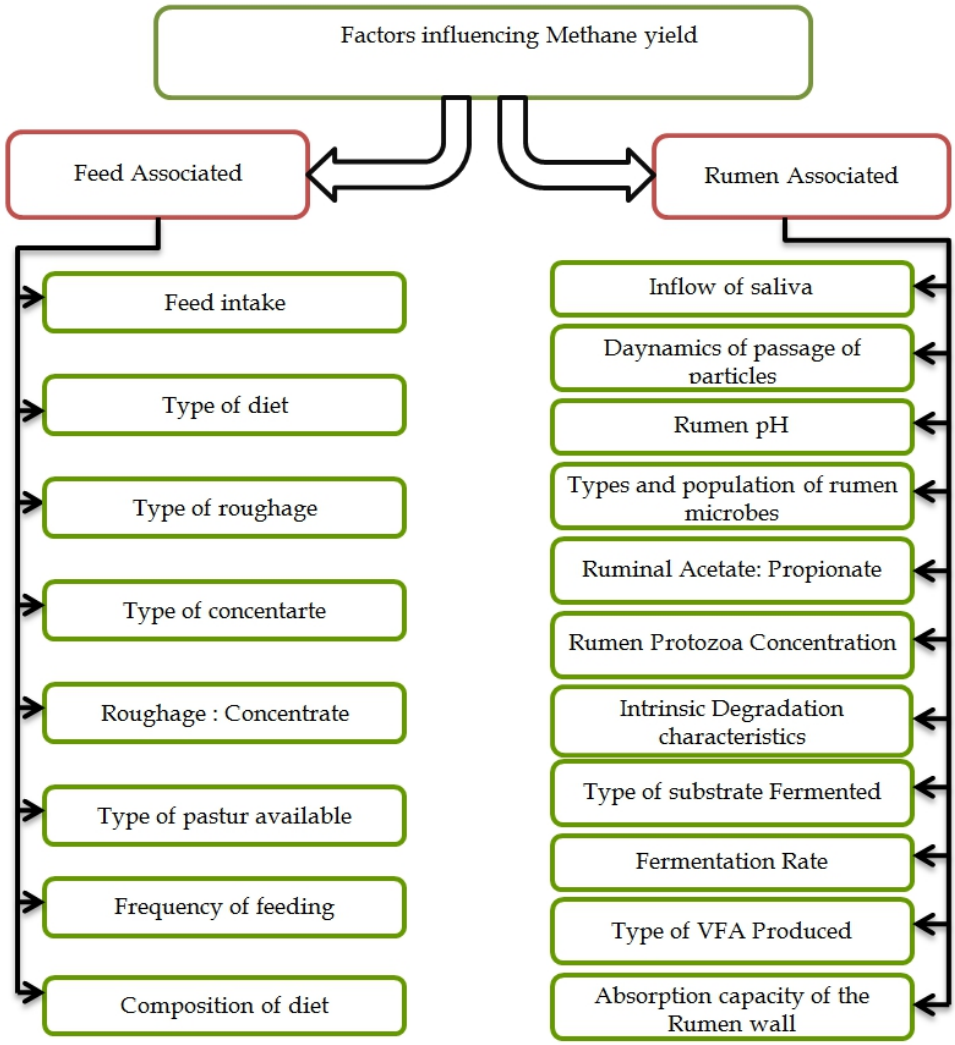

Fig. 1. Different factors influencing enteric methane production

5.3 Different prediction model for enteric methane emission

5.3.1 Empirical models

Although many statistical models have been fairly successful in predicting CH_4 production, many variables in these models are not commonly measured which may lead to difficulties in predicting CH_4 production outside the range of values used for model development (Johnson et al., 1996). These problems may be addressed by using equations with common input variables and by developing models with minimum input variables from multiple

sources. The limitation of using some of the extant models, such as the equation of Moe & Tyrrell (1979), is the difficulty of obtaining reliable model input variables, which might have compromised the predictive ability of the model in the study. Ellis et al. (2007) formulated the most accurate equations which could be useful to the livestock industry for accurately predicting CH_4 production from a minimum set of inputs. Although the extant models evaluated performed well, the new equations developed in the study was more user-friendly and reliable prediction than extant models and therefore a preferable model for generating national CH_4 emissions inventory. Sejian et al. (2011a) have described the different types of regression/prediction equations for enteric methane emission for domestic livestock.

5.3.2 Mechanistic models

There are various emission models available to predict accurately enteric methane emission for farm households (Sejian et al., 2011a). Yan et al. (2000) improved on the earlier representation of methanogenesis in the mechanistic model, and outlined some likely reasons for the differences between observed and predicted values for CH_4 production. One of these is the error attributable to dietary composition, not only in the analysis, but also due to variation in nutrient composition between samples of the same feedstuff. This knowledge of the dietary components, not only of typical feeds but also alternative feeds that are under consideration for CH_4 emission reduction purposes, is a prerequisite for successful use of the models to compare the effect of different feeds on CH_4 production (Palliser & Woodward, 2002). Nonlinear mechanistic model of CH_4 production provides a significant opportunity to enhance scientific ability to estimate CH_4 emissions from cattle (Mills et al., 2003; Kebreab et al., 2008). In addition researchers identified that mechanistic models can be used to generate Ym values that can be used in national CH_4 emission inventory models. It was suggested that if incentives are introduced to mitigate CH_4 emissions at farm level, mechanistic models would be excellent tools to make reliable estimates of enteric CH_4 emissions. The advantage of mechanistic models compared with empirical models is that mitigation options implemented at a farm or national level can be assessed for their effectiveness.

5.3.3 Whole farm model (WFM)

Computer simulation can provide a cost-effective and efficient method of estimating CH_4 emissions from dairy farms and analyzing effects of management strategies on CH_4 emissions. Invariably all whole farm models (WFM) are mechanistic models. A commonly used simulation is the one proposed by Rotz et al. (2007). The model is an Integrated Farm System Model (IFSM) which is a potential tool for simulating whole-farm emissions of CH_4 and evaluating the overall impact of management strategies used to reduce CH_4 emissions. The IFSM was further refined into a process-based whole-farm simulation including major components for soil processes, crop growth, tillage, planting and harvest operations, feed storage, feeding, herd production, manure storage, and economics (Rotz et al., 2009). Incorporation of the CH_4 module with IFSM in addition to modules simulating N_2O emissions, provides an important tool for evaluating the overall impact of management strategies used to reduce GHG emissions in dairy farms.

Farm System Simulation Framework (FSSF) is another type of WFM which uses pasture growth and cow metabolism for predicting CH_4 emissions in dairy farms. Also included in the WFM is climate and management information. Some other WFMs are also developed by Neil et al. (1997), and Bright et al. (2000). However these models are adequate only for predicting CH_4 production by non-lactating Holstein cows. Prediction rates for lactating cows are less accurate and WFMs currently described in the literature seem inappropriate (IPCC, 1997). Hence development of WFMs are required for the prediction of nutrient and GHG emissions and better estimates of enteric CH_4 production. Currently available WFMs may incorrectly estimate CH_4 emission levels because they cannot predict the wide range enteric CH_4 emissions as affected by DMI and diet. The low prediction accuracy of CH_4 equations in current WFMs may introduce substantial error into inventories of GHG emissions and hence lead to incorrect mitigation recommendations. If regression equations examined here and elsewhere continue to explain only a small fraction of the variation in observed values, moving towards regression equations including more nutritional informations and details on a subanimal level, or towards a dynamic mechanistic description of enteric CH_4 emission, will improve predictions (Ellis et al., 2010).

6. Manure methane production

Manure from confined livestock operations is most often stored in solid or liquid form before being applied to agricultural land. Increasingly, however, manure is composted before land application or anaerobically digested to produce CH_4 as bio-fuel. Methane emissions from anaerobic digestion can be recovered and used as energy by adapting manure management and treatment practices to facilitate methane collection. Depending on the management system used, greenhouse gas emissions (mainly CH_4 and N_2O) from manure vary considerably. Strategies to mitigate net emissions aim to change manure properties or the conditions under which CH_4 and N_2O are produced and consumed during manure storage and treatment. The selection of successful methane emissions reduction options from manure depends on several factors, including climate; economic, technical and material resources; existing manure management practices; regulatory requirements; and the specific benefits of developing an energy resource (biogas) and a source of high quality fertilizer.

7. Mechanism of methane reduction

There are two mechanisms available by which methane production can be reduced in livestock. These mechanisms influence the availability of H_2 in the rumen and subsequent production of enteric CH_4 emissions by livestock. Processes that yield propionate act as net proton-using reactions while those that yield acetate result in a net increase in protons. Hence mitigation strategies aiming at reducing CH_4 production must work towards increasing the propionate production. This will reduce CH_4 production by removing some of the H_2 produced during ruminal fermentation. Another mechanism by which CH_4 production may be reduced during the rumen fermentation process is through the provision of alternative hydrogen acceptors or sinks. Another mechanism widely accepted is to supplement anti-methanogenic agents which will inhibit the process of methanogenesis either by directly inhibiting the methanogenic microbe in the rumen or by increasing more propionate production. In addition, strategies to mitigate net emissions from livestock

manure aim to change manure properties or the conditions under which CH_4 and N_2O are produced and consumed during manure storage and treatment. Such strategies aim to manipulate livestock diet composition and/or include feed additives to alter manure pH, concentration and solubility of carbon and nitrogen, and other properties that are pertinent to CH_4 and N_2O emissions.

In the anaerobic conditions prevailing in the rumen, the oxidation reactions required to obtain energy in the form of ATP release hydrogen. The amount of hydrogen produced is highly dependent on the diet and type of rumen microbes as the microbial fermentation of feeds produces different end products that are not equivalent in term of hydrogen output. For instance, the formation of propionic acid consumes hydrogen whereas the formation of acetic and butyric acids releases hydrogen.

$$\text{Pyruvate} \dashrightarrow \text{acetate } (C_2) + CO_2 + 2H$$
$$\text{Pyruvate} + 4H \dashrightarrow \text{propionate } (C_3) + H_2O$$
$$2C + 4H \dashrightarrow \text{butyrate } (C_4) + 2H_2O$$

From this it can be concluded that if ruminal fermentation patterns are shifted from acetate to propionate, both hydrogen and methane production will be reduced. This relationship between methane emissions and the ratio of the various VFA has been well documented and it provides opportunities to reduce methane emissions. This ratio may, for example, be influenced by the type of carbohydrate consumed by the animal. Cereal-based diets that are high in starch favour propionate production and consequently tend to produce less methane per unit of feed consumed than forage-based diets.

Another mechanism by which methane production may be reduced during the rumen fermentation process is through the provision of alternative hydrogen acceptors or sinks. Compounds such as unsaturated fatty acids provide alternative hydrogen acceptors, consuming hydrogen in limited quantities, during biohydration. Dicarboxylic acids (such as fumaric and malic acids), which are intermediates in the propionic acid pathway, may also serve as alternative electron sinks for H_2. If H_2 accumulates, re-oxidation of NADH is inhibited inhibiting microbial growth, forage digestion and the associated production of acetate, propionate and butyrate. Thus any mitigation strategy aimed at reducing methanogen populations must include an alternative pathway for H_2 removal from the rumen as well. It should therefore be possible to reduce CH_4 production by inhibiting H_2 liberating reactions or by promoting alternative H_2-using reactions or routes for disposing of H_2 during fermentation.

8. Methane mitigation strategies

CH_4 mitigation strategies can be broadly divided into preventative and 'end of pipe' options. *Preventative measures* reduce carbon/nitrogen inputs into the system of animal husbandry, generally through dietary manipulation and, while a reduction in the volume of CH_4 emitted per animal may result, this is often secondary to the (primary) objective of improved productive efficiency. Alternatively, '*end of pipe*' options reduce—or inhibit—the production of CH_4 (methanogenesis) within the system of animal husbandry (Sejian et al., 2011a). Any reduction strategies must be confined to the following general framework viz.,

development priority, product demand, infrastructure, livestock resource and local resources. The most attractive emissions mitigation projects must balance the needs in all of these areas, so that no one factor creates a constraint on continued improvement in production efficiency, and the resulting CH_4 emissions reductions. Within this framework, CH_4 emissions mitigation options for enteric fermentation can encompass a wide range of activities across these areas. However, underlying these activities must be specific options for improving the production efficiency of the livestock. Without these options, CH_4 emissions cannot be reduced. The technologies that can reduce the amount of methane production in rumen or total release of methane into atmosphere are useful for efficient use of feed and making the environment more favourable. Several options have been considered for mitigating methane production and emitting in atmosphere by the livestock. All approaches point towards either reduction of methane production per animals or reduction per unit of animal product. There are several factors which need to be considered for selection of best options for methane emission reduction: these include climate, economic, technical and material resources, existing manure management practices, regulatory requirements etc. Generally the methane mitigation strategies can be grouped under three broader headings viz., managemental, nutritional and advanced biotechnological strategies (Sejian et al., 2011a). Figure 2 describes the salient enteric methane mitigation strategies.

8.1 Dietary manipulation

The chemical composition of diet is an important factor which affects rumen fermentation and methane emission by the animals. Methane production was significantly lower in the sheep fed on green sorghum and wheat straw in the ratio of 90:10 as compared to where the ratio was 60:40 (31.5*vs*46.91/kg). Improvement in the digestibility of lignocellulose feeds with different treatments also resulted in lower methanogenesis by the animals (Agrawal & Kamra, 2010). Wheat straw treated with urea (4kg urea par 100kg DM) or urea plus calcium hydroxide (3kg urea+3 kg calcium hydroxide per 100kg DM) and stored for 21 days before feeding, reduced methane emission from sheep. The treatment of straw with urea and urea molasses mineral block lick caused a reduction of 12-15% methane production and the molar proportion of acetate decreased accompanied with an increase in propionate production (Agrawal & Kamra, 2010). On inclusion of green maize and berseem in the ration, methanogenesis decreased significantly. By increasing the concentrate level in the paddy straw based diet there was a depression in methane production accompanied with an increase in propionate concentration in the rumen liquor. Castor bean cake and karanj cake inhibited methanogenesis significantly, but these two oil cakes also affected in *vitro* dry matter degradability of feed adversely, which might be due to the presence of anti-nutritional factors (kumar at al., 2007). Fumaric acid is a precursor of propionic acid in the fermentation of feed in the rumen and can act as an alternate sink for consumption of hydrogen generated in the rumen. The levels of fumaric acid required to inhibit methanogenesis to a significant extent may cause a drop in P^H which might affect feed fermentation adversely. Free fumaric acid (10% in the ration) and an equivalent amount of encapsulated fumaric acid decreased methane emission to the extent of 49% and 75% compared to control sheep without supplementation of fumaric acid (Agrawal & Kamra, 2010).

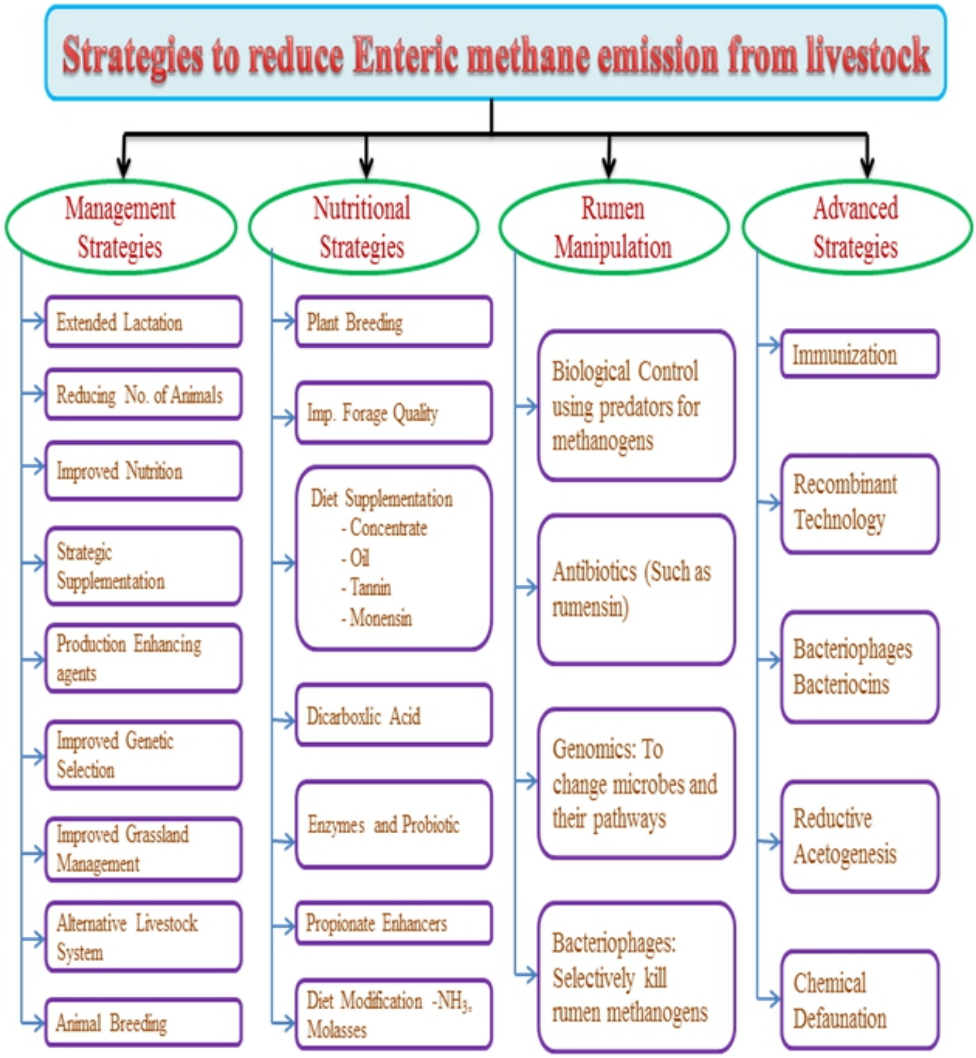

Fig. 2. Different enteric methane mitigation strategies

8.2 Increased proportion of concentrates in the diet

A higher proportion of concentrate in the diet leads to a reduction in CH4 emissions as a proportion of energy intake (Yan et al., 2000). The relationship between concentrate

proportion in the diet and methane production is curvilinear (Sauvant & Giger- Reverdin, 2007) with a marked decrease in methane observed when dietary starch is higher than 40%. Replacing plant fibre in the diet with starch induces a shift of VFA production from acetate towards propionate occurs, which results in less hydrogen production (Singh, 2010). A positive response to high levels of grain based concentrate on methane reduction has also been reported by others (Beauchemin & McGinn 2005; McAllister & Newbold, 2008). The metabolic pathways involved in hydrogen production and utilization and the activity of methanogens are two important factors that should be considered when developing strategies to control methane emissions by ruminants. Reduction of hydrogen production should be achieved without impairing feed fermentation. Reducing methanogens activity and/or numbers should ideally be done with a concomitant stimulation of pathways that consume hydrogen to avoid the negative effect of the partial pressure increase of this gas. Many mitigating strategies proposed have indeed multiple modes of action (Martin et al., 2008). Hydrogen gas produced during microbial fermentation of feed is used as an energy source by methanogens, which produce methane. Efficient H_2 removal is postulated to increase the rate of fermentation eliminating the inhibitory effect of H2 on the microbial degradation of plant material (McAllister & Newbold, 2008). The rate of CH4 formation is determined by the rate at which H2 passes through the dissolved pool, and the amount of CH4 formed is determined by the amount of H2 that passes thought the pool. The absolute amount of CH4 formed per animal on different diets is related to characteristics of the feed in complex ways incuding the nature and amount of feed, the extent of its degradation, and the amount of H2 formed from it (Singh, 2010).

8.3 Adding lipid to the diet

Dietary fat seems a promising nutritional alternative to depress ruminal methanogenesis without decreasing ruminal pH as opposed to concentrates (Sejian et al., 2011b). Addition of oils to ruminant diets may decrease CH4 emission by up to 80% in vitro and about 25% in vivo (Singh, 2010). Lipids cause depressive effect on CH4 emission by toxicity to methanogens, reduction of protozoa numbers and therefore protozoa associated methanogens, and a reduction in fibre digestion. Oils containing lauric Acid and myrstic acid are particulary toxic to methanogens. Beauchemin et al. (2008) recently reviewed the effect of level of dietary lipid on CH4 emissions over 17 studies and reported that with beef cattle, dairy cows and lambs, for every 1%(DMI basis) increase in fat in the diet, CH4 (g/kg DMI) was reduced by 5.6 %. In another review of fat effects on enteric CH4, (Martin et al., 2010) compared a total of 67 in vivo diets with beef, sheep and dairy cattle, reporting an average of 3.8% (g/kg DMI) less enteric CH4 with each 1% addition of fat (Singh, 2010).

8.4 Ionophores

Ionophores (e.g. monensin) are antimicrobials which are widely used in animal production to improve performance. Tadeschi et al. (2003) reported in a recent review that on feedlot and low forage diets, tend to marginally increase average daily gain whilst at the same time reducing DMI, thus increasing feed efficiency by about 6%. Monensin should reduce CH4 emissions because it reduces DMI, and because of a shift in rumen VFA proportions towards propionate and a reduction in ruminal protozoa numbers (Singh, 2010). In vivo

studies have shown that animals treated with monensin emit reduced levels of CH4 (e.g. McGinn et al., 2004; van Vugt at al., 2005) but others have reported no significant effect (e.g. Waghorn et al., 2008 van Vugt et al., 2005). Monensin causes a direct inhibition on H-producing bacteria (Russell and Houlihan, 2003) that results in a decrease in methane production due to shortage of molecular H. Monensin also favours propionate producing bacteria (Newbold et al., 1996).

8.5 Plant secondary metabolites

The term plant secondary metabolite is used to describe a group of chemical compounds found in plants that are not involved in the primary biochemical processes of plant growth and reproduction (Agrawal & Kamra, 2010). These compounds might function as a nutrient store and defence mechanisms which ensures survival of their structure and reproductive elements protecting against insect or pathogen predation or by restricting grazing herbivores. Several thousand of plant secondary metabolites have been reported in various plants and many of them have found their use in traditional Indian and Chinese system of medicine (Kumar at al., 2007).

8.5.1 Saponins

Numerous studies have demonstrated that Saponins and Saponin –containing plants have toxic effects on protozoa. Forages containing condensed tannins have been shown to decrease methane production by the ruminants. Tannins present in C*alliandra calothyrus* reduced nutrient degradation and methane release per gram of organic matter degraded in *in vitro* experiments with rumen simulation technique (RUSITEC) (Hess et al., 2003). Woodward et al. (2002) investigated the effect of feeding of sulla on methane emission and milk yield in Friesian and Jersey dairy cows. Cows feed sulla produced less methane per kg DM intake (19.5 vs. 24.6 g) and per kg milk solid yield (243.3 vs. 327.8 g). Similar trends in methane emission and milk production have been observed in sheep fed on lotus silage (Woodward et al., 2001).there was also 16 % reduction in methane production in lambs fed on *Lotus pedunculatus* (lotus), which might be due to the presence of condensed tannins (Waghorn et al., 2002). Another condensed tannins containing forage *Sericea lespedeza* (17.7% CT) decreased methane emission (7.4 vs. 10.6 g/d and 6.9 vs. 16.2 g/kg DMI for *sericea lespedeza* and crabgrass /tall fescue, respectively) in angora goats (Puchala et al., 2005; Agrawal & Kamra, 2010). *Bergenia crassifolia, Emblica officinalis, Peltiphyllum peltatum, Populus deltoids, Quercus Incana,rheum Undulatum, Terminalia belerica, Terminalia chebula* and *Vaccinium vitis-idaea* are some other plants containing high tannin contents and have a potential to inhibit *in vitro* as well as *in vivo* methane emission by the rumen microbes (Patra et al., 2006; kumar et al., 2009).

8.5.2 Essential oils

Allium sativum, Coriandrum sativum, Eucalyptus globules, Foeniculum vulgare, Mentha piperita, Ocimum sanctum, Populus deltoids and Syzygium aromaticum are some of the plants which contain high concentration of essential oils and are effective against methane emission and protozoa growth in the rumen, but some of them also have adverse effects on degradability of feed and nutrient utilization by the animals. The results of in vivo

experiments with these plants are also variable and need further experimentation before their practical application in the livestock production (Agrawal & Kamra, 2010).

8.6 Bacteriocins

Some bacteriocins are known to reduce methane production *in vitro* (Callaway et al., 1997, Lee et al., 2002). Nisin is thought to act indirectly, affecting hydrogen producing microbes in a similar way to that of the ionophore antibiotic monensin (Callaway et al., 1997). A bacteriocin obtained from a rumen bacterium, bovicin HC5, decreased methane production *in vitro* up to 50% without inducing methanogens adaptation (Lee et al., 2002). Klieve and Hegarty (1999) also suggested the use of archaeal viruses to decrease the population of methanogens.

8.7 Organic acids

Organic acids are generally fermented to propionate in the rumen, and in the process reducing equivalents are consumed. Thus they can be an alternative sink for hydrogen and reduce the amount of hydrogen used in CH4 formation. Newbold et al. (2005) reported fumarate and acrylate to be the most effective in batch culture and artificial rumen. There have been some recent in vivo studies. Newbold et al. (2002) reported a dose-dependent response to fumarate in sheep. Wallace et al. (2006) described a proportional reduction of 0.4-0.75 when encapsulated fumaric acid (0.1 % of diet) was fed to sheep. While the level of reduction in CH4 emissions that could be achieved is somewhat uncertain, the main impediment to this strategy is the current cost of organic acids which makes their use uneconomical. Integrated research investigating animal, plant, microbe and nutrient level strategies might offer a long term solution of methane production. At the animal level, genetic selection is the area of research with the best chance of finding a solution. At the microbe level, vaccination and probiotics are the promising approaches for future research. Any mitigation strategy that reduces methanogen populations must also include an alternative pathway for H2 removal from the rumen. Improvement and breeding of plants is another helpful way to control of methanogenesis, but the estimation of time required must be realistic. Strategies must however suit particular classes of livestock. Advances brought about through rumen metagenomic projects and the utilization of new technologies will broaden our understanding of the mechanisms involved in methanogenesis and other metabolic H2- consuming and releasing processes, and will help find new tools for mitigation (Morgavi et al., 2010). The sustainability of methane suppressing strategies is an important issue. There is an urgent need for support model that is capable of evaluating the effectiveness of both existing and new technologies for reducing methane emission.

9. Methane mitigation strategies from livestock manure

Manure from confined livestock operations is most often stored in solid or liquid form before being applied to agricultural land. Increasingly, however, manure is composted before land application or anaerobically digested to produce CH_4 as bio-fuel. Methane emissions from anaerobic digestion can be recovered and used as energy by adapting manure management and treatment practices to facilitate methane collection. This methane

can be used directly for on-farm energy, or to generate electricity for on-farm use or for sale. The other products of anaerobic digestion, contained in the slurry effluent, can be utilized in a number of ways, depending on local needs and resources. Successful applications include use as animal feed and aquaculture supplements, in fish farming, and as a crop fertilizer. Additionally, managed anaerobic decomposition is a very effective method of reducing the environmental and human health problems associated with manure management. The controlled bacterial decomposition of the volatile solids in manure reduces the potential for contamination from runoff, significantly reduces pathogen levels, removes most noxious odors, and retains the organic nitrogen content of the manure.

Depending on the management system used, greenhouse gas emissions (mainly CH_4 and N_2O) from manure vary considerably. Strategies to mitigate net emissions aim to change manure properties or the conditions under which CH_4 and N_2O are produced and consumed during manure storage and treatment. The selection of successful methane emissions reduction options depends on several factors, including climate; economic, technical and material resources; existing manure management practices; regulatory requirements; and the specific benefits of developing an energy resource (biogas) and a source of high quality fertilizer.

One such strategy is to manipulate livestock diet composition and/or include feed additives to alter manure pH, concentration and solubility of carbon and nitrogen, and other properties that are pertinent to CH_4 and N_2O emissions.

Another manure management option is to change the material used for bedding the animals, which could also affect manure pH and soluble C and N levels, and thus the emissions during manure storage and treatment.

Composting technology, control of aeration, use of amendments, or co-composting livestock manure with other organic waste could also potentially modify conditions for GHG production and emission. The use of covers may also help retain N nutrients during storage.

Manure mitigation includes both low-tech strategies like covering and cooling manure lagoons during storage and alternative techniques for manure dispersion and application (Weiske et al., 2006; IPCC, 2007b). More advanced technologies include frequent manure removal from animal housing into covered storage using scraping systems (Weiske et al., 2006) as well as farm scale or centralized digesters for biogas generation and utilization (DeAngelo et al., 2006, USEPA, 2006). In small-scale farm digesters, biogas from local manure may be used for electricity and/or heat production. Larger, centralized digesters can also take in additional organic wastes. There are many different digester designs ranging from low-tech small-scale to high-tech large-scale models, for example polyethylene bag or covered lagoon digesters for cooking fuel, light flexible-bag digesters, and large-scale dome digesters (USEPA, 2006). With the use of liquid-based systems, the primary method for reducing emissions is to recover the methane before it is emitted into the air. Methane recovery involves capturing and collecting the methane produced in the manure management system. This recovered methane (a medium Btu gas with about 500-600 Btu/ft^3) can be flared or used to produce heat or electricity. Because most of the manure facility methane emissions occur at large confined animal operations (primarily dairies and hog farms), the most promising options for reducing these emissions involve recovering the

methane at these facilities and using it for energy. Three methane recovery technologies are available:

9.1 Covered anaerobic digesters

These are the simplest form of recovery system, and can be used at dairy or swine farms in temperate or warm climates. Manure solids are washed out of the livestock housing facilities with large quantities of water, and the resulting slurry flows into an anaerobic primary lagoon. The average retention time for the manure in the lagoon is about 60 days. The anaerobic conditions result in significant methane emissions, particularly in warm climates. The covered lagoons are air-tight and provide the anaerobic conditions under which methane is produced and recovered which can be used as energy. Lagoons are most commonly used at large confined dairy and swine facilities in North America, Europe, and regions of Asia and Australia.

9.2 Complete mix digesters

This type of digesters presents a methane recovery option for all climates. They are heated, constant-volume, mechanically-mixed tanks that decompose medium solids swine or dairy manure (3-8% total solids) to produce biogas and a biologically stabilized effluent. The manure is collected daily in a mixing pit where the percent total solids can be adjusted and the manure can be pre-heated. A gas-tight cover placed over the digester vessel maintains anaerobic conditions and traps the methane that is produced. The produced methane, representing about 8 to 11 percent of the total manure, is removed from the digester, processed, and transported to the end use site.

9.3 Plug flow digesters

This type of digesters only works with dairy scraped manure and cannot be used with other manures. These are constant volume, flow-through units that decompose high solids dairy manure (>11% solids) to produce biogas and a biologically stabilized effluent. The basic plug flow digester design is a long tank, often built below ground level, with a gas-tight, expandable cover. A gas-tight cover collects the biogas and maintains anaerobic conditions inside the tank. The amount of methane produced is about 40 cubic feet per cow per day.

10. Conclusions

Given that the livestock production system is sensitive to climate change and at the same time itself a contributor to the phenomenon, climate change has the potential to be an increasingly formidable challenge to the development of the livestock sector. Responding to the challenge of climate change requires formulation of appropriate adaptation and mitigation options for the sector. Although the reduction in GHG emissions from livestock industries are seen as high priorities, strategies for reducing emissions should not reduce the economic viability of enterprises if they are to find industry acceptability.

11. Future scope of research

Prioritized research need to address using of advanced molecular technology to reduce livestock methane emission. Both conventional and non-conventional feed resources need to

be tried for their potential to affect methane emission by the animals. Further, the research addressing chemical feed additives need to ensure that there are no side effects on feed utilization and no residues left in the livestock products like meat and milk. In addition, while attempting to use plant secondary compounds to reduce enteric methane emission care needs to be taken to ensure optimum dose of such compounds so that there is no toxic effects on rumen microbes. Finally, in depth research need to be undertaken to identify the microbial feed additives such as reductive acetogenic bacteria, yeasts and other microbes which may manipulate rumen fermentation and reduce methane emission.

12. Acknowledgement

The authors are highly thankful to the Senior Research Fellows Miss Saumya Bahadur, Mr. Anoop Kumar, Miss Indu Shekhawat and lab assistant Mr.Ajay Kumar Singh for their valuable help in preparing this manuscript.

13. References

Agrawal, D.K & Kamra, D.N (2010). Global warming: Role of livestock and mitigation strategies. In: International conference on "Physiological capacity building in livestock under changing climate scenario". Physiology and Climatology division, Indian Veterinary Research Institute, Izatnagar, 243122, Uttar Pradesh, India, November 73-80, pp 27-39.

Beauchemin, KA & McGinn, SM (2005) Methane emissions from feedlot cattle fed barley or corn diets. *Journal of Animal Science,* 83, pp 653-661.

Beauchemin, K.A., Kreuzer, M., O'Mara, F & McAllister, T.A (2008). Nutritional management for enteric methane abatement: a review. *Australian Journal of Experimental Agriculture*, 48(1-2), pp 21–27.

Bright, KP., Sherlock, RA., Lile, J & Wastney ME (2000). Development and use of a whole farm model for dairying, Applied Complexity:From Neural Nets to Managed Landscapes, NZ Institute for Crop and Food Research,Christchurch, NZ, pp 382-389.

Callaway, TR., Carneiro, De Melo, AMS & Russell, JB (1997). The effect of nisin and monensin on ruminal fermentations in vitro. *Current Microbiology,* 35, pp 90–96.

Chhabra A, Manjunath KR, Panigrahy S & Parihar JS (2009). Spatial pattern of methane emissions from Indian livestock. *Current Science,* 96(5), pp 683-689.

DeAngelo, B.J. de la Chesnaye, FC., Beach, RH., Sommer, A & Murray, BC (2006). Methane and Nitrous Oxide Mitigation in Agriculture, *The Energy Journal*, Multi-Greenhouse Gas Mitigation and Climate Policy, Special Issue 3, 89-108.

Ellis, JL., Kebreab, E., Odongo, NE., McBride, BW., Okine, EK & France, J (2007). Prediction of methane Production from Dairy and Beef Cattle. *Journal of Dairy Science*, 90, pp 3456–3467.

Ellis, JL., Bannink, A., France, J., Kebreabz, E & Dijkstra J (2010). Evaluation of enteric methane prediction equations for dairy cows used in whole farm models. *Global Change Biology*, doi: 10.1111/j.1365-2486.2010.02188.x

FAO (Food and Agricultural Organization of the United Nation), (2008). FAOSTAT.

FAO (Food and Agriculture Organization of the United Nations), 2006. Livestock a Major Threat to the Environment: Remedies Urgently Needed. Available: http://www.fao.org/newsroom/en/news/2006/1000448/index.html

Gibbs, M & Johnson, D E (1994). Methane Emissions from Digestive Processes of Livestock', In: *International Anthropogenic Methane Emissions: Estimates for 1990,* EPA 230R-93-010, pp.*2-1-2-44.*

Gleik, PH., Adams, R.M. & Amasino R.M., (2010). Climate Change and the Integrity of Science. *Science,* 328, pp 689-691.

Hess, HD., Monsalve, L.M., Lascano, C.E., Carulla, J.E., Diaz, T.E & Kreuzer, M (2003). Supplementation of a tropical grass diet with forage legumes and Sapindus saponaria fruits: effect on in vitro ruminal nitrogen turnoverand methanogenesis. *Australian Journal of Agricultural Research,* 54, pp 703–713.

IPCC (Intergovernmental Panel on Climate Change), (1997) Guidelines for National GHG Inventories: Workbook and Reference Manual. Agriculture (Chapter 4) and Waste (Chapter 6). OECD, Paris, France.

IPCC (Intergovernmental Panel on Climate Change), (2001) Climate change 2001: the scientific basis. Intergovernment panel on climate change. Cambridge, UK: Cambridge University Press.

IPCC (Intergovernmental Panel on Climate Change), (2007a). Brussels: Intergovernmental Panel on Climate Change. Climate Change 2007: Impacts, Adaptation and Vulnerability.

IPCC (Intergovernmental Panel on Climate Change), (2007b). Climate Change: Synthesis Report; Summary for Policymakers. Available: http://www.ipcc.ch/pdf/assessment-report/ar4/syr/ar4_syr_spm.pdf.

IPCC, (2001). Technical Summary: contribution of working group I to the Third Assessment Report. Intergovernmental Panel on Climate Change. http://ipcc.org.third assessment report/.

Johnson, DE., Ward, GW & Ramsey, JJ (1996). Livestock methane:Current Emissions and Mitigation Potential. Lewis Publishers, New York, NY.

Johnson, KA & Johnson, DE (1995). Methane emissions from cattle. *Journal of Animal Science,* 73, pp 2483–2492.

Johnson, D.E., Phetteplace, H.W &. Seidl, A.F (2002). Methane, nitrous oxide and carbon dioxide emissions from ruminant livestock production systems. In GHGes and animal agriculture. Proceeding of the 1st International Conference on GHGes and Animal Agriculture, Obihiro, Japan, November 2001 (eds. J. Takahashi and B.A. Young), pp. 77-85.

Kebreab, E., Johnson, KA., Archibeque, SL., Pape, D & Wirth, T (2008). Model for estimating enteric methane emissions from United States dairy and feedlot cattle. *Journal of Animal Science,* 86, pp 2738-2748.

Klieve, AV & Hegarty. RS (1999). Opportunities of biological control of ruminant methanogenesis. *Australian Journal of Agricultural Research*, 50, pp 1315-19.

Kumar, R., Kamra, DN Agarwal N. &. Chaudhary, L C (2007). *In vitro* methanogenesis and fermentation of feeds containing oil seed cakes with rumen liquor of buffalo. Asian-*Aust. J. Anim. Sci.,* 20, pp 1196-1200.

Kumar, S., Puniya, A., Puniya, M., Dagar, S., Sirohi, S., Singh, K & Griffith, G. (2009). Factors affecting rumen methanogens and methane mitigation strategies. *World Journal of Microbiology and Biotechnology.* 25, 1557-1566.

Lassey, K.R (2007). Livestock methane emission: From the individual grazing animal through national inventories to the global methane cycle. *Agric For Meteorol.,* 142, 120–132.

Lee, SS, Hsu, JT, Mantovani, HC & Russell, JB (2002). The effect of bovicin HC5, a bacteriocin from *Streptococcus bovis* HC5, on ruminal methane production *in vitro*. *FEMS Microbiol. Lett.,* 217, pp 51–55.

Leng, R.A., (1993). The impact of livestock development on environmental change. FAO corporate documentary repository, pp 1-14.

Martin, C., Rouel, J., Jouany, JP., Doreau, M & Chilliard, Y (2008) methane output and diet digestibility in response to feeding dairy cows crude linseed, extruded linseed, or linseed oil. *J Anim Sci.,* 86, pp 2642-2650.

Martin, C., Morgavi, D.P & Moreau, D (2010). Methane mitigation in ruminants: from microbe to the farm scale. *Animal,* 4, pp 351–365.

McAllister, TA. & Newbold, CJ (2008). Redirecting rumen fermentation to reduce methanogenesis. *Australian Journal of Experimental Agriculture,* 48 (1-2), pp 7-13.

McAlpine, CA., Syktus, JI., Deo, RC., Ryan, JG., McKeon, G., McGowan, HA & Phinn, S, (2009). An Australian continent under stress: A conceptual overview of processes, feedbacks and risks associated with interaction between increased land use pressures and a changing climate. *Global Change Biology*, doi: 10.1111/j.1365-2486.2009.01939.x.

McGinn, SM., Beauchemin, KA., Coates, T & Colombatto, D (2004). Methane emissions from beef cattle: Effects of monensin, sunflower oil, enzymes, yeast, and fumaric acid. *J Anim Sci*., 82, pp 3346–3356.

McMichael, AJ., Powles, JW., Butler WCD & Uauy, R (2007). Food, livestock production, energy, climate change, and health. The Lancet, 370(9594): 1253 – 1263.

Meadows, DH., Meadows, DL & Randers, J (1992). Beyond the Limits. Earthscan Publications Ltd., London.

Mills, JAN., Kebreab, E., Yates, CM., Crompton, LA., Cammell, SB., Dhanoa, MS., Agnew, RE & France, J (2003). Alternative approaches to predicting methane emissions from dairy cows. *J Anim Sci.,* 81, pp 3141-3150.

Moe, PW., Tyrrell, HF (1979). Methane production in dairy cows. *J Dairy Sci.,* 62, 1583–1586.

Morgavi, DP., Forano, E., Martin, C & Newbold, CJ (2010). Microbial ecosystem and methanogenesis in ruminants. *Animal* 4, pp 1024-1036.

Moss, AR., Jounany, JP & Neevbold, J (2000). Methane Production by ruminants: Its Contribution to Global warming. *Ann Zootech.,* 49, pp 231-253.

NASA (National Aeronautics and Space Administration)2006. 2005 Warmest Year in Over a Century.

Neil, PG., Bright ,KP & Sherlock RA (1997). Integrating legacy subsystem components into an object-oriented model, MODSIM 97 – Proceedings of the International Conference on Modelling and Simulation, Modelling and Simulation Society of Australia, Hobart, AU., pp 1133-1138.

Newbold, CJ., López, S., Nelson, N., Ouda, JO., Wallace, RJ & Moss, A.R (2005). Propionate precursors and other metabolic intermediates as possible alternative electron acceptors to methanogenesis in ruminal fermentation in vitro. *Br. J. Nutr*., 94, pp 27–35.

Newbold, CJ., Ouda, JO., López, S., Nelson, N., Omed, H., Wallace, RJ & Moss, A.R., 2002. Propionate precursors as possible alternative electron acceptors to methane in ruminal fermentation. In: Takahashi, J., Young, B.A., Soliva, C.R., Kreuzer, M. (Eds.), The 1st International Conference on Greenhouse Gases and Animal Agriculture GGAA2001. Elsevier Health Sciences, Tokachi Plaza, Japan, pp. 272–279.

Newbold, CJ., Wallace, RJ & McIntosh, F.M (1996). Mode of action of the yeast Saccharomyces cerevisiae as a feed additive for ruminants. *Br. J. Nutr*., 76, pp 249–261.

NOAA (National Oceanic and Atmospheric Administration) (2007). NOAA Says U.S. Winter Temperature Near Average, Global December-February Temperature Warmest on Record [Press release].

Palliser, CC & Woodward, SL (2002). Using models to predict methane reduction in pasture fed dairy cows. Proceedings Integrating Management and Decision Support. Coordinated by Susan M. Cuddy (CSIRO, Australia). Parte 1, vol. 482, p.162-167.

Patra, AK., Kamra, D & Agarwal, N (2006). Effect of plant extract on *in vitro* methanogenesis, enzyme activities and fermentation of feed in rumen liquor of buffalo, *Animal Feed Science and Technology*, 128, pp 276–291.

Puchala, R., Min, BR., Goetsch, AL & Sahlu, T (2005). The effect of a condensed tannin-containing forage on methane emission by goats. *J Anim Sci.,* 83, 182-186.

Rotz, CA., Corson, MS & Coiner CU (2007). Integrated Farm System Model: Reference Manual. Pasture Systems and Watershed Management Research Unit, USDA Agricultural Research Service: University Park, PA. Available at: http://www.ars.usda.gov/Main/docs.html?docid=8519.

Rotz, CA., Corson, M S., Chianese, DS & Coiner, CU (2009). *The Integrated Farm System Model: Reference Manual*.University Park, Pa.: USDA-ARS Pasture Systems and Watershed Management research unit: www.ars.usda.gov/SP2UserFiles/Place/19020000/ifsmreference.

Russell, J & Houlihan, A (2003). Ionophore resistance of ruminal bacteria and its potenial impact on human health. *FEMS Microbiol. Rev*., 27, pp 65-74.

Sarmah, B.C (2010). Impending climate changes on animal production and health. In: International conference on "Physiological capacity building in livestock under changing climate scenario". Physiology and Climatology division, Indian Veterinary Research Institute, Izatnagar, 243122, Uttar Pradesh, India, November 11-13, pp 81-88.

Sauvant, D & Giger-Reverdin, S (2007). Empirical modelling meta-analysis of digestive interactions and CH4 production in ruminants. In: Energy and Protein Metabolism and Nutrition, EAAP publication 124, p 561, Wageningen Academic Publishers, the Netherlands.

Sejian, V., Lakritz, J., Ezeji, T & Lal, R (2011b). Forage and Flax seed impact on enteric methane emission in dairy cows. *Research Journal of Veterinary Sciences*, 4(1), pp 1-8.

Sejian, V., Lal, R., Lakritz, J and Ezeji, T (2011a). Measurement and Prediction of Enteric Methane Emission. *International Journal of Biometeorology*, 55, pp 1-16.

Singh, B (2010). Some nutritional strategies for mitigation of methane emissions. In: International conference on "Physiological capacity building in livestock under changing climate scenario". Physiology and Climatology division, Indian Veterinary Research Institute, Izatnagar, 243122, Uttar Pradesh, India, November 11-13, pp 142-158.

Steinfeld, H., Gerber, P., Wassenaar, T., Castel, V., Rosales, M & de Haan, C (2006). Livestock's Long Shadow: Environmental Issues and Options. Rome: Food and Agriculture Organization of the United Nations.

Tamminga, S (1996) Areview on environmental impacts of nutritional strategies in ruminants. *J Anim Sci.*, 74, pp 3112–3124.

Tedeschi, L., Fox, D., Tylutki, T. 2003. Potential Environmental Benefits of Ionophores in Ruminant Diets. *Journal of Environmental Quality,* 32, pp 1591-1602.

Topping JC, Jr (2007). Summit Aftermath: Study by NASA and University Scientists Shows World Temperature Reaching a Level Not Seen in Thousands of Years and Raises Grave Concern of Irreparable Harm.

UNFCCC (1998). Kyoto protocol to the United Nations Framework Convention on Climate Change. United Nations, pp 1-20.

UNFCCC (2008). National greenhouse gas inventory data for the period 1990–2006. United Nations, pp 1-12.

USEPA, (2006). Global Mitigation of Non-CO2 Greenhouse Gases. U.S. Environmental Protection Agency, Office of Atmospheric Programs (6207J), Washington, DC.

van Vugt, S.J., Waghorn, G.C., Clark, D.A & Woodward, S.L (2005). Impact of monensin on methane production and performance of cows fed forage diets. *Proc. N.Z. Soc. Anim. Prod.* 65, pp 362–366.

Waghorn, GC., Tavendale, M & Woodfield, DR (2002). Methanogenesis from forages fed to sheep. *Proc New Zealand Grassland Assoc.*, 64, pp 167-171.

Waghorn, G.C., Clark, H., Taufa, V & Cavanagh, A (2008). Monensin controlledrelease capsules for methane mitigation in pasture-fed dairy cows. *Aust.J. Exp. Agric.*, 48, pp 65–68. doi:10.1071/EA07299.

Wallace, R J., Wood, TA., Rowe, A., Price, J., Yanez, DR., Williams, SP & Newbold, CJ (2006). Encapsulated fumaric acid as a means of decreasing ruminal methane emissions. *Int. Congr. Ser.*, 1293, pp 148–151.

Weiske, A., Vabitsch, A., Olesen, JE., Schelde, K., Michel, J., Friedrich, R & Kaltschmitt, M (2006). Mitigation of greenhouse gas emissions in European conventional and organic dairy farming, *Agriculture, Ecosystems and Environment,* 112, pp 221-232.

Woodward, SL., Waghorn, G C. , Lassey, KR & Laboyrie, PG (2002). Does feeding sulla (*Hedysarum coronarium*) reduce methane emission from dairy cows? *Proc. N.Z. Soc. Anim. Sci.,* 62, pp 227–230.

Woodward, SL., Waghorn, G C., Ulyatt, MJ & Lassey, KR (2001). Early indications that feeding Lotus will reduce methane emission from ruminants. *Proc. N.Z. Anim. Prod.*, 61, 23–26.

Yan, T., Agnew, RE., Gordon, FJ & Porter, MG (2000). Prediction of methane energy output in dairy and beef cattle offered grass silage based diets. *Livest Prod Sci*., 64, 253-263.

12

General Equilibrium Effects of Policy Measures Applied to Energy: The Case of Catalonia

Maria Llop
Universitat Rovira i Virgili and CREIP
Spain

1. Introduction

In the last decades, the negative externalities caused by the economic activity on the environment have become a crucial subject in most countries. In particular, it has emerged a debate focused on and the measures that need to be taken to mitigate the adverse effects of human kind on the natural ecosystems. This debate has been intensified during the last twenty years because of climate change (Stern, 2006). Nowadays, there exists the consensus that climate change is a problem that affects the whole world and, accordingly, the solution requires a global response.

On the other hand, researchers have developed a conceptual set to define and implement pollution abatement measures to be successful in preserving the environment and to mitigate the negative effects of humans on the environment. Nowadays, policy makers have at hand different policy measures, which can alternatively be applied in an economy, aimed at reducing the pollution generation. This leads to the question of which are the effects of the different measures, how agents are affected and which are the positive effects on the environment. Then, there is the need of using analytical instruments able to calculate the impacts caused by the alternative policy interventions in order to get the maximum positive effects on environment compatible with the minimum affectation on the economic activity.

Modelling an economy with all its interrelations, agents and sectors is complex. In an economic system, there is a large number of agents, goods and markets, each one characterised by its corresponding optimisation behaviour, that are difficult to be jointly captured in an economic model. For this reason, environmental policies have usually been studied in a partial equilibrium context. However, we must bear in mind that many of the measures have also an impact on variables not directly related with the interventions, because of the indirect effects that have to be added to the immediate (direct) effects. Then, in order to understand the entire impacts of economic policies on the environment or, on the contrary, the effects of environmental protection on macroeconomic variables, we need to use models able to capture the complex interrelations existing between the different sectors and agents of the economy.

The computable general equilibrium (CGE) models are useful instruments to analyse the effects of policy measures and changes in the economic scenarios on the main economic indicators, such as the level of sectoral production, the consumption price index, the GDP,

the private income, the public deficit or the level of public activity. Moreover, CGE models can also be used to show the effects on environmental variables such as water consumption, greenhouse emissions and waste generation. One of the main advantages of general equilibrium, compared with partial equilibrium models, is that it allows to capture all the economic agents and their economic optimisation. Given that all the markets and agents are included, the CGE models provide a solution not only taking into account the direct impacts between variables and agents but also taking into account the indirect effects explained by the interdependence between agents and markets.

Recently, computable general equilibrium analysis has become a promising method to assess the impact of different energy and environmental policies on economic and environmental variables. The CGE framework allows to calculate the effects of a certain policy on pollutant emissions, the economic costs associated with this policy, and the economic and social costs and benefits stemming from such public intervention. One of the first studies were Goulder (1992) for the USA, Pireddu and Dufournand (1996) for Italy, and Böhringer and Rutherford (1997) for Germany.

For Spanish applications, Labandeira and Rodríguez (2004) studied the impact of an environmental tax on carbon dioxide emissions. Manresa and Sancho (2005) analysed the costs and benefits of a tax policy aimed at reducing the CO_2 pollution in Spain. Faehn et al. (2009) analysed fiscal and environmental aspects using a general equilibrium model with imperfect competition. At the regional level, André, Cardenete and Velázquez (2005) and González and Dellink (2006) assessed the impact of an environmental tax reform on the regional economies of Andalusia and the Basque Country, respectively.

With regard to the emission objectives, the European Union (EU) signed in 2008 a climate change agreement known as "20-20-20 European Directive". This agreement is aimed at reducing the Union's greenhouse gas emissions by 20% before the year 2020. Additionally, this plan also establishes that 20% of the energy used in Europe has to come from renewable sources, and that energy efficiency has to be improved by 20% in 2020.

Taking into account the recent European directive, it seems crucial to study the different options that policy makers have at hand to reduce the pollutant gas emissions. In this chapter, it is used a CGE model to analyse the economic effects on the regional economy of Catalonia of the implementation of policies applied on the energy activities.[1] Similarly to the present objective, Llop and Pié (2008) analysed the economic impact associated to alternative policies designed to reduce pollutant emissions in the Catalan economy with the use of a linear model of prices based on an input-output framework. This paper analysed the effects caused by a new taxation on the energy consumption and a reduction in the energy used by agents. The present study is a further analysis than that in Llop and Pié (2008) because, as it is based on a general equilibrium model, it reflects not only the structure of production but also the rest of economic agents (consumers, government and foreign sector) in the determination of prices in the economy. The present model also assumes a non-linear technology of production that, differently to the input-output model, allows to show substitution possibilities between the elements that compound the structure of production.

[1] The region of Catalonia is located in the North-East of Spain. It is a very dynamic region representing around 20% of the Spanish GDP and 18% of the Spanish population.

The rest of the chapter is organised as follows. The next section describes the characteristics of computable general equilibrium models and the construction phases which are common in CGE modelling. The third section describes the model for the Catalan economy and the fourth section presents the database used to calibrate all the exogenous parameters. The fifth section shows the main results of the simulations. At the end of the paper, some concluding remarks are pointed out.

2. Description of computable general equilibrium models

In the last decades, it has been developed a useful set of analytical instruments which have helped economists and policy makers to improve their knowledge about the relationships between economic agents, such as firms, public institutions, consumers and foreign agents. Partial equilibrium models have largely been used to analyse the economic impact of changes in economic scenarios and policy interventions. However, partial equilibrium approaches are focused on the immediate effects existing in a specific economic environment, and do not take into account the indirect effects which, in most cases, can be of importance. Therefore, partial equilibrium approaches do not capture the complete chain of impacts of public interventions and, consequently, the results of partial equilibrium analysis can be inaccurate and incomplete. The consequence is that the outcomes of partial equilibrium studies can lead to imprecise conclusions. Recently, computable general equilibrium models have become useful tools to analyse the effects caused by public interventions and other changes in the economic systems. Generally, general equilibrium approaches make an extensive representation of an economy including all the agents and their decisions of optimisation. Moreover, CGE models make a complete and systematic representation of the way in which agents interrelate among them, and this allows to capture the complete sequence of impacts when there is some alteration in one part of the economic system.

The computable general equilibrium techniques are based on the concept of general equilibrium, which at the same time responds to the Walrasian idea of interrelation and interdependence between agents and markets, to analyse the effects of different economic measures or changes in the economic relations. In fact, a CGE model is an empirical representation of an economy in which all the markets are interrelated and in which the prices of goods, services and primary factors guarantee a situation of equilibrium in this economy.

It is important to bear in mind that under the CGE analysis there is no a unique way of representing an economy, its agents and their optimization behaviour, and this in turn greatly determines the models' final characteristics. From a practical point of view, the structure and characteristics of a particular model will depend, to a greater extent, on both the problem under analysis and the data availability to researchers.

The institutional classification of the economic agents and their optimisation behaviour are crucial aspects in determining the final characteristics of the general equilibrium models. Despite there is a large set of possibilities in designing a CGE model, we can describe some steps that are common within the process of computable equilibrium techniques. Figure 1 schematically reflects the sequence in the construction of an applyed general equilibrium model.

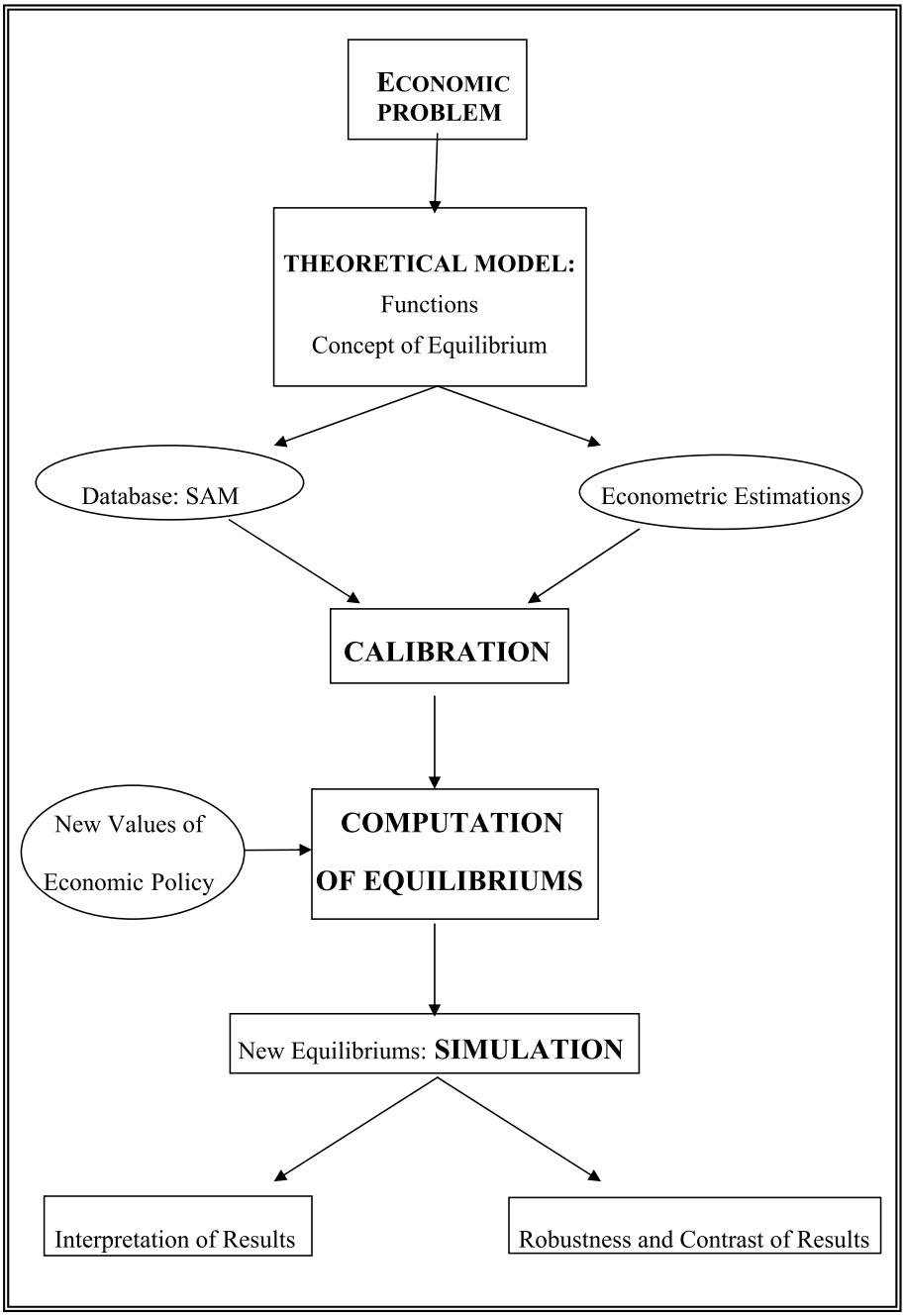

Source: own elaboration.

Fig. 1. Construction of a CGE Model

The construction of a CGE model starts with the definition of a theoretical set that is a simplified representation of the economy under study (Kehoe (1996) and Manresa (1996)). This step is very relevant because, among other decisions, it have to be determined the type of agents in the model and the degree of disaggregation that should be used when representing the economy's agents and institutions and the optimization rules that characterise such agents. As it is logical, the objectives of the analysis will determine the definition of agents and their economic behaviour and, additionally, the availability of information to researchers will force to use a disaggregation according to data.

A second step consists in designing the analytical context in which the economic behaviour of consumers, producers, government and foreign agents is to be identified. Consumers have some initial endowments (of goods and factors of production), and a set of preferences, which allow to obtain the final demand functions for each good. The market demand is the result of adding the individual demands, and it has some important properties; it is continuous, non-negative and accomplishes the Walras' law. As it is well-known, Walras's law says that for any set of prices, the total value of consumers' expenditures equals consumers' revenues. The resulting market demands are homogeneous of grade zero, and this means that only the relative prices are significant in the decisions of consumption and saving of private agents. This is an important property because it means that the changes in the absolute level of prices have no impact on the resulting equilibrium, and only the changes in relative prices modify the agents' decisions.

The production functions of CGE models usually define constant-returns-to-scale, and producers choose those quantities of both primary inputs and factors of production that ensure the maximum level of profits. Despite this is the normal representation of technology, the literature of CGE models can also show increased returns to scale in some sectors and companies as well as imperfect competition (an example of these modifications to the normal model's specification can be found in Bonano (1990)). On the other hand, the equilibrium must guarantee that demand equals to supply in all markets of goods and factors of production. In other words, the equilibrium is characterised by a set of relative prices and levels of production in each industry for which the demand equals to supply in all markets. Despite this is the normal market situation, it can also be defined an excess of supply or surplus in some markets. With constant-returns-to-scale, the objective of maximum profit implies that the only possible solution for sectors is the one that gives null sectoral profits.

CGE models also incorporate the public agent or government, that transfers income to the rest of agents (households and firms), and supplies public goods through the public expenditure activity. As any economic agent, government maximizes its utility, subject to their income restriction. This agent collects taxes, which are the main source of public income, and may have a public deficit which, in this case, is financed by the rest of economic agents.

General equilibrium models also define the external sector, that includes all the income relations of the economy with foreign agents and foreign markets. As there are many different ways to define the external relations of the economy, computable general equilibrium models can differ widely depending not only on the number of foreign agents involved but also on the type of behaviour assumed to this part of the model.

Once the theoretical model and its basic characteristics have been defined, the type of the functional forms of each part of the model has to be decided. The choice of functional forms depends on both the availability of data and the objectives of the analysis. Functions like Cobb-Douglas, Constant Elastic Substitution (CES), Leontief, or Lineal Expenditure Systems (LES) are frequently used because the parameters involved can be easily obtained compared with other analytical expressions that, despite being more general and flexible, have the inconvenient of requiring a large amount of data not always available to researchers.

At this point, when the complete structure of the model and its functional forms have been defined, we need to specify all the values of the parameters (or exogenous variables) involved in the model's structure. These parameters can be obtained by using both econometric estimations and calibration (for instance, Mansur and Whalley (1984) made a complete description of calibration). The method of calibration requires a database that consistently reflects all the flows of goods, services and income between the economic agents during a specific period, which will be considered the reference situation of the economy (benchmark equilibrium). This database is a social accounting matrix (or SAM) which has a structure of a double-entry table containing all the income flows of agents in rows and the corresponding expenditures in columns. Usually, the information required to construct a SAM comes from different sources, such as national product accounts, input-output matrices and other economic surveys (Pyatt (1988)). It is necessary to remark, however, that there are CGE models that do not use any SAM to calibrate their parameters and they use macroeconomic data directly from statistical sources but this is not the normal practice in applied general equilibrium research.

The calibration method has been criticised by econometricians because there is no any statistical test to determine the reliability of the values obtained for the parameters of CGE models (see Hansen and Heckman (1996) for an argument against calibration). Despite these methodological problems, calibration has many advantages given that it requires much less data than economic estimations. This explains why calibration is the most commonly used method in computable general equilibrium research. Related to this subject, Whalley (1991) described the main advantages of using calibration in CGE modelling in contrast with econometric estimations, which can be summarised in the following ideas:

- The large number of parameters of any computable general equilibrium model requires a great number of observations if econometric estimations have to be undertaken.
- There is a difficulty in treating value, and its separation between prices and quantities in observations makes it difficult to estimate the parameters econometrically.
- The large dimension of CGE models implies that the construction of equilibrium datasets (that is, reference equilibrium databases) requires a large set of statistical information; hence the research could not be viable if the construction of time series is needed to econometrically estimate all the parameters involved in CGE models.

Despite the disadvantages of using statistical methods, econometric estimations of parameters can also be used in CGE models (Jorgenson, 1984). Specifically, the literature shows some models that use statistical estimations while other models combine calibration and econometric estimation to obtain all the exogenous variables required.

Once the exogenous parameters have been obtained, the model can be represented as a system of equations where the variables to be determined (i.e. the endogenous variables) are

the prices of goods, the prices of services, the prices of factors, the levels of sectoral activity, as well as other relevant variables. At this point, the system can be solved by using a computer program such as MPS/GE, GEMODAL, GEMPACK or GAMS. The computation of the model provides an initial solution, which is considered the starting point of the analysis. This initial solution, or benchmark equilibrium, can be compared with new situations that will be analysed in the model.

The simulation analysis consists of applying new values for the exogenous variables of the model. This procedure, which is in fact an experiment of comparative statics, has the objective of calculating which would be the consequences of adopting economic measures without putting such measures into practice or, in case of being applied, which are the entire economic effects on agents and markets.

The following step in the CGE construction is the analysis and interpretation of the results. In fact, this is a very important phase given that it is crucial to analyze the robustness that must be attributed to the results obtained with the model. Robustness means, on the one hand, whether the variables are sensitive to small variations in some of the parameters of the model, and on the other hand, if the variables are sensitive to certain specifications of the functional forms (see Harrison and Vinod (1992) for a discussion about this problem). This is an important analysis because it allows to identify relevant aspects of the economy that could influence the outcomes of the model.

Finally, whenever possible, the results of the model must be contrasted with reality. For instance, Kehoe, Polo and Sancho (1995) contrasted the model used to study the introduction of VAT in Spain (Kehoe, Manresa, Noyola, Polo and Sancho (1988)). In general, the original study was good for predicting industrial prices, levels of production, and prices of factors of production, even though the predictions of the prices of goods were not so good. This last step is not a frequent practice in applied general equilibrium research. The main difficulty in make an ex post evaluation of the models is that usually the measures simulated are never put into practice. However, contrasting the results is very important because it allows us to understand the degree of trust we should attribute to a given model and its results. In this respect, the ex post performance evaluation has to take into account that the model is built from a set of hypothesis that, if not reproduced in the economy, will necessarily invalidate its conclusions.

3. The model

The CGE model for the Catalan economy is a static representation of the regional economy and assumes perfect competition and demand equal to supply in all markets. The model contains fifteen sectors of production, an aggregated consumer, a level of public administration and a consolidated foreign agent, reflecting all the regional relations with abroad. In what follows, I describe the characteristics of the economic agents and the optimization behaviour captured in the model.

3.1 Production

Each sector of production, j = 1,...,15, obtains a homogenous good and presents a nested constant-returns-to-scale function. Figure 2 schematically shows the structure of the production function.

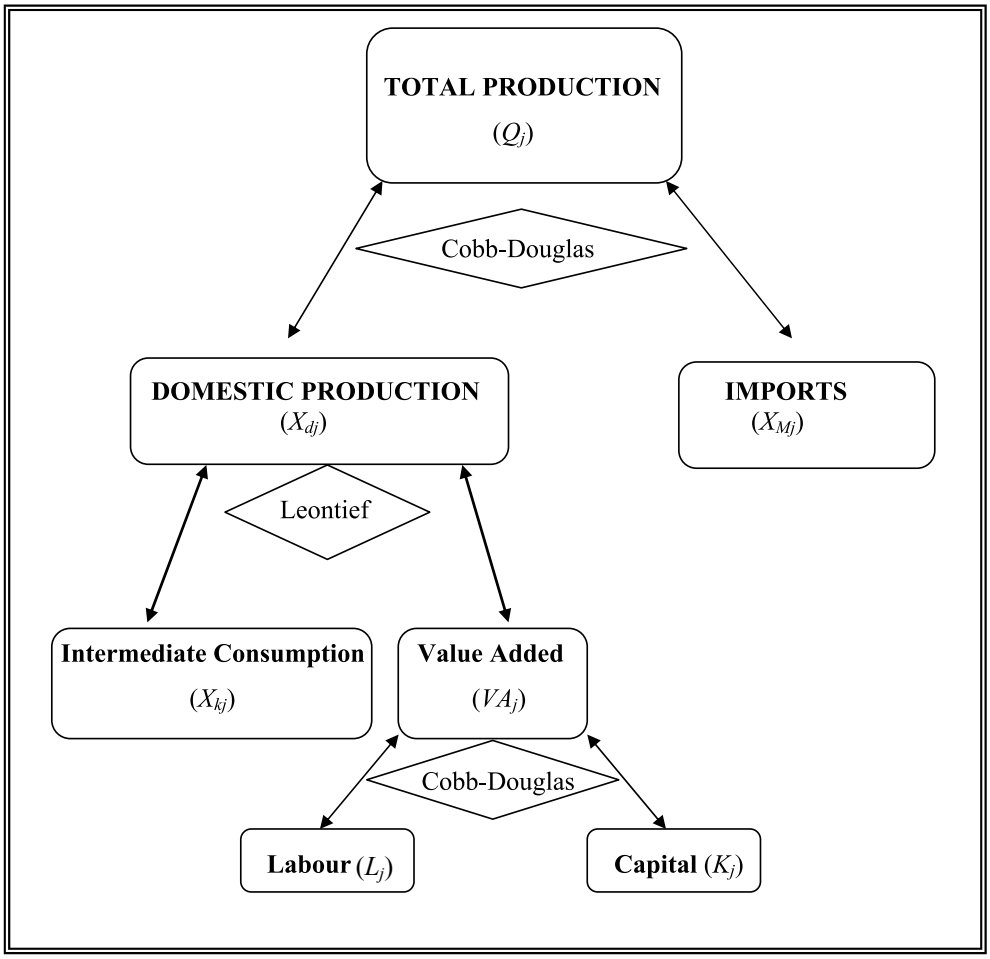

Source: own elaboration.

Fig. 2. Nested Structure of the Production Function

The first level of the production function follows the Armington hypothesis (Armington, 1969), in which imports and domestic output are assumed to be partially substitutive. Specifically, the total output in each sector (Q_i) is a Cobb-Douglas aggregator combining domestic production (X_{dj}) and regional imports (X_{Mj}) from abroad:

$$Q_j = \delta_j X_{dj}^{\gamma_j} X_{Mj}^{1-\gamma_j}, \quad 0 < \gamma_j < 1 \qquad j = 1,...,15, \tag{1}$$

where δ_j is a scale parameter.

The second level of the production function defines the domestic output by using a Leontief aggregator with constant-returns-to-scale:

$$X_{dj} = \min\left[\frac{X_{1j}}{a_{1j}}, \cdots, \frac{X_{15j}}{a_{15j}}, \frac{VA_j}{v_j}\right], \quad j = 1,...,15 . \tag{2}$$

In this expression, X_{kj} is the amount of k used in the domestic production of j and a_{kj} and v_j are parameters obtained by calibration.

Finally, the third level of the production function calculates the sectoral value added according to a Cobb-Douglas expression:

$$VA_j = \beta_j L_j^{1-\alpha_j} K_j^{\alpha_j}; \qquad 0 < \alpha_j < 1 \qquad j = 1,...,15 , \tag{3}$$

where β_j is a scale parameter and L_j, K_j are the quantities of labour and capital, respectively, used by sector j.

Producers are competitive in both the input and the output markets and their objective consists of minimising production costs, subject to a given level of output. From this optimisation behaviour, I obtain the demand functions of inputs in each sector and, given that I assume constant-returns-to-scale, the corresponding sectoral profits will be zero.

3.2 Consumers

The model reflects an aggregated consumer that has Cobb-Douglas utility function in logarithms, in which consumption and saving (or future consumption) are combined in the following way:

$$U = \sum_{h=1}^{9} \gamma_k \ln c_k + \gamma_s \ln c_s ; \quad \gamma_h, \gamma_s > 0; \quad \sum_{h=1}^{9} \gamma_h + \gamma_s = 1 , \tag{4}$$

where c_h is the consumption of good h and c_s is the private saving. The model distinguishes between production and consumption goods. The consumption goods are obtained by a conversion matrix of fixed coefficients that consequently defines a direct (and linear) relationship between production prices and consumption prices.

The budget restriction of consumers (expression (5)) imposes that the total consumption and saving cannot exceed the household's disposable income. Private income comes from the household's endowments of labour and capital and from transfers, that come from public sector and from abroad. All these revenues are subject to direct taxation on income.

$$\sum_{h=1}^{9} P_h(1+t_h)c_h + P_I c_s \le \left(wL + rK + PTcpi + ETP_F\right)\left(1-\tau\right) . \tag{5}$$

The left side in (5) shows the final consumption: t_h is the effective tax rate on the consumption of h and P_h is the corresponding price. Additionally, the left side of (5) shows private saving that it is valued at the investment price: P_I. The right side in the budget restriction shows the disposable income: wL is the labour income (w is the wage and L is the endowment of labour or total supply), rK is the capital income (K is the endowment of capital and r is the corresponding price), PT_{cpi} shows the public transfers (indexed with the

consumption price index: *cpi*), and *ET* are the external transfers from abroad (indexed with the price of external sector P_F). Finally, τ is the effective tax rate on household's income.

The model assumes that the consumer maximises its utility function subject to the budget constraint. From this behaviour, I obtain the demand functions for all the consumption goods and for private saving.

3.3 Government

The government produces public goods and public services that, at the same time, are demanded by himself. The model defines a Leontief utility function for the government, which combines public consumption and public investment in fixed proportions:

$$U^G = \min\left[C_{15}^G, \gamma^G C_I^G\right], \tag{6}$$

where C_{15}^G is the amount of public consumption (in the model, j = 15 is the sector that represents the public services production) and C_I^G is the public investment. The parameter γ^G >0 shows a constant proportion between public consumption and public investment.

The government's budget restriction imposes that public consumption and public investment cannot exceed public revenues. These revenues come from the taxation system and must be reduced by the amount of public transfers to households. Specifically, the public budget is defined as:

$$P_{15}C_{15}^G + P_I C_I^G \leq I^G + \omega_I^G P_I . \tag{7}$$

In expression (7), ω_I^G is the amount of debt that government can have in the event of deficit and I^G is the income coming from taxation, containing the following taxes:

$$I^G = VAT + DT + PrT + SST - PT_{cpi}, \tag{8}$$

where VAT is the indirect taxation on consumption ($VAT = \sum_{h=1}^{9} P_h t_h c_h$). The direct taxation on private income (DT) is calculated as $DT = (wL + rK + PTcpi + ETP_F)\tau$. Additionally, $PrT = \sum_{j=1}^{15} s_j \left(\frac{P_{dj} X_{dj}}{1 + s_j}\right)$ is the taxation on domestic production, with s_j being the tax rate on domestic production. Finally, the social security contributions $SST = \sum_{j=1}^{15} ss_j w L_j^D$, where ss_j is the social security contribution rate in j and L^D_j is the sectoral labour demand, complete the tax figures of the model.

3.4 Foreign agent

In the CGE model, the relations of the economy with abroad are represented using an aggregated agent that includes all the regional transactions of income (revenues and expenditures) with the external markets. This foreign agent produces a traded good by

using the regional exports as inputs, and following a fixed coefficients technology. Additionally, the economy can both receive transfers from abroad and make transfers abroad at the same time.

The model can reflect a situation of external deficit that must consequently be balanced with the corresponding foreign agent's saving, in order to preserve the macroeconomic equilibrium between total savings and total investment in the regional economy.

3.5 Definition of equilibrium

In the CGE model for the Catalan economy, the definition of equilibrium is based on the Walrasian concept, which it has been extended not only to include producers and consumers, but also government and foreign agents. Specifically, the equilibrium is defined as a vector of prices, a vector of activity levels and a set of macroeconomic indicators that clear all markets and allow all agents to achieve their optimization plans. Mathematically, the model is represented as a set of equations containing the equilibrium conditions in all markets.

With respect to the macroeconomic closure rules used in the model, it have been defined the same for both the government and the foreign sector. These closure rules consist of a variable activity level of government and a fixed public deficit, and a variable activity level of the foreign agent and a fixed trade deficit.

4. Database

The parameters or exogenous variables of the CGE model for the Catalan economy have been calculated by applying the standard calibration procedure. This procedure allows to reproduce an initial equilibrium, or benchmark situation, in which all the prices and activity levels are unitary and the solution of the model coincides with the empirical information shown in the social accounting matrix (or SAM) database. That is, the situation reflected in the data of the regional SAM used is assumed to be an equilibrium situation of the economy.

A SAM is a double-entry square matrix in which each agent is represented simultaneously in a row and a column. This database contains the economic transactions within the production system (as in an input-output table) and, additionally, it also contains all the other transactions of the circular flow (factorial and personal income distribution). Therefore, a SAM completes the typical information of the input-output tables by adding the other relationships of income taking place within the circular flow.

By agreement, the rows of a SAM show the revenues of the economic agents and the columns show the corresponding expenditures. To preserve the accounting equilibrium, the value of income must be equal to the value of expenditure in each agent. This means that the total sum of a row must be equal to the total sum of the corresponding column to preserve the equilibrium between origin and destination of income in all the economic agents.

Table 1 shows the list of accounts included in the regional database, that takes the 2001 as temporal reference. Given the information deficiencies at the regional level, the 2001 SAM for the Catalan economy (SAMCAT) has a simple structure that is described in Llop (2011).

Specifically, the production system is divided into 15 sectors (1 agricultural sector, 9 industrial sectors and 5 service sectors). The SAMCAT also shows nine consumption goods, different than the goods obtained in the production processes. Additionally, the regional

Production Sectors	1. Agriculture
	2. Energy
	3. Chemistry
	4. Metals and electric equipment
	5. Automobiles
	6. Food production
	7. Textiles
	8. Paper
	9. Other industries
	10. Construction
	11. Commerce
	12. Transports and communications
	13. Finance
	14. Private services
	15. Public services
Consumption Goods	16. Food
	17. Tobacco and alcohol
	18. Clothes and shoes
	19. Housing
	20. Furniture
	21. Medical assistance
	22. Transports and communications
	23. Culture and education
	24. Other consumption goods
Factors of production	25. Labour
	26. Capital
Consumers	27. Consumers
Saving-investment	28. Capital account
Public sector	29. Production taxes
	30. Social Security taxes on employers
	31. Direct taxes on income
	32. Consumption taxes
	33. Government
Sector exterior	34. Foreign sector

Table 1. List of accounts in the SAMCAT

database shows two production factors, labour and capital, and a generic account containing the income relations of private consumers. In the SAMCAT, the capital account shows all the sources of saving and investment in the regional economy. The government's accounts involve four different taxes (on production, on personal income, on consumption and, finally, Social Security contributions) and an account that contains the income flows of public administration. Finally, the foreign agent is aggregated into a consolidated account showing imports, exports and income transactions of the regional economy with abroad.

5. Results

The first computation of the model involves the calculation of the reference equilibrium (benchmark situation), in which all the prices and activity levels are unitary and the model exactly reproduces the numerical information contained in the social accounting matrix. Then, the model is used to show the effects of different policies applied to the energy sector that have usually been identified as potentially successful for controlling pollutant emissions.

The simulation analysis consists of making three alternative modifications to the benchmark equilibrium. First, it has been introduced a 10% tax on intermediate energy uses. Second, it has been analysed the effects of a greater efficiency in the energy uses, consisting of a reduction in intermediate energy uses of all sectors of production by 10%. Third, it has also been calculated the joint effects: that is to say, a 10% tax on intermediate energy uses together with a 10% decrease in energy requirements by sectors of production. The simulations undertaken are quantitatively defined for the sake of illustration of the effects involved. Despite the numerical values used can be seen not easily applicable at the reality, the reason why I choose them is simply to clearly show the intensity and the direction of the associated economic impacts.

Before showing the numerical results of the simulations, an additional aspect of the analytical context used should be taken into account. Given that the Walras' law implies that one of the equations in the model is redundant, the wage is considered as numéraire and the price of labour is consequently fixed to one in all the simulations performed. This means that in the new equilibriums the prices are in fact relative prices with respect to the numéraire (the wage).

Table 2 shows the changes in sectoral prices, the changes in the prices of consumption goods and the changes in other prices of the model (price of investment and price of external sector).

The first scenario simulates the effects of a new 10% tax on the energy used in the production system. The new taxation on energy causes a general increase in production prices. Logically, the energy price is the most affected by this policy intervention and its price rise by 11.17%. The effects on chemistry (2.86%), transport and communications (2.47%) and other industries (2.33%) are also significant and show a great reaction of the production prices under the policy simulated. On the contrary, finance and private services are the sectors whose prices are less affected by the taxation on energy (0.47% and 0.77%, respectively).

	Situation 1	Situation 2	Situation 3
SECTORS			
1. Agriculture	1.20%	-0.98%	-0.11%
2. Energy	11.17%	-9.13%	-0.10%
3. Chemistry	2.86%	-2.34%	-0.35%
4. Metals and electric equipment	0.99%	-0.81%	-0.09%
5. Automobiles	1.07%	-0.87%	-0.10%
6. Food production	1.17%	-0.93%	-0.11%
7. Textiles	1.34%	-1.10%	-0.12%
8. Paper	1.32%	-1.09%	-0.12%
9. Other industries	2.33%	-1.90%	-0.21%
10. Construction	1.16%	-0.95%	-0.10%
11. Commerce	1.11%	-0.91%	-0.10%
12. Transports and communications	2.47%	-2.02%	-0.22%
13. Finance	0.47%	-0.38%	-0.04%
14. Private services	0.77%	-0.63%	-0.07%
15. Public services	1.02%	-0.84%	-0.09%
CONSUMPTION GOODS			
16. Food	1.14%	-0.94%	-0.11%
17. Tobacco and alcohol	1.13%	-0.93%	-0.10%
18. Clothes and shoes	1.20%	-0.98%	-0.11%
19. Housing	1.28%	-2.25%	-0.25%
20. Furniture	1.13%	-0.93%	-0.10%
21. Medical assistance	1.09%	-0.89%	-0.10%
22. Transports and communications	1.28%	-2.33%	-0.25%
23. Culture and education	1.13%	-0.93%	-0.10%
24. Other consumption goods	0.90%	-0.73%	-0.08%
OTHER PRICES			
Consumption Price Index (*cpi*)	1.51%	-1.23%	-0.14%
Price of Investment (P_I)	1.10%	-0.90%	-0.01%
Price of External Sector (P_F)	1.80%	-1.40%	-0.02%
Price of Capital (*r*)	-0.01%	-0.01%	-0.01%
Price of Labour (*w*)	0.00%	0.00%	0.00%

Situation 1: 10% taxation on intermediate energy uses
Situation 2: 10% reduction in intermediate energy requirements
Situation 3: 10% taxation on energy uses and 10% reduction in intermediate energy requirements

Table 2. Changes in prices (%)

As the consumption goods are a combination of the production goods, the increase in production prices are transmitted to the prices of consumption goods. At the same time, this is reflected in the consumption price index that shows an increase by 1.51%. The inflationary effect of the taxation on energy can also be seen in the investment price and in the price of the external sector (that increase by 1.10% and 1.80%, respectively). The relative price of factors suffers practically no changes, and the price of capital shows an insignificant reduction by 0.01%.

The second modification to the benchmark equilibrium consists of analysing the effects of a 10% reduction in the intermediate uses of energy, that can be driven by greater consumer awareness for more sustainable energy uses or by efforts to increase the efficiency in production processes in terms of the energy requirements. This simulation will give us some idea of how a change (reduction) in energy consumption will affect the main economic variables. From table 2, the reduction in water uses shows a generalised decrease in production prices. Specifically, the prices of energy decrease by 9.13%, the prices of transport and communications decrease by 2.02% and the prices of chemistry decrease by 2.34%. These are the activities most affected by the reduction in energy uses, while the other sectoral prices are less sensitive to the reduction in energy demand.

The prices of consumption also decrease, mainly housing (-2.25%) and transport and communications (-2.33%). The consumption price index, that is compounded by the prices of the consumption goods, shows a significant reduction (1.23%). Finally, table 2 shows that the investment price and the external price also present reductions (being of 0.90% and 1.40%, respectively).

The third simulation examines the effects of a combined policy consisting in a new 10% taxation on the intermediate energy uses and a 10% reduction in sectoral energy uses. A result is that the increased efficiency of energy uses together with a tax on energy has practically no effects on production prices and on consumption prices. Under this situation, the consumption price index shows a small reduction of 0.14%. In fact, this negligible variability in prices suggests that the inflationary effects of the new taxation are practically compensated by the deflationary effects of the decrease in energy requirements. This is an interesting result, mainly if the aim is to avoid inflation of prices.

Table 3 contains the changes in the activity levels of sectors of production and consumption goods in each new situation analysed in the model. As expected, the new tax on energy (situation 1) causes a general decrease in the sectoral activity levels that it is also transmitted to the consumption goods. It is also remarkable that the investment is negatively affected by the decrease in the activity of sectors, and shows a reduction by 1.33%.

The second column in table 3 shows that the decrease in the energy requirements is associated with a positive effect on the activity levels of all sectors with the exception of energy that, once all the interactions in the model have been concluded, reduces its activity level by 7.85%. In the consumption goods, it is interesting to remark the positive effects on the activities of transport and communications and housing that reflect positive effects by 2.36% and 2.28% respectively. The price reductions lead to a greater demand that can be seen in the positive effects on the activity levels of production and consumption. Finally, we can observe that the investment is positively affected by the reduction in energy demand (1.11%).

	Situation 1	Situation 2	Situation 3
SECTORS			
1. Agriculture	-0.39	0.31	0.02
2. Energy	-0.80	-7.85	-9.42
3. Chemistry	-0.02	-0.07	-0.05
4. Metals and electric equipment	-0.27	0.12	-0.08
5. Automobiles	-0.23	0.18	0.01
6. Food production	-0.26	0.21	0.01
7. Textiles	-0.03	0.01	-0.01
8. Paper	-0.07	0.02	-0.02
9. Other industries	-0.24	0.11	-0.07
10. Construction	-1.24	0.65	-0.27
11. Commerce	-0.78	0.62	0.04
12. Transports and communications	-0.75	0.52	-0.04
13. Finance	-0.59	0.41	-0.03
14. Private services	-0.87	0.67	0.02
15. Public services	-0.94	0.78	0.08
CONSUMPTION GOODS			
16. Food	-1.11	0.93	0.10
17. Tobacco and alcohol	-1.10	0.92	0.10
18. Clothes and shoes	-1.13	0.97	0.10
19. Housing	-2.66	2.28	0.24
20. Furniture	-1.10	0.92	0.10
21. Medical assistance	-1.06	0.88	0.10
22. Transports and communications	-2.75	2.36	0.25
23. Culture and education	-1.10	0.92	0.10
24. Other consumption goods	-0.87	0.72	0.08
OTHER ACTIVITY LEVELS			
Investment (Y_I)	-1.33	1.11	0.12
External Sector (Y_F)	0.52	-0.44	-0.05

Situation 1: 10% taxation on intermediate energy uses
Situation 2: 10% reduction in intermediate energy requirements
Situation 3: 10% taxation on energy uses and 10% reduction in intermediate energy requirements

Table 3. Changes in activity levels (%)

The last column of table 3 illustrates the effects of a combined measure of taxation and reduction in the demand for energy. This situation shows a limited modification in the activity levels of the production system with the unique exception of the energy activity, that it has a negative impact of 9.42%. Also the effects on the consumption goods, investment and external sector are very limited.

Table 4 contains some additional aggregated indicators, which allows to complete the understanding of the economic impact of the various scenarios. Specifically, it shows the changes in the real GDP and two measures of the effects on the private agents (changes in the real disposable income of consumers and equivalent variation).

	Situation 1	**Situation 2**	**Situation 3**
Real GDP	-1.18%	0.99%	0.11%
Real Private Disposable Income	-1.46%	1.23%	0.13%
Equivalent Variation (Thousands of Euro)	-1,355.69	1,141.76	122.93

Situation 1: 10% taxation on intermediate energy uses
Situation 2: 10% reduction in intermediate energy requirements
Situation 3: 10% taxation on energy uses and 10% reduction in intermediate energy requirements

Table 4. Changes in other variables (%)

As table 4 shows, the measures cause different impacts on the regional production. The GDP suffers from a reduction in case of applying a new tax on the intermediate uses of energy. On the contrary, the increase in the efficiency of energy uses has a positive effect on the production in real terms. Finally, the combination of a price intervention and a decrease in energy requirements leaves the real GDP practically in the benchmark levels.

The effects on the private agents are also opposite depending on the type of intervention analysed. As the new tax on energy causes an increase in prices, private welfare is negatively affected and both the real private income and the equivalent variation are negative in table 4. On the other hand, the reduction in the demand for energy is associated to a significant improvement in private welfare; the private real income increases by 1.23% and the equivalent variation is around 1,142 thousand of euro. From table 4, it is interesting that the combination of a tax on energy with a reduction in the energy requirements mitigates the negative effects on consumers of the traditional taxation and allows to ensure the benchmark levels of private welfare. This is an important finding and it suggests that price effects should be accompanied with a more sustainable consumption of the energetic goods to avoid the negative impacts of the intervention on households.

The simulation analysis shows that alternative energy policies, which are available to policy makers, cause different effects on the main economic indicators. This is an important finding

as it suggests that the economic consequences of environmental measures are not trivial and depend, to a greater extend, on the type of policy implemented.

6. Conclusions

This chapter has defined a computable general equilibrium model, following the walrasian tradition, that has been applied to the Catalan economy with the use of a social accounting matrix for the year 2001. The objective of the analysis has been the study of the economic impact of various policies implemented on the energy sector. The reason why I focus on energy is because the consumption and production of energy is associated with important negative impacts on the environment, as it causes most of the pollutant emissions and, consequently, it negatively affects the process of climate change.

The results show that a tax on intermediate energy uses increases the regional prices (production prices, consumption prices, consumer price index, investment price and external price) and this has a clear negative effect on private welfare (real disposable income and equivalent variation) and on regional production (real GDP). On the other hand, when energy uses are reduced, the regional prices decrease and this causes a positive effect on private welfare and on regional GDP. When a tax is combined with a reduction in the intermediate demand for energy, production prices and the consumer price index are very close to zero. Additionally, the effects on GDP and private welfare are slightly positive.

Policy makers have a set of measures to be applied that can help to accomplish environmental goals. The analytical method presented in this chapter provides interesting insights about the economic consequences of policy interventions aimed at reducing the negative impacts on the environment. The results in this paper show that different policies can have different effects on production prices, consumer price indices, GDP and private welfare.

7. Acknowledgements

The author acknowledges the financial support of the Spanish Ministry of Culture (grant ECO2010-17728) and of the Catalan Government (grant SGR2009-322 and "Xarxa de Referencia d'R+D+I en Economia i Polítiques Públiques").

8. References

Allan, G.; Hanley, N.; McGregor, P.; Swales, K. and Turner, K. (2007). The Impact of Increased Efficiency in the Industrial Use of Energy: A Computable General Equilibrium Analysis for the United Kingdom., *Energy Economics*, Vol. 29, pp. 779-798.

André, F. J.; Cardenete, M. A. and Velázquez, E. (2005). Performing an Environmental Tax Reform in a Regional Economy. A CGE Approach. *Annals of Regional Science*, Vol. 39, pp. 375-392.

Armington, P. (1969). A Theory of Demand for Products Distinguished by Place of Production. *International Monetary Fund Staff Papers*, Vol. 16, pp. 159-178.

Bergman, L. (1991). General Equilibrium Effect of Environmental Policy: A CGE Modeling Approach. *Environmental and Resource Economics*, Vol. 1, pp. 43-61.

Bhattacharyya, S. C. (1996). Applied General Equilibrium Models for Energy Studies: a Survey. *Energy Economics,* Vol. 18, pp. 145-164.

Böhringer, C. and Rutherford, T. F. (1997). Carbon Taxes with Exemptions in an Open Economy: A General Equilibrium Analysis of the German Tax Initiative. *Journal of Environmental Economics and Management,* Vol. 32, pp. 189-203.

Böhringer, C.; Conrad, K. and Löschel, A. (2003). Carbon Taxes and Joint Implementation. *Environmental and Resource Economics*, Vol. 24 (1), pp. 49-76.

Böhringer, C. and Löschel, A. (2006). Computable General Equilibrium Models for Sustainability Impact Assessment: Status Quo and Prospects. *Ecological Economics*, Vol. 60, pp. 49-64.

Bonanno, G. (1990). General Equilibrium Theory with Imperfect Competition. *Journal of Economic Surveys*, Vol. 4 (4), pp. 297-328.

Bovenberg, A. L. (1999). Green Tax Reforms and the Double Dividend: An Updated Reader's Guide. *International Tax Public Finance,* Vol. 6, pp. 421-443.

Bovenberg, A. L. and Goulder, L. H. (2002). Environmental Tax Policy. in A. J. Auerbach, M. Feldstein (eds.), *Handbook of Public Economics*, Elsevier Press, Amsterdam, pp. 1471-1545.

Conrad, K. and Schröder, M. (1993). Choosing Environmental Policy Instruments Using General Equilibrium Models. *Journal of Policy Modeling,* Vol. 15 (5-6), pp. 521-543.

Devarajan, S. (1988). Natural Resources and Taxation in Computable General Equilibrium Models of Developing Countries. *Journal of Policy Modeling*, Vol. 10 (4), pp. 505-528.

Dissou, Y. (2005). Cost-effectiveness of the Performance Standard System to Reduce CO_2 Emissions in Canada: A General Equilibrium Analysis. *Resource and Energy Economics*, Vol. 27, pp. 187-207.

Edwards, T. H. and Hutton, J. P. (2001). Allocation of Carbon Permits within a Country: A General Equilibrium Analysis of the United Kingdom. *Energy Economics*, Vol. 23, pp. 371-386.

Faehn, T.; Gómez, A. and Kverndokk, S. (2009). Can a Carbon Permit System Reduce Spanish Unemployment?. *Energy Economics*, Vol. 31(4), pp. 595-604.

Glomsrod, S.; Vennemo, H. and Johnsen T. (1992). Stabilization of Emissions of CO_2: A Computable General Equilibrium Assessment. *Scandinavian Journal of Economics*, Vol. 94 (1), pp. 53-69.

González, M. and Dellink, R. (2006). Impact of Climate Policy on the Basque Economy. *Economía Agraria y Recursos Naturales,* Vol. 6 (12), pp. 187-213.

Gottinger, H. W. (1998). Greenhouses Gas Economics and Computable General Equilibrium. *Journal of Policy Modeling*, Vol. 20 (5), pp. 537-580.

Goulder, L. H. (1992). Do the Cost of Carbon Tax Vanish when Interactions with Other Taxes Are Accounted for?. NBER, Documento de Trabajo 4061.

Goulder, L. H. (1995). Enviromental Taxation and the "Double Dividend": A Reader's Guide. In: *Public Economics and the Environment in an Imperfect World,* Dordrecht, L. Bovenberg and S. Cnossen (eds.), Kluwer Academic Publishers.

Goulder, L. H. and Schneider, S. (1999). Induced Technological Change, Crowding Out, and the Attractiveness of CO_2 Emissions Abatement. *Resource and Environmental Economics,* Vol. 21 (3-4), pp. 211–253.

Haji Hatibu Haji Semboja (1994). The Effects of Energy Taxes on the Kenya Economy. *Energy Economics*, Vol. 16 (3), pp. 205-215.

Hanley, N. D.; McGregor, P. G.; Swales, J. K. and Turner, K. (2006). The Impact of Stimulus to Energy Efficiency on the Economy and the Environment: A Regional Computable General Equilibrium Analysis. *Renewable Energy,* Vol. 31, pp. 161-171.

Hansen, L. P. and Heckman, J. J. (1996). The Empirical Foundations of Calibration. *Journal of Economic Perspectives*, Vol. 10 (1), pp. 87-104.

Harrison, G. W. and Vinod, H. D. (1992). The Sensitivity Analysis of Applied General Equilibrium Models: Completely Randomized Factorial Sampling Designs. *Review of Economics and Statistics*, Vol. 74 (2), pp. 357-362.

Jorgenson, D. W. (1984). Econometric Methods for Applied General Equilibrium Analysis. In: *Applied General Equilibrium Analysis,* H. Scarf and J. B. Shoven (eds.), pp. 139-203, Cambridge University Press.

Kehoe, T. J.; Manresa, A.; Noyola, P. J.; Polo, C. and Sancho, F. (1988). A General Equilibrium of the 1986 Tax Reform in Spain. *European Economic Review*, Vol. 32 (2-3), pp. 334-342.

Kehoe, T. J.; Polo, C. and Sancho, F. (1995). An Evaluation of the Performance of an Applied General Equilibrium Model of the Spanish Economy. *Economic Theory*, Vol. 6 (1), pp. 115-141.

Kehoe, T. J. (1996): Social Accounting Matrices and Applied General Equilibrium Models. *Unpublished Manuscript*.

Labandeira, X. and Rodríguez, M. (2004). Green Taxes Reforms in Spain. *European Environment*, Vol. 14, pp. 14.

Leontief, W. (1970). Environmental Repercussions and the Economic Structure: An Input-Output Analysis. *Review of Economics and Statistics*, Vol. 52, pp. 262-271.

Llop, M. (2012). The Role of Saving and Investment in a SAM Model of Prices. *Annals of Regional Science*, Vol. 48, pp. 339-357.

Llop, M. and Pié, L. (2008): Input-output Analysis of Alternative Policies Implemented on the Energy Activities: An Application for Catalonia. *Energy Policy*, Vol. 36, pp. 1642-1648.

Manresa, A. (1996). Equilibrio General Computable: Un Instrumento de la Economía Aplicada. *Unpublished Manuscript*.

Manresa, A. and Sancho, F. (2005). Implementing a Double Dividend: Recycling Ecotaxes Towards Lower Labour Taxes. *Energy Policy*, Vol. 33 (12), pp. 1577-1585.

Mansur, A. and Whalley, J. (1984). Numerical Specification of Applied General Equilibrium Models: Estimation, Calibration, and Data, In: *Applied General*

Equilibrium Analysis, H. Scarf and J. B. Shoven (eds.), pp. 69-127, Cambridge University Press.

Naqvi, F. (1998). A Computable General Equilibrium Model of Energy, Economy and Equity Interactions in Pakistan. *Energy Economics*, Vol. 20, pp. 347-373.

Nestor, D. V. and Pasurka, C. A. (1995). CGE Model of Pollution Abatement Processes for Assessing the Economic Effects of Environmental Policy. *Economic Modelling*, Vol. 12 (1), pp. 53-59.

Nugent, J. B. and Sarma, C. V. S. K. (2002). The Three E's-efficiency, Equity, and Environmental Protection-in Search of "win-win-win" Policies - A CGE Analysis of India. *Journal of Policy Modeling*, Vol. 24 (1), pp. 19-50.

Oladosu, G. and Rose, A. (2007). Income Distribution Impacts of Climate Change Mitigation Policy in the Susquehanna River Basin Economy. *Energy Economics*, Vol. 29, pp. 520-544.

Otto, V.; Löschel, A. and Dellink, R. (2007). Energy Biased Technical Change: A CGE Analysis. *Resource and Energy Economics,* Vol. 29, pp. 137-158.

O'Ryan, R.; De Miguel, C. J.; Millar, S. and Munasinghe, M. (2005). Computable General Equilibrium Model Analysis of Economywide Cross Effects of Social and Environmental Policies in Chile. *Ecological Economics*, Vol. 54, pp. 447-472.

Parry, I. W. H. and Williams, R. C. (1999). A Second-Best Evaluation of Eight Policy Instruments to Reduce Carbon Emissions. *Resource and Energy Economics,* Vol. 21, pp. 347-373.

Parry, I.; Williams, R. C. and Goulder, L. H. (1999). When Can Carbon Abatement Policies Increase Welfare? The Fundamental Role of Distorted Factor Markets. *Journal of Environment Economics and Management*, Vol. 37 (1), pp. 52-84.

Pearce, D. (1991). The Role of Carbon Taxes in Adjusting to Global Warming. *The Economic Journal*, Vol. 101, pp. 938-948.

Pyatt, G. (1988). A SAM Approach to Modeling. *Journal of Policy Modeling*, Vol. 10 (3), pp. 327-352.

Scrimgeour, F.; Oxley, L. and Fatai, K. (2005). Reducing Carbon Emissions? The Relative Effectiveness of Different Types of Environmental Tax: The Case of New Zealand. *Environmental Modelling and Software*, Vol. 20 (11), pp. 1439-1448.

Shoven, J. B. and Whalley, J. (1984). Applied General Equilibrium Model of Taxation and International Trade: An Introduction and Survey. *Journal of Economic Literature*, Vol. 22, pp. 1007-1051.

Steininger, K. W.; Friedl, B. and Gebetsroither, B. (2007). Sustainability Impacts of Car Road Pricing: A Computable General Equilibrium Analysis for Austria. *Ecological Economics*, Vol. 63, pp. 59-69.

Stern, N. (2006). *Stern review: The economics of Climate Change*, Cambridge University Press, New York.

Whalley, J. (1991). La Modelización del Equilibrio General Aplicado. *Cuadernos Económicos del ICE, Vol.* 48, pp. 179-195.

Whalley, J. and Wigle, R. (1991). Cutting CO_2 Emissions: The effects of Alternative Policy Approaches. *Energy Journal*, Vol. 12 (1), pp. 109-124.

Wissema, W. and Dellink, R. (2007). AGE Analysis of the Impact of a Carbon Energy Tax on the Irish Economy. *Ecological Economics*, Vol. 61, pp. 671-683.

Xie, J. and Saltzman, S. (2000). Environmental Policy: An Environmental Computable General-Equilibrium Approach for Developing Countries. *Journal of Policy Modeling*, Vol. 22 (4), pp. 453-489.

13

Carbon Dioxide Geological Storage: Monitoring Technologies Review

Guoxiang Liu
Department of Civil and Environmental Engineering West Virginia University
USA

1. Introduction

With anthropogenic activities, the concentration of CO_2, one of the greenhouse gases along with CH_4, NO_2, NO etc., is increasing in the atmosphere. As shown in Davison et al. (2004), the most abundant greenhouse gas, CO_2, has risen from a preindustrial level of 270 parts per million by volume (ppmv) to over 380 ppmv (Keeling & Whorf, 1998; Metz, Davidson, Coninck, Loos & Meyer, 2005) with an accumulation rate of about 1.5 ppmv per year (Halmann & Steinberg, 1999; Hansen et al., 1997). At the current increasing rate, CO_2 concentration in the atmosphere could be more than 700 ppmv by the end of this century (Halmann & Steinberg, 1999; Hansen et al., 1997; Metz, Davidson, Coninck, Loos & Meyer, 2005; Metz, Davidson, de Coninck, Loos & Meyer, 2005) due to around 6 Gt CO_2 emissions globally from fossil-fuel combustion used for generating electricity, transportation and some industrial processes etc. each year (Metz, Davidson, de Coninck, Loos & Meyer, 2005). The enormous CO_2 amounts injected into the environment have resulted in a series of global problems, such as warming of the Earth's surface, increasing extreme weather, polar ice melting, and desert size increasing. For example, the global average surface temperature of the Earth has increased by approximately $0.74 \pm 0.18\,^{\circ}C$ over 1906-2005 (Trenberth & Jones, 2007). The Intergovernmental Panel on Climate Change (IPCC) has predicted an average global rise in temperature of about 1.4 to 5.8 $^{\circ}C$ between 1990 and 2100 (Metz, Davidson, Coninck, Loos & Meyer, 2005). Although the cause and effect relation between the atmospheric concentration of CO_2 and global warming is still uncertain, the increase in emissions of CO_2 and other greenhouse gas has caused public concern worldwide (EPA, 2005; Metz, Davidson, de Coninck, Loos & Meyer, 2005).

However, the concentration of CO_2 in the atmosphere can be reduced by capturing and disposing of the produced CO_2 in geological formations for a long time (Herzog & Drake, 1996; Metz, Davidson, de Coninck, Loos & Meyer, 2005; Reichle et al., 1999). This is called carbon capture and sequestration (CCS). CCS may bring other benefits, such as coal-bed methane recovery, enhanced oil recovery, enhanced gas recovery, or even water production. At present, there are several options of CO_2 sequestration being discussed. One is to inject the CO_2 into deep coalbeds, where it will be adsorbed by the coal, typically replacing methane that can be recovered. Another option is to pump the CO_2 into saline formations where the CO_2 dissolves into the ambient fluid (Bergman & Winter, 1995; Gunter et al., 1996; Metz, Davidson, de Coninck, Loos & Meyer, 2005). Storing the CO_2 in depleted oil or natural gas reservoirs where it replaces the residual oil or gas is another option (Davison et al., 2004).

Moreover, the CO_2 can be sequestered in oceans and ecosystems (Lorenz & Lal, 2010; Metz, Davidson, Coninck, Loos & Meyer, 2005; Metz, Davidson, de Coninck, Loos & Meyer, 2005; Voormeij & Simandl, 2002). The potential capacity of CO_2 storage in these sites is estimated as 20,000 billion tons (Herzog & Golomb, 2004).

Once CO_2 is injected into a geological formation, it can be trapped in the pore spaces by four main processes. The first process is stratigraphic and structural trapping. This means that the CO_2 is trapped in the pore space by overlying low permeability rock-cap (caprock) seal(s). This trapping depends on the strata and structure of the geological formation. Another process is residual gas trapping, which means that the CO_2 is sequestered in the matrix of media. Capillary pressure is the main factor providing the stability of this trapping. Solubility trapping refers to CO_2 dissolving into the fluid of the geological formations, such as water. Finally, CO_2 can react with solid materials and become mineralized. Since the mineralization process depends on factors like pH and chemical species, it takes longer than other mechanisms, but of the four processes, this trapping is more stable over time (Bachu et al., 1994; Gunter et al., 1993). However, whatever the mechanism of CO_2 sequestration in different media such as saline basins or coal reservoirs, the basic idea for the geological sequestration is to find suitable geological structures that have sufficient pore space to hold the CO_2, and an impermeable cap-rock to seal CO_2 within the storage reservoir without long-term leakage (Metz, Davidson, de Coninck, Loos & Meyer, 2005).

As the literature reports, there are several modes of CO_2 leakage back to the atmosphere. For example, injected CO_2 can leak out along fractures and faults, especially with large pressure gradients and high injection rates (Metz, Davidson, de Coninck, Loos & Meyer, 2005). If the effective stress of the reservoir rises to its maximum limitation due to CO_2 injection, there is a large potential risk of structural deformation and fracture, resulting in CO_2 leakage from the reservoir. Ultimately, this means CO_2 sequestration failure of the site (Lee et al., 2005; Liu & Smirnov, 2008; 2009; Pekot & Reeves, 2003). Injected CO_2 may escape through poorly plugged and/or old abandoned wells, even due to corrosion within the well, plugging cement and surrounding material. Moreover, ground water can bring dissolved CO_2 out of a geological formation. Figure. 1 shows these potential leakage mechanisms from geological sequestration, as well as related remedial methods (Metz, Davidson, de Coninck, Loos & Meyer, 2005). In addtion, there are also some meteorological factors, such as atmospheric pressure variations, wind near the ground surface, temperature variation, and rainfall (Chen & Nash, 1994; Guo et al., 2008; Liu, 2010; Neeper, 2001; Oldenburg, Lewicki & Hepple, 2003; Oldenburg, Unger, Hepple & Jordan, 2003; SEAI, 1996; Sturman, 1992; Taylor, 1970) that have effects on the CO_2 leakage, especially in the near-surface of vadose zone. These potential leakages of injected CO_2 mainly result from the reasons below (NETL, 2011).

- Undetected faults, fracture and/or potential fast flow paths.
- Fracture or fault change caused by stress or geochemical reactions.
- Confining penetration by geochemical reactions.
- Unintended lateral flow.
- Wellbore failure events.
- Natural disasters such as earthquake etc.

These will require deep and shallow monitoring by geophysical techniques, well related facilities, and modeling simulations to confirm the behaviors of CO_2 which cover:

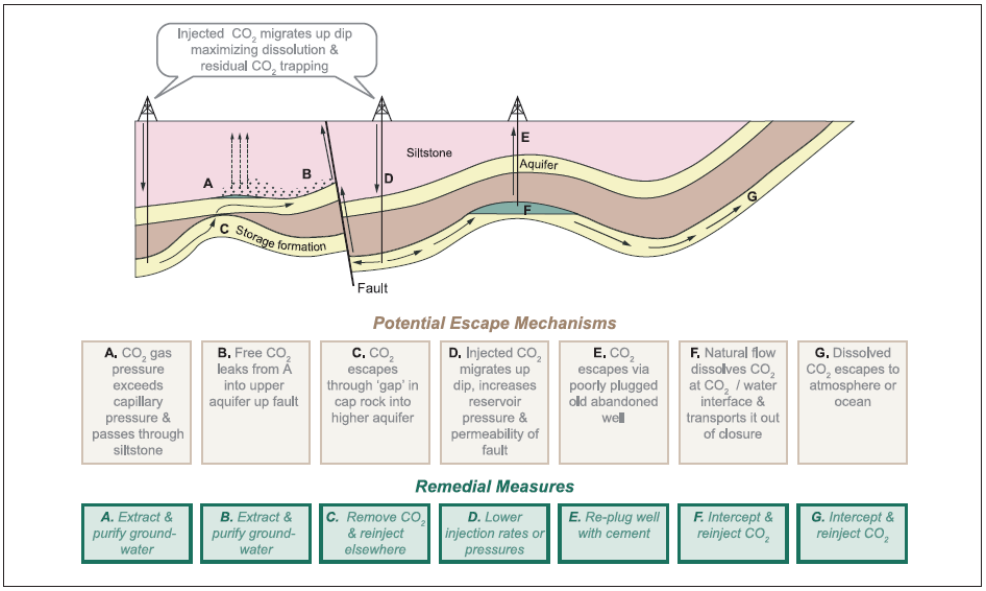

Fig. 1. Potential CO_2 escape mechanisms from geological formations and remediation techniques (Metz, Davidson, de Coninck, Loos & Meyer, 2005).

- CO_2 movement in the storage reservoir over time.
- Pressure changes in and around the storage reservoir due to CO_2 injection.
- CO_2 migration from primary storage reservoir.
- CO_2 migration in shallow depths through overburden.
- CO_2 detection/measurement near/at the surface.

Moreover, CO_2 leakage may happen not right above of the storage site but kilometers away, which strongly depends on the local geological structure. The upward migration dipping the high permeable formation such as sandstone and thus appear the leakage several kilometers away from storage site. Depending the leakage path and permeability, the leakage may occur after hundreds of years but it still highly significant. All of statements above require a CO_2 monitoring system which combine with the processes of site characterization, modeling prediction, risk assessment, and remediation and regulation.

For sake of monitoring and predicting CO_2 leakages stated above, there are more and more methods that have been developed in recently years (Abu-Khader, 2006; Dasgupta, 2006; Gale, 2004; Liu, 2010; Liu & Smirnov, 2009; Smith, 2004; Sweatman & McColpin, 2009). The potential leakage can be surveyed by monitoring variation values of the formation pressure, stress, CO_2 plume, CO_2 density, and chemical component by numerical simulations, seismic methods, gravimetric strategies, and electromagnetic technologies. The monitoring also focuses on the near-surface and surface monitoring by flux measurement tools, remote sensing equipments, acoustic image and sonar methods, and numerical simulations.

In this chapter, all of the above mentioned methods, strategies, technologies, and tools for CO_2 monitoring will be reviewed in details. Their applications to CO_2 storage in fields will

be presented based on the recently projects and practices in worldwide such as Sleipner in the North Sea, Salah in Algeria, Weyburn in Canada, Gorgon in Australia, seven Regional Carbon Sequestration Partnerships in United States etc. Inducting suggestions would be discussed through the reviewing of monitoring technologies based on the comparisons of these field applications.

2. Review of monitoring technologies

The main purpose of monitoring CO_2 is to confirm the storage of the CO_2 without significant leakage for a long-term period to meet the regulation and environmental policy. In view of the monitoring, there are various methods such as geophysics based, geochemistry based, well based etc. that rely on the specific storage location and monitoring objective as follows (IEA, 2007):

- Reservoir location: on-shore or off-shore
- Reservoir type: brine, oil, gas, or coal-bed
- Reservoir depth
- Quantity of injected CO_2
- Land use at proposed storage site: populated, agricultural, wooded, arid, or protected
- Monitoring phase: pre-injection, injection, post-injection, post-closure
- Monitoring objective: plume, top-seal, migration, quantification, efficiency, calibration, leakages, seismicity, integrity, or confidence

Moveover, the monitoring can be focused on the deep and/or shallow formation(s) even though the surface leakage flux or the atmospheric concentration of CO_2. The purpose of the deep monitoring is to track the movement of CO_2 within the storage reservoir and its migration into surrounding formations. This can help to confirm how much CO_2 is stored in the target reservoir. It further helps to adjust and optimize the storage and injection options. Another main objective of the deep monitoring is to track the passway of CO_2 migration from deep to shallow to avoid leaking. Deep monitoring system can be implemented by the surface-based techniques such as surface seismic and/or deep-based methods like monitoring well. The main purpose of the shallow monitoring is to detect CO_2 that has migrated into shallow overburden or surface/atmoshpere. So, most of the techniques based on the gas and flux detection can be used for this monitoring purpose.

The potential monitoring technologies are listed in Figure 2 (CO_2STORE, 2007). However, many of them have not been tested on the real sites of CO_2 storage. These technologies can be grouped based on the monitoring purpose such as deep and shallow, plume tracking, fine-scale processes etc (CO_2STORE, 2007). In this section, most of the monitoring technologies that have been used in the CO_2 storage fields will be reviewed.

2.1 Seismic technologies

The seismic technology was started in the 1930s for the 2D geological data acquirement. However, the real ability to acquire and process 2D seismic data was developed in the 1950s (Davies et al., 2004). With the acquisition of multiple closely spaced lines such as 25 m with 2D seismic image, the data can provide the 3D migration during processing. These lead to a volume from which lines, planes, and slices in any orientation for three dimensions, which are 3D seismic data (Lonergan & White, 1999). The 3D close line spacing has a potential to

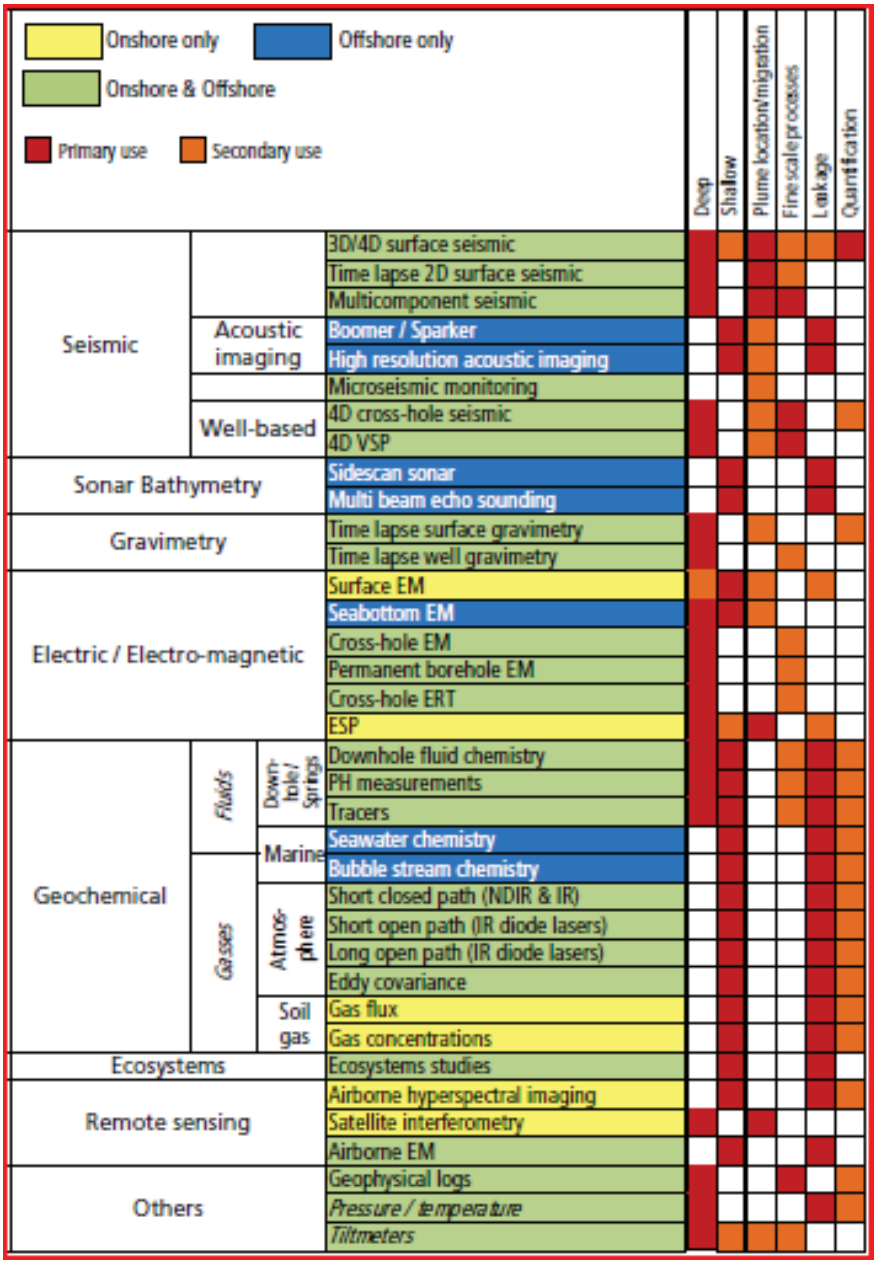

Fig. 2. Potential CO_2 monitoring methods and tools (CO_2STORE, 2007).

produce stratigraphic resolution, imaging of structural and depositional dips, and migration by the automatic or semi-automatic tracking of density of the surface reflection. It means that the characteristics such as fault systems can be mapped in much more detail than one only with 2D seismic data (Freeman et al., 1990).

With development of the seismic technology, the interpretation of seismic data become more accurate and powerful to reflect geoscience, such as identification of stratigraphy, structural geology, igneous geology. Some new techniques, such as 4D seismic and 4C seismic have been applied to investigate the characteristic changes over time to strength the static image from 3D data by introducing time lapse and longitudinal (P-) waves and transverse (S-) waves (Davies et al., 2004). These techniques can be used both at the surface and downhole. The following sections will provide more details of the seismic technologies.

2.1.1 4D seismic technologies

4D seismic is a time-lapse seismic survey, which involves acquisition, processing, and interpretation of the repeated seismic surveys (3D seismic) with time intervals for field site. The major applications of the seismic technologies in monitoring include two types of reservoir property identification due to spatial sensitivity of seismic images. The first one is the static geology properties such as porosity, lithology, shale content. The second one is the dynamic properties based on the fluid flow, such as pressure, temperature, fluid saturation (Lumley & Behrens, 1998). As well known, the operation of seismic survey is to generate the seismic sources, such as dynamite, airguns, vibrators at/near earth surface, and then record the reflected seismic waves from subsurface by receivers (hydrophones or geophones) at/near surface, using a wave-equation-imaging algorithm to create seismic image of the fluids and reservoir properties by contrasting the reflections (Claerbout, 1985).

The time-lapse signal is affected by compressibility of the reservoir rock and the pore fluids because acoustic impedance is the production of velocity and density. So, if the fluids with big difference of density such as gas-water,gas-oil, light oil, the monitoring is much easier than the one with small difference of density such as heavy oils (Lumley, 2001). The basic relationships among porosity, rock property, and fluid property for 4D seismic monitoring were suggested by Lumley and Behrens (Lumley & Behrens, 1998). As shown in Figure 3, the top one indicates how the seismic impedance varying with the change of porosity for oil-full to water-swept conditions; the bottom one shows that compressible and high porosity geological formations are better options than the other rigid, low porosity ones for 4D seismic monitoring (Lumley & Behrens, 1998).

Before a seismic survey is performed, usually, four steps were suggested to be followed for the feasibility and risk assessment on whether 4D seismic is able to image the desired reservoir and fluid properties (Lumley & Behrens, 1998).

• Evaluating the primary critical variables of the seismic technique and reservoir for the success of 4D seismic survey. Mostly, there are three questions to help to figure out the criteria. What is the compressibility range (high, medium, and/or low) of the reservoir rock? Is there sufficient fluid saturation changes to be surveyed over time? Is there a highly probability to obtain high quality 3D seismic data in the study area (Lumley & Behrens, 1998; Lumley et al., 1997)?

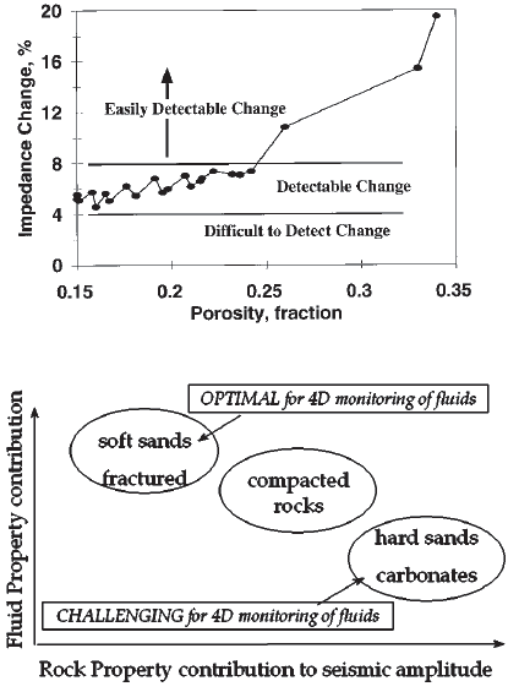

Fig. 3. The basic relationships among porosity, rock property and fluid property for 4D seismic monitoring (Lumley & Behrens, 1998). The bigger porosity media is easier to be detected by 4D seismic survey as shown in the top of the figure. The bottom of the figure indicates that the more soft media is more suitable for 4D seismic to monitor the fluids.

• Determining the properties (static geological characteristics and dynamic fluid-related properties) of specific reservoir rocks in reservoir conditions by core measurements with reference of Figure 3 (Lumley & Behrens, 1998; Wang, 1997) .

• Pre-testing the range of properties of the study area, seismic frequency content, full waveform effects, reflection angle and amplitude effects by modeling seismic traces from core data and well logs to calibrate seismic data at possible well locations (Lumley & Behrens, 1998).

• Computing time-lapse 3D synthetic seismic images by using detailed reservoir and flow simulations (Lumley & Behrens, 1998).

Beyond above four steps for helping decision-making in the procedure of 4D seismic survey, the risk of 4D seismic may reduce during the acquire in the field investigation if with consideration of the new proposed workflow as shown in Figure 4 (Lumley & Behrens, 1998). This workflow integrates the 4D seismic survey (with seismic history matching) in the reservoir modeling procedure to improve the reservoir characteristics. This means that the monitoring methods based on the modeling (simulation) correspondingly are improved.

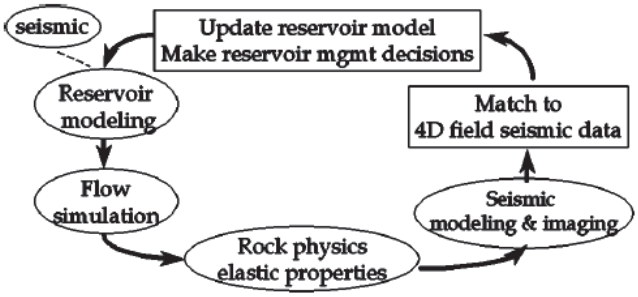

Fig. 4. A workflow proposed for reservoir applications of 4D seismic technologies (Lumley & Behrens, 1998).

In CO_2 monitoring, the purpose of seismic technique is to determine the changes in seismic properties (mostly acoustic impedance) that resulted from CO_2 injection by comparing the surveys among time-lapse seismic data set. An example in Figure 5 shows the results of CO_2 plume during injection from a 4D seismic simulation study in a West Texas carbonate reservoir (Lumley & Behrens, 1998).

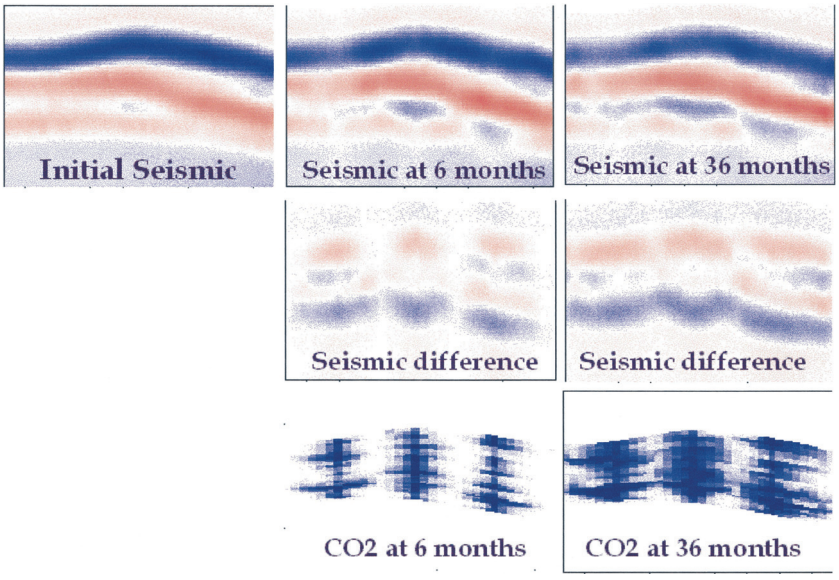

Fig. 5. An example of CO_2 migration using time-lapse seismic techniques for six and 36 months monitoring (Lumley & Behrens, 1998).

2.1.2 Other seismic techniques

Micro-Seismic Technique: Micro-seismic also called passive seismic or minute tremors which is an option to monitor pore pressure and geomechanical stress variations due to CO_2 injection. One of the wide applications is to characterize the zones of weakness (such as overburden) in the storage site and tracking the flow pathways for CO_2 movement (including movement of contaminants due to CO_2 injection) and/or leakage monitoring (Dasgupta, 2006; DTI, 2005). This includes caprock/seal integrity and pre-existing fault or fracture networks identification. An example for fluid pathway tracking by micro-seismic is provided in Figure 6 (Dasgupta, 2006). Moreover, micro-seismic demonstrated the possibility on geomechanical behavior such as deformation monitoring by acquiring real-time events of the seismic survey (Verdon, 2010).

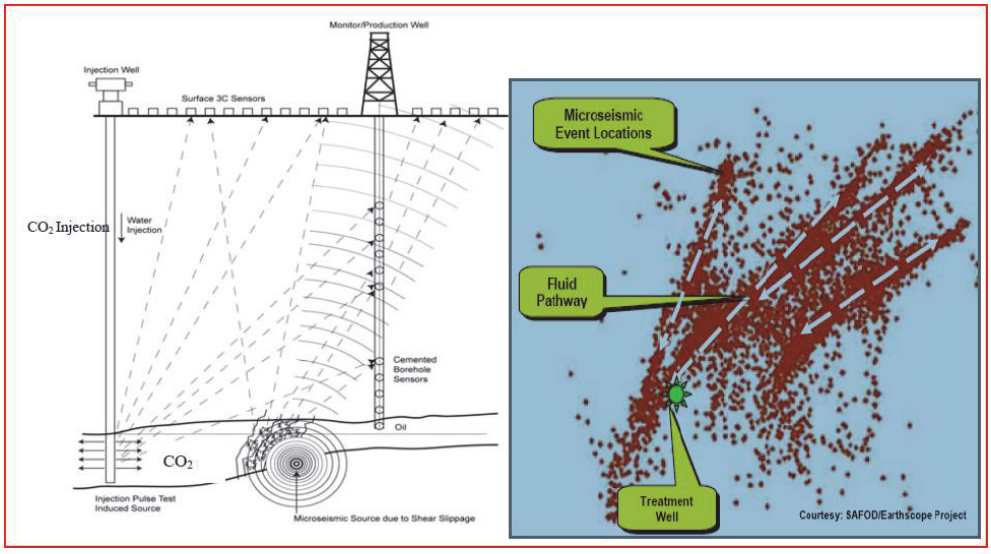

Fig. 6. An example of fluid pathway monitoring by micro-seismic technique with seismic events (Dasgupta, 2006).

Although the example of micro-seismic in Figure 6 is at the surface, micro-seismic also can be used in downhole if it is required (DTI, 2005). The micro-seismic technique is mostly used in the low permeability reservoirs where the pressure changes are sensitive according to the CO_2 injection (CO_2STORE, 2007).

Multi-component Seismic Technique: The main idea of this method is to introduce longitudinal (P-) waves and transverse (S-) waves to survey more fluid and reservoir properties (Davies et al., 2004). For the monitoring onshore, there are three polarised s-wave sources and three-component geophones for full-wave survey with total nine-component data. For an offshore purpose, because the s-waves do not propagate through water, converting waves from S- to P- wave is needed to map the sea bed by sensor package. S-waves are more sensitive to fractures than P-waves but less effective to the fluid content than P-waves (DTI, 2005). As a potential application, this technique was introduced to the Vacuum, Weyburn, and West Queen fields as an critical method to monitoring CO_2 movement (Benson, 2010).

Well-based Seismic Technique: The seismic technique with receivers in the wellbore are named as well-based seismic technique. The seismic sources can be at the surface (named as downhole method) or from another wellbore (named as cross-hole method). Downhole seismic survey is a simple and cheap method since it requires only one borehole. The basic idea is to record the velocity profiles from a fixed seismic source point to the downhole points by gradually moving down in the wellbore. The reservoir properties are interpreted from these records. Crosshole requires at least two wells around to the CO_2 storage site. The seismic sources are mounted in one wellbore and receivers are in the other one. Velocity and attenuation variations according to the travel-time and seismic amplitude changes, are mapped and analyzed for CO_2 plume and pressure change between two wells (DTI, 2005). An example of crosshole seismic used in Frio-II for CO_2 plume monitoring is demonstrated in Figure 7 (Daley et al., 2007; Freifeld et al., 2008). Moreover, this technique is useful to assess how much pore space is effective for the CO_2 storage.

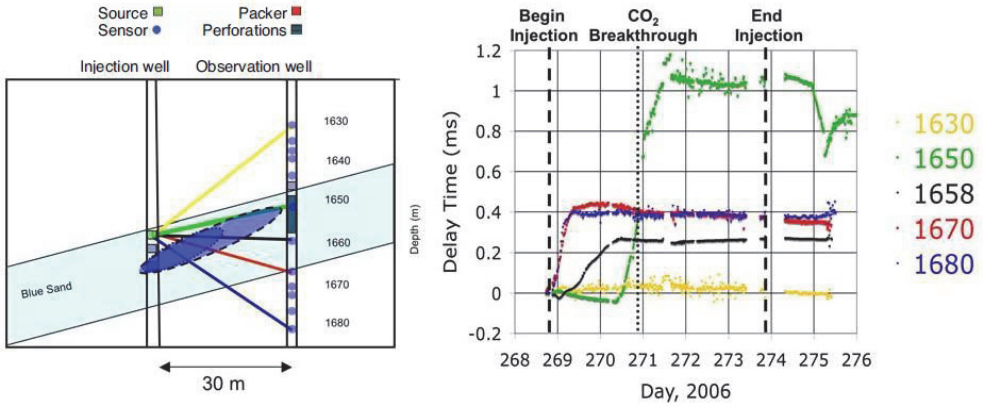

Fig. 7. An example of crosshole seismic used in Frio-II for CO_2 plume monitoring. The figure was modified by Freifeld et al. (2008) based on the original work (Daley et al., 2007). Two eclipses on the left are the CO_2 for one day (inner) and two day (outer) after injection. The measurements of delay time for five sensor depths (1630, 1650, 1658, 1666, and 1680 meters) are on the right plots. These plots show the progressively later increasing in delay time with decreasing depth except the shallowest depth 1630 meters during the monitoring period.

Depending on the site, beyond two receiver wellbores can be located near the energy sources wellbore to detect CO_2 plume around the whole storage reservoir. A scheme with four monitoring wells around the injection well (the distance range from injection well to monitoring wells is 40 to 120 meters) was designed to demonstrate CO_2 monitoring with a small scale injection at a rate of 10-48 tonnes per day in Nagaoka, Japan by Kikuta et al. (2004). The results confirm the benefits of the crosshole seismic technique that even a small amount (hundreds to thousands of tonnes) of CO_2 can be detected. However, the CO_2 beyond the region of the system of the seismic source and receive wells cannot be detected. This is the main limitation of the well-based techniques.

Vertical Seismic Profiling (VSP): This is another method usually using borehole to vertically monitor the property variations of the reservoir and fluid. Mostly, the CO_2 plume and pressure changes due to CO_2 injection can be well detected in- and post-injection periods. This technique show the good abilities in the storage site with big vertical differences of geological characteristics because the down-going wave and up-going wave can be separated by VSP.

As a summary, seismic technologies play a curial role in the CO_2 monitoring for leakage and risk assessment especially in- and post-injection period. Most of the technologies stated above can be used at the surface or subsurface through borehole based on the specific CO_2 monitoring site. The technologies can be cooperated together for monitoring purpose from deep to shallow, in-injection to post-injection, small scale to large scale. Even based on the specific conditions of the storage site, the properties of the seismic technologies, such as resolution of acoustic imaging and amplitude of the seismic source can be changed as various seismic techniques, such as high resolution acoustic imaging (DTI, 2005). More applications of these technologies will be stated in the section 3 Field Applications of Monitoring Technologies.

2.2 Electromagnetic technologies

The idea of the electromagnetic technologies is to transmit an electric (magnetic) source to the CO_2 storage site by grounded dipole and receive response of the source for figuring out the conductivity by contrasting the response difference from subsurface. Because the resistivity of CO_2 is lower than water, the conductivity change due to CO_2 injection can be detected by the electromagnetic technologies. A resistivity results of the CO_2 and water were confirmed under the reservoir pressure and temperature in the laboratory tests by Borner et al. (2010) as shown in Figure 8. The conclusion of the experiments indicates that the resistance decreases with CO_2 injection increasing. The pure CO_2 does not show any relevant electric conductivity even when the pressure increased to 130 bar (Borner et al., 2010).

Based on the resistance differences between CO_2 and others in the reservoir, a typical scheme of the electromagnetic method for CO_2 plume monitoring is suggested in Figure 9 (LLNL, 2005). In this scheme, electrical current being offered between two casings for mapping voltage distribution is measured on the remaining casings, repeating the mapping process with different pairs of casing until the whole CO_2 volume being figured out (LLNL, 2005).

Field tomographic data was acquired at the site in April 2001, October 2001, July 2002, and October 2003. Due to some reasons, the CO_2 injection was stopped in December 2002. The results of CO_2 plume are provided in Figure 11 based on the proposed system in Figure 10 (Kirkendall & Roberts, 2004). These observations are time-lapse set of two-dimensional images between transmitting and receiving in Figure 11. A) is the background distribution before CO_2 injection. B) is the imaging with five months of CO_2 injection. And C) is the difference image between A) and B). This difference clearly shows the CO_2 movement where located in the top left from injection perforation which is red color areas. Dark blue is the replaced water by injected CO_2. The region with yellow color is distinguished as oil movement. These conclusions confirmed the laboratory tests that is the resistivity values playing crucial in brine delineating from CO_2 and oil. Moreover, CO_2 and oil also can be recognized by the similar method based on their resistibility (Kirkendall & Roberts, 2004).

Moreover, Ishido published a direct correspondence between water saturation change and electric field amplitude change by Ishido & Mizutani (1981). Electromagnetic technology was

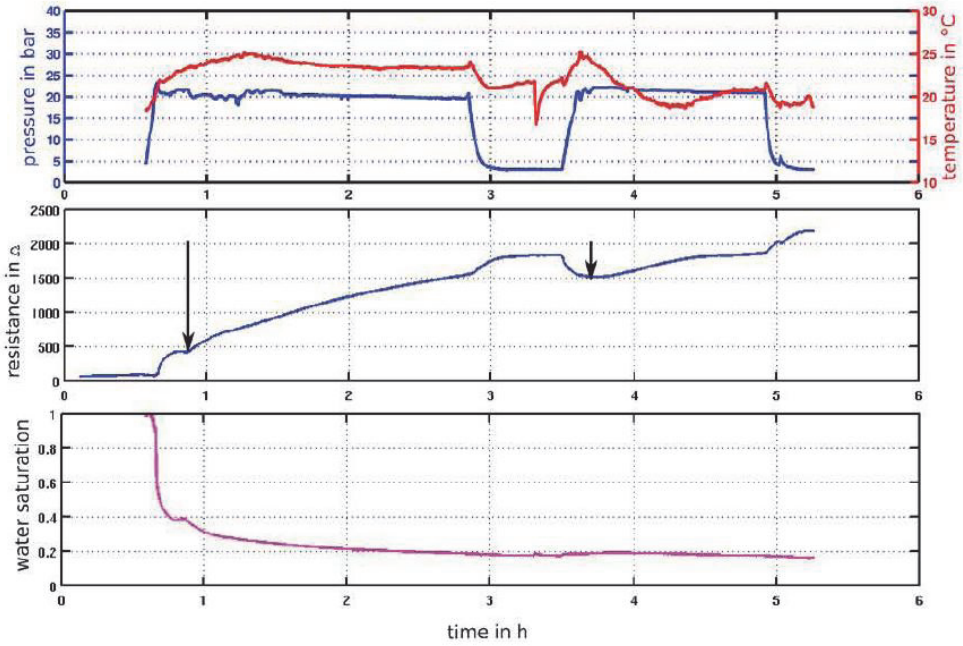

Fig. 8. Resistance results of the CO_2 and water under the reservoir pressure and temperature in the laboratory tests by Borner et al. (2010). Two arrows are the start point of CO_2 injection. With more CO_2 injection, the resistance becomes higher.

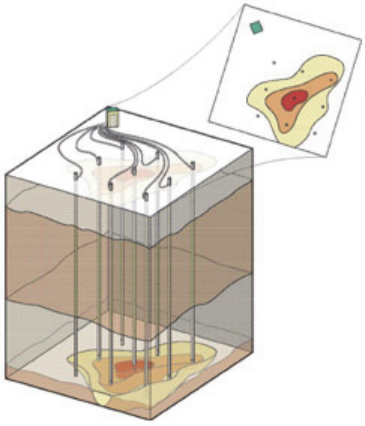

Fig. 9. A typical scheme of the electromagnetic method for CO_2 plume monitoring by measuring the electrical resistivity distribution in the subsurface (LLNL, 2005).

reported as monitoring method to detect CO_2 leakage through permeable fractures by various frequencies electromagnetic sources (Mikhailov et al., 2000). Electromagnetic technologies indicate the ability to monitor offshore CO_2 storage seabed at depths up to several kilometers.

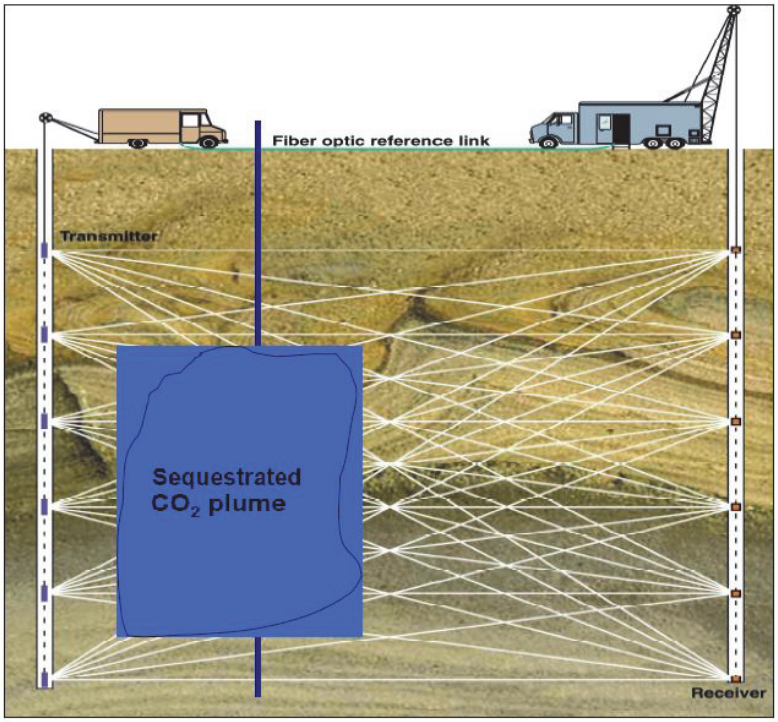

Fig. 10. The system used for CO_2 plume mapping in Lost Hills anticline in San Joaquin Valley, California by electromagnetic technologies (Kirkendall & Roberts, 2004).

For this application, electromagnetic technique is called seabed-logging (Johansen et al., 2005). However, the work of Johansen et al. (2005) suggested that seabed logging was supposed to work at least 300 meters of deep water for obtaining enough mapping signals based on the current study.

2.3 Gravimetric technologies

Gravimetric technologies can detect variations of the rock and fluid density due to CO_2 injection in the subsurface through measuring the gravitational acceleration. As reported by Goldberg (2011), a typical workflow of the techniques for downhole measurement includes the following:

- Determine the various vertical depths according to the monitoring task;
- Install gravimetric sensors with sidewall of the borehole in the geological formations;
- Measure the local gravitational field or gravity gradient as the baseline gravimetric data;
- Measure the local gravitational field or gravity gradient again as post-baseline data with time intervals from baseline measurement;
- Quantify the difference between baseline data and post-baseline data to monitoring CO_2 movement on both vertical and horizontal directions.

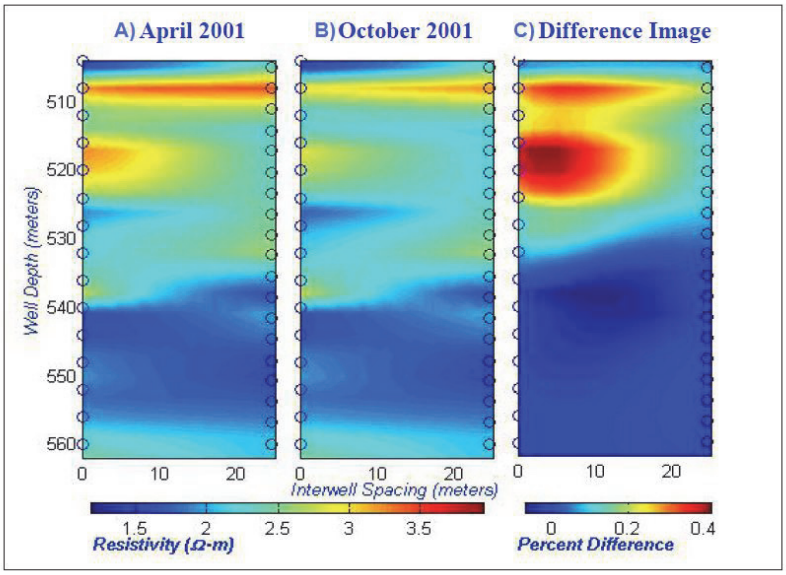

Fig. 11. Field tomographic data was acquired by electromagnetic technique in Lost Hills anticline in San Joaquin Valley, California in four date periods, April, 2001, October, 2001, July, 2002, and October, 2003. A) is the background distribution before CO_2 injection. B) is the imaging with five months of CO_2 injection. And C) is the difference image between A) and B) (Kirkendall & Roberts, 2004).

Moreover, the author pointed out a range of the density changes of CO_2-aquifer over depth (Goldberg, 2011). The density contrast is around 500 kg/m^3 at the shallow depth within 1000 meters. With depth increases to 2500 meters, CO_2 will be in a supercritical phase. Correspondingly, the density difference decreases to about 200 kg/m^3. If deeper than 2500 meters, the density of CO_2 becomes heavier than aquifer; the difference is about 40-50 kg/m^3. Regarding the minimum sensitivity (mostly is around 10 μGal) of gravimetric sensor, these contrasts over the depth are enough to be measured of gravimetric technologies (Goldberg, 2011).

Estimating the amount of dissolved CO_2 is one of the challenge problems because some technologies, such as seismic are not effective for such changes. However, gravimetric technologies can monitor these amount of changes by quantifying mass differences between baseline data and multiple post baseline data (CO_2STORE, 2007). Moreover, gravimetric measurement can be installed both at the surface and downhole for onshore and offshore monitoring purposes (Chadwick et al., 2009; CO_2STORE, 2007; Stenvold, 2008).

2.4 Surface and near surface technologies

Compared to the technologies stated above, this section more focuses on the shallow to surface monitoring. There are many technologies for surface and near-surface which mainly include soil flux monitoring based on the chamber equipments (LI-COR Bioscience, 2004; Madsen

et al., 2009) or enhanced vent-based scheme (Liu, 2010; Liu et al., 2009), micrometeorological flux monitoring (Burba & Anderson, 2010; Madsen et al., 2009), tracers monitoring (Phelps et al., 2007; Wells et al., 2007), surface deformation monitoring (Davis & Marsic, 2010b; Sweatman & McColpin, 2009), surface water monitoring (Darby et al., 2008; Emberleya et al., 2004).

2.4.1 Chamber-based soil CO_2 flux monitoring

Chamber-based soil CO_2 flux measurement is a direct method at the surface to monitor CO_2 leakage. Roughly, there are two types of chambers named as closed top and open top as reported in the papers (Edwards & Riggs, 2003; LI-COR Bioscience, 2004; 2011; Madsen et al., 2009; Vanaja et al., 2006). In view of the applications to the field monitoring, closed-chambers appears to have wider usage than open ones. As an example, closed-chamber methods developed by LI-COR Bioscience are reviewed in this section. A schematic of this chamber is shown in Figure 12 (LI-COR Bioscience, 2004; Madsen et al., 2009). This system includes two main parts as closed-chamber and analyzer. The small portion of air is collected firstly in the chamber, and then piped to the analyzer for CO_2 flux monitoring by an infrared gas analyzer.

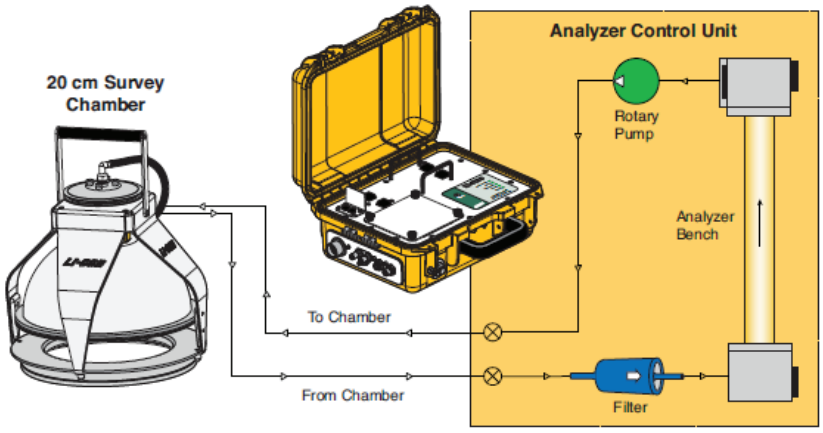

Fig. 12. An example of closed-chamber schematic (LI-8100) developed by LI-COR Bioscience (LI-COR Bioscience, 2004).

For this type of instrument, four main criteria were suggested by LI-COR Bioscience (2004) for accurate measurement: firstly, keeping the pressure equilibrium inside the chamber; secondly, ensuring a good mixing of the air in chamber; thirdly, handling an altered diffusion gradient inside the chamber; and the last one is to minimize the disturbance from the environment (LI-COR Bioscience, 2004). The new version of instruments with solution of such criteria has been applied to field tests, such as Soybean field in Nebraska, Central Appalachian Coal Seam Project of the Southeast Regional Carbon Sequestration Partnership, CO_2SINK and Midwest Geological Sequestration Consortium Illinois Basin-Decatur Illinois Site Project (LI-COR Bioscience, 2004; 2011; Madsen et al., 2009). One of the CO_2 soil flux monitoring results with fluctuated temperature in Soybean field in Nebraska is shown in Figure 13 (LI-COR Bioscience, 2004). The diurnal soil CO_2 flux was observed in July, 2006. The flux

range varying from 2 to 7 $\mu mol(m^{-2}s^{-1})$ was comparable with other published data at the same location (LI-COR Bioscience, 2004).

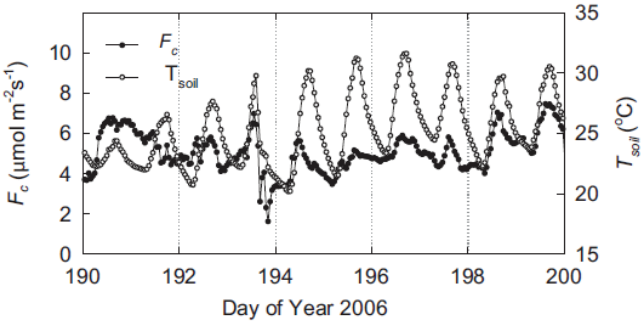

Fig. 13. Soil CO_2 flux monitoring results in Soybean field at the University of Nebraska-Lincoln Agricultural Experimental Station Near Mead in Nebraska (LI-COR Bioscience, 2004).

2.4.2 One-way vent-based CO_2 flux detection

Regarding to the CO_2 monitoring in the near-surface, it is important to realize that the CO_2 flux is not only affected by geological properties but also by barometric pumping. Periodic variation of the atmospheric pressure drives a natural "breathing"between the atmosphere and sub-surface (Martinez & Nilson, 1999; Neeper, 2001; Olson et al., 2001; Tillman & Smith, 2005). With the periodic increase of barometric pressure, gas is pushed downward into the soil; this is known as "inhaling". Conversely, "exhaling"occurs when the soil pressure is higher than the barometric pressure, which drives the air-flow upwards (Choi & Smith, 2005; Martinez & Nilson, 1999; Neeper, 2001; SEAI, 1996). As an example, hourly observations of pressure and the air flowrate during a 4-day period at Castle Airport in the summer of 1998 (NFESC, 2004) is shown in Figure 14. Although the records are not strictly periodic, the diurnal nature in the pressure variation is obvious. Figure 15 is a modeling demonstration of "air breathing"with a periodic sinusoidal barometric change (Liu, 2010).

To predict the CO_2 ground surface flux with considering barometric pumping to determine if this quasi-periodic pressure variation significantly affects near-surface CO_2 in the vadose zone, a scheme was suggested to address the effect of a one-way vent valve on the control of CO_2 flux during barometric pumping. In many leakage scenarios, CO_2 will escape at low concentrations over wide areas. The purpose of the suggested scheme is to concentrate the low CO_2 flux leakage from a large area so that the number of detectors and their required sensitivity can be reduced for the detections (Liu, 2010; Liu et al., 2009).

An example was given in Figure 16 based on the proposed scheme. The vent valve system includes a one-way vent valve, buffer (plenum), and membrane for coverage of the surface for impermeable purpose. One-way vent valve is controlled by the pressure difference between subsurface gas pressure and barometric pressure as shown in Figure 16. The domain used in the tests is the 20 $\times$ 20 meter axi-symmetric two-dimensional geometry, including two soil layers. The thickness of topsoil is 3.5 meters from the surface. Another 16.5 meters is cobble.

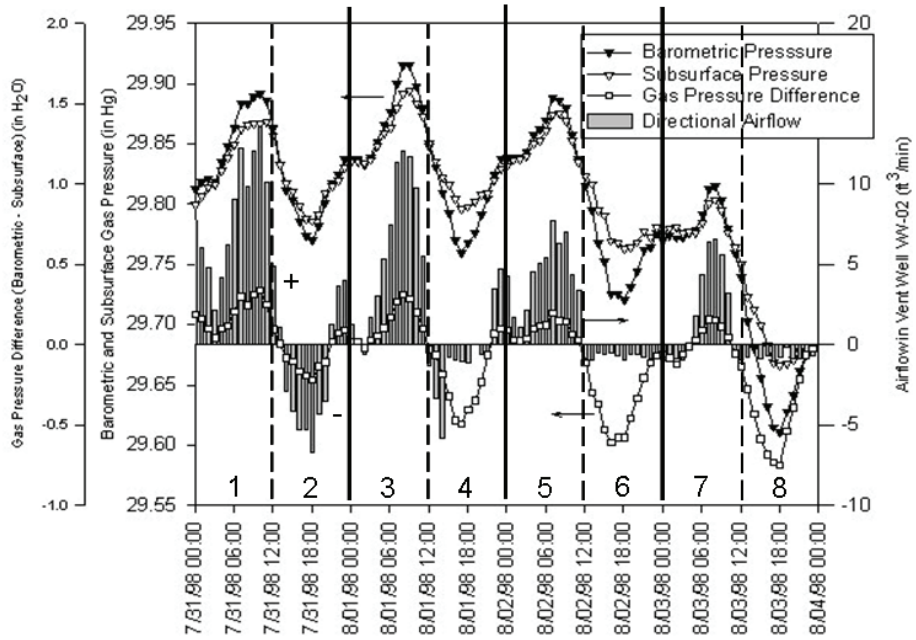

Fig. 14. Airflow, barometric, and subsurface pressures during 4 days monitored through a well at Castle Airport (NFESC, 2004).

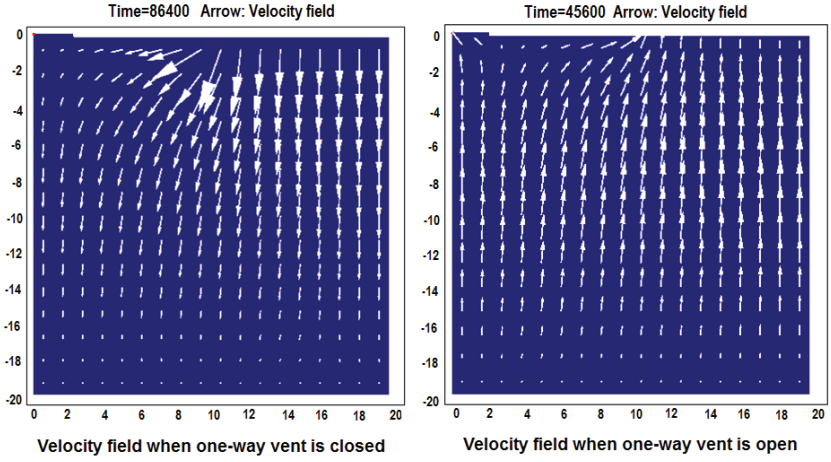

Fig. 15. Example of velocity fields controlled by one-way vent control with barometric pumping (Liu, 2010).

The CO_2 source point is located at 5 meters deep marked by the red dot, and the water table is 4.25 meters deep along the white line in Figure 16. The region above the water table is the

vadose zone. The right section of Figure 16 is the scheme and grid used in the simulations (Liu, 2010; Liu et al., 2009).

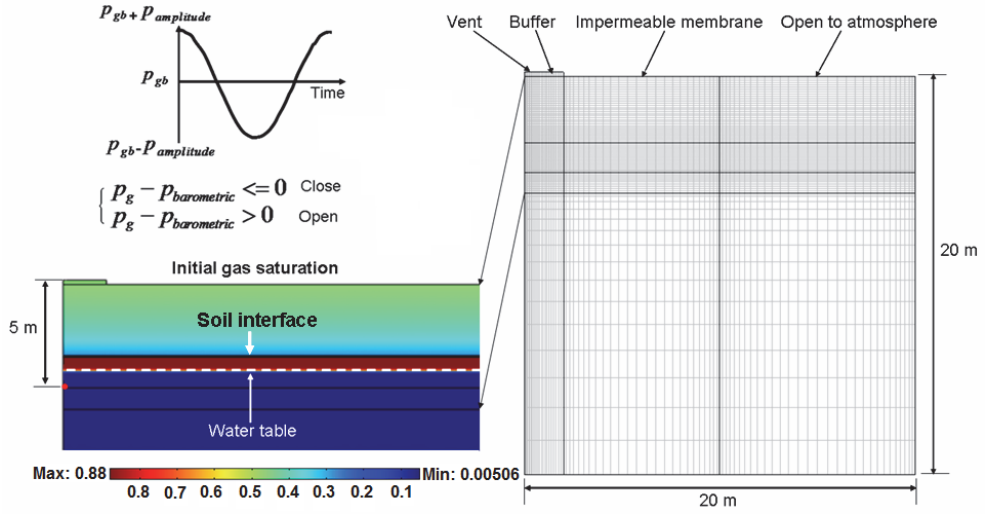

Fig. 16. Domain and the vent valve system coupled on the top boundary for investigation of the proposed method. The red point is the CO_2 source point. Besides, the soil interface line and the horizontal cross lines are for local grid refinement while the verticals are boundaries of the buffer and the impermeable membrane (Liu, 2010; Liu et al., 2009).

To demonstrate on how the proposed scheme enhances CO_2 leakage monitoring is effective, a series of the cases was designed in Table 1 for comparisons of the total CO_2 mass out from the one-way vent in Figure 17(a).

Case No.	Barometric Pumping	Impermeable Membrane (m)	Vent	Buffer & Size (m)	Δ P (Pa)	Period (day)
1	no	no	no	no	no	no
2	yes	no	no	no	800	1
3	yes	no	yes	no	800	1
4	yes	10	yes	no	800	1
5	yes	10	yes	yes, 0.2	800	1

Table 1. Summarized Investigation Cases

Through comparisons in Figure 17(a), the proposed concept was confirmed to use an impermeable membrane and a one-way vent valve to concentrate gas from a large region at the vent so that fewer sensors, and sensors of lesser sensitivity, could be used for detection of CO_2 leaking from geological storage. This is the reason why the accumulated CO_2 mass out from the vent is the highest than the other 4 cases. Figure 17(b) shows the details on why the sensor on the vent was easier and quicker to catch CO_2 leakage because high percentage (more than 85%) of total leaked CO_2 was collected and flowed out from the vent.

Moreover, another 22 cases (a total of 27 cases) were designed to address the effects from the other related factors: the properties of barometric pressure (amplitude and period), variations

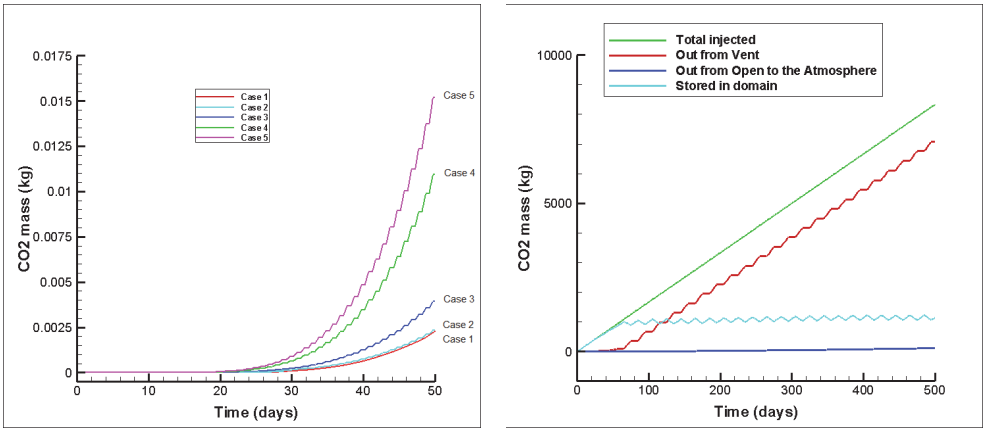

(a) Comparisons among five cases (b) Comparisons among CO_2 mass balance

Fig. 17. Comparisons of the CO_2 mass out from the vent (Liu, 2010).

of impermeable membrane and buffer zone size, and meteorological phenomena (rainfall and wind) under the various soil permeability and leakage source rate. All of the tests draw the consistent conclusion that the proposed scheme, one-way vent valve system by Liu (2010), is efficient at the near-surface CO_2 flux monitoring.

2.4.3 Eddy covariance based CO_2 flux monitoring

The first eddy covariance method was suggested by Swinbank Swinbank (1951). This methods was proposed to directly measure the detailed structure of temperature, vapor pressure, and total wind speed and its vertical component of the air passing a fixed point, which are brought about by eddy movement in the lower atmosphere through a apparatus (Swinbank, 1951). This method relies on a combination of wind velocity and CO_2 concentration measurements based on the derivation of the turbulent eddies and corresponding scalar from the fast measurement average values (Burba & Anderson, 2010; LI-COR Bioscience, 2006). Recent years, this method has been applied to CO_2 leakage monitoring in the atmosphere (Benson, 2006; Cooka et al., 2004; Goulden et al., 1996; Lewicki et al., 2009; LI-COR Bioscience, 2004; 2006; 2011; Miles et al., 2004). As examples, CO_2 emissions were monitored in the Barrow Island site in Alaska and Willow Creek site in Wisconsin in 2002 and 2005 respectively (Benson, 2006; Cooka et al., 2004). The conclusions indicate that the resolution of proposed instruments show the good abilities in CO_2 monitoring with excluding the natural background fluxes (Benson, 2006; Cooka et al., 2004; Miles et al., 2004).

2.4.4 Surface deformation monitoring technologies

Because of CO_2 injection and related extraction of fluids, the pressure underground changes which means that the corresponding strain changes and results in the displacement. Surface deformation monitoring technologies are based on measuring this displacement (swelling and shrinkage) for the purpose of monitoring (Davis & Marsic, 2010a; Sweatman & McColpin, 2009). The technologies integrate three parts, which are satellite-based interferometric

synthetic aperture radar (InSAR), surface tiltmeters, and differential global positioning system (DGPS). InSAR is used to provide periodic updates of the ground deformation within a typical coverage area about 10,000 km^2 by imaging large swaths of the earth's surface (Davis & Marsic, 2010a; Davis et al., 2008; Du et al., 2005; Kherroubi et al., 2009; Lewicki et al., 2009; Sweatman & McColpin, 2009). Tiltmeter is built with a highly sensitive electrolytic bubble level to measure tilt movements in a one nanoradian of radian level. DGPS monitoring is usually used to supply InSAR and tiltmeter arrays in acquisition areas. At least two GPS receivers and sophisticated Kalman filters are used to exam the horizontal and vertical motions in typical differential method. One receiver is placed in an area where non-deformation is a reference; another receiver(s) is located in the region(s) where the deformation needs to be monitored. The difference between the reference and the receiver is the surface deformation as shown in Figure 18. The accuracy of the surface deformation monitoring technologies can be millimeter level for both land and subsea instruments (Davis & Marsic, 2010c; Sweatman & McColpin, 2009). The applications of the technologies covered CO_2 storage in a coal-bed and deep saline aquifer (Davis & Marsic, 2010c; Sweatman & McColpin, 2009). Moreover, surface deformation monitoring technologies are useful in well stimulation efforts to map hydraulically created fractures (Gladwin, 1984; Sweatman & McColpin, 2009).

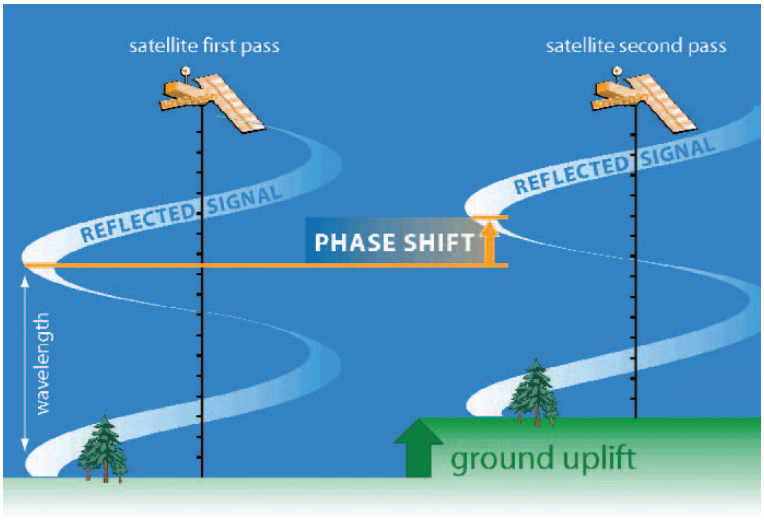

Fig. 18. Example of satellite-based InSAR technology for earth's surface deformation monitoring (Sweatman & McColpin, 2009).

2.4.5 Geochemical and tracer monitoring technologies

Geochemical monitoring involves measuring of the changes of the groundwater and/or associated gas content, such as CO_2, in and around storage site. The measurement is frequently done to detect the water composition differences, pH value changes, and electrical conductivity various, which is caused by the dynamic equilibrium of dissolution and mineralization systems, such as $Na^+ - Ca^{2+} - HCO3^{-1} - Cl^{-1}$. This detection also includes monitoring the changes of isotopic element, such as ^{13}C, ^{14}C, ^{18}O, and ^{2}H (Benson & Gasperkova, 2004). The samples of the water can be collected from surface, wellhead,

and/or downhole. These samples are usually taken from different locations in frequent time intervals. Similar to the time-lapse technologies, geochemical monitoring methods can be used in the whole process of CO_2 storage, such as pre-injection, injection, and post-injection. As an example, geochemical monitoring technologies have been used in the CO_2 storage in the Otway site in Australia (Caritat et al., 2009; Hortle et al., 2011). More than 70 groundwater compositions (elements/compounds) and seven isotopes from 28 sampling locations (stations) in various depths were tested. The preliminary results indicate that there is not much significant changes by contrasting the pre- and post-injection though some compositions varied a little based on some seasons. The mostly interesting factors, HCO_3^- and pH values were shown in Figure 19 (Caritat et al., 2009; Hortle et al., 2011). It means that there is not any significant CO_2 leakage within the monitoring period.

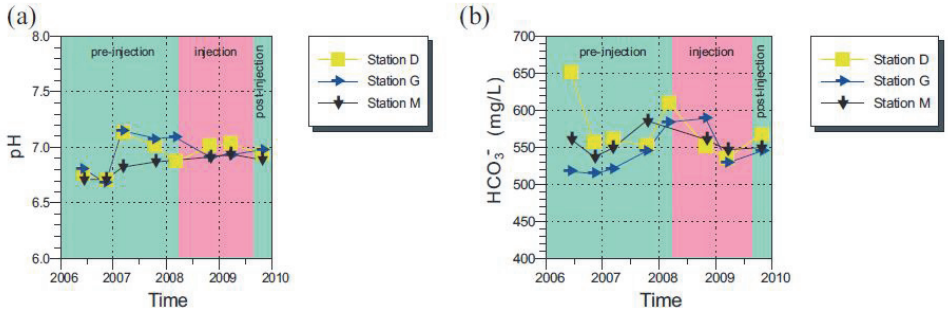

Fig. 19. The comparisons of HCO_3^- and pH values from pre-injection, injection, and post-injection (Hortle et al., 2011).

Monitoring CO_2 by inspecting tracers is another option which can be used in the groundwater and vadose zone for the migration identification. The systemic study of the tracers in the field was discussed by Zemel (1995). The potential choices of the tracers include natural and artificial elements/compounds. Isotopes, such as C, O, H noble gases are the natural tracers, which have been widely used in different CO_2 storage sites (Bachelor et al., 2008; Stalker et al., 2009). SF_6, CD_4, and perfluorocarbons are good choices of artificial tracers (Hortle et al., 2011; McCallum et al., 2005). However, any tracer needs to be evaluated based on the occupational health, environmental safety, and suitability for the monitoring and analysis concerns (Stalker et al., 2009). As guidelines, a total of 13 points for tracer choice was suggested by Stalker et al. (2009). These points are briefly summarized as follows: 1. highly physical and chemical stability (without significant degrade, microbial, and reaction) for the selected CO_2 storage site (even under the high pressure and high temperature conditions); 2. Availability (even for large-scale of CO_2 injection) with competitive cost; 3. Collaborations in the CO_2 storage system which work with other tracers during different monitoring phases; 4. Easy detection and analysis during monitoring even in different monitoring depths with a background level of tracer self (Stalker et al., 2009). As part of the monitoring project of Zero Emissions Research and Technology (ZERT), a pilot site was selected in the West Pearl Queen, southeast of New Mexico, USA (Wells et al., 2007). In this monitoring program, several tracers, such as Perfluorocarbon tracers (PFTs), perfluoro-1,2-dimethylcyclohexane (PDCH), perfluorotrimethylcyclohexane (PTCH) and perfluorodimethylcyclobutane (PDCB) were used to detect CO_2 leakage in a series of six concentric circles (with different radius)

centered injection well as shown in Figure 20(a). Authors reported a total of four sets of measurement data with the monitoring schematic design. As an example, only third set of the test results are cited in Figure 20 (Wells et al., 2007). One of the conclusions pointed out that these tracers show a excellent ability in CO_2 monitoring (Wells et al., 2007).

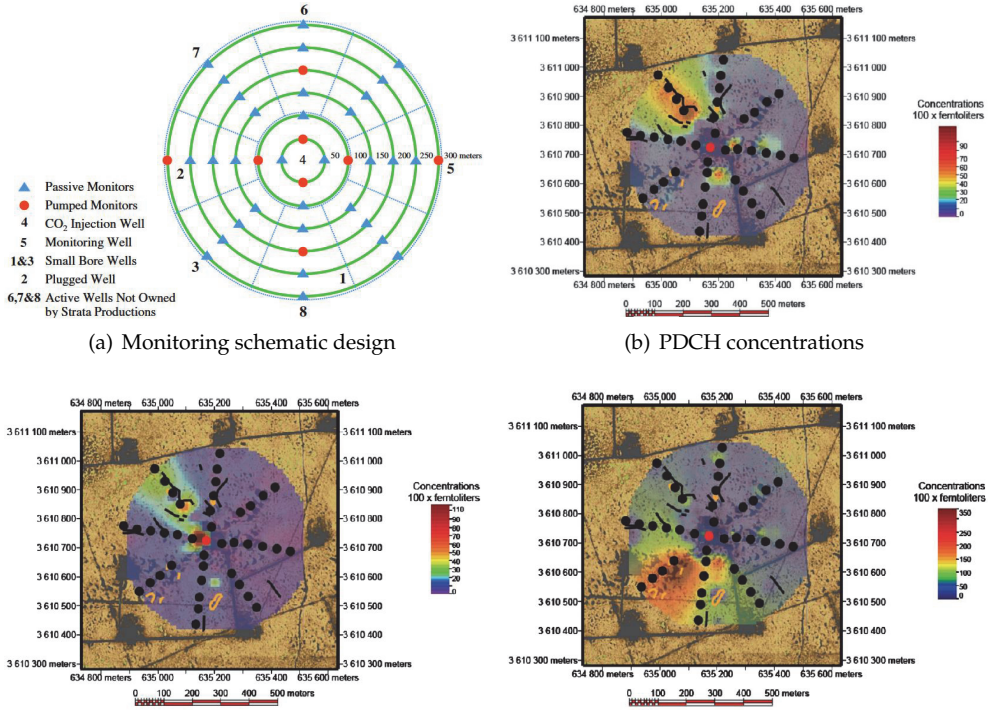

(a) Monitoring schematic design

(b) PDCH concentrations

(c) PTCH concentrations

(d) PDCB concentrations

Fig. 20. Orthophoto view of tracers concentration (third set of total four sets) measured over 54 days. Red dot is the injection well and black dots are the adsorbent tubes for sampling (Wells et al., 2007).

2.5 Terrestrial ecosystem monitoring technologies

CO_2 monitoring technologies in terrestrial ecosystems are not reviewed in this chapter since most methods are based on the CO_2 flux measurement and carbon biomass (Ebinger et al., 2001; Jacobs & Graham, 2000). However, the related knowledge are available through the publications by Betts et al. (2004); Brovkin et al. (2004); D. & E. (2003); Ebinger et al. (2001); Jacobs & Graham (2000); Lehmann et al. (2006); Wisniewski et al. (1993)

2.6 Cost of monitoring technologies

The cost for some monitoring technologies were summarized in Figure 21 by Benson & Gasperkova (2004). Besides, based on monitoring phases (pre-operational monitoring, operational monitoring, and closure monitoring), three options (low residual gas saturation

saline formation (LRG), high residual gas saturation saline formation (HRG), and reservoir with EOR) of CO_2 storage were estimated by choices "basic monitoring package" and "enhanced monitoring package". The cost for "basic monitoring package" and "enhanced monitoring package" for three storage options are listed in Table 2 (Benson & Gasperkova, 2004; Zahid et al., 2011).

3. Field applications of monitoring technologies

The selection of monitoring technologies is specifically based on the CO_2 storage site, such as geological characteristics, which covers onshore or offshore, saline aquifers, or oil/gas reservoir. Moreover, the selection also depends on the monitoring phase, such as pre-injection, injection, and post-injection. In addition, the monitoring technologies selection starts from the beginning of CO_2 storage site selection. This is because two primary factors of storage capacity and cap-rock sealing ability are always investigated in the procedure of CO_2 storage from site characteristics, injection location determination, injection rate, and period to the monitoring detection during injection and post-injection. This procedure is also an optimization of determining low risk (such as leakage) with integrating injection location, injection rate, and injection period in the sink-seal system. Similarly, Seto & Mcrae (2011) suggested a framework for integrated monitoring design based on technologies and cost for risk reduction. In this section, only CO_2 monitoring technologies in several projects were reviewed to demonstrate how these technologies work in fields, rather than checking all injection and planned injection projects of worldwide in Figure 22.

- **Sleipner**

The site at Sleipner, Norway North Sea has been developed for CO_2 storage by 1 Mt per year injection rate. The initial identification of the site for this project was investigated in 1994 and commenced with CO_2 by Statoil and the partners in 1996. The CO_2 injected in the storage formation "Utsira Sand" has been monitored by introducing seismic surveys, time-lapse seafloor gravity technologies, and surface/near-surface methods, such as soil gas and satellite remote sensing (Aleksandra et al., 2010; Arts et al., 2008). As an example, the results of 2D cross seismic surveys were shown in Figure 23 (Arts et al., 2008). By comparing the bright reflections in all images of Figure 23, the changes of the saturation due to CO_2 injection within the period is clear.

- **Salah**

The project of CO_2 storage located In Salah, Algeria, has been operated by BP, Sonatrach, and Statoil for 1.2 Mt per year of CO_2 injection rate in Jurassic saline formation around 1850 meters deep (Aleksandra et al., 2010; Mathieson et al., 2010). The technologies used for the CO_2 monitoring were summarized in Figure 24 (Mathieson et al., 2010).

Based on the technologies above, some monitoring results, such as surface deformation, satellite imaging, time lapse 3D seismic survey, and shallow aquifer tests were reported (Aleksandra et al., 2010; Chadwick et al., 2009; CO_2STORE, 2007; Onuma et al., 2009; Mathieson et al., 2011; 2010; Wildenborg, 2011). As an example, a ground deformation results from In Salah is shown in Figure 25 (Wildenborg, 2011). The period of the deformation tracking is from November 29, 2003 to August 29, 2009.

Technique		Costs
Wellhead Pressure	[T1]	$4,500/$5,500 without/with remote transmission (http://www.pioneerps.com)
Formation Pressure	[T2]	open hole, depth 5,000 ft, 20 tests, Texas: $10,450, Alaska: $32,800 (http://www.reeves-wireline.com)
Injection and Production Rate	[T3]	Production well: Gas/water separator w/meters: $35,000 (cheaper version: $15,000), remote monitoring with satellite feed $4,500; Injection well: gas meter: $4,500,remote monitoring with satellite feed $4,500, continuous gas analysis: $50,000, it's cheaper if only periodic analysis is used (J. Robinson, Alberta Reseach Council)
Well Logs	[T4]	Basic Combo (caliper, gamma ray, neutron, resistivity): $29,600; Sonic DeltaT Long-Spacing: $8,910; UltraSonic Cement/ Casing Imager: $13,500; Dipole Sonic Imager: $12,328; Combinable Magnetic Resonance: $19,849; RST (Saturation Tool): $17,238 (Schlumberger)
Fluid and Gas Composition	[T5]	Complete compositional analysis of gas samples: $100/sample; ^{14}C analysis of gas component by AMS: $650/component (http://www.isotechlabs.com); isotopes in CO_2 sample: $30; isotopes in water sample: $50-$100 (M. Conrad, LBL); Chromatograph +RTU: $30,000 (G. Wright, ExxonMobil)
Seismic Monitoring	[T6]	$10-25 k / km^2 acquisition + $800-1,000/$km^2$ processing (SACS and W. King (ChevronTexaco) and seismic contracting company)
Electrical and Electromagnetic Monitoring	[T7]	$1,000/site ($200/site) (M. Hoversten, LBNL)
Gravity Monitoring	[T8]	$1,000/site ($200/site) (J.Hare, ZongeEnginnering and T. Niebauer, Micro-g)
Land Surface Deformation	[T9]	InSAR: $10,000/image (http://www.npagroup.com)
Tilt Measurements	[T10]	downhole: existing well, 5 days, $94K acquisition + $37K interpretation (array of 12 tools) (Pinnacle Technologies)
		surface:($45-60K construction + $15k/day analysis)/20-30 stations (Pinnacle Technologies)
Airborne or Satelite Imaging	[T11]	$70K for 300-500 km^2 for hyperspectral imaging; $20-40K for satelite imaging; if seasonal view -> 3 times/year; mobilization: $30K; baseline imaging will take 3 years; interpretation: 3* ($96K+$300K) = $1,188K (W. Pickles, LLNL)
Soil Gas and Vadose Zone Monitoring	[T12]	Vadose zone: $40k (http://www.sandia.gov/ Subsurface/factshts/ert/vzms.pdf)
Surface Flux Monitoring	[T13]	$35k equipment + $25k installation + 10k interpretation/year + 5k maintenance/year (M. Fischer, LBNL)
Atmospheric CO_2 Concentration	[T14]	1ppm: < $10k, 0.1 ppm: $120k (M. Torn, LBNL)
Micro Seismicity	[T15]	10 stations: $400k + $50-75k/year (E.Majer, LBNL)

Fig. 21. Cost evaluations for monitoring technologies (Benson & Gasperkova, 2004; Zahid et al., 2011). [T#] stands the index numbers which is used in the table 2.

	Basic Monitoring Package			Enhanced Monitoring Package		
Technologies	Saline Formation (LRG), $	Saline Formation (HRG), $	EOR Reservoir $	Saline Formation (LRG), $	Saline Formation (HRG), $	EOR Reservoir $
Pre-operational Monitoring						
[T4]	1,064,250	1,064,250	0	1,064,250	1,640,250	0
[T1]	55,000	55,000	0	55,000	55,000	0
[T2]	328,000	328,000	0	328,000	328,000	0
[T3]	550,000	550,000	0	550,000	550,000	0
[T6]	3,828,000	2,387,000	0	3,828,000	2,387,000	0
[T7]	N/A	N/A	N/A	225,000	225,000	360,000
[T8]	N/A	N/A	N/A	225,000	360,000	360,000
[T15]	475,000	475,000	475,000	475,000	475,000	475,000
[T14]	100,000	100,000	320,000	100,000	100,000	320,000
[T13]	N/A	N/A	N/A	700,000	700,000	700,000
[T5]	N/A	N/A	N/A	1,000,000	1,000,000	1,000,000
Management (15%)	960,038	743,888	119,250	1,282,538	1,066,388	482,250
Sub-Total:	7,360,288	5,703,138	914,250	9,832,788	8,310,638	3,697,250
Operational Monitoring						
casing Logs	N/A	N/A	N/A	6,000,000	6,000,000	13,200,000
[T6]	9,493,000	9,493,000	15,840,000	9,493,000	9,493,000	15,840,000
[T7]	N/A	N/A	N/A	936,000	936,000	1,440,000
[T8]	N/A	N/A	N/A	936,000	936,000	1,440,000
[T1]	1,665,000	1,665,000	1,500,000	1,665,000	1,665,000	1,500,000
[T3]	3,351,000	3,351,000	6,450,000	3,351,000	3,351,000	6,450,000
[T14]	1,800,000	1,800,000	2,460,000	1,800,000	1,800,000	2,460,000
[T13]	N/A	N/A	N/A	4,800,000	4,800,000	4,800,000
[T15]	3,675,000	3,675,000	3,675,000	3,675,000	3,675,000	3,675,000
[T5]	N/A	N/A	N/A	570,000	570,000	570,000
Management (15%)	2,997,600	2,997,600	4,488,840	4,983,900	4,983,900	7,706,340
Sub-Total:	22,981,600	22,981,600	34,414,440	38,209,900	38,209,900	59,081,940
Closure Monitoring						
[T6]	15,983,000	11,935,000	7,920,000	15,983,000	11,935,000	7,920,000
[T7]	N/A	N/A	N/A	1,519,000	1,125,000	720,000
[T8]	N/A	N/A	N/A	1,519,000	1,125,000	720,000
[T1]	N/A	N/A	N/A	277,500	277,500	1,250,000
[T13]	N/A	N/A	N/A	8,000,000	8,000,000	3,200,000
[T5]	N/A	N/A	N/A	950,000	950,000	380,000
Management (15%)	2,397,450	1,790,250	1,188,000	4,237,275	3,511,875	1,978,500
Sub-Total:	18,380,450	13,725,250	9,108,000	32,485,775	26,924,375	15,168,500
Total Cost:	48,722,338	42,409,988	44,436,690	80,528,463	73,444,913	77,947,690
Total Cost at 10% discount	13,697,010	12,023,781	12,683,389	20,927,707	19,250,724	23,319,093
Total CO_2	2.58e8	2.58e8	2.58e8	2.58e8	2.58e8	2.58e8
Cost/CO_2 Tonne	0.189	0.164	0.172	0.312	0.284	0.295
Discount Cost per CO_2 Tonne	0.053	0.047	0.049	0.081	0.075	0.090

Table 2. Cost of monitoring packages modified from the works of Benson & Gasperkova (2004)

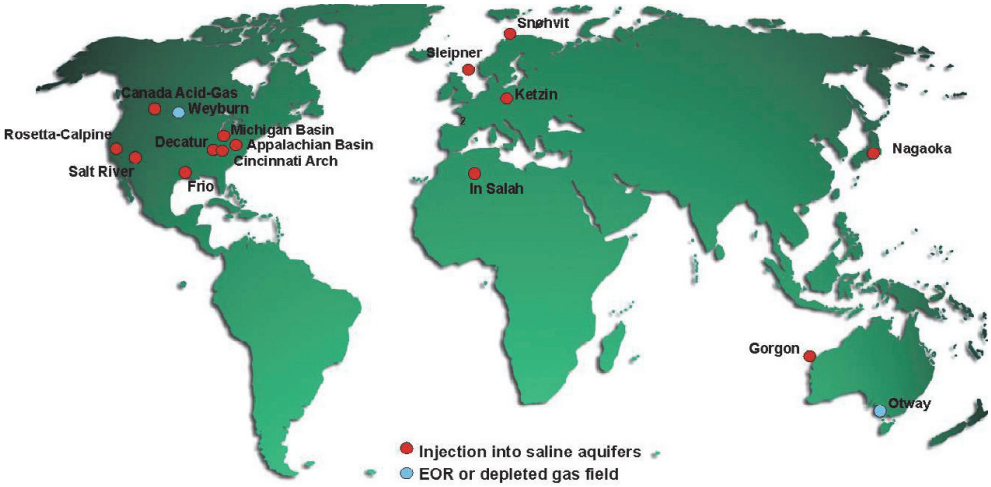

Fig. 22. Worldwide CO_2 injection and planned injection projects (Michael et al., 2009; 2010).

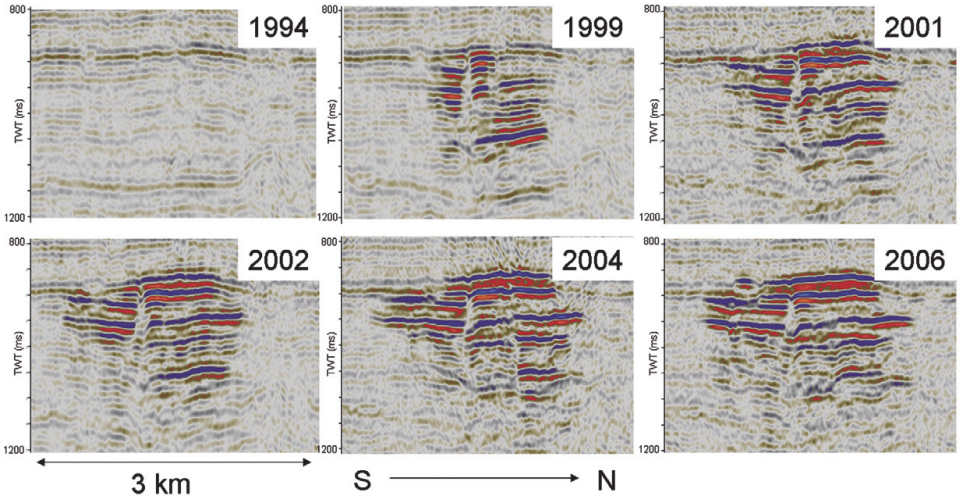

Fig. 23. 2D seismic cross view of the CO_2 storage site, Sleipner, Norway North Sea (Aleksandra et al., 2010; Arts et al., 2008).

- **Gorgon**

Storage CO_2 in the Gorgon field, Australia, was designed for large-scale of the CO_2 injection by the rate of 4.9 Mt per year. This project has been operated by Chevron, Royal Dutch Shell, and ExxonMobil and was approved for injection in August 2009. The technologies introduced for the monitoring include injection well monitoring by well head pressure, flow rate, and

Monitoring technology	Risk to monitor	Action
Wellhead/annulus sampling	Wellbore integrity Plume migration	• Twice-monthly sampling since 2005
Tracers	Plume migration	• Implemented 2006
Wireline logging/sampling	Subsurface characterization	• Overburden samples and logs collected in new development wells
Soil gas/surface flux	Surface seepage	• Preinjection surveys in 2004 • Repeat survey in 2009
3D-4D seismic	Plume migration	• Initial survey in 1997 • High-resolution survey acquired in mid-2009. Provides feasibility evaluation for 4D
Deep-observation wells	Plume migration	• Not planned at present due to cost
Microseismic	Cap rock integrity	• Test well drilled mid-2009 above KB-502 injector • Depth 500 m, 1500 m above injection zone, 50 geophones array (10 three-component) • Recording ongoing
Electromagnetic surface and wellbore	Plume migration	• Not useful at Krechba due to subsurface architecture and logistics • Wells too widely spaced
Gravity	Plume migration	• Modeling suggests surface response negligible • May be tested in 2011 • Borehole gravity possible if suitable access available
VSP	Cap rock integrity Plume migration Fracture evaluation	• Modeling results inconclusive • Decision pending 3D VSP into microseismic array
Shallow aquifer wells	Contamination of potable aquifer Cap rock breach	• Seven shallow aquifer wells drilled • Sampling twice per year
Microbiology	Surface seepage	• First samples collected in late 2009
Eddy covariance flux towers and LIDARs	Surface seepage	• Reviewed, but weather conditions and potential equipment theft ruled this out • Reviewing potential for deployment in 2011
InSAR monitoring	Plume migration Cap rock integrity Pressure development	• Used extensively, contributions and commissioned work from several providers • Images captured every 28 days
Tiltmeters/GPS	Plume migration Cap rock integrity Pressure development	• To calibrate InSAR deformations • 70 tiltmeters deployed around KB-501 in late 2009

Fig. 24. The summarized monitoring technologies and status In Salah, Algeria (Aleksandra et al., 2010; Mathieson et al., 2010).

continuous bottom-hole pressure; reservoir surveillance wells by saturation logs and pressure changes above well perforations; surface seismic monitoring over plume area and time lapse 3D; and surface monitoring by soil gas flux sampling grids and seepage points (Aleksandra et al., 2010; Flett et al., 2009). A integrated reservoir surveillance was planned as shown in Figure 26 (Aleksandra et al., 2010; Flett et al., 2009).

- **Weyburn**

Weyburn CO_2 project is a commercial scale site with 2.7 Mt per year injection rate. The Weyburn Oilfield was stimulated by water injection in 1996 after 20 years production. For CO_2 storage, there are two projects. One is for CO_2 enhanced oil recovery managed by EnCana; another is International Energy Agency Greenhouse Gas Weyburn-Midale CO_2 Monitoring and Storage project run by Petroleum Technology Research Center (Aleksandra et al., 2010; Hutcheon et al., 2003; Stalker et al., 2009). The main technologies used to monitor in the first

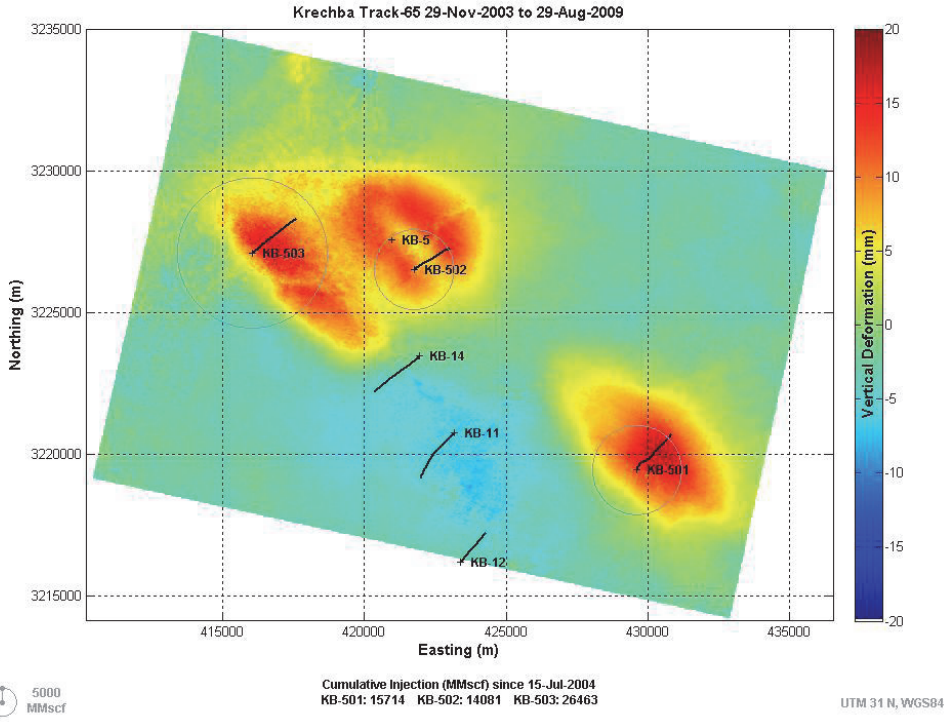

Fig. 25. An example of ground deformation monitoring In Salah, Algeria (Wildenborg, 2011).

phase of the Weyburn are seismic images and geochemical methods from CO_2 injection in September 2000. As an example, results of geochemical monitoring were reported in Figure 27 (Hutcheon et al., 2003; Stalker et al., 2009). In this figure, (a) and (b) indicate the changes of $\delta^{13}CHCO_3$, (c) and (d) show the variations of calcium, and (e) and (f) are the increasing of total alkalinity within 289 and 980 days from the beginning of injection.

- **Frio**

The storage site of Frio is located in the South Liberty oilfield, southeast of Houston. This project started from 2002 for the pilot demonstration of CO_2 storage with funding by the National Energy Technology Laboratory of US DOE. The injection rate of the project was designed as 160 tonnes per day for fating to the brine-bearing sandstone-shale system. Regarding the CO_2 monitoring, there is a list summarize the techniques being used in Figure 28 (Aleksandra et al., 2010; Doughty et al., 2008; Myer et al., 2003).

4. Gaps in knowledge of monitoring technologies

In the past decade, CO_2 monitoring technologies have been making significant progress in subsurface and at surface, based on the geophysical equipments, geochemical experiments, and modeling methods. Particularly, based on the Special Report on CO_2 Capture and Storage by the IPCC (Metz, Davidson, Coninck, Loos & Meyer, 2005), the knowledge gaps

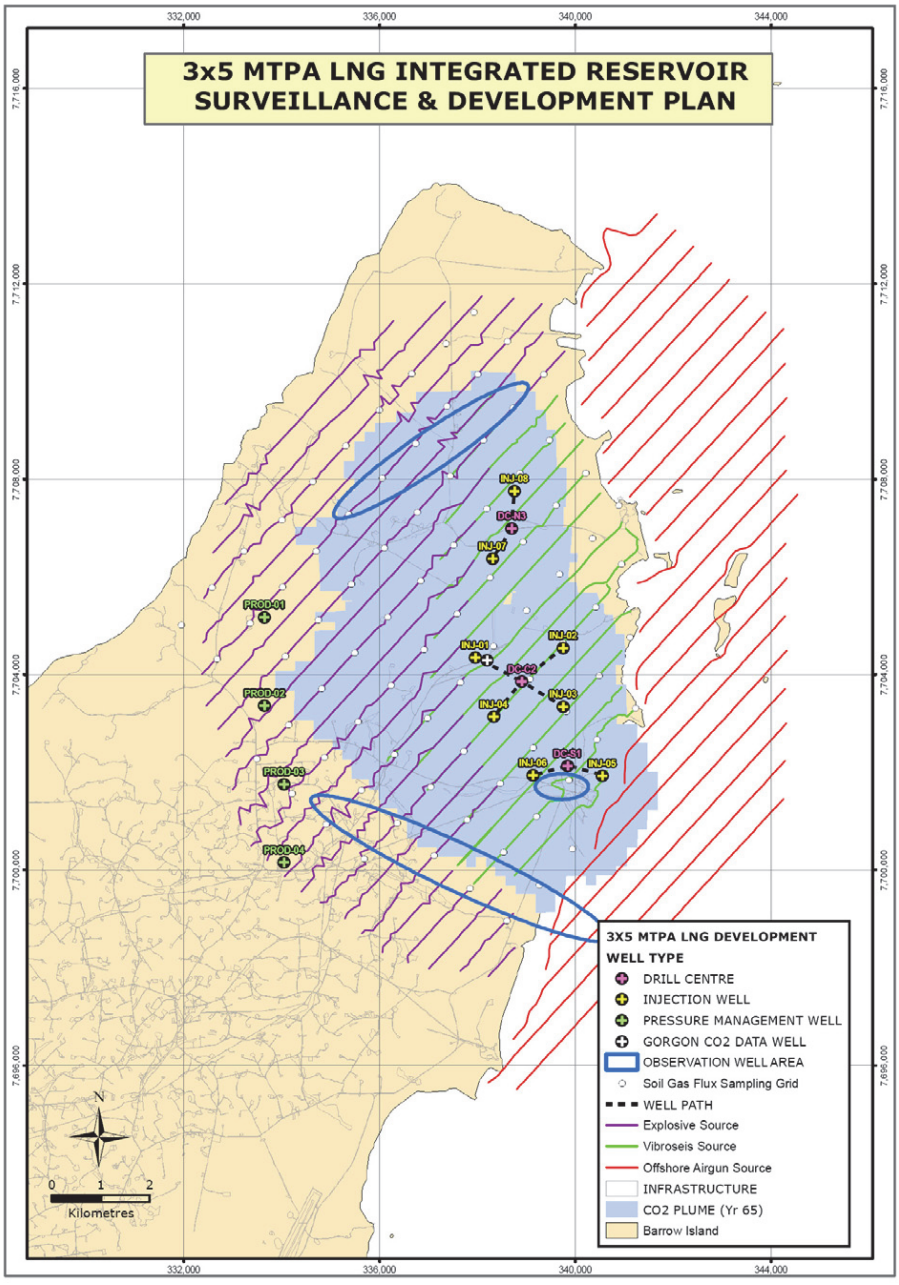

Fig. 26. An integrated reservoir surveillance design for the Gorgon project in Australia (Wildenborg, 2011).

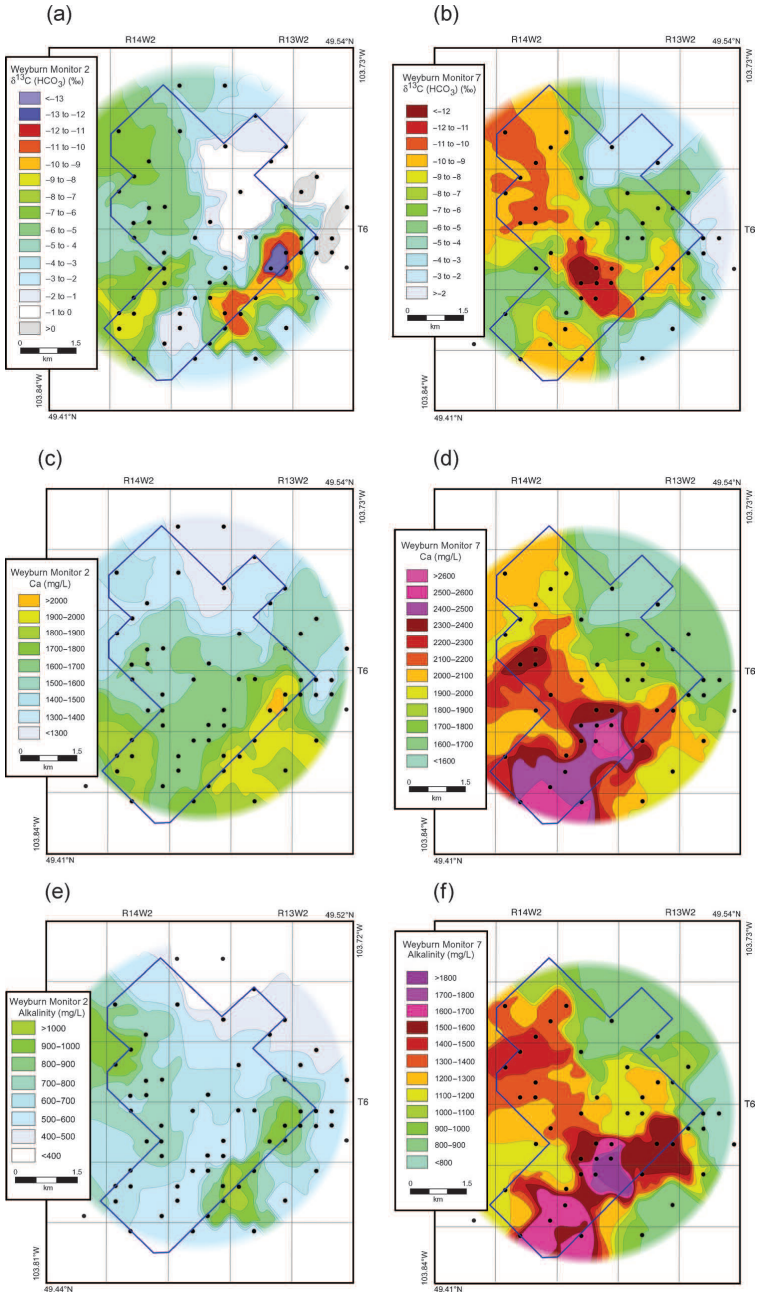

Fig. 27. Geochemical monitoring results at Weyburn, Canada (Hutcheon et al., 2003; Stalker et al., 2009).

	New well logs	New well core	Seismic and electrical geophysics	Surface tilt	Pressure transient tests	Wellbore fluid sampling	Wellbore pressure	Tracers
Rocks type, thickness, dip	+	+	+	+				
Layer continuity			+		+	+	+	+
Faulting and fracturing	+	+	+	+	+	+	+	+
Porosity and permeability	+	+	+		+	+		+
Baseline mineral and fluid composition	+	+				+		
Evolution of fluid pressure			+	+	+	+	+	
Evolution of CO_2, brine saturation	+		+		+	+		+
Mineral dissolution, precipitation; fluid chemistry changes						+		+

Fig. 28. Monitoring technologies used in the Frio CO_2 storage (Aleksandra et al., 2010; Myer et al., 2003).

of monitoring technologies have been addressed frequently (Aleksandra et al., 2010; Michael et al., 2009; CO_2STORE, 2007; IEA, 2007; 2009; Michael et al., 2009; 2010; NETL, 2009; Zahid et al., 2011).All of the technologies reviewed in this chapter show abilities (or potential abilities) in field application with pre-demonstration. However, though some improvements were suggested to fill some of knowledge gaps, the main problems of developing practical and cost-effective technologies for field-scale monitoring application are still open for more explorations (Michael et al., 2009; IEA, 2009; Michael et al., 2009; 2010; NETL, 2009). The main aspects of the technologies are summarized as below (Benson & Gasperkova, 2004):

- **Seismic Technologies**

Seismic technologies, as a very good and popular monitoring set, have been applied to several worldwide CO_2 storage projets because of the high spatial resolution and high sensitivity on small CO_2 amounts in the subsurface. However, seismic techniques cannot reflect the CO_2 information where the seismic source, such as impedance cannot distinguish the variation like the low porosity geological media, consolidated or cemented sandstone, rigid carbonates etc as discussed in Figure 3. In particular, when the small amount of CO_2 near the gaseous phase, it is hard to monitor such CO_2 migrations by seismic techniques. On the other hand, the interpretation of seismic data in the pore space needs to be much quantized, which would help to figure out the CO_2 behaviors in the formation accurately.

- **Electromagnitic Technologies**

Electromagnitic technologies show the potential ability on monitoring of CO_2. However, the accuracy of hardware needs to be improved, especially on the distinguish of mixture fluids

such as CO_2 and water. On the other hand, because electromagnitic technologies are relatively new, the demonstrations of the technologies are expected to show the real capacity of the large-scale of CO_2 monitoring and develop experience for the applications.

• Gravity Technologies

Gravity monitoring technologies are better options for dissolved CO_2 that are used in the Sleipner, Norway, and Schrader Bluff, Alaska. However, the technologies still need more research for the mature field application. First of all, the instrument for the gravity measurements need to be improved with avoiding noise, measuring gravity change accurately, and cost competence. Second, if using the potential ability of gravity technologies to estimate the saturation changes, the quantitative methods need to be more efficient based on the inversion algorithms.

• Surface/Near-Surface Fluxes Technologies

Most of the current technologies for surface/near-surface CO_2 monitoring with supposing of the known leakage location so that the ground-based or airplane based technologies can be successfully used to detect the CO_2 compositions. However, the monitoring of CO_2 footprint probably hundreds of square kilometers, according to the suggestion by Benson & Gasperkova (2004). It means that the monitoring locations and quantifications are very tough by local technologies. Moreover, the background CO_2 varies over the monitoring location and time. So, the better methods for surface/near-surface monitoring may more depend on the development of the technologies of remote sensing and satellite-based observing (Benson & Gasperkova, 2004).

• Geochemical and Tracers Monitoring Technologies

The main works of the geochemical and tracers monitoring technologies lie on the sensitivity of tests and regulations management. Moreover, the geochemical reactions between the well (including abandoned well) and surrounds need more work on figuring out the mechanisms. These reactions include what may happen among annulus cement, plug cement, casing wall over the pH value, which particularly depends on the compositions of the injected CO_2.

Moreover, some more specific techniques applied in the above technologies need to be more addressed.

• Sensors used in the borehole for onshore and offshore monitoring technologies need to consider the temperature and pressure changes over the depth of the well. Specifically, the CO_2 sensor and pH sensor strongly require such considerations because of their sensitivity.

• The fingerprint recognitions of tracers, including gas tracers and hydrogeological tracers, need more works on figuring out the leakage of CO_2.

• The modeling of CO_2 monitoring requires an integrated system, which couples various physical phenomena, such as geochemical reactions, geomechanical behaviors, and geothermal effects into the dynamic model to comprehensively and accurately evaluate the sink-seal system. On the other hand, the related data sets for this integrated system are far away to meet the requirements of the modeling. More field measurements and laboratory tests definitely improve the reliability of the model predictions.

As stated, the CO_2 monitoring is a integrated process which start from the beginning of the geological exploration, site characteristics, and storage formation(s) identifications lasting to

the phases of CO_2 injection and post-injection. Generally, the designs of CO_2 monitoring and choices of technologies need to be considered with the integrated process. As a general guideline, IEAGHG released a monitoring selection tool based on the potential technologies with considering storage options and periods (IEAGHG, 2010). Moreover, Myer (2000) suggested that the strategy for development of monitoring technologies with a focus on the CO_2 monitoring is a three step approach, involving (1) numerical simulation and laboratory experiments to assess technique sensitivities, (2) field testing at different scales in different formations, and (3) analysis and integration of complimentary data. This iterative approach will permit selection of the most cost-effective combination of techniques for the particular formation and sequestration activity being considered by Myer (2000). However, the more details on systemic strategies and optimizations of CO_2 monitoring are still open for further research and field investigations, especially location-based strategy and optimization designs. The suggestion for such designs would be based on the knowledge databases of the world and regulations of the location with cost-effective consideration.

5. Conclusions

In this study, the most recent CO_2 monitoring technologies were reviewed with their applications in fields as examples. The cost of each CO_2 monitoring technology was compared based on the previous research. According to the CO_2 monitoring technologies being used, several CO_2 storage sites in worldwide were analyzed. All of reviews shown that the technologies for CO_2 monitoring have been enhanced more by compared in past decade. Though some of the technologies are still in the beginning stage, they indicate the positive potential of applications in the near-future. Moreover, the general gap of knowledge related to the technologies were partly resealed. With the suggestions for the gap of knowledge, these technologies will play more important roles in CO_2 monitoring by a accurate and cost-effective way.

6. Acknowledgements

The author would like to thank Dr. Donald D. Gray for the advising during the research and thank the funding support of the National Energy Technology Laboratory, U.S. Department of Energy, under task order 41817M2124/003.

7. References

Abu-Khader, M. M. (2006). Recent progress in CO_2 capture/sequestration: A review., *Energy Sources, Part A: Recovery, Utilization, and Environmental Effects* 28(14): 1261–1279.

Aleksandra, H., Esentia, M., Stewart, J. & Haszeldine, S. (2010). Benchmarking worldwide CO_2 saline aquifer injections, *Technical report*, Scottish Center for Carbon Capture and Storage, SCCS.

Arts, R., Chadwick, A., Eiken, O., Thibeau, S. & Nooners, S. (2008). Ten years' experience of monitoring CO_2 injection in the utsira sand at sleipner, offshore norway, *First Break* 26: 65–72.

Bachelor, P., McIntyre, J., Amonette, J., Hayes, J., Milbrath, B. & Saripalli, P. (2008). Potential method for measurement of CO_2 leakage from underground sequestration fields using radioactive tracers, *Journal of Radioanalytical and Nuclear Chemistry* 277: 85–89.

Bachu, S., W., G. & E., P. (1994). Aquifer disposal of CO_2: Hydrodynamic and mineral trapping, energy conversion & management, *Energy Conversion & Management* 35: 269–279.

Benson, H. & Gasperkova, E. (2004). Overview of monitoring techniques and protocols for geological storage of CO_2, *Technical report*, Prepared for the IEA Greenhouse Gas R&D programme.

Benson, R. (2010). Multicomponent seismic monitoring of CO_2-enhanced oil recovery, *SPE International Conference on CO_2 Capture, Storage, and Utilization*, New Orleans, Louisiana.

Benson, S. (2006). Monitoring carbon dioxide sequestration in deep geological formations for inventory verification and carbon credits, spe 102833, San Antonio, Texas.

Bergman, P. & Winter, E. (1995). Disposal of carbon dioxide in aquifers in the U.S., *Energy Conversion & Management* 36: 523–526.

Betts, R., Cox, P., Collins, M., Harris, P., Huntingford, C. & Jones, C. (2004). The role of ecosystem-atmosphere interactions in simulated amazonian precipitation decrease and forest dieback under global climate warming, *Theoretical and Applied Climatology* 78: 157–175.

Borner, J., Herdegen, V., Borner, R. & Spitzer, K. (2010). Electromagnetic monitoring of CO_2 storage in deep saline aquifersIc numerical simulations and laboratory experiments, Berlin, Germany.

Brovkin, V., Sitch, S., Bloh, W., Claussen, M., Bauer, E. & Cramer, W. (2004). Role of land cover changes for atmospheric co2 increase and climate change during the last 150 years, *Global Change Biology* 10: 1253–1266.

Burba, G. & Anderson, D. (2010). *A Brief Practical Guide to Eddy Covariance Flux Measurements: Principles and Workflow Examples for Scientific and Industrial Applications*, LI-COR Biosciences, Lincoln, USA.

Caritat, P. d., Kirste, D. & Hortle, A. (2009). Composition and levels of groundwater in thecrc otway project area, victoria, australia: Establishing a pre-injection baseline, pp. 667–670.

Chadwick, A., Arts, R., Bentham, M., Eiken, O., Holloway, S., Kirby, A., Pearce, M., Williamson, P. & Zweigel, P. (2009). Review of monitoring issues and technologies associated with the long-term underground storage of carbon dioxide in: Evans, d.j.; chadwick, r.a., (eds.) underground gas storage : worldwide experiences and future development in the uk and europe. london, uk., *geological Society Special Publications* 313: 257–275.

Chen, Y. & Nash, A. (1994). Diurnal variation of surface airflow and rainfall frequencies on the island of hawaii, *Monthly Weather Review* 122: 34–56.

Choi, J. & Smith, J. (2005). Geoenvironmental factors affecting organic vapor advection and diffusion fluxes from the unsaturated zone to the atmosphere under natural conditions, *Environmental Engineering Science* 22(1): 95–108.

Claerbout, J. (1985). *Imaging the Earth's Interior*, Blackwell Scientific Publications Inc.

Michael, K., Arnot, M., Cook, P., Ennis-King, J., Funnell, R., Kaldi, J., Kirste, D. & Paterson, L. 2009). CO_2 storage in saline aquifers I – Current state of scientific knowledge *Energy Procedia* 1(1): 3197 – 3204.

CO_2STORE (2007). Best practice for the storage of CO_2 in saline aquifers - observations and guidelines from the SACS and CO_2STORE projects, *Technical report*, Edited and

compiled by: Andy Chadwick, Rob Arts, Christian Bernstone, Franz May, Sylvain Thibeau, and Peter Zweigel.

Cooka, B., Davisb, K., Wang, W., Desai, A., Berger, B., Teclaw, R., Martin, J., Bolstad, P., Bakwin, P., Yi, B. & Heilman, W. (2004). Carbon exchange and venting anomalies in an upland deciduous forest in northern wisconsin, usa, *Agricultural and Forest Meteorology* 126(3-4): 271–295.

D., L. & E., F. (2003). A review and evaluation of stemflow literature in the hydrologic and biogeochemical cycles of forested and agricultural ecosystems, *Journal of Hydrology* 274: 1–29.

Daley, T., Solbau, R., Ajo-Franklin, J. & Benson, S. (2007). Continuous active-source seismic monitoring of CO_2 injection in a brine aquifer, *Petroleum Geoscience* 72(5): A57.

Darby, E., Bumgarner, J. & Hovorka, S. (2008). Geochemical modeling of nearsurface, CO_2 interactions: The critical element in cost-effective long-term monitoring, Washington, D.C.

Dasgupta, S. (2006). Monitoring of sequestered CO_2: Meeting the challenge with emerging geophysical technologies, *First Regional Symposium on Carbon Management*, Dhahran, Saudi Aramco.

Davies, R. J., Stewart, S. A., Cartwright, J. A., Lappin, M., Johnston, R., Fraser, S. I. & Brown, A. R. (2004). 3D seismic technology: Are we realising its full potential?, *Geological Society, London, Memoirs* 29(1): 1–10.

Davis, E. & Marsic, S. (2010a). Geodesy via gps and insar integration, *U.S. Patent 7768441*.

Davis, E. & Marsic, S. (2010b). Interpretation of CO_2-sequestration-induced surface deformation at krechba, algeria, New Orleans, Louisiana.

Davis, E. & Marsic, S. (2010c). Use of deformation based reservoir monitoring for early warning leak detection, Amsterdam.

Davis, E., Marsic, S. & Roadarmel, W. (2008). Deformation monitoring through multi-platform integration, Lnce, Lisbon.

Davison, J., Freund, P. & Smith, A. (2004). Putting carbonback into the ground, *Technical report*, IEA Greenhouse Gas R & D Centre.

Onuma, T., Okada, K. & Ohkawa, S. (2008). Detection of surface deformation related with CO_2 injection by DInSAR at In Salah, Algeria, *Energy Procedia* 1(1): 2177 – 2184.

Doughty, C., Freifeld, B. & Trautz, R. (2008). Site characterization for CO_2 geologic storage and vice versa: the frio brine pilot, texas, usa as a case study, *Environmental Geology* 54(8): 1635–1656.

DTI (2005). monitoring technologies for the geological storage of CO_2, *Technical report*, Cleaner Fossol Fules Programme.

Du, J., Brissenden, S., McGillivray, P., Bourne, S., Hofstra, P., Davis, E., Wolhart, S., Marsic, S. & Wright, C. (2005). Mapping reservoir volume changes during cyclic steam stimulation using tiltmeter based surface deformation measurements, spe 62577, Calgary, Alberta, Canada.

Ebinger, M., Cremers, D., Breshears, D., Unkefer, P., Kammerdiener, S. & Ferris, M. (2001). Total carbon measurement in soils using laser-induced breakdown spectroscopy: results from the field and implications for carbon sequestration, *Los Alamos National Laboratory*, Los Alamos, NM.

Edwards, N. & Riggs, J. (2003). Automated monitoring of soil respiration: A moving chamber design, *Soil Sci. Soc. Am. J.* 67: 1266–1271.

Emberleya, S., Hutcheonb, I., Shevalierb, M., Durocherb, K., Gunterc, W. & Perkinsc, E. (2004). Geochemical monitoring of fluid-rock interaction and CO_2 storage at the weyburn CO_2-injection enhanced oil recovery site, saskatchewan, canada, *Energy* 29(9-10): 1393–1401.

EPA (2005). Inventory of U.S. greenhouse gases emissions and sinks: 1990-2003.

Flett, M., Brantjes, J., Gurton, R., McKenna, J., Tankersley, T. & Trupp, M. (2009). Subsurface development of CO_2 disposal for the gorgon project, *Energy Procedia* 1(1): 3031 – 3038.

Freeman, B., Yielding, G. & Badley, M. (1990). Fault correlation during seismic interpretation, *First Break* 8(3): 87–95.

Freifeld, B., Daley, T., Hovorka, S., Henninges, J., Underschultz, J. & Sharma, S. (2008). Recent advances in well-based monitoring of CO_2 sequestration, *9th International Conference on Greenhouse Gas Control Technologies (GHGT-9)*, Washington, D.C.

Gale, J. (2004). Geological storage of CO_2: What do we know, where are the gaps and what more needs to be done?, *Energy* 29(9-10): 1329–1338.

Gladwin, M. T. (1984). High-precision multicomponent borehole deformation monitoring, *Review of Scientific Instruments* 55(12): 2011 –2016.

Goldberg, D. (2011). Methods of long-term gravimetric monitoring of carbon dioxide storage in geological formations, *Patent US 20110042074*.

Goulden, M., Munger, J., Fan, S., Daube, B. & Wofsy, S. (1996). Measurements of carbon sequestration by long-term eddy-covariance: Methods and a critical evaluation of accuracy, *Global Change Biology* 2: 169–182.

Gunter, W., Bachu, S., Law, D., Marwaha, V., Drysdale, D., Macdonald, D. & McCann, T. (1996). Technical and economic feasibility of CO_2 disposal in aquifers within the alberta sedimentary basin, *Energy Conversion & Management* 37: 1135–1142.

Gunter, W., Perkins, E. & McCann, T. (1993). Aquifer disposal of CO_2-rich gases: reaction design for added capacity, *Energy Conversion and Management* 34: 941–948.

Guo, H., Jiao, J. & Weeks, E. (2008). Rain-induced subsurface airflow and lisse effect, *Water Resour. Res.* W07409: doi:10.1029/2007WR006294.

Halmann, M. & Steinberg, M. (1999). *Greenhouse gas carbon dioxide mitigation: Science and technology*, Lewis Publishers.

Hansen, J., Sato, M., Ruedy, R., Lacis, A. & Oinas, V. (1997). Global warming in the twenty first century: An alternative scenario, *Proc. Natl. Acad. Sci.* 97(18): 9875–9880.

Herzog, H. & Drake, E. (1996). Carbon dioxide recovery and disposal from large energy systems, *Annual Review of Energy and the Environment* pp. 145–166.

Herzog, H. & Golomb, D. (2004). Carbon capture and storage from fossil fuel use, c.j. cleveland, editor, *Encyclopedia of Energy* pp. 277–287.

Hortle, A., de Caritat, P., Stalvies, C. & Jenkins, C. (2011). Groundwater monitoring at the otway project site, australia, *Energy Procedia* 4(0): 5495 – 5503.

Hutcheon, I., Durocher, K., Shevalier, M., Mayer, B., Gunter, W. & Perkins, E. (2003). Carbon isotope evidence for CO_2 dissolution and fluid-rock interaction at the weyburn CO_2 injection enhanced oil recovery site: Saskatchewan, canada, *Proceedings of 2nd National Conference on Carbon Sequestration*, Pittsburg, PA.

IEA (2007). Monitoring selection tool - interactive design of monitoring programmes for the geological storage of CO_2.

IEA (2009). Iea ghg monitoring network, *CO_2 Geological Storage Modeling Workshop*, Orleans, Frence.

IEAGHG (2010). Interactive design of monitoring programmes for the geological storage of CO_2, *Technical report*, IEAGHG.

Ishido, T. & Mizutani, H. (1981). Experimental and theoretical basis of electrokinetic phenomena in rock-water systems and its applications to geophysics, *J. Geophys. Res.* 83: 1763–1775.

Jacobs, G. & Graham, R. (2000). Carbon sequestration in terrestrial ecosystems: A status report on r&d progress, *Carbon sequestration and bioenergy feedstock production seminar*, National Laboratory, Oak Ridge, TN.

Johansen, S., Amundsen, H., Rosten, T., Ellingsrud, S., Eidesmo, T. & Bhuyian, A. (2005). Subsurface hydrocarbons detected by electromagnetic sounding, *The First Break* 23: 31–26.

Keeling, C. & Whorf, T. (1998). Atmospheric CO_2 records from sites in the sio air sampling network, *Technical report*, in Trends: A Compendium of Data on Global Change, Carbon Dioxide Information Analysis Center, Oak Ridge National Laboratory.

Kherroubi, A., Deverchere, J., Yelles, A., Lepinay, B., Domzig, A., Cattaneo, A., R., B., Gaullier, V. & Graindorge, D. (2009). Recent and active deformation pattern off the easternmost algerian margin, western mediterranean sea: New evidence for contractional tectonic reactivation, *Marine Geology* 261: 17–32.

Kikuta, K., Hongo, S., Tanase, D. & Ohsumi, T. (2004). Field test of CO_2 injection in nagaoka, japan, *7th International Conference on Greenhouse Gas Control Technologies (GHGT-7)*, Vancouver.

Kirkendall, B. & Roberts, J. (2004). Electromagnetic imaging of CO_2 sequestration at an enhanced-oil-recovery site, *Technical report*, Lawrence Livermore National Laboratory, Paper UCRL-TR-202407.

Lee, H., Torres-Verdin, C. & Sepehrnoori, K. (2005). Near well bore pressure transient simulation with geomechanical deformation for formation evaluation in weak reserviors, *Technical report*, The University of Texas at Austin, Austin, Texas.

Lehmann, J., Gaun, J. & Rondon, M. (2006). Bio-char sequestration in terrestrial ecosystems - a review, *Mitigation and Adaptation Strategies for Global Change* 11: 395–419.

Lewicki, J., Hilley, G., Fischer, M., Pan, L., Oldenburg, C., Dobeck & Spangler, L. (2009). Eddy covariance observations of leakage during shallow subsurface CO_2 releases, *J. Geophys. Res.* 114(D12302).

LI-COR Bioscience (2004). Surface monitoring for geologic carbon sequestration monitoring - methods, instrumentation, and case studies, *Technical report*, LI-COR Bioscience, 980-10283.

LI-COR Bioscience (2006). Automated soil CO_2 flux system & li-8150 multiplexer - instruction manual, document #53-07671, *Technical report*, LI-COR Bioscience, 980-11916.

LI-COR Bioscience (2011). Surface monitoring for geologic carbon sequestration monitoring - vol. 2. methods, instrumentation, and case studies, *Technical report*, LI-COR Bioscience, 980-11916.

Liu, G. (2010). *Numerical modeling of near-surface CO_2 migration with barometric pumping effects*, Ph.D. dissertation, Civil and Environmental Engineering, West Virginia University.

Liu, G., Gray, D. & Bromhal, G. (2009). Scheme to enhance near-surface carbon dioxide monitoring using barometric pumping, *84th Annual Meeting of West Virginia Academy of Science*, Glenville, WV.

Liu, G. & Smirnov, A. (2008). Modeling of carbon sequestration in coal-beds: A variable saturated simulation, *Energy Conversion and Management* 49(10): 2849–2858.

Liu, G. & Smirnov, A. (2009). Carbon sequestration in coal-beds with structural deformation effects, *Energy Conversion and Management* 50(6): 1586–1594.

LLNL (2005). locked in rock sequestering carbon dioxide underground, *Technical report*, Lawrence Livermore National Laboratory.

Lonergan, L. & White, N. (1999). Three-dimensional seismic imaging of a dynamic earth, *Philosophical Transactions: Mathematical, Physical and Engineering Sciences* 357(1763): 3359–3375.

Lorenz, K. & Lal, R. (2010). *Carbon Sequestration in Forest Ecosystems*, Springer-Verlag.

Lumley, D. (2001). Time-lapse seismic reservoir monitoring, *Geophysics* 66(1): 50–53.

Lumley, D. & Behrens, R. (1998). Practical issues of 4d seismic reservoir monitoring: What an engineer needs to know, *SPE Reservoir Evaluation & Engineering* 1(6): 528–538.

Lumley, D., Behrens, R. & Wang, Z. (1997). Assessing the technical risk of a 4D seismic project, *Leading Edge* 16(9): 1287–1291.

Madsen, R., Xu, L., Claassen, B. & McDermitt, D. (2009). Surface monitoring method for carbon capture and storage projects, *Energy Procedia (Greenhouse Gas Control Technologies 9)* 1(1): 2161–2168.

Martinez, M. & Nilson, R. (1999). Estimates of barometric pumping of moisture thgourgh unsaturated fractured rock, *Transport in porous media* 36: 85–119.

Mathieson, A., Midgely, J., Wright, I., Saoula, N. & Ringrose, P. (2011). In salah co2 storage jip: CO_2 sequestration monitoring and verification technologies applied at krechba, algeria, *Energy Procedia* 4(0): 3596 – 3603.

Mathieson, A., Midgley, J., Dodds, K. & Wright, I. (2010). CO_2 sequestration monitoring and verification technologies applied at krechba, algeria, *The Leading Edge* 29: 216–222.

McCallum, S., Riestenberg, D., Cole, D., Freifeld, B., Trautz, R., Hovorka, S. & Phelps, T. (2005). Monitoring geologically sequestered CO_2 during the frio brine pilot test using perfluorocarbon tracers, *Fouth Annual Conference on Carbon Capture and Sequestration DOE/NETL*, Pittsburg, PA.

Metz, B., Davidson, O., Coninck, H., Loos, M. & Meyer, L. (2005). *Special Report on Renewable Energy Sources – IPCC Special Report on Carbon Dioxide Capture and Storage*, Camberidge University Press.

Metz, B., Davidson, O., de Coninck, H., Loos, M. & Meyer, L. (2005). Carbon dioxide capture and storage, *Technical report*, Switzerland.

Michael, K., Allinson, G., Golad, A., Sharma, S. & Shulakova, V. (2009). CO_2 storage in saline aquifers ii – experience from existing storage operations, *Energy Procedia* 1(1): 1973–1980.

Michael, K., Golab, A., Shulakova, V., Ennis-King, J., Allinson, G., Sharma, S. & Aiken, T. (2010). Geological storage of CO_2 in saline aquifers – a review of the experience from existing storage operations, *Int. J. Greenhouse Gas Control* 4(4): 659–667.

Mikhailov, O., Queen, J. & Toksoz, M. (2000). Using borehole electroseismic measurements to detect and characterize fractured (permeable) zones, *Geophysics* 65: 1098–1112.

Miles, N., Davis, K. & Wyngaard, I. (2004). Using eddy covariance to detect leaks from CO_2 sequestered in deep aquifers, Vancouver, Canada.

Myer, L. (2000). A strategy for monitoring of geologic sequestration of CO_2, *Technical report*, Lawrence Berkeley National Laboratory.

Myer, L., Benson, S., Doughty, C., Hovorka, S., Hoversten, G., Majer, E., Pruess, K., Knauss, K., Phelps, T., Cole, D., Knox, P., Gunter, W., Newmark, R., Vasco, D. & Foxall, W.

(2003). Monitoring and verification at the frio pilot test, *Proceedings of 2nd National Conference on Carbon Sequestration*, Pittsburg, PA.

Neeper, D. (2001). A model of oscillatory transport in granular soils, with application to barometric pumping and earth tides, *Journal of Contaminant Hydrology* 48: 237–252.

NETL (2009). Doe publishes best practices manual for public outreach and education for carbon storage projects, the first version, *Technical report*, National Energy Technology Laboratory, US. DOE.

NETL (2011). Best practices for: Risk anakysis and simulation for geological storage of CO_2, *Technical Report DOE/NETL-2011/1459*, National Energy Technology Labratory.

NFESC (2004). Cost and performance report for natural pressure-driven passive bioventing, *Technical report*, Engineering Service Center, Port Hueneme, California.

Oldenburg, C., Lewicki, J. & Hepple, R. (2003). Near-surface monitoring strategies for geologic carbon dioxide storage verification, *Technical report*, Lawrence Berkeley Laboratory, Berkeley, CA.

Oldenburg, C., Unger, A., Hepple, R. & Jordan, P. (2003). On leakage and seepage from geologic carbon sequestration sites, *Technical report*, Lawrence Berkeley Laboratory, Berkeley, CA.

Olson, M., Jr. Tillman, F., Choi, J. & Smith, J. (2001). Comparison of three techniques to measure unsaturaed-zone air permeability at picatinny arsenal, nj, *Journal of Contaminant Hydrology* 53: 1–19.

Pekot, L. & Reeves, S. (2003). Modeling the effects of matrix shrinkage and differential swelling on coalbed methane recovery and carbon sequestration, *International Coalbed Methane Symposium*, number 0328, Tuscaloosa, AL.

Phelps, T., McCallum, S., Cole, D., Kharaka, Y. & Hovorka, S. (2007). Monitoring geological CO_2 sequestration using perfluorocarbon gas tracers and isotopes, Pittsburgh, PA.

Reichle, D., Houghton, J., Kane, B. & Ekmann, J. (1999). Carbon sequestration: Research and development, *Technical report*, U.S. DOE report.

SEAI (1996). Barometric pumping with a twist: Voc containment and remediation without boreholes, phase 1, *Technical report*, Science and Engineering Associates, Inc., Santa Fe, NM.

Seto, C. & Mcrae, G. (2011). Reducing risk in basin scale CO_2 sequestration: A framework for integrated monitoring design, *Environ. Sci. Technol.* 45: 845–859.

Smith, P. (2004). Monitoring and verification of soil carbon changes under article 3.4 of the kyoto protocol, *Soil Use and Management* 15(20): 264–270.

Stalker, L., Boreham, C. & Perkins, E. (2009). A review of tracers in monitoring CO_2 breakthrough: Properties, uses, case studies, and novel tracers, *Technical report*, in M. Grobe, J. C. Pashin, and R. L. Dodge, eds., Carbon dioxide sequestration in geological mediamdashState of the science: AAPG Studies in Geology 59.

Stenvold, T. (2008). *Offshore Gravimetric and Subsidence Monitoring*, Phd dissertation, Norwegian University of Science and Technology.

Sturman, A. (1992). Dynamic and thermal effects on surface airflow associated with southerly changes over the south island, new zealand, *Meteorology and Atmospheric Physics* 47: 229–236.

Sweatman, R. & McColpin, G. (2009). Monitoring technology enables long-term CO_2 geosequestration, *E&P* November: 5–6.

Swinbank, C. (1951). The measurement of vertical transfer of heat and water vapor by eddies in the lower atmosphere, *Journal of Atmospheric Sciences* 8(3): 135–145.

Taylor, P. (1970). A model of airflow above changes in surface heat flux, temperature and roughness for neutral and unstable conditions, *Boundary-Layer Meteorology* 1: 18–39.

Tillman, F. J. & Smith, J. (2005). Site characteristic controlling airflow in the shallow unsaturated zone in response to atmosphere pressure canges, *Environmental Engineering Science* 22(1): 25–37.

Trenberth, K. & Jones, P. (2007). Chapter 3: Observations: Surface and atmospheric climate change, IPCC fourth assessment report.

Vanaja, M., Maheswari, M., Ratnakumar, P. & Ramakrishna, Y. (2006). Monitoring and controlling of CO_2 concentrations in open top chambers for better understanding of plants response to elevated CO_2 levels, *Indian Journal of Radio and Space Physics* 35: 193–197.

Verdon, J. (2010). *Microseismic Monitoring and Geomechanical Modelling of CO_2 Storage in Subsurface Reservoirs*, Phd dissertation, University of Bristol.

Voormeij, D. & Simandl, G. (2002). Geological and mineral CO_2 sequestration options: A technical review, *Technical report*, Geological Fieldwork.

Wang, Z. (1997). Feasibility of time-lapse seismic reservoir monitoring: the physical basis, *Leading Edge* 16(9): 1327–1329.

Wells, A., Diehl, J., Bromhal, G., Strazisar, B., Wilson, T. & White, C. (2007). The use of tracers to assess leakage from the sequestration of CO_2 in a depleted oil reservoir, new mexico, usa, *Applied Geochemistry* 22(5): 996–1016.

Wildenborg, T. (2011). CO_2 geological storage: Research into monitoring and verification technology - eu project co2remove, *Technical report*, TNO-NATIONAL GEOLOGICAL SURVEY, DELFT, NEDERLAND.

Wisniewski, J., Robert, D., Sampson, R. & Lugo, A. (1993). Carbon dioxide sequestration in terrestrial ecosystems, *Climate Research Clim. Res.* 3: 1–5.

Zahid, U., Lim, Y., Jung, J. & Han, C. (2011). CO_2 geological storage: A review on present and future prospects, *Korean Journal of Chemical Engineering* 28(3): 674–685.

Zemel, C. (1995). *Tracers in the Oil Field*, Develop. Petrol. Sci.